The Influence of Different Time Varying Antecedent Flows On The Stability of Mixed Grain Size Deposits

by

Yusron Saadi

B.Sc. (Eng) Mataram, M.Sc. (Eng) Newcastle upon Tyne

Thesis submitted in partial fulfilment of the requirements for the Degree of Doctor of Philosophy

University of Sheffield
Department of Civil and Structural Engineering

October 2002

DEDICATION

This thesis is dedicated to

my parents
who create an atmosphere
full of inspiration and belief

and
to my teachers
who have guided me
through the tunnels of knowledge

DECLARATION

I declare that the work in this thesis has been composed by myself and no portion of the work has been submitted in support of an application for another degree or qualification of this or any other university or other institute of learning. The work has been my own except where indicated and all quotations have been distinguished by quotation marks and the sources of information have been acknowledged.

25/10/02

SUMMARY

The objective of this work was to examine the impact of unsteady flows on the erosion and movement of mixed grain size sediment. Time varying flows were examined as flowrates in natural rivers are rarely constant. There are very few reported studies on the movement of sediment in unsteady open channel flow and most of those used single sized sediment. River reach has its own sedimentological character and non-uniform beds exhibit very different behaviour from that of single sized material. Therefore it was thought important to examine the impact of time varying flow on the stability of water worked mixed grain size sediment beds.

The thesis reports on a series of laboratory experiments in which a bimodal sediment bed was exposed to different flow hydrographs. The flow hydrographs consisted of constant flowrate with different duration and time varying flows with different rising and falling limb but had the same peak flowrate. Each experiment was followed by a stability test in which a standard "triangular shaped hydrograph" was used to assess the stability of each water worked deposit. The stability observation demonstrated that grain size fractions have different thresholds of motion when beds are formed by different antecedent flow patterns. The bed stability increased as the antecedent constant flow hydrograph progressed. The rising and falling limbs of the flowrate hydrographs were found to have a significant effect on the bed stabilisation process. It revealed that the shortest rising limb of flow hydrograph formed the weakest bed while the longest recession limb of flow hydrograph formed the most stable bed. It is believed that the short period of flowrate acceleration did not allow the coarse grains to stabilise with numerous exposed large grains spread on the bed. In a longer duration of recession limb of hydrograph, the coarse grains moved and eventually deposited over a length of time. As the flowrate declined the finer grains also rolled and then deposited forming a strong bond with the coarse grains.

These experiments also provided important information on the flow structures and the changes in the bed topography as the tests progressed. There is strong evidence that only upward interactions (ejections) with high momentum magnitude were able to transport coarser grains. The lack of change in the distribution of downward looking-bed interactions (sweeps) in all tests indicated that these features are not important in determining transport. Changes in bed topography were also measured and characteristics of the distribution of bed surface elevation were linked to the observed changes in bed stability.

ACKNOWLEDGEMENTS

This study is only possible with the assistance and support of others. I therefore would like to take this opportunity to express my appreciation and to acknowledge the efforts of the people involved.

I wish to thank Indonesian Government for their full financial support of this research through the Engineering Education Development Project (EEDP).

Sincere thanks must go to Dr. Simon J. Tait for his able supervision and support during this work. I have appreciated not only his advice but also his encouragement and confidence in me which has allowed me to pursue this work with a level of independence that I had not anticipated and from which I derived great benefit. Without his enthusiasm and patience there would not have been sufficient resources for the production of this work.

My thanks are extended to my fellow in the Water Engineering Research Group, Department of Civil and Structural Engineering University of Sheffield. It is not only for the smile we have shared but also for their understanding of my condition, which limited me from joining their "day out" and other non-academic activities.

The works have not been possible without the support from the departmental technician. I would like to thank Mr. Paul Osborne, Mr. Darren Unwin and others who kindly helped me in preparation of the laboratory works including the "quarry hunting" for the material used in the experiments.

Finally, I would like to express my appreciation to my wife Nini, who was in her early pregnancy to my first son Haytham, had helped me with her patience and encouragement throughout. It was a truly great source to replenish my energy to face all the long hours of experiments.

CONTENTS

LIST OF FIGURES

LIST OF TABLES

I. INTRODUCTION

1.1. BACKGROUND

Natural rivers are rarely free of sediment. Although at low discharges sediment movement is rare, most rivers are regularly subjected to sediment-transporting flows. In nature it is rare for a river to contain only one type of sedimentary material, as its morphology is the result of continuing processes of erosion along reachs with numerous different sediment sources. Factors, such as the characteristics of the catchment, its topography, land use practices and river characteristics, such as bank materials, grain size distributions and the structure and topography of the bed, control the supply, transport and storage of water and sediment into and through a river reach. Sediment transport in natural streams can vary continuously over time and in space even within small catchment areas. The short term variability in the rate and composition of transported sediment makes a significant contribution to the long-term channel evolution. The variation in sediment transport is controlled by the rate of sediment entrainment for each size fraction, the amount of sediment available for transport in a reach and by the transport length of individual particles. Particularly troublesome as regards prediction are streams with sediment size distributions that are bimodal mixtures of sand and gravel where the median D_{50} of the overall distribution may be virtually absent from the bed (Sear, 1996).

Early research on gravel-bed rivers was concerned with stable or regime channels. It is understandable that this approach was taken, as the basic knowledge of the flow and sediment transport processes was poor. Many research studies focused on predicting sediment response to steady flows. However, in order to develop appropriate modelling techniques to forecast river response to changing environmental conditions at different space and time scales, it is vital to understand the dynamic adjustment of the gravel-bed rivers as most of these rivers are inherently unstable. Parker (1991) noted that a major change of thinking concerning sediment transport in rivers began in the decade of the 1980's. The decade was the starting point of research on sediment mixtures. Until then, research tended to be focused on single size material and the published sediment

transport rate relationships were developed using a "uniform" grain size. This was done so that the effects of the 'average' sediment size on transport rates could be determined. The obvious fact is that each reach of a single river has its own sedimentological character and that reliable predictions in such systems cannot be made with such sweeping assumptions. Most natural channels are also subject to a range of time varying flows. It is during periods of large changes in flowrate that most sediment movement occurs. However, engineering predictive techniques have traditionally been developed by simplifying such systems as to contain single sized sediment and being at a series of steady flow discharges for long enough to assume the system is in "quasi equilibrium". Whilst this may be the case for the hydraulic conditions in rivers due to the time scale of river floods, it is unlikely that the grain sorting processes active during the mobilisation of gravel beds would reach "equilibrium" in the short times available during typical storm flows.

1.2. PREVIOUS EXPERIMENTS

There are very few reported studies on the movement of sediment in unsteady open channel flows. Those studies that have been reported have all used single sized sediment despite growing evidence that grain size mixtures and single sized material do not move in the same fashion. Although unsteady flows are expected to have high levels of acceleration, and thus generate a hysteresis type pattern in the relation between water surface slope, and flow depth when discharge is unsteady, the water surface slope is almost never treated as a variable even in sophisticated research projects (Meirovich et al., 1998). This has occurred because of the difficulty in obtaining this data in the field, especially during flood flows. However the degree of variability in sediment movement during the course of a flood-wave in some cases has been shown to be considerable (Reid et al., 1985). Most of the existing sediment transport relations only predict the total sediment discharge and, therefore, are not suitable for predicting changes in the size distribution of bed materials in riverbeds undergoing degradation or aggradation (Karim, 1998). In addition, the relationships developed are empirical and site-specific and thus they are not suitable for general application to the different streams. Temporal flow changes, variations of cross-section, and changes in the bed composition and texture almost always produce conditions in which the sediment input to a particular

reach is not in equilibrium with the transporting capacity of that reach. Little work has been carried out to examine the grain sorting behaviour during unsteady flows. One of those works (e.g. Graf and Suszka, 1985), indicated that time varying flows did influence the amount and rate of sediment transport. However, their tests were conducted with uniformly sized grains so that no investigation was possible of the impact of time varying flows on grain sorting.

In the last two decades many researchers (e.g. Klingeman and Emmet, 1982 ; Misri et al., 1984 ; Reid and Frostick, 1987 ; Wilcock and Southard, 1989 ; Barta et al., 1994 ; Molinas and Wu, 1998; Karim, 1998 ; Shvidchenko and Kopaliani, 1998) carried out experiments involving measurement of the bed load transport rates of different size fractions in a mixture. Renewed interest in the transport of mixed size sediment has produced important new empirical and theoretical results. Discussion of the interaction between the grain size population of the bed and the fractional transport rates have been included in some of the past works (e.g. Parker and Klingeman, 1982 ; Andrews and Parker, 1987 ; Iseya and Ikeda, 1987 ; Sutherland, 1987). However a consensus on the most suitable method of prediction has not been obtained. An example of this, is the discussions in the use of the particle size distribution of surface sample or volumetric samples of the transported material to scale overall bedload transport (Wilcock and Southard, 1988).

1.3. OBJECTIVES OF THIS STUDY

The objective of this study was to examine the impact of time varying antecedent flows on the stability of mixed grain size sediment and to characterise the gravel bed surface by grain size distribution analysis and bed texture measurements. The grain sorting and the development of armoured bed surface during different time varying flow patterns were investigated. This was intended to examine the impact of time varying flows on the development of bed stability which would be very important in determining the behaviour of a riverbed in a subsequent floods.

In order to investigate the links between time varying flows and sediment transport rates for a variety of conditions, experiments with simultaneous measurements of near-bed

flow and transported sediment at relatively high frequency were conducted. Experiments were divided into three groups consisting of ten different combinations of hydrographs. The first group was steady flow experiments with different time lengths of constant discharge. The aim of these experiments was to quantify the changes in stability caused by an increase in the length of time as a mixed grain sediment bed was exposed to a uniform flowrate. The second group was the combination of steady flow and unsteady flow with different time lengths of decreasing discharge. The aim was to assess the impact that different rates of decline in flood hydrographs have on sorting and stability. The third group was unsteady flow where three different hydrographs with different rising limb but the same peak discharge and the same recession limb were applied. The aim of this series of tests was to examine the effect that different rate of increase of flow discharge has on the stability of a water-worked sediment bed. Bed topography measurements in a selected area were also carried out in all experiments to examine the impact of different hydrograph and flow duration to the changes in the bed surface structure.

II. LITERATURE REVIEW

2.1. INTRODUCTION

Sediment transport within a river reach varies spatially and with time in response to changes in the imposed flow discharge and upstream sediment input. Transport is controlled by the rate of sediment entrainment, the amount of sediment available for entrainment in a reach and by the transport length of individual particles (Sear, 1996). Transport of sediment by the river flows occurs in two modes : a contact mode, where the particle rolls or slides along in contact with the rough bed, and a non-contact mode, where the particle is suspended in the moving fluid supported by fluid turbulence (Kelsey et al, 1994) or a combination of the two ways where sediment leaps into the flow and then rests on the bed (Gyr, 1983). The mode of transport of the material depends on the sediment characteristic such as its size and shape, density of particle and the prevailing flow condition (Featherstone and Nalluri, 1988).

The erosion and transport processes of non-uniform sediment are much more complex than those of uniform sediments. Both types of sediment respond very differently to the imposed fluid forces (Raudkivi, 1993). Since the pioneering work of Einstein (1950), it has been recognised that calculating sediment transport rates of highly nonuniform sediments using a single representative size of the bed material is not appropriate (Ranga Raju et al., 1991). Therefore, in order to predict the response of mixed size sediment to flow, it has been thought necessary to predict the transport rates of individual grain size fraction in the mixture and then sum them up to get the total transport rate.

According to Di Silvio (1992), all existing experimental formulae show that for a given hydraulic condition the transport rate of a uniform material increases if its grain size increase. As there is no significant changes in bed roughness, it can be assumed that the movement of each particle of the sediment bed compose of the finer grains is not greatly affected by the presence of the others. In the coarser bed, the erodibility of the grain is expected to be increased due to the grain relative projection above the mean bed and the

exposure relative to the upstream grain. In a mixture the mobility of different grain sizes is strongly equalised by the fact that finer particles are protected by the coarser ones and, therefore, are less subjected to the hydraulic forces than in a uniform-size bed, and that the coarser ones suffer an enhanced exposure to the flow, in comparison to a uniformly sized deposit.

2.2. CHARACTERISING NATURAL SEDIMENTS

Most natural river reaches contain sediment beds with a continuous grain size distribution depending on the characteristics of the river channel and catchment. Rivers are often considered to have either cohesive, sand, gravel, cobble or boulder beds. Broadly speaking, rivers can be subdivided into gravel bed and sand bed rivers (Simons and Simons, 1987). The traditional method of particle size analysis divided material into six categories : clay, silt, sand, gravel, cobbles and boulders. Very similar classifications were proposed by British Standard BS 1377 and by the Subcommittee on Sediment Terminology of the American Geophysical Union (Raudkivi, 1991). Einstein (1971) claimed that the grain size has probably the greatest influence on the ability of a flow to move sediment. The transport of sediment by water flow is frequently divided into bed load and suspended load, but for practical reasons (Einstein, 1971), the term wash load for the very fine part of sediment load have also been introduced by engineers.

Natural sediments normally consist of distributions of particle sizes. The "Udden-Wentworth" grain size scale is widely accepted and used as the practical standard for objective and detailed description of grain size needed for communicating observations about sediment grain size distributions. This scale recognises three fractions, gravel, sand, and mud. However the scale is most detailed in the sand and mud fractions, and inadequately covers gravel, the dominant fractions in many fluvial environments (Blair and McPherson, 1999). Textural classification of sediment and sedimentary rocks that is widely used because of its objectivity and practicality is suggested by Folk (1974). This classification is a flexible polynomial scheme in which various sediments attributes are systematically listed. Folk et al (1970) also offered a field method for estimating the sorting class of sediment without the benefit of quantitative size analysis (Blair and

McPherson, 1999).

A better focus on gravelly sediment has developed because of an expanded interest in the deposits of rivers. According to Blair and McPherson (1999), Udden (1914) devised more detailed subclasses called "grades", with boundaries defined by a logarithmic scale using 1 mm as the starting point. Coarser grade boundaries were established by progressive multiples of 2, and finer ones by progressive multiples of 0.5. The use of sieves for size analysis dictates that the intermediate axial length (d_I) of a grain is the one that determines classification. Krumbein (1934, 1938) also devised the phi scale (ϕ) to convert the sediment grade boundary values from fractional numbers to more simple whole numbers (Blair and McPherson, 1999).

The phi-index scale that divides the sediment into arbitrary class intervals is defined as

$$\phi = -\log_2 d_I \text{ (mm)} = -\log d_I / \log 2 \qquad (2.1)$$

$$d_I = 2^{-\phi}$$

where :

ϕ = phi values

d_I = intermediate axial length of the grain (grain diameter)

The negative sign in the equation causes an unnecessarily complicated inverse relationship between ϕ and d_I, rather than a direct one (Blair and McPherson, 1999). It was added so that phi values in most of the sand fraction are positive, exemplifying the historical emphasis on sand and the limited consideration of gravel. As the result of this emphasis, five divisions for the small size range covered by sand shows more formal division than four divisions that have been established for the gravel fraction (granule, pebble, cobble and boulder). Table 2.1. shows the sedimentary grain size scale that is widely used as the practical standard in engineering practice. It is similar to the classification used by British Standard (BS 1377) and American Geophysical Union (AGU) on the basis of particle size.

Sediment of uniform grain size responds differently from one with a broad grain size distribution. It has been recognised that calculation of sediment transport rates of highly nonuniform sediments using a single representative size of the bed material is not

appropriate. Samaga et al (1985) have shown that large errors can result in the computed transport rates if a single representative size like the median size of the bed material is used in several of the standard methods available. Therefore, it is necessary to divide the bed material into different fractions and compute the fractional transport to get the total transport rate. From a hydraulic point of view, two simple criteria have been used to determine that a sediment mixture is uniform. Those criteria are the ratio of ninety five percent finer (d_{95}) and five percent finer (d_5), and the geometric standard deviation (σ_g), which is the square-root of the ratio of eighty four percent finer (d_{84}) and sixteen percent finer (d_{16}). The mixture can be categorised as uniform if the value of d_{95}/d_5 is less than 4 and $\sigma_g = \sqrt{\left(\frac{d_{84}}{d_{16}}\right)} < 1.35$ (Raudkivi, 1993).

Table 2.1. Sedimentary grain size scale (after Udden, 1914 ; Folk, 1954, 1974 ; Folk et al., 1970 ; and Blair and McPherson, 1999)

Grain size		Grade	Class	Fraction	
d_1 (mm)	ϕ			Unlithified	Lithified
4096	-12		Boulder	Gravel	Conglome-rate
1024	-10	large and very large			
		small and medium			
256	-8	small and large	Cobble		
64	-6	coarse and very coarse	Pebble		
16	-4	fine and medium			
4	-2	very fine	Granule		
2	-1	very coarse	Sand	Sand	Sandstone
1	0	coarse			
0.500	1	medium			
0.250	2	fine			
0.125	3	very fine			
0.063	4	coarse	Silt	Mud	Mudstone or Shale
0.031	5	medium			
0.016	6	fine			
0.008	7	very fine			
0.004	8	coarse	Clay		
0.002	9	medium			
		fine			
		very fine			

2.3. SEDIMENT TRANSPORT OF NATURAL RIVERS

2.3.1. Transport Rate

Most of the existing sediment transport relations only predict the total sediment discharge and, therefore, are not suitable for predicting changes in the size distribution of bed materials in riverbeds undergoing degradation or aggradation (Karim, 1998). Many investigators have proposed several empirical equations calibrated from different laboratory flume data sets with the assumptions that the sediment is homogeneous and noncohesive (Yang, 1973 ; Ackers and White, 1973 ; van Rijn, 1984). The prediction methods of many existing published sediment transport rate relationships have therefore been developed using data from "uniform" sized sediment. This was done so that the effects of the 'average' or 'representative' sediment size on transport rates could be determined.

Experiments involving measurement of the bed load transport rates of different fractions in a mixture and the effect of size gradation have been carried out by several researchers (e.g. Klingeman and Emmet, 1982 ; Misri et al., 1984 ; Reid and Frostick, 1987 ; Wilcock and Southard, 1989 ; Barta et al., 1994 ; Molinas and Wu, 1998; Karim, 1998 ; Shvidchenko and Kopaliani, 1998). Since the experiments were mostly based on specific conditions, such as the original grain size distribution, and the rate and composition of the incoming sediment, it has proved difficult to apply the developed relationships to different streams in the field. It is therefore apparent given the lack of generality of many of the existing transport rate relationships, that have either been modified for mixed grain transport, or developed from mixed grain data sets, that understanding of some of the principle variables is missing. The problem of finding a universal bedload transport equation therefore lies in improving understanding of the dominant physical factors that control particle movement in natural channels.

Some authors (Yang, 1973 ; Ackers and White, 1973) believed that the unit stream power is the dominant physical factor in determination of total sediment concentration. Water discharge, average velocity, energy slope and shear stress have all been taken to be the dominant independent variables in sediment transport equations. As the rate of transport is very sensitive, the use of available predictive equations may result in very different answers and some are complicated to apply (Ackers and White, 1973). Those

existing equations are mostly derived under the assumption that there is always a determinate relationship between sediment discharge and a dominant independent variable (Yang, 1973). Molinas and Wu (1998) proposed that the transport rate functions of Engelund and Hansen (1967), Ackers and White (1973) and Yang (1973) can be used to demonstrate the effect of grain size on the transport of sediment. They claimed that these functions represent the transport phenomenon adequately. However, for a given flow condition and a range of sediment sizes, considerable scatter exists around the regression equation proposed by Molinas and Wu (1998). The presence of a range of grain sizes introduced many effects into sediment transport processes. The effects that are of particular importance in the mixed grain size beds occur when a coarse surface layers develop. The development of these coarser surface layers, normally termed "armouring", alters both the surface grain size distribution and the grain surface geometry. Attempts have been made to account for the development of coarse armour layer using empirical devices called 'hiding functions' (Sutherland, 1991). Hiding functions have been empirically determined under a number of different experimental and field conditions and have been used to numerically adjust the predicted threshold conditions or predicted transport rates. The original predictions having been made using traditional single-sized threshold of motion of transport rate relationships. The effectiveness of hiding functions has been demonstrated by Proffitt and Sutherland (1983) who obtained the improvement in the size distributions of the transported sediment (Sutherland, 1991). However, these functions are site-specific and do not attempt to simulate individual physical processes (sheltering, protrusion and grain arrangement) caused by the interaction between different grain size fractions when a mixed grain size is mobilised. Generally their successful application requires knowledge of the result so that the most appropriate "hiding function" can be selected.

The supply of transportable sediment during high flows might not be uniformly distributed across and along the channel, but will probably be concentrated in local areas. In boulder-bed streams, gravel is typically found in isolated pockets protected by local flow obstructions (Barta et al., 1994) and its deposition and entrainment is depend strongly on the local geometry of boulders and banks. Cao (1997) proposed that the proportion of the bed exposed to vigorous turbulent bursts may be a significant factor in determining transport. According to Hubbell (1987), observations of laboratory and

field measurements of sand and gravel transport demonstrate that, even at constant-flow conditions, transport rates at a point vary with time from zero (or near zero) to approximately four times the mean rate. It is therefore very important in field investigation or laboratory experiments to measure bedload transport rate at the same position over a sufficiently long sampling period in order to cover a distribution of "instantaneous" transport rate which may occur during a short period of observation.

2.3.2. Sediment Transport under Unsteady Flow Conditions

Unlike steady flows where it is believed that the level of turbulence can be scaled and thus characterised by the bed shear stress, in unsteady flows the turbulent fluctuation even close to the bed do not necessarily scale with the local average bed shear stress (Nelson et al, 1995). It is therefore necessary to define an unsteadiness parameter that can reasonably characterise the effect on velocity profiles and turbulence in flood flows (Nezu, et al., 1993). Graf and Suszka (1985) proposed that the overall characteristic of hydrograph should be expressed by an unsteadiness parameter, Γ_{HG}, in the form of

$$\Gamma_{HG} = \frac{1}{u_*}\frac{\Delta h}{\Delta T} \tag{2.2}$$

where :

u_* = base flow friction velocity ($= \sqrt{gh_bS_o}$)

Δh = depth variation (difference between maximum flow depth and the base flow depth

ΔT = total time duration of the hydrograph

h_b = base flow depth

S_o = bed slope

Song and Graf (1996) noted that from the definition of the unsteadiness parameter, Γ_{HG}, for a certain base flow, the larger the Γ_{HG} value, the more unsteady the flow. The value of Γ_{HG} also depends on the base flow variables describing the hydraulic conditions before any increase in discharge.

Referring to Graf and Suszka (1985), for a given cross sectional shape, the sediment discharge for steady uniform flow, Q_{so}, can be given as a function of flow depth while

the sediment discharge for an unsteady flow (a hydrograph), Q_s, is given as a function of the instantaneous flow depth and of the depth variation,

$$Q_{so} = f(h) \quad \text{and} \quad Q_s = f(h, {}^{\partial h}/_{\partial t}) \tag{2.3}$$

the relationship between steady flow sediment transport and unsteady flow sediment transport becomes

$$\frac{Q_s}{Q_{so}} = f_1\left(\frac{\partial h}{\partial t}.\frac{1}{u_*}\right) \tag{2.4}$$

the relative error of the sediment discharge

$$\frac{Q_s - Q_{so}}{Q_{so}} = f_2\left(\frac{\partial h}{\partial t}.\frac{1}{u_*}\right) \tag{2.5}$$

where :

Q_{so} = calculated sediment discharge (steady uniform flow)

Q_s = measured sediment discharge (unsteady flow)

$\frac{\partial h}{\partial t}$ = depth variation

u_* = base flow friction velocity

Graf and Suszka (1985) obtained a hydrograph with a certain base flow depth upon which the unsteady part of the hydrograph's wave was superimposed having a peak depth. This hydrograph was characterised by a base flow parameter and ratio of the rise and fall of the water depth, compared to the hydrograph's wave period. They found that during the passage of the hydrographs, the measured sediment discharge, Q_s, and calculated sediment discharge, Q_{so}, were different. The measured sediment discharge being always larger than the calculated one for the rising branch of the flow hydrograph, whereas for the descending branch, the measured sediment discharge was not always larger but sometimes equal to that of the calculated sediment discharge. These results may be explained by the shear stress measurements made by Tu and Graf (1992) and Nezu et al (1993) in laboratory channels with fixed rough boundaries. Tu and Graf (1992) found that the shear stress in the rising branch can be considerably larger than the one in the falling branch at the same water height, where the vertical shear stress profiles for the rising branch were concave, implying accelerating flows, and for the

falling branch were convex, implying deceleration flows. Nezu et al (1993) compared the observation and theoretical values of shear stress. Their observed values were in a good agreement with the theoretical ones and the shear stress increased in the rising stage, whereas it decreased in the falling one.

More interestingly, Graf and Suszka (1985) pointed out that an increase of the $(\Delta h/\Delta T)/u_*$ values which implies a steeper hydrograph, was considerably more evident in the rising than in the descending branch which lead to an important consequence that the rising branch of the hydrographs bears all the important information no matter what the slope of the descending branch. The limitation of this study is that the experiment was conducted for uniform sediment. Although Graf and Suszka (1985) presented two real cases that coincide with their study, the cases were very specific where the observation was done during flushing operations at a river diversion for a power station and during a flash flood with a very short duration hydrograph.

2.3.3. Sediment Sampling Techniques

Different procedures have been developed for sampling and analysing bed material. Traditionally this has been directly measured by sampling small incremental river widths using some type of bucket or similar equipment. This technique provides bulk material samples. Traditionally, bulk sieve analysis has been considered as the standard sampling procedure. Standards for sieving mineral aggregates samples have also been established by several organisations (e.g. ASTM, ISO, BS). When the grain size distribution of bed surfaces are required, other techniques such as areal, grid, or transcet sampling and volumetric sampling are used (Church et al, 1987 ; Diplas and Sutherland, 1988). These surface sampling techniques produce samples that are unique and, thus, results from the different sampling methods are not directly comparable (Diplas and Fripp, 1992). Estimates of the grain size distribution of a bed surface are required for investigations of flow resistance and the initiation of bed material movement, while bulk samples that include the underlying sediment are required for investigations of bed load transport (Hey and Thorne, 1983).

A meaningful sample must be drawn from a homogeneous body of sediment. The

sampling time and its interval that elapses between consecutive samples are temporal elements involved in bed load sampling as well as the period of sampling (Gomez, 1991). Some studies (e.g. Hubbel, 1987) found that errors can be great in cross-sections where the lateral distribution of mean transport rates is extremely non-uniform, whereas errors are relatively moderate where high and low mean transport rates occupy similar proportions of the width or where most of the width has transport rates higher than the mean rate for the entire cross-section. In order to minimise errors, sampled rates obtained with all tested samplers may require some degree of adjustment and if possible it is advisable to do repetitive sampling. It is also considered that more reliable results can be obtained by long sampling times than that of short sampling times.

2.4. STABILITY OF MIXED GRAIN SIZE SEDIMENT

2.4.1. Introduction

Accurate estimation of incipient motion of grains is still a significant problem in sediment transport studies. For a long time this problem has been considered using only the mean grain size of the sediment bed. Shields (1936) introduced the best-known treatise on initial bed grain instability. He linked incipient motion with the mean boundary shear stress and mean grain diameter. The relationship he proposed was mainly based on experiments carried out in laboratory flumes with fully developed two-dimensional turbulent flows over flat beds of single sized sediment. He non-dimensionalised his data with respect to a grain Reynolds number and a unique relationship was proposed to describe the threshold of sediment entrainment. However, the approach is unable to explain the great scatter of experimental data since it does not provide an insight into the mechanism that determine bed instability (Dittrich et al., 1996). Hence the application is only satisfactory for problems which have similar boundary conditions. Later study by Shvidchenko et al (2001) indicated a further finding on the application of mean grain size. They suggested that the shear stress at incipient motion of median sized grains in mixtures was found to be the same as for uniform sediment of this size and was consistent with available flume and field data.

A range of friction angles demonstrating that grains within a size fraction can generate a range of resisting forces. This variability was at its greatest with the finer size fractions

and when the sediment beds were water worked, with no upstream sediment supply rather than on mechanically scrapped flat beds. In mixed grain size deposits, the initiation of motion of a given size of sediment of various grain size fractions is affected by the presence of the other sizes. This adjusts the entrainment thresholds and thus the transport of sediment mixtures in open channels. In summary, the finer fractions are sheltered by the coarse fractions, and the coarser particles, in turn, are exposed more to the action of flow past them due to their more exposed position (Samaga et al, 1986). Determining the threshold of sediment movement is particularly important. Incipient motion studies have been carried out for over eight decades by previous researchers. Their works have been systematically analysed by Buffington and Montgomery (1997). Although their reanalysis and stratification of incipient motion values reveal systematic methodological biases and highlight fundamental differences of median grain size type and the associated values of dimensionless critical shear stress, the list of non-dimensional critical shear stress for different grains with the explanation on experimental conditions applied to each experiment are very useful for the present researcher who intends to investigate this further.

Current prediction methodologies rely on the calculation of time-averaged quantities of flow in order to predict sediment movement. It is believed that the incipient motion of sediment particles is sensitive to the fluctuating fluid forces. Modern equipment used for flow velocity measurement now allow researchers to investigate near bed turbulence over sediment deposits and to link these more detailed measurement with the movement of individual sediment fractions. However, the problem of defining critical flow conditions associated with the initial instability and entrainment of bed sediment particles is not as simple as thought. It has long been realised that different threshold methods give different values of the critical shear stress for initiation of grain motion. This has mainly been due to the different methods of defining the threshold of movement (Wilcock, 1988). Even in the relatively simple case of sediments that are nearly uniform in size variations in the fluid shear stress grains have been observed (Grass, 1971). Wiberg and Smith (1987) discussed that particles at the surface of a poorly sorted bed can have critical shear stresses that differ significantly from the critical shear stress associated with that particle when placed on a well sorted bed of the same size. The difference is primarily due to the relative protrusion of the particle into

the flow along with differences in the particle angle of repose or bed pocket geometry, that results from having a mixture of grain sizes on the bed. This work was confirmed by Kirchner et al (1990). In this study, friction angles for a range of individual grains from different size fractions was estimated. Their observations indicated that for a given grain size on a given bed the critical shear stress is a wide distribution rather than a single value. A more fundamental problem is that the bed shear stress is a fluctuating quantity, and one cannot precisely define a value below which there is no motion (Wilcock, 1988). Therefore, the criterion of initial motion needs to be defined so that determinations of the critical shear stress for different fraction of sediment mixture are comparable.

The prediction of bed instability concerns a definition of the boundary condition between single phase fluid flow and the complex two-phase interaction process involving both the fluid flow and the sediment motion (Grass, 1970). Fluctuations with high magnitudes and low frequencies are important in the entrainment and movement of sediment, but not to the degree that those with higher frequencies can be neglected. When the velocity of the fluid increased sufficiently, individual particles on the bed begin to move in an intermittent and random fashion. According to Grass (1970) the initial bed instability is the result of an interaction between two statistically distributed random variables. The first variable is that for a particular fluid density and viscosity, every grain on the bed surface can be assumed to be potentially susceptible to a local instantaneous critical bed shear stress which cause the grain to become unstable while the second variable is a result of flow turbulence close to boundary, which produces randomly varying local instantaneous bed shear stresses (Grass, 1970). The resisting shear stresses that the bed can generate has a probability distribution because of the random shape, weight and placement of individual grains, and flow boundary conditions also have a distribution of instantaneous shear stresses. The initial movement characteristics of the bed material can be defined if the distributions can be measured.

In mixed size sediment, there are two general methods for determining the critical shear stress; the largest grain method and reference transport method (Wilcock, 1988). The first one associates the critical shear stress with the largest grain in the mixture that can be moved by a given flow. This method has a disadvantage in that the grain coarser than

the largest transported grains must be available in the bed, a condition often not met in the limited observation area. The latter approximates the critical shear stress that produces a fixed small value of transport rate for each fraction. Unfortunately different researchers have used different fixed values to define the threshold of motion. Knowledge of the proportion of each grain size available on the bed surface is also required. Direct comparison of the two methods is prevented by the problem that both are typically applied to very different portions of a transported sample. Estimation of critical shear stress by the largest grain method uses only a single grain per sample whilst the reference transport method, estimation incorporates the transport rate of all grains available in a sample (Wilcock, 1988).

2.4.2. Stability Criteria for Mixed Grain Size

In hydraulic engineering, determining the critical condition for sediment incipient motion and the sediment transport rate is very important. Natural river sediments are generally non-uniform and the bedload movement in such case is quite complex. In this condition, the coarse particles on the bed are easier to be entrained than the uniform sediment of equivalent sizes, because they have higher chance of exposure to the flow and experience larger fluid dynamic forces than they would if they were in a uniform sediment bed. The situation is reversed for the fine particles that transport of a particular size of smaller particles will be less than that if the bed were composed of uniform sediments of the same size. This condition is likely to occur due to the fact that the finer particles are more likely sheltered and entrapped behind or below coarser particles. The smaller particles remain immobile for certain period of time until set in motion by turbulent burst or dislodgement of sheltering particles (Misri et al, 1984 ; Karim, 1998 ; Wu et al, 2000). Therefore, the effect of the presence of one size on the transport rate of another in case of non-uniform sediment must be very carefully taken in the modelling of non-uniform sediment transport.

Until recently, most of the studies on the non-uniform sediment transport are based on introducing some kind of correction factors to modify the existing formulas of uniform sediment transport. However, the state-of-art for estimating the non-uniform sediment transport is still inadequate. Karim (1998) categorised the past investigations on

fractional sediment transport into two groups : the modification of critical or applied bed-shear stress for each size fraction through a correction factor, and the application of a correction factor directly to uniform-size sediment discharge equation used for a representative size fraction. Early research that fractionally calculates the non-uniform bedload transport was attributed to Einstein (1950). It was followed by Egiazarrof (1965), Ashida and Michiue (1971), Hayashi et al (1980), Misri et al (1984), Samaga (1986), Parker (1990), Parker and Sutherland (1990) and Wilcock (1993) who all developed several formulas to determine the incipient motion or transport rate of non-uniform sediment mixtures (Wu et al, 2000).

The used of correction factors was first introduced by Einstein (1950) who proposed a function to adjust the shear stress at the threshold of motion for different grain fractions. However checks on his method using data for non-uniform sediment, subsequent to the publication of his paper, have shown that the agreement between the measured and computed total bedload is not satisfactory (Misri, et al, 1984). Einstein (1950) overestimated the stability of fine grains and underestimated the stability of coarse grains. Later investigations were carried out with the object of evolving a method of computing the bedload transport of a sediment mixture. Misri et al (1984) developed a correction factor expressed as a function of the grain shear stress for individual grain sizes, with respect to the critical shear stress for the mean sediment size. Their study reported good agreement for flume data but poor agreement for river data except at intermediate shear stresses (Karim, 1998). Wiberg and Smith (1987) developed an equation for the critical shear stress non-cohesive sediment that is derived from the balance of forces of individual particles on the surface of a bed. This equation agrees well with data for beds composed both of uniform and of heterogeneous sediment. They suggested that the particle angle of repose, one of two factors in the initial motion problem in mixed grain size bed other than the relative protrusion of the grains into the flow, decreased when the diameter of moving grain, D, was larger than the length scale of the bed roughness, k_s. From the experimental and the calculated results, the critical shear stress for a particle on a poorly sorted bed can differ significantly from that appropriate for a well sorted bed.

Similar approach as developed by Misri et al (1984) was utilised by Samaga et al (1986)

but they modified their correction factor through a graphical procedure for application to a wide range of flows. Samaga et al (1986) proposed the procedure for the calculation of bed load by dividing the bed material into various size fractions to find the fraction by weight of each size in the bed mixture. The critical shear stress for each size was calculated on the basis of Shields' criterion and the multiplying correction factors based on the index of the non-uniformity of the original bed mixture. The total transport rate is the sum of the transport rates of individual fractions. They claimed that the observation have confirmed the findings of Misri et al (1984) about the limitations of Einstein's method in calculating the transportation rates of sediment mixtures as well as the suggestion that all relevant parameters must be taken into account to reduce the inadequacies of the correction factor proposed by Proffitt and Sutherland (1983).

Karim (1988) introduced a "partial transport" factor in the case that the bed of non-uniform sediments was partially armoured by immobile particles. The factor represents the fraction of bed area not armoured. The interaction between different fraction was taken into account through the formulation of a weighing function for each fraction, consisting of two components : areal fraction of each grain size on bed, and sheltering factor. The accuracy of this method in estimating sediment discharge for each size fraction, had been evaluated by applying it to four sets of field data and one set of laboratory data. A careful examination of the results for the data sets indicates that, of the two correction factors in the weighting function for each size fraction, the areal fraction factor had a bigger effect in adjusting the size distribution of transported materials, whereas the sheltering factor influenced the adjustment of size distribution as well as the total sediment discharge. However, Karim (1988) pointed out that although a good agreement was found between computed and observed values for both total sediment discharge and the size distribution of transported sediment, in application to the field and laboratory data sets, prediction was less accurate for flows with a partially armoured bed surface, indicating the need for further research of such flows. It also remains to be seen whether the relative influence of the correction factors indicates a general trend or will be different for other data sets with different flow and sediment characteristics (Karim, 1988).

2.4.3. Critical Shear Stress of Sediment Mixtures

The critical shear stress or the initiation of sediment motion at which individual size fractions in mixed-size sediments begin to move has been investigated by a number of researchers. In recent years much effort has been devoted to investigate the critical shear stress both for well-sorted and poorly sorted sediment. These effort has also been motivated by the realisation, supported by a growing body of data, that the critical shear of individual fractions in mixed-size sediment is considerably different from that of unisize sediments and from many earlier attempts to model it (Wilcock and Southard, 1988). Miller et al (1977) provide a comprehensive review and critique of the various initial motion studies (Wiberg and Smith, 1987) while Buffington and Montgomery (1997) produce a systematic analysis of incipient motion studies with special reference to gravel-bedded rivers. Although Buffington and Montgomery (1997) calculate dimensionless critical shear stress values of the median grain size, $\tau^*_{c_{50}}$, the analysis that resulted from the compilation of eight decades of incipient motion studies in a common format is useful. The authors provided some recommendation on the reliability of different data sets. They pointed out that numerous additions, revisions, and modifications of the Shields' curve since its original publication have been done using sufficient data sets which are grouped into the four most common methods of estimating the treshold of motion. First method is the extrapolation of bed load transport rates to either a zero or low reference value (e.g. Shields, 1936 ; Day, 1980 ; Parker and Klingeman, 1982). This method determines dimensionless critical shear stresses based on critical shear stresses associated with either zero or low reference transport rate extrapolated from paired shear stress and bedload transport measurements. The second method is visual observation that is direct but can be subjective depending on definition of how much movement constitutes initial motion (e.g. Gilbert, 1914 ; Kramer, 1935 ; Neill and Yalin, 1969 ; Yalin and Karahan, 1979 ; Wilcock, 1988). The third method is the development of competence functions that relate shear stress to the largest mobile grain size, from which one can establish the critical shear stress for a given size of interest. The competence function, used in this method, are sensitive to the size and efficiency of the sediment trap, sample size, sampling strategy, availability of coarse grain sizes, and curve-fitting technique (e.g. Andrews, 1983 ; Carling, 1983 ; Komar, 1987 ; Wilcock, 1992 ; Wathen et al., 1995). And the last group is theoretical calculation that utilise simple force balance arguments to predict initial motion

thresholds and is sensitive to model parameters such as grain protrusion, packing, and friction angle (e.g. White, 1940 ; Wiberg and Smith, 1987 ; Jiang and Haff, 1993). In compilation of Buffington and Montgomery (1997), the median grain size dimensionless critical shear stress values, $\tau^*_{c_{50}}$, corresponding to these four methods of measuring incipient motion are symbolised as $\tau^*_{c_{r50}}$ for the first method (reference), $\tau^*_{c_{v50}}$ for the second method (visual), $\tau^*_{c_{q50}}$ for the third method (competence), and $\tau^*_{c_{t50}}$ for the fourth method (theoretical). The dimensionless critical shear stress or Shields parameters of grain sizes other than median grain size will vary as a function of size-specific friction angle, grain protrusion, and mobility of neighbouring grains (Buffington and Montgomery, 1997).

The initial motion threshold, or critical shear stress for incipient motion of individual fractions τ_{cri} is estimated by producing a least square trend of τ_{cri} which is fitted to the estimated reference shear stress line. The reference transport method requires nominating the value of a transport rate parameter and fitting lines to data from each size fraction to determine the corresponding dimensionless critical shear stress τ_{cri}*. The

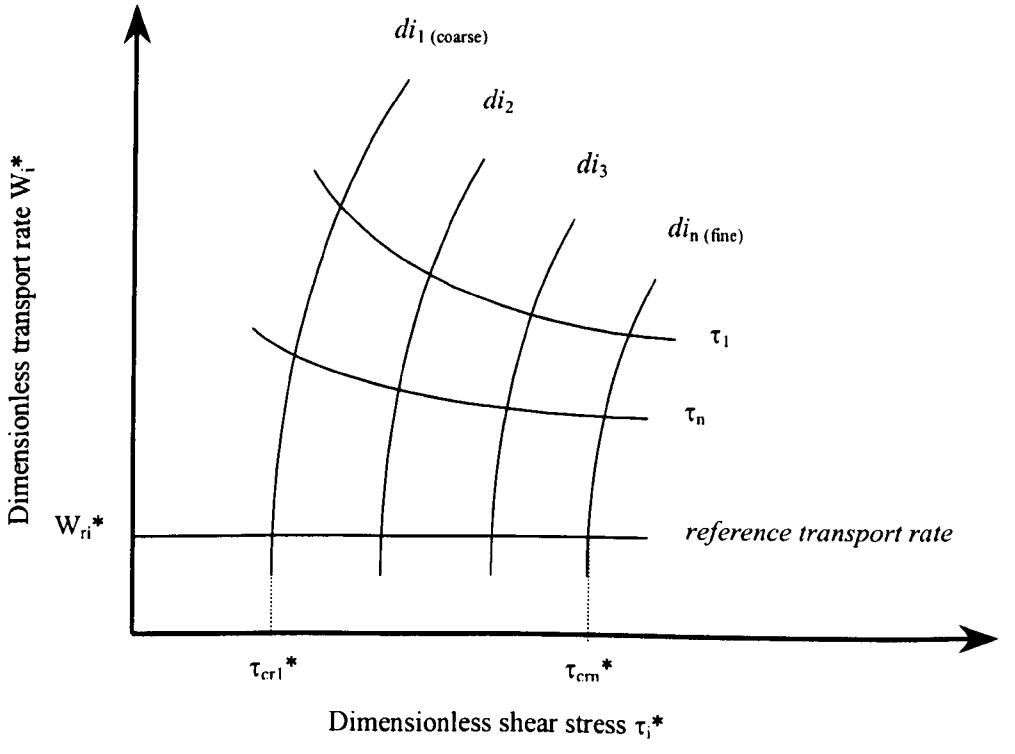

Figure 2.1. Fractional transport rate as function of shear stress (after Sutherland, 1991)

values of τ_{cri}* should be decreased for the larger fractions and increased for the smaller fraction with respect to values appropriate for the size being considered in a homogenous bed (Sutherland, 1991). This method that has been used to estimate incipient conditions for a variety mixed-size sediments (Parker et al., 1982 ; Wilcock, 1992), has the advantages that it may be measured for all fractions in a mixture regardless of the distribution of τ_{cri} within the mixture. It does not depend on sampling individual, rare, large grains in transport and because it is based on a transport rate, it is on a consistent basis with the threshold between partial transport and fully mobile transport (Wilcock and McArdell, 1993).

There are different reference transport criteria have been previously used (Parker et al., 1982 ; Day, 1980). The first author define the reference transport rate in terms of a constant value of the fractional transport parameter W_{ri}* (Wilcock, 1988 ; Wilcock and Southard, 1988). The value of W_{ri}* is arbitrarily chosen to be equal to 0.002 and was formalised by the use of least-squares log-log regression to fit each dimensionless bedload parameter, W_{ri}*, and Shield stress correlation, τ_{ri}* (Parker et al., 1982). Other reference transport rate was formulated by Day (1980) who defines it using the Ackers and White (1973) transport model. The Ackers and White reference transport rate, G_{gr}, is equal to 10^4 (Wilcock, 1988 ; Wilcock and Southard, 1988).

2.4.4. Modification of Thresholds of Motion using Hiding Functions

Hiding functions are an empirical device to account for the many effects introduced into sediment transport processes by the presence of a range of grain size (Sutherland, 1991). Hiding functions modify the mobility of size fractions with respect to their single size mobilities as determined by the Shields curve to values more appropriate to mixed grain size beds. Unlike Shields' entrainment function that applies strictly to uniform sediment, a hiding functions is used to define threshold conditions for a sediment mixture as a whole by substituting the median size for other representative size. A "reduced" hiding function, expressed as a function of the ratio of individual grain size to the median size of surface based-bed sediments was developed by Parker (1990) and Parker and Sutherland (1990). Their works notes that surface grains are subject to selective transport, which may lead to a coarse surface layer and formation of mobile armour

layer, or static armour layer in the limiting case of zero transport rate.

According to Armanini (1992), it is desirable to introduce a proper hiding factor in order to account for possible hiding effects. This factor reduces the transport capacity of the finer fraction of the mixture and increases the transport capacity of the coarser fraction. In the literature (Egiazaroff, 1965 ; Day, 1980 ; Andrews, 1983 ; Ranga Raju et al, 1991; Andrews and Parker, 1987 ; Ferguson et al., 1989 ; Pender and Li, 1995) different expressions for the hiding factor have been proposed to be applied to different kind of sediment transport formulas but in general it is a function of the ratio between the diameter of interest and the scaling size.

A hiding function can be defined as

$$\tau_{ci}^{*} = \varepsilon_i \tau_{cu}^{*} \tag{2.6}$$

$$\varepsilon_i = \frac{\tau_{ci}^{*}}{\tau_{cu}^{*}} = \left(\frac{d_i}{d_u}\right)^{-b} \tag{2.7}$$

where :

ε_i = hiding function (empirical adjustment factor)

τ_{ci} * = Shields' number for size fraction i in a mixture

τ_{cu}* = Shields' number for a size fraction in a uniform sediment (Shields' values)

d_i = grain size fraction i in a mixture

d_u = scaling grain size fraction in a mixture

b = empirical coefficient

The median size of mixture d_{50} has been applied as scaling size d_u by Wilcock and Southard (1988) and Ashida and Michiue (1971) in order to determine the hiding function for non-uniform sediment whilst others studies have reported that it is variable in static armouring experiments (Proffitt and Sutherland, 1983). Many researchers used different scaling size as the representative size. A scaling size of $d_u = 0.77d_{65}$ was used by Einstein (1950) and Shen and Lu (1983) with the consideration that larger grains would be unaffected by hiding and placed the upper limit for hiding at $d_i/d_u = 0.5$. Komar and Li (1988) used a function of d_i/d_{50} to obtain τ_{ci} * while Wiberg and Smith

(1987) determined τ_{ci}* by adopting the scaling size of roughness length representative of the bed (d_i/k_s).

2.5. BED ARRANGEMENT

2.5.1. Particle Size Distributions

The particle size distribution of the bed material found in gravel streams is usually highly variable, so that it is very difficult to provide a representative description of the materials as they exhibit large spatial variation in the size distribution, both in the horizontal as well as in the vertical direction (Diplas, 1987). White and Day (1982), plotted several grain size distributions for both sand-bed and gravel-bed stream in terms of D_{50} (Parker, 1991). The size distributions of sand-bed stream, with D_{50} ranging from 0.2 to 0.9 mm, are symmetric S-curves with relatively low spreads, suggesting that they might be approximately log-normal whilst the curves of gravel-bed streams, with D_{50} ranging from 30 to 70 mm, are essentially concave upward except near the coarsest tail, and are thus strongly asymmetric, deviating substantially from log-normal (Parker, 1991). More extensively, Shaw and Kellerhals (1982) produced 174 grain size distributions to characterise the downstream variation in grain size in twelve rivers in Alberta, Canada (Parker, 1991). The gravel-bed and sand-bed reaches are easily distinguished according to their grain size distribution where the sand-bed reaches contain little material coarser than 1 mm. The gravel bed reaches may contain substantial amounts of sand, but the relative paucity of material in the range from 1 to 10 mm is evidenced by the plateau in the size distribution, indicating bimodality (Parker, 1991). Based on the observation by White and Day (1982) and Shaw and Kellerhals (1982), an important point raised by Parker (1991) that although various hypotheses have been proposed, the cause of the deficiency of grains in the granule (1 to 10 mm) remains incompletely understood and so that, it is about time that researchers try to solve it, or at least it serves to illustrate that the problem of grain sorting can have significant morphological implications.

The availability of material on the bed strongly influences the composition transported sediment. It is believed that the transported bedload size distributions are identical to that of the material available for transport. This means no systematic change in the

composition between the bed material available for transport and the transported sediment. Sutherland and Williman (1977) observed the development of armoured surfaces in alluvial channels. They observed that the size distribution curves of eroded material being very similar to the original material size distribution although the rapid erosion occurred and particles of all sizes were in motion. Suzuki and Hano (1991) investigated grain size change of the surface layer of a riverbed with gravel and sand mixture. The laboratory experiment for this purpose was carried out through the flume with equilibrium conditions of sediment discharge. They found that although in certain condition bedload transport governed by hydraulic conditions rather than availability, the grain size composition of the transported sediment should be the same as that of input sediment even if the volume of the transported sediment changes largely.

Leopold (1992) in his studies of 12 gravel-bar streams in the mountains of Colorado and Wyoming showed that the bulk or largest volume of bedload is of smaller size sand the size seen in the bed materials and on the bars. This means the difference between transported sediment and the bed material is in the size classes larger than the median. However, distribution analysis of material finer than 50 % by weight portion is nearly the same for the transported sediment and the bed material.

2.5.2. Hydraulic Roughness

An important aspect of any streambed surface is its roughness. The roughness may be expressed using the Darcy-Weisbach friction factor or an equivalent sand grain roughness (Sutherland and Williman, 1977). In open channel flow computations, the Manning equation, which was derived from the Chezy equation, is widely used in addition to the Darcy-Weisbach equation (Featherstone and Nalluri, 1986). As the roughness of a streambed may varies from place to place within a given channel reach, the equivalent values must be determined in the application of Manning formula to the whole section of a stream (Chow, 1959). However, no reliable methods exist by which one could calculate the roughness from direct measurement of either grain size or bed topography. In a small number of armouring experiments, Tait and Willetts (1991) observed that the rise in the calculated hydraulic roughness did not coincide with the increased coarseness of the bed surface. In an alluvial channel, the roughness varies with

flow and is only indirectly related to the grain size and grain size distribution of the boundary material. On gravel, cobble and boulder-bed rivers, bed elevation changes can be significant, but they are not usually as dramatic, or as large as in sand-bed rivers (Simons and Simons, 1987).

In the turbulent-rough-flow range the resistance to flow depends primarily upon the size, shape and arrangement of the granular material making up the boundary. The transport of mixed-size sediments by running water leads to the development of a bed surface that has a different grain size distribution than the original sediment bed. Studies have indicated that it is the grain arrangement on the bed that can have a significant impact on the stability exhibited by mixed grain sediment bed (Kirchner et al, 1990). Kirchner et al., 1990 pointed out that among other factors, the erodibility of a grain on a rough bed is controlled by its relative projection above the mean bed, its exposure relative to upstream grains, and its friction angle. In particular, they analysed how the surface topography is controlled by grain packing on poorly sorted beds, and how that surface shapes the near-bed flow over individual grains. They found that the distribution of bed elevations in water-worked gravel bed was fairly close to normal. This agrees with Nikora et al (1998) who found the bed elevation distribution for natural beds was skewed positively, while that for manually created gravel beds was skewed negatively and both types of bed elevation distribution were close to Gaussian. This agreement suggested that the shape of the bed elevation distribution might be a statistical measure of bed particle arrangements. However, additional studies of both particle arrangements and bed elevation distribution are required to develop this hypothesis properly (Nikora et al, 1998).

2.5.3. Armouring of Non-Uniform Sediment

Under a wide range of flow conditions, the transport of heterogeneous sediment leads to the development of a bed surface that is coarser than the subsurface bed material. This coarse surface layer is normally called a bed armour surface. The prevalence of bed armour in gravel bed rivers has led to interest in the evolution of stable armours (Parker and Sutherland, 1990). Regarding the stable armours evolution, Gomez (1994) found that the development of a stable armour is normally associated with the winnowing of fine grain sizes from the bed. Armour layers also form under conditions of partial

bedload transport, in which the composition of transported fraction is not the same as the bed surface composition.

The bed is said to be armoured if the concentration of immobile material is dense enough to stabilise the bed surface and prevent the further removal of any of the finer underlying material (Bray and Church, 1980) or in some circumstances the transport rate is reduced to zero (Tait et al, 1992). Armouring process is possibly occurred at sufficiently low shear stress where only part of the smaller grain sizes has been removed. As the result of this removal, coarser material will accumulate in the surface layer, which is protected from further erosion at the prevailing flow condition. At this point the bed has developed a stable armour coat. The stable grain can not be found in the condition that the critical shear stress higher than the critical value is applied to the bed, e.g. during flood in natural rivers. The erosion process will continue until for some reason the shear stress is reduced. If the constant discharge is applied to the laboratory flume, the erosion will eventually lead to a reduction of the bed slope (Gessler, 1991). As the consequences the bed shear stress will drop to some extent allowing the stabilisation process become possible.

In the early period of the formation of knowledge on sediment transport studies it was assumed (Du Boys, 1879) that the transport of granular material occurs in "carpet like" form (Yalin, 1977). When the shear stress exceeds its critical values ($\tau_o > \tau_{cr}$) the flow drags one grain diameter thick (top grain carpet) induces the motion of the grain in the second layer (second grain carpet). Subsequently the motion of grain carpet makes the next layer move. It was even suggested that the velocity of the top carpet was higher and decrease according to the linear relation (Yalin, 1977).

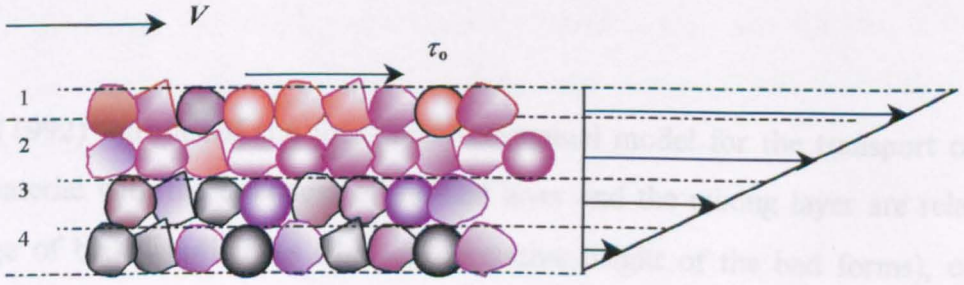

Figure 2.2. "Carpet like" form of material transport processes as described by Du Boys,1879 (after Yalin, 1977).

Later investigation found that the actual motion of the grains has nothing in common with form described by Du Boys. According to Velikanov (1955) it was apparently Krey in 1910 who first observed and disagreed with the "mechanical model" of Du Boys. Krey and many others (Bettes and White, 1981 ; Willetts et al., 1987; Gessler, 1991) revealed that it is only the grain forming the uppermost layer which can be brought into motion by the flow and contributes to the transported sediment. Bettes and White (1981) made the active layer thickness proportional to the hydraulic roughness height, and thus sensitive to bed forms as well as to grain size. Willetts et al (1987) adopted two-layer active depth based on the present of largest grain d_{100} where each layer equal in thickness to half of the largest grain (see Figure 2.3). In terms of armouring various definitions of armour coat have been proposed mostly motivated by practical consideration but Gessler (1991) claimed that it has been documented many times that the armour coat is "one grain thick". Other researchers made the active layer thickness equal to a multiple of a representative grain size which become larger for more vigorous flow regime (Borah et al, 1982), so that the active layer thickens with increased flow (Willetts et al, 1987).

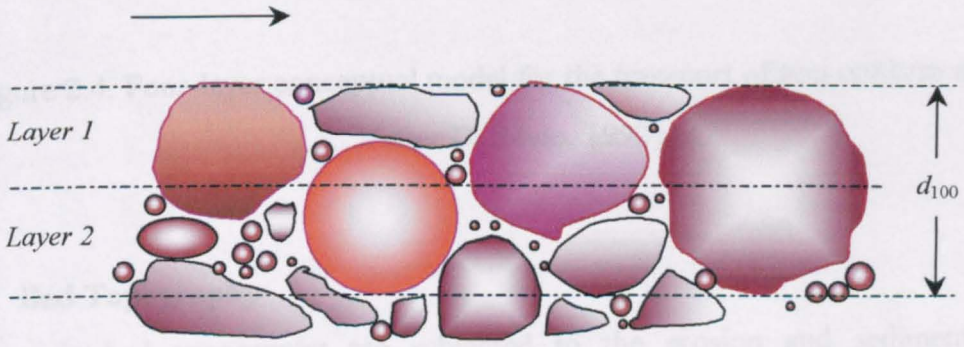

Figure 2.3. Active layers (after Willetts et al., 1987)

Di Silvio (1992) introduced the four-layer conceptual model for the transport of non-uniform material with the thickness of the bed layer and the mixing layer are related to the average of bed disturbances (the representative height of the bed forms), or to a representative grain size for a plane bed. The first layer is water stream containing particles exclusively transported in suspension. Particles that are transported as bedload

exist in the second layer called bed layer. The third layer is mixing layer, containing particles that are presently not in movement, but are liable to frequent vertical movements into the moving bed layer. Below the third layer is the intrusion layer. This layer containing particles liable to occasional vertical movements to and from the upper "transport" layer. Unfortunately the relationships used to control the vertical movement of sediment are theoretical and no attempt have been made to verify these relationships with observation. The particles below the intrusion layer are never disturbed, unless degradation processes take place. The four layer conceptual model by Di Silvio is presented in Figure 2.4.

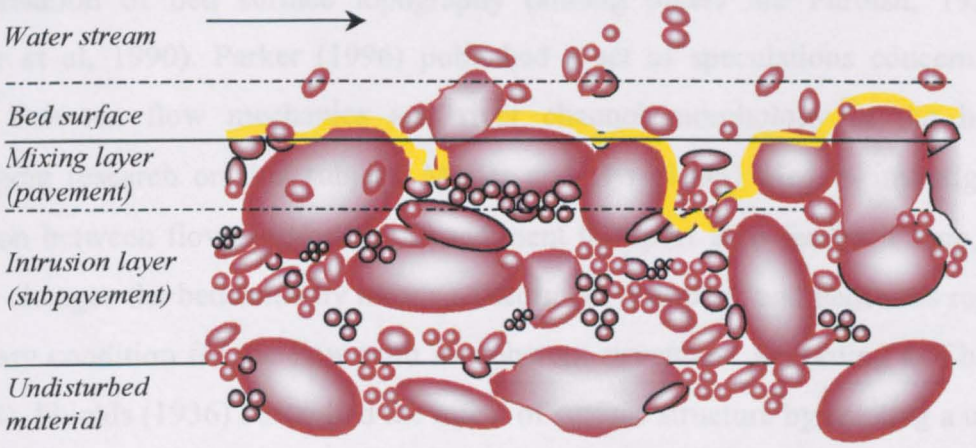

Figure 2.4. Four-layer conceptual model for the transport of non-uniform material (after Di Silvio, 1992)

2.5.4. Bed Topography

Changes in bed topography are subjected to the erosion and sediment transport processes. The evolution of a streambed, both in composition by size fraction and variation in elevation with time, is determined not only by the magnitude of the total sediment discharge, but also by how much sediment in each size fraction is transported by the flow (Karim, 1988). In order to fully characterise a gravel bed surface, some researchers have claimed that the measurement of bed texture is necessary as well as a grain size distribution analysis. However, it appears unlikely that the grain size distribution of the bed surface can be linked directly to its surface topography as the bed topography of a surface will also be dependant on the flow history and the type and amount of sediment moved over it (Tait and Willetts, 1991). Natural streams exploit

widely graded materials to create critically stable conditions at the bed, but the condition is not simply maintained because of the fluctuating flows (Church et al., 1998). It is believed that the degree of structural development depends on the history of recent flows. Therefore the effect of flow history may be important on the behaviour of bed material transport in natural rivers. The grain size distribution of surfaces gives indirect indications of the relative proportions of sheltered to sheltering grains. Topographical measurements will hopefully indicate the potential for nearbed flow adjustment and the degree of efficiency of the sheltering bed features.

Many attempts have been carried out to formulate direct measurement and quantitative characterisation of bed surface topography (among others are Furbish, 1987 and Kirchner et al, 1990). Parker (1996) published a set of speculations concerning the relation between flow mechanics and river channel morphology in the hope of encouraging research on this subject. Muller and Gyr (1996) tried to investigate the interaction between flow, bedforms and sediment transport by a feedback loop, where the flow changes the bedforms by means of sediment transport, and bedforms represent a boundary condition for the flow with its coherent structures. According to Church et al. (1998), Shields (1936) controlled the effect of surface structure by creating a uniform particle arrangement prior to taking each set of measurements by using narrowly graded materials and by following the same starting procedure for each run. If particle arrangement is held constant, bed strength is a reliable function of particle weight, and if it is not, the development of an interlocked structure dominates the bed strength in mixed size sediments. Some new techniques have been evaluated by De Jong (1992) for measuring micro and macro-roughness over mobile gravel-bed boundaries both before, during and after flood flows. Observation by Church et al (1998) suggested that stable and reticulate stone cells developed on the bed surface in cobble-gravel streams with relatively widely graded sediments. These structures promoted streambed, and therefore channel stability by dramatically reducing the transport of bed material. However, a range of material sizes is obviously necessary for recognisable structures to develop.

The development of surface structure is a self-organised, critical phenomenon, the emergent product of stochastic encounters among many individual grains. The timescale

for the development of surface structures, which occurs at relatively low rates of sediment transport, is long in comparison with typical fluctuations in water discharge. Most of the time, conditions are either subcritical, in the sense that the flow is insufficient to disturb the bed significantly, or the stresses applied by the flow create a transient situation in which the bed is adjusting toward a new critical state. A consequence is that most gravel bed streams are probably not in equilibrium with imposed flows of typically limited competence (Church et al., 1998). It is hoped that further study of the phenomena associated with the development of bed structures will reveal a satisfactorily parameterisation of this aspect of the sediment transport problem. There is a lot more work to be done on the subject of water-sediment interaction and resulting morphology.

2.6. TURBULENT FLOW

2.6.1. Background

An understanding of the turbulence characteristics of open channel flow is needed to explain the natural phenomenon of sediment erosion and transport processes. Field studies show that during the passage of a flood, the bed load movement and the suspended load distribution as well as the river processes are different from those in steady flow. Turbulent flow is the key role to the entrainment process that determines the variation of bed configuration. Previous studies in this area included detailed measurement of turbulent velocity fluctuation characteristics close to rigid boundaries of varying roughness in two dimensional water channel flows. Grass (1971) and Kim et al. (1971) investigated the production of turbulence near a smooth wall in turbulent boundary layers. Other studies of the structure of turbulent flow, mainly over fixed rough boundaries, have been conducted by Nowell and Church (1979), Nezu and Nakagawa (1993), and Nikora and Goring (1999b), who studied the characteristic of turbulence structure in quasi 2-D flows with static and weakly mobile bed in an irrigation canal. An important point indicated by these studies is that the vertical distribution of turbulence characteristics is split into three main layers in the flow depth: a near water surface region, an intermediate flow region and a near bed layer.

It has been recognised that in the turbulent boundary layer over smooth beds or entirely flat-bed boundaries, the majority of the turbulent energy is generated in the near-bed

region where bursting processes generate intermittent high shear stress events (Nowell and Church, 1979 ; Roy et al, 1996 ; Garcia et al, 1996). Nowell and Church (1979) in their study of turbulent flow in a depth-limited boundary examined the influence of roughness density on turbulent characteristic particularly in the near bed layer. Bed roughness density was defined as $^{nA_e}/_{A_t}$, the ratio of the plan area of n roughness elements of individual area, A_e, to the total bed area of the flume, A_t. They noted that roughness density clearly had an influence on the streamwise turbulent kinetic energy production and on the rate of turbulent energy dissipation particularly in the nearbed flow region. They found variations of turbulence intensity, which is the square root of streamwise turbulent kinetic energy in three regions : $y/D > 0.35$, $0.35 > y/D > 0.20$ and $y/D < 0.20$ where y is the distance from the bed to measurement position and D is the total flow depth. In the first region, comprising most of the outer flow region, identified by the velocity profiles, turbulent intensity decreased steadily and approximately linearly toward the surface. In the second region, corresponding to the transition region of the mean velocity profiles, turbulent intensities were approximately constant near $u'/u_* \approx 2$ where u' is streamwise velocity fluctuation and u_* is friction or shear velocity. In the third region (sometimes called the roughness sub layer), turbulent intensity was a maximum near $y/D = 0.25$ and then decreased toward the bed. This agrees with Song and Graf (1996) who found that turbulent intensity decreases with an increase of y and the maximum value is just above the bed. The work of Nowell and Church (1979) also clearly demonstrated that the value of turbulence intensity scaled with shear velocity varied depending on the roughness density within the roughness sublayer. The largest values were seen when the roughness density was equal to $\frac{1}{8}$. For values below or above $\frac{1}{8}$, the levels of turbulence reduce. This clearly showed that the bed surface arrangement could influence the near bed turbulence.

2.6.2. Bursting Events

Over the last three decades, experimental work has identified a quasi-ordered coherent structure in turbulent wall-layer flow, which is characterised by the bursting process. This consists of a sequence of repeatable and cyclic fluid motions referred to as ejection and sweep events (Cao, 1997). These organised features are called coherent structures.

According to Robinson (1991) the meaning of coherent structures is a three-dimensional region of the flow over which at least one fundamental flow variable exhibits significant correlation with itself or with another variable over a range of space and or time that is significantly larger than the smallest local scales of the flow (Garcia et al., 1996). Alfredsson and Johansson (1984) described the cycle of bursting event, which is caused by the interaction between the outer and inner regions of the flow. This cycle of events was originally proposed by Offen and Kline (1974). The bursting process as a cyclic downstream flow pattern occurs near the wall irrespective of the roughness although its exact dimension and frequency may be modified by the wall roughness.

According to Smith (1996) a burst is conceptualised as the local breakdown and the ejection into the outer region of wall-layer fluid in proximity to a low-speed streak followed by a sweep which is the three-dimensional inflow of high-speed fluid from the outer region due to the formation and presence of hairpin-like vortices. Despite the importance of bursting processes for initiating particle motion and sediment transport (Drake et al., 1988), the characteristic and structure of turbulence above natural gravel beds remain poorly quantified and understood (Roy et al., 1996). The existence of turbulent coherent structures similar to those present in the turbulent boundary layer over a smooth boundary, was first observed over a rough bed by Grass (1971). The presence of structural features over a rough beds was confirmed by observation from several other researchers (Grass et al., 1991 ; Defina, 1996 ; Grass and Mansour-Tehrani, 1996; Tait et al., 1996). These intermittent events were similar in nature to the ejections and sweeps present over smooth beds of homogeneous roughness and over rough walls in that the production of turbulence in the near wall region was dominated by quasi-periodic bursts events consisting of violent outward ejections of low speed fluid and then inrushes of high speed fluid towards the boundary (Garcia et al., 1996).

Sweeps event ($u' > 0$, $v' < 0$) occurred when high speed fluid from the outer region of the boundary layer moves toward the wall and penetrate the wall layer. At the initial stage, the wall layer is very thin, and then it continuously becomes thicker due to viscous diffusion during a relatively long quiescent period. This quiescent state ends in the bursting process, which is normally related to a wall-layer streak. To start with, the low-speed streak lifts away from the wall, and oscillations in both the spanwise and

normal directions appear. A break down occurs in the form of a violent and chaotic upward eruption of the low-speed fluid in the wall-layer into the outer layer termed as the "ejection" ($u' < 0$, $v' > 0$), after the oscillations have increased in amplitude and scale to a certain limit. A sweep soon follows the ejection, in which process the chaotic motion is swept away, the wall-layer streaks reappear at different spanwise locations, and a new quiescent period begins (Nelson et al., 1995).

The occurrence of bursting events are regarded as an important class of coherent structures in open channel flows and determine momentum and energy transfer between the near bed region and the outer flow (Nikora and Goring, 1999b). Flow visualisations have shown the existence of diverse vortical structures, with inclined 'horseshoes' or 'hairpins', although more recently a funnel shape has also been proposed (Kaftori et al., 1994), whilst numerical data bases (e.g., Jimenez et al., 1988 ; Guezennec et al., 1989) as well as particle image velocimetry (e.g., Liu et al., 1991 ; Urushihara et al., 1993) reveal the existence of inclined, thin shear layers of concentrated spanwise vorticity (Garcia et al., 1996).

Limited experimental observations of sediment particle motions within the nearbed roughness layer have suggested a close association between movement and the turbulent bursting cycle (Gyr and Muller, 1996). It has now been suggested that the intermittent bursting process could play a key role in sediment transport (Cao, 1997). Since the discovery of bursting events and their importance for the turbulence production, much effort has been spent to elucidate the underlying mechanism and find a scaling law for their frequency of occurrence (Alfredsson and Johansson, 1984). Although Jimenez and Pinelli (1997) have confirmed that wall turbulence is maintained by a cycle in which streamwise vortices extract energy from the mean flow to create alternating streaks of longitudinal velocity, and that the streaks in turn give rise to the vortices, presumably by inflectional instabilities, the work on this mechanism has been hindered by the difficulty in experimentally detecting these flow structures.

2.6.3. Detection of Bursting Events

A major problem has been the non-availability of velocity measurements collected

simultaneously over a 3-D space to identify the flow structures. Generally only time series of flow velocity measurements, either of 1, 2 or 3 directional components made at a single position in space are available. The methods used to detect ejections and sweeps have been developed to use these limited data sets. Among those methods are the variable-interval time-averaging (VITA) technique proposed by Alfredsson and Johansson (1984) and quadrant method used by many researchers (e.g. Lu and Willmarth, 1973 ; Alfredsson and Johansson, 1984 ; Luchik and Tiederman, 1987 ; Nezu and Nakagawa, 1993 ; Nelson et al., 1995 ; Nikora and Goring, 1999b). The VITA technique can be used to detect the frequency of occurrence as well as duration of the events whereas the quadrant method, which is said to be one of the most effective methods (Nikora and Goring, 1999b), is used to detect bursting event characteristics. This method gives the best agreement with visual detection of a burst. However, it is now often used in several environments far removed from the near-wall region of the turbulent boundary layer (Biron et al., 1993). In the *uv*-quadrant method the amplitude of the *uv*-signal is used to determine the occurrence of these events, which consequently must be associated with considerable contributions to the time average Reynolds stress (Alfredsson and Johansson, 1984).

According to Alfredsson and Johansson (1984) the conditional averages obtained by VITA technique and the method of Willmarth and Lu (1972) show strong *uv*-activity close to detection times, giving confidence in their ability to detect turbulent-producing coherent flow structures. They suggested that consideration to determine the relevance of the various methods may be judged from their ability to detect events associated with large contributions to the Reynolds stress. More importantly, they recognised that when comparing results from different studies on the bursting frequency, one should bear in mind that most detection methods employ some kind of threshold, the value of which affects the measured frequency of occurrence of detected events.

Roy et al. (1996) gives an example of the results of using different burst detection techniques to characterise the scales of turbulent structures. Those techniques, i.e. the Quadrant, U-Level, VITA and VITA with slope, are used to identify the presence of an ejection if the velocity signals respond to specific conditions (Figure 2.5). Roy et al. (1996) suggested that although the burst frequency differs from one detection technique

to another and decreases with sensor size, average frequency is not significantly different between the measurements in near-bed and the outer region. In the near-bed region, shear stress production appears to be dominated by strong sweep-like motions while the outer region is dominated by ejection events.

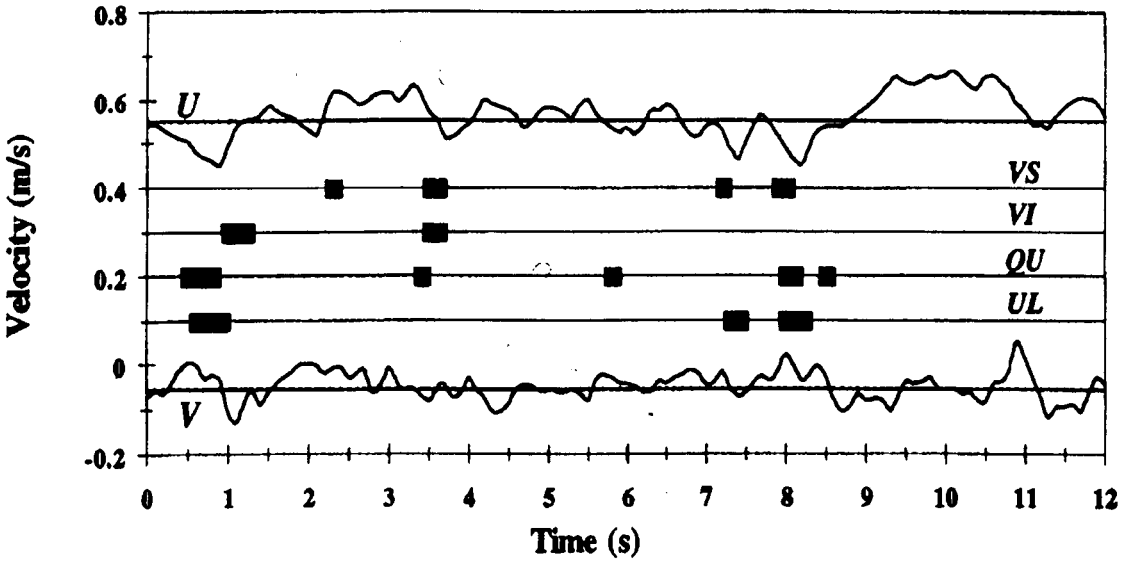

Figure 2.5. Identification of ejections by four detection techniques on a typical set of streamwise and vertical velocity measurement (after Roy et al., 1996)

According to Roy et al. (1996) the strongest events are generally picked up by all techniques although the duration of the event may vary while the smaller events can pass undetected, especially with the VITA technique. In the estimation of burst frequency, quadrant analysis appears very consistent and reliable. Quadrant analysis showed a clear dominance of the ejection (quadrant-2) and sweep (quadrant-4) events in both the near-bed and outer regions (Roy et al., 1996). As observed by Nakagawa and Nezu (1977) who documented in detail the changes in the structural features of turbulence when the bed surface roughness is gradually increased, Roy et al. (1996) suggested that shear stress production in the near-bed region is clearly sweep dominated although ejection motion appears to dominate in terms of the percentage of time spent in each quadrant. Krogstad et al (1992) has also shown ejections and sweeps dominate shear stress production in a laboratory flume with rough and smooth bed, but events are stronger and more frequent over rough beds where sweeps tend to dominate shear stress

production (Roy et al., 1996).

2.6.4. Scaling of Turbulent Flow Features

Grass and Mansour-Tehrani (1996) estimated the mean transverse spacing or spanwise wavelength, λ, between the low-speed streaks from images of hydrogen bubble traces taken during laboratory experiments. Following the hypothesis of Grass (1971) that λ should scale with the roughness dimension, k, it was seen that the ratio of λ/k is constant for geometrically similar roughness elements. This is confirmed with measured λ/k values of 3.25 for 6 mm spheres and λ/k values of 3.18 for 12 mm spheres derived from figures produced by Grass et al (1991). For the pebble roughness the dominant spanwise wavelength produced a corresponding λ/k ratio of 3.11 which is in close agreement with the corresponding values for the spherical roughness element. The measurement of the mean spacing between the low-speed streaks formed over a bed comprised of spherical roughness elements with an average diameter of 10 mm measured by Grass and Mansour-Tehrani (1996) is also in remarkably good agreement with measurements by Defina (1992) where $\lambda/k = 3.4$ was observed.

The transverse spacing between low-speed streak is also formulated by Defina (1996) based on the equivalent sand roughness height of 6.7 mm where $k_s/D = 0.67$ for grain diameter of 10 mm. Under fully rough wall conditions Defina (1996) found that the mean streaks spacing, λ, scaled with the size of the wall roughness, k_s, similar to what previously suggested by Grass (1971) where $\lambda/k_s \approx 4.5$.

Dimensionless transverse spacing between low-speed streaks as proposed by Defina (1996) is defined as follows

$$k_s^+ = k_s u_* / \upsilon \qquad (2.11)$$

k_s^+ = roughness Reynolds number

u_* = bed shear velocity $=\sqrt{(\tau/\rho)}$

k_s = equivalent sand roughness height (= 6.7 mm)

The non-dimensional mean streak spacing, λ^+, formulated by Grass and Mansour-

Tehrani (1996) is defined as the following

$$\lambda^+ = \lambda U_\tau / \upsilon \qquad (2.10)$$

where :

λ^+ = dimensionless transverse spacing between low-speed streaks

λ = mean transverse spacing between low-speed streaks (spanwise wavelength)

U_τ = bed shear velocity $=\sqrt{\tau/\rho}$

υ = fluid kinematic viscosity

In the case of smooth wall flow, they observed λ^+ values of 101 is in good agreement with previous measurement by Kline et al. (1967) and Smith and Metzler (1983). However their measurements of streak spacing for rough beds indicated a range of λ^+ values from A to B. Grass (1992) and Grass and Mansour-Tehrani (1996) proposed a universal scaling length as the ratio between a local 'effective eddy viscosity', υ_t, and bed shear velocity u_*, such that $\lambda=100\upsilon_t/ u_*$ irrespective of the wall roughness condition (Defina, 1996).

Smith (1996) also noted that sediment streaks are subject to varying spacing depending on the sediment grain size (i.e. smaller grain sizes form more closely-spaced streaks). At flow rates, the flow-dominated sediment flows generally undergo a metamorphosis to a sediment-dominated flow, wherein the sediment collects into larger ridges of transverse extent (Williams and Kemp, 1971) or the sediment is of significantly large dimension (Grass et al., 1991; Kirkbride, 1993) such that the vertical turbulence scale of these sediment irregularities exceeds $k^+ = u_\tau k/\upsilon > 50 - 90$ (where k^+ is roughness Reynolds number and k is roughness height or the sediment size), which classifies the wall as fully rough (Smith, 1996). Several researchers (Grass, 1992 ; Weedman and Slingerland, 1985 ; Best 1992) have illustrated that the wall-region vortex interaction can give rise to the formation of sediment 'streaks' along a flat wall. Grass et al. (1991) and Grass and Mansour-Tehrani (1996) show that the region above fixed roughness elements displays a somewhat organised spanwise pattern akin to streaks, but with a spanwise spacing scaling on the roughness dimension (roughly three times k), which suggests that the spaanwise spacing of the flow patterns scales with the roughness size (Smith, 1996). It is well known (Ligrani,1989) that the flow above a fully-rough wall still displays a mean

velocity profile with a characteristic logarithmic scaling and the turbulence Reynolds stress distribution in the outer region undergoes only minor variations (Smith, 1996).

The criteria used by Nikora and Goring (1999b) to classify bursting events was also used in most previous studies of bursting phenomena which is based on the dispersion of instantaneous streamwise and vertical velocity in the form of

$$\left|u'v'\right| \geq H_t \sigma_u \sigma_v \tag{2.12}$$

where :

u' = the streamwise velocity fluctuation from the mean

v' = the vertical velocity fluctuation from the mean

H_t = the threshold value

σ_u = the standard deviation of the instantaneous streamwise velocity

σ_v = the standard deviation of the instantaneous vertical velocity

Nikora and Goring (1999b) underlined that two threshold values of 0 and 1.2 have been selected on the basis of the first value used to make their data comparable with a number of previous studies using similar value and the second value was used as suggested by Luchik and Tiederman (1987) gives the best agreement with visually detected events. An event is recognised if the product of the velocity fluctuations exceeds $H_t \sigma_u \sigma_v$, otherwise it is discarded as noise. The threshold value of 1.2 is also applied by Roy et al. (1996) for quadrant analysis.

A study by Nikora and Goring (1999a), which was concentrated on the effects of bed mobility on turbulence properties and flow resistance in a gravel bed irrigation canal, also found several important features in which their study differs from fixed-bed flows. They revealed that the normalised frequency of bursting event $\left({}^{H}/_{T_E \bar{u}_{max}}\right)$, where H is cross sectional depth, T_E is the mean time between ejection and $\bar{u}_{max}$ is the maximum mean velocity, detected by quadrant method were appreciably less than those for fixed-bed flows. For weakly mobile bed the values of the normalised frequency were 0.25 ± 0.006 whereas for fixed-bed were ranging from 0.33 to 0.66. This suggests that the bed particle motion modify the parameters of bursting events. Their analysis also shows that

the relative turbulence intensity $K^{0.5}/\bar{u}$, where K is the turbulence energy and $\bar{u}$ is the mean velocity, was lower than that for flows over fixed gravel beds. These results indicated a greater variation in burst frequency for stable beds exhibiting different roughness.

2.6.5. Impact of Turbulent Flow on Sediment Transport

Motivated by the observations of Vanoni (1964), Sutherland (1967) speculated that the mechanism for entraining sediment grains into suspension would involve interactions between turbulent vortices and particles in the near-bed region of the flow (Garcia et al., 1996). Although the details of his concept of such interactions, revisited by Wells (1992), are not totally correct in the light of present knowledge of turbulence structure in the near-bed region of boundary layer flows, his hypothesis delineates the basic mechanics of such phenomena which has been verified more recently by a number of experimental studies (Garcia et al., 1996).

It was believed that one of the factors which may control the grain entrainment rate is the temporal and spatial distribution of the flow structures close to the bed (Tait et al., 1996). Several studies (e.g. Sumer and Oguz, 1978 ; Sumer and Deigaard, 1981 ; Ashida and Fujita, 1986), with the application of different experimental techniques, have investigated the implication of the bursting phenomenon on the mechanics of particle transport in the near-bed region of boundary layers. Garcia et al. (1996) visualised

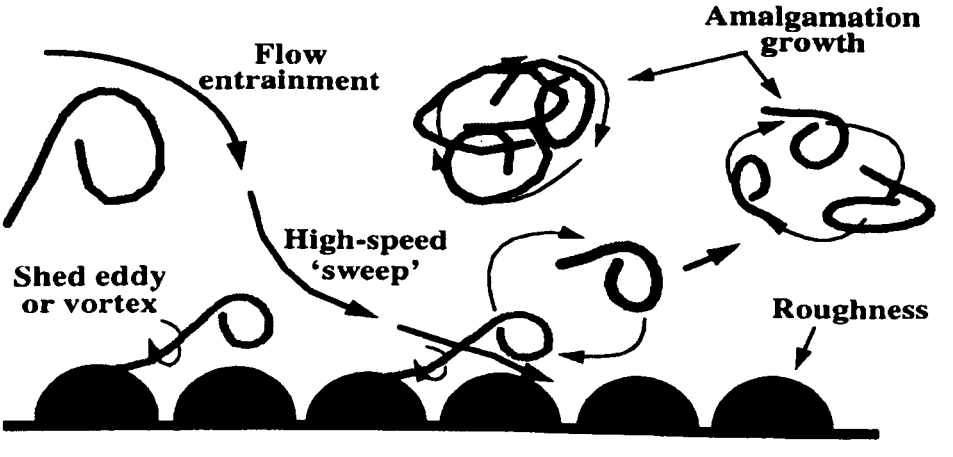

Figure 2.6. Conceptual model of turbulence generation in the presence of a fully-rough wall (after Smith, 1996)

particle motion in the near-bed region of the smooth flows. It showed that particles tend to be picked up from low-speed streaks, lifted away from the bed by some kind of ejection mechanism, and deposited back to the bed along the high speed-streaks. In the case of the transitionally rough flows, they found that the particles did not tend to sort along bed streaks although they were observed to be entrained by a similar ejection mechanism as in the case of smooth flows.

According to Garcia et al. (1996), both the present work and much of past research, primarily based on experimental evidence, suggests a consensus on the mechanism that causes ejection of particles away from the bed. Such particle ejections are related to interactions between particles and intermittent flow events associated with turbulent bursting during which low-momentum fluid is ejected towards the outer regions. Kirkbride (1993) pointed out that for large roughness flows comprised of large sediment (clasts) of fully rough scale, the low-speed streaks of a smooth wall essentially disappear and are replaced by wakes shed by the clasts (Smith, 1996). The scale of the initial hairpin-like vortices for a fully-rough wall as shown in Figure 2.6, will increase proportionally with the roughness scale, and an increase in wall roughness will elevate the wall drag and overall momentum exchange process (Smith, 1996). Grass (1971) demonstrated that the presence of roughness accentuates the amplitude of sweeps and ejections in proximity to the rough surface, which clearly reflect an increased level of momentum exchange (Smith, 1996).

Nelson et al. (1995) claimed that sweeps collectively move more sediment than outward interactions, primarily because they are much more common, not because they are individually more effective. In fact, the efficacy of either sweeps or outward interactions is easily argued. They argued that strong correlation with large fluctuation of streamwise velocity can be expected because the particle motions are dominated by lift, drag, and gravity and both upward lift and downstream drag are dominantly function of streamwise velocity (e.g., Wiberg and Smith, 1985). During sweeps, downward flow enhances transport by advecting fluid with higher streamwise velocities toward the bed, and during outward interactions, upward flow tends to move particles away from the bed into regions of higher streamwise velocity, thereby increasing their speed and hence the transport rate (Nelson et al., 1995).

2.7. SUMMARY OF LITERATURE REVIEW

Although the experiments involving measurement of the bedload transport rates and the entrainment thresholds of different fractions in a mixture have been carried out for a number of years, little work has examined the behaviour of mixed grain size sediment beds. The effect of size gradation and the understanding of the basic physical processes associated with unsteady flow sediment transport over mixed grain bed is still of particular importance to explore. The factors that control particle movement in natural channels has been a major issue in this field particularly in the problem of finding a universal bedload transport equation. It was widely recognised that the previous experiment mostly conducted in a certain condition so that the effects of complexity can be simplified. Although there are some encouraging results in partial sediment transport investigation, that under some condition the grains size distribution of bedload can be predicted, the amount of sediment transport per unit time remains unsolved. The result of these studies which was often ambiguous and contradictory, are not suitable for general application to the different streams, and then emphasising the need for further studies.

Steady flow experiments have identified the physical processes such as adjustment of the nearbed flow, size selective sorting of surface grain sizes and the rearrangement of the surface grain positions relative to each other, as significant in the development of deposit stability, particularly in situations of low upstream sediment supply. Existing work has indicated that the timescale for each physical process is different and that these timescale are different from the variation of flowrates observed in rivers in flood. Sediment movement in most natural rivers is intermittent and occurs infrequently, generally at high flowrates during unsteady flows. Therefore it is important to discover the way in which the highlighted physical processes, nearbed flow adjustment, size selective sorting and surface grain position operate under unsteady flows. This is necessary as the different time scales associated with each process to reach an equilibrium state. Given the evidence available in the literature it was decided to develop a program of laboratory test to examine the aspects of mixed grain sediment transport under unsteady flows.

III. EXPERIMENTAL APPARATUS AND PROCEDURES

3.1. INTRODUCTION

Work over the last two decades has attempted to examine the influence of mixed grain sizes on sediment transport. There have been several investigations of the phenomenon of bed armouring and its consequences. However there are few studies which have examined the underlying processes in detail when a mixed grain sediment bed is exposed to a mobilising flow. Engineering predictive techniques have been developed by simplifying the complexity of natural channels system by assuming that they contain mainly single sized sediments, and are at steady flow discharges for long enough time periods to assume a system in "quasi-equilibrium". Several studies have indicated that there are significant differences in the way in which mixed grain size sediment and uniformly sized sediment behave even if the average grain size is similar.

Little work has been carried out to examine the grain sorting behaviour during periods of time varying flows. Previous investigations with mixed grain size investigating dynamic armour formation have been conducted at a short time scale. Longer tests have been conducted to examine the formation of a static armour layer. However these tests have always had a duration of mobilising steady flows much longer than would be observed in a natural river.

The aim of this study was to examine the impact of different patterns of 'short term' time varying flows on the grain sorting and movement of mixed grain size sediment. To meet these objectives a series of laboratory tests was conducted. Each test was split into two parts. In the first part a sediment deposit was subjected to an initial 'flood event', afterwards the water worked surface was exposed to a larger flood in order to examine sediment stability that had developed. The bedload transport rate, its composition, the near bed flow velocity and the local bed surface topography were all monitored. These data were collected in order to describe the grain sorting experienced during different patterns of flow hydrograph and to quantify the adjustment in the critical entrainment conditions for different grain size fractions after being subjected to the different flows in

the initial 'storm events'.

3.2. EXPERIMENTAL APPARATUS

3.2.1. Laboratory Flume

The laboratory experiments were carried out in the Sediment Transport Laboratory at the University of Sheffield. A re-circulating glass sided tilting flume which was 18.4 metres long, 0.5 metres wide and 0.5 metres deep was used (Figure 3.1). The first 2.5 m of the flume bed was composed of coarse gravel particles ($d_{50} \approx 20$ mm) glued to the flume base in order to provide repeatable and uniform turbulent flow conditions at the upstream edge of the mobile bed section. Downstream of the static bed section, a 12.5 m length of mobile bed was placed in the flume. The gradient of the flume was altered by the use of hydraulic jack and flowrates were controlled by use of a computer-controlled pneumatic valve located in the inlet pipe flume. An adjustable gate at the downstream end of the flume acted as a control of the flow depth allowing the gradient of the water surface to be altered.

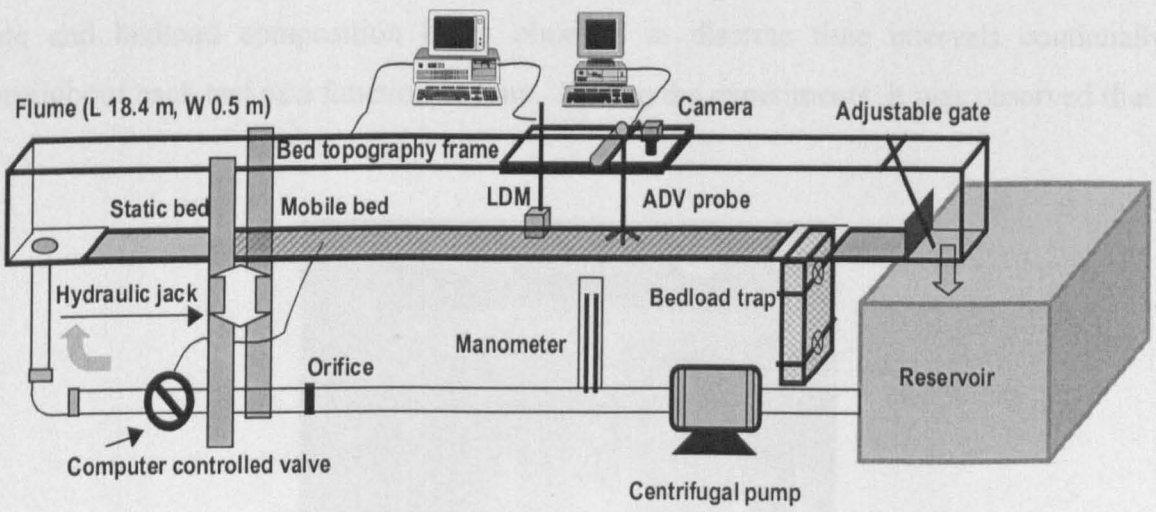

Figure 3.1. Sketch of the experimental layout

Different flowrates were obtained based on a correlation between discharge and the percentage of valve opening. This correlation was found in preliminary tests using a manometer and a pre-calibrated orifice plate in the inlet pipe. The same volume of water was used for each test so that this relationship would remain the same. The discharge of 0.0338 m^3/s was selected as the highest discharge applied in all the antecedent flow

tests. It was achieved by setting the valve at 75 % opening. For the unsteady antecedent flow hydrographs the increasing and decreasing discharges were achieved by employing a computer program to control the valve opening with time. The different level of valve opening creates different flow discharges up to the 100 % of valve opening during which the maximum discharge of 0.0375 m^3/s was provided. During the operation of valve, the downstream control was fixed so that similar floodwave was observed, providing the time variation in discharge was the same.

3.2.2. Bedload Trap

A slot type sediment trap located 12.7 m from the flume inlet was provided to collect the material being transported as bedload. It was positioned in the centre of the flume with the size of 420 mm in lateral direction and 70 mm in the streamwise direction. The bedload trap was originally split into three lateral sections (Figure 3.2 and Figure 3.3). It was equipped with two valves and interchangeable collection boxes to allow an interrupted collection of bedload samples but only the middle section of 190 mm width was used to trap the moving bedload. This allowed a continuous record of the transport rate and bedload composition being obtained at discrete time intervals continually throughout each test as a function of time. During the experiments it was observed that

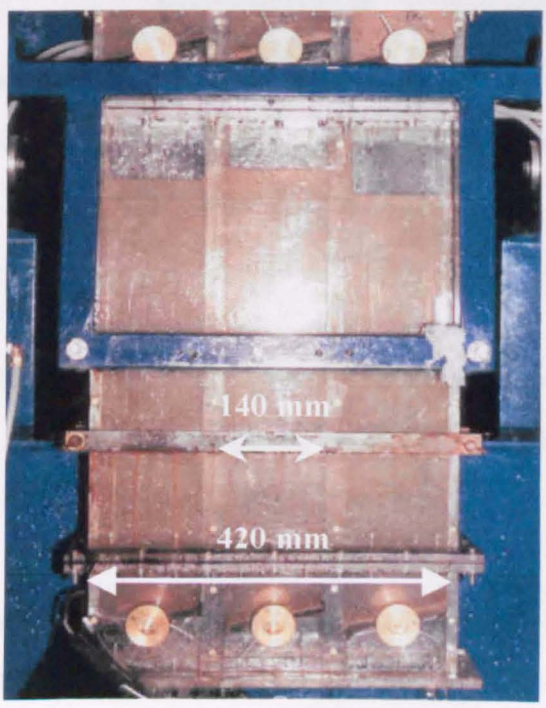

Figure 3.2. Photograph of sediment collection box

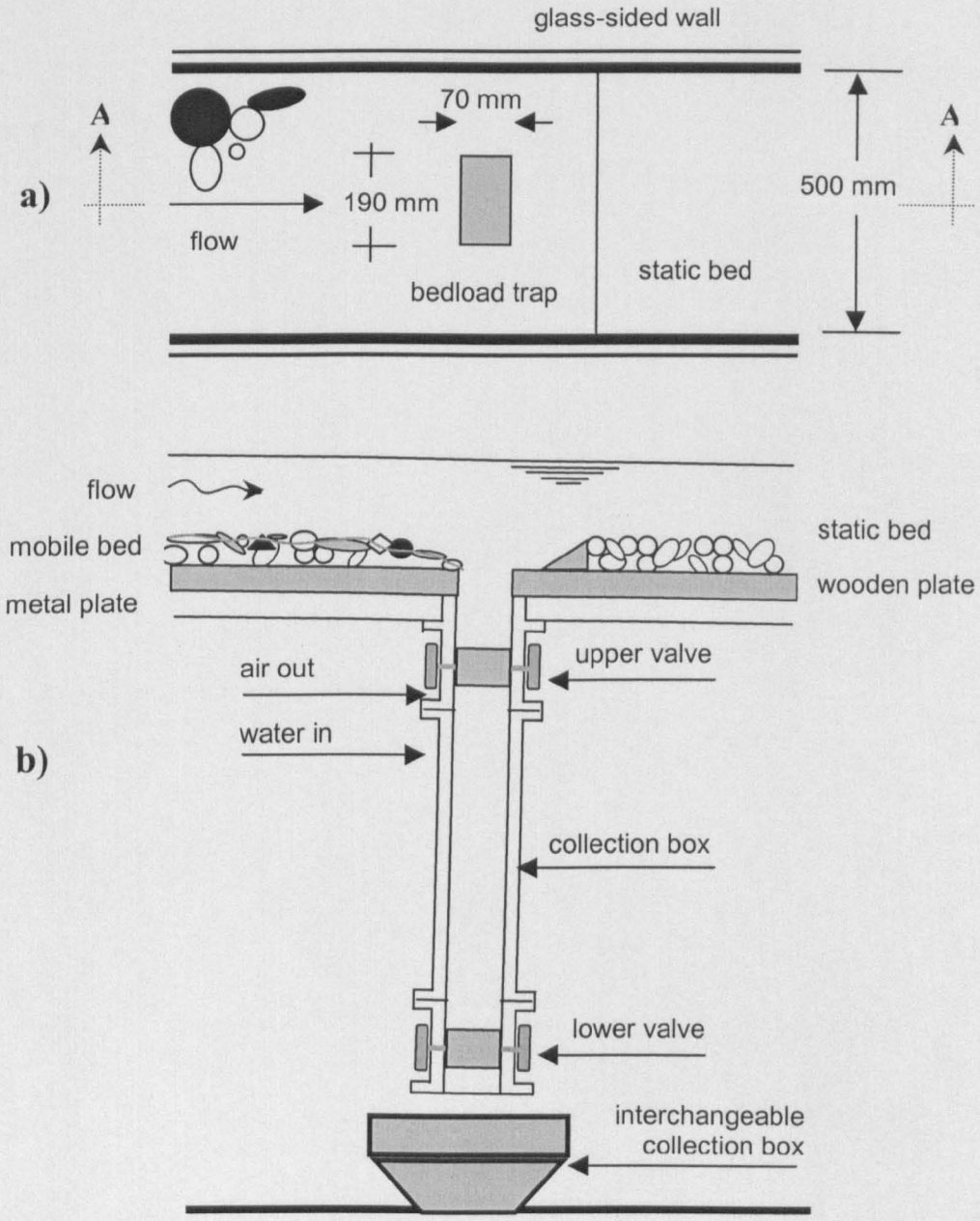

Figure 3.3. Sketch of bedload trap attached to the flume, a). plan view, b). cross section A - A

the movement of the bedload was not affected by the operation of the trap so that the pattern of transported bedload was believed to strongly reflects the actual pattern of transport phenomenon in the central section of the flume.

A section of uniformly sized fixed sediment grains was located downstream of the trap (see Figure 3.3). Examination of this area at the end of tests indicated no grains that could have come from the mobile sediment bed. It was therefore concluded that the trap

was highly efficient at collecting all the grain sizes in motion. These observations suggested that the dimension of the trap used is suitable to reliably collect the moving bed material. Preliminary experiments showed that the movement of particles was concentrated in a zone centred along the centreline of the flume. This was reflected by the existence of valley-formed bed along the centreline of the flume as shown in Figure 3.4. The average width of the valleys formed on the bed matched the width of the bedload trap. It was also matched the width of measurement grid for the velocity and bed surface measurements (180 mm).

Figure 3.4 a). Valleys formed along the centreline of the flume, and
b). the width of the valley as indicated by the ruler

The mode of sediment supply is one of the most important controls that can be exercised in mixed grain size sediment transport experiments. Parker and Wilcock (1993) outlined the fundamental difference between operating a flume in a sediment feed or a re-circulating mode. Operating a flume in re-circulating mode is useful for examining the transport capacity of different grain size fractions at a particular hydraulic condition. However, there is effectively no grain size sorting with time when the flume is run in

this mode. When a flume is run with an imposed feed rate and size distribution, the final conditions are heavily dependent on the feedrate and size distribution selected. This system does take time to attain the final equiblirium conditions. It was the intention of this work to examine how time varying flowrates at a time scale commonly found in rivers, would affect the way in which such a system attains a final equilibrium, and to examine if these are significant differences in the final equilibrium state even though the sediment feed conditions were not changed. The simplest feed system was selected, that of a zero feed. This type of operation develops static armour rather than the dynamic armour formed in re-circulating or feed systems with a non zero feed. This mode of operation does however have a time in which the system tends to a final equilibrium in a manner similar to a non-zero sediment feed experiment. In all the tests performed, no sediment was feed into the flume at the upstream boundary.

3.2.3. Acoustic Doppler Velocimeter and Mounting Arrangement

It has been recognised that the near bed flow environment can be significant in the entrainment and movement of sediment particles (Grass, 1971). In order to quantify the pattern of near-bed flow and to investigate the variation in time-averaged shear stress, an Acoustic Doppler Velocimeter (ADV-SonTek) was used to carry out a series of near-bed flow velocity point measurements. The ADV probe is a versatile, high-precision instrument that measures three flow velocity components of streamwise, lateral and vertical direction. The ADV probe measured the flow in these three directions by measuring the Doppler shift of acoustic signals transmitted from the probe and reflected back to the probe receivers off scatters in the flow. The probe periodically emits a short acoustic signal, and three receivers measure the changes in frequency of the echo by Doppler effect. The ADV has been used to estimate the near-bed shear stress in open channel (Kim et al., 2000) as well as measurement in combined sewer (Ahyerre et al., 2001) with reasonable success. Analysis by Voulgaris and Trowbridge (1998) indicated that the ADV sensor could measure mean velocity and Reynolds stress within 1 % of the estimated true value. Snyder and Castro (1999) run the test in the stratified tank to verify the usability of the ADV. As suggested by Kraus et al (1994) the accuracy of the probe to horizontal flow fields was generally within the range of $\pm$ 0.25 % $\pm$ 0.25 cm/s. Note that the first figure (0.25 %) is a relative accuracy, being a percentage of the value

indicated, and the second (0.25 cm/s) is an absolute accuracy, providing a lower limit or minimum resolution related to the inherent Doppler noise.

The ADV probe consists of three acoustic receivers and a transmitter at the base of the probe, which all must be fully submerged to ensure proper operation (Figure 3.5.). The red receiver arm on the 3-D down-looking probe is aligned in the direction of the x-axis and the value for velocity Vx in the software refers to the velocity along this axis. The directions of y-axis and z-axis are based on the definitions of a right-handed co-ordinate system (SonTek, 1995). An important advantage of the ADV is that it measures the flow in a small sampling volume of approximately 0.25 cm^3 or approximately 5 cm away from the sensing elements (Nikora and Goring, 1998).

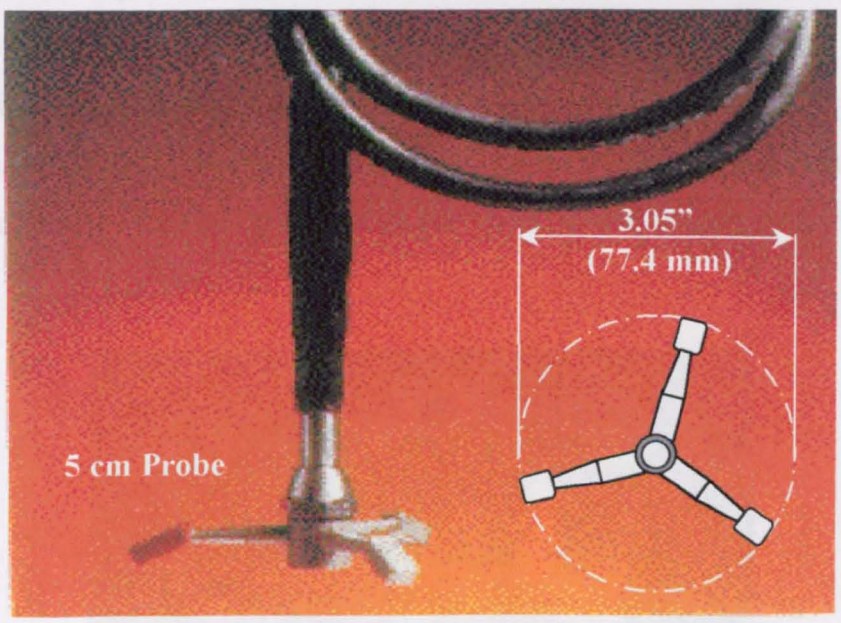

Figure 3.5. 3-D down-looking Acoustic Doppler Velocimeter SonTek

One advantage of the ADV probe is that it measures the flow at a distance from the sensing elements. It has a small sampling volume, a cylinder with 3 to 9 mm length and 6 mm diameter, allowing the ADV to be less affected by severe attenuation in the variance of vertical velocities. In this experiment, the distance from the sensor head to the sampling volume was approximately 50 mm. The manufacturer advised that in most flow regimes, this distance is sufficient to avoid interference from the probe in the flow (SonTek, 1994). The requirement that the probe always be submerged, and that the

measurement volume was 50 mm from the transmitter head meant that a minimum flow depth was required. This was set at 60 mm. This constrained the hydraulic conditions that were possible during the testing program.

Before data collection was started, the velocity range and the sampling rate were set. As a general rule, the velocity range should always be set as small as possible. It was observed that the maximum discharge applied in the experiments produced maximum velocity that was slightly above 60 cm/s. This velocity occurred when the flowrate was approaching its peak during the stability test. In this case, the velocity range of $\pm$ 100 cm/s was a reasonable choice. The reason for this was that the noise in the data increases with increasing velocity range. If the velocity range is set higher than 100 cm/s and the actual velocity is only 60 cm/s the data will appear excessively noisy and resulting in a loss of precision at high sampling rates.

In this experiment the ADV probe was clamped on a trolley with adjustable movement in the streamwise, lateral and vertical directions (Figure 3.6). This arrangement allowed the ADV measurement volume to be moved accurately and remotely once its initial

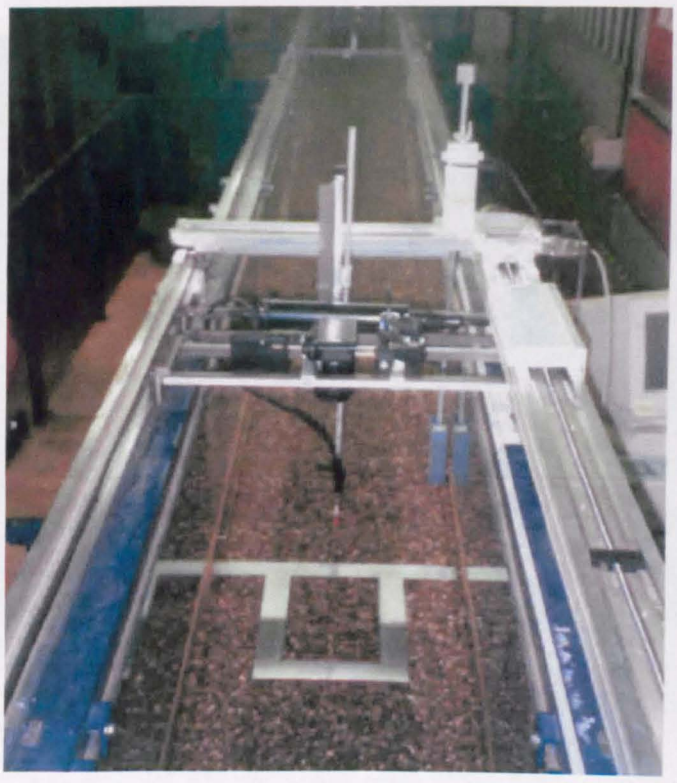

Figure 3.6. Clamping arrangement over the measurement grid

position had been established. All measurements were carried out at sampling rate of 25 Hz. This sampling rate was selected in order to examine the structure and variation in turbulence over rough water worked gravel beds. Previous flow visualisation work by Tait et al (1996) and measurement in the field by Nikora and Goring (1998b) and Smart (1999) have indicated that the coherent flow structures observed over gravel beds appeared to have a frequency of occurrence of around 2 -3 Hz. A sampling frequency with higher magnitude would be able not only to identify such structures but also give some insight into their development.

3.2.4. Laser Displacement Meter and Movement Frame

The changes of bed surface structure will be observed by measuring the elevation of the bed surface at a large number of points organised on an orthogonal grid. These measurements took place at the beginning and end of the initial part of each test and also after the 'stability test'. The laser displacement meter used for this purpose was attached to a computer controlled motion frame that could be programmed with a certain movement pattern.The displacement sensor traversed the sample area of 280 by 180 mm

Figure 3.7. Laser Displacement Meter (LDM) in use

at intervals of 1.0 mm in both streamwise and lateral directions (Figure 3.7). A single bed position reading was taken at each grid point. A grid interval of 1.0 mm was determined in order to cover the close range of variations in the bed elevation. Although the mixture was also composed of sand with grain size less than 1.0 mm, this fraction made up only a small proportion of the bed. After the test, as the finer grains were transported and the bed become more coarser, the 1.0 mm grid interval of LDM movement is still sufficient to pick the variation of elevation with the assumption that it would be able to pick at least five information points on grains of the average grains d_{50} = 5.19 mm. Due to the long operation time (12 hours and 55 minutes) to cover the large number of steps (50400 rows of data for each experiment), the sensor was left to run overnight unattended.

The laser displacement sensor was a model LC 2400 manufactured by Keyence. It has a measurement range of ± 9 mm with the zero datum position being located at fixed distance 50 mm from the sensor head. The sensor had a measurement spot diameter of 45 x 20 μm and had a stated vertical resolution of 0.5 μm. Given this level of vertical accuracy, and spatial precision coupled with its measurement range in comparison to the typical grain size, it was believed that this sensor would be suitable to obtain detailed information on grain arrangement as the water worked sediment beds developed.

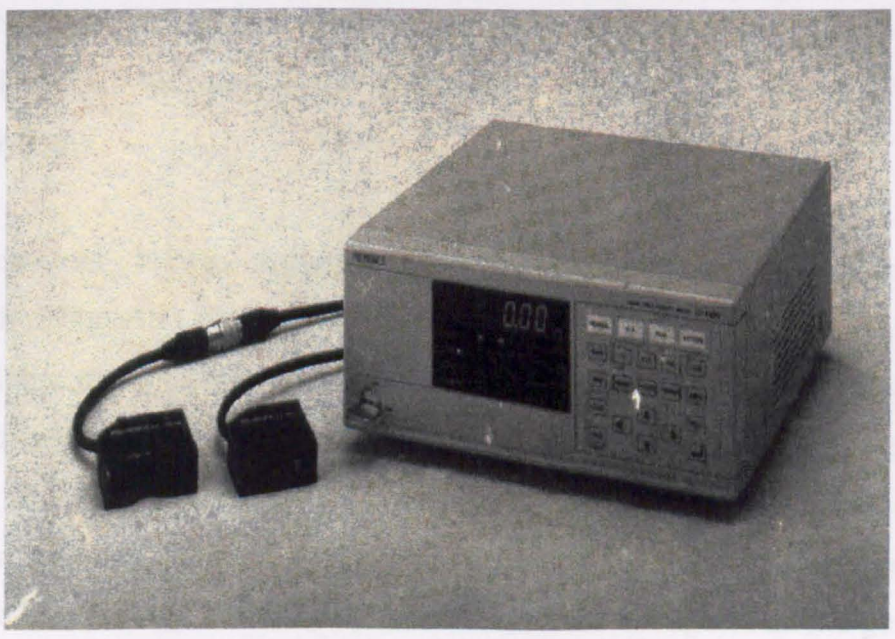

Figure 3.8. Laser Displacement Meter Keyence 2400

The vertical position of the sensor was adjusted at the start of each test to a reasonable height above the bed surface with the consideration of the measurement range of the sensor, so that it would pick up maximum detail of the variation in bed surface level within the measurement area. Grid points within sample area were marked on the measurement rails so that the bed topography measurements could be related to measurement locations used by the ADV probe. The bed topography frame had been designed in such a way that ADV probe can be moved easily in the selected area. All data values are recorded by a computer to allow the bed structures to be analysed at a later stage.

3.3. SELECTION OF SEDIMENT MIXTURES

The primary requirement used to select the sediment for this experiment is that the mixture must have a range in grain sizes and must be similar in nature to the natural sediment mixtures that exists in many rivers. Unlike the uniform sediment that has been extensively investigated and where the transport mechanisms are reasonably well understood (Wu et al, 2000) the transport processes in non-uniform sediment are much more complex. In a broad grain size distribution, sediment responds differently from one with uniform grain size and the critical shear stress of individual friction depends on mixture characteristics (Wilcock, 1993). Bimodal sediment have been used in this experiment as this form of grain size distribution has been found in many gravel-bed rivers (Shaw and Kellerhals, 1982) and has been used by other researchers, notably Wilcock (1993) in his work on the behaviour of bimodal mixtures in a recirculating laboratory flume.

A sediment mixture was manufactured from three different grain size sediments supplied from quarries located on river floodplains in Nottinghamshire. There were mixed using a mechanical mixer to form a well mixed material that contained mixed sized sand (sediment A), a 6 mm fine gravel (sediment B) and a 10 mm coarse gravel (sediment C). This was called Mix 1 (0.33 A + 0.33 B + 0.33 C). This mix was initially tested in a series of simple experiments to examine its mobility. The mixtures were exposed to five different discharges that accommodate a range of discharges. This was intended to obtain information to ensure that the mix selected had a range of mobilities at the possible final test discharges. The bedload transport rate was measured for both a

freshly scrapped bed and an armoured bed, which was a deposit that had been exposed to the flowrate for at least three hours. The phi-index scale of 0.5 was used to divide the sediment sieve size into class intervals to adequately describe the bimodal sediment mixtures (Table 3.1).

Table 3.1. The ϕ-index and the sediment class intervals

No.	Phi-index (ϕ)	d (mm)	Sieve size (mm)	Remarks
1.	2.5	0.177	0.150	
2.	2.0	0.250	0.250	
3.	1.5	0.354	0.355	
4.	1.0	0.500	0.500	
5.	0.5	0.707	0.710	$\phi = -\log_2 d$
6.	0.0	1.000	1.000	(d in mm)
7.	-0.5	1.414	1.400	
8.	-1.0	2.000	2.000	
9.	-1.5	2.828	2.800	
10.	-2.0	4.000	4.000	
11.	-2.5	5.657	5.600	
12.	-3.0	8.000	8.000	
13.	-3.5	11.314	10.000	

This mixture gave a good transport rate pattern during each run, with sufficient material being entrained and transported to ensure accurate transport rate measurement using the bedload trap. Table 3.2 confirms the common behaviour of the freshly laid sediment in that the larger the discharge applied to the bed the higher the amount of material being transported. All armoured beds transported significantly less than the corresponding freshly laid bed. An interesting feature presented by experiments with discharges Q_4 and Q_5. Both produced significantly different values in transport rate of the fresh sediment bed but transported almost similar amounts from the armoured bed. This led to the hypotheses that Q_4 was capable to progressively disrupt the bed and accommodate the similar level of armouring as displayed by the maximum discharge. It was then decided to apply Q_4 with discharge of 0.0338 m^3/s to all antecedent flow experiment and the maximum discharge of 0.0375 m^3/s was applied to the second stability experiments. These values of flow gave a measurable range of bedload transport rates on both freshly laid and armoured bed.

Table 3.2. Average sediment transportation rate of Mix 1

No.	Valve opening	Discharge	Average transportation rate (gr/s per m)	
			Fresh bed	Armoured bed
1.	30	$Q_1 = 0.0123$	0.1542	0.1742
2.	45	$Q_2 = 0.0220$	0.4590	0.0574
3.	60	$Q_3 = 0.0305$	0.4721	0.0732
4.	75	$Q_4 = 0.0338$	0.6621	0.0905
5.	100	$Q_5 = 0.0375$	1.2826	0.0932

Unfortunately, due to the limited stock and to ensure sufficient sediment was available for all the main tests, a new batch of sediment was purchased. A new mixture of material from Langford quarry was then selected to replace the existing one. The mixture composition was designed to match Mix 1. Using similar ϕ-index applied for Mix 1, both the grain size distributions and sorting coefficients were obtained by sieving analysis and the data of typical grading curve of new materials for each composition was examined and compared to get the closest to grading curve for Mix 1.

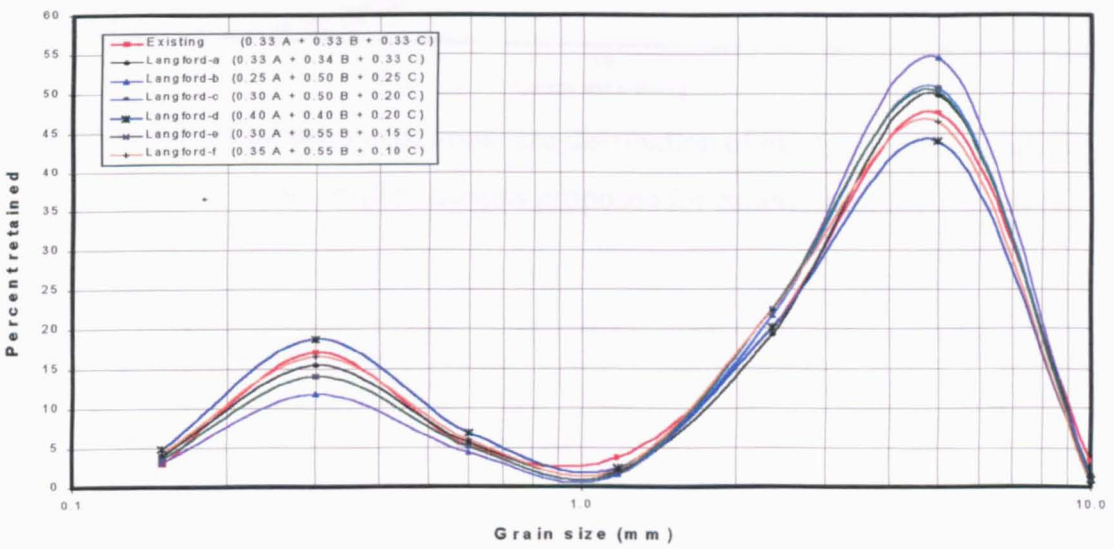

Figure 3.9. Grading curve comparison of existing material and six different compositions of new material

Figure 3.10 presents six different composition obtained using the sediment from Langford closest to the existing mixture. The grading curve of mixture Langford-f

with composition of 35 % sand, 54 % 6 mm gravel and 10 % 10 mm gravel (0.35 A + 0.55 B + 0.10 C) seems to be the closest to the existing material when examining the average grain size. But further examination of the entire grain size distribution led to the decision that mixture Langford-c has a closest grain size distribution compare to Langford-f (see Figure 3.10). Mixture Langford-c (0.30 A + 0.50 B + 0.20 C) was then selected to be used for all the main experiments (see Figure 3.11). This mixture has two modes with finer mode and coarse mode being at approximately 0.355 mm and 5.60 mm with d_{16} = 0.65 mm, d_{50} = 5.19 mm and d_{84} = 7.61 mm. The geometric standard deviation, σ_g = 3.42.

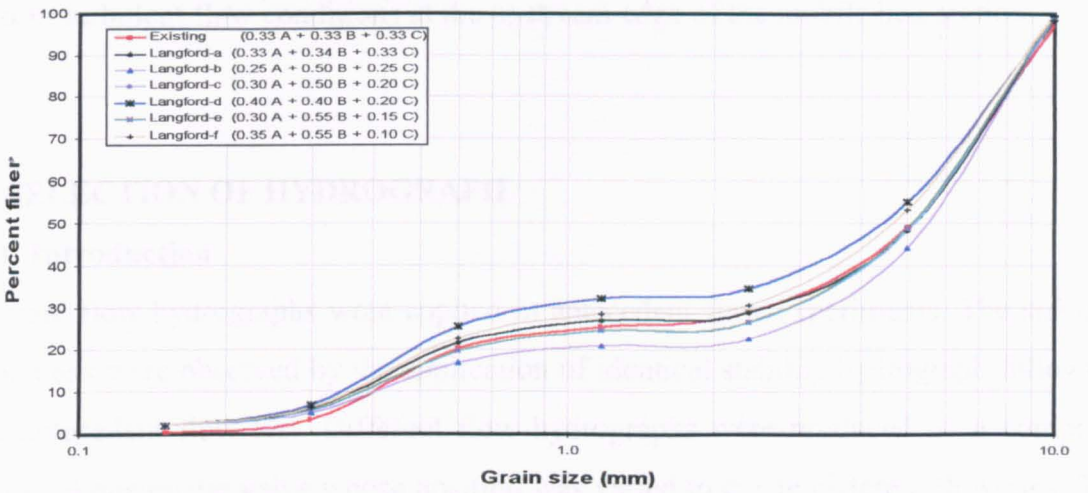

Figure 3.10. Comparison of grain size distribution of existing material and six composition designs proposed for experiments

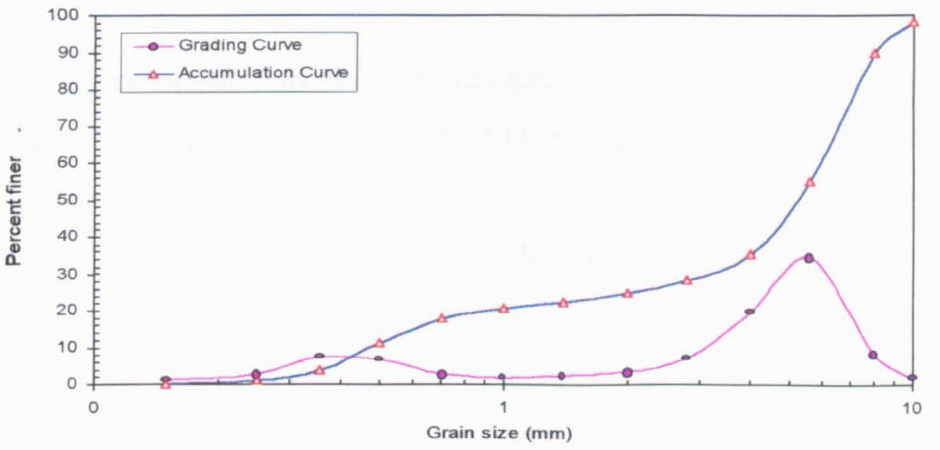

Figure 3.11. Grading curve and cumulative distributions of mixture Langford-c (0.30 A + 0.50 B + 0.20 C)

In all tests no sediment was input at the upstream inlet to the flume. The concept was to carefully place the mixture that was fully mixed using the electric mixer. The mixing time length was long enough to produce a well-mixed sediment bed. One mixing contained 18 kg of sediment A, 30 kg of sediment B and 12 kg of sediment C. The mixing process was repeated until the amount of mixture was sufficient enough to fill the 12.5 m length of mobile bed section in the flume. The total mass of sediment used for each experiment was approximately 310 kg. The sediment bed was scrapped flat using a metal scrapper, which ran on two parallel measurement rails to give a bed surface with the same slope of the flume, i.e. 1 in 250. This was done before the bed was exposed to a flow hydrograph. The first 2.5 m of the flume bed was composed of coarse gravel particles ($d_{50} \approx 20$ mm) glued to the flume base in order to provide repeatable and uniform turbulent flow conditions at the upstream edge of the mobile bed section.

3.4. SELECTION OF HYDROGRAPH

3.4.1. Introduction

Different flow hydrographs were applied in antecedent flow experiments. The stability of the beds were observed by the application of identical stability hydrograph following each antecedent flow test. Different flow hydrographs were produced by a computer controlled pneumatic valve whose position was varied to create different flowrates. The length of steady flow experiment was divided into four different duration while time varying flow with or without steady flow was separated into three different duration as indicated by the number given in the name of experiment.

In details the experimental work was characterised by three groups of hydrographs :

1. Steady flow experiments SF I in which the discharge was held at a steady value throughout the test. Four different durations were applied, namely Experiment SF 1-3 (3 hours), Experiment SF 1-6 (6 hours), Experiment SF 1-9 (9 hours) and Experiment SF 1-12 (12 hours) respectively.
2. Steady flow with time varying flow experiments UF II in which the flowrate was initially held at a steady flowrate for three hours followed by a period of linear decline in flow discharge. Three selected different durations of declining flow were identified as Experiment UF 2-6 (3 hours steady and 3 hours declining

flow), Experiment UF 2-9 (3 hours steady and 6 hours declining flow) and Experiment UF 2-12 (3 hours steady and 9 hours declining flow).

3. Time varying flow experiments UF III with a different duration of increasing discharge but similar 3-hour duration of decline in flow discharge. Those were identified as Experiment UF 3-6 for 3 hours increasing and 3 hours declining flow, Experiment UF 3-9 for 6 hours increasing and 3 hours declining flow, and Experiment UF 3-12 for 9 hours increasing and 3 hours declining flow.

3.4.2. Steady Flow Experiments SF I

The aim of these experiments was to examine how the armour bed developed and also to quantify the additional stability caused by an increase in the length of time as a mixed grain sediment bed was exposed to a uniform flowrate. The gate at downstream end of the flume was adjusted during the initial stage of all the steady flow experiments so that experiment was started with a uniform flow depth and a uniform average shear stress was applied to the bed. A flowrate of 0.0338 m^3/s was applied to four different run times of three, six, nine and twelve hours respectively (see Figure 3.12).

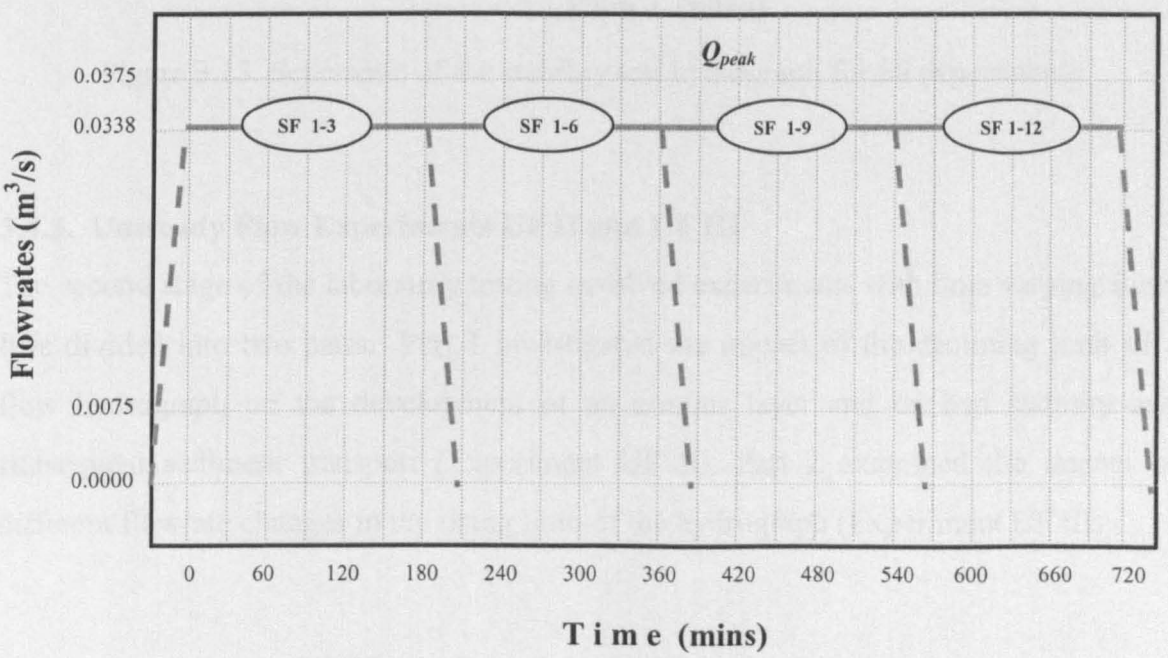

Figure 3.12. Schematic of antecedent flow hydrograph for steady flow Experiments SF I

The stability of the water worked beds formed during the steady flow experiments need to be estimated to study the processes that control the development of stability in gravel

bed rivers. The stability of the water worked deposits was examined by applying a relatively short hydrograph (Figure 3.13). This hydrograph was the same in each test. The flowrate increased from base flow of 0.0075 m3/s to a peak flowrate of 0.0375 in a time of 60 minutes. It then took a further 60 minutes to return to the base flowrate. The level of bed stability was assesed by examining the temporal pattern of the eroded sediment at 10 minutes intervals.

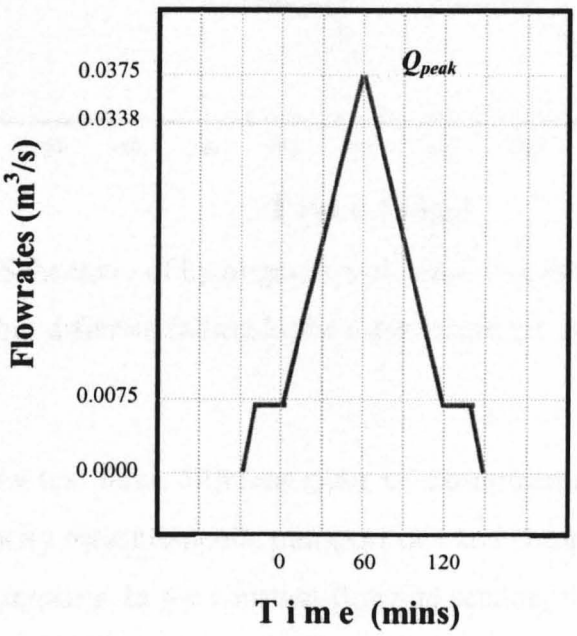

Figure 3.13. Schematic of the stability test hydrograph for all experiments

3.4.3. Unsteady Flow Experiments UF II and UF III

The second stage of the laboratory testing involved experiments with time varying flow. It is divided into two parts. Part 1 investigated the impact of the declining limb of a flow hydrograph on the development of an armour layer and on bed stability and subsequent sediment transport (Experiment UF II). Part 2 examined the impact of different flowrate changes in the rising limb of the hydrograph (Experiment UF III).

3.4.3.1. The Impact of Different Duration of Falling Limbs

The aim of the experiments was to assess the impact that different rates of decline in flood hydrographs have on grain sorting and bed stability. Three antecedent flow experiments had an identical initial section of constant flowrate followed by a decline in flow discharge with different duration (Figure 3.14.).

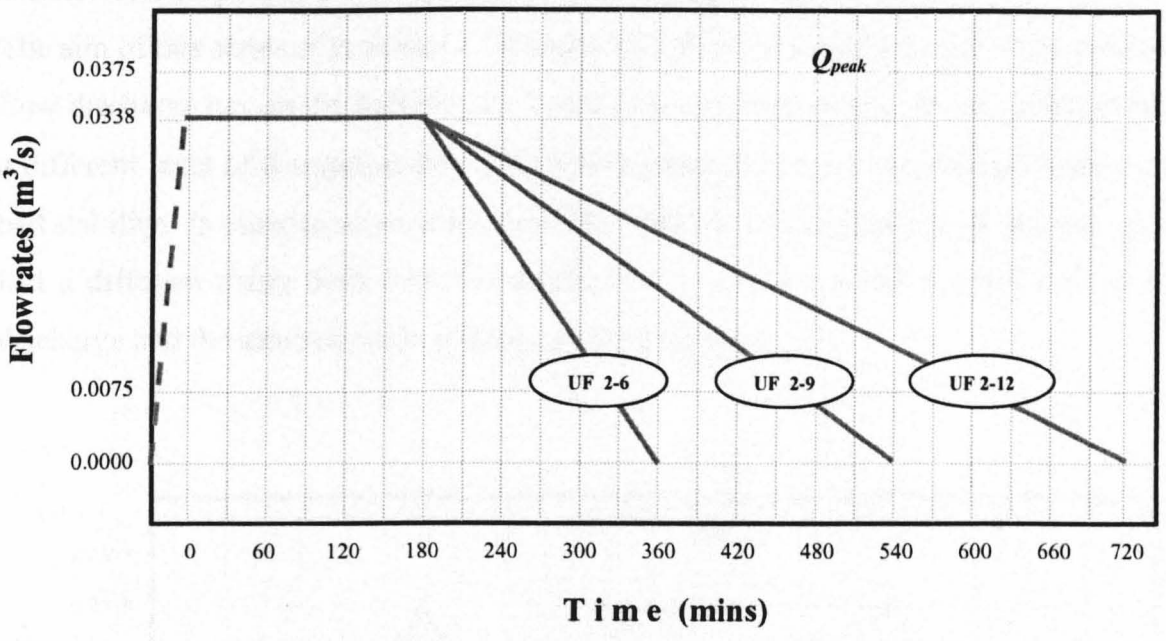

Figure 3.14. Schematic of hydrograph with similar constant discharge but different falling limbs Experiment UF II

As with the steady flow test three different types of experimental measurements were made. These were velocity measurements, transport rate and composition measurements and bed surface measurements. In the constant flowrate section, the nearbed streamwise velocity measurements were measured at a single point in the centreline of the flume with an interval 10 minutes and also at different points in the measurement grid. During the decelerating flowrate, measurements were taken at a single point 10 mm from bed so that the near bed flow environment at the same point can be compared as the discharge declines.

The flow was stopped at the end of the test and the flume slowly drained. The bed surface over a 280 mm by 180 mm was measured using the bed topography frame. Photographs were taken to visually observe the bed changes between the start and the end of the tests. The second stability hydrograph as applied to the steady antecedent flow experiments (Figure 3.13) was introduced to the armoured bed after each run to quantify its stability by measuring the resulting transport rates at 10 minutes intervals. This allows the stability of the armoured beds formed by the different hydrographs of UF 2-6, UF 2-9 and UF 2-12 to be quantified.

3.4.3.2. The Impact of Different Duration of Rising Limbs

The aim of this series of tests was to examine the effect that different rates of increase of flow discharge has on the stability of a water worked sediment bed. It was believed that a different level of disruption during the initial phase may have a significant impact on bed stability. In order to accomplish this, three different hydrographs were applied, each had a different rising limb with the duration of 3, 6 and 9 hours but the same peak discharge and the same duration of recession limb (Figure 3.15).

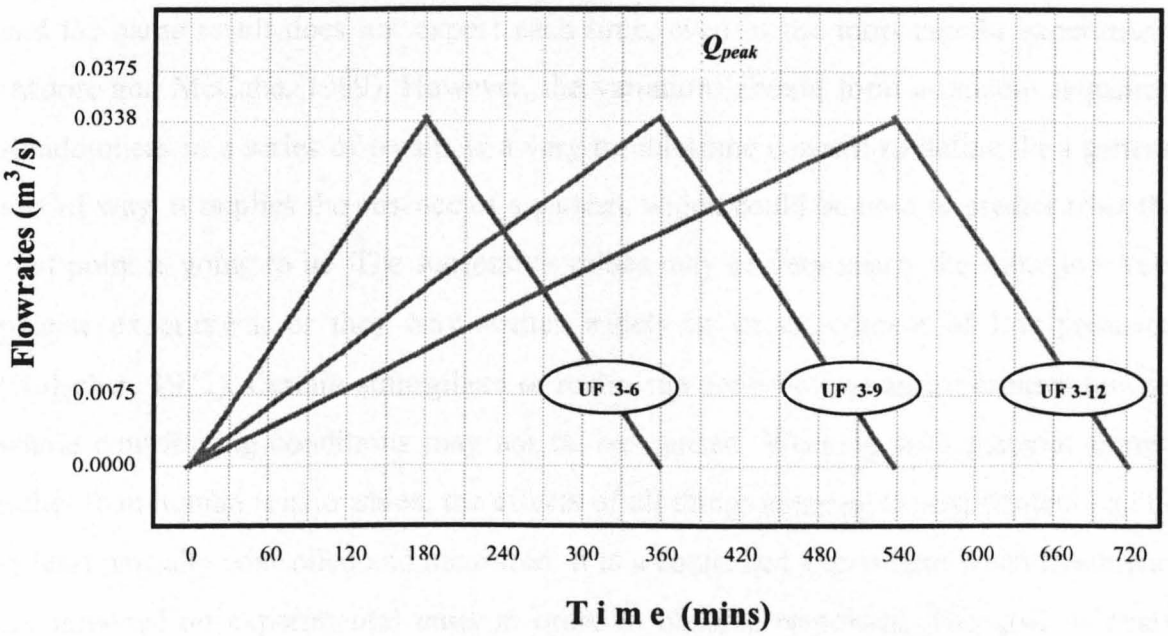

Figure 3.15. Schematic of hydrographs with different rising limb but similar falling limbs (Experiment UF III)

Similar to the other two series of tests, measurements made during these experiments were divided into three different activities ; near bed flow velocity measurement at the central point of the measurement grid (10 mm above the bed), transport rate and composition measurement, and bed surface measurement. The flow was stopped at the end of the test and the bed surface profile of 280 mm by 180 mm was measured using the bed topography frame. Again, the second stability hydrograph with the higher maximum discharge of 0.0375 m^3/s (Figure 3.13) was introduced to the armoured bed after each run to quantify its stability by measuring the resulting transport rates at 10 minutes intervals. This allows the stability of the armoured beds formed by the different antecedent flow hydrographs of UF 3-6, UF 3-9 and UF 3-12 to be quantified.

3.5. THE USE OF STATISTICS

3.5.1. Introduction

Statistical analysis provides methods of treating data so that the maximum information can be obtained with a predetermined risk of drawing false conclusions. It can be said that no method, including statistic, can draw conclusion from experimental data with zero risk of error. According to Holscher (1971) the sources of error which are universal to almost all experimentation may be summarised into three factors : the variability of the material or sample used, the uncontrolled conditions of the testing, and the measurement errors of instruments and people. Sources of variability are always exists and the same result does not expect each time, even in the most careful experiments (Moore and McCabe, 1999). However, the variations should form a random sequence. Randomness in a series of results is a very troublesome concept to define. In a general sort of way, it implies the absence of a pattern, which could be used to predict what the next point is going to be. The successive values may be very nearly the same in a very precise experiment, or they may scatter widely in an experiment of low precision (Holscher, 1971). Certain atmosphere or realm can contribute to an experiment but the whole contributing conditions may not be recognised. Working with material things, rather than human relationships, the effects of all things entering the experiment can be at least partially controlled and measured. It is a controlled experiment when treatments are imposed on experimental units in order to observe responses. The goal of every controlled experiment is to establish a cause-and-effect relationship between treatments and outcomes specified by the response variable (Petruccelli et al., 1999). In fact, only a properly designed and conducted controlled experiment can establish a cause-and-effect relationship. The problem in developing an experiment under control is that it may or may not be economically feasible (Holscher, 1971). However it should always be done if there is a strong tendency that it is feasible.

3.5.2. Random and Discrete Variables

A random variable, or a variate if its distribution is known, is a variable whose value is uncertain or unpredictable or non-deterministic (Kottegoda and Rosso, 1998). It is a phenomenon that usually encountered because of its inherent randomness and consequent unpredictability. A random phenomenon is an occurrence that results in one

of a known set of definite, identifiable outcomes, but whose actual outcome can not be predicted with certainty in advance (Petruccelli et al., 1999). Hence, the effects caused by unexpected and unpredicted variable enter in an experiment must be carefully checked. Randomness of experimental order is a fundamental procedure for good results. It prevents some overlooked effect from becoming identified with an experimental factor and also ensures that any small overlooked effects are impartially distributed among the comparisons (Holscher, 1971). Random variables may assume some value, the magnitude of which depends on a particular occurrence or outcome of an experiment. A random variable can be statistically specified by its distribution or probability law using a mathematical function where the variable can be the discrete or continuous type. Continuous variables can take any value in a given range while discrete variables can take only certain distinct values or isolated values such as integers in a given range so that both distribution are necessarily different.

3.5.3. Probability Distributions and Bin Size

Over the years, statisticians and scientists have noticed that certain data distribution patterns occur repeatedly in nature. These pattern has arisen the idea of theoretical distributions : mathematical curve that serve as models for these observed data distribution patterns (Petruccelli, 1999). One of the great advantages of mathematics is that the essential features of quite different phenomena can be described by the same mathematical model. Mathematical model is a form of probability theory to describe events in the real word. Probability or a measure of uncertainty can be defined as the extent to which an event is likely to occur, measured by ratio of the favourable cases to the whole number of cases possible (Rees, 2001). Therefore, the possibility of the occurrence of events that may influence experimental outcomes and estimate their likelihood must be considered. The application of probability models is often necessity since the solutions of physical problems in engineering are associated with random factors that can greatly influence outcomes. The models are classified separately according to whether the variables are continuous or discrete. The parameters of the model vary from one case to another.

A data distribution is a summary of the variation in a set of data, which lists each data value and its frequency. A mean for a data distribution translates into the mean of a

distribution model which may be represented graphically by a probability histogram, a standard tool for displaying the variation in numerical data (Petruccelli et al., 1999). Construction of a histogram begins by breaking the range of data values into a number of intervals or classes and counting the frequencies of observations in each interval.

The number of the classes can be determined by method as suggested by Freedman and Diaconis (1981) as follows (Kottegoda and Rosso, 1998) :

$$n_c = \frac{rn^{\frac{1}{3}}}{2i_{qr}} \tag{3.1}$$

The number of classes is then used to determine the width of the classes or recognised as the bin size, which is the difference between the largest and smallest value per number of cells :

$$binsize = \frac{r}{n_c} \tag{3.2}$$

where :

n_c = the number of classes

r = range of the observation (the difference between max_{values} and min_{values})

n = number of data

i_{qr} = interquartile range = Q_3 - Q_1

Q_1 = the median of the lower half of the data

Q_3 = the median of the upper half of the data

The interquartile range is a measure of variability that is resistant to the effect of outliers, an individual value that falls outside the overall pattern. It is based on quantities called quartiles that are obtained by dividing the number of observations into a lower half and an upper half. The lower quartiles separate the bottom 25 % of the data set from the upper 75 % and the upper quartile separates the top 25 % from the bottom 75 % (Figure 3.16). The middle of quartile is the median, which is included in both halves if the number of observation is odd. The quartiles together with the median give some indication of the centre, spread, and shape of a distribution.

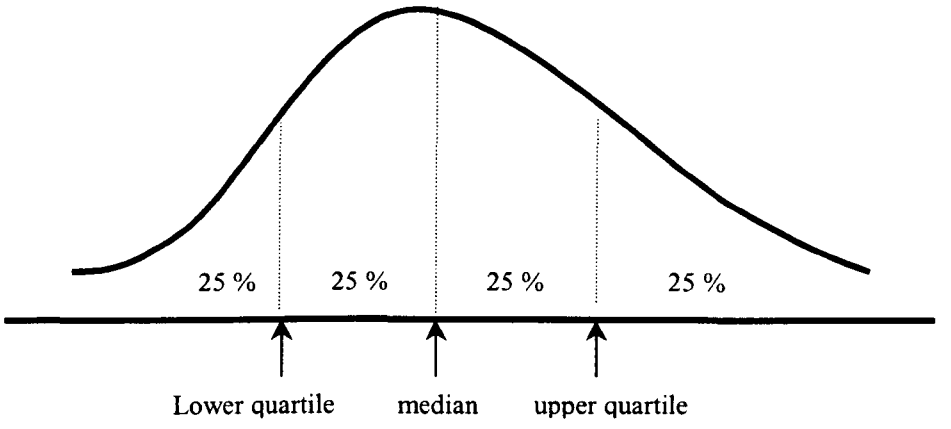

Figure 3.16. The quartiles for a smoothed histogram

The quartiles and the interquartile range are not affected by changes in either tail of the distribution. The resistant nature of the interquartile range follows from the fact that up to 25% of the smallest sample observation and up to 25% of the largest can be made more extreme without affecting its value, changes in a few data points have no further effect once the points move outside the quartiles (Devore and Peck, 1994 ; Moore and McCabe,1999). The relationship between the interquartile range and the standard deviations is roughly $\sigma = i_{qr}/1.35$ if a histogram of the observation data can be reasonably well approximated by a normal curve. The larger values of σ suggest that the histogram have a longer tails or heavier than a normal curve (Devore and Peck, 1994).

In a particular case, the shape of the distribution is considered before deciding whether to apply mean, median or mode (Rees, 2001). If the shape of the distribution is roughly symmetrical about a vertical centre line, the mean is the preferred average. If the shape of the distribution is not symmetrical, there will be a small number of extremely high values (positive skewness) or low values (negative skewness), which are not balanced by values on the other said of the distribution. These extreme values influence the mean more than the median so that the median is preferred in this case. The mode is rarely used for either continuous or discrete data, since it may not exist at all. It is useful only for categorical data (nonnumerical).

3.5.4. Standard Deviations, Skewness and Kurtosis

A standard deviation may be informally interpreted as the size of a "typical" deviation

from the mean. It is a measure of how widely values are dispersed from the average value. The value of standard deviation can be greatly affected by the presence of even single unusually small or large observation. The standard way to prevent negative and positive deviations from counteracting one another is to square all data before combining them. This method allows the deviations with opposite signs but the same magnitude to make identical contributions to variability.

Standard deviation can be determined using the following equation :

$$\sigma = \sqrt{\frac{n\sum x^2 - \left(\sum x\right)^2}{n(n-1)}} \tag{3.3}$$

where :

n = number of data,

x = individual data value

Skewness characterizes the degree of asymetry of a distribution around its mean. Positive skewness indicates a distribution with an asymmetric tail extending toward more positive values while negative skewness indicates a distribution with an asymmetric tail extending toward more negative values. The mean exceeds the median in positive skewness, while the mean is less than the median for negatively skew data. If the measure of skewness lies between -1 and +1, the distribution can be said to be roughly symmetrical. Kurtosis characterizes the relative peakedness or flatness of a distribution compared with the normal distribution. Positive kurtosis indicates a relatively flat distribution.

Skewness and kurtosis can be determined using the equation as follows :

$$Skew = \frac{n}{(n-1)(n-2)}\sum\left(\frac{x_i - \bar{x}}{SD}\right)^3 \tag{3.4}$$

$$Kurt = \left[\frac{n(n+1)}{(n-1)(n-2)(n-3)}\sum\left(\frac{x_i - \bar{x}}{SD}\right)^4\right] - \frac{3(n-1)^3}{(n-2)(n-3)} \tag{3.5}$$

where :

n = number of data

x_i = individual data value

$\bar{x}$ = average of data

SD = standard deviation

3.6. NEARBED FLOW VELOCITY MEASUREMENT

3.6.1. Selected Location and Type of Measurement

One of the major aims of this experiment was to study the influence of the near-bed flow velocity and the bed shear stress variations caused by turbulent fluctuations and their influence on the movement of different size fractions. Therefore nearbed flow velocity measurements weremade to discover the pattern of near-bed flow so that changes in the fluid force distribution on a mixed grain size bed as it armours could be estimated.

All nearbed flow velocity measurements were taken using the ADV probe over a relatively small area of 280 mm x 180 mm (Figure 3.17) located 9.14 m from the flume inlet. The first type of measurement was single point velocity measurements. These measurements were conducted at the centreline of the flume (point E3) 10 mm above the bed with measurement interval of 10 minutes. This resulted in 278 velocity time series data being available for analysis (Table 3.3). The second type of measurement was nearbed flow velocity measurements at different points within the selected area. These measurements were carried out only during constant flowrate so that no measurement was conducted during the antecedent flow experiment UF III. All velocity measurements were made at the centreline of the flume (row 3) and another two adjacent rows (row 1 and row 5). Row 1 and row 5 were relatively close to the centre line to minimise side-wall effects (Figure 3.17). The probe was positioned at 10 mm above the average bed surface and moved in a grid pattern of three streamwise rows 60 mm apart (row 1, row 3 and row 5). Each row had three measurement position 120 mm apart (line A, line E and line I). These velocity time series were used to investigate the variation in time averaged and instantaneous shear stress over the 280 mm x 180 mm measurement area and to deduce if there is any link between the pattern of shear stress and changes in bed surface arrangement. Details of the number of measurements made in each experiment are presented in Table 3.3.

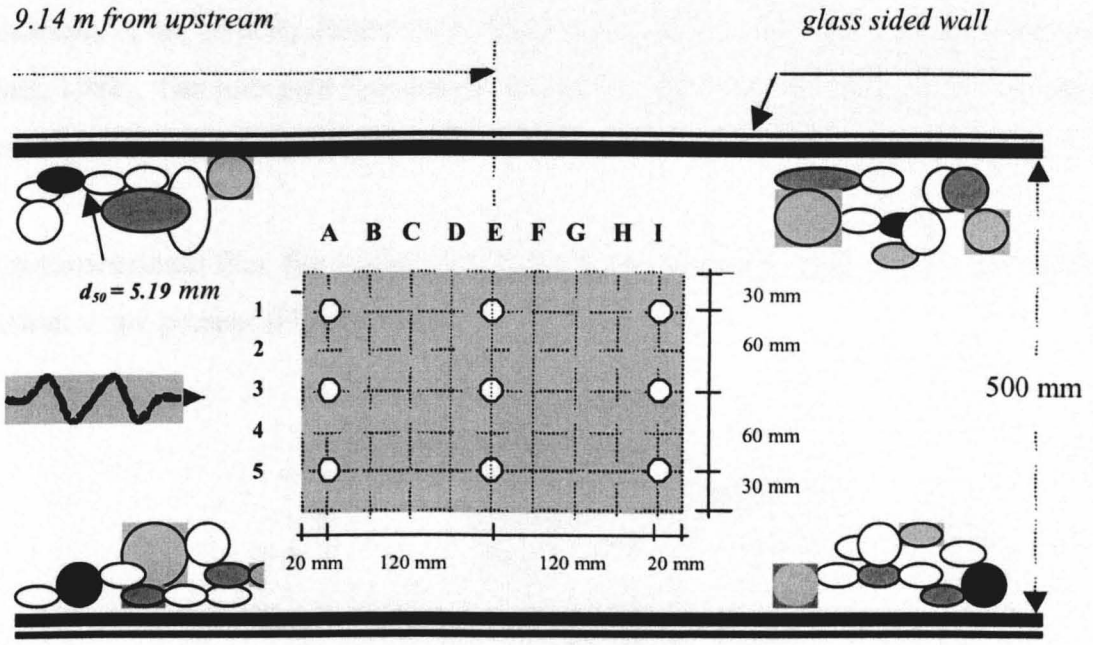

Figure 3.17. Grid spacing and location of nearbed flow velocity measurement

Table 3.3. Summary of nearbed flow velocity measurements for all experiments

Experiment No.	Measurement at a single point							Measurement of grid points during antecedent flow			
	Antecedent flow test				Stability test						
	R	C	F	T	R	F	T	1st	2nd	3rd	T
SF 1-3	-	3	-	3	5	5	10	9	7	-	16
SF 1-6	-	17	-	17	5	5	10	9	9	-	18
SF 1-9	-	32	-	32	5	5	10	9	9	-	18
SF 1-12	-	41	-	41	5	5	10	9	9	9	27
UF 2-6	-	3	12	15	5	5	10	9	9	-	18
UF 2-9	-	3	25	28	5	5	10	9	9	-	18
UF 2-12	-	3	39	42	5	5	10	9	9	-	18
UF 3-6	10	-	11	21	5	5	10	-	-	-	-
UF 3-9	23	-	12	35	5	5	10	-	-	-	-
UF 3-12	33	-	11	44	5	5	10	-	-	-	-
T o t a l				278			100				133

Note: R = rising limb section, C = constant flowrate section, F = falling limb section, T= total number of measurement, 1st = first measurement, 2nd = second measurement, 3rd = third measurement

3.6.2. Estimation of Instantaneous and Time-Averaged Shear Stress

The most common flow encountered in engineering practice is turbulent flow. In this flow, the motion of fluid particles is complex and erratic causing instantaneous

fluctuations in the velocity components (Chadwick and Morfett, 1993 ; Featherstone and Nalluri, 1988). The turbulent fluctuations cause an exchange of fluid momentum setting up internal shear stresses within the fluid.

In two-dimensional flow the velocity component in streamwise direction, u, and vertical direction, v, are present (Figure 3.18).

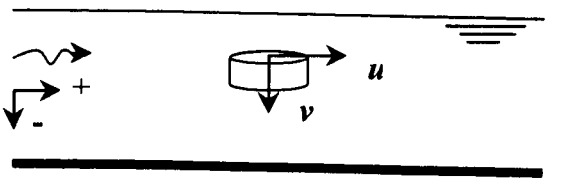

Figure 3.18. The movement of particle of fluid in two-dimensional flow field

Considering a turbulent boundary layer in which a small particle moves in vertical direction through a small horizontal element of area δA in a short time δt, the mass δm moving through the area is given by

$$\delta m = -v \times \rho \times \delta A \times \delta t \tag{3.6}$$

the momentum δM is

$$\delta M = \delta m \times u = -v\rho\delta A\delta t u \tag{3.7}$$

The existence of momentum implies the existence of a corresponding force within the fluid

$$\delta F = \frac{\delta M}{\delta t} = -v\rho\delta A u \tag{3.8}$$

The instantaneous shear stress τ' is equal to the force over the area

$$\frac{\delta F}{\delta A} = \tau' = -\rho u v \tag{3.9}$$

The fluctuating components recognised in turbulent flow are u' in streamwise direction, and v' in vertical direction. From Figure 3.18 the mass has an instantaneous streamwise

velocity $\bar{u}+u'$ and an instantaneous vertical velocity $\bar{v}+v'$, the momentum δM is given by

$$\begin{aligned}\delta M &= -(\bar{v}+v')\delta A\,\delta t(\bar{u}+u') \\ &= -\bar{v}\bar{u}\rho\delta A\,\delta t - \bar{v}u'\rho\delta A\,\delta t + v'\bar{u}\rho\delta A\,\delta t + v'u'\rho\delta A\,\delta t \end{aligned} \tag{3.10}$$

The average values of u' and v' are $\overline{u'}$ and $\overline{v'}$ in two-dimensional random turbulent. Therefore, the momentum equation can be rewritten as

$$\delta M = -\bar{v}\bar{u}\rho\delta A\,\delta t - \overline{v}\,\overline{u'}\rho\delta A\,\delta t + \overline{v'}\bar{u}\rho\delta A\,\delta t + \overline{v'}\overline{u'}\rho\delta A\,\delta t \tag{3.11}$$

Normally, when momentum transfer due to turbulence is considered over a long time period, $\overline{u'}$ and $\overline{v'}$, must both be zero but the product $\overline{u'v'}$ may not be zero. In two-dimensional flow, net movement of average velocity in vertical direction, $\bar{v}$, is also zero. Therefore δM can reduce to

$$\delta M = \overline{v'u'}\rho\delta A\,\delta t \tag{3.12}$$

The existence of momentum implies the existence of a corresponding force within the fluid

$$\delta F = \frac{\delta M}{\delta t} = \rho\overline{u'v'}\delta A \tag{3.13}$$

Since the stress is equal to the force over the area, the time averaged shear stress τ'', which is the derivation of the Reynold's shear stress, becomes

$$\tau'' = \frac{\delta F}{\delta A} = \rho\overline{u'v'} \tag{3.14}$$

Another equation was applied to calculate the time averaged shear stress $(\bar{\tau})$ in an attempt to avoid using the 'random' turbulence assumption that $\overline{u'}$, $\overline{v'}$ and $\bar{v}$ are zero. The value of time-averaged shear stress was then calculated by averaging the large number of values of calculated "instantaneous" shear stress at each measurement point.

$$\bar{\tau} = \sum_{i=1}^{n}\frac{\tau'}{n} \tag{3.15}$$

$$\overline{\tau''} = \sum_{i=1}^{n} \frac{\tau''}{n} \tag{3.16}$$

where :

n = large number of measurement

3.6.3. Determination of the Number of Velocity Data Required

The data used for analysis were time series of instantaneous streamwise, lateral and vertical velocities that have been collected with a sampling rate of 25 Hz. Two measurements at the same point were taken with an interval between measurement in order to observe the consistency of streamwise velocity distribution.

Initially, the distributions of streamwise velocity were recorded for two short durations of forty seconds. Each record gave 1000 samples of velocity in three different directions. The length of each time series was then extended by increasing the sampling time to three minutes. This increased the number of data to 5000 instantaneous streamwise velocity values. The probability distribution of different number of sample was observed to obtain the number applied for all experiments to provide a representative sample of the turbulence. The inspection of the "instantaneous" velocity distributions showed that the distributions predicted from 1000 data values was significantly different than that of 2000, 3000 or the larger number of data (Saadi, 2000). By examining the data from two measurement at same point but in different time elapsed of the experiment, it was seen that there was a tendency that the larger the number of data the more likely the probability distributions were similar. The differences between distribution reflect the effect of sampling for only short time periods. The curve obtained from 4000 data values was very similar to those of the larger number. It suggested that the data numbers larger than 4000 produced similar distribution curves indicating sufficient data to adequately represent the overall population of fluid velocities. By comparing the differences in probability distribution for 3000, 4000 and 5000 samples, it was observed that a record of 3 minutes, that contains 5000 values of instantaneous streamwise velocity was likely to give sufficient data so that probability of a particular value of streamwise velocity could be predicted with a resolution of ± 1 % even at the tails of the probability distributions.

Similar observation was carried out to "instantaneous" shear stress (Saadi, 2000). This observation strengthen the conclusion that the larger the number of data, the smaller the difference in instantaneous shear stress distribution. As a result, 5000 data values were chosen as the standard number of data points in any velocity time series.

3.6.4. Determination of Class Interval of Data

The number and the width of the classes of the streamwise velocity and the instantaneous shear stress were determined using Equation 3.1 and Equation 3.2. The range of observation was obtained from the difference between the largest and the smallest values. Several data measurements from four experiments were sampled to obtain the class width or bin size used for experiments (see Table 3.4). It can be seen that the variation of bin size for instantaneous nearbed streamwise velocity is less than 0.2 m/s while the variation in bin size for the instantaneous bed shear stress is slightly larger. For uniformity, the bin size of 1.5 m/s for instantaneous nearbed streamwise velocity and 2.5 N/m^2 for instantaneous bed shear stress were applied in all experiments.

Table 3.4. Summary of statistical parameters used to estimate bin size of instantaneous nearbed streamwise velocity and instantaneous bed shear stress

Test No.	Interquartile range		Range of observations		Number of classes or cells		Width of the class (bin size)		Time elapsed (mins)
	V_x (m/s)	τ' (N/m^2)	V_x	τ' (N/m^2)	V_x	τ'	V_x (m/s)	τ' (N/m^2)	
SF 1-3	13.600	22.774	60.540	140.639	38.060	52.800	1.591	2.664	10
	14.180	22.720	59.340	150.250	35.779	56.541	1.659	2.657	80
	13.505	23.230	61.740	150.525	39.087	55.402	1.580	2.717	180
SF 1-6	13.315	23.718	65.930	133.175	42.335	48.006	1.557	2.774	10
	14.930	22.310	68.210	158.070	39.061	60.577	1.746	2.609	120
	13.320	20.857	57.420	152.617	36.857	62.563	1.558	2.439	80
SF 1-9	13.290	25.666	53.820	159.759	34.624	53.220	1.554	3.002	160
	13.880	23.117	77.150	145.807	47.523	53.928	1.623	2.704	250
	13.265	21.756	59.500	111.398	38.350	43.778	1.551	2.545	400
SF 1-12	13.730	23.215	63.090	162.227	39.287	59.746	1.606	2.715	170
	14.230	23.189	64.100	143.536	38.514	52.923	1.664	2.712	200
	14.730	23.129	80.400	117.160	46.667	43.309	1.723	2.705	300
	14.790	23.644	62.450	142.315	36.101	51.462	1.730	2.765	680

3.7. BED TOPOGRAPHY MEASUREMENTS

3.7.1. Laser Displacement Meter

The laser displacement meter reads the variation in height of the bed surface, in relation to the pre-set datum, and returns it as a voltage via an A/D board. The voltage value was converted to a height value once the sensor has been calibrated. Figure 3.19 gives the correlation between the voltage values and height values. The sensor was set to zero at a reasonable datum height within the bed surface and the readings obtained were positive or negative differences from this original pre-set datum.

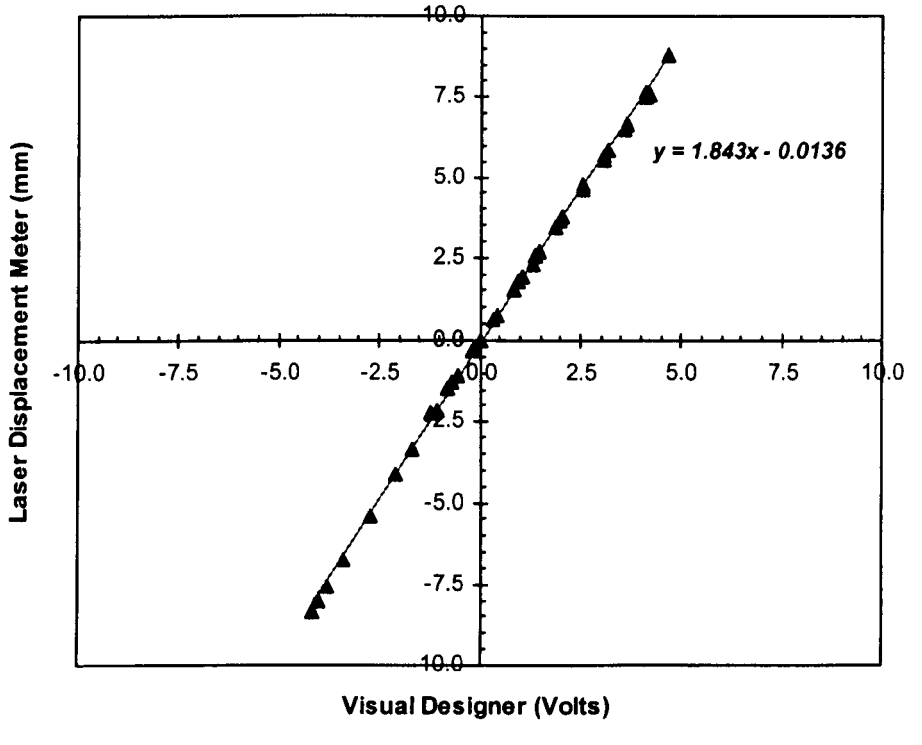

Figure 3.19. Correlation between voltage measurement (VD in volt) and real measurement (LDM in mm)

3.6.2. Bed Topography Data Format

A small area of 280 mm by 180 mm was selected to be measured by laser displacement meter. This area was located 9.14 m from upstream end of the flume. The displacement meter traversed the sample area and took readings at grid intervals of 1 mm in both the streamwise and lateral directions. The data set is arranged such that the starting point is at the upstream left end of the grid. To reduce the possible error during operation, the program was created in such a way that the displacement meter would return to a

defined starting point every ten rows of operation completed. This allowed for the quality of the data to be checked periodically during the measurement of a grid. The streamwise co-ordinate is known as x and ranges from 0 to 280 mm. The lateral co-ordinate is y and ranges from 0 to 180 mm. This generates a matrix with 280 columns and 180 rows as described in Figure 3.20.

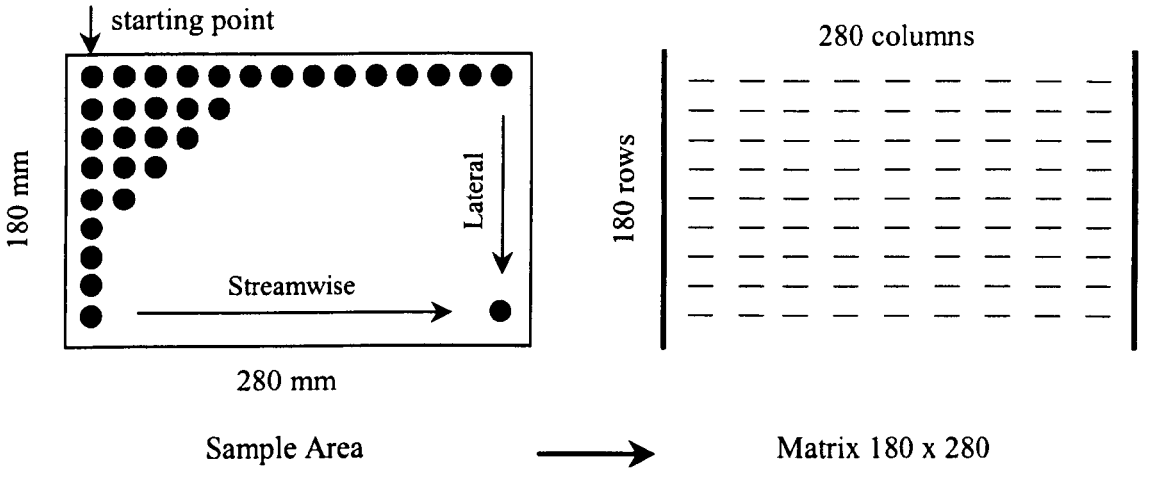

Figure 3.20. Diagram of measurement for bed topography data

Difficulties were experienced in that incomplete data was collected for the topographical sample areas. It was expected that each measurement of 280 by 180 mm grid would give 50400 data points. In fact, from closer inspection of the data obtained for each experiment, it was noticed that some of the z values were not within the expected range of $\pm$ 9 mm. It was suspected that when the sensor was unable to take reading, i.e. the bed surface was out of range, the statement *too far/too near* appeared and no values recorded. In this case, the recorded number of data points are less than 50400 and the structure of the matrix can not be maintained by keeping all columns and rows at length of 280 and 180 data.

In order to maintain the structure of the data matrix, these were distributed equally to all rows as there was no data set in which less than 0.5 % of data was missing. This resulted in a new matrix with the dimension of 279 columns by 179 rows. The total number of data values use for analysis was then 49941. Further analysis of this data is described in the next three chapters.

IV. EXPERIMENTAL RESULTS OF STEADY FLOW EXPERIMENTS SF I

4.1. INTRODUCTION

In this chapter, the results from four steady-antecedent flow experiments with different duration are reported along with their subsequent stability tests. The flow duration ranged from 3 hours to 12 hours with an identical flow discharge of 0.0338 m^3/s. The results of each experiment which have been identified as SF 1-3 (3 hours duration), SF 1-6 (6 hours duration), SF 1-9 (9 hours) and SF 1-12 (12 hours duration), are described and then discussed together with the observations made during the stability test.

The aim of these experiments was to examine the influence flow duration has on developing bed stability in a mixed grain size sediment. This chapter is divided into four parts, each associated with a different type of observations. The first section is focused on stability analysis of the water worked sediment beds. It describes the results of the short duration of 'standard' hydrograph applied to all experiments to assess the stability of water worked bed at the end of the steady antecedent flow. The standard "stability" hydrograph has a peak discharge larger than the constant discharge applied during antecedent flows. It rose from a base flow of 0.0075 m^3/s to a peak flowrate of 0.0375 m^3/s in a time of 60 minutes. The flowrate then declined to the base flowrate again in a time of 60 minutes.

The second part describes the observations of bedload and composition made during each antecedent flow test. This part is also contains the investigation of momentum in bursting events. As each water worked bed developed the changes in the average "instantaneous" nearbed streamwise flow velocity and bed shear stress were analysed by comparing measurement results carried out at different time elapsed. To complete the second part, the bed topography analysis was included in each antecedent flow test observation. The third section describes the comparative results of all antecedent flow and the stability tests. The results of the two initial sections were linked in order to investigate the influence of the length of time to the sediment transport processes, the development of bed stability and the changes in bed configuration. The final part of this chapter is the summary of experiments where

conclusions are drawn as to the impact different duration of steady flow can have on the behaviour of river or actual events.

4.2. STABILITY TESTS OBSERVATIONS SF I

4.2.1. Transport Rate Measurement SF I

Figure 4.1 shows the bedload transport rates measured during the stability tests carried out after all the steady antecedent flow tests. The observation of high transport rates throughout the stability test after antecedent flow tests SF 1-3 indicates that the bed formed by the shortest duration of constant flowrate was the weakest. When the duration of antecedent flow increased to six hours (Experiment SF 1-6), the transport rate during the stability hydrograph was still moderately high but noticeably less than the shorter test. The transport rate reduced slightly for longer duration (Experiment SF 1-9) and a much lower level of transport was experienced in experiment SF 1-12. This suggests that the longer tests (with a constant discharge) established a more stable bed. However the increase in stability was not linear.

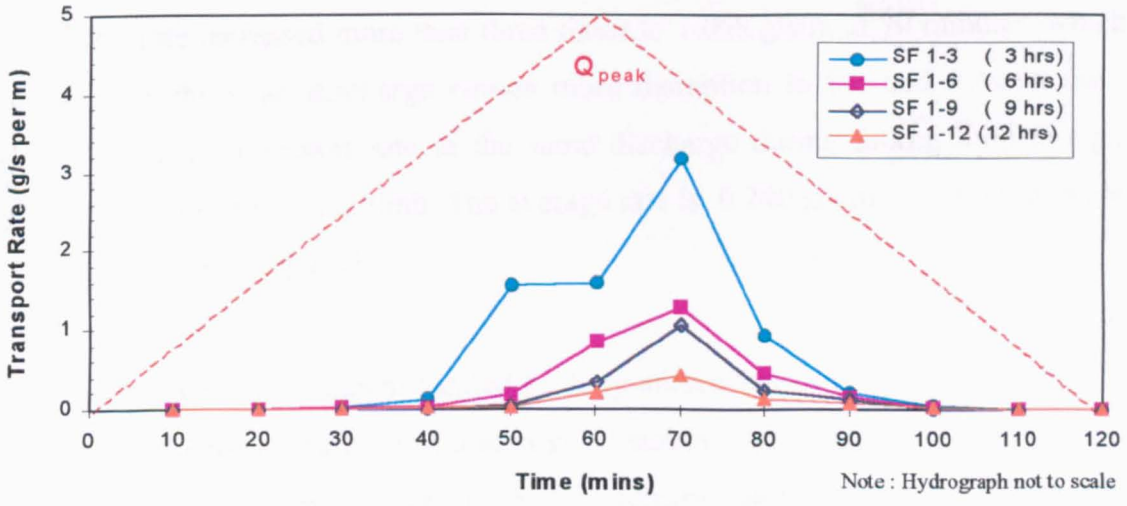

Figure 4.1. Bedload transport rate pattern during stability tests SF I

Figure 4.1 also shows that although the four antecedent flow experiments produced different level of bed stability, only the higher discharges during the stability tests were able to destabilise the previously formed armoured bed. The transport rate during the stability tests

generally increased with increasing discharge. However at the peak discharges the peak value of transport rate was not attained. It was only when the discharge passed its peak, at time elapsed 60 minutes, that the transport rate was significantly increased. In stability test SF 1-3 at the beginning of falling limb (time elapsed 60-70 minutes) the transport rate is 3.188 g/s/m or more than 100 % higher from 1.576 g/s/m observed during the similar level of discharge at the end of rising limb (time elapsed 50-60 minutes).

The peak discharge of stability test after antecedent flow experiment SF 1-6 produced a maximum transport rate of 1.257 g/s/m (time elapsed 60-70 minutes). This was 50 % above the transport rate shortly before the discharge attained its peak (0.833 g/s/m at time elapsed 50-60 minutes). The transport rates measured at the same level of discharges during the falling limb are always higher than those in the rising limb. Overall, the average transport rate during 60 minutes of the rising limb (time elapsed 0-60 minutes) is 0.180 g/s/m and this increased to 0.319 g/s/m during the same period of falling limb (time elapsed 60-120 minutes).

The transport rate for stability test SF 1-9 when the discharge approaching its peak is 0.339 g/s/m. The rate increased more than three times to 1.068 g/s/m at 70 minutes, which was 10 minutes after the peak discharge causes more disruption to the bed. As in the previous stability tests, the transport rate at the same discharge during falling limb is significantly higher than that of the rising limb. The average rate is 0.240 g/s/m in falling limb compare to 0.068 g/s/m in the rising limb.

The armoured bed or pavement formed by long antecedent flow of experiment SF 1-12 was also only weakened at the highest discharge of stability test (time elapsed 60 minutes). This was shown by an increase in transport rate in comparison between the similar period before and after peak discharge. During the last ten minutes of rising limb, or just before the peak discharge was reached (time elapsed 50-60 minutes), the transport rate was 0.214 g/s/m. Within the same period at the beginning of falling limb, the bedload rate then increased to 0.425 g/s/m. The average bedload transport rate during falling limb (time elapsed 60-120 minutes) increased more than 100 % than the rate of that during the rising limb at

corresponding discharges (time elapsed 0-60 minutes). The average bedload transport rate during the rising limb and the falling limb are 0.044 g/s/m and 0.110 g/s/m respectively.

4.2.2. Grain Size Distribution of Transported Bedload SF I

Observations of the grain size distribution of the transported bedload during all the stability tests were made and compared with the transport rate pattern described above. The stability test observations for SF 1-3 suggest that during the initial low discharges the flow eroded only the finer grains (Figure 4.2). Although there was coarse grains of 5.6 mm sieve size transported at time elapsed 30 minutes, the fluid forces during time elapsed 0 to 30 minutes in the rising limb were not sufficient to transport considerable amounts of grains in the coarser mode. The increasing percentage of coarser grains at time elapsed 40 minutes in Figure 4.2 is not the reflection of high transport in the coarser mode but solely because of the small amount of total bedload. When water discharge increased at time elapsed 50 minutes or 10 minutes before the peak discharge was reached, significantly more coarse particles on the bed moved. The coarse mode dominated the transported bedload until time elapsed 80 minutes. This suggests that the grains in the coarse mode start to move when the fluid forces are strong enough to transport them, therefore the transport was highly size selective.

The removal of sheltered smaller grains continued as the flow strength increases. An increasing proportion of the grains in the fine mode was entrained into transport and the level of exposure of larger grains increased and becoming less stable and easy to remove. This can be explained by examining the pattern of transport during the increasing flowrates and declining flowrates. In the last 10 minutes of rising limb the proportion of transport in the finer mode to the total transport is 5.17 % (45.13 grams) and this increased to 7.710 % (67.28 grams) in the first 10 minutes of falling limb. Within the same duration and at similar level of discharge, the proportion of grains in the coarse mode in transport increased significantly from 12.35 % (107.78 grams) in the last 10 minutes of rising limb to 28.07 % (244.92 grams) in the first 10 minutes of falling limb. Supporting this observation was the fact that the lower available fluid forces at time elapsed 80 minutes in the falling limb were able to move and transport more grains in the coarse mode than in the fine mode (see Figure 4.2). At time elapsed 90 minutes the proportion of grains transported in the coarse mode decreased to

almost similar level of grains in the fine mode. The proportion of coarser grains was gradually reduced within the next 30 minutes and transported bedload was then fine grains dominated until the stability hydrograph ended. It is worth noting that a decrease in the coarse fraction of transported bedload in the falling limb is believed to be solely due to the decreasing fluid forces rather than the changes in the availability of coarse grains on the bed surface.

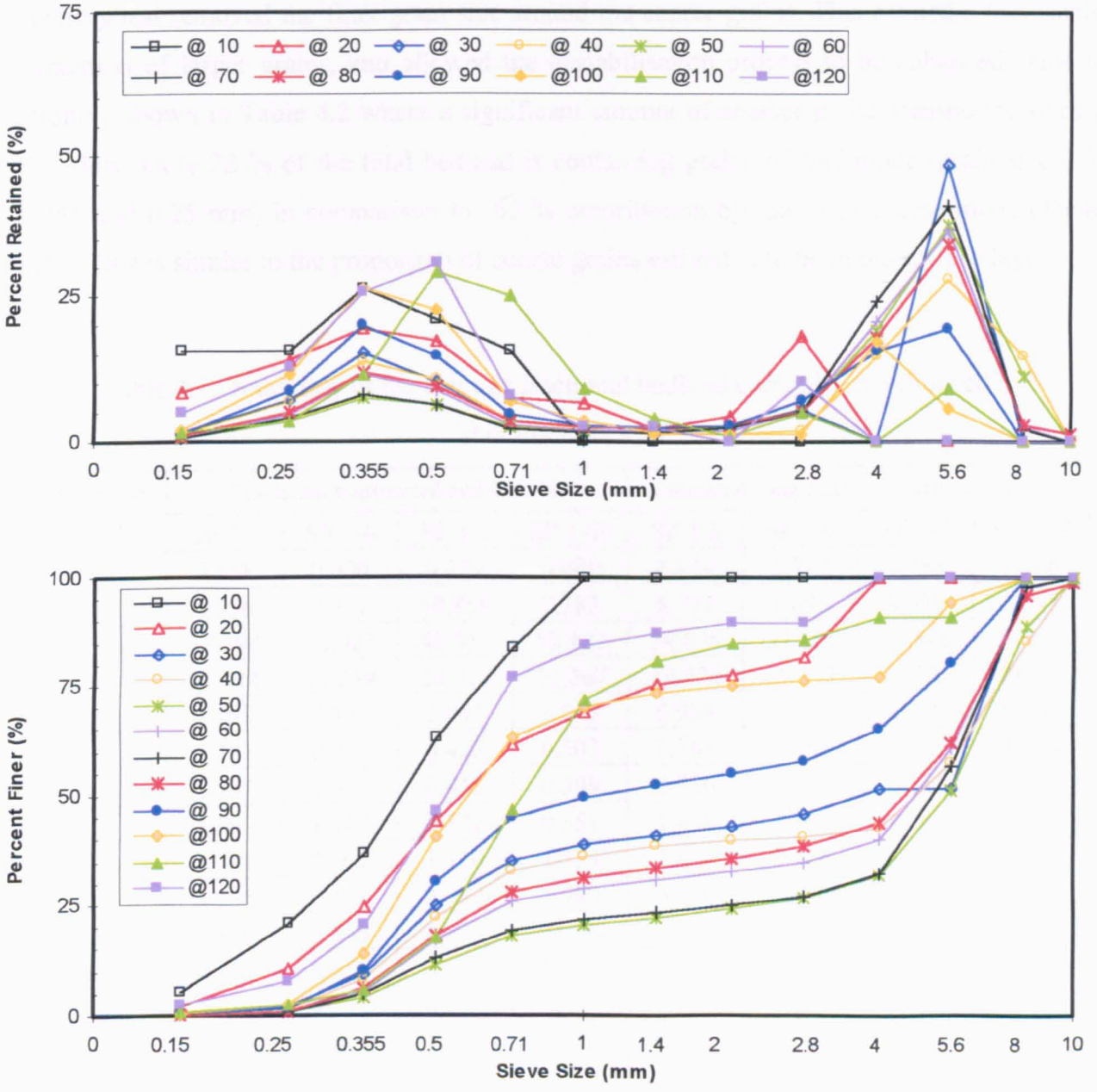

Figure 4.2. Grain size distribution of transported bedload for stability flow Experiment SF 1-3

It is apparent that during the stability test of Experiment SF 1-3 the larger grain is more important than finer grain. Although grains in the coarse mode (grain size 4, 5.6 and 8 mm) did not make a continues contribution to the bedload and they only started to move when the fluid forces had increased sufficiently, their contribution in the total amount of bedload is considerably higher than would be expected from their availability in the surface. This enhanced level of mobility of the coarser grains was thought to be due to their enhanced exposure. The level of exposure left by antecedent flow increased when the peak discharge of stability test removed the finer grain size around the coarse grains. This created a less stable formation of larger grains, and allowed the destabilisation process to be enhanced. This is strongly shown in Table 4.2 where a significant amount of coarser grains transported during this flow. Only 22 % of the total bedload is containing grains of fine mode (grain size 0.5, 0.355 and 0.25 mm) in comparison to 63 % contribution by grains of coarse mode (Table 4.1). This is similar to the proportion of coarse grains estimated to be in the surface layer.

Table 4.1. Summary of the average fractional bedload composition produced by stability tests SF I

Sieve size (mm)	Fractional transported bedload (%)				Estimated composition of surface layer (%)			
	SF 1-3	SF 1-6	SF 1-9	SF 1-12	SF 1-3	SF 1-6	SF 1-9	SF 1-12
10	0.158	0.000	0.759	0.000	1.774	1.772	1.758	1.766
8	4.256	8.341	10.858	7.385	8.752	8.696	8.636	8.695
5.6	37.594	46.027	46.357	52.482	34.835	34.857	34.846	34.901
4	21.124	15.259	24.817	11.267	19.528	19.723	19.573	19.785
2.8	5.290	2.838	3.045	1.025	6.908	6.964	6.929	6.961
2	2.387	0.996	0.422	0.503	3.563	3.584	3.578	3.590
1.4	1.855	1.031	0.413	0.399	2.526	2.535	2.543	2.547
1	1.899	1.347	0.522	0.551	1.835	1.842	1.860	1.857
0.71	2.731	2.569	1.110	1.538	2.652	2.626	2.662	2.635
0.5	7.566	7.404	3.349	5.990	6.746	6.645	6.731	6.619
0.355	9.875	9.346	4.824	10.878	7.241	7.139	7.245	7.065
0.25	4.440	4.051	2.808	6.474	2.604	2.586	2.615	2.557
0.15	0.755	0.732	0.669	1.357	0.937	0.931	0.925	0.921
receiver	0.069	0.059	0.047	0.152	0.101	0.100	0.098	0.100
Total	100	100	100	100	100	100	100	100

Data form the stability test SF 1-6 suggests that the transport at the lowest flowrates (time

elapsed 10, 110 and 120 minutes) was again composed entirely of grains in a single fine mode. At time elapsed 20 minutes a small amount of grain size 4 mm was found in transport. The contribution of 4 mm is proportionally dominant only because of the overall amount of bedload transported at this time elapsed was very small (Figure 4.3). It is also shown that at time elapsed 30 and 40 minutes the coarse mode was represented only by grains of 5.6 mm in transport with the amount less than grains in the fine mode. It was at time elapsed 50 minutes when all grains in coarse mode appeared. The coarse mode started to dominate the transport. This occurred at a latter time than experienced in the stability test SF 1-3. Following the disruption by peak discharge (time elapsed 60 minutes) the contribution of coarse grains in bedload transport was immediately evident at time elapsed 70, 80 and 90 minutes respectively, and then diminished during the lower discharges (see Figure 4.3).

The significant amount of increased in coarse mode is apparent as the flowrate approaching its peak. It was followed by the increased in the proportion to the total bedload transported in each time elapsed. At time elapsed 50 minutes the amount of grains in the coarse mode is 13.4 grams (60 %) and subsequently increased to 69.11 grams (73 %) at time elapsed 60 minutes and 108.71 grams (76 %) at time elapsed 70 minutes. Although the amount of grains in the fine mode was also increased in the corresponding time elapsed, this grains was proportionally decreased. The amount of transported grains in the fine mode at time elapsed 50 minutes is 6.85 grams (31 %) and increased to 18.37 grams (19 %) at time elapsed 60 minutes. After the peak flowrates, a small increased is noticed when 21.70 grams (15 %) was transported at time elapsed 70 minutes. At the lower flowrates (time elapsed 80 minutes) the amount of grains in the coarse mode decreased to 33.75 grams (66 %). The amount of finer mode is also decreased (11.73 grams) but proportionally increased (23 %). Although the flowrates had similar level between time elapsed 50 and 80 minutes, the higher amount of transport at the latter time indicates the influence of destabilising process during the peak flowrates. In the last 30 minutes of the falling limb (time elapsed 90 to 120 minutes) the transported bedload was clearly finer mode dominated.

In term of the total amount of bedload transported, Table 4.1 shows that the stability flow during Experiment SF 1-6 transported 70 % grains in the coarse mode in comparison to 21 %

of grains in the fine mode. This finding suggests that the stability flow was very efficient at moving the coarse material. It leads to the conclusion that during the stability flow of Experiment SF 1-6 coarser grains are more mobile than anticipated than finer grains.

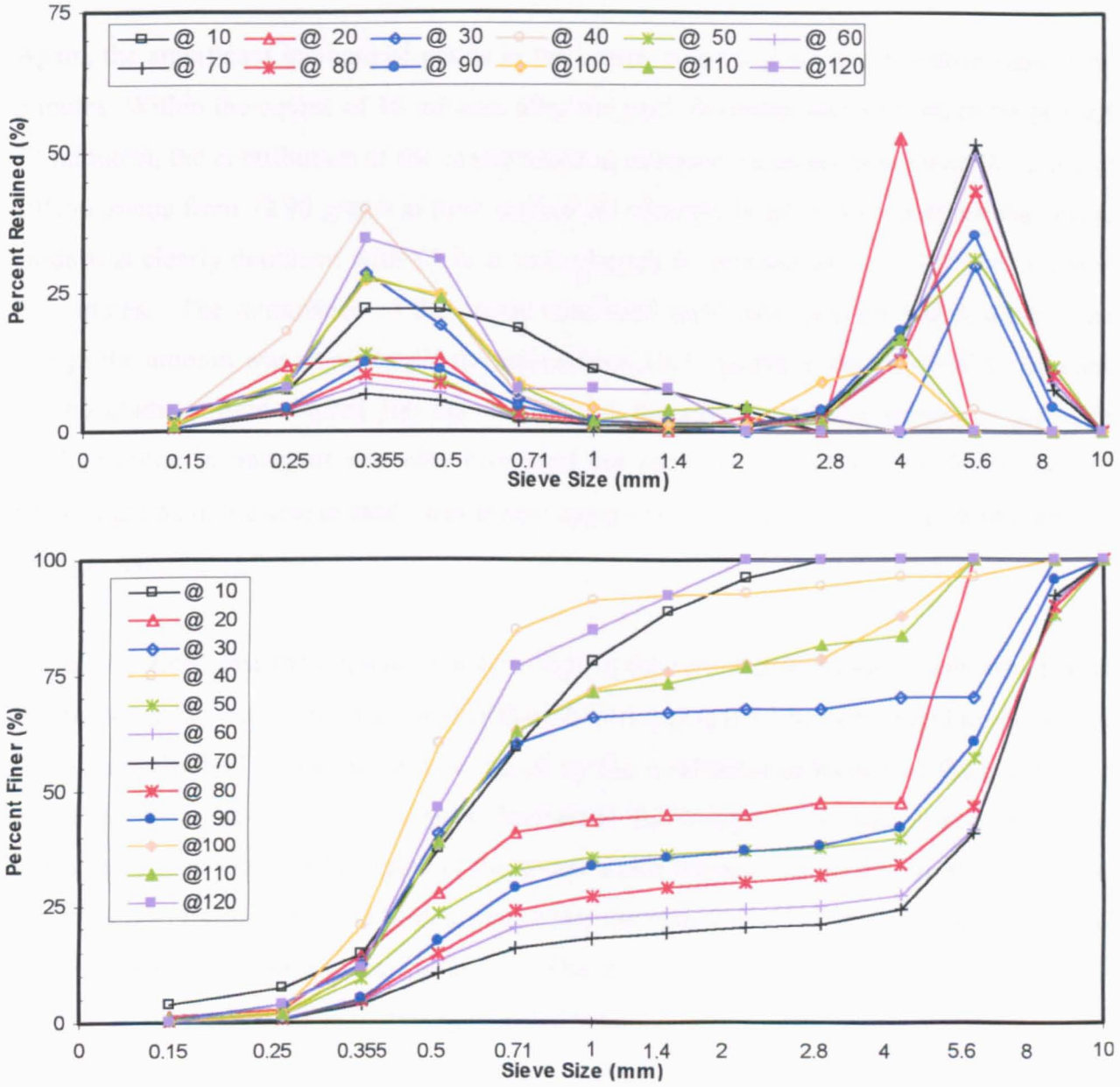

Figure 4.3. Grain size distribution of transported bedload for stability flow Experiment SF 1-6

In the stability test of Experiment SF 1-9, the grains in the coarse mode started to move at time elapsed 30 minutes. More erratic changes in the fine mode are noticed in the rising limb. Figure 4.4 shows that the lower discharges (time elapsed 10 and 20 minutes) carried grains in

the fine mode and also larger grains of 1 mm and 1.4 mm. Grains size 4 mm appeared at time elapsed 30 and 40 minutes but still less than the amount of grains in the fine mode. It was at time elapsed 50 minutes all grains in the coarse mode existed in transport with the proportion exceeded the grains in the fine mode.

Again, the significant increase of grains in the coarse mode was occurred at time elapsed 60 minutes. Within the course of 10 minutes after the peak flowrates was attained (time elapsed 70 minutes), the contribution of the coarse mode in transport increased more than threefold to 105.56 grams from 32.90 grams at time elapsed 60 minutes. In term of proportion, the coarse mode was clearly dominant with 85 % at time elapsed 60 minutes and 87 % at time elapsed 70 minutes. The dominance of this mode continued until time elapsed 100 minutes even though the amount was significantly decreased from 19.97 grams at time elapsed 80 minutes to 0.65 grams at time elapsed 100 minutes. During the same period the amount of grains in the fine mode in transport was also decreased but proportionally increased. In the last 20 minutes grains in the coarse mode was absent suggesting that the transport was dominated by finer grains.

It is also noticed that the amount of grains both in the fine and the coarse mode which was transported in the falling limb are higher than that transported in the corresponding discharge in the rising limb. This increased was caused by the weakening processes of the bed by the peak flowrate. The influences of peak flowrate to the transport can also be seen from the transport pattern. Only 18 % grains in the coarse mode transported during the rising limb in comparison to 64 % during the falling limb while the contribution of grains in the fine mode is also increased but not in a similar fashion. During the rising limb, grains in the fine mode contributed only 3 % with an increased to 8 % during the falling limb.

Table 4.1 shows the overall composition of each fraction in stability test Experiment SF 1-9. More than 80 % of the total transported bedload contain grains in the coarser mode (4 mm, 5.6 mm and 8 mm) compare to the small amount of 10 % contribution of grains in the fine mode (0.25 mm, 0.355 mm and 0.5 mm). Although there is higher proportion of course grains moving, in terms of total mass they are still smaller than that transported during the stability test of Experiment SF 1-6.

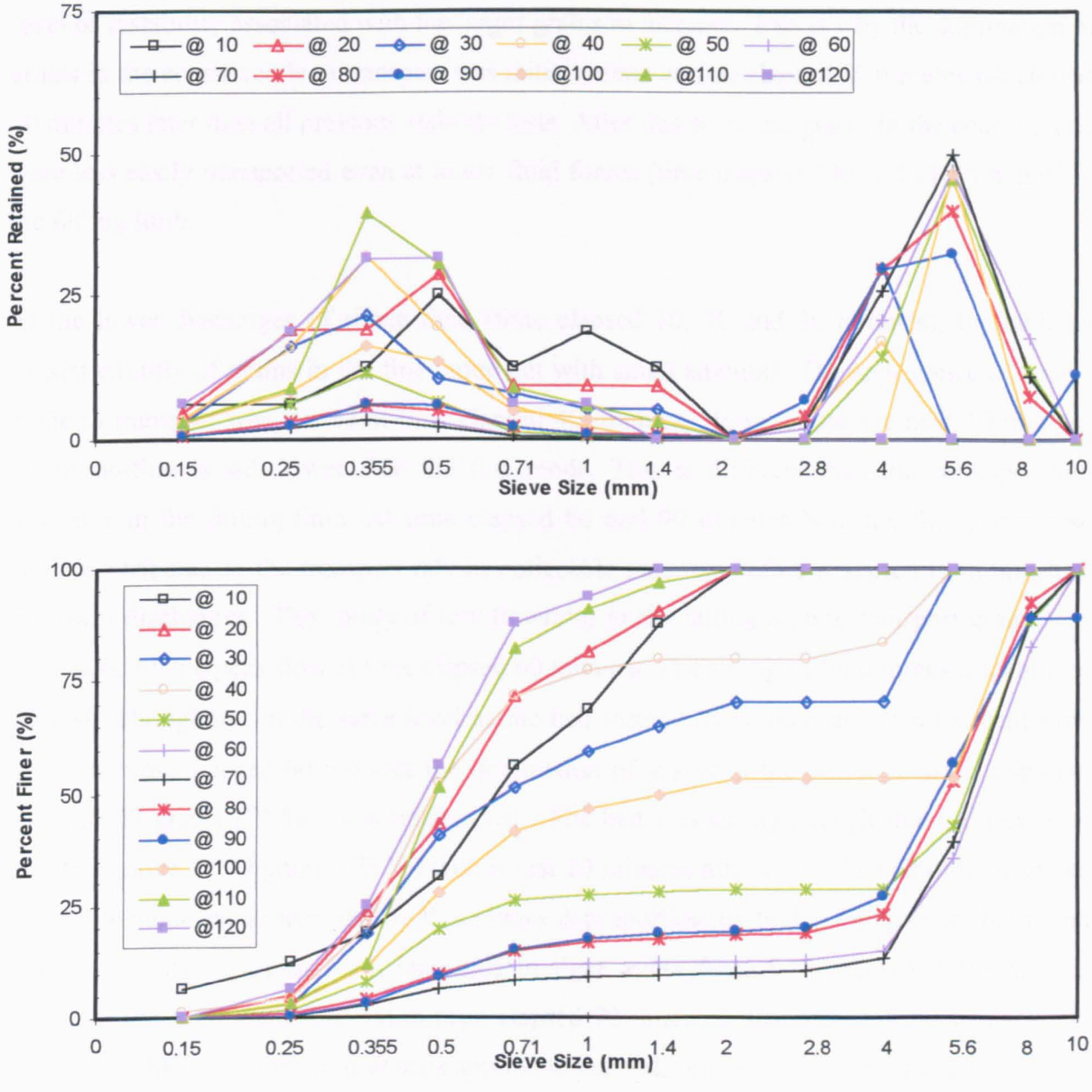

Figure 4.4. Grain size distribution of transported bedload for stability flow Experiment SF 1-9

The pattern of transported bedload during the stability test of experiment SF 1-12 is described in Figure 4.5. A very low transport rate of bedload was experienced throughout the stability test. The low transport rate suggests that both the finer and coarser grains were strongly bounded as the results of the long and constant antecedent flows. The increasing loss of finer grains during the rising limb, particularly when the discharge approaching its peak, caused the

level of instability associated with the larger grains to increase. This is why the domination of grains in the coarse mode in transport was initially seen at time elapsed 60 minutes which was 10 minutes later than all previous stability tests. After this stage the grains in the coarse mode were less easily transported even at lower fluid forces (time elapsed 100 and 110 minutes) in the falling limb.

At the lower discharges of rising limb (time elapsed 10, 20 and 30 minutes), the bedload consist entirely of grains in the fine mode but with small amounts. The appearance of coarse mode in transport was started at time elapsed 40 minutes. However for the next 10 minutes the proportion is still lower than the fine mode. This is different than the corresponding flowrates in the falling limb. At time elapsed 80 and 90 minutes both the fine and coarse mode contributed to the transport rate in noticeable amounts before it started to diminish at the lower discharges. The ability of low flowrates in the falling limb to transport grains was influenced by the peak flow at time elapsed 60 minutes. The strongest fluid forces destabilised the bed although not in the same level as the bed formed by shorter steady antecedent flow tests. At time elapsed 60 minutes the domination of grains in the coarse mode is apparent when 17.39 grams (72 %) was transported. The bed was strong enough that the flow was able to remove 37.60 grams (78 %) within just 10 minutes afterwards. The amount of grains in the fine mode transported during these times is proportionally higher compare to that found in the other stability tests. An increased in finer mode from 5.73 grams (24 %) at time elapsed 60 to 8.78 grams (18 %) at time elapsed 70 minutes, distinguished the stability test Experiment SF 1-12 from similar tests applied to the bed formed by shorter duration of steady antecedent flow tests. The proportion of grains of the fine mode in transport for the whole duration of stability test Experiment SF 1-12 is higher than those tests.

When the fractional bedload transport for the whole duration of stability test is observed, it is found that the different pattern as mentioned earlier is apparently shown. The contribution of grains in the coarse mode, i.e. 4 mm, 5.6 mm and 8 mm is 71 % of total transported bedload whilst grains in the fine mode is 23 %. The increasing rate of grains in the fine mode is a strong indication that the more stable the formation of the bed is caused by more stable coarser grains. The fluid forces were only able to remove more grains in the fine mode rather than to increase the transport rate of grains in the coarse mode.

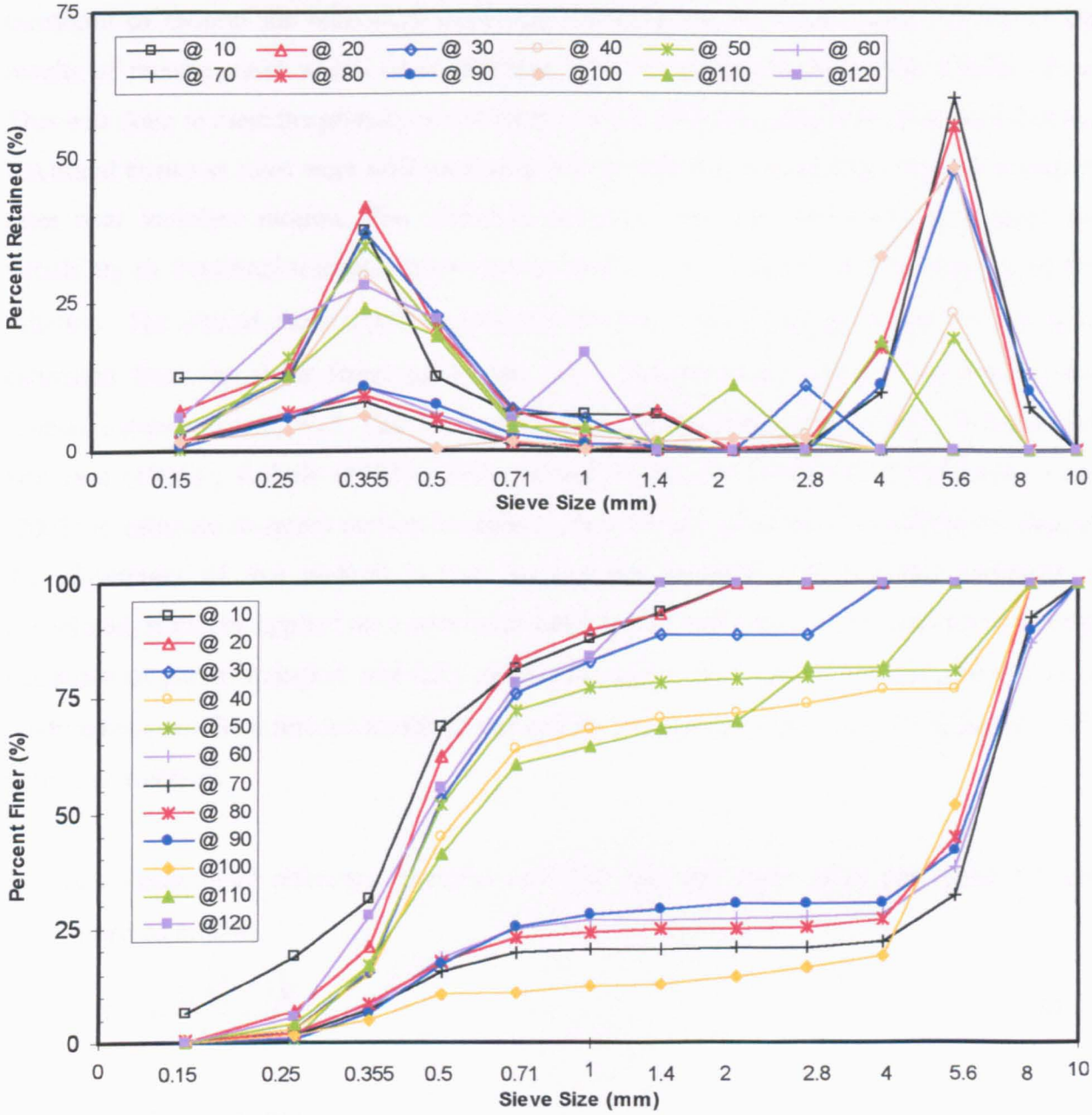

Figure 4.5. Grain size distribution of transported bedload for stability flow Experiment SF 1-12

4.2.3. Fractional Threshold of Motion SF I

It was clear in the previous section that the threshold of motion of individual grain size fraction, particularly of the coarse mode fractions, is an important factor in determining whether a water worked deposit would remain stable. It was therefore decided to examine the

threshold of motion for individual grain size fractions for each test. Table 4.3 shows the results of measurement which cover different level of discharges during the stability flow. This was done to meet the primary requirement used to select the data to be examined that the fractional transport rates were well measured over a wide range, including very low transport rates near incipient motion. The sufficient sampling was also performed to account for variability of fractional transport rates over a variety of time elapsed with an interval of ten minutes. The critical shear stress for incipient motion of individual grain size fraction τ_{ci} is estimated from the shear stress parameter, τ_{ri}*, that produces a small, non-dimensional reference transport rate, W_{ri}*. This method has been used by Parker et al (1982) ; Wilcock and Southard (1988) ; Kuhnle (1993) ; Wilcock and McArdell (1993) and Shvidchenko et al (2001) to estimate incipient motion conditions for a variety of mixed-size sediments. One of the advantages of this method is that because the proportion of available sediment is considered, it can be applied on a consistent basis for the estimation of threshold during both situations of partial transport and fully mobile transport. With the aid of appropriate data, a relation between the reference transport rate and the critical shear stress can be found for each grain size fraction.

The non-dimensional reference transport rate W_{ri}* and the shear stress parameter τ_{ri}* are determined as follows

$$W_{ri}^{*} = \frac{q_{bi}\left(\frac{\rho_s}{\rho}-1\right)g}{f_i \rho_s U_*^{3}} \tag{4.1}$$

$$\tau_{ri}^{*} = \frac{\tau_o}{\left(\frac{\rho_s}{\rho}-1\right)\rho g D_i} \tag{4.2}$$

where :

q_{bi} = fractional bedload transport rate for grain size fraction i (gr/s/m)

ρ_s = sediment density (kg/m^3)

ρ = fluid density (kg/m^3)

g = acceleration due to gravity (m/s^2)

f_i = proportion of grain size fraction i on the bed surface (estimated at the end of the antecedent flow tests)

U_* = bed shear velocity = $(\tau_o/\rho)^{1/2}$

τ_o = average bed shear stress estimated from ADV velocity measurements $(= -\rho\overline{u'v'})$ (N/m^2)

D_i = grain size fraction i (mm)

This technique involves fitting a transport function to the sediment transport data for each fraction. Then the values of τ_{ri}^* is defined such that W_{ri}^* equals a low reference value of 0.002 for each grain size fraction (see Figure 4.6, Figure 4.7, Figure 4.8 and Figure 4.9). The curve was fitted by eye as nonlinear least square fitting method did not always give the best visual match to the data because it was overly influenced by small errors in the shear stress term for points near initial motion, where the transport function is very steep (Wilcock and Southard, 1988). However, a conservative estimate of the error in the measured values of τ_{ri}^* was necessary as the curve fitting was to some extent subjective. The error was estimated by using a similar method applied by Wilcock and Southard (1988). The reading of τ_{ri}^* values when the curved was placed as far as possible to the right and left of the measured τ_{ri}^* was used as the error bounds. This estimation is analogous to a confidence interval for an estimated intercept in that the true values of τ_{ri}^* is highly likely to fall within the error bounds (Wilcock and Southard, 1988). Table 4.2 reports the values and error bounds for all size fractions in the stability tests SF 1, SF 1-6, SF 1-9 and SF 1-12. These values were obtained from Figure 4.6, Figure 4.7, Figure 4.8 and Figure 4.9.

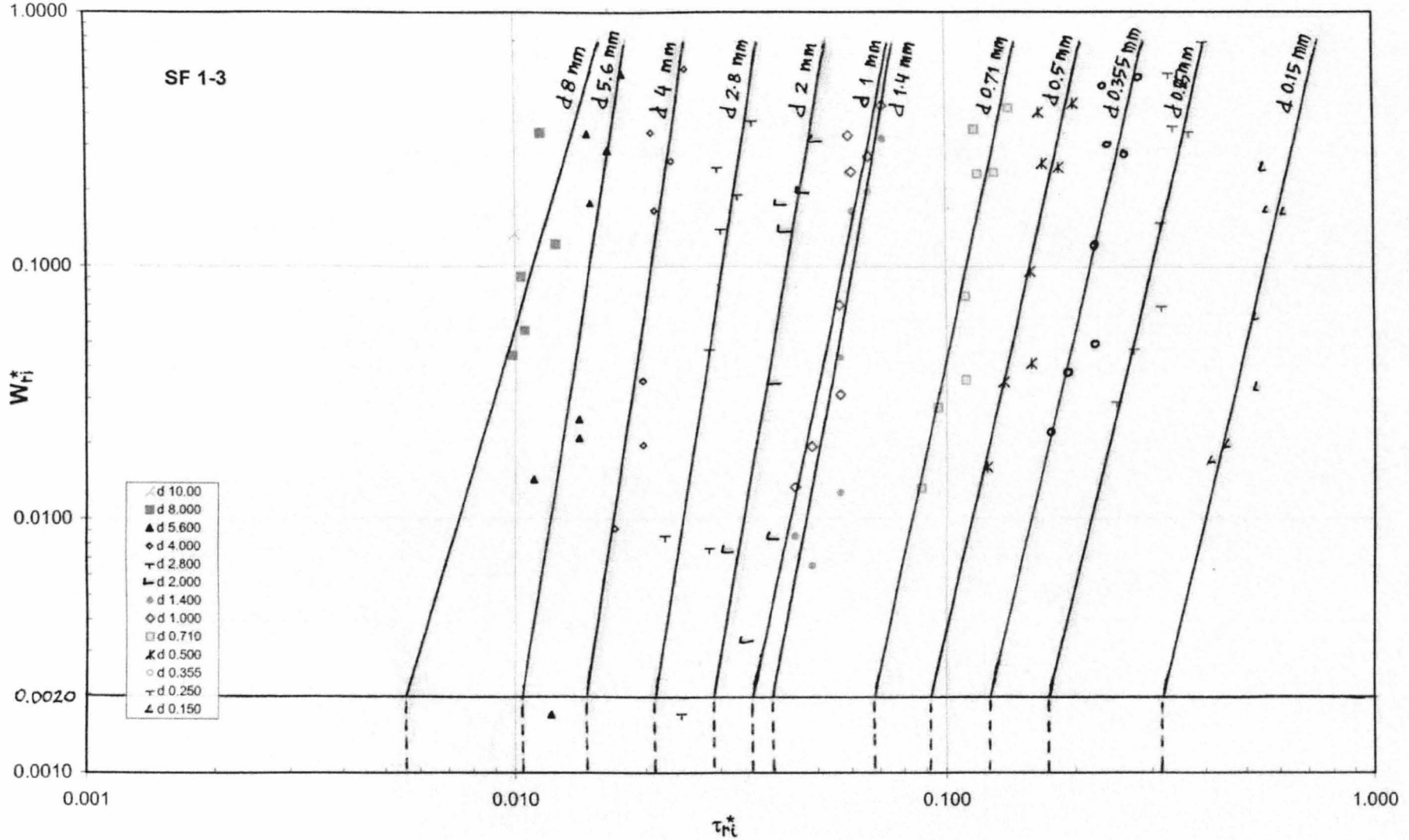

Figure 4.6. The non-dimensional shear stress parameter, τ_{ri}^*, determined from the low reference transport rate, $W_{ri}^* = 0.002$, for stability tests SF 1-3

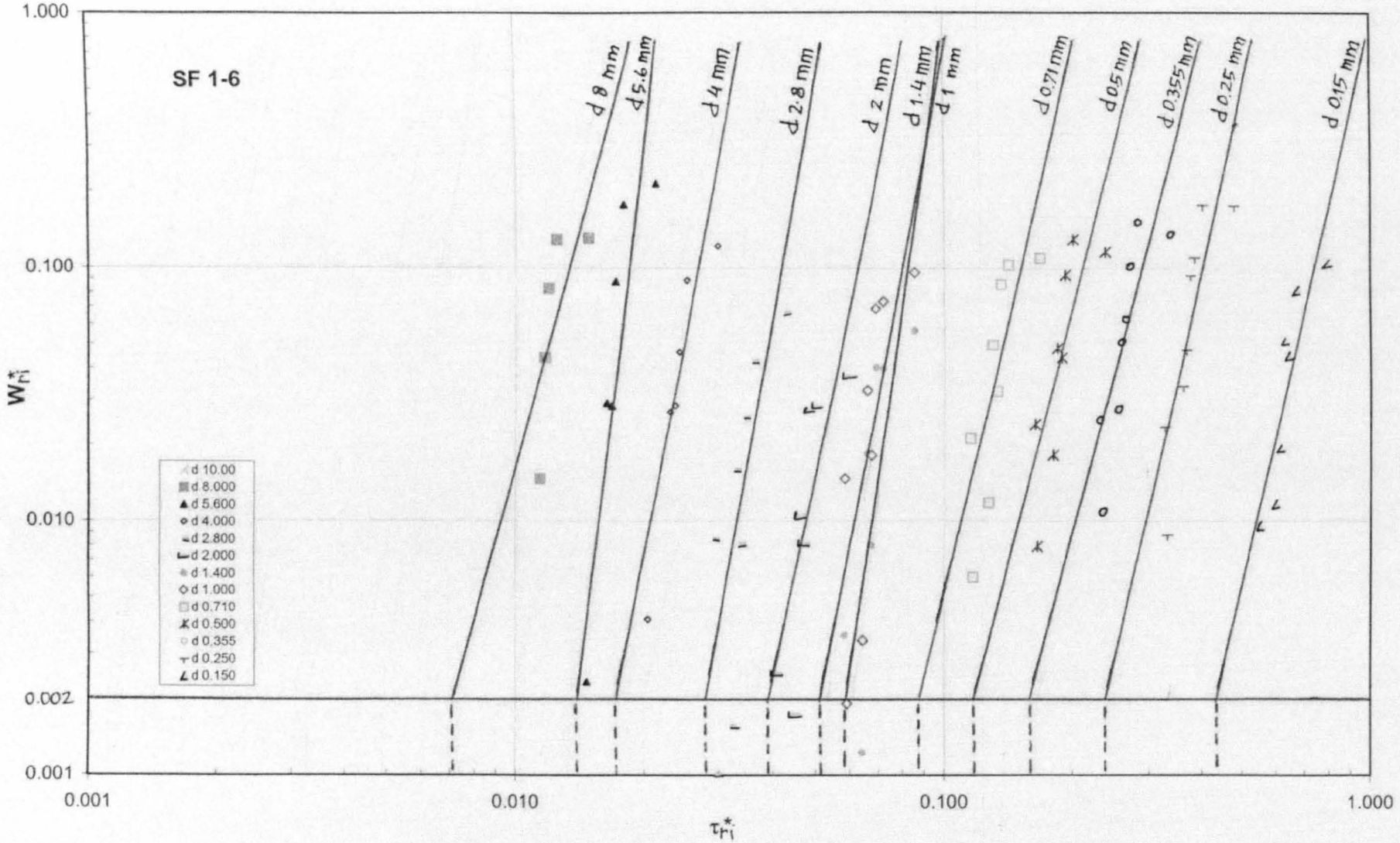

Figure 4.7. The non-dimensional shear stress parameter, τ_{ri}^*, determined from the low reference transport rate, $W_{ri}^* = 0.002$, for stability tests SF 1-6

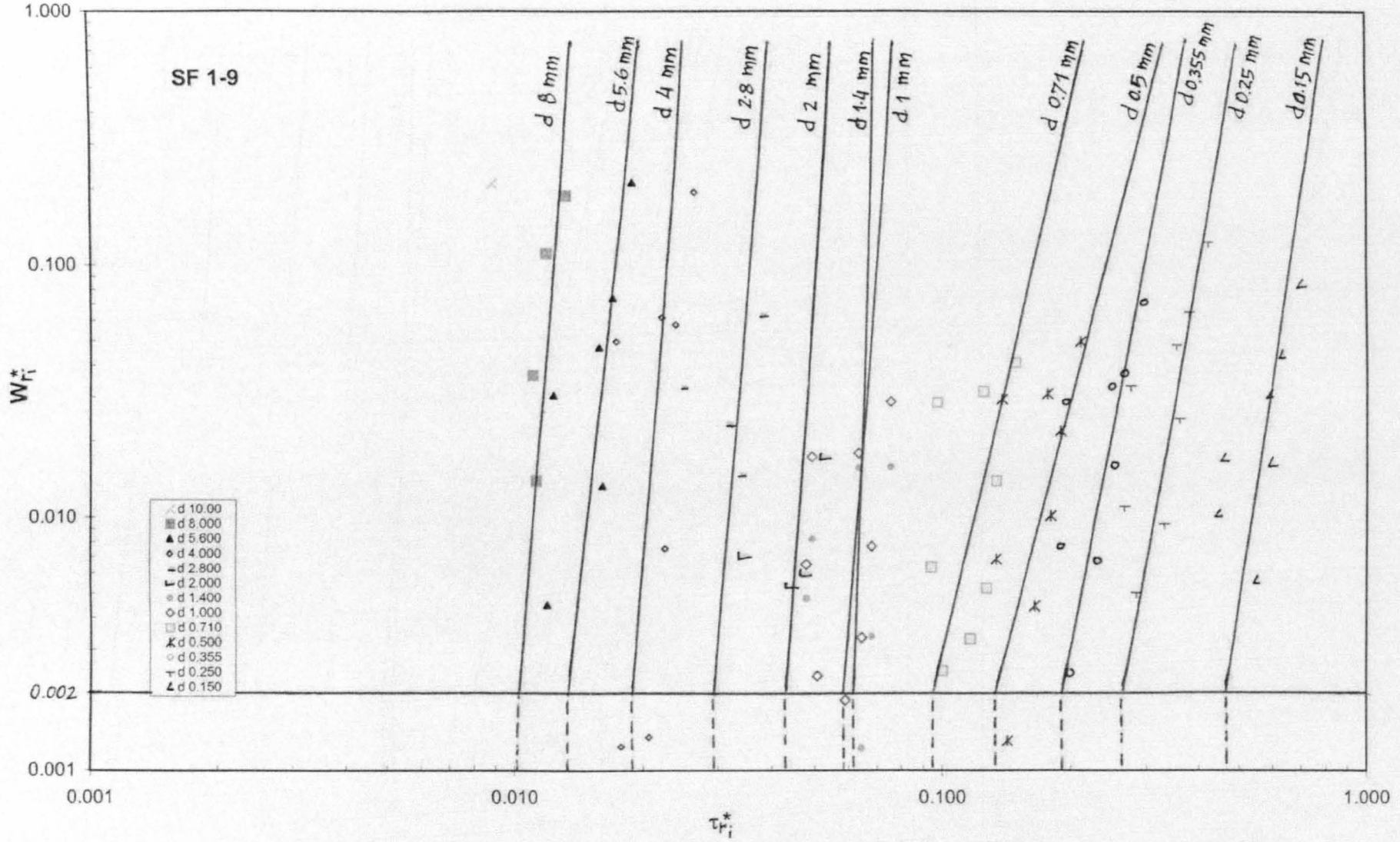

Figure 4.8. The non-dimensional shear stress parameter, τ_{ri}^*, determined from the low reference transport rate, $W_{ri}^* = 0.002$, for stability tests SF 1-9

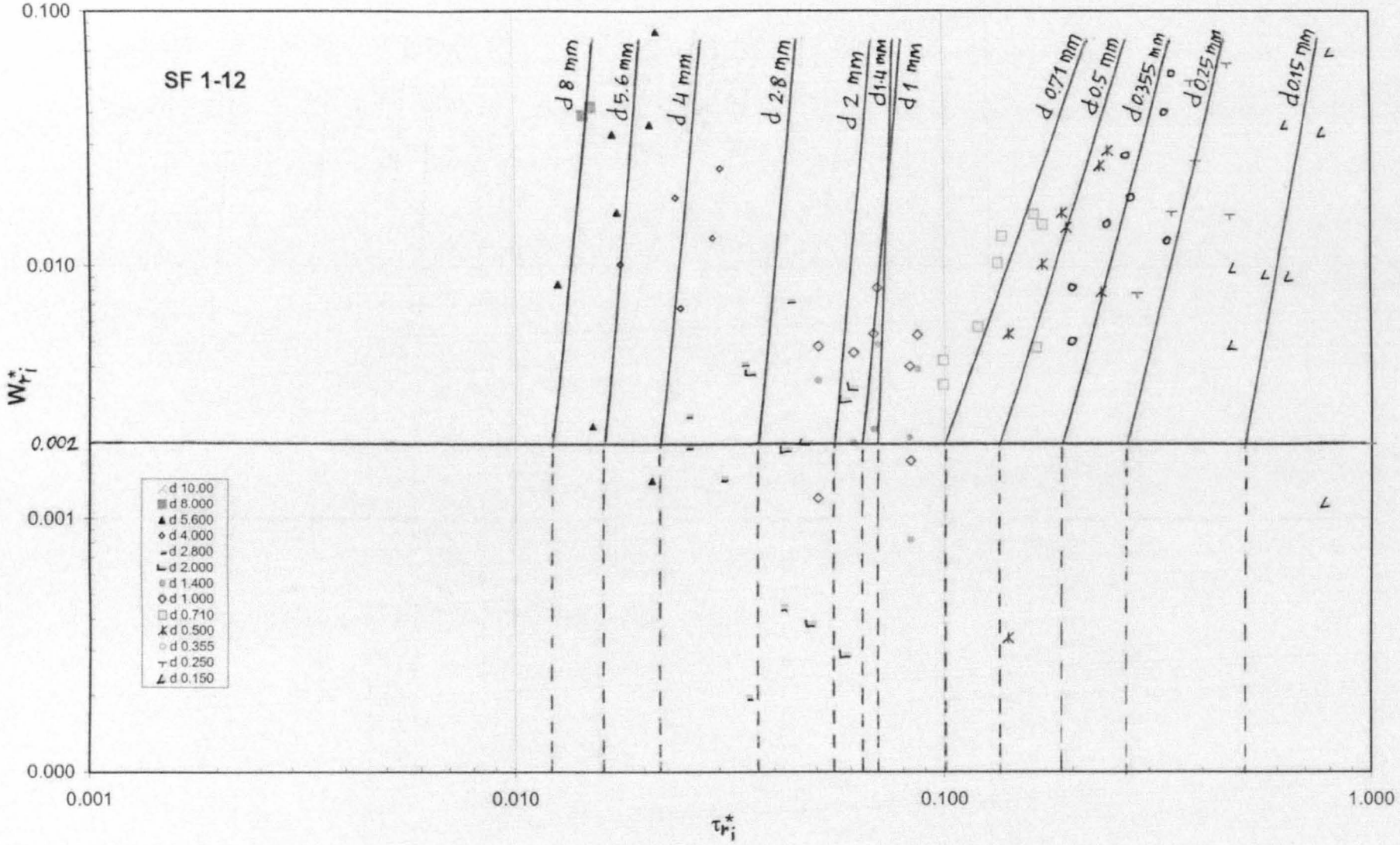

Figure 4.9. The non-dimensional shear stress parameter, τ_{ri}*, determined from the low reference transport rate, W_{ri}* = 0.002, for stability tests SF 1-12

Table 4.2. Non dimensional shear stress parameter, τ_{ri}*, and the error bounds for grain size fractions of stability tests SF I

Grain size	SF 1-3		SF 1-6		SF 1-9		SF 1-12	
	τ_{ri}*	Error bounds	τ_{ri}*	Error bounds	τ_{ri}*	Error bounds	τ_{ri}*	Error bounds
10 mm	-	-	-	-	-	-	-	-
8	0.0054	0.0053 - 0.0057	0.0071	0.0068 - 0.0074	0.0105	0.0100 -0.0104	0.0120	0.0118 - 0.0121
5.6	0.0100	0.0101 - 0.0105	0.0130	0.0128 - 0.0134	0.0130	0.0128 - 0.0131	0.0150	0.0138 - 0.0150
4	0.0140	0.0132 - 0.0141	0.0160	0.0156 - 0.0170	0.0180	0.0180 - 0.0186	0.0220	0.0206 - 0.0220
2.8	0.0210	0.0205 - 0.0217	0.0270	0.0260 - 0.0280	0.0280	0.0280 - 0.0300	0.0350	0.0344 - 0.0363
2	0.0290	0.0280 - 0.0300	0.0380	0.0370 - 0.0408	0.0420	0.0420 - 0.0430	0.0530	0.0517 - 0.0530
1.4	0.0400	0.0390 - 0.0410	0.0570	0.0570 - 0.0600	0.0620	0.0600 - 0.0620	0.0700	0.0700 - 0.0726
1	0.0340	0.0330 - 0.0350	0.0510	0.0505 - 0.0520	0.0570	0.0570 - 0.0600	0.0620	0.0620 - 0.0635
0.71	0.0670	0.0640 - 0.0707	0.0860	0.0830 - 0.0930	0.0930	0.0930 - 0.0970	0.1000	0.0937 - 0.1028
0.5	0.0920	0.0900 - 0.0960	0.1160	0.1130 - 0.1201	0.1260	0.1250 - 0.0130	0.1270	0.1200 - 0.1300
0.355	0.1220	0.1200 - 0.1250	0.1500	0.1430 - 0.1550	0.1880	0.1880 - 0.0190	0.1800	0.1800 - 0.1820
0.25	0.1600	0.1550 - 0.1700	0.2300	0.2228 - 0.2400	0.2500	0.2500 - 0.2560	0.2450	0.2430 - 0.2720
0.15	0.3100	0.3067 - 0.3200	0.4200	0.4160 - 0.4340	0.4500	0.4330 - 0.4500	0.5050	0.4720 - 0.5205

Table 4.3. Critical Shear Stress, τ_{ci} , of grain size fractions for stability tests SF I

Grain size (mm)	SF 1-3	SF 1-6	SF 1-9	SF 1-12
	τ_{ci} (N/m^2)	τ_{ci} (N/m^2)	τ_{ci} (N/m^2)	τ_{ci} (N/m^2)
10	-	-	-	-
8	0.699	0.919	1.360	1.554
5.6	0.906	1.178	1.178	1.360
4	0.906	1.036	1.165	1.424
2.8	0.952	1.224	1.269	1.586
2	0.939	1.230	1.360	1.716
1.4	0.906	1.292	1.405	1.586
1	0.583	0.826	0.923	1.004
0.71	0.770	0.988	1.069	1.149
0.5	0.745	0.971	1.052	1.052
0.355	0.690	0.862	1.092	1.034
0.25	0.647	0.931	1.012	1.012
0.15	0.753	1.020	1.093	1.238

The variation of critical shear stress τ_{ci} with grain size indicates that the individual grain fractions moves at different level of flow strength (Table 4.3). As expected from the measurement of bedload transport rates (Figure 4.1) the stability test applied to antecedent

flow SF 1-3 indicated lower critical shear stresses for all grain sizes than that of stability test applied to the bed which previously formed by antecedent flow SF 1-6, SF 1-9 and SF 1-12 respectively.

The interesting features are shown in Figure 4.10. Grains in the fine mode for stability test of antecedent flow SF 1-6, SF 1-9 and SF 1-12 have a relatively consistent increase with very close values of the threshold of motion. A much lower threshold of motion for fine grains is presented by the curve of stability test SF 1-3. It is suspected that the antecedent flow test with the duration of 3 hours still produced a bed with many unsheltered fine grains. Relatively stable and sheltered fine grains are only likely to be obtained with a duration longer than 3 hours as the three other stability tests applied to three different duration of antecedent flow present a very close curve.

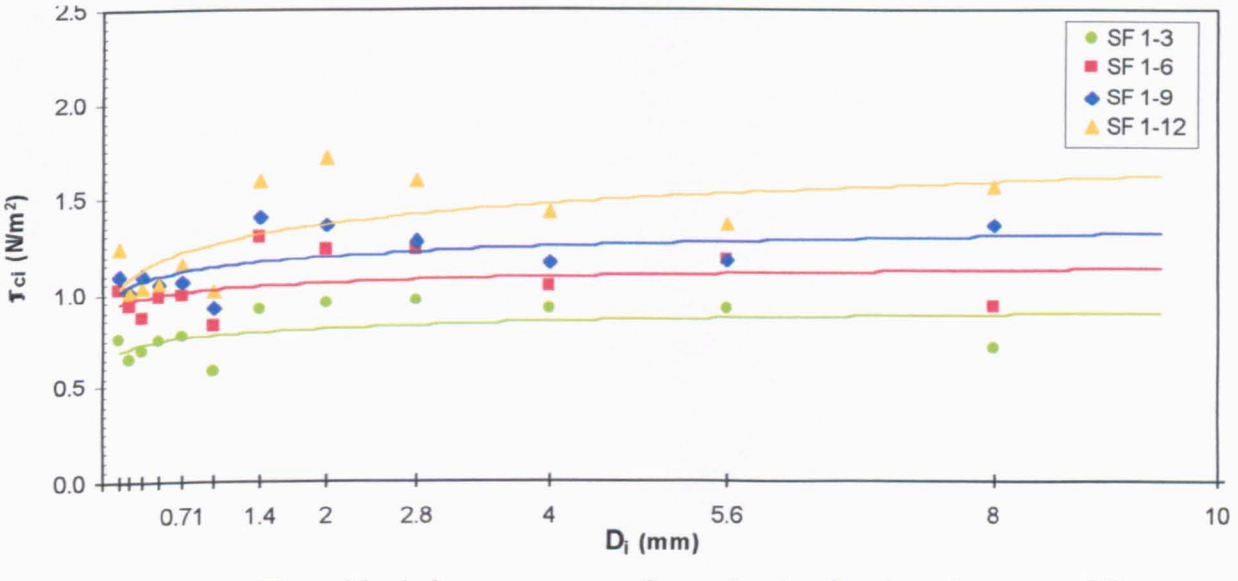

Figure 4.10. The critical shear stress, τ_{ci}, for grain size fractions in terms of D_i for the stability tests SF I

The coarser grains produced a simple pattern in which the level of increase in the threshold of motion coincides with the increasing duration of antecedent flow test. Values of the critical shear stress for grains in the coarse mode for stability test SF 1-12 are at least two times

higher than the increase from SF 1-3 to SF 1-6. The increase in stability of the coarse grains also seems to be continuing whereas the increase in stability of finer grains stabilised between 3 and 6 hours.

The data of the critical shear stress thresholds was used to plot hiding functions in a manner described by Sutherland (1992) as the following

$$\varepsilon_{is} = \frac{\tau_{ci}}{\tau_{i\,Shields}} \tag{4.3}$$

where

τ_{ci} = critical shear stress threshold for grain size i estimated from measured transport rate and shear stress data $= \tau_{ri}^{*}(s-1)\rho g D_i$ (N/m^2)

$\tau_{iShields}$ = critical shear stress for grain size i estimated using Shields relationship $= \theta(s-1)\rho g D_i$ (N/m^2)

τ_{ri}* = non dimensional shear stress parameter derived from a low reference transport rate value $W_{ri}^{*} = 0.002$

θ = Shields' entrainment function (= 0.056)

ρ = fluid density (kg/m^3)

g = acceleration due to gravity (m/s^2)

D_i = grain size fraction i (mm)

s = specific density of sediment (= 2.65)

Higher values of hiding functions, calculated using Equation 4.3, indicate that smaller grains on the bed were more hidden from the flow and also more impeded in their motions than coarser grains. This is supported by the transport pattern in the stability test that grains in the coarse mode were dominance in transport. Table 4.4 and Figure 4.11 show that the mobility of finer grains decreases while the mobility of coarser grains increases relative to homogenous single size bed. This suggests that the finer grains are sheltered and trapped below the larger

grains. The relative grain sizes of the finer grains to the coarser bed are very small and then even smaller as the bed coarsen after antecedent flow. As applied by Wilcock and Southard (1988), the size ratio of the fraction (D_i/D_{50}) is one of variables used to describe the relative grain size. It has a central role in mixed size sediment transport because of the size of each grain relative to others in the mixture controls the variation from fraction to fraction of both the value of bed shear stress acting on individual grains and the resistance of those grains to movement.

Table 4.4. Hiding Function ε_{is} of grains size fractions for stability tests SF I

Grain size (mm)	SF 1-3	SF 1-6	SF 1-9	SF 1-12
	ε_{is}	ε_{is}	ε_{is}	ε_{is}
10	-	-	-	-
8	0.096	0.127	0.188	0.214
5.6	0.179	0.232	0.232	0.268
4	0.250	0.286	0.321	0.393
2.8	0.375	0.482	0.500	0.625
2	0.518	0.679	0.750	0.946
1.4	0.714	1.018	1.107	1.250
1	0.643	0.911	1.018	1.107
0.71	1.196	1.536	1.661	1.786
0.5	1.643	2.143	2.321	2.321
0.355	2.143	2.679	3.393	3.214
0.25	2.857	4.107	4.464	4.464
0.15	5.536	7.500	8.036	9.107

It can be seen from Figure 4.11 that the hiding functions in the region $D_i/D_{50} < 0.15$ for SF 1-6, SF 1-9 and SF 1-12 are similar. In the stability test SF 1-3 these grains are less stable than in the other three stability tests. The hiding function value reduces with time in the region $0.25 < D_i/D_{50} < 1.6$. All this data suggest that after 3 hours the finer grains have achieved their maximum stability. However the processes, which control the stability of the coarse grains, are much slower and are still active even after 12 hours of flow.

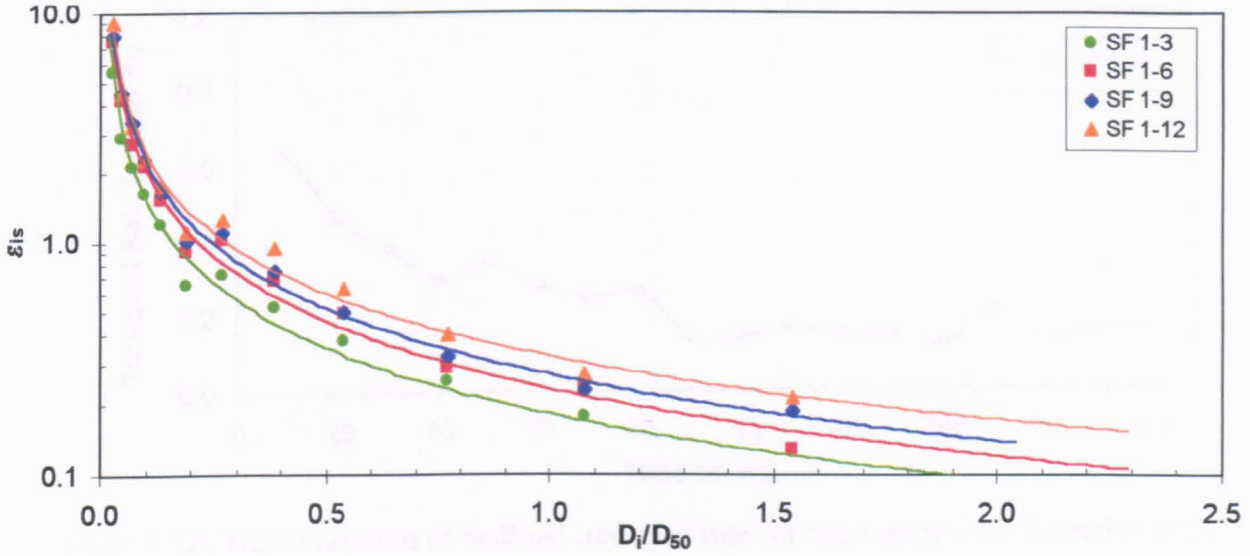

Figure 4.11. Hiding function, ε_{is}, derived from fractional threshold conditions for stability tests SF I

In order to explain why different stabilising behaviour were found in the fine and the coarse grain fractions, a detailed examination of the laboratory observations was made during the steady antecedent flow experiments.

4.3. OBESERVATIONS OF ANTECEDENT FLOW EXPERIMENTS SF I

4.3.1. STEADY ANTECEDENT FLOW EXPERIMENT SF 1-3

4.3.1.1. Bedload Transport Rate and Composition SF 1-3

Bedload transport rates changes significantly during the initial hour of experiment SF 1-3. Figure 4.12 shows the bed was highly mobile during the first 60 minutes with the average transport rate of 0.397 g/s/m. This suggests that the transport processes involve sporadic release of material as bed adjustments take place. Within the early stage the bed rearranging themselves as the water flow disrupted them and led to the high initial transport rate. The movement of particles was very active reflecting the progressive development of bed surface caused by a high constant discharge. The average transport rate reduced to 0.179 g/s/m during the second hour or more than half of the initial rate. As the armouring process continued the transport rate continued to decrease, but at a slower rate reflecting the diminishing supply of dislodgeable grains. This was indicated by the almost constant transport rate during the last 60 minutes at 0.150 g/s/m.

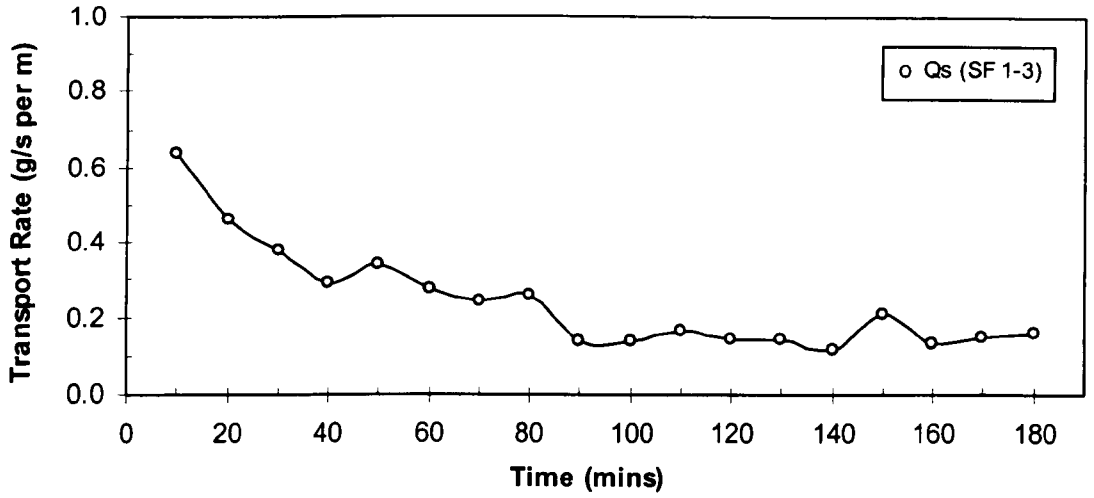

Figure 4.12. Time variation of bedload transport rate for antecedent flow Experiment SF 1-3

During the antecedent flow experiment SF 1-3, the bedload composition shows systematic changes. Observations of grain distribution curve of the bedload indicate that the degradation phase occurred during initial stages of antecedent flow (Figure 4.13). In term of modal grain size the finer mode experience a similar pattern of transport throughout the 3 hours whilst the coarser mode shows variations. The grain size of 0.355 mm is dominant in the fine mode for the whole duration of the test. In the coarse mode, the grain size of 4 mm is dominant during the very first part of the test. These grains were thought to represent very loose or exposed grains, whose lack of stability had been caused by the mechanical scraper used to originally form the bed. Once these grains has largely been transported, larger grains of 5.6 mm in size becoming more exposed. The modal grain size in the coarse mode therefore increased. After about 30 minutes (time elapsed 90 minutes) the proportion of 5.6 mm grains with sufficient exposure declined so much that the modal grain size reduced to 4 mm. This remained constant until time elapsed 130 minutes when the coarse modal grain size varied from 5.6 mm to 4 mm periodically. The inconsistency in coarser mode was believe to indicate the increasing exposure of larger grains as the result of decreasing amounts of finer grains left on the bed.

The active depth of bed has been found to less than half of the largest grain size present. After antecedent flow the average bed surface measured by the vernier depth gauge had reduced by 4.3 mm. This decrease is approximately half the size of the largest grain size. A layer in the prediction of sediment available for transport was assumed using the two layer active depth

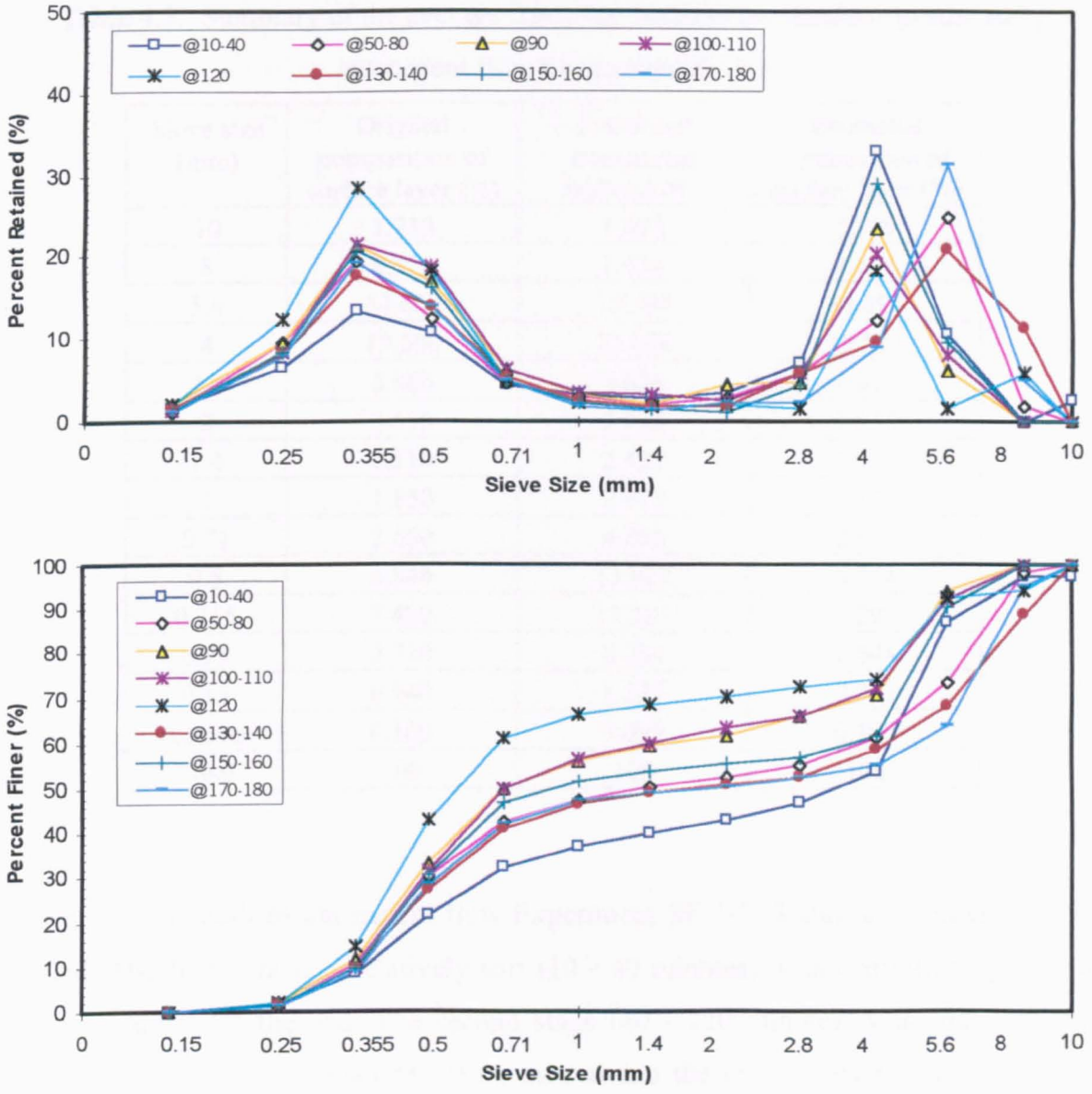

Figure 4.13. Grains size distribution of transported bedload for antecedent flow SF 1-3

available for transport in a mixing layer as suggested by Willetts et al. (1987). In this case the active depth based on the present of largest grain d_{100} where each layer is equal in thickness to half of the largest grain is coincide with the actual decreasing bed surface level. By considering the bedload trap width, the mixing layer contains 40.9 kg sediment mixture available for transport. The composition of the total bedload transported was calculated from laboratory observations so that the bed surface composition at the end of the test could be estimated (Table 4.5).

Table 4.5. Summary of the average fractional bedload composition produced by antecedent flow Experiment SF 1-3

Sieve size (mm)	Original composition of surface layer (%)	Fractional transported bedload (%)	Estimated composition of surface layer (%)
10	1.730	1.023	1.739
8	8.570	1.634	8.655
5.6	34.660	15.594	34.894
4	19.600	22.676	19.562
2.8	6.860	5.826	6.873
2	3.530	2.925	3.537
1.4	2.510	2.422	2.511
1	1.850	2.975	1.836
0.71	2.680	4.806	2.654
0.5	6.840	13.022	6.764
0.355	7.420	17.387	7.297
0.25	2.710	8.084	2.644
0.15	0.940	1.527	0.933
receiver	0.100	0.099	0.100
Total	100	100	100

Looking at the overall of antecedent flow Experiment SF 1-3, 3 stages of activity has been identified. The first, which is relatively sort (10 - 40 minutes), was controlled by the initial artificial condition of the bed. The second stage (40 - 120 minutes) was characterised by increasing amounts of fine material being moved and the coarse modal grain size moving from 5.6 mm to 4 mm and then size of the coarse mode reducing. In the third phase, the fine grain proportion started to reduce. The proportion of coarse mode increased and its behaviour become more erratic, with the coarse modal grain size alternating between 5.6 mm and 4 mm.

4.3.1.2. Variations of Average Nearbed Streamwise Velocity and Bed Shear Stress SF 1-3

Observation to the time averaged nearbed streamwise velocity and the time averaged bed shear stress during the antecedent flow Experiment SF 1-3 confirm relatively unchanged values throughout the duration of experiment. This is satisfactorily conforms by a straight-line in Figure 4.14. Limited measurement of nearbed streamwise velocity was carried out due to

the short duration of experiment to allow sufficient time for another measurement on the grid. The similarity of both the average values of nearbed streamwise velocity and bed shear stress can be accepted as the same discharges were applied. However, the small changes possible in bed shear stress may not directly be used to claim that the bed surface roughness was not different during the erosion process because of the results are not representing a sufficient data of observation. However, the similarity or possibly a small variation in the bed shear stress supports the argument that sediment transport increases or decreases nonlinearly with bed shear stress and the sum of local transport rates across a section may be considerably different from the transport rate calculated from section-averaged parameters (Smart, 1999).

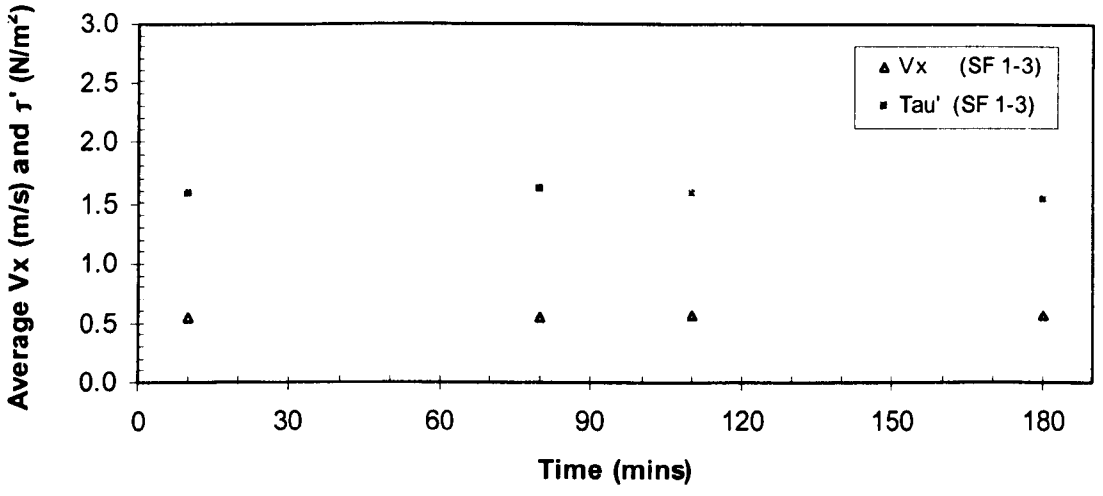

Figure 4.14. Variation of time averaged nearbed streamwise velocity and bed shear stress during antecedent flow of experiment SF 1-3

Investigation of the changes in the average nearbed streamwise velocity at different locations on the measurement grid was observed by repeatedly measuring the streamwise nearbed flow velocity. For experiment SF 1-3 the duration required to complete each set of measurements was 30 minutes. This short period was required to allow a sufficient time allocation for the measurement of vertical flow distribution and measurement of nearbed flow velocity at each grid point. However, due to time constraints not all of the measurements at selected grid points could be measured with the last two points I3 and I5 were measured once only at the beginning of the run (Table 4.6). The elapsed time for the first and second set of measurements was 60 minutes and 150 minutes.

Table 4.6. Variations of the average nearbed streamwise flow velocity and the standard deviation in antecedent flow Experiment SF 1-3

Points	First measurement (time elapsed 60 minutes)		Second measurement (time elapsed 150 minutes)		Changes of Vx (%)
	V_x (m/s)	σ (m/s)	V_x (m/s)	σ (m/s)	
A1	0.568	0.097	0.568	0.097	0
A3	0.562	0.094	0.564	0.099	0.356 (+)
A5	0.498	0.086	0.495	0.090	0.602 (-)
E1	0.551	0.102	0.571	0.092	3.630 (+)
E3	0.550	0.099	0.553	0.095	0.545 (+)
E5	0.458	0.094	0.472	0.093	3.057 (+)
I1	0.530	0.102	0.552	0.106	4.151 (+)
I3	0.540	0.103	n/a	n/a	n/a
I5	0.455	0.094	n/a	n/a	n/a
Average	0.524	0.097	0.539	0.096	-

The results of average streamwise nearbed flow velocity at each grid point presented in Table 4.6 and Figure 4.15 show that the average values measured at different grid points with short time intervals between measurement are relatively similar. The changes in velocity at the same grid point are very small with the range of variations from -0.6 % to +4 % between the two measurement times. At most measurement points the velocity increased while at point A5 velocity decreased slightly. The standard deviations of average nearbed streamwise velocity in Table 4.6 show the presence of relatively similar level of fluctuations. It can be said that the nearbed streamwise nearbed flow velocities at different points with the same depth from the boundary are quite similar. The individual values were not widely dispersed from the mean.

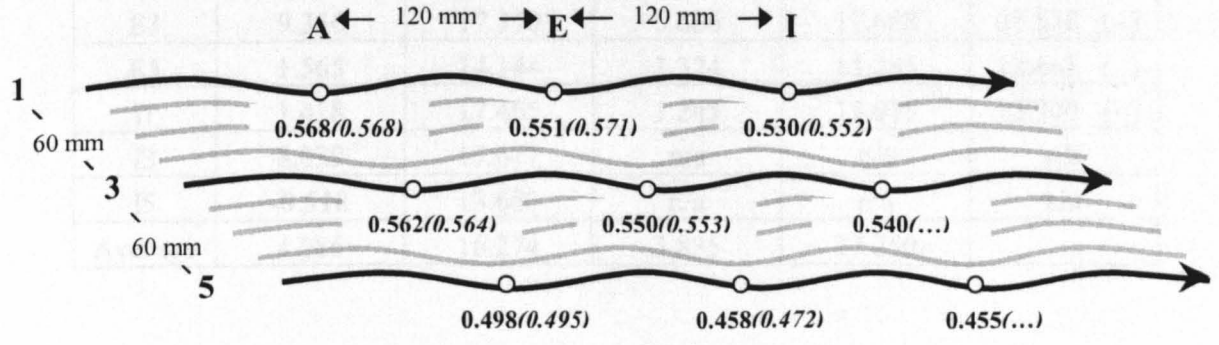

Figure 4.15. Distribution of average nearbed streamwise velocity (m/s) in antecedent flow Experiment SF 1-3 (first measurement in bold, second measurement in brackets)

A different pattern of variation to the average nearbed streamwise velocity is experienced by the average bed shear stress, $\overline{\tau}$. This is the estimation of the average instantaneous bed shear stress over the small area, which was averaged over the time of measurement (see Equations 3.9 and 3.15). The average values of bed shear stress showed significant change from location to location (Table 4.7 and Figure 4.16). Some points indicate very high values of shear stress and significant temporal variation. The different patterns of vertical flow fluctuations at the different grid points are thought to contribute to these changes. This is indicated by the results that they do not follow the changes in average nearbed streamwise velocity. In the condition that the average nearbed streamwise velocities increased, the average bed shear stresses may increased (points A3 and E1) but the other points show a decreasing value (points E3, E5 and I1). Decreasing value of average bed shear stress is likely the indication that the vertical velocity component was being increasingly dominated by the upward direction. The variation between the two measurement (time interval 90 minutes) ranges from a 76 % decrease to almost 94 % increase with almost all grid points experiencing a significant variation.

Table 4.7. Variations of the average bed shear stress and the standard deviation in antecedent flow Experiment SF 1-3

Points	First measurement (time elapsed 60 minutes)		Second measurement (time elapsed 150 minutes)		Changes of $\overline{\tau}$ (%)
	$\overline{\tau}$ (N/m^2)	σ (N/m^2)	$\overline{\tau}$ (N/m^2)	σ (N/m^2)	
A1	2.757	16.366	3.916	17.483	42.038 (+)
A3	2.673	16.756	5.185	17.988	93.977 (+)
A5	4.087	14.514	0.975	14.879	76.144 (-)
E1	7.396	18.631	7.513	18.452	1.582 (-)
E3	9.356	17.310	6.686	17.688	28.538 (-)
E5	1.565	14.144	1.324	15.245	12.665 (-)
I1	1.418	17.465	1.245	19.018	12.200 (-)
I3	8.039	17.677	n/a	n/a	n/a
I5	-0.518	13.600	n/a	n/a	n/a
Average	4.086	16.274	3.835	17.250	-

Closer examination of the distribution of average nearbed streamwise velocity at various grid points has shown that there is no systematic pattern in the way the average nearbed stream-

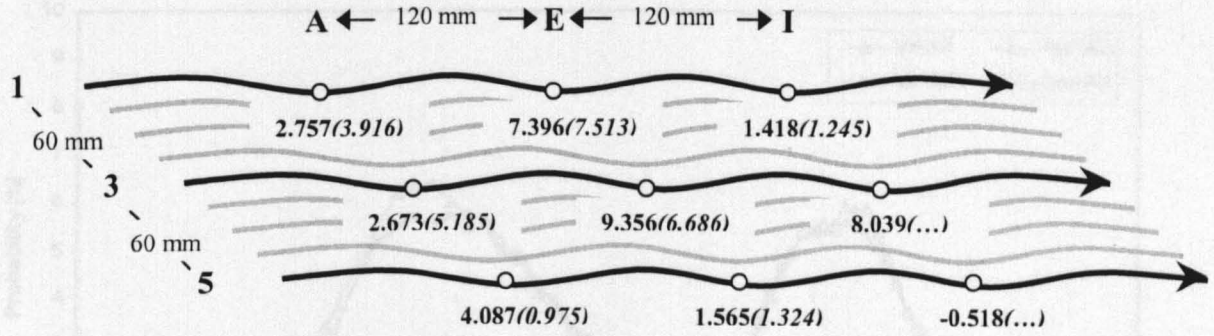

Figure 4.16. Distribution of average bed shear stress, $\overline{\tau}$, (N/m^2) in antecedent flow Experiment SF 1-3 (first measurement in bold, second measurement in brackets)

wise velocity changes with regard to the average bed shear stress distribution. For example, two grid points that have demonstrated small decreases and increases in average nearbed streamwise velocity with very small variation in their standard deviations are examined (Table 4.7). Distribution of measured nearbed streamwise velocity and calculated bed shear stresses are shown in Figure 4.17 and Figure 4.18. Point A3 produced a difference in which the distribution of "instantaneous" bed shear stress in the second measurement is shifted to the right particularly for larger values as shown in the tail section of the distribution curve in Figure 4.17. This means the second measurement at 150 minutes produced larger number of "instantaneous" nearbed streamwise velocity that result in the range of observation of the first measurement (r_1) is smaller than the second measurement (r_2) as the difference between the largest and the smallest value during this run is higher. This also produces the higher inter-quartile range (i_{qr}) during the second experiment. Meanwhile, point A5 shows a consistent pattern of "instantaneous" nearbed streamwise velocity at both measurement times. Although the range of observation (r_1) < (r_2) and inter-quartile range (i_{qr1}) < (i_{qr2}) as experienced by point A3, there is a strong similarity in the distribution of "instantaneous" nearbed streamwise flow velocity as shown in Figure 4.17.

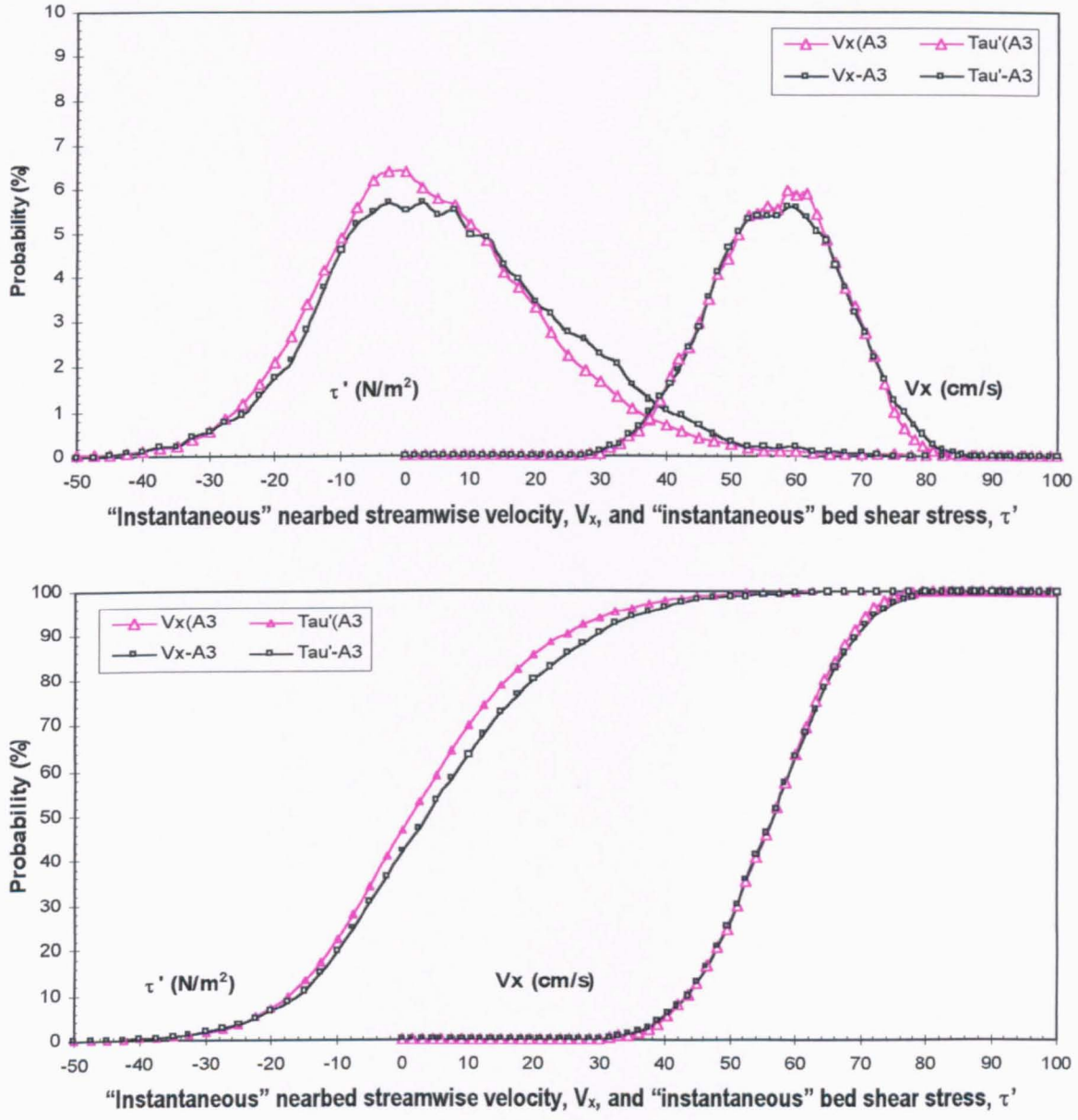

Figure 4.17. Variation of "instantaneous" nearbed streamwise velocity and "instantaneous" bed shear stress at Point A3 (the first and the second measurement indicated by "(" and "-")

Different patterns are presented by the distribution of "instantaneous" bed shear stress. Point A3 exhibits variation in which the second measurement produced more higher values as indicated by a big difference in its range of observation ($r_1 > r_2$). The distribution curve and the cumulative distribution of "instantaneous" bed shear stress of the second measurement are then shifted to the right. Point A5 experienced different pattern. As the range of observation of the second measurement is larger than the first measurement ($r_2 > r_1$) the distribution curve

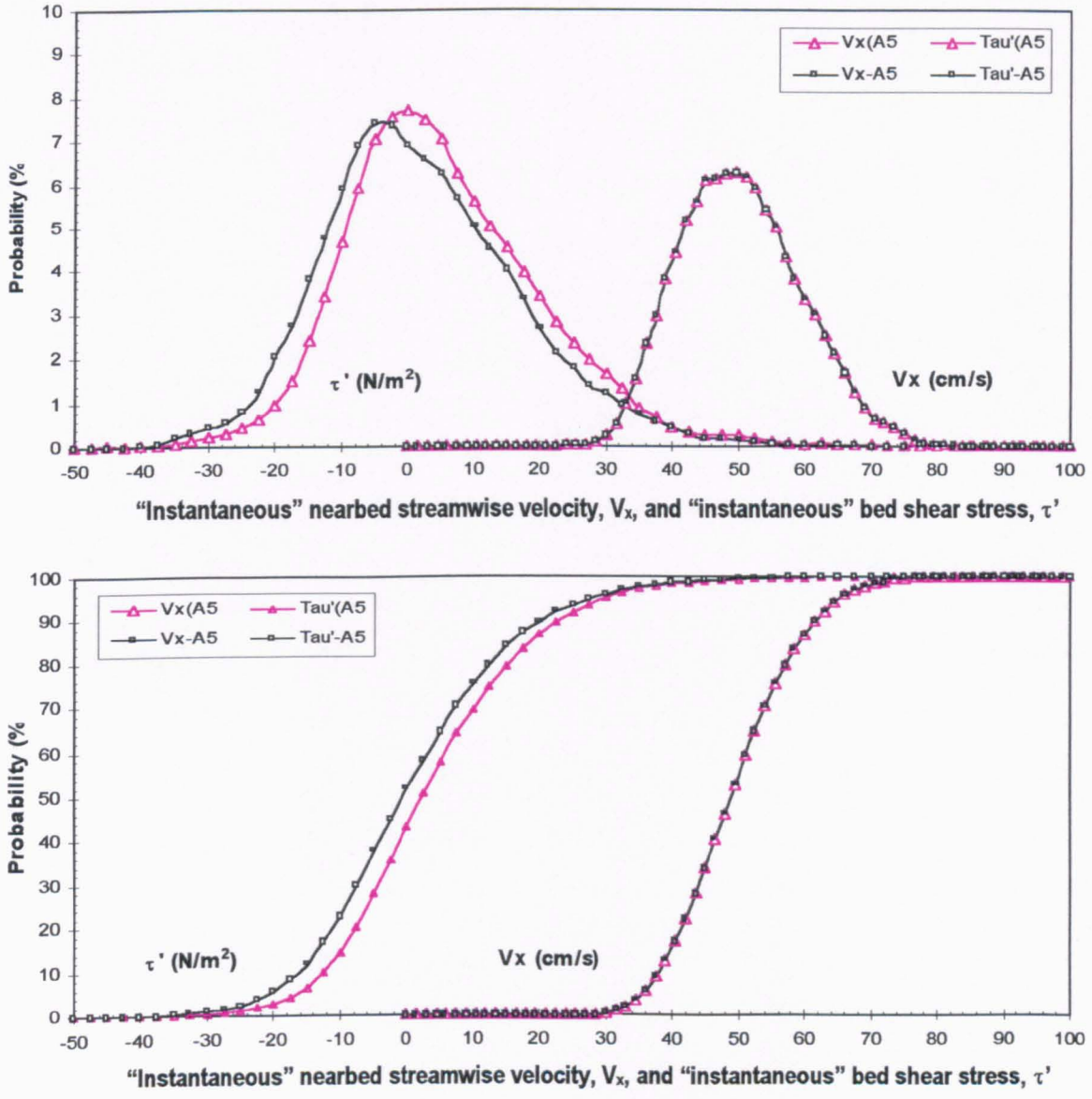

Figure 4.18. Variation of "instantaneous" nearbed streamwise velocity and "instantaneous" bed shear stress at Point A5 (the first and the second measurement indicated by "(" and "-")

and cumulative distribution are skewed to the left (see Figure 4.18) although the inter-quartile range of both points were increased at different level ($i_{qr1} < i_{qr2}$).

4.3.1.3. Bursting Events and Flow Momentum SF 1-3

The reducing transport rate in antecedent flow Experiment SF 1-3 is assumed to be primarily caused by the changes in the bed formation, which become stronger after certain time exposed

to the flow. However it is very important to remember that the bedload transport rate observation cannot be separated from turbulent flow, which has a key role in the grain entrainment process. The temporal and spatial distribution of the flow structure close to the bed is believed to be one of factors that control the grain entrainment rate. The majority of the turbulent energy is generated in the near-bed region where bursting processes generate intermittent high shear stress events.

Observation of the bursting events during experiment SF 1-3 found that the occurrences of ejections and sweeps are relatively balance with the proportion of ejections is 49.6 % in comparison to 50.4 % sweeps. In this observations events are recognised if the threshold values of 1.2 $\sigma_u\sigma_v$ was exceeded. It is distinguished into ejections ($u`<0$ ; $v`>0$) and sweeps ($u`>0$ ; $v`<0$). The threshold values of observed time elapsed ranging from 0.0070 to 0.0074 show that the dispersion of streamwise and vertical velocity were sensibly constant reflecting the steady uniform flow during the experiment. In Table 4.8 two observed time elapsed are presented. The results was obtained by the application of a Matlab program called Momentum.m, which can be seen more detail in the Appendix.

The observation from limited time elapsed in Table 4.8 shows that the frequency of both ejections and sweeps are not stable. At the start of the test (time elapsed 10 minutes) the frequency of ejections and sweeps is similar. However, the average duration of ejections is slightly less than the average duration of sweeps. This is caused by different number of observation of both events during this time elapsed. Less events exceeding the threshold values in the upward interactions was observed while the events exceeding the threshold values in the downward-looking bed interactions was slightly more frequent. At time elapsed 110 minutes sweeps was more frequent than ejections but the average duration is shorter than the average duration of ejections.

As only general information on the bursting events is provided in Table 4.8, the strength of either ejections and sweeps are not known. Therefore the magnitude of momentum caused by the upward and downward-looking bed interactions was then observed. The momentum was calculated using Equation 3.7 applied in Momentum.m. It can be seen from Figure 4.19 that the magnitude of momentum per unit area (dM/dA) produced by ejections ranging from a low

Table 4.8. Summary of bursting events at selected time elapsed in antecedent flow Experiment SF 1-3

Parameter descriptions	Time elapsed (minutes)	
	10	110
Threshold values (m^2/s^2)	0.0074	0.0070
Number of ejections	206	195
Number of sweeps	206	202
Frequency of ejections (Hz)	1.0300	0.9750
Frequency of sweeps (Hz)	1.0300	1.0100
Average duration of ejections (s)	0.0522	0.0529
Average duration of sweps (s)	0.0530	0.0509

value to high value in comparison to the magnitude of momentum during the sweeps. But the similar number of ejections and sweeps lead to the conclusion that the high momentum produced by ejections in Figure 4.20 is also caused by the distribution of high values of streamwise and vertical velocities at the times of measurement.

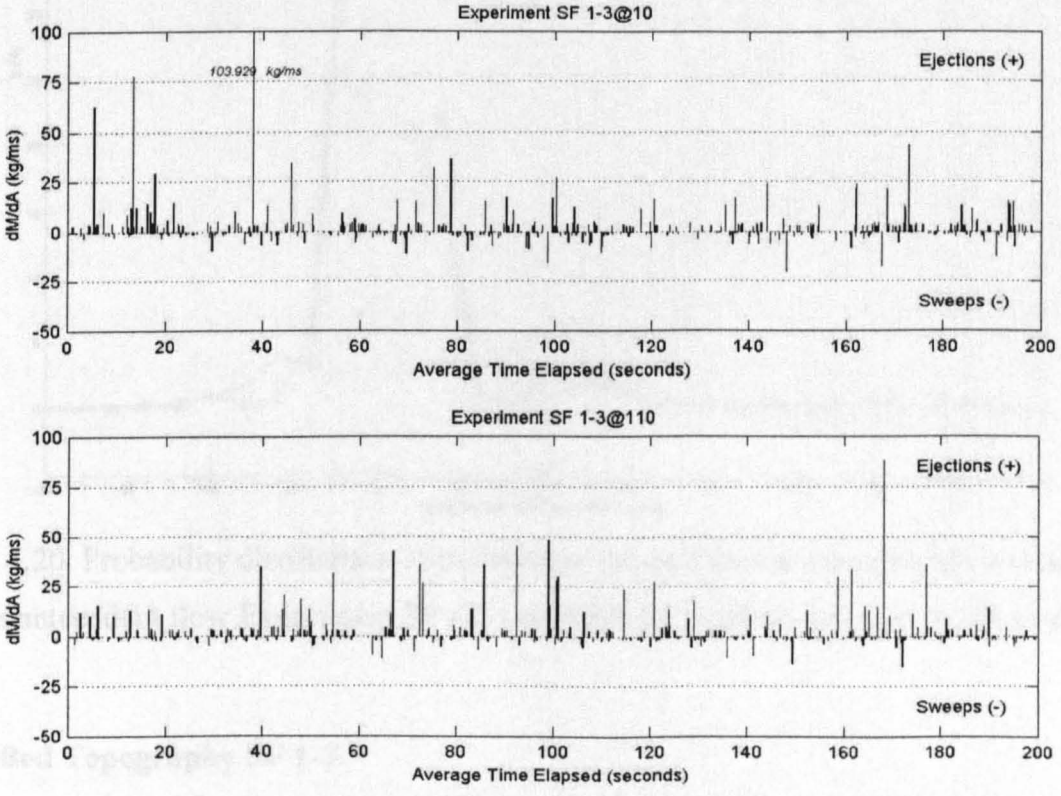

Figure 4.19. The sequence of momentum per unit area and its magnitude at time elapsed 10 and 110 minutes antecedent flow Experiment SF 1-3

In order to obtain further information the probability distribution of ejections and sweeps for selected time elapsed were observed (Figure 4.20). The most frequent momentum of ejections is the magnitude in the range between 1 and 5 kg/ms whereas the sweeps produced fairly densely populated distribution between -5 to -1 kg/ms. The occurrences of outward interactions and downward looking bed interactions at time elapsed 10 minutes, which is more frequent than time elapsed 110 minutes is likely the reason in the difference of transported bedload grains size distribution at both time elapses. These flow momentum are strong enough to transport more coarser grains which dominated the transported bedload at time elapsed 10 minutes whereas time elapsed 110 minutes produced a fairly similar proportion in finer and coarser mode (see Figure 4.13).

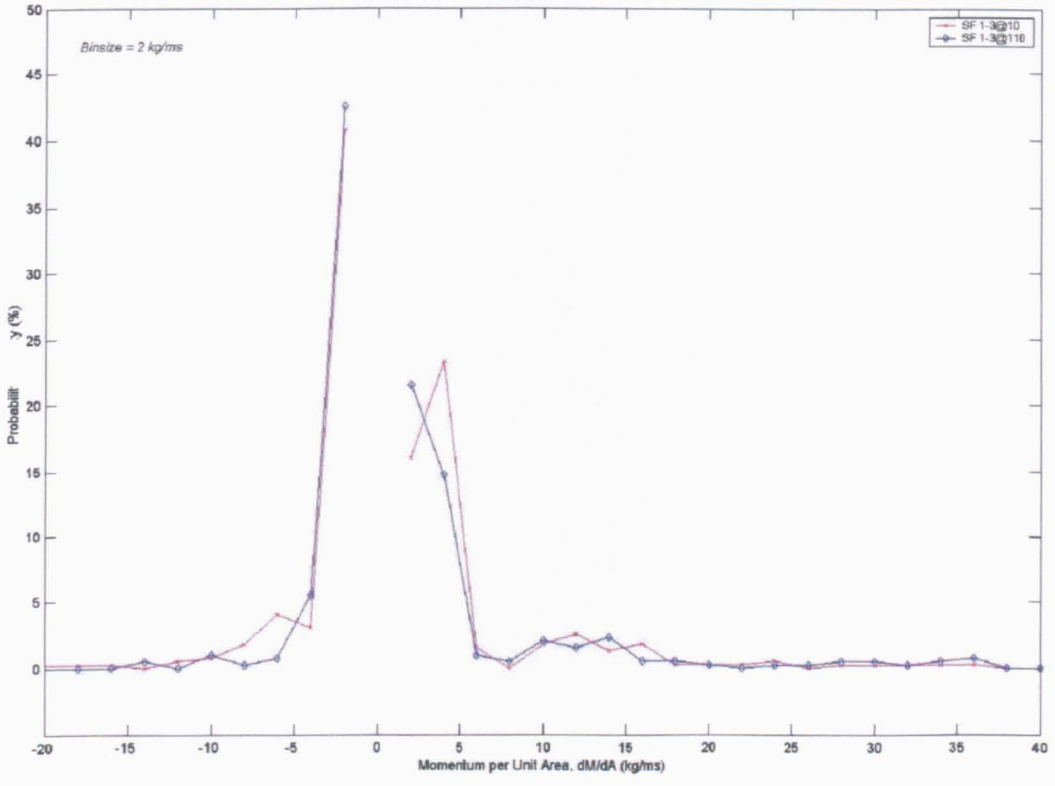

Figure 4.20. Probability distribution of momentum per unit area at time elapsed 10 and 110 minutes antecedent flow Experiment SF 1-3 (ejections are positive and sweeps are negative)

4.3.1.4. Bed Topography SF 1-3

In order to examine the changes in the bed surface structure, the bed elevation data obtain from the series of measurement were analysed. The topography of the bed surface of the

velocity measurement grid was measured before and after the flow applied to the bed. The changes were investigated by employing the software package of Matlab. The output of the program shows the changes of bed topography in the measurement grid from original bed condition to the final form in Experiment SF 1-3. The patterns of changes can easily be recognised by looking at the represented plot of bed surface for each stage of Experiment SF 1-3 (see Figure 4.21, Figure 4.22 and Figure 4.23).

The bed surface seen in Figure 4.21 shows little valley formed bed formation. This is because of the initial mechanical scrapping of the surface was done so that the surface would be relatively flat. However, the size composition of sediment mixture on the bed left some pore spaces, which the initial scrapping process did not completely fill. The spacing measurement of 1 mm also allowed more details in bed surface elevation to be plotted so that small differences in the bed surface are visible. The average bed surface level of original bed of experiment SF 1-3 is 1.923 mm above the arbitrary zero datum.

It is clear in Figure 4.22 that the original bed has eroded and the bed surface structure has changed significantly during antecedent flow. The average bed surface elevation is 0.869 mm below the zero datum, which means that the average bed surface level has reduce by almost 2.8 mm from the average original bed level. Figure 4.22 also shows the irregularity in the erosion processes with some small areas of higher elevation indicating the presence of several isolated larger grains. Further erosion continued during the stability test. A valley formed on the bed surface after antecedent flow in the area of 125 to 200 mm in streamwise direction (x-direction) and 50 to 75 mm in lateral direction (y-direction). As the result of erosion process during the stability test, lower bed surface elevations were found over the area of existing valley (Figure 4.23). It is also noticed that highly exposed areas that were appear on the bed formed by antecedent flow test, e.g. at point (100,150) and (200,125) in Figure 4.22, are removed and no longer exist after stability test (Figure 4.23). The higher flowrates during stability test not only removed high exposed grains but also produced exposed areas at different points within the measurement grid. However, it is very clear from all figures that the level of erosion during antecedent flow test was different than that during stability test. Three hours of antecedent flow armoured the bed to some extent so that the stability test could not eroded and changed the bed surface topography to the same extent as the antecedent flow

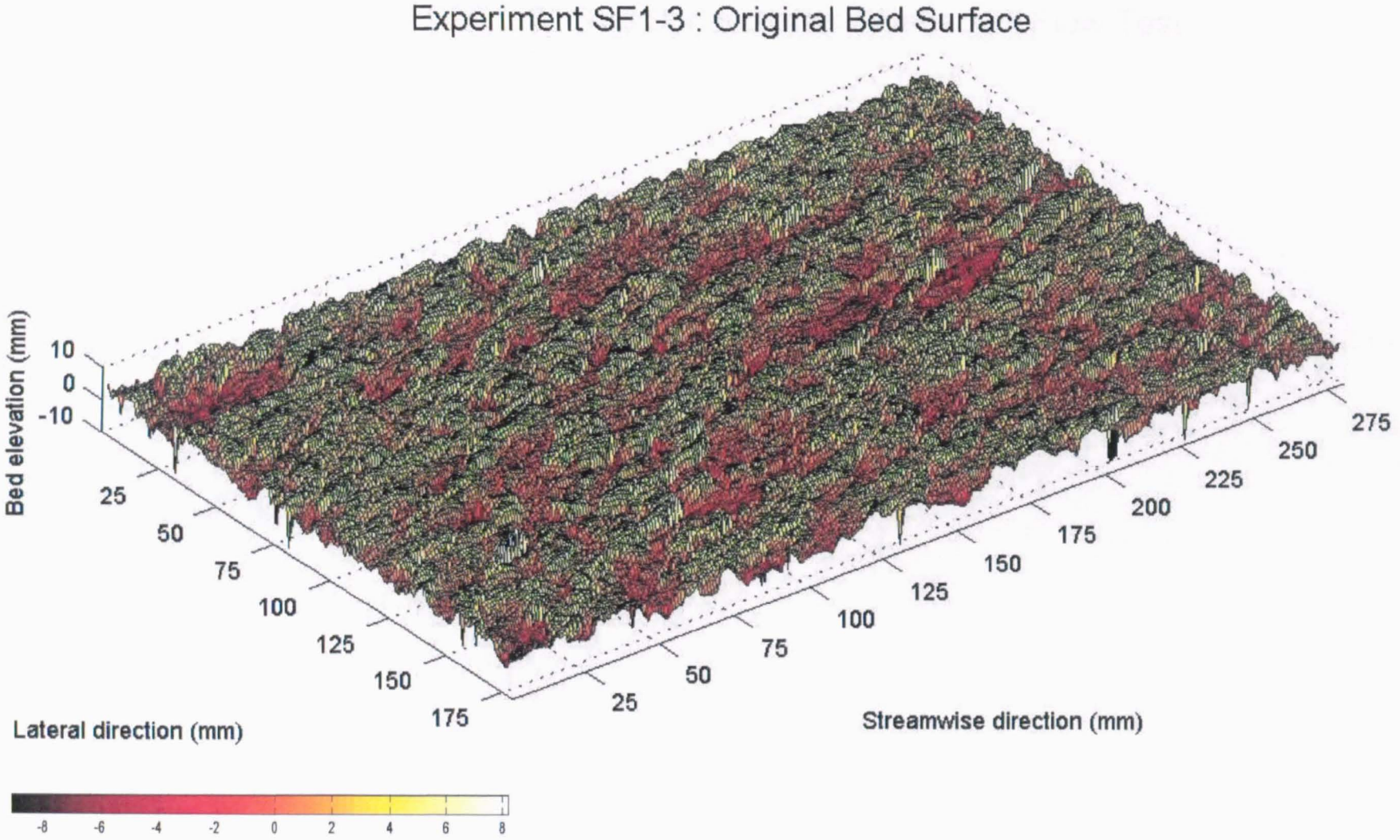

Figure 4.21. Original bed surface topography of the measurement grid Experiment SF 1-3

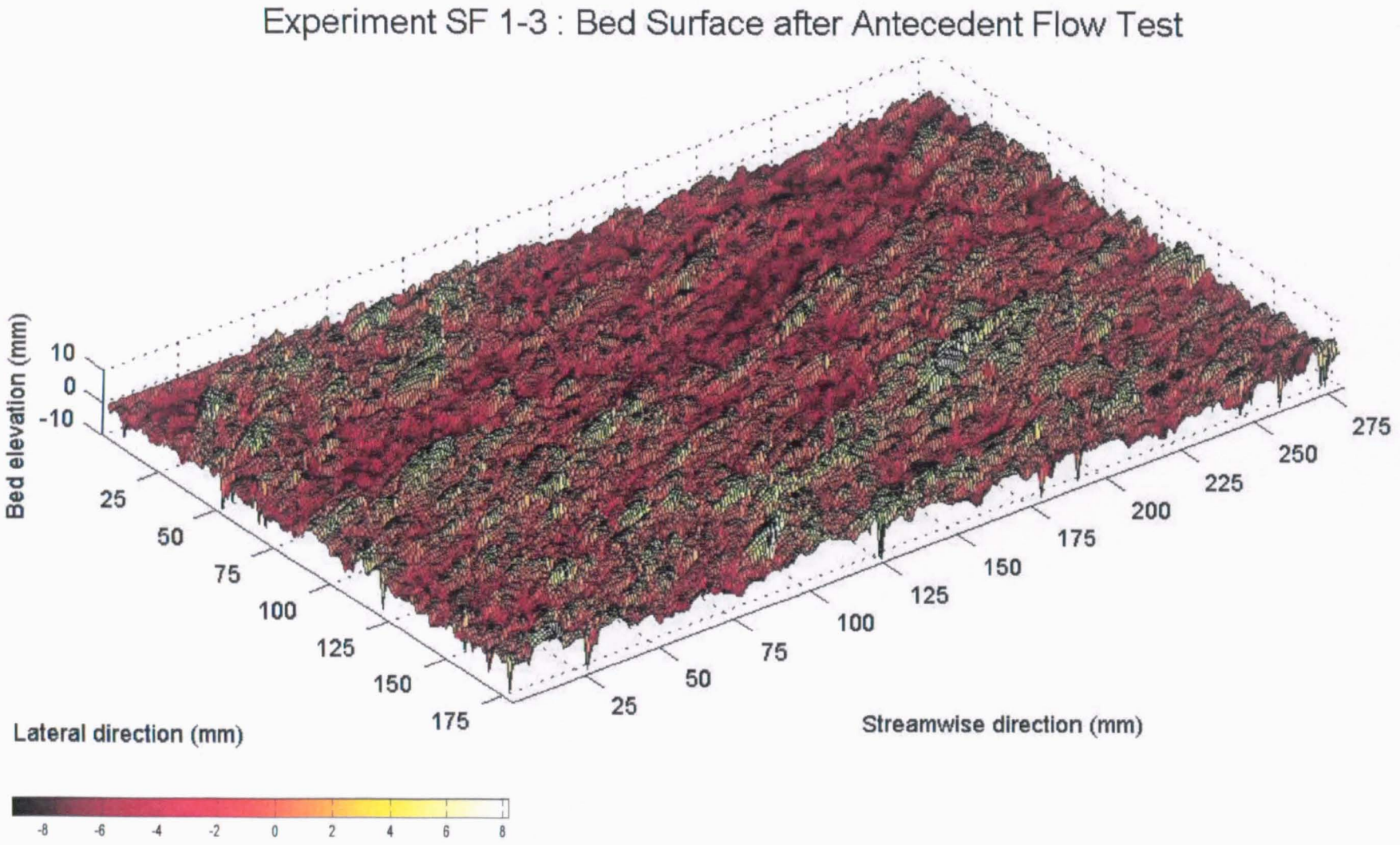

Figure 4.22. Bed surface topography of the measurement grid after antecedent flow Experiment SF 1-3

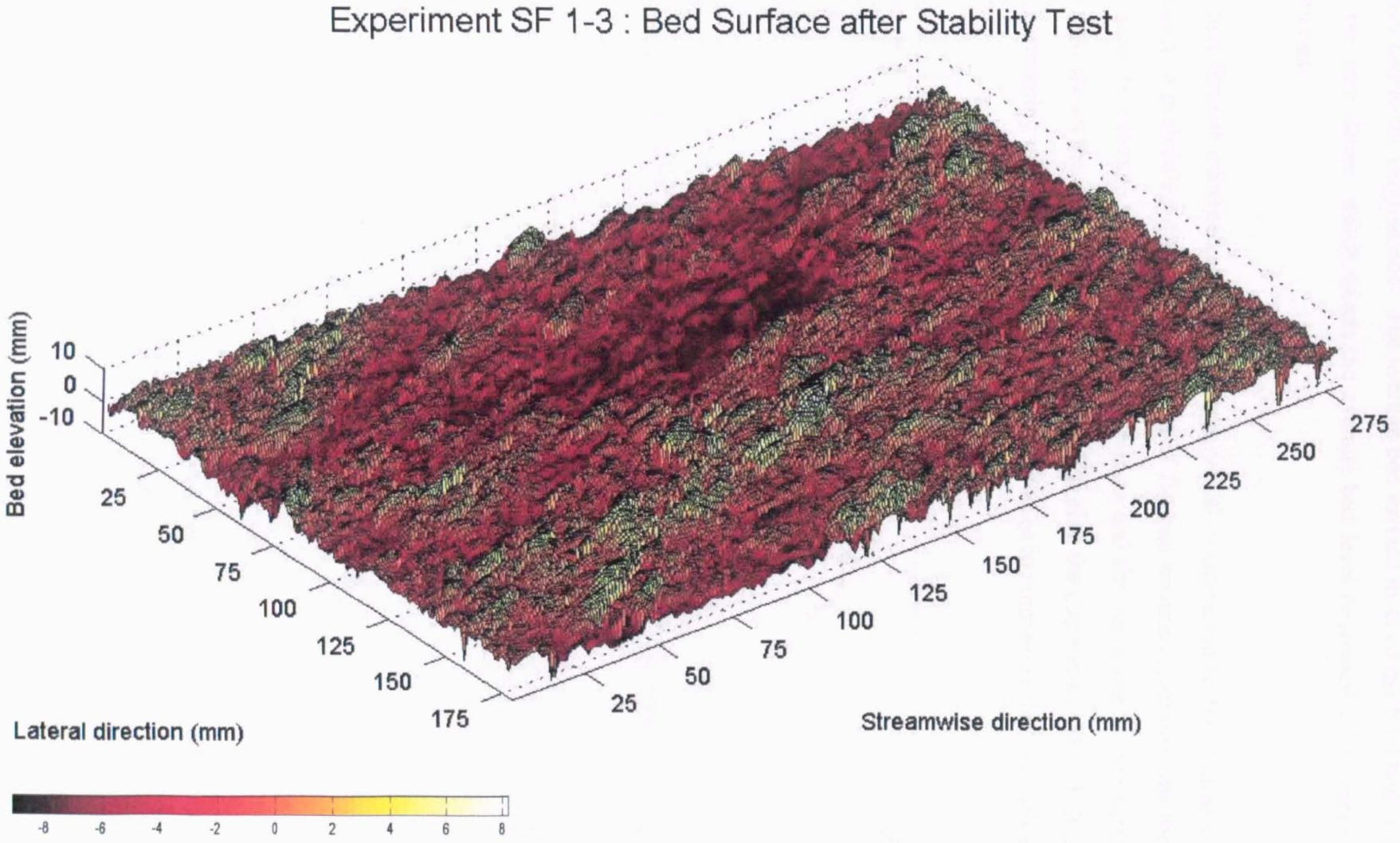

Figure 4.23. Bed surface topography of the measurement grid after stability test Experiment SF 1-3

test have had to the original bed. The average bed surface level of the final bed is 1.999 mm below the zero datum, which means the average bed level decreased 0.331 mm during the stability test.

Given that limited information available from visual examination to the figures of the bed topography, a probability distribution analysis of the bed surface elevations was then carried out in order to estimate the level of grain exposure and the variations in bed surface level. Figure 4.24 shows the bed surface level evolution during the Experiment SF 1-3. It is realised that a shortcoming of this method arises from difficulties in comparing the level of variation

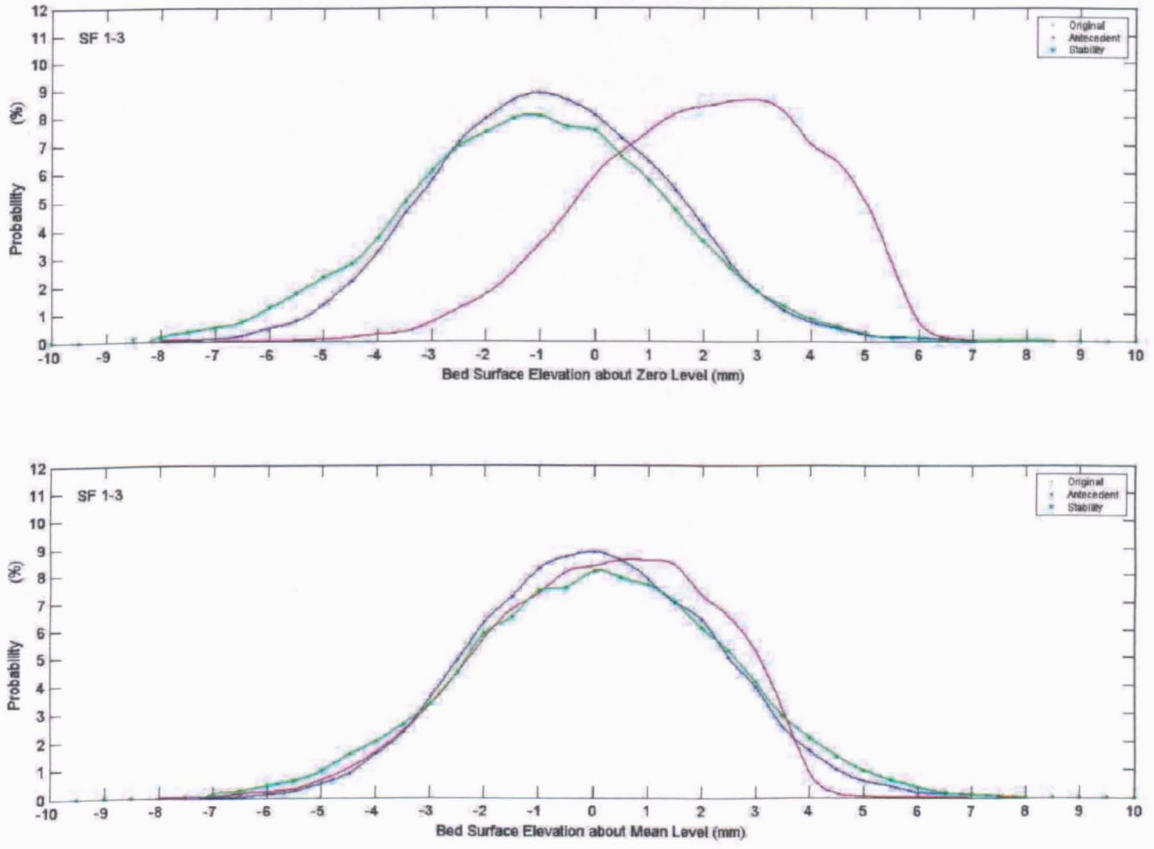

Figure 4.24. Probability distribution of bed surface elevation about zero and mean level for Experiment SF 1-3

of the bed surface between different time. This plot indicates the level of degradation with zero as the datum for all distributions. Another method is then applied by examining the distribution of deviation of bed elevations from the mean bed surface with the mean level

being taken as the zero datum at each time. However, the use of this reference level which has no major physical significance may cause all grains within a particular area of the bed to be positioned above or below the mean bed surface even though when examined in detail they may occupy very similar topographic positions in relation to their immediate neighbours. However this method still allows the differences in the bed surface arrangement to be examined by comparing the shape of distribution for different stages of the experiment.

The bed elevation distribution curve of the original bed is not symmetrical (Figure 4.24). The distribution skews to the right indicating the domination of positive bed elevation. After the bed exposed to three hours of antecedent flow the shape of distribution changes. It skews dramatically to the left. A substantial amount of bed material has been transported during antecedent flow test. The distribution is now quite symmetrical in shape. However there is a large tail on the positive side started about 4 mm above the mean level. This tail indicates the presence of a number of isolated larger grains resting on the bed surface.

At the end of stability test, the bed surface elevation distribution indicates that further and probably different degradational processes occurred. The number of both large positive and negative bed elevations from the mean increases. An increase in exposure of large grains was continued during stability test for antecedent flow SF 1-3. However, the level of increase is relatively small in comparison to antecedent flow test. This is caused by the degradation processes that was continued but without any replacement of fine material to fill the gaps. This phenomenon is reflected by the changes in the negative tail which is evident at the end of stability test. In the previous antecedent flow the changes are very small indicating that there were many fine grains filling gaps on the bed surface.

4.3.2. STEADY ANTECEDENT FLOW EXPERIMENT SF 1-6

4.3.2.1. Bedload Transport Rate and Composition SF 1-6

There was a significant change in bedload transport rate during the initial stages of antecedent flow. The bedload drops rapidly within the course of one hour to a rate of about 0.2 g/s/m. In the next hour the rate fluctuated but still very closed to this value with a range of ± 0.05 g/s/m.

Another rapid drop took place again in the third hour of the test. At this stage the bedload transport rate decreased to approximately half of the previous hour to 0.1 g/s/m. Figure 4.25 shows that after this period the bedload transport rate was low and almost constant during the remaining hours. This pattern of transport suggests that bed was highly mobile during the first 180 minutes involving significant release of material from bed during the first 60 minutes of time elapsed. Re-arrangement of the bed is the result of sediment movement As the armouring process continued the transport rate continued to decrease. It is believed that after 180 minutes, the bed started to develop differently. This is reflected in the slower and almost constant rate of bedload transportation.

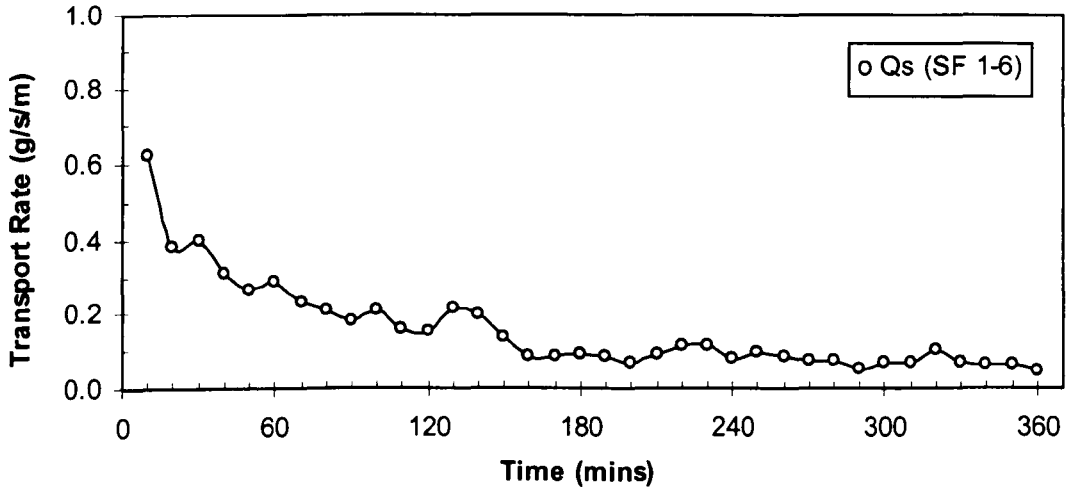

Figure 4.25. Time variation of transport rate for antecedent flow Experiment SF 1-6

The composition of the transported bedload during initial stage of antecedent flow was dominated by finer mode. As can be seen from Figure 4.26, throughout antecedent flow Experiment SF 1-6, more sediment was transported in the finer mode than in the coarse mode. In the last hour the rate of this mode reduced as the consequences of the availability of this material left on the bed becoming less. However, the contribution of this mode was still higher than the coarse mode. The finer mode also shows a similar pattern of grain size distribution with the modal size of finer grains was 0.355 for the whole duration of the test. More interesting features are shown by the changes in the coarse mode. As the test progresses the modal size of coarse grain shifts to the right from a grain size of 5.6 mm to the larger grain

sizes. This suggests that the level of exposure of the larger grains increases with time. This leads to the flow being able to transport the larger grains. Although the percentage of finer grain transported during the test was dominant, this is not an indication that the coarser mode was more stable. It is the reflection of the ability of the flow to continuously remove the finer grain for the whole duration of the test.

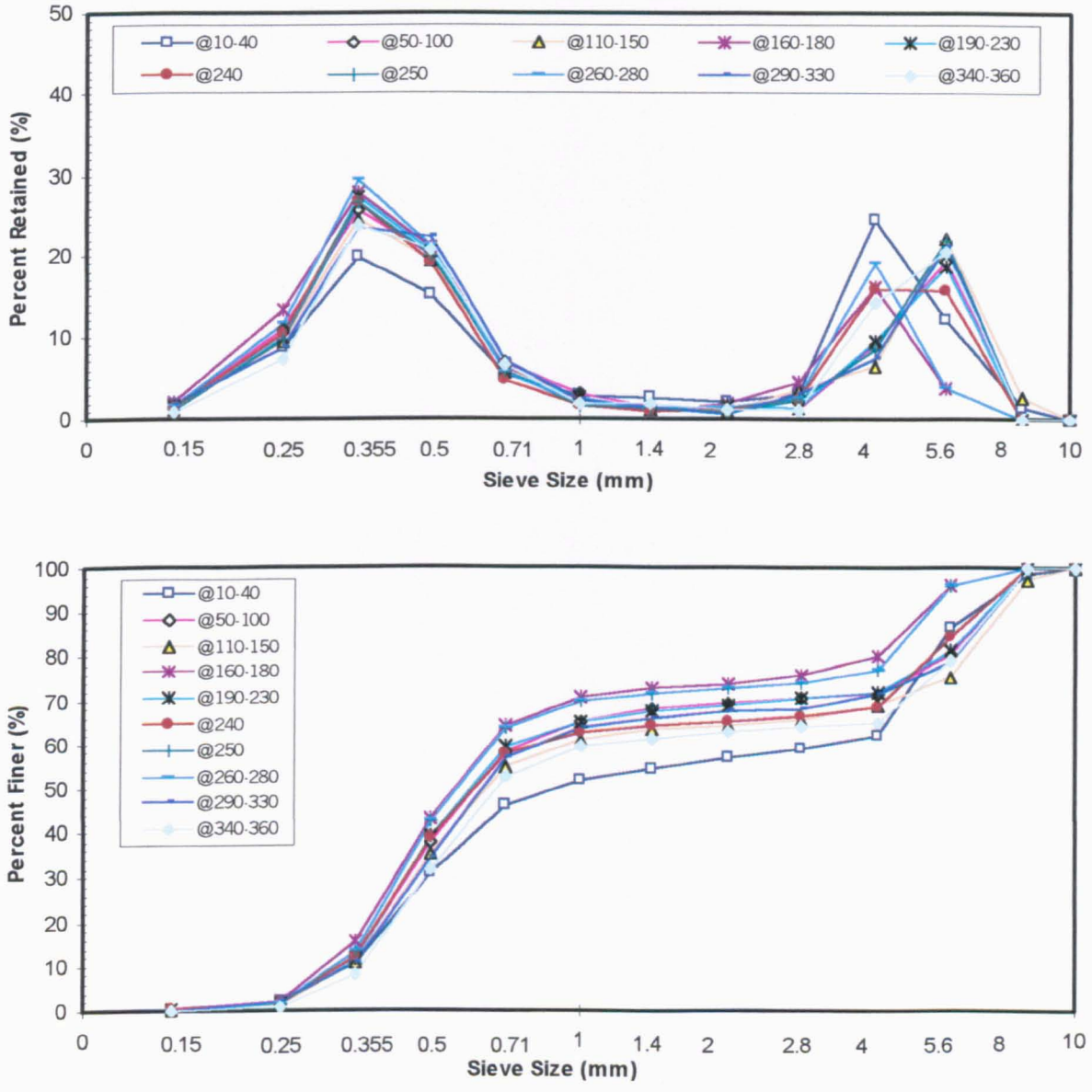

Figure 4.26. Grain size distribution curve of transported bedload for antecedent flow Experiment SF 1-6

The surface grain size distribution was estimated in a similar manner as in Experiment SF 1-3. From the original mixing layer available for transport, 640 grams or 1.6 % was transported. Table 4.13 shows that grains in the fine mode contributed more than grains in the coarse mode in transport rate as suggested by the distribution curve in Figure 4.28. In summary there appears that after 40 minutes the proportion of finer mode was relatively stable whereas the modal grain size of the coarse mode started to fluctuate. Overall the bedload is finer than the original bed material so the bed surface has coarsened during the antecedent flow test.

Table 4.9. Summary of the average fractional bedload composition produced by antecedent flow Experiment SF 1-6

Sieve size (mm)	Original composition of surface layer (%)	Fractional transported bedload (%)	Estimated composition of surface layer (%)
10	1.730	0.000	1.757
8	8.570	0.830	8.693
5.6	34.660	16.212	34.952
4	19.600	14.238	19.685
2.8	6.860	2.518	6.929
2	3.530	1.489	3.562
1.4	2.510	1.728	2.522
1	1.850	2.628	1.838
0.71	2.680	6.098	2.626
0.5	6.840	18.743	6.652
0.355	7.420	23.991	7.158
0.25	2.710	9.780	2.598
0.15	0.940	1.612	0.929
receiver	0.100	0.132	0.099
Total	100	100	100

4.3.2.2. Variations of Average Nearbed Streamwise Velocity and Bed Shear Stress SF 1-6

Longer duration of the antecedent flow Experiment SF 1-6 allowed more measurements of nearbed streamwise velocity to be collected. These measurement were carried out by ADV probe at central point of the measurement grid. No data available at time elapsed when the measurement was replaced by observation to each point of the grid, i.e. at times between 10 -

90 minutes and 270 - 340 minutes, so that only the results of measurement available for central point are presented.

It can be seen in Figure 4.27 that the average nearbed streamwise velocities are sensibly constant. A small variations in the individual values of both streamwise velocity (u) and vertical velocity (v) produced fluctuation in the average bed shear stresses with the range of 20 % from the average value over the whole test. However, this variation cannot be used to claim as the important factor in the variation of transport rate. In order to obtain the characteristic of the flow in regard to the contribution in grain entrainment process, the turbulent energy near the bed was observed.

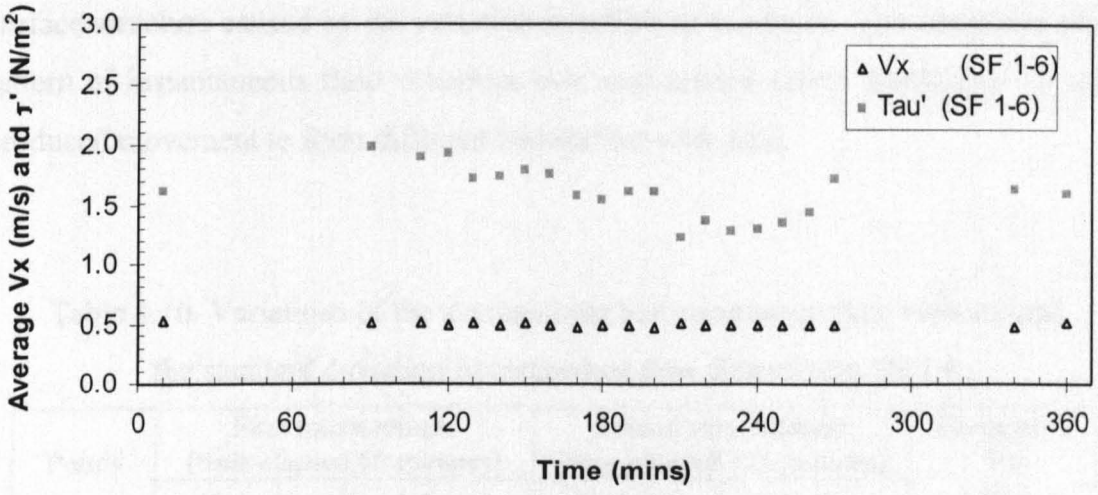

Figure 4.27. Variation of time averaged nearbed streamwise velocity and bed shear stress during antecedent flow of Experiment SF 1-6

A longer time interval of 255 minutes between two measurement of the streamwise nearbed flow velocity on the measurement grid was applied in experiment SF 1-6. It was done in an attempt to observe the differences of the average streamwise velocity of the grid, which may occur during a longer time than in experiment SF 1-3. Table 4.10 shows that the average streamwise flow velocity measured at different time elapsed with longer interval between measurement are more fluctuated. The variations of changes are slightly wider with the range from 4.7 % decrease to 4.6 % increase except at Point A5. This point experience a big

difference with the value reduces to 17.6 %. It can be seen that the standard deviation of the second measurement at Point A5 is very high compare to the other points.

The velocity decreased at the majority of the measurement points while points A1, E1 and I1 show an increase. This is interesting, as these points (A1, E1 and I1) were located in the same line in the streamwise direction (Figure 4.28). In line 3, a different pattern of change occurred with decreasing values of average streamwise velocity found in the second measurement, while in the rest of the area (line 5), the upstream point A5 experienced a decrease in average streamwise velocity as well as the next point E5. The furthest downstream point (I5) has a constant value of average velocity. These patterns indicate that there is a possibility that variations in nearbed velocities occur over a relatively small area. As flow discharge was kept constant, it is suspected that variations in average streamwise were due to the changes in the bed surface structure caused by the variation in sediment transport. The integrated effects of the pattern of instantaneous fluid velocities over and around grains destabilise the sediment and produced movement to form different bed surface with time.

Table 4.10. Variations of the average near bed streamwise flow velocity and the standard deviation in antecedent flow Experiment SF 1-6

Points	First measurement (time elapsed 60 minutes)		Second measurement (time elapsed 313 minutes)		Changes of Vx (%)
	V_x (m/s)	σ (m/s)	V_x (m/s)	σ (m/s)	
A1	0.542	0.098	0.551	0.102	1.661 (+)
A3	0.502	0.104	0.490	0.105	2.390 (-)
A5	0.490	0.102	0.404	0.249	17.551 (-)
E1	0.523	0.100	0.547	0.095	4.589 (+)
E3	0.511	0.104	0.487	0.100	4.697 (-)
E5	0.498	0.100	0.489	0.094	1.807 (-)
I1	0.521	0.101	0.533	0.099	2.303 (+)
I3	0.532	0.104	0.523	0.106	1.692 (-)
I5	0.487	0.102	0.487	0.092	0
Average	0.512	0.102	0.500	0.116	-

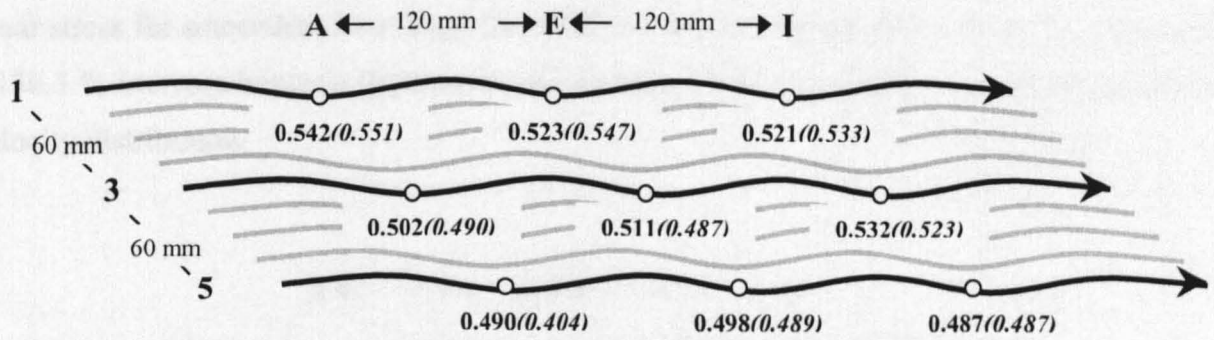

Figure 4.28. Distribution of average nearbed streamwise flow velocity (m/s) in antecedent flow Experiment SF 1-6 (first measurement in bold, second measurement in brackets)

Table 4.11. Variations of the average bed shear stress and the standard deviation in antecedent flow Experiment SF 1-6

Points	First measurement (time elapsed 60 minutes)		Second measurement (time elapsed 313 minutes)		Changes of $\overline{\tau}$ (%)
	$\overline{\tau}$ (N/m^2)	σ (N/m^2)	$\overline{\tau}$ (N/m^2)	σ (N/m^2)	
A1	2.152	17.194	4.746	18.274	120.539 (+)
A3	-2.260	15.716	0.826	16.336	136.549 (+)
A5	5.084	16.301	2.704	16.142	46.814 (-)
E1	10.221	17.732	7.907	18.073	22.640 (-)
E3	9.698	18.297	5.027	15.664	48.165 (-)
E5	2.555	17.302	4.779	16.585	87.045 (+)
I1	4.574	18.252	-0.359	17.539	107.849 (-)
I3	2.010	17.040	0.956	17.086	52.438 (-)
I5	1.815	15.167	-1.059	15.304	158.347 (-)
Average	3.983	17.000	3.661	16.778	-

Table 4.11and Figure 4.29 show that the patterns of bed shear stress calculated using Equation 3.10 do not automatically follow the pattern in streamwise velocity. These variations appear to have no systematic pattern. The wide variation is caused by the variation in vertical velocity. The level of fluctuation influenced the level of bed shear stress and produced inconsistency in the spread of bed shear stress over the observation area. It is very clear that the scattered values of bed shear stress in Table 4.11 is an indication of the continuous fluctuation of flow velocity in vertical direction. It is then assumed that the variation of bed

shear stress for antecedent flow Experiment SF 1-6 which ranging from a 158.3 % decrease to a 136.5 % increase between the measurements are primarily caused by adjustment in vertical velocity distribution.

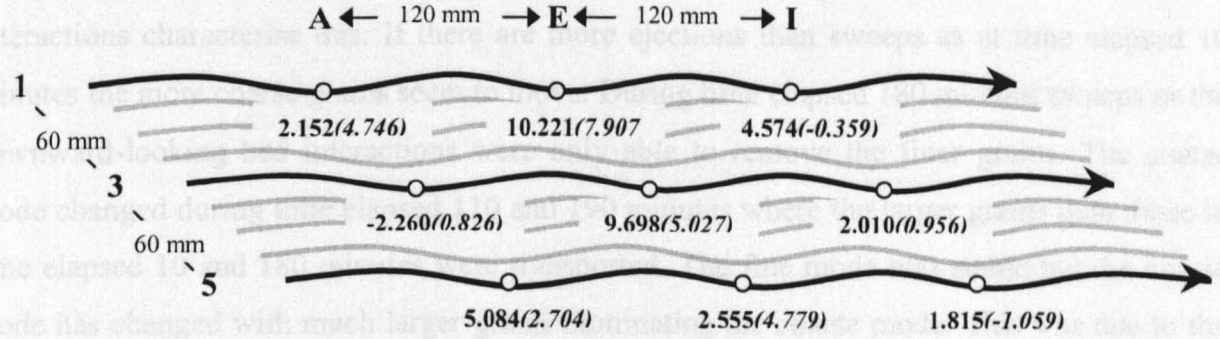

Figure 4.29. Distribution of average bed shear stress (N/m^2) in antecedent flow Experiment SF 1-6 (first measurement in bold, second measurement in brackets)

4.3.2.3. Bursting Events and Flow Momentum SF 1-6

The effect of the number and size of near bed bursting events was also examined using data collected in SF 1-6. The observation shows that the occurrences of ejections were more often than sweeps. The average frequency of ejections throughout the test is 0.9867 Hz while the average frequency of sweeps is 0.8800 Hz. This suggests that almost 53 % of events is containing the ejections while the sweeps is about 47 %. This finding opposes the point stated by Nelson (1995), who claimed that sweeps are more common although he underlined that sweeps are not individually more effective in moving the sediment. The dominance of ejections and their longer duration is thought likely to contribute more to the bed shear stress production rather than sweeps. These measurements do not agree with the early findings and assumption by Roy et al (1996) that the shear stress production in the near-bed region is clearly sweeps dominated.

In antecedent flow Experiment SF 1-6 it is also observed that the average duration of ejections is 0.0582 seconds. This is longer than the average duration of sweeps, which has 0.0500 seconds. In Table 4.12 four different times elapsed are selected to observe the pattern of

momentum transfer by ejections and sweeps in relation to the change in the grain size distribution of transported bedload. Although at time elapsed 10 and 180 minutes the bedload has similar modal grain sizes (Figure 4.30), there is different pattern in which more coarser bedload is transported at time elapsed 10 minutes while finer grains were more dominant during time elapsed 180 minutes. It is suspected that the outward and downward-looking bed interactions characterise this. If there are more ejections than sweeps as at time elapsed 10 minutes the more coarse grains seem to move. During time elapsed 180 minutes sweeps or the downward-looking bed interactions were only able to remove the finer grains. The coarse mode changed during time elapsed 110 and 190 minutes where the larger grains than those in time elapsed 10 and 180 minutes were transported. The fine mode was stable but the coarse mode has changed with much larger grains dominating the coarse mode. This was due to the more ejection in comparison to the sweeps event. It seems that the grain size distribution of bedload have a correlation with the bursting event. Time elapsed 110 and 190 minutes had been dominated by ejections with the proportion higher than that of time elapsed 10 and 180 minutes. The more frequent ejections allowed for the removal and transportation of larger coarse grains.

Table 4.12. Summary of bursting events at selected time elapsed in antecedent flow Experiment SF 1-6

Parameter descriptions	Time elapsed (minutes)			
	10	110	180	190
Threshold values (m^2/s^2)	0.0082	0.0091	0.0075	0.0081
Number of ejections	192	203	200	212
Number of sweeps	187	196	206	171
Frequency of ejections (Hz)	0.9600	1.0150	1.0000	1.0600
Frequency of sweeps (Hz)	0.9350	0.9800	1.0300	0.8550
Average duration of ejections (s)	0.0542	0.0520	0.0530	0.0521
Average duration of sweps (s)	0.0537	0.0498	0.0493	0.0503

It is suspected that the high level of turbulence that is resulted from fluctuation in vertical velocity transported not only finer grains but also removed the considerable amount of larger grains. High fluctuations in vertical velocity produce outward interaction and lead to positive momentum in the flow. The examples of momentum distribution during both of ejections and

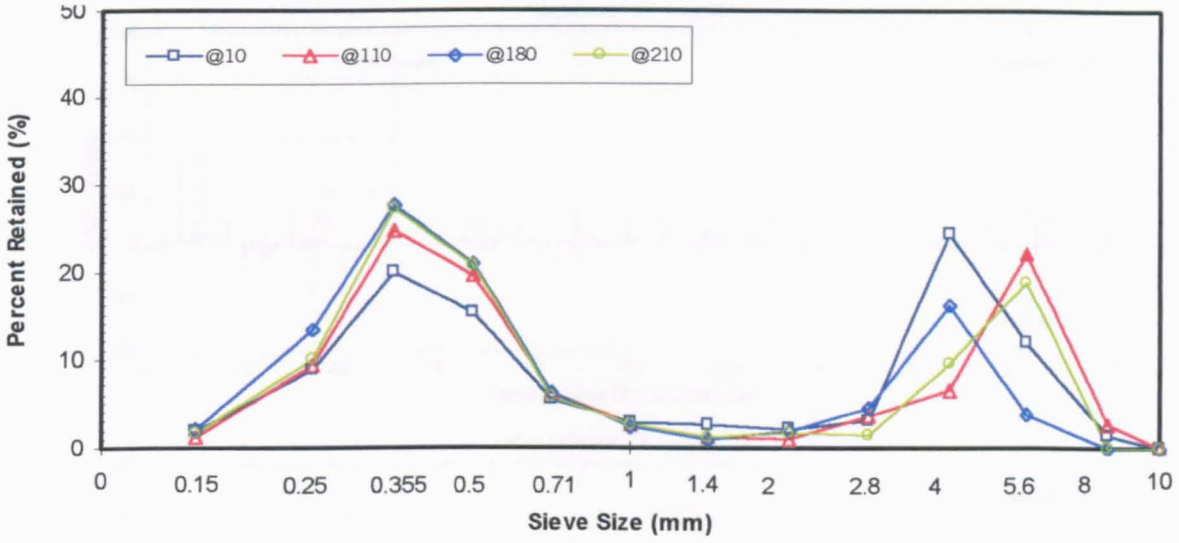

Figure 4.30. Grain size distribution of transported bedload at selected time elapsed in antecedent flow Experiment SF 1-6

sweeps are presented in Figure 4.30. It shows that the bursting events during Experiment SF 1-6 are clearly dominated by ejections. The low magnitude of momentum of downward-looking bed interaction is also noticeable from Figure 4.31.

Further investigation shows that the probability distribution of momentum magnitudes of the ejections and sweeps (Figure 4.32) have a much stronger correlation with the bedload pattern mentioned above. There is no significant difference in the distribution of sweeps with low values of momentum in the range of up to 5 kg/ms dominates the events in all observed time elapsed. Major differences are observed in the probability distribution of ejections in the range between 5 to 25 kg/ms.

The grain size distribution curves that show the consistent mode of finer grains indicates that momentum available during experiment were sufficient enough to transport these grains. However, the higher values are recognised to be responsible for removal of larger grains. This is indicated by the changes in the coarse modal grain size at time elapsed 110 and 190 minutes during which the larger magnitudes of momentum per unit area took place. Time elapsed 110 has more momentum around 20 kg/ms while time elapsed 190 containing more momentum with the magnitude of around 22 kg/ms. The probability density of a relatively high

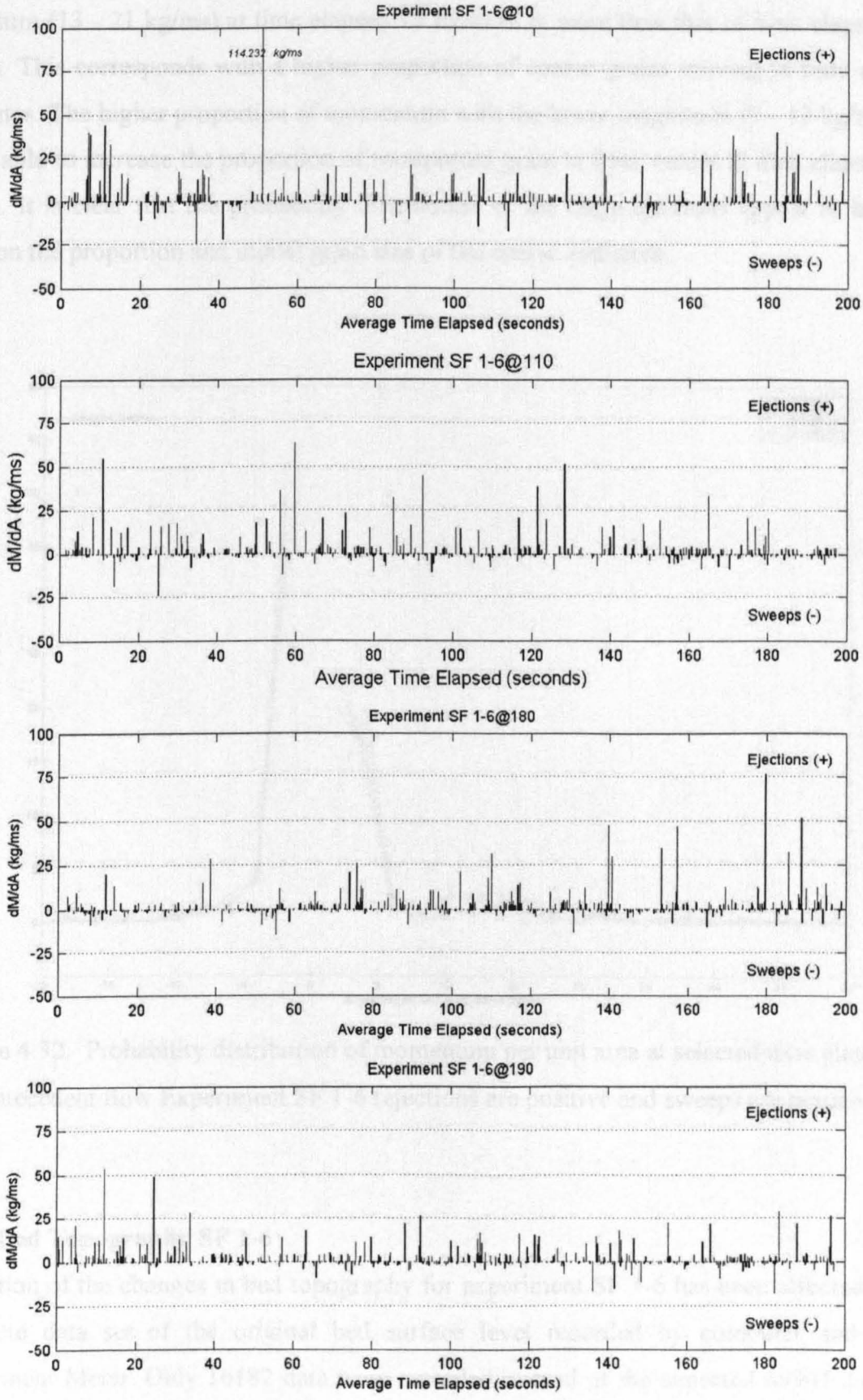

Figure 4.31. The sequence of momentum per unit area and its magnitude at selected time elapsed in antecedent flow Experiment SF 1-6

momentum (13 - 21 kg/ms) at time elapsed 10 minutes is more than that of time elapsed 180 minutes. This corresponds with a higher proportion of coarse grains moving at time elapsed 10 minutes. The higher proportion of momentum with the lower magnitude (9 - 13 kg/ms) can only be able to increase the proportion of transported grain in finer modes at time elapsed 180 minutes. It is clear that the probability distribution of the large ejections appear to have an impact on the proportion and modal grain size of the coarse sediment.

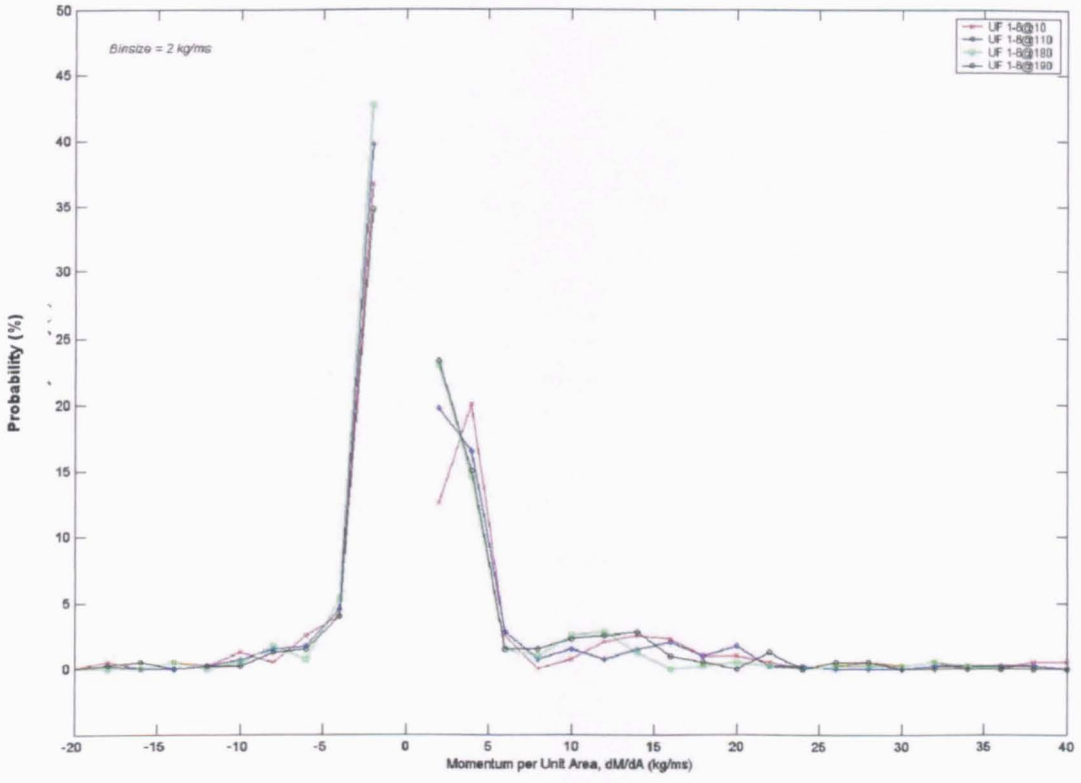

Figure 4.32. Probability distribution of momentum per unit area at selected time elapsed in antecedent flow Experiment SF 1-6 (ejections are positive and sweeps are negative)

4.3.2.4. Bed Topography SF 1-6

Observation of the changes in bed topography for experiment SF 1-6 has been affected by an incomplete data set of the original bed surface level recorded by computer and Laser Displacement Meter. Only 16182 data were recorded instead of the expected 49941 data. As the result of this problem, only the bed surfaces after antecedent flow and final bed after stability test were plotted.

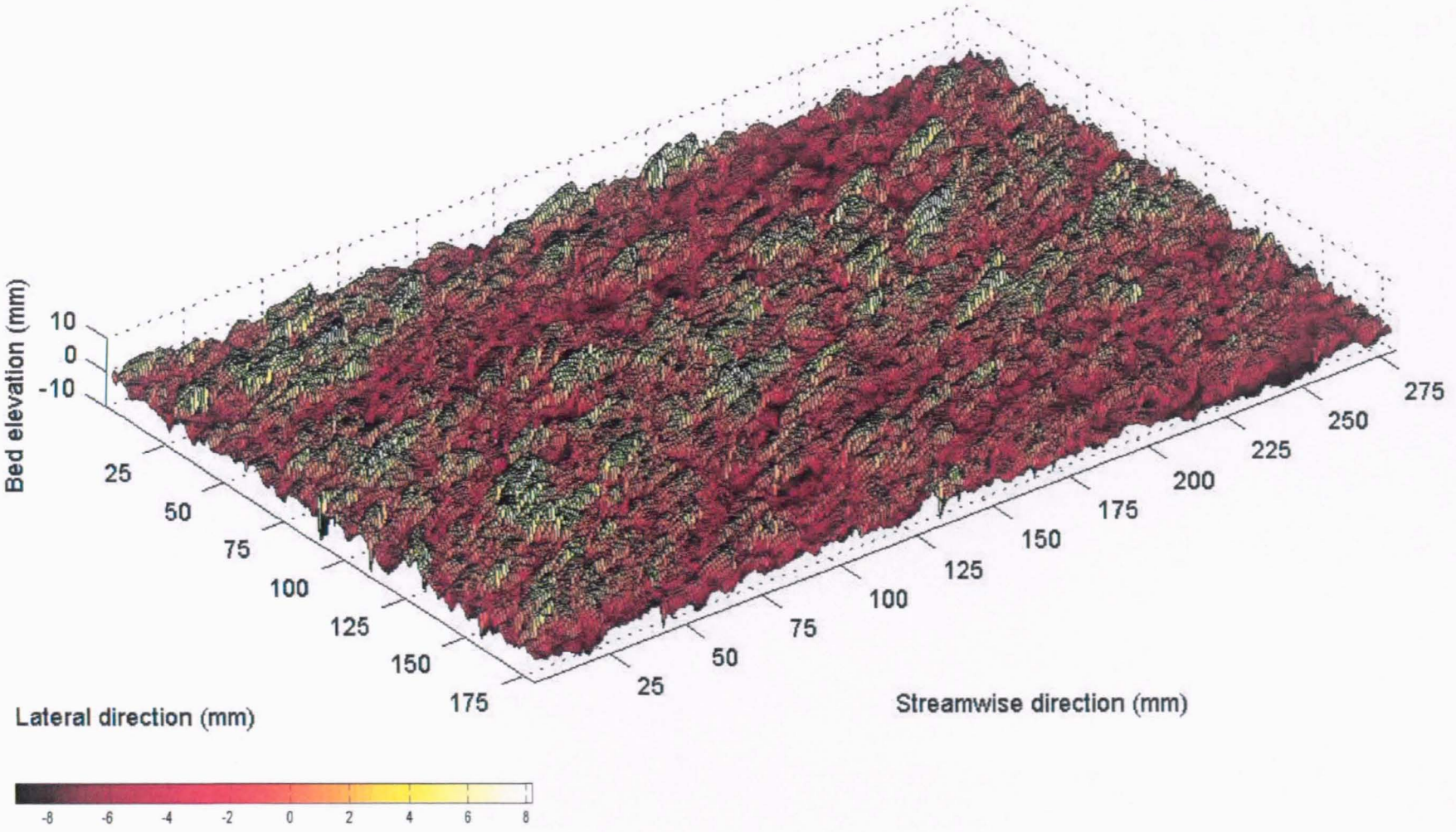

Figure 4.33. Bed surface topography of the measurement grid after antecedent flow Experiment SF 1-6

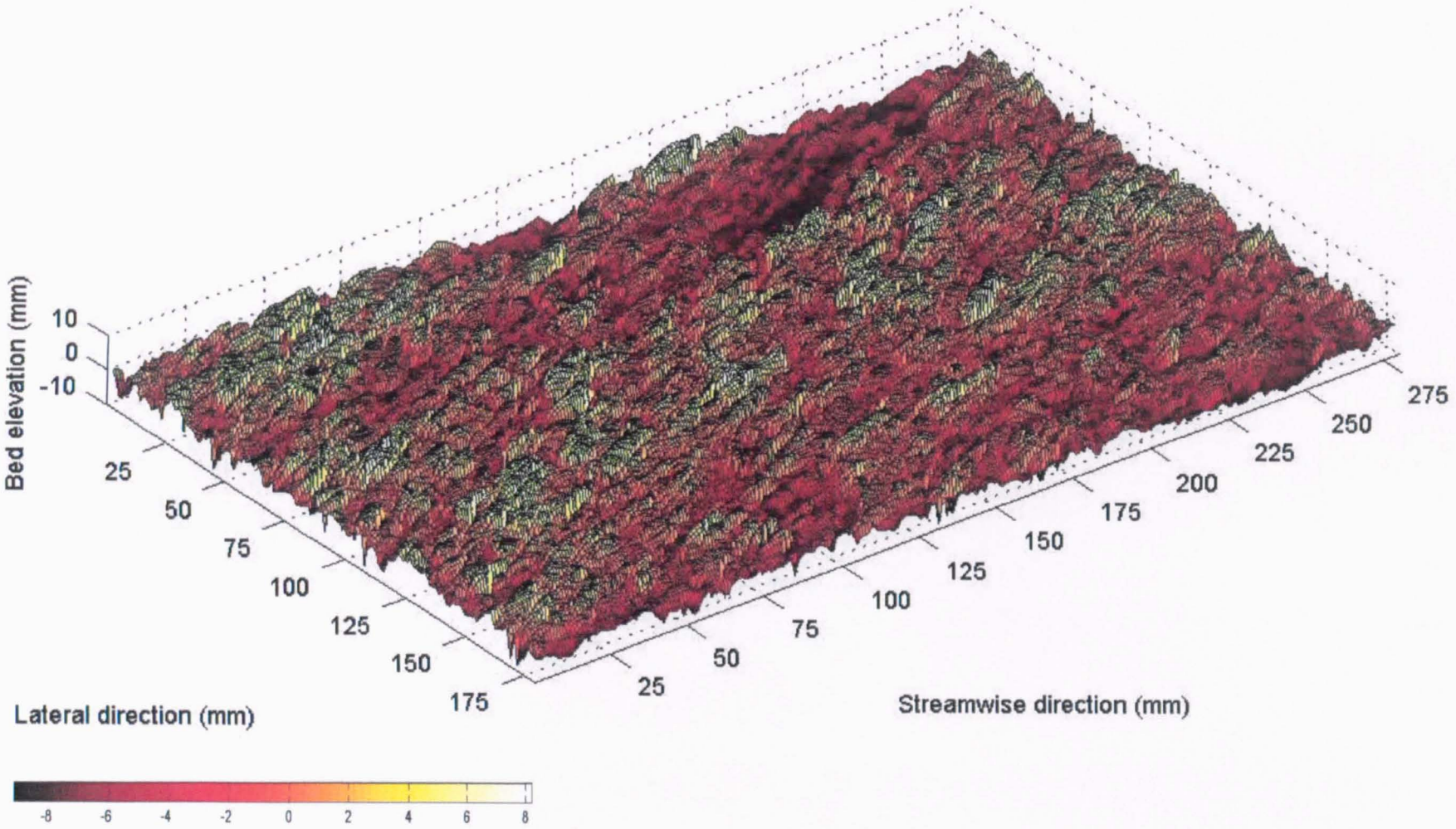

Figure 4.34. Bed surface topography of the measurement grid after stability test Experiment SF 1-6

As shown in Figure 4.33 and Figure 4.34 a relatively similar pattern in bed surface topography formed by the 6 hours antecedent flow and stability test have been found. The average bed surface elevation decreased from 2.032 mm to 2.054 mm below the zero datum. This indicates that there was a small amount of further degradation occurred during the stability test with the increasing darker spots covering some areas. However, some peaks with high exposure, e.g. at points (30,70), (50,15), (60,100), (135,90), (210,90) and (220,50), show permanent appearances in both stages. The similar levels of valley-formed structures in some areas before and after stability test are also found in this experiment. The resistances of these features indicate that the 6 hours antecedent flow had formed a more stable bed than the bed exposed to the 3 hours antecedent flow test.

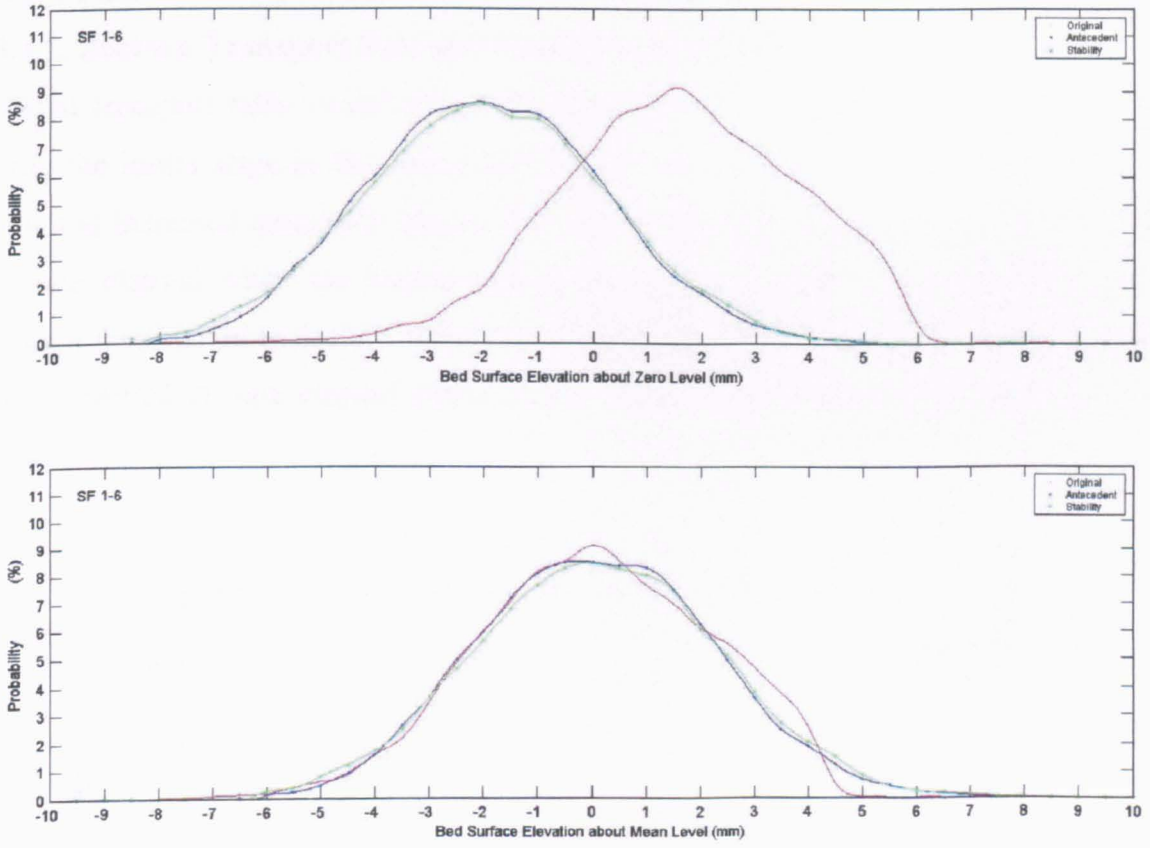

Figure 4.35. Probability distribution of bed surface elevation about zero and mean level for Experiment SF 1-6

The level of grain exposure was investigated by examining the probability distribution curve of bed elevations (Figure 4.35). The original bed distribution could be adequately described

by the available 16182 data because of the relatively homogeneous nature of the bed surface. Figure 4.35 shows that the level of exposure either about zero level and average bed level before and after stability test produced almost identical curves. However it is not very difficult to distinguish between them. A small variation about the zero value describes the small range in the bed elevation. This coincides with a relatively similar pattern mentioned earlier in relation to those appears in Figure 4.34. Figure 4.35 indicates that there is an increase in both negative and positive tail. Although these increases are less than those in stability test SF 1-3 (see Figure 4.24), the negative tail indicates that to some extent the degradation phase was taking place during the stability test SF 1-6. A number of isolated grains also exist on the bed.

4.3.3. STEADY ANTECEDENT FLOW EXPERIMENT SF 1-9

4.3.3.1. Bedload Transport Rate and Composition SF 1-9

Bedload transport rates variation in experiment SF 1-9 indicated a more complex pattern during the initial stage of the antecedent flow. It started with a low transport rate of 0.057 g/s/m and increased quickly to almost four times within 80 minutes (Figure 4.36). This was the time elapsed when the bedload transport reached its peak rate of 0.227 g/s/m. The transport then started to decline, which continued until very low transport rates of 0.019 g/s/m were measured at time elapsed 540 minutes. These transport rates were 8 % of the peak value.

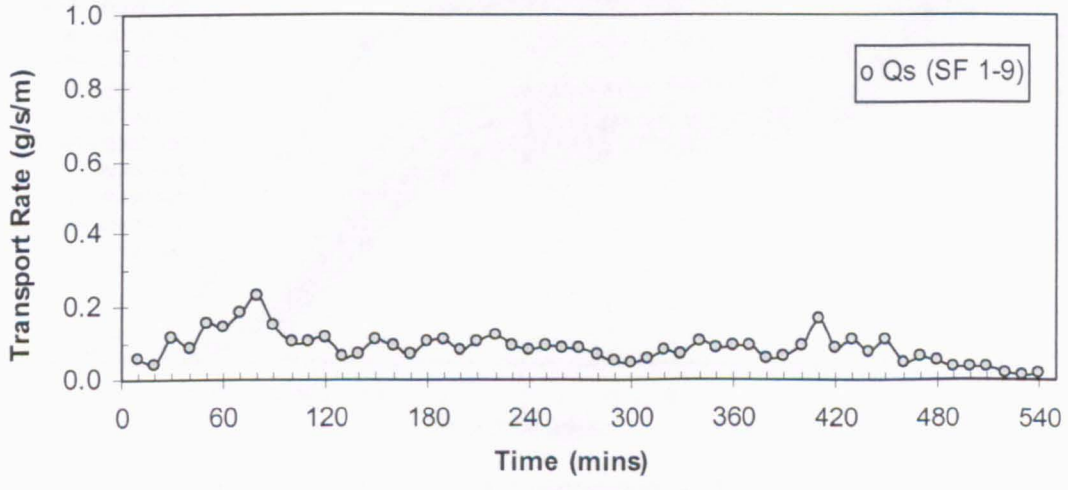

Figure 4.36. Time variation of transport rate for antecedent flow Experiment SF 1-9

In term of grain size, grains in both the fine and the coarse mode give similar contributions in the transported bedload during the high transport rate (time elapsed 50 - 100 minutes) as shown in Figure 4.37. However, the finer grains were dominant in the very initial stage of antecedent flow. Figure 4.39 shows that during the first 40 minutes of time, grain sizes of 0.25 mm and 0.15 mm contributed significantly to the transported bedload compared to the latter time in the test. In the next stage the finer mode was constant with the highest contribution from 0.355 mm grain size. Grains in the coarse mode present different pattern. Grain of size 4.0 mm gave maximum contribution for certain times elapsed but the modal grain size in the

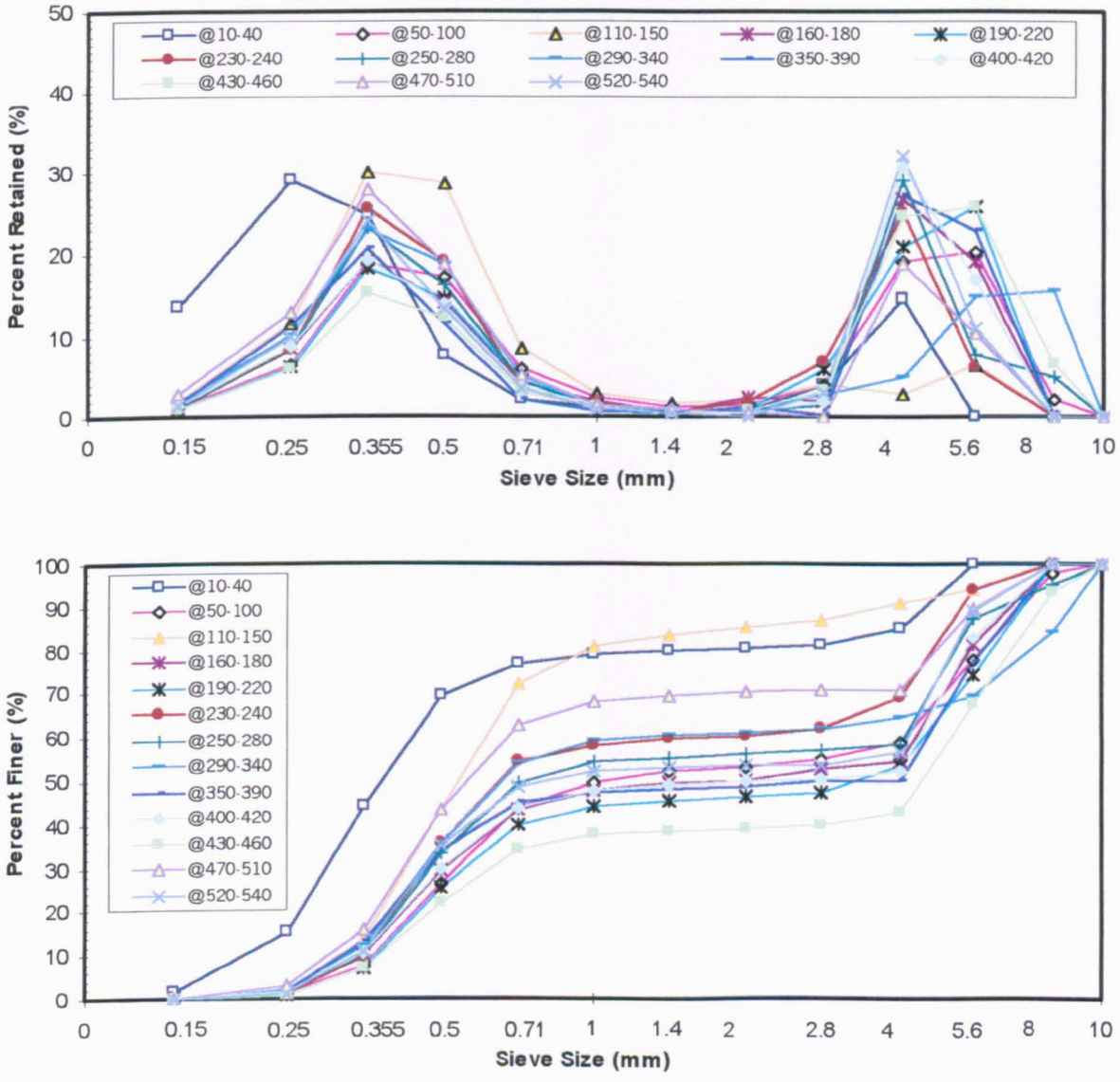

Figure 4.37. Grain size distribution of transported bedload for antecedent flow Experiment SF 1-9

coarse mode changed at different time elapsed. This leads to the conclusion that the larger grains experienced phases of increasing exposure making them less stable so that their mobility increases and decreases periodically in the later stages of this test.

Table 4.13. Summary of the average fractional bedload composition produced by antecedent flow Experiment SF 1-9

Sieve size (mm)	Original composition of surface layer (%)	Fractional transported bedload (%)	Estimated composition of surface layer (%)
10	1.730	0.000	1.753
8	8.570	2.642	8.648
5.6	34.660	15.931	34.906
4	19.600	19.583	19.600
2.8	6.860	3.160	6.909
2	3.530	1.126	3.562
1.4	2.510	0.821	2.532
1	1.850	1.651	1.853
0.71	2.680	4.695	2.653
0.5	6.840	16.454	6.714
0.355	7.420	21.672	7.233
0.25	2.710	9.868	2.616
0.15	0.940	2.154	0.924
receiver	0.100	0.243	0.098
Total	100	100	100

Overall, the finer mode contributed more than coarser mode in transported bedload leaving the bed generally. The consistency of the finer mode is also evident in Table 4.13. The grain size of 0.355 mm produced the highest contribution to the transported bedload compared to the nearest grain sizes of 0.5 mm and 0.25 mm respectively. More than 20 % of transported bedload containing 0.355 mm grains. This is clearly presented by the curve in Figure 4.37. Different features are described by grains in the coarse mode. The grain size of 4 mm is the dominant among the coarser grains. It contributes to almost 20 % of total transported bedload. However a moderately high contribution by the coarser mode of 5.6 mm grain size indicates that the level of exposure established during antecedent flow demonstrated that the flow was sufficient enough to move these larger grains.

4.3.3.2. Variations of Average Nearbed Streamwise Velocity and Bed Shear Stress SF 1-9

Similar to that applied in the previous two test, the nearbed streamwise velocities measured in antecedent flow Experiment SF 1-9 were also observed (Figure 4.38). Again, these measurement were carried out by ADV probe at central point of the measurement grid so that no data was represented by time elapsed where different type of measurement was carried out. It can be seen in Figure 4.38 that the average nearbed streamwise velocities in antecedent flow Experiment SF 1-9 are relatively constant throughout the test. The variations of the average nearbed streamwise velocity values of each time elapsed to the average nearbed streamwise velocity for the whole observations is very small with the range from - 5 % to + 4 %. However, in the average values of the bed shear stress of each time elapsed, the range of variation to the average values of the whole observation is wider. The lowest average values of time elapsed is -14 % from the average values of the whole observation while the highest values is + 19 % more. A small variation in the individual values of nearbed streamwise velocity caused the variation in the average values. The variation in vertical velocity also produced fluctuation, which leads to the higher variation in the average bed shear stress.

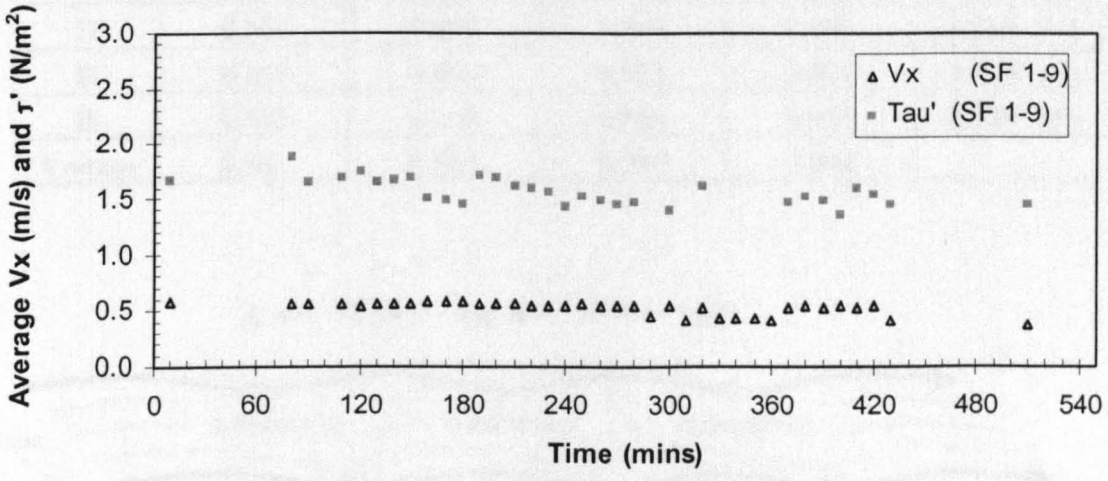

Figure 4.38. Variation of time averaged nearbed streamwise velocity and bed shear stress during antecedent flow Experiment SF 1-9

In antecedent flow Experiment SF 1-9 the average nearbed streamwise velocities were measured over the measurement grid point with a time interval between two series of

measurement was 420 minutes. The changes in the time-averaged values of streamwise nearbed velocity are very small with the range of variations from a 6.1 % decrease to 3.8 % increase. Although the difference in standard deviation presented in Table 4.14 are very small, it shows that during the first measurement period the nearbed streamwise velocities were more widely dispersed. This suggests that there were disturbances that contributed to the fluctuated velocity. The disturbances may be caused by rigorous disruption of the bed at initial stage of experiment. The level of disturbances decreased during the second measurement taken 420 minutes after the first measurement.

Table 4.14. Variations of the average nearbed streamwise flow velocity and the standard deviation in antecedent flow Experiment SF 1-9

Points	First measurement (time elapsed 64 minutes)		Second measurement (time elapsed 484 minutes)		Changes of Vx (%)
	V_x (m/s)	σ (m/s)	V_x (m/s)	σ (m/s)	
A1	0.556	0.098	0.574	0.088	3.237 (+)
A3	0.532	0.104	0.539	0.095	1.316 (+)
A5	0.522	0.102	0.532	0.096	1.916 (+)
E1	0.546	0.100	0.563	0.093	3.114 (+)
E3	0.559	0.104	0.525	0.095	6.082 (-)
E5	0.530	0.103	0.550	0.091	3.774 (+)
I1	0.561	0.095	0.549	0.096	2.139 (-)
I3	0.558	0.096	0.525	0.097	5.914 (-)
I5	0.523	0.104	0.526	0.093	0.574 (+)
Average	0.543	0.101	0.547	0.094	

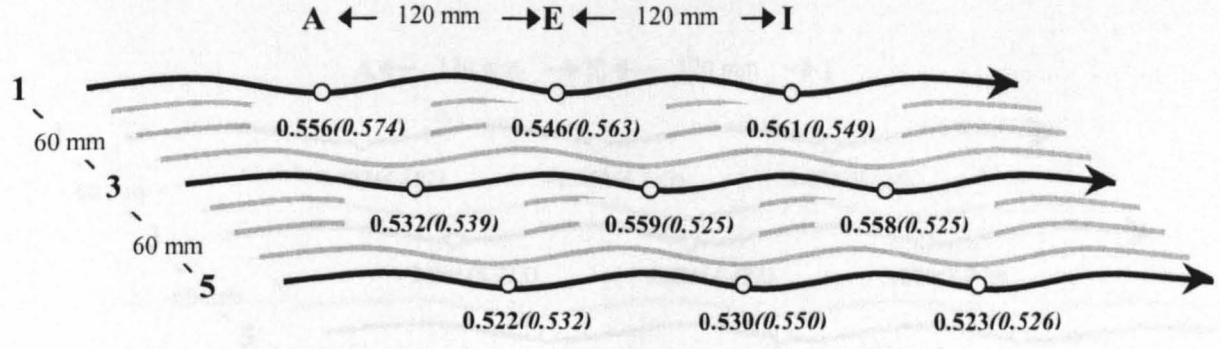

Figure 4.39. Distribution of average nearbed streamwise velocity (m/s) in antecedent flow Experiment SF 1-9 (first measurement in bold, second measurement in brackets)

The pattern of variation of time average bed shear stress calculated by summation of the bed shear stress at different points over the measurement area (see Equation 3.9 and Equation 3.15), are presented in Table 4.15 and Figure 4.40. Although the data show increasing values of average shear stress, no systematic pattern was found as the changes are inconsistently different from point to point. Rather unexpectedly, it is found that the first measurement of point E1 has a negative value. This condition may raise a question that there was a mistake in the measurement or it may be the ADV probe did not perform properly. Investigation on this problem suggested that such problem did not exist. Examination of the nearbed velocity both in streamwise and vertical direction found that the probability distributions both for

Table 4.15. Variations of the average bed shear stress and the standard deviation in antecedent flow Experiment SF 1-9

Points	First measurement (time elapsed 64 minutes)		Second measurement (time elapsed 484 minutes)		Changes of $\overline{\tau}$ (%)
	$\overline{\tau}$ (N/m^2)	σ (N/m^2)	$\overline{\tau}$ (N/m^2)	σ (N/m^2)	
A1	4.983	17.808	4.892	18.734	1.826 (-)
A3	2.891	17.981	5.715	17.356	97. 682 (+)
A5	2.408	17.893	6.873	18.251	185. 424 (+)
E1	-1.752	17.487	6.143	17.678	492.295 (+)
E3	9.436	19.422	4.492	16.469	52.395 (-)
E5	2.233	18.647	4.039	18.625	80.878 (+)
I1	9.036	19.030	9.868	18.578	42.408 (+)
I3	3.670	18.479	7.279	17.773	98.338 (+)
I5	1.892	17.483	1.677	17.574	11.364 (-)
Average	0.543	18.248	0.547	17.893	

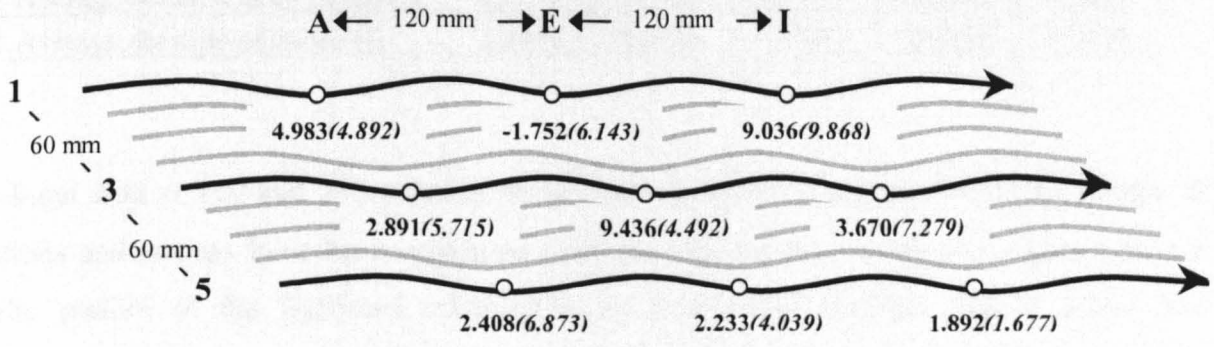

Figure 4.40. Distribution of average bed shear stress (N/m^2) in antecedent flow Experiment SF 1-9 (first measurement in bold, second measurement in brackets)

streamwise and vertical velocity are normal distributions as expected (Saadi, 2000). The calculation of average vertical velocity indicated that the upward direction was dominant at this point and thus produced negative values of shear stress.

4.3.3.3. Bursting Events and Flow Momentum SF 1-9

It is not very clear whether the variation in the average nearbed streamwise velocity and nearbed shear stress contribute to the variation in transport rate during the test. It is therefore underlines the important to explore the role of bursting events. Although at certain times the number of sweeps exceeds ejections during experiment SF 1-9, it is generally upward interactions (ejections) that are more common in bursting events. This is in agreement with the findings in experiments SF 1-3 and SF 1-6. Observation of 27 times during this test indicated that the outward interactions are 54.4 % of bursting events compared to 45.6 % for sweeps. This means that the probability of ejections taking place is almost 10 % higher than sweeps.

Table 4.16. Summary of bursting events at selected time elapsed in antecedent flow Experiment SF 1-9

Parameter descriptions	Time elapsed (minutes)				
	10	110	190	320	420
Threshold values (m^2/s^2)	0.0075	0.0079	0.0081	0.0080	0.0076
Number of ejections	205	196	220	219	208
Number of sweeps	210	206	197	201	210
Frequency of ejections (Hz)	1.0250	0.9800	1.1000	1.0950	1.0400
Frequency of sweeps (Hz)	1.0500	1.0300	0.9850	1.0050	1.0500
Average duration of ejections (s)	0.0535	0.0567	0.0502	0.0586	0.0583
Average duration of sweps (s)	0.0551	0.0524	0.0542	0.0523	0.0520

The burst data at 110 and 190 minutes, which have a different pattern in the occurrence of ejections and sweeps have been compared with the bedload data. Both time elapsed have a similar pattern of the fractional contribution in transported bedload (Figure 4.41). The difference between the two is that the overall transported bedload at time elapsed 110 minutes was dominated by finer grains whilst the coarse grains were most transported at time elapsed

190 minutes. It is believed that this pattern was caused by the ability of the outward interactions of the flow to remove the larger grains. Although the average duration of both ejections and sweeps at 190 minutes are slightly shorter than at 10 minutes, the ejections are more frequent at 190 minutes, most notably in the range of momentum between 9 and 15 kg/ms (Figure 4.43). This suggests that ejections frequency can have an impact on the entrainment of coarse grains. More observations of other selected times strengthen this conclusion. Examination of the data at 320 and 420 minutes show a similar pattern. At 320 minutes larger coarse grains are in motion than at 420 minutes. At 420 minutes the frequency of ejections and sweeps are the same. However at 320 minutes there are more ejections than sweeps. This demonstrates that when the ejections are more frequent, the fluid forces seem to be able to move even larger grains (grain size 8 mm at 320 minutes time elapsed) although the average duration of ejections and sweeps at both time elapsed are similar.

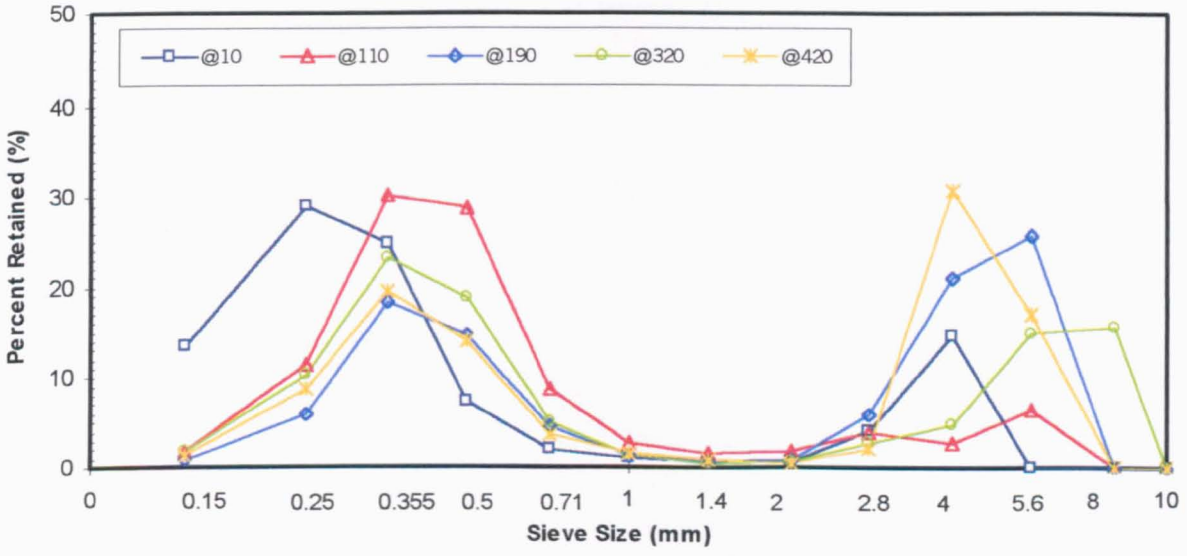

Figure 4.41. Grain size distribution of transported bedload at selected time elapsed antecedent flow Experiment SF 1-9

Figure 4.42 shows the sequence of momentum per unit area at selected time elapsed, which have different pattern in transported bedload. It has clearly been shown that the higher number and also size of ejections are more evident at time elapsed 320 minutes compared to time elapsed 110 minutes. During this time, the available fluid forces were sufficiently strong to remove the larger grains, which dominated the transported bedload at 320 minutes in comparison to the bedload at 110 minutes.

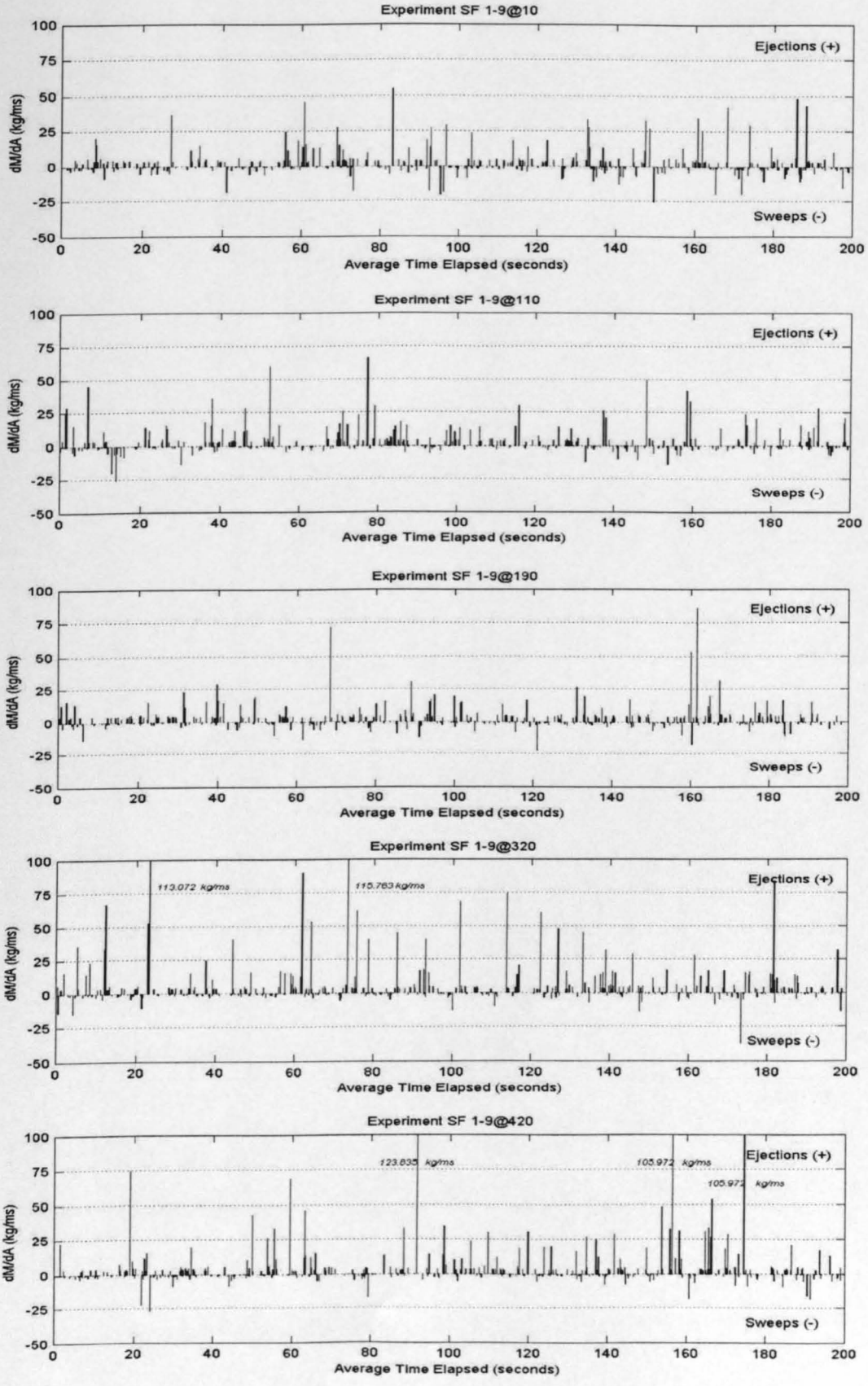

Figure 4.42. The sequence of momentum per unit area and its magnitude at selected time elapsed in antecedent flow Experiment SF 1-9

There is a higher proportion of ejections with a magnitude of momentum in the range of 9 - 15 kg/ms at time elapsed 320 minutes than at time elapsed 110 minutes, particularly in the range between 13 and 15 kg/ms (Figure 4.43). Thus, the outward interactions of fluid forces with high proportions of larger momentum ejections are more capable and likely to entrain the larger grains. At time elapsed 320 minutes, both fine and coarse material were transported with the proportion of larger grains increased as the neighbouring larger grains (8 mm) are also transported (Figure 4.41). The significantly higher proportion of the ejections momentum in the range between 13 - 15 kg/ms is believed to be responsible in transporting 8 mm grains.

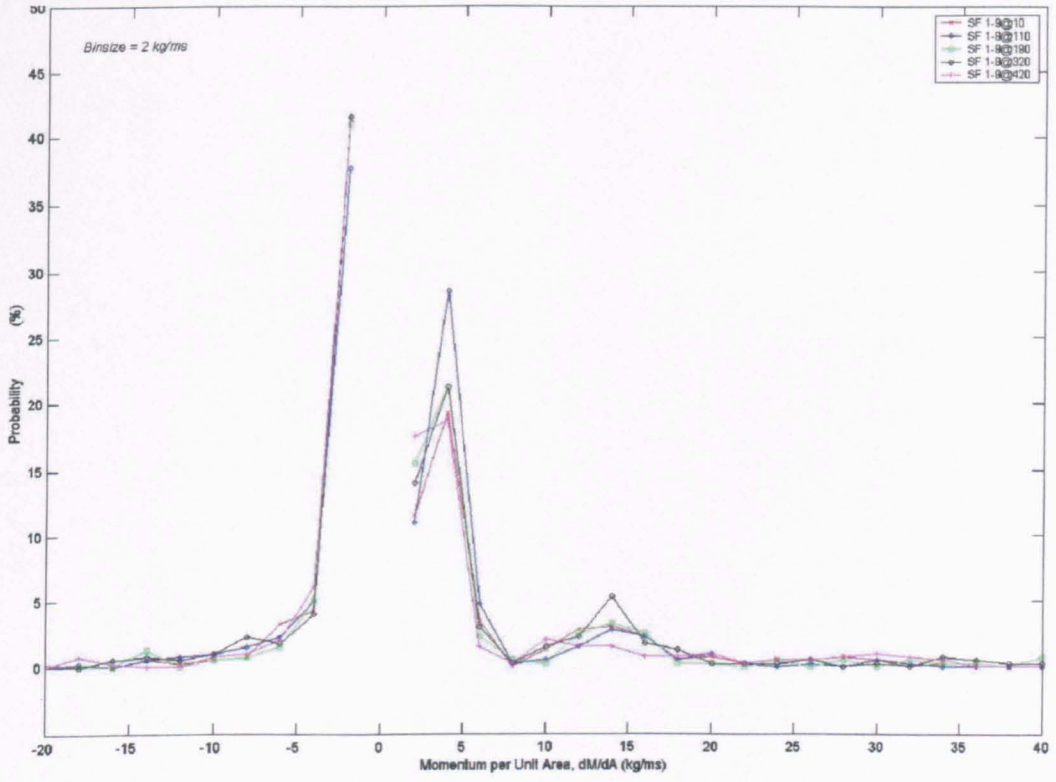

Figure 4.43. Probability distribution of momentum per unit area at selected time elapsed in antecedent flow Experiment SF 1-9 (ejections are positive and sweeps are negative)

In all the proceeding analysis, the role of sweeps is believed to be less important. The frequency and momentum magnitude of sweeps (Figure 4.43) appear to remain consistent through the rest even though significant changes in the bedload transport and composition were observed (Figure 4.41). The analysis also demonstrates the important of the frequency of

ejections and the magnitude of momentum caused by these events. The more frequent the ejections with the high magnitude of outward interactions the more larger grains transported irrespective of the average duration of both ejections and sweeps at observed time elapsed.

4.3.3.4. Bed Topography SF 1-9

The original bed shown in Figure 4.44 indicates the influence of the scrapping process. A relatively flat surface is shown with streamwise lines on top of the bed. It is also noticed that this flat surface formed at a slightly higher elevation than the scrapped beds for experiment SF 1-3 and SF 1-6. The average bed surface elevation of this original bed is 2.396 mm.

The application of 9 hours antecedent flow to the original bed produced diagonal patch of valley in the bed surface (Figure 4.45). Areas of high elevation are also produced as well as few very high isolated large grains resting on top of the bed. The plot shows that the reduction in the bed surface elevation covered most of the surface area. This was a result of destabilisation and dislodgement of grains during the antecedent flow test. After 9 hours of flow the average bed level decreased almost 2.5 mm to 0.080 mm below the zero datum.

An interesting feature is shown by comparing Figure 4.45 and Figure 4.46. The armoured bed formed by 9 hours antecedent flow was stable and the patchiness is not destroyed by stability test. The patches are now moved upstream and are more organised. This can be explained as the following. The valley formed in the bed reduced the resistance of the grains at upstream edges and they move forward during the stability test. Even at the peak flowrates in the stability test the flow was not able to entrain these grains and transport them far downstream. This is because of the sufficient level of stability formed by long antecedent flow test. The fluid forces only removed the grains in a rolling fashion over short distances. The grains only rolled a short distance downstream either to fill the lower levels or to increase the level of bed surface. These movement made the patches (valleys) to move progressively upstream. The average bed surface level after stability test indicates almost no difference than the average bed surface before stability test. It changes to 0.111 mm below the zero datum, a decrease of only 0.031 mm.

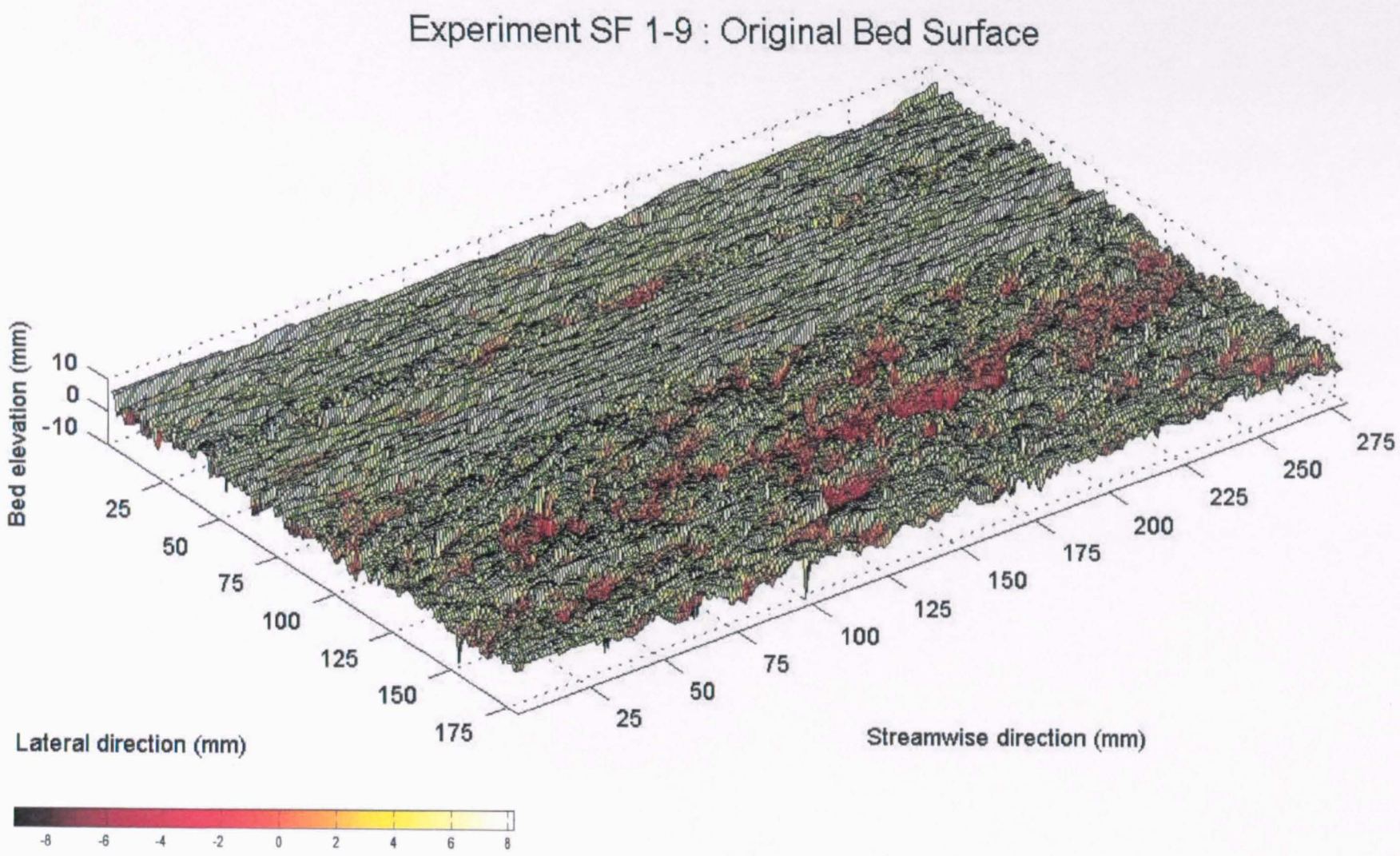

Figure 4.44. Original bed surface topography of the measurement grid Experiment SF 1-9

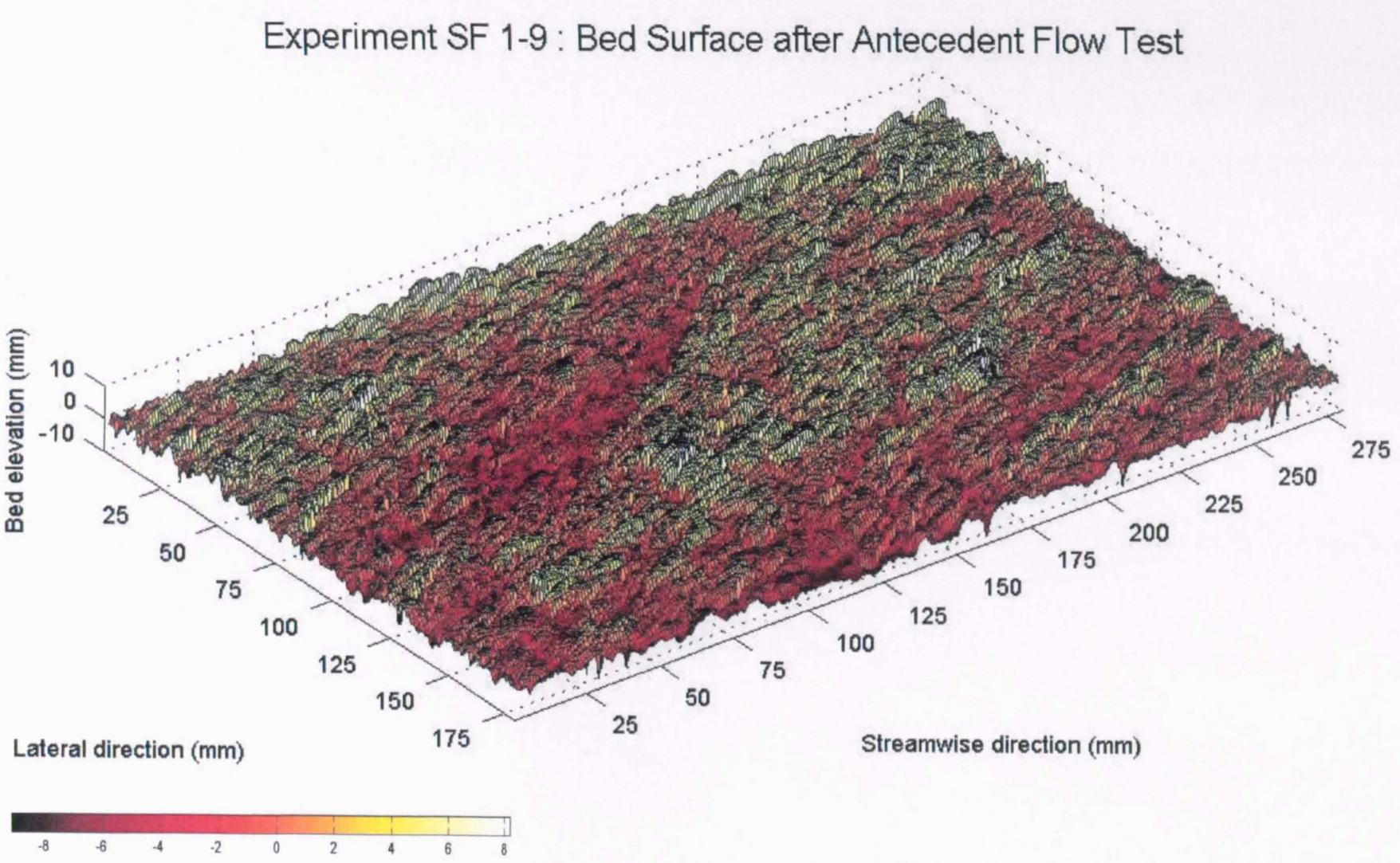

Figure 4.45. Bed surface topography of the measurement grid after antecedent flow Experiment SF 1-9

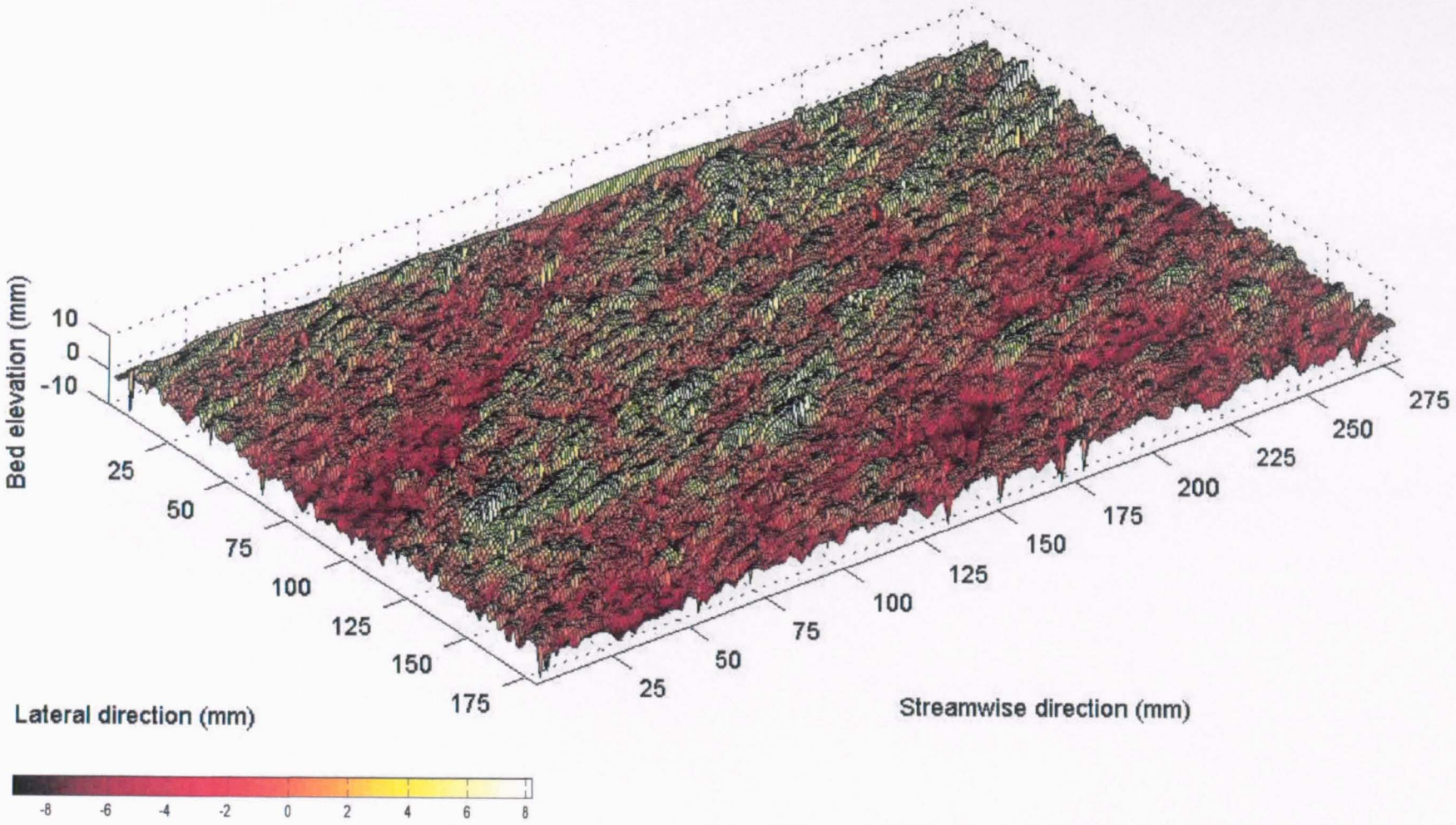

Figure 4.46. Bed surface topography of the measurement grid after stability test Experiment SF 1-9

The original bed elevation distributions of Experiment SF 1-9 shows a different pattern from the original bed elevation distribution in SF 1-3 and SF 1-6. In this bed surface there is a high proportion of elevations in the range from the zero datum. This unusual concentration of 5 mm elevation is thought to be due to the variability of the bed placing process. During 9 hours of antecedent flow the erosion processes rearranging the bed surface. The curve of elevation distribution becomes more symmetrical. The bed surface elevations are relatively balanced in which the elevations below and above the average bed surface are quite similar. However it is thought that the high proportion of 5 mm was not physically disappeared. In this case the fluid forces of antecedent flow were only able to lower the level during the readjustment processes of the bed surface rather than transported them downstream.

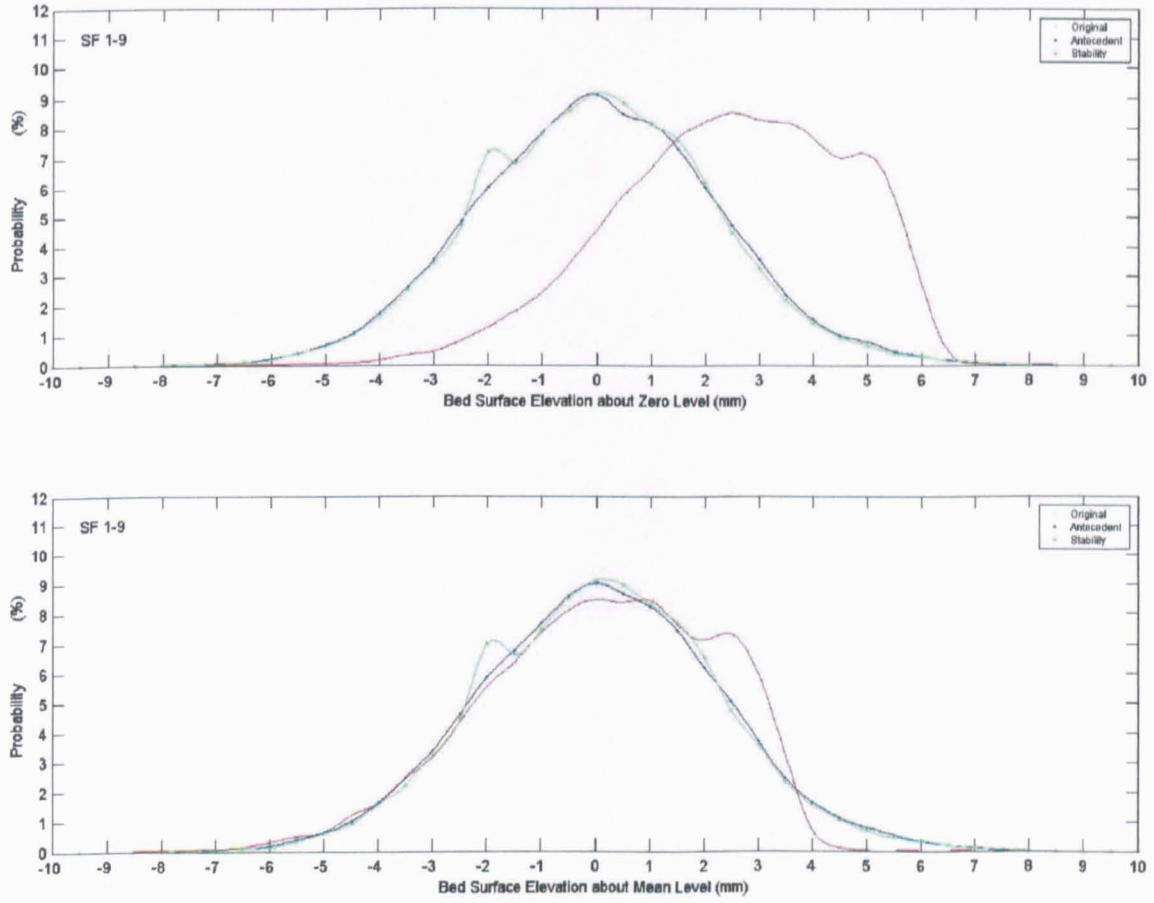

Figure 4.47. Probability distribution of bed surface elevation about zero and mean level for Experiment SF 1-9

It was when the higher flowrates above 0.0338 m^3/s during the stability test that the influence of the irregularities formed by the original bed surface distribution can be seen. The "over proportion" of elevation with 5 mm height from zero datum in the original bed surface distribution have significant impacts to the distribution curve of stability flow. Following the removal of finer grains during the low flowrates at initial stage of stability test, these grains more exposed. The stronger fluid forces about the peak hydrograph of stability test with flowrates higher than the constant flow rate during antecedent flow test, completely removed the exposed grains which was initially 5 mm height in the original bed but lowered after antecedent flow test. This transformation is evident in Figure 4.47. The bed surface elevation distribution after stability tests shows the irregular form similar to the distribution curve of original bed surface. This time is in the left hand side of the peak distribution curve indicating the level of decrease of about -5 mm with similar proportion to + 5 mm height in the original bed.

Apart from the considerable amount of 5 mm deep valley-formed by the stability test, the changes of the shape of the elevation distribution from post-antecedent flow to the end of the subsequent stability test are generally very small. This indicates a more stable bed than in experiment SF 1-3 and SF 1-6 is obtained in experiment SF 1-9 with no substantial amount of bedload transported during the observation stability test. It is very clear from the distribution of bed surface elevation that a generally very small degradational process took place during the stability test. The hump in the final distribution curve is created by the similar form in the original bed surface, which was temporarily "hidden" and adjusted by the available fluid forces during the antecedent flow test. Only the higher flowrates during the stability test could destabilise and then transported this structure.

4.3.4. STEADY ANTECEDENT FLOW EXPERIMENT SF 1-12

4.3.4.1. Bedload Transport Rate and Composition SF 1-12

Bedload transport rates variation with time in experiment SF 1-12 indicated a similar pattern with the transport rate variations produced by experiment SF 1-3 and SF 1-6. Initially the transport rate was high and then declined significantly with a sharp decrease occurred in the early stage of the test (Figure 4.48). In the first 10 minutes the transport rate was 0.355 g/s/m

indicating the ability of water flows to destabilise, entrain and transport the sediment bed. Within 80 minutes the rate drops to 0.124 g/s/m and then fluctuated with the tendency to transport lower amount of sediment. During the third and fourth hours, the average transport rate was 0.103 g/s/m. The fluctuation continued during the next two hours with slightly higher transport rate at 240 and 270 minutes of time elapsed. The average transport rate within this period indicates a lower average rate of 0.071 g/s/m or decreased more than 30 % from the rate of the previous two hours. The average transport rate continued to decrease every 2 hours to 0.068 g/s/m, 0.050 g/s/m and 0.034 g/s/m respectively. There was a noticeable increase in transport at time elapsed 680 minutes, which leads to the slight increased in the average transport rate within the last two hours from 0.026 g/s/m to 0.043 g/s/m in the last hour of the test.

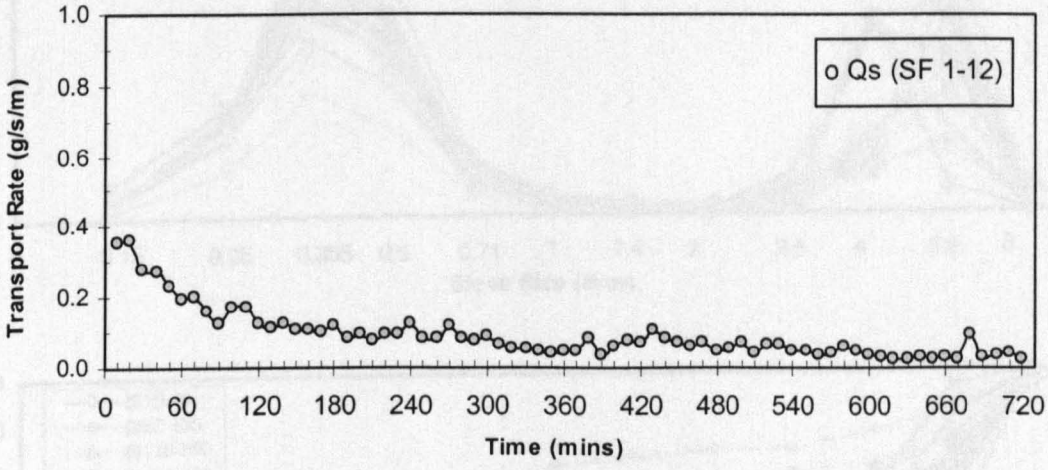

Figure 4.48. Time variation of transport rate for antecedent flow Experiment SF 1-12

The importance of finer grains that was transported during initial high transport rate is shown in Figure 4.49. It is very clear that the finer grains were dominant from the start until time elapsed 270 minutes. The distribution curve of the finer mode is constant with the modal grains size of 0.355 mm. Different pattern is shown by grains in the coarse mode. After 150 minutes the modal grain size of coarse grains changed from 5.6 mm to 4 mm. The coarse modal grain size increase again to 5.6 mm until time elapsed 300 minutes. In Figure 4.49 it is apparent that grains size of 8 mm are rarely seen in transport. This grain size appear in transport at the early stage of the experiment (10 - 40 minutes) and also at time elapsed 350 -

460 minutes. There is an inconsistency between time elapsed 310 to 410 minutes where the modal grains size of the coarse mode changed erratically. After 2 hours constant with 5.6 mm, the coarse modal grain size decrease to 4 mm again at time elapsed 310 - 340 minutes. At time elapsed 350 - 400 minutes the modal size of the coarse grains even larger with 8 mm. This is the only times when the contribution of 8 mm dominates the coarse mode in transport. At the following times the coarse modal grain size decrease and constant at 5.6 mm until the end of the antecedent flow Experiment SF 1-12.

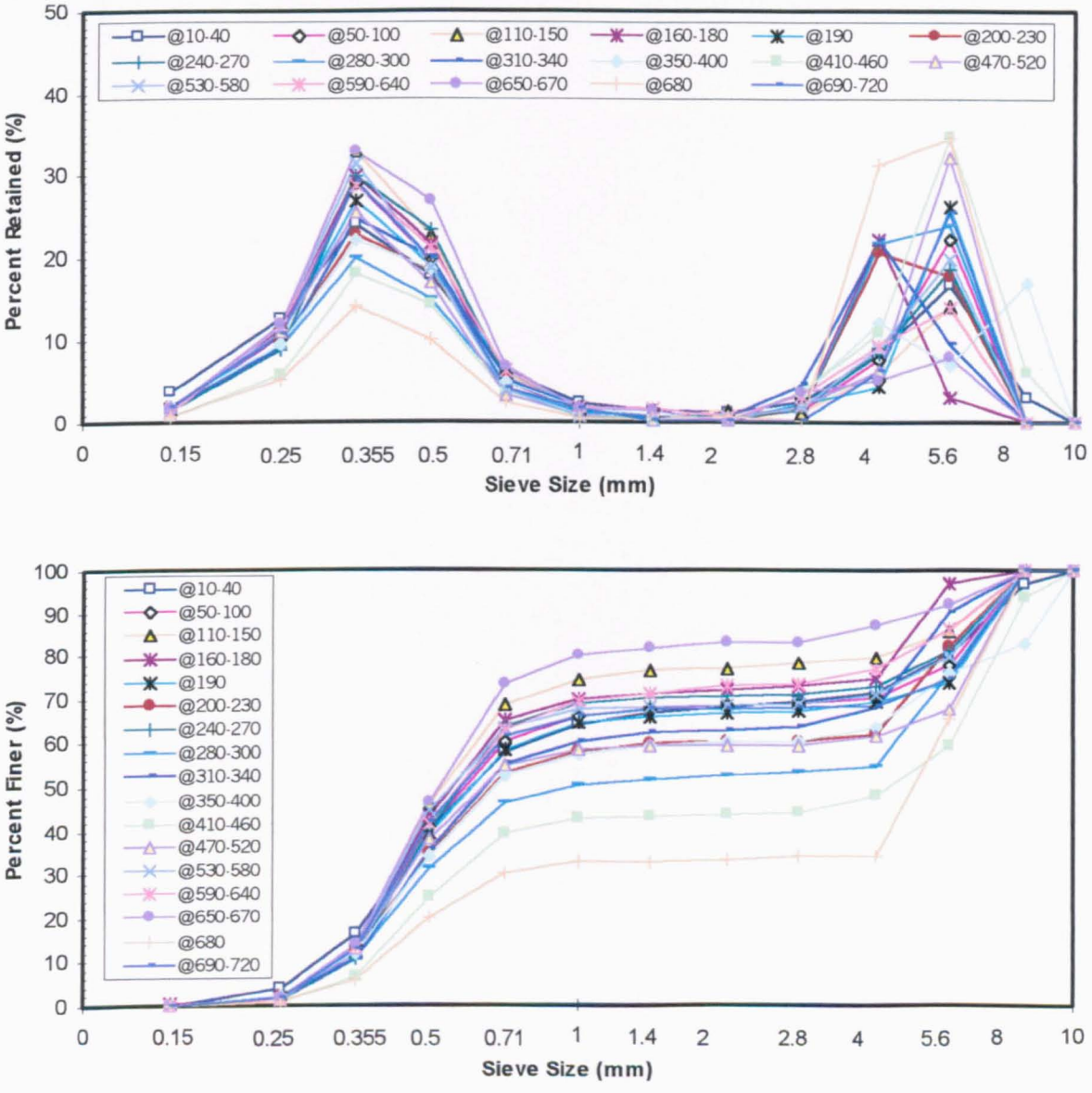

Figure 4.49. Grain size distribution of transported bedload for antecedent flow Experiment SF 1-12

It is very clear from Table 4.17 that the finer mode is more important than the coarser mode. More than half of the transported sediment contained the grains in the fine mode (56 %) whilst the grains in the coarse mode contributed only 31 % of the total transported bedload. Transported material was always much finer than the bed which tended to coarsen throughout the test. The absence of the larger coarse grains of 8 mm for in the majority of the observation suggest that this grains were relatively resistance to the fluid forces during the antecedent flow Experiment SF 1-12. It is thought that the appearances of these grains in transport were due to the exposure level of these grains at the beginning and at time elapsed 350 - 460 minutes. The level of exposure between 350 and 460 minutes was supported by the erosion process of finer grains, which transformed the bed into the coarser surface condition in comparison to the original bed surface.

Table 4.17. Summary of the average fractional bedload composition produced by antecedent flow Experiment SF 1-12

Sieve size (mm)	Original composition of surface layer (%)	Fractional transported bedload (%)	Estimated composition of surface layer (%)
10	1.730	0.000	1.762
8	8.570	1.894	8.692
5.6	34.660	18.885	34.947
4	19.600	10.667	19.763
2.8	6.860	2.190	6.945
2	3.530	0.676	3.582
1.4	2.510	0.771	2.542
1	1.850	1.648	1.854
0.71	2.680	5.330	2.632
0.5	6.840	19.071	6.617
0.355	7.420	26.328	7.075
0.25	2.710	10.550	2.567
0.15	0.940	1.920	0.922
receiver	0.100	0.071	0.101
Total	100	100	100

4.3.4.2. Variations of Average Nearbed Streamwise Velocity and Bed Shear Stress SF 1-12

As experienced in the shorter steady antecedent flow tests, a relatively constant values of the

average nearbed streamwise velocity was found in steady antecedent flow Experiment SF 1-12 (Figure 4.50). The highest range of variation is found at time elapsed 10 minutes. At this time elapsed the average values of nearbed streamwise velocity is 9 % more than the average values for the whole observation. The lowest average velocity is found at time elapsed 590 minutes where the values is 3.5 % lower than the average values of the whole observation. A wider range of variation was experienced by the average bed shear stress. During the constant flowrates, the highest value of average bed shear stress, estimated using Equation 3.16, is 11 % more than the average value for the whole observation. This is at 220 minutes time elapsed. The lowest average value is at 180 minutes time elapsed with less than 9 % of the average bed shear stress measured throughout the antecedent flow experiment SF 1-12 (Figure 4.50). The difference in the range of variation between the average nearbed streamwise velocity and the average bed shear stress is likely caused by the variations in the vertical velocity as the straight line formed by the average nearbed streamwise flow velocity indicates that the flow in streamwise direction were relatively constant throughout the test.

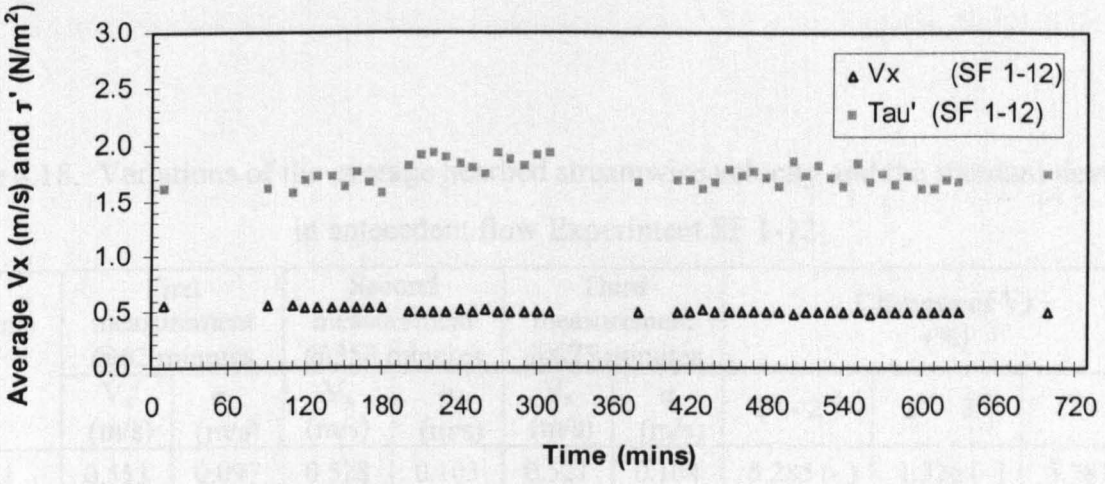

Figure 4.50. Variation of time averaged nearbed streamwise velocity and bed shear stress during antecedent flow Experiment SF 1-12

The longer duration of the antecedent flow experiment SF 1-12 made possible to carry three series of ADV measurement within the measurement grid. This allows the comparison of the changes in the near bed flow between a short and a long time interval in one experiment. Table 4.18 shows that the average values of nearbed streamwise velocity of all points are

decreased after almost 6 hours of the flow. In the third measurement, a further 5 hours later, the average nearbed streamwise velocity values continued to decrease at some points but increased slightly in other points. This indicates that there is no strong pattern in the nearbed streamwise velocity in correlation to the time. However when comparing the average values for a longer time interval, i.e. more than 10 hours between the first and the third measurement it is found that the average values of nenarbed streamwise velocity decreased in the majority of grid points. Although there is a slight increase in the average values of all points in the measurement grid from the second to the third measurement (+0.4 %), the average values of the final measurement was still lower than the average values of the first measurement (-5 %). Although similar values in the average standard deviation of the measurement grid indicate a relatively similar level of variation in the average nearbed streamwise velocity throughout the experiment, it can be suggested that the average flow velocity is reducing as it is difficult to expect the streamwise nearbed flow velocity would perform in a similar manner throughout the experiment. The mobile bed as it deforms would have different bed roughness at different observed time elapsed.

Table 4.18. Variations of the average nearbed streamwise velocity and the standard deviation in antecedent flow Experiment SF 1-12

Points	First measurement @62 minutes		Second measurement @358 minutes		Third measurement @675 minutes		Changes of Vx (%)		
	V_x (m/s)	σ (m/s)	V_x (m/s)	σ (m/s)	V_x (m/s)	σ (m/s)	1^{st} - 2^{nd}	2^{nd} - 3^{rd}	1^{st} - 3^{rd}
A1	0.553	0.097	0.528	0.103	0.521	0.104	5.285 (-)	1.326 (-)	5.787 (-)
A3	0.549	0.093	0.499	0.098	0.509	0.095	9.107 (-)	2.004 (+)	7.286 (-)
A5	0.479	0.095	0.472	0.094	0.467	0.092	1.461 (-)	1.059 (-)	2.505 (-)
E1	0.557	0.098	0.523	0.098	0.532	0.101	6.104 (-)	1.721 (+)	4.488 (-)
E3	0.555	0.099	0.498	0.099	0.496	0.103	10.270(-)	0.402 (-)	10.631(-)
E5	0.458	0.097	0.449	0.096	0.472	0.097	1.965 (-)	5.122 (+)	3.057 (+)
I1	0.563	0.091	0.526	0.105	0.525	0.101	6.572 (-)	0.190 (-)	6.750 (-)
I3	0.532	0.098	0.504	0.098	0.482	0.101	5.263 (-)	4.365 (-)	9.398 (-)
I5	0.483	0.096	0.473	0.092	0.492	0.098	2.070 (-)	4.017 (+)	1.863 (+)
Average	0.525	0.096	0.497	0.098	0.499	0.099			

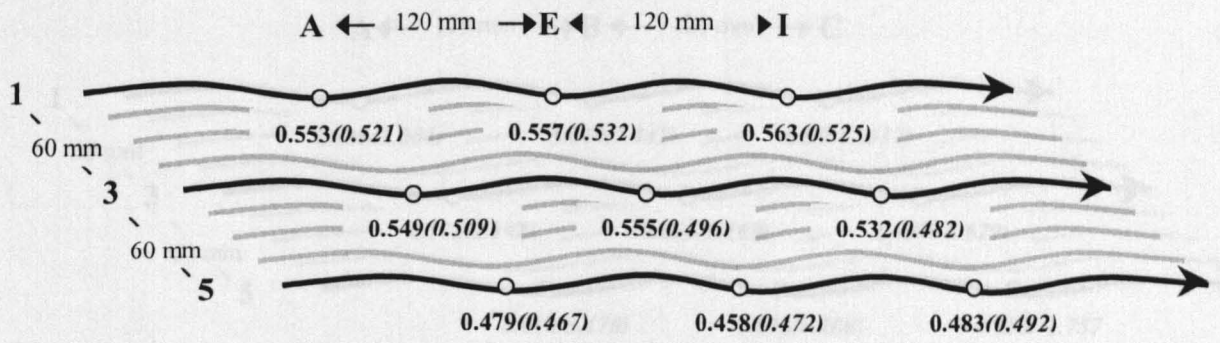

Figure 4.51. Distribution of average nearbed streamwise velocity (m/s) in antecedent flow Experiment SF 1-12 (first measurement in bold, third measurement in brackets)

Table 4.19 shows the complexity in the changes of average bed shear stress calculated directly from the ADV data using Equation 3.15. Selected points have significantly lower or higher values than the others. Certain points exhibit relatively small variation of the average values throughout the observed times. Given that the changes in average nearbed streamwise flow velocity are relatively small, it is suspected that the fluctuation of vertical velocity occurred and presence during the whole duration of antecedent flow experiment. It is believed

Table 4.19. Variations of the average bed shear stress and the standard deviation in antecedent flow Experiment SF 1-12

Points	First measurement @62 minutes		Second measurement @358 minutes		Third measurement @675 minutes		Changes of $\overline{\tau'}$ (%)		
	$\overline{\tau'}$ (N/m^2)	σ (N/m^2)	$\overline{\tau'}$ (N/m^2)	σ (N/m^2)	$\overline{\tau'}$ (N/m^2)	σ (N/m^2)	1st - 2nd	2nd - 3rd	1st - 3rd
A1	2.936	18.582	5.197	17.873	5.004	18.007	77.010(+)	3.714 (-)	70.436(+)
A3	4.182	17.385	2.245	16.307	2.998	15.917	46.318(-)	33.541(+)	28.312(+)
A5	3.018	15.517	3.392	15.124	3.470	14.509	12.392(+)	2.299(+)	14.977(+)
E1	5.004	19.281	6.666	19.618	7.441	19.323	33.213(+)	11.626(+)	48.701(+)
E3	9.828	18.142	8.049	16.385	9.160	16.675	18.101(-)	13.803(-)	6.797 (-)
E5	2.678	16.551	4.533	15.304	6.208	15.961	69.268(+)	36.951(+)	131.815(+
I1	6.539	19.640	6.030	19.703	7.517	19.093	7.784(-)	24.660(+)	14.956(+)
I3	2.498	17.922	-0.411	16.712	-0.629	16.574	116.453(-)	53.041(-)	125.180(-)
I5	-4.235	16.282	-2.625	14.749	-1.757	16.069	38.017(+)	0.331(+)	58.512(+)
Average	3.605	17.700	3.675	16.864	5.971	16.903			

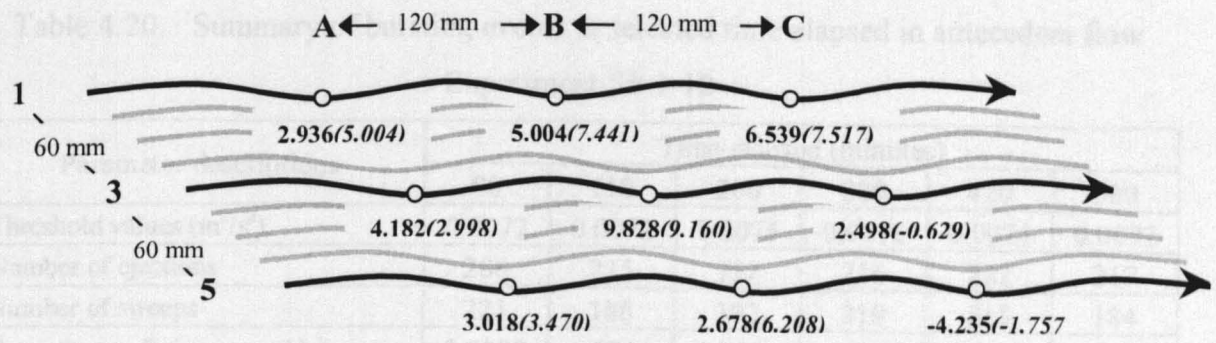

Figure 4.52. Distribution of average bed shear stress (N/m^2) in antecedent flow Experiment SF 1-12 (first measurement in bold, third measurement in brackets)

that different level of turbulence at different points caused by the variations of bed roughness even at a small adjacent area within the measurement grid. It is worth noting that the measurement was carried out at 10 mm from the bed surface so that the influence of either isolated exposed grains or valley-formed bed features would be relatively closed and would therefore be likely to affect the nearbed flow. Overall, the average values of the measurement grid increased with time while the average standard deviations is slightly decreased indicating the more fluctuated pattern in the vertical flow velocity.

4.3.4.3. Bursting Events and Flow Momentum SF 1-12

Information on bursting events (ejections and sweeps) was examined at 44 stages time elapsed during Experiment SF 1-12. Overall, the frequency of occurrence of ejections is still higher (51 %) than that of sweeps (49 %). At this stage, it is too early to conclude whether fully armoured bed balances the frequency of outward and downward looking bed interactions. It is necessary to investigate if this sediment bed that had been exposed to flow over a considerably longer period, produced a more organised pattern of outward and downward-looking bed flow turbulence structures. The data in Table 4.20 suggest that this may not be the case. It is seen that before 420 minutes the frequency of occurrence of the sweeps is not always higher than the frequency of occurrence of ejections. The frequency of ejections and sweeps do not correspond with time as well as the average duration of both events.

Table 4.20. Summary of bursting events at selected time elapsed in antecedent flow Experiment SF 1-12

Parameter descriptions	Time elapsed (minutes)					
	90	110	200	280	420	580
Threshold values (m^2/s^2)	0.0072	0.0072	0.0076	0.0076	0.0074	0.0072
Number of ejections	206	215	192	216	222	217
Number of sweeps	221	186	192	219	215	184
Frequency of ejections (Hz)	1.0300	1.0750	0.9600	1.0800	1.1100	1.0850
Frequency of sweeps (Hz)	1.1050	0.9300	0.9600	1.0950	1.0750	0.9200
Average duration of ejections (s)	0.0561	0.0538	0.0544	0.0520	0.0562	0.0538
Average duration of sweps (s)	0.0538	0.0574	0.0508	0.0504	0.0501	0.0550

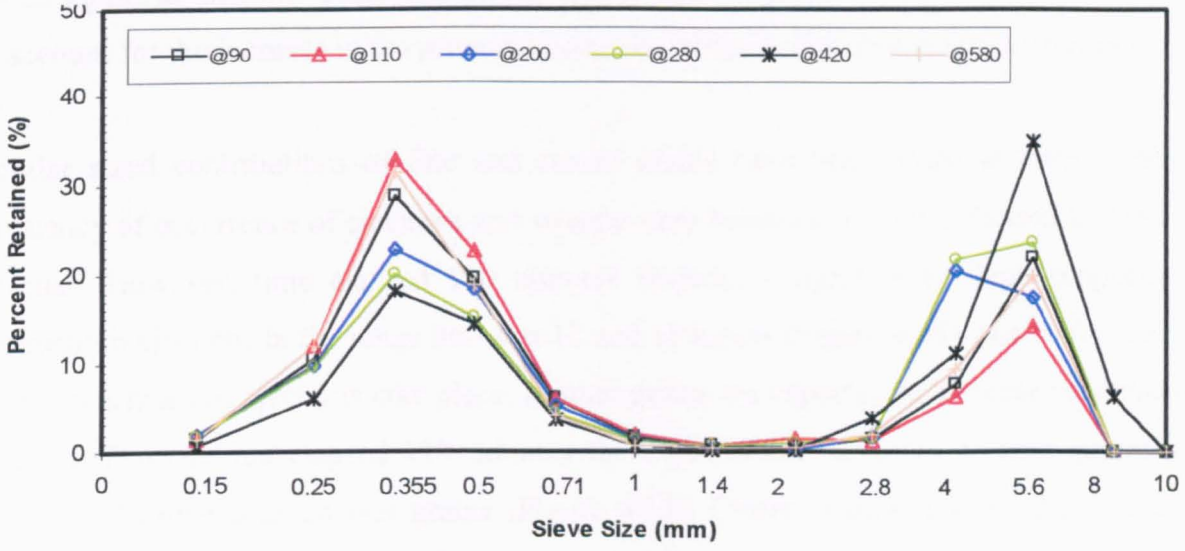

Figure 4.53. Grain size distribution of transported bedload at selected time elapsed in antecedent flow Experiment SF 1-12

To some extent the tendency found in shorter experiments is also observed in this test. At time elapsed 90 minutes the occurrence of ejections is lower than sweeps (Table 4.20). During this time the bedload transport was dominated by the finer grains (Figure 4.53) and the transport rate was high. This is a similar pattern found in experiments SF 1-3, SF 1-6 and SF 1-9. As the bedload transport rate diminished, the bursting events were expected to alter, potentially in the frequency of occurrence of the bursting events and also their magnitudes.

At time elapsed 420 minutes, a different pattern in grain size distribution of transported bedload is observed (Figure 4.53). During this period the frequency of occurrence of the outward interactions was considerably higher than the downward-looking bed interaction compared to the time elapsed 280 minutes. As a result the grains are coarser and make a more dominant contribution to the transport bedload. A different pattern is shown at time elapsed 580 minutes. Lower proportion of coarser grains than that at time elapsed 420 minutes was moving. However, the transported bedload during this time elapsed was still relatively high with the considerable amount of grains in the coarse mode. It can be seen from Figure 4.55 that high magnitude of momentum ejections were occurring at time elapsed 420 minutes particularly in the range between 15 - 23 kg/ms. The overall proportion in the range between 9 - 23 kg/ms at this time elapsed is higher than at time elapsed 580 minutes. This is believed to account for the increase in the proportion and the amount of coarse grains in transport.

Similar sized contributions of fine and coarse grains have been found at times when the frequency of occurrence of ejections and sweeps were balanced, i.e. time elapsed 200 and 280 minutes. However, time elapsed 110 minutes features a significantly high proportion of momentum ejections in the range between 13 and 15 kg/ms (Figure 4.55). Normally when the high momentum of ejections take place, coarser grains are expected to increase in transported bedload. During time elapsed 110 minutes the considerable amounts of finer grains were transported rather than coarser grains (Figure 4.53). Closer examination of the momentum distribution at this time indicates few structures with momentum greater than 15 kg/ms. This suggests that ejections, with momentum less than this threshold, appear to be less able to move coarse grains.

Again, as in the other tests, the momentum distribution in the sweeps events shows low magnitude and little variation during the antecedent flow experiment (see Figure 4.54 and Figure 4.55). This indicates that it is the character of the ejections events, particularly in terms of momentum per unit area, that determines the ability of the fluid to measure grains movement.

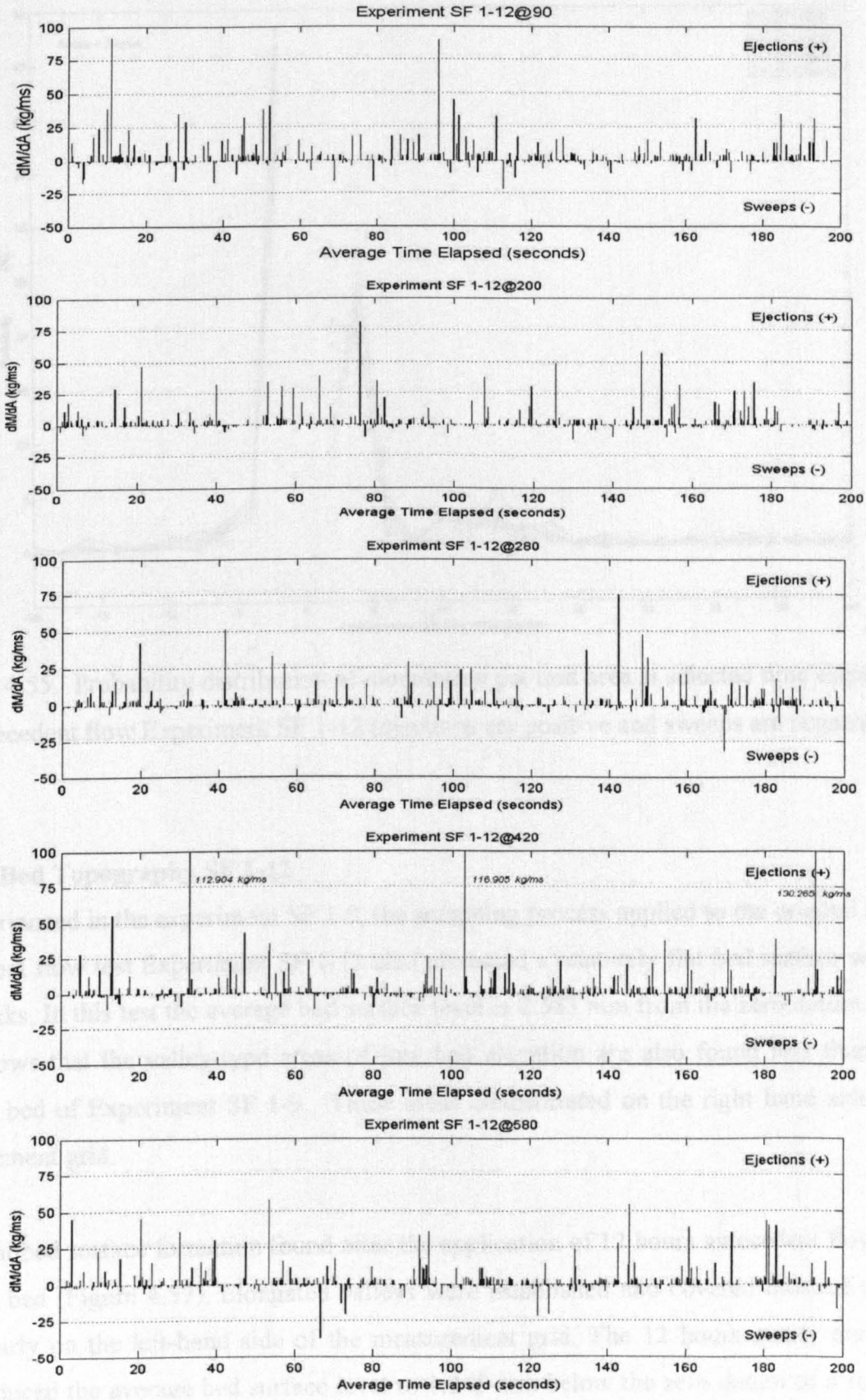

Figure 4.54. The sequence of momentum per unit area and its magnitude at selected time elapsed in antecedent flow Experiment SF 1-12

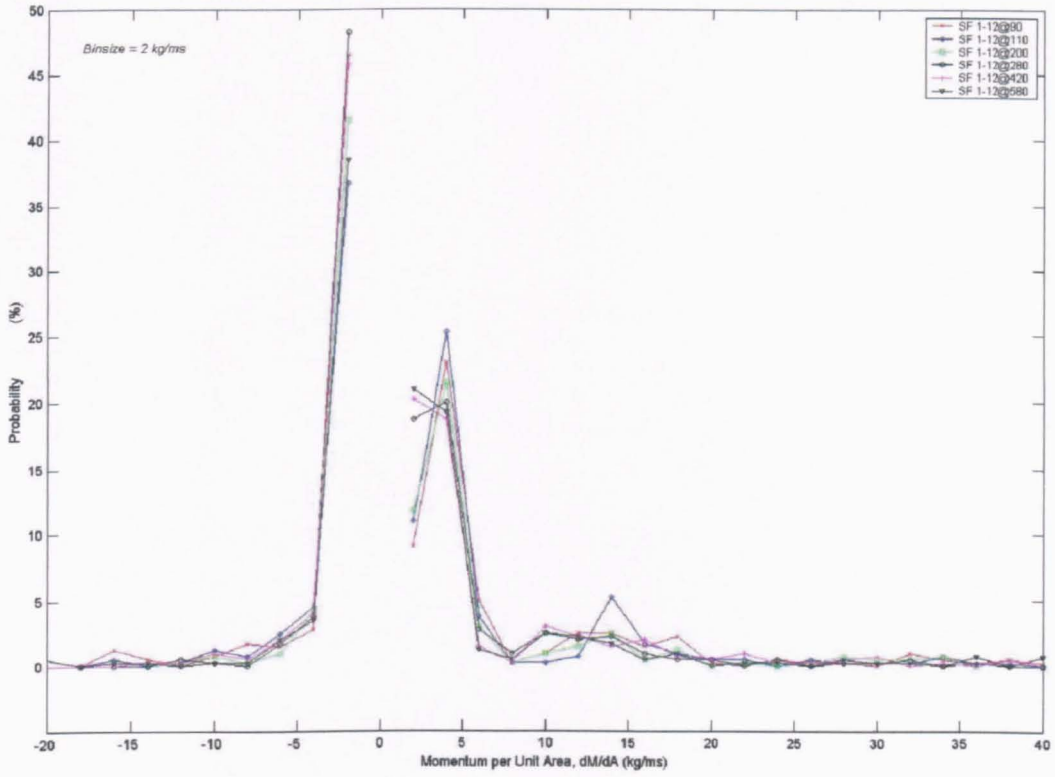

Figure 4.55. Probability distribution of momentum per unit area at selected time elapsed in antecedent flow Experiment SF 1-12 (ejections are positive and sweeps are negative)

4.3.4.4. Bed Topography SF 1-12

As experienced in the experiment SF 1-9, the scrapping process applied to the original bed for antecedent flow test Experiment SF 1-12 also produced a relatively flat bed surface with few high peaks. In this test the average bed surface level is 2.583 mm from the zero datum. Figure 4.56 shows that the valley-type areas of low bed elevation are also found less than in the original bed of Experiment SF 1-9. These areas concentrated on the right hand side of the measurement grid.

Different bed surface formation found after the application of 12 hours antecedent flow to the original bed (Figure 4.57). Elongated valleys were established and covered most of the area particularly on the left-hand side of the measurement grid. The 12 hours steady antecedent flow reduced the average bed surface level to 1.245 mm below the zero datum or a reduction of 3.828 mm from the average level of original bed. The level of decreased is more than that caused by steady antecedent flow experiments SF 1-3, SF 1-6 and SF 1-9. Points with high

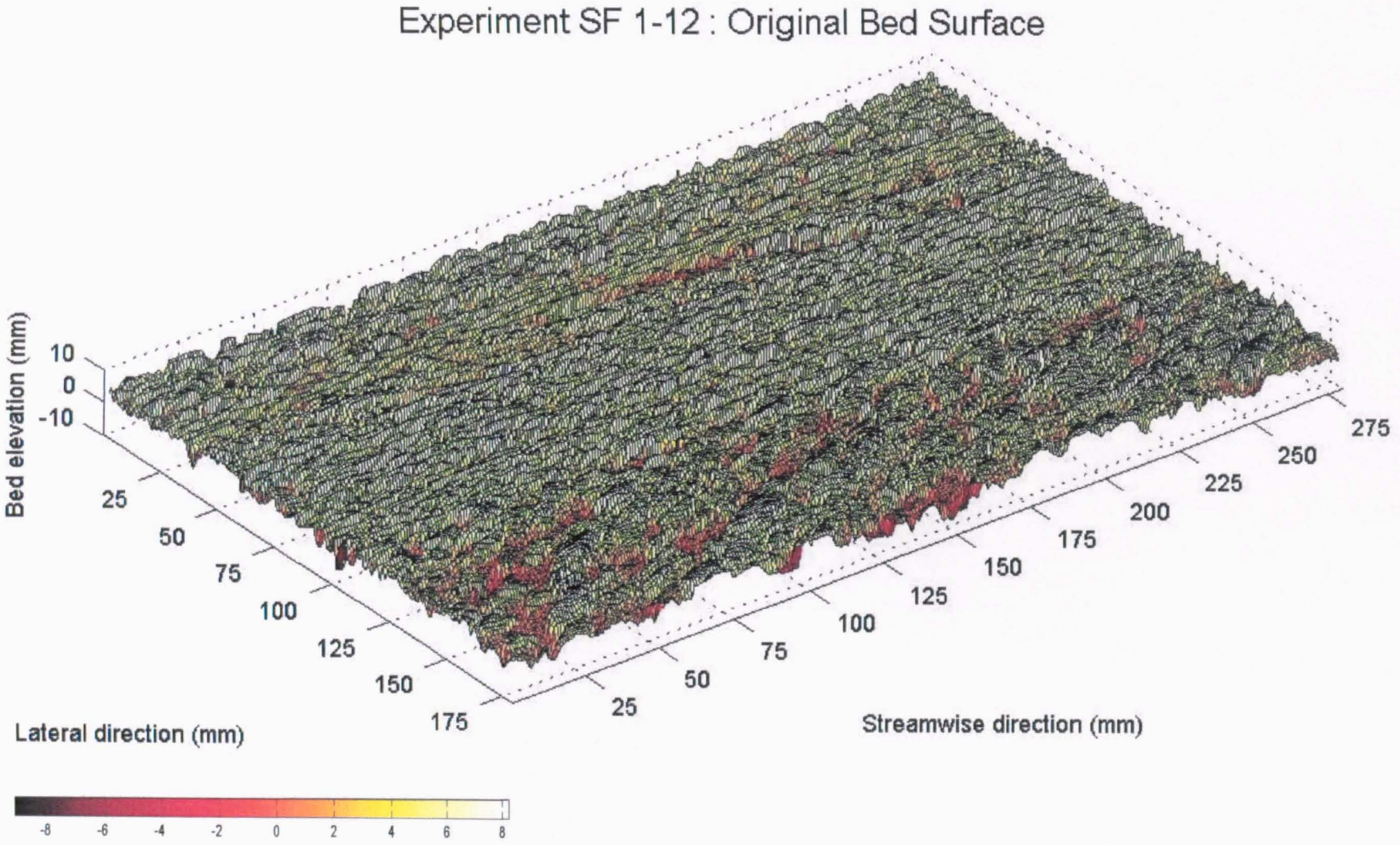

Figure 4.56. Original bed surface topography of the measurement grid Experiment SF 1-12

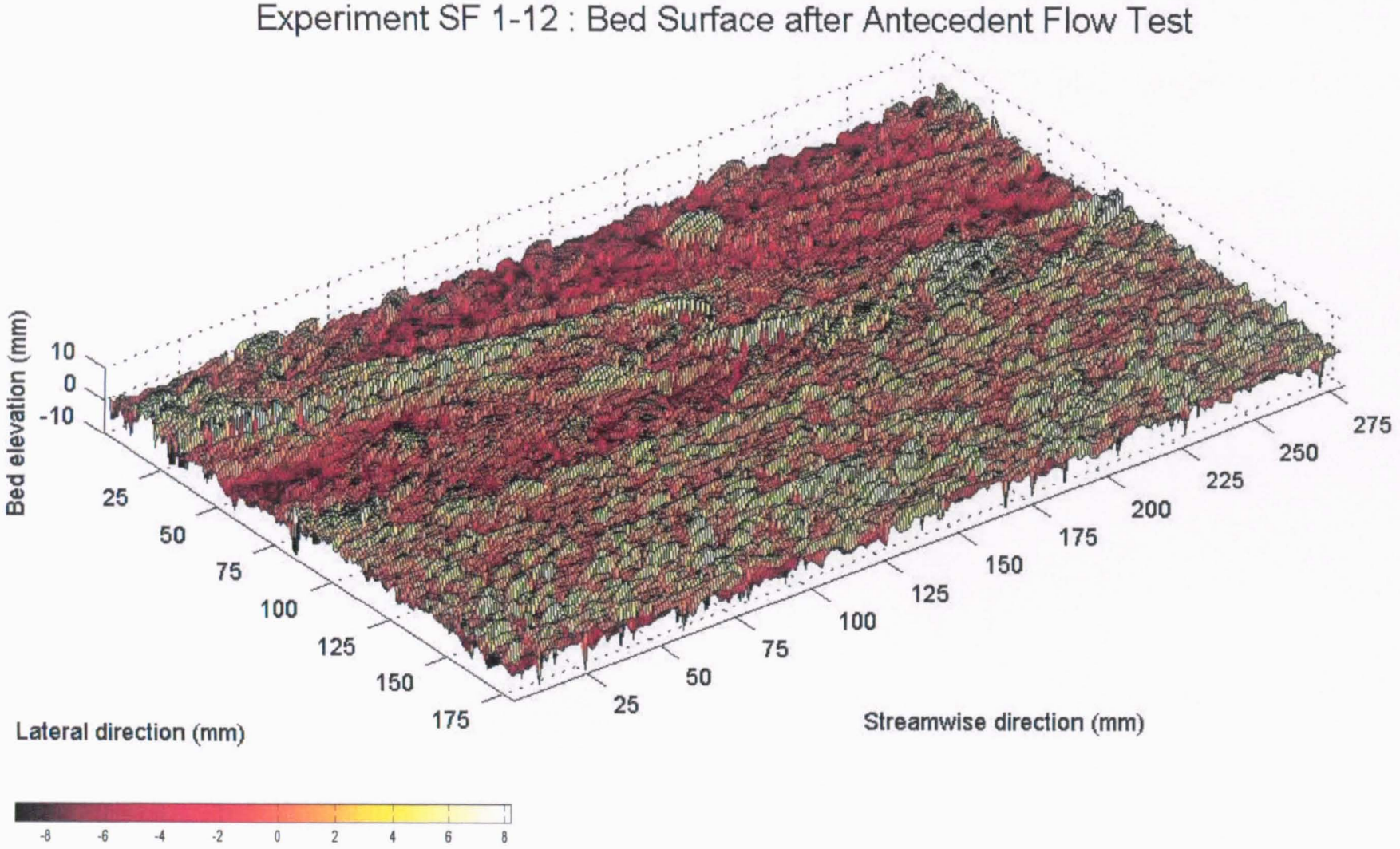

Figure 4.57. Bed surface topography of the measurement grid after antecedent flow Experiment SF 1-12

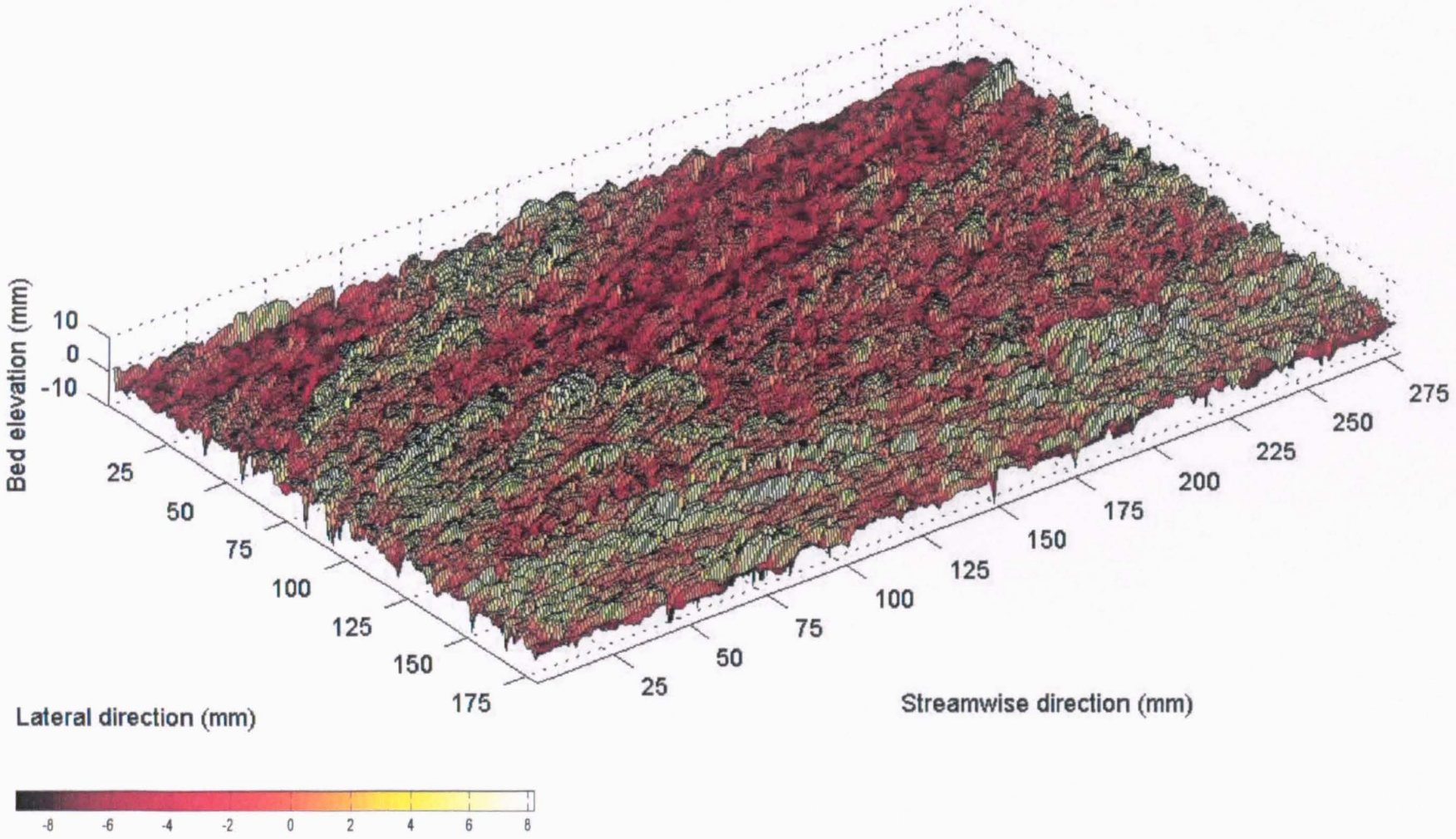

Figure 4.58. Bed surface topography of the measurement grid after stability test Experiment SF 1-12

exposures before stability test were partially kept in existence after stability test (Figure 4.58). Although the valley-formed area more spread, there are some indication that the stability test of Experiment SF 1-12 was only able to remove grains in similar fashion to those in stability test Experiment SF 1-9. For instance, the low level in the area of point x100 to x125 and y0 to y25 (Figure 4.57) was increased after stability test because of the movement of grains forward in rolling fashion. Further down to this area the level of the bed surfaces decreased, indicating the removal process took place. Similar patterns but in a smaller scale was found along the centreline of the measurement grid. Before the stability test applied, the relatively exposed areas in the downstream part of the measurement grid were slightly reduced after stability test and vice versa in the upstream part.

It has been shown in Figure 4.1 that the most stable bed is formed by 12 hours antecedent flow test. As in the previous experiment, the degradational stage can be seen when the antecedent flow test was applied to the original bed. The coarsening process caused the variation in the bed surface, most notably in the positive side from the mean. After 12 hours antecedent flow was run over the bed, the number of grains resting on the bed, with at least 4 mm exposure from the mean level increased. It is also noticed that the proportion of bed surface level between 1 mm to about 4 mm height decreased suggesting that the number of grains with moderate exposure has reduced. The tail of the distribution with negative excursions from the mean bed has little variation from the original and armoured bed. However, as the armoured bed condition was achieved after sufficient time of antecedent flow only bed surface elevation around the mean level was changing during the stability test. In this test the bed surface elevation of higher values both above and below the average level did not deviate markedly from the mean (Figure 4.59). A stable bed configuration appears to be one in which there are few large negative and positive excursions from the mean bed. In a stable bed the number of moderate positive excursions is reduced. It appears that in stable bed there are a few well-sheltered and stable large grains. The other exposed medium or coarse grains have been moved into these larger structures. The negative excursions follow the pattern of the original bed suggesting that the fine grains have not filled the "holes" in the original bed but are somehow connected with the larger grain structures.

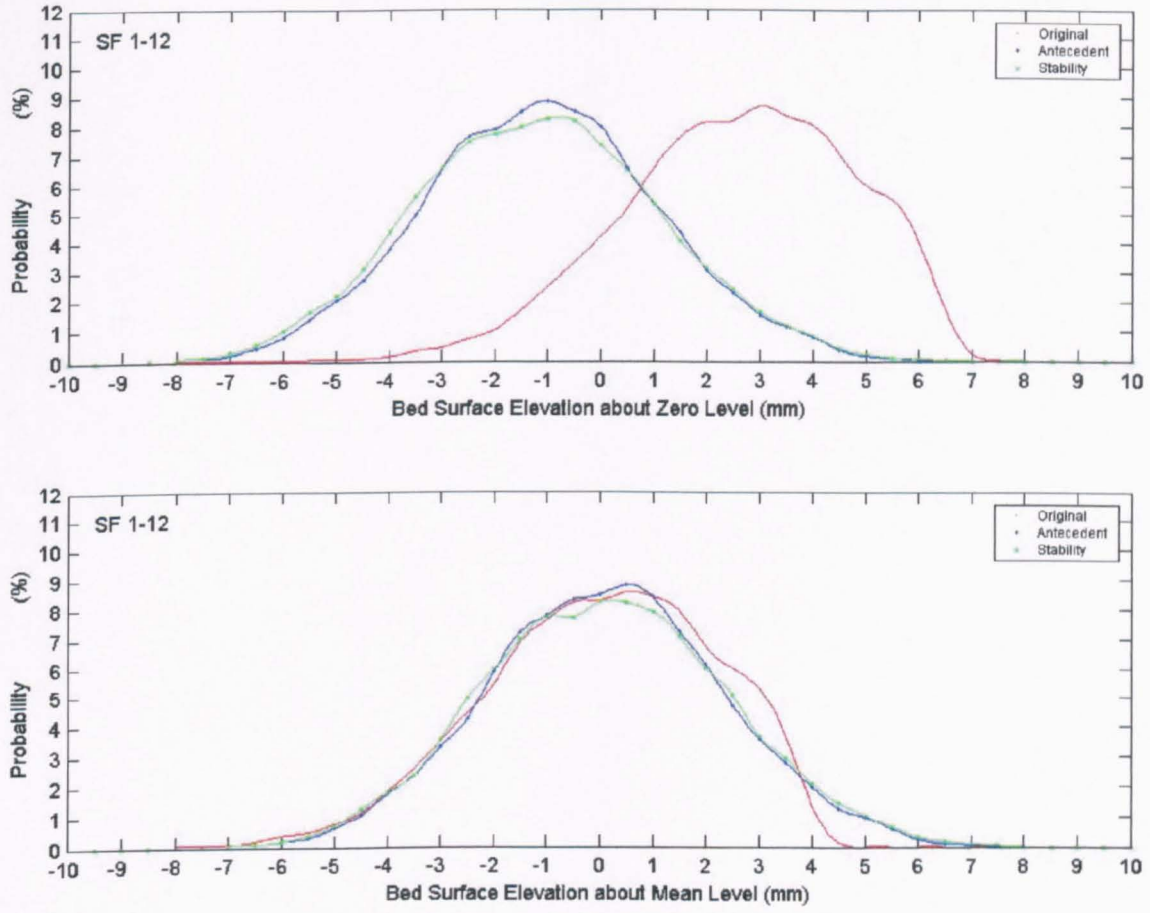

Figure 4.59. Probability distribution of bed surface elevation about zero and mean level for Experiment SF 1-12

4.4. COMPARARATIVE RESULTS AND DISCUSSIONS OF SF I

4.4.1. Transport Mode of Steady Antecedent Flow Experiments SF I

The application of a relatively high constant discharge to freshly laid bimodal sediment beds has a different effect on the coarse and fine modes of transported sediment. Bedload collected at 10 minute intervals were sieved to show the changes in the amounts transported in each mode. It is evident that this sieving analysis applied to the transported bedload produced by steady antecedent flow tests SF 1-3, SF 1-6, SF 1-9 and SF 1-12 show a pattern of change.

In the initial hour of each test, large amount of grains in both the fine mode and the coarse mode were transported. As regards composition a relatively consistent pattern was seen. Initially the proportion of grains in the fine mode was more dominant than grains in the coarse

mode. The first observation in Experiment SF 1-3 indicated that grains in the coarse mode were more transported than grains in the fine mode (Figure 4.60). This was believed to be due to the artificial nature of the initial bed. After about 360 minutes the proportion of grains in the coarse mode started to become larger than the amount of sediment in the finer mode. However this pattern was not consistent for the rest of these tests, with the fine mode dominating and then the coarse mode and vice versa.

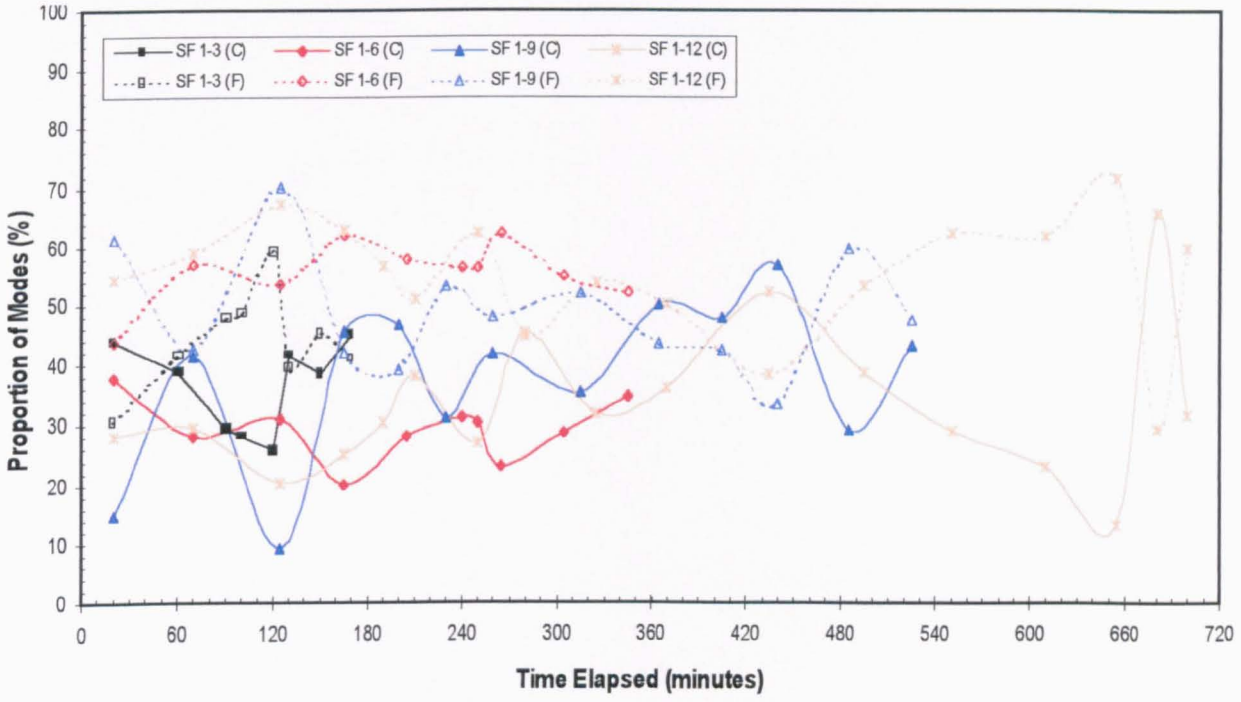

Figure 4.60. Proportion of two modes during steady antecedent flow Experiments SF I (coarse and fine mode are represented by solid and dotted line)

Normally when a constant flow discharge is applied, the transport rate, with no upstream sediment feed, is a function of time. The transport rate is expected to decreased rapidly and then remained at a low value. In this case the amount of bedload may be higher for the longer duration of experiments but this is not as a result of any increase in the transport rate. This is because after a set time the bed had reached an armoured stable condition and very low transport rates existed. However, Table 4.21 suggests that after the period of 6 hours a slightly different behaviour was observed. It can be seen that the total amount of bedload transported during 9 hours of constant flowrates less than the amount of bedload transported during 6 hours with similar condition.

Table 4.21. Summary of bedload for steady antecedent flow Experiments SF I

Experiment No.	Bedload transport		Mass and proportion of mode			
	Mass (g)	Rate (g/s/m)	Fine mode		Coarse mode	
			(g)	(%)	(g)	(%)
SF 1-3	496.930	0.242	191.282	38.493	198.300	39.905
SF 1-6	637.600	0.155	334.827	52.514	199.440	31.280
SF 1-9	531.220	0.086	254.952	47.994	202.690	38.156
SF 1-12	732.140	0.089	409.619	55.948	230.224	31.445

Observation of the temporal pattern in transport rates suggested that the armoured stable bed condition was achieved between time elapsed 6 and 9 hours as the transport rate dropped dramatically after 6 hours of exposed to the flow. Therefore the last 3 hours of antecedent flow SF 1-9 would only have small bedload production. This assumption is not fully accepted as the longer duration of antecedent flow opposes it. Antecedent flow experiment SF 1-12 indicates that the bed destabilisation is continued after 9 hours of flow exposure. During this time the low transport rate is expected as indicated by small transport rate in antecedent flow SF 1-12. Having observed this situation, two assumptions raised. The first one is that the antecedent flow SF 1-9 experienced different condition and hence the pattern of transport found in other antecedent flow experiments was not in existence in SF 1-9. This assumption is also supported by the fact that SF 1-9 features a contradict pattern in the proportion of mode of grains transported during the 9 hours of antecedent flow experiment (Table 4.21).

The second assumption is that the stable armoured bed had been achieved between 6 and 9 hours of flow exposure. The grains in the fine mode were better sheltered after 6 hours so that the rates dropped in the following hours. The grains in the coarse mode were also thought to have reached the stable condition. This is indicated by the relatively constant amount transported in 9 hours. Table 4.21 shows that only small increased found in three different duration of antecedent flow. However the application of relatively high flowrates of 0.0338 m^3/s continually imposed the bed after 9 hours. Further erosion took place and considerable amount of grains in the fine mode transported. If there is an increase in the amount of grains in the coarse mode transported at this stage, it was because of the transported finer grains changed the surface of "initial stable bed" and increased the exposure of larger grains to some extent.

4.4.2. Stability of the Antecedent Flow Beds and Mode of Transport SF I

The different levels of transport rate during the identical stability tests SF I indicated the influence of flow duration in each antecedent flow test. It is found that the beds formed by a constant flowrate with the shortest duration is the weakest. It is very important to bear in mind that the level of bed stability established by all the four stability tests did not form a linear relationship with duration of antecedent flow tests. However, the stability tests show that after a certain duration of antecedent flow, the transport rate decreased in an almost regular fashion. The amount of bedload transported during stability test after 3 hours antecedent flow test is 872.58 grams (0.638 g/s/m). Similar tests applied to the bed formed by 6 hours, 9 hours and 12 hours antecedent flow test eroded 341.43 grams (0.250 g/s/m), 210.82 grams (0.154 g/s/m) and 105.35 grams (0.077 g/s/m) respectively. Therefore it can be assumed that the bed exposed to the constant flow rate of 0.0338 m^3/s needs at least 6 hours to form a relatively strong pavement. This is confirmed by the values of hiding functions of stability test SF 1-3, which had considerably lower values than the other stability tests. The hiding function values of grains size fractions increased in the stability test SF 1-6. The finer grains seemed to stabilise after 6 hours as indicated by a small increase in hiding function values for the longer experiments of SF 1-9 and SF 1-12. The finer grains gained their stable position after 6 hours while the stability of the coarser grains were continuing as the tests progressed.

The grain size distribution curve also reveals the different mode of transport in stability test than the mode found in the antecedent flow tests. In stability test SF 1-3 grains in the coarse mode (grain sizes 5.6 mm and neighbouring 4 mm and 8 mm) started to dominate the transport at time elapsed 30 minutes whilst stability test SF 1-6 and SF 1-9 at the latter time elapsed. Both stability tests started to transport more grains in the coarse mode than in the fine mode (grain sizes 0.355 mm and neighbouring 0.25 mm and 0.5 mm) at time elapsed 50 minutes. The most stable bed formed by 12 hours antecedent flow test is confirmed when the stability test applied to this bed could only transported more grains in the coarse mode at the end of rising limb. This means the coarser grains in the bed of antecedent flow SF 1-12 were destabilised only by higher flowrates. Generally, for all stability tests the fluid forces in the early stages of rising limb (time elapsed 0 to 20 minutes) transported only grains in the fine mode. Apart from the stability test SF 1-6, the introduction of grains of the coarse mode in transport was started at time elapsed 30 minutes with the very low amount and proportion.

The period of domination of the coarse mode lasted for about 40 - 50 minutes depending on the starting time elapsed of domination (Table 4.22).

Table 4.22. Transport mode of the stability tests applied to antecedent flow-formed bed SF I

Stability Test	Time elapsed of coarse grain domination (mins)	Bedload proportion (%)				Total (%)	
		Fine mode		Coarse mode		Fine mode	Coarse mode
		Rising	Falling	Rising	Falling		
SF 1-3	@30 - @80	9.37	12.51	27.22	35.76	21.88	62.97
SF 1-6	@20 & @50 - @90	8.54	12.27	24.45	45.17	20.80	69.63
SF 1-9	@50 - @100	3.19	7.79	17.98	64.05	10.98	82.03
SF 1-12	@60 - @100	9.08	14.27	17.41	53.73	23.35	71.13

Table 4.22 shows that the grains in the coarse mode dominated the bedload. The falling limb produced higher bedload than the rising limb. This is understandable as it reflects the influence of the peak flowrates of 0.0375 m^3/s in destabilising the armoured bed structure formed by antecedent flow tests. However, there is a significant difference shown by the stability test SF 1-9. It is found that lower proportion of grains in the fine mode transported during the rising and falling limb of this stability test whilst a significant proportion of grains in the coarse mode were transported in the falling limb. This produces a significantly low proportion of grains in the fine mode transported throughout the stability test. It can also be seen that the proportion of grains in the coarse mode transported during the whole duration of stability test SF 1-9 is significantly higher than three other stability tests.

As previously described in Section 4.4.1 the relatively stable bed after 9 hours exposed to the constant flowrates of 0.0338 m^3/s still exhibit the transport in the last 3 hours of antecedent flow experiment SF 1-12. This means the application of flowrates higher than 0.0338 m^3/s to the bed formed by 9 hours antecedent flow experiment caused further disruption to the bed, in particular the exposed larger grains resting on it. In Table 4.22 a significant increased of grains in the coarse mode transported after the peak discharge was attained in stability test applied to the bed formed by 9 hours steady antecedent flow test. These grains were weak so that their appearances in transport lasted longer and continued to dominate the transport until

time elapsed 90 minutes. No wonder that the proportion of grains in the coarse mode produced by stability test SF 1-9 is higher than in stability test SF 1-3, SF 1-6 and SF 1-12 respectively.

4.4.3. The Distribution of Average Nearbed Streamwise Flow Velocity and Average Bed Shear Stress SF I

In all steady antecedent flow tests SF I, relatively constant values of the average nearbed streamwise velocity were found throughout each test (Figure 4.61). This suggests that no extreme disturbances in the nearbed flow during the experiments. The range of variations of the time averaged nearbed streamwise velocity from the average values of all observations in a test is less than 10 %. It is found that the range of variation for the shorter tests is lower than for the longer tests. The variation of the point averaged nearbed streamwise velocity from the average velocity in antecedent flow Experiment SF 1-3 is in the range of ± 2 % while in the experiments SF 1-6 and SF 1-9 the variation is wider but in the range between +7 % and -5 %. The variation increased slightly during SF 1-12 with the range being between +9 % and -4 %. It can be seen in Figure 4.61 that the time averaged nearbed streamwise velocities are generally decreased towards the end of each test. This suggests that the armoured beds become hydraulically rougher with time.

A wider range of variation was found in the time averaged bed shear stresses (Figure 4.62). In antecedent flow SF 1-3 the variation of time averaged bed shear stress to the average value for the whole duratiuon of the test ranges from +3 % to -3 %. Wider variations are found in SF 1-6, SF 1-9 and SF 1-12. These observations indicate that the pattern of "constant" values of time averaged streamwise nearbed velocity is not followed by the average bed shear stress. This is thought to be due to the variation in the distribution of vertical velocity. It is suspected that the changes in the bed roughness have an influence on the vertical velocity distribution and as the bed roughness increases the vertical velocity distribution becomes more varied. As seen in Figure 4.62, although there is fluctuations in time averaged bed shear stresses, the values are generally decreased towards the end of the experiments. The decrease is not large enough to explain the reduction in transport rate.

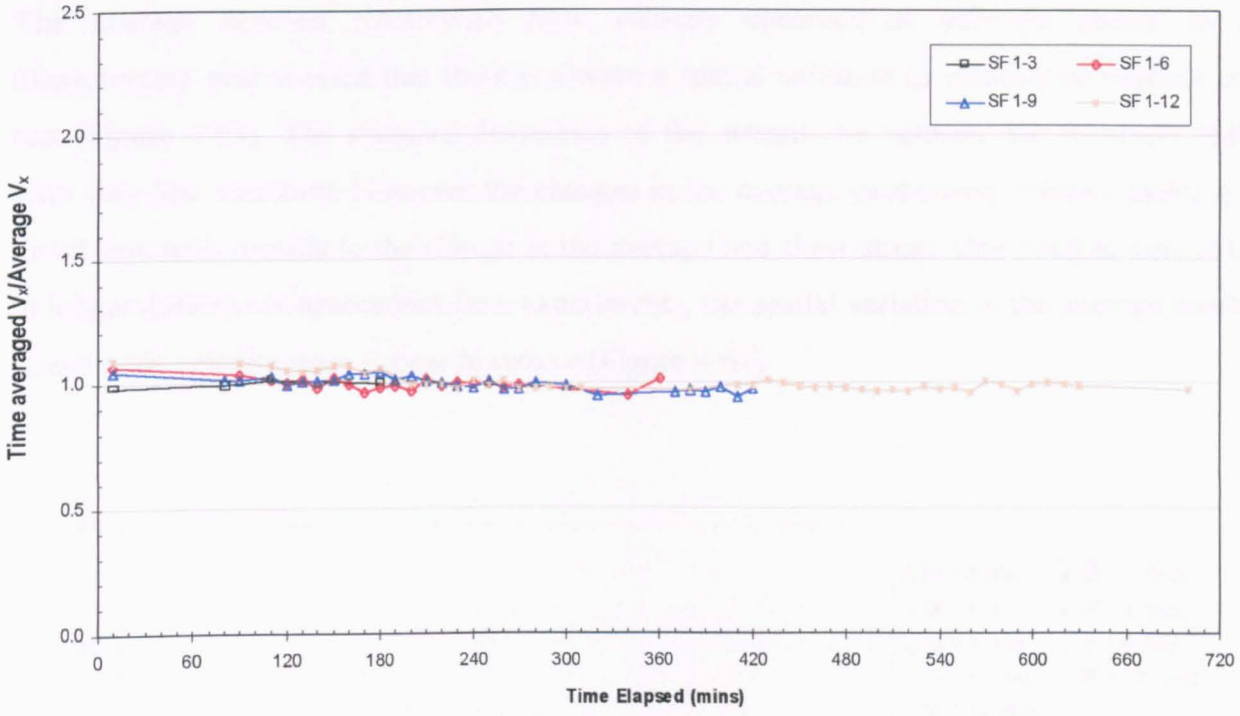

Figure 4.61. Variation of time averaged nearbed streamwise velocity during the steady antecedent flow Experiments SF I

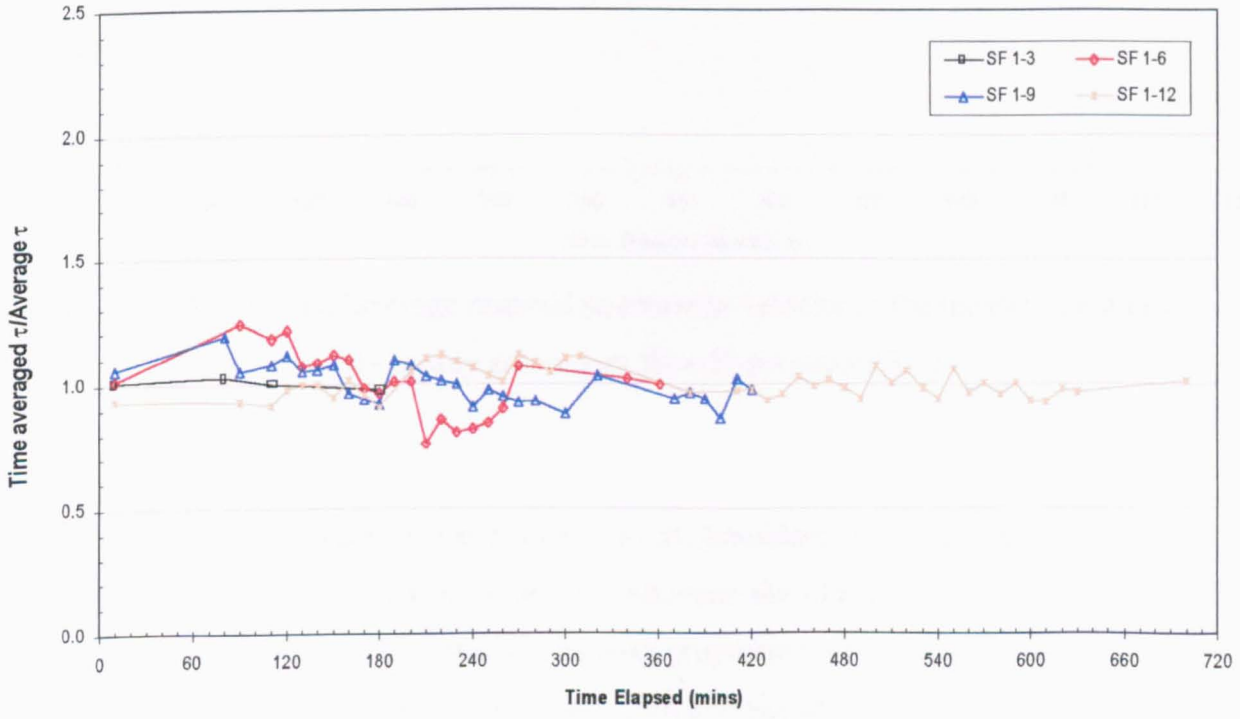

Figure 4.62. Variation of time averaged bed shear stress during the steady antecedent flow Experiments SF I

The average nearbed streamwise flow velocity observed at different points in the measurement grid showed that there is always a spatial variation in velocity throughout each test (Figure 4.63). The standard deviations of the streamwise velocity are relatively stable with very low variation. However the changes in the average streamwise velocity indicate no direct link with regards to the change in the average bed shear stress. One point to note is that in longer duration of antecedent flow experiments, the spatial variation in the average nearbed streamwise velocity does appear to reduce (Figure 4.64).

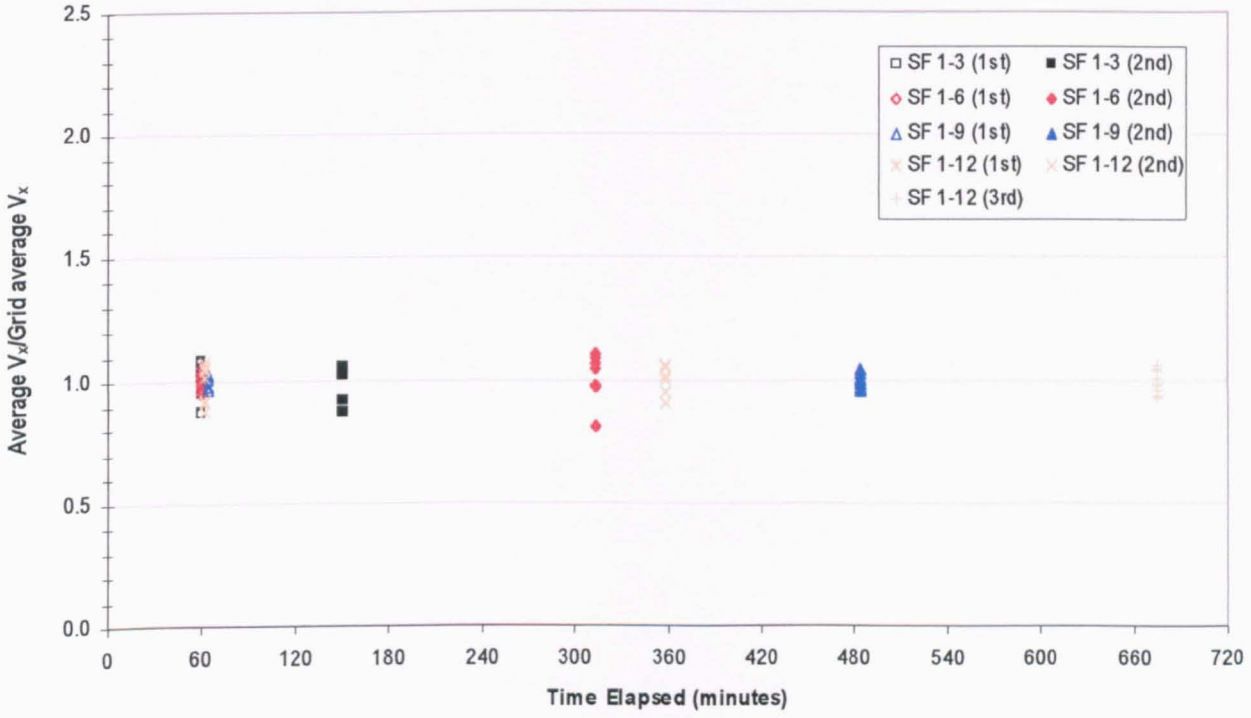

Figure 4.63. Variation of average nearbed streamwise velocity in the measurement grid during the steady antecedent flow Experiments SF I

As the measurements were carried out close to the boundary, it is reasonablee to assume that changes in the bed roughness are likely to influence the changes in the distribution of bed shear stress. Figure 4.64 shows that as the tests progressed, the spatial variation in bed shear stress reduced. In particular the areas of very high average shear stress reduced in number.

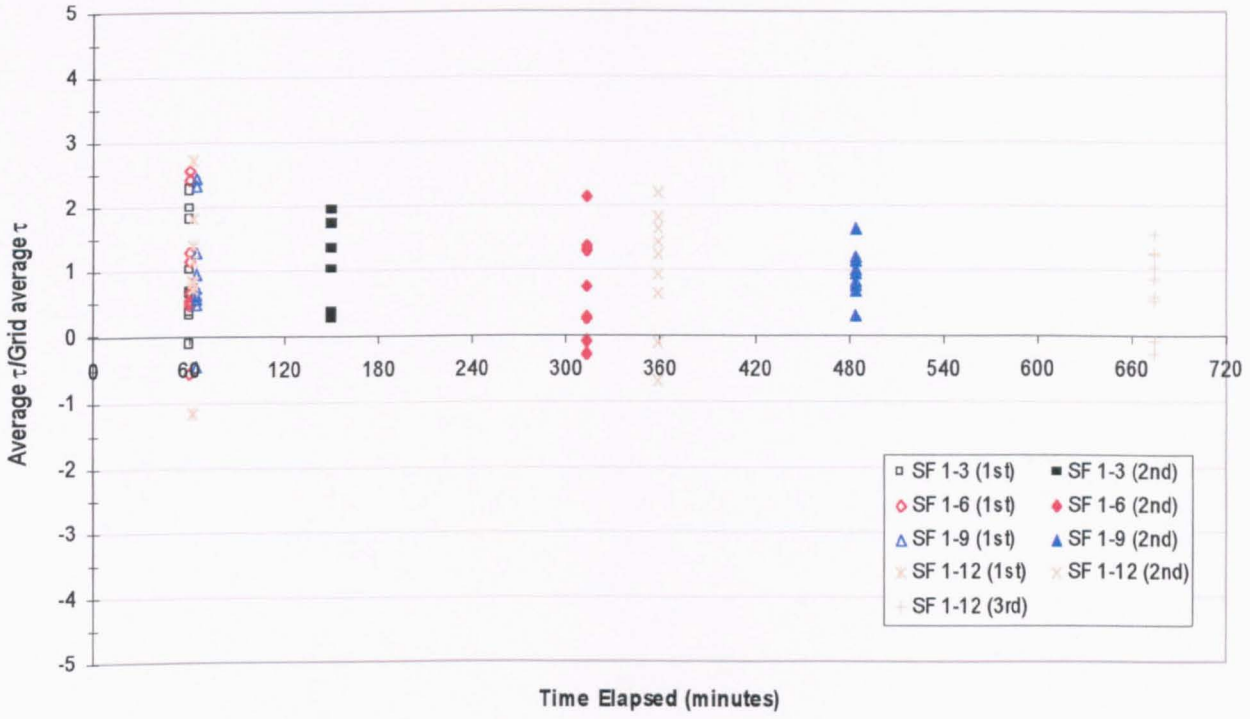

Figure 4.64. Variation of average bed shear stress in the measurement grid during the steady antecedent flow Experiments SF I

4.4.4. Bursting Events and Flow Momentum SF I

In steady antecedent flow experiments it is found that the average duration of both ejections and sweeps are quite similar (Table 4.23). This suggests that the duration of the events is not determining the transport behaviour as each antecedent flow test has different pattern in transport rate. Closer examination to the flow momentum suggests that the proportion of occurrence of high magnitude of momentum must be considered as the most important factor in grain entrainment process, particularly the coarse grains. The lowest frequency of ejections is found in the antecedent flow experiment SF 1-9. It is believed that the upward interactions with the smallest occurrence of 0.838 Hz in this experiment caused the incapability of antecedent flow to transport more material than that produced by the antecedent flow with shorter duration, i.e. antecedent flow experiments SF 1-3 and SF 1-6. As seen in Table 4.21 the irregularity in transport, where the transport rate is not as expected, is created by antecedent flow Experiment SF 1-9. It is also apparent in this test that the proportion of ejections in bursting events is the lowest among other tests (45.6 %). This is underlines the important of turbulence bursting pattern in determining the transport rate.

Table 4.23. Summary of bursting events of steady antecedent flow Experiments SF I

Parameter descriptions		Steady antecedent flow experiments			
		SF 1-3	SF 1-6	SF 1-9	SF 1-12
Ejections	Proportion (%)	49.567	52.857	45.602	50.486
	Frequency (Hz)	1.003	0.987	0.838	1.107
	Average duration (s)	0.053	0.058	0.055	0.051
Sweeps	Proportion (%)	50.433	47.143	54.398	49.514
	Frequency (Hz)	1.020	0.880	0.999	1.086
	Average duration (s)	0.052	0.050	0.052	0.051

In all steady antecedent flow experiments, it has been found that the most popular magnitude of momentum is in the range between -5 to +7 kg/ms. The momentum of downward looking-bed interactions with the low magnitude between -1 to -5 kg/ms was the most frequent. More than 35 % of downward looking-bed interactions at this strength is found in all steady antecedent flow experiments. The most common upward interactions are those with the magnitude of momentum less than 7 kg/ms. It is found that in all antecedent flow experiments the proportion of these ejections is in the range of 10 - 25 %. The existence of lower values in all antecedent flow experiments indicated that there is no coincidence with the different pattern of transport found in the same experiments. It is thought that the different pattern of momentum distribution in the higher magnitude determines the pattern of bedload transport. The observations show that the magnitude of momentum per unit area in the region above 7 kg/ms removed grains in considerable amounts. The increasing proportion of momentum in the range between 9 and 21 kg/ms increased the entrainment of grains in the coarse mode. This was seen in all tests (Figure 4.20, 4.32, 4.43 and 4.55). It is also found that the higher proportion of high momentum caused the removal of the largest grains available in the bed. This is indicated by the changes in the modal grain size of the coarse mode.

4.4.5. Bed Topography SF I

The pattern of bed surface topography after steady antecedent flow test SF 1-3, SF 1-6 and SF 1-9 tend to form diagonal patches. Different bed surface formation than that in the original bed becomes apparent, particularly elongated valleys and peaks are established in the

measurement area. Different patterns were produced by steady antecedent flow SF 1-12 with the concentration of eroded bed in certain areas and the patches are more elongated in the streamwise direction. However after the application of the stability test to this bed, a similar pattern with the other antecedent flow tests was observed in which diagonal patches are formed. Although the antecedent flow Experiment SF 1-12 had the most stable bed, the bed features were observed to be continually developing to some extent. The fluid forces in the stability test SF 1-12 were still able to remove grains with an increasing proportion in the fine mode. Some of these grains were transported downstream and trapped in the collection box whilst other grains, mainly coarse, moved in a rolling fashion changed the surface of the adjacent area.

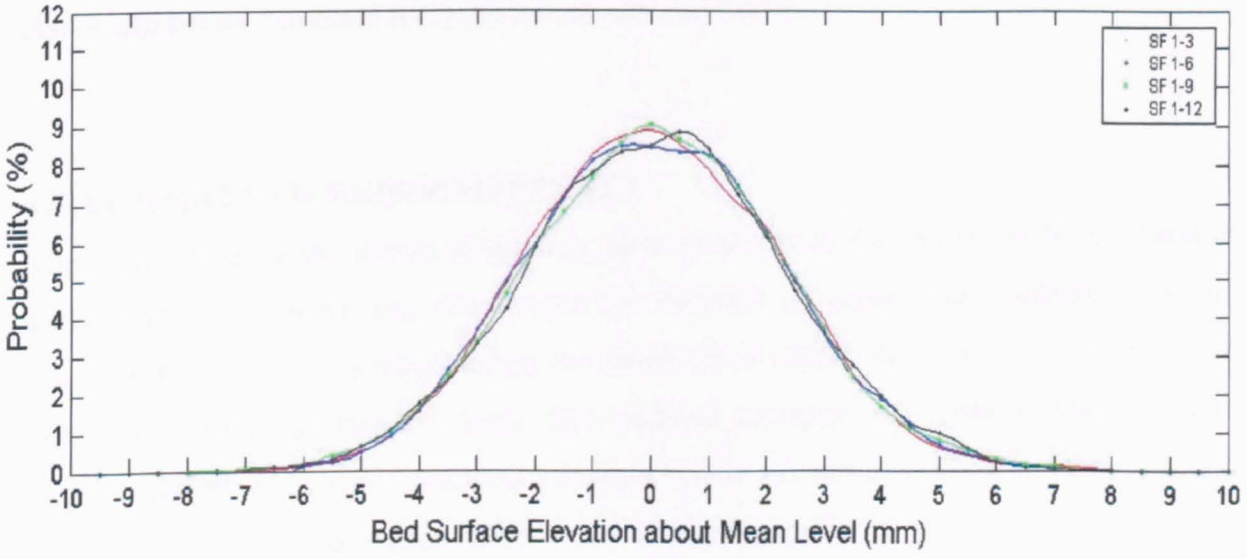

Figure 4.65. The comparison of the bed surface distribution about mean level after antecedent flow tests Experiments SF I

Although the distribution curves of the original bed surface for each test were not exactly similar, the antecedent flow tests produced almost identical distribution curves. Looking at the distribution of bed surface about the mean (Figure 4.65) it can be seen that there are differences in the bed surface caused by slightly different original bed levels. The proportion of high exposed bed and the proportion of valleys are identical to each other although closer examination indicated that more stable bed of SF 1-9 and SF 1-12 have slightly more large

positive and negative excursions from the mean. They also have slightly fewer elevations close to the mean. It appears that the number of high positive and negative values is related to bed strength, however the pattern is subtle.

The level of stability formed by antecedent flow with different durations is also reflected by the distribution curves after stability test. The difference between the distribution curve before and after stability test was easily recognised in experiment SF 1-3 (see Figure 4.24). The differences between the two curves indicate the destabilisation process was very intense during the stability test. The differences decreased for the stability tests applied to the bed formed by longer antecedent flow tests, with the least difference between curves found in experiment SF 1-12 (Figure 4.59). In stability test SF 1-12 only the distribution of bed surface elevation around the mean level changed whilst the bed surface elevation at the higher values above and below the mean level did not deviate markedly.

4.5. SUMMARY OF EXPERIMENTS SF I

The application of the identical stability tests to the beds formed by different duration of antecedent flow shows that the longer the duration of antecedent constant flowrate the stronger the bed. This is supported by the threshold of motion data for individual size fraction collected during the stability tests. The bedload transport rate pattern suggests that the stability test SF 1-3 transported a significantly higher amount of bedload in comparison to the other stability tests. During the stability test SF 1-6 the transport rate was less than half of that in the stability test SF 1-3. The transport rate was then decreased almost linearly in the stability tests for the longer antecedent flow bed SF 1-9 and SF 1-12. This suggests that beds were expected to be in a relatively stable condition after they were exposed to at least 6 hours of constant flowrates at 0.0338 m^3/s.

It is worth noting that from the threshold of motion observations of all stability tests in Experiments SF I the finer grains seem to take a shorter time to gain the maximum stability than the coarser grains. In fact the threshold of motion of the coarse grains was still increasing even after 12 hours of constant flow. In general, the domination of coarse grains in transport during the stability test lasted 40 - 50 minutes. The weaker the bed, the earlier the period of

domination started. The considerably higher transport rates were found after the peak discharge and higher average bedload transport rate in the later half of stability tests was common to all tests. This pattern of behaviour demonstrates that in each stability test the bed is progressively becoming weaker once sediment starts to move. This shown by the fact that the bedload transport rates in the falling limbs were always larger than the transport rates in the rising limbs. Given that there was little or no transport at the end of each of the steady antecedent flow test, it is reasonable to assume only the flowrates about 0.0338 m^3/s have caused significant disruption to the bed surface. Despite having similar hydrographs, the level of disruption was different in each stability test. This was thought to be another characteristic of the different levels of bed stability inherent in the beds at the end of each steady antecedent flow test.

The disruption caused by the higher flowrates in the stability test is also believed to characterise the changes in the bed surface elevations. The bed surface distribution curves before and after stability test are relatively similar compared to the distribution of original bed surface. This is very interesting because of the amounts of material transported during the stability test was considerably higher than that transported during the antecedent flow test. It is believed that the disruption not only eroded and then transported the bed material downstream, particularly the exposed grains, but also deposited the material from the upstream part. This suggests that the level of bed stability also appeared to be linked to the bed surface topography. The more stable beds were characterised by a closer distribution of bed surface elevations before and after the stability test. These identical bed surface distributions indicated that the variations of peaks and valleys are relatively balanced before and after the stability test.

There are no significant changes in the average nearbed streamwise velocity throughout the antecedent flow tests. The average values of nearbed streamwise velocity are reduced slightly particularly for the shorter time interval between measurements. This pattern was found not only for the single measurement point in the centreline of the measurement area but also from measurements of different points in a grid. These measurements indicated that there could be spatial variation in average nearbed velocity. Although these variations reduced with time, they do not follow the transport rate pattern. A similar pattern was seen for the average bed

shear stress, but with a slightly wider variation. This is thought to be due to the distribution of instantaneous vertical velocity. There was a variation in the vertical velocity distribution as the bed surface structure was continually changing during the experiment. By looking at the flow behaviour in the bursting events, it was found that during the antecedent flow tests Experiment SF I the upward interactions or ejections were more frequent than the downward-looking bed interactions or sweeps. The average duration of these events is relatively similar. This suggests that the duration of bursting events is not a good measure of their potential impact on transport. It was observed that the high momentum of ejections are responsible for transporting the coarse grains. The existence of ejections with high magnitude of momentum not only transports a considerable amount of bedload but also determines which mode of transport (coarse or fine) dominates the bedload composition.

V. EXPERIMENTAL RESULTS OF UNSTEADY FLOW EXPERIMENTS UF II

5.1. INTRODUCTION

In this chapter three antecedent flow tests with a short steady flow and with different duration of declining flow are observed. The duration of the steady flow was 3 hours with a similar steady flow discharge of 0.0338 m^3/s. This was followed by declining flow of 3, 6 and 9 hours in duration to form experiments with total duration of 6, 9 and 12 hours respectively. The results of each experiment which have been identified as UF 2-6 (6 hours duration), UF 2-9 (9 hours duration) and UF 2-12 (12 hours duration), are described and then discussed together with the observations made during their subsequent stability tests.

The aim of these experiments was to examine the influence of different declining rates of flow discharge on grain sorting and bed stability. Similar to the Experiment SF I this chapter is also divided into four sections based on the type of observations made. This was intended to make a comprehensive comparison between different type of flow hydrograph. The first section is focused on stability analysis. It describes the results of short duration of 'standard' hydrographs applied to all experiments to assess the stability of water worked bed at the end of the antecedent flow tests. The standard hydrograph used in these experiments is identical to that used in Experiment SF I. It has a peak discharge larger than the maximum discharge applied during the antecedent flow experiments. The discharge rose from a base flow of 0.0075 m^3/s to a peak flowrate of 0.0375 m^3/s in a time of 60 minutes.

The second section describes the results of each antecedent flow to obtain the condition before the stability test is applied. The observations consist of transport pattern and bedload composition that characterise the bed surface at the end of antecedent flow test. In this section bursting events was also investigated, as well as the changes in the average "instantaneous" nearbed streamwise velocity and bed shear stress. The bed topography analysis was then carried out to complete this section. The third section is containing the comparative results of all antecedent flow and the stability test, which linked and discussed those observed in the first and the second section. The fourth section is the summary of Experiment UF II.

5.2. STABILITY TESTS OBSERVATIONS UF II

5.2.1. Transport Rate Measurement UF II

Different features than those found in stability test of steady antecedent flow are experienced by stability test of unsteady antecedent flow Experiment UF II. The result of stability tests in Figure 5.1 shows that the bed formed by 3 hours constant flow rate and 6 hours declining flow rate UF 2-9 is the weakest. The transport rate increased significantly after the flow reached its peak discharge. At this stage the amount of material removed at similar level of flow rate in the rising limb and the falling limb is noticeably different. The transport rate during the last 10 minutes of the rising limb is 3.2 g/s/m compared to 4.6 g/s/m transported during the initial 10 minutes of the falling limb. This means that after peak discharge passed the transport rate is 43.4 % higher within the same period of observation. The transport rate at different time elapsed during falling limb are also higher than those transported at the similar level of discharges during rising limb.

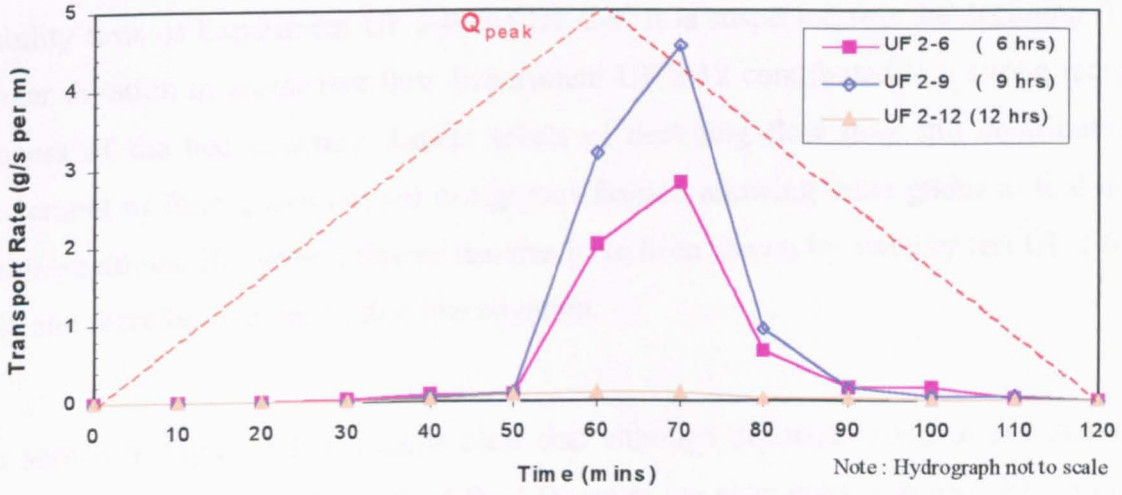

Figure 5.1. Bedload transport rate pattern during stability tests Experiments UF II

Stability test applied to antecedent flow with shorter declining flow UF 2-6 shows that although the average transported bedload during falling limb is higher than rising limb, the peak discharge caused less disruption to the bed. The transport rate during the last 10 minutes of the rising limb is 2.0 g/s/m compare to 2.8 g/s/m transported during the initial 10 minutes

of the falling limb. This means the transport rate increased 39.3 % within the same period of observation shortly after the peak discharge passed. This is a lower rate than in the stability test UF 2-9, which indicates that the beds were more resistant to the fluid forces at the peak discharge for this experiment. The transport rate at different time elapsed during the falling limb are also higher than those transported at similar level of discharges during the rising limb.

The most stable bed in this group was produced by the longest declining antecedent flow. A very low transport rate was measured during the stability test with the longest declining flow duration UF 2-12. This suggests the bed that previously exposed by the combination of 3 hours constant flow and 9 hours of slowly declining flow was very stable. A mere transport rate of 0.099 g/s/m was produced during the last 10 minutes of the rising limb and slightly lower rate at 0.094 g/s/m during the first 10 minutes of falling limb. This is very interesting as the transport rate during the similar level of flow discharge before and after the peak discharge is slightly lower rather than significantly increased as experienced in the other two stability tests of Experiment UF 2-6 and UF 2-9. It is suspected that the declining flow with longer duration in antecedent flow Experiment UF 2-12 contributed to a strong reorganising process of the bed structure. Lower levels of declining flow may still contributed to the movement of finer grains but not in rigorous fashion allowing these grains to find numerous stable positions. However different features have been shown by stability test UF 2-6 and UF 2-9, and therefore require further investigation.

As shown in Figure 5.1 it is quite clear that although different levels of bed stability have been found, only the high levels of fluid forces at the peak discharge was able to destabilise the previously formed armoured bed. As mentioned earlier the transport rate is generally increased with increasing discharge but the rates of increase were sporadic when the flow passed its peak discharge. The stability test of UF 2-6 and UF 2-9 have indicated that the beds were intensely disrupted at the highest discharge and exhibit even higher transport rates shortly afterwards. Different features, which were experienced by the stability test Experiment UF 2-12, and the pattern that the duration of the antecedent flow test did not automatically coincide with the level of stability leads to the assumption that there is an influence of the

type of declining flow hydrograph on the bed stability. The influences of rapid declining flow in stability test UF 2-6, the medium duration of declining flow in stability test UF 2-9 and the longer duration of decline in stability test UF 2-12 will be examined further in the next section of this chapter.

5.2.2. Grain Size Distribution of Transported Bedload UF II

In order to compare the transport rate pattern and the grain size distribution, it is necessary to observe the pattern of transported bedload during the stability tests. This data for the stability test Experiment UF 2-6 suggests that at the initial stage of the stability flow only finer grains were carried. The grains in the coarse mode started to appear in transport at time elapsed 40 minutes. It was when the flow reach its peak discharge at time elapsed 60 minutes the dominance of coarser grains is clearly apparent with 72.1 %. At this time only 17.3 % of transported bedload was the grains in the fine mode. At similar levels of flowrates in the falling limb, the amount of coarser grains in transport increased but the proportion is decreased because of the finer grains also increased considerably. At this time elapsed the proportion of grains in the coarse mode is 70.4 % while grains in the fine mode is 17.6 %. Interestingly grains in the coarse mode continuously dominated the transport from time elapsed 60 minutes to the end of the stability test. This underlines the importance of the coarser grains in determining the overall bed. It is believed that the rapid decrease during the antecedent flow stops all grains motion relatively quickly. This resulted in a low degree of sheltering of grains irrespective of the size.

It is noticeable that the finer grain sizes of 0.25 mm, 0.355 mm and 0.5 mm gave a consistent and significant contribution during the initial stages of the stability test (Figure 5.2). From time elapsed 60 minutes, it was the turn of grains of size 4 mm, 5.6 mm and 8 mm to contribute most to the transported bedload. In terms of total bedload transport, the importance of larger grains during the stability test of experiment UF 2-6 becomes more apparent. Table 5.1 shows that the percentage of grains in the coarse mode and grains in the fine mode of the total bedload transported during stability test are 67.4 % and 20.3 % respectively. The composition of the total bedload transported was also calculated so that the bed surface composition at the end of the test can be estimated.

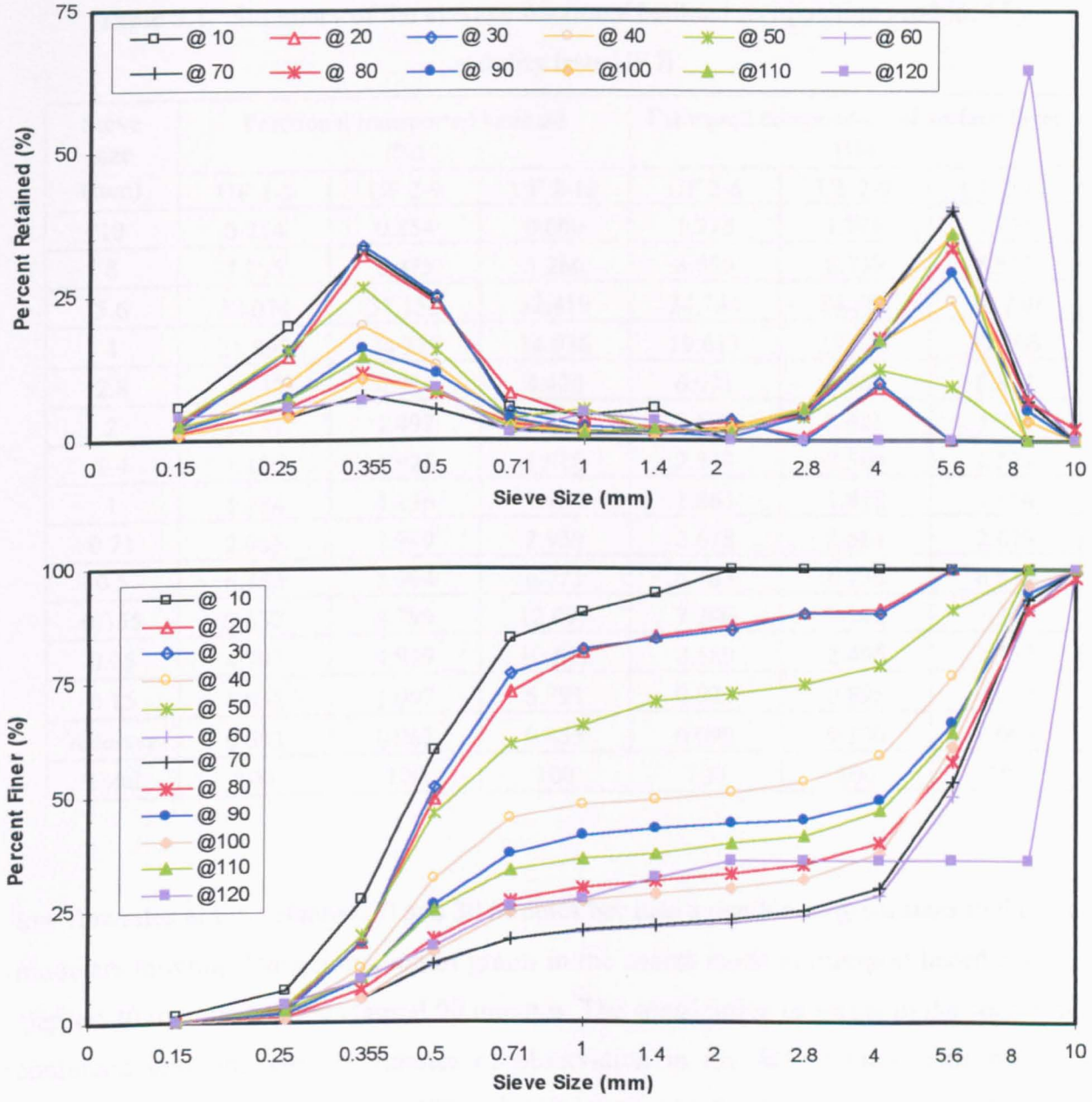

Figure 5.2. Grain size distribution of transported bedload for stability flow Experiment UF 2-6

A different feature in transport pattern is experienced by stability test UF 2-9. The grain size distribution of transported bedload suggests that the coarse mode started to move at the lower level of flowrates in comparison to the stability test UF 2-6. The presence of grain of size 5.6 mm in the coarse mode at time elapsed 10 minutes can be discounted as the possibility of only a single grain in this size fraction was accidentally transported and hence produced the "false" proportion in Figure 5.3. However this assumption is unlikely to be valid at other stages of

Table 5.1. Summary of the average fractional bedload composition produced by stability tests UF II

Sieve size (mm)	Fractional transported bedload (%)			Estimated composition of surface layer (%)		
	UF 2-6	UF 2-9	UF 2-12	UF 2-6	UF 2-9	UF 2-12
10	0.214	0.854	0.000	1.773	1.778	1.733
8	7.395	6.475	3.266	8.656	8.739	8.573
5.6	38.074	37.153	32.419	34.744	34.855	34.710
4	21.895	24.279	14.936	19.613	19.534	19.665
2.8	4.747	4.924	4.420	6.931	6.962	6.892
2	1.781	1.497	2.286	3.582	3.621	3.546
1.4	1.136	0.921	1.916	2.547	2.580	2.522
1	1.284	1.136	1.981	1.863	1.878	1.854
0.71	2.065	1.949	2.939	2.678	2.684	2.679
0.5	6.350	5.904	6.771	6.763	6.736	6.810
0.355	9.137	8.799	12.693	7.240	7.142	7.346
0.25	4.797	4.949	10.647	2.589	2.496	2.652
0.15	1.032	1.097	5.291	0.923	0.895	0.919
receiver	0.093	0.062	0.435	0.099	0.100	0.098
Total	100	100	100	100	100	100

low flowrates at time elapsed 20 and 30 minutes because a number of grain sizes in the coarse mode are moving. The domination of grains in the coarse mode in transport lasted from time elapsed 20 minutes to time elapsed 90 minutes. The contribution of grains in the coarse mode continued until the last 10 minutes of observation in the falling limb. This means the corresponding low discharges at 100 and 110 minutes in the falling limb were also able to remove grains in the coarse mode but with very low transport rate. As shown in Figure 5.3 only finer grains were transported during the last 10 minutes of the falling limb (time elapsed 120 minutes).

As experienced by stability test UF 2-6 the extreme increase of transport rate occurred in the last 10 minutes of the rising limb. The proportion of grains in the fine mode transported during this time elapsed is 16.6 %. This is almost similar to that transported during the same time in stability test UF 2-6. The proportion increased to 18.8 % during the corresponding flowrates in the falling limb. Stability test UF 2-9 also transported more material in the coarse

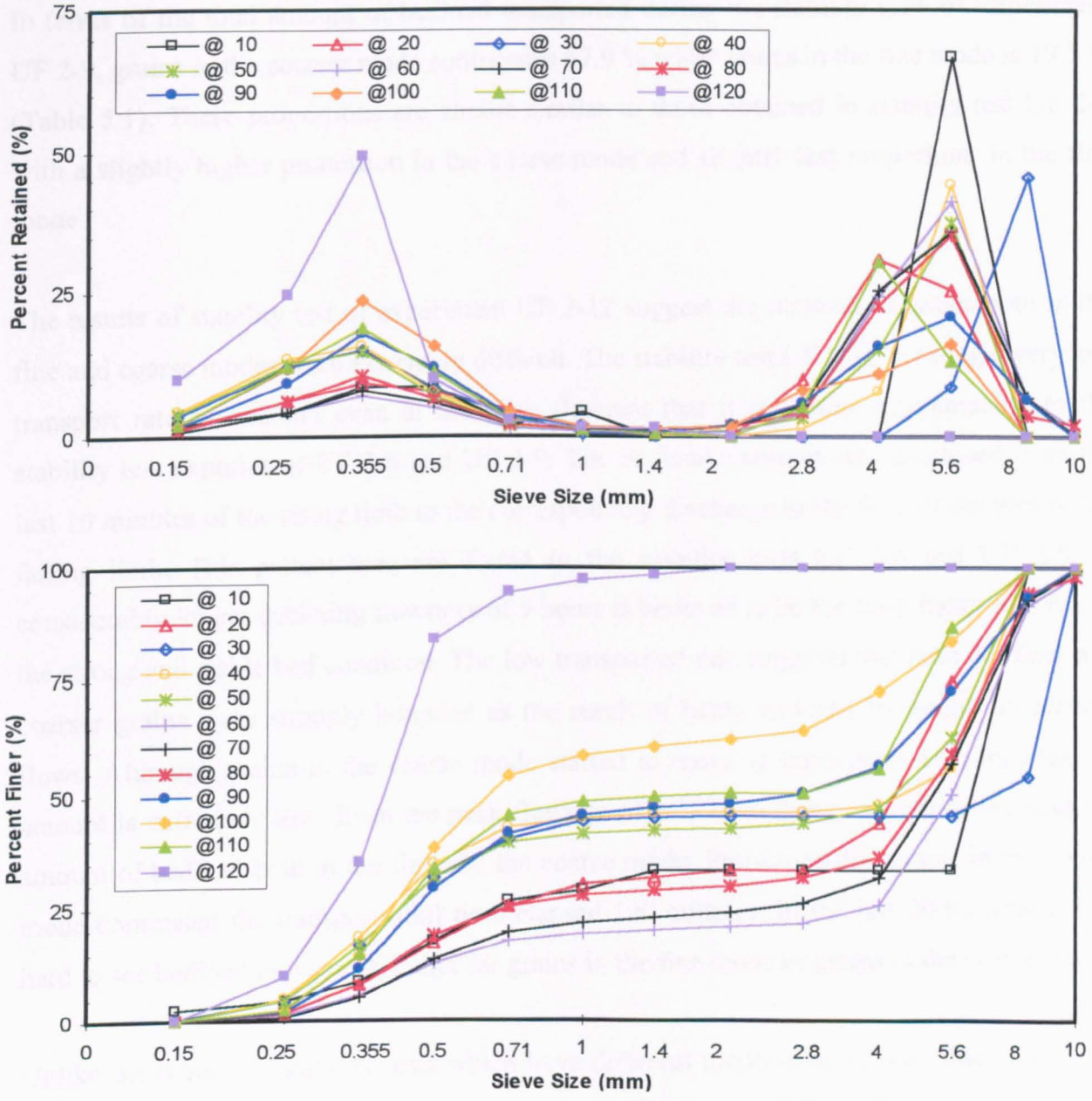

Figure 5.3. Grains size distribution of transported bedload for stability flow Experiment UF 2-9

mode than in stability test UF 2-6. The proportion at time elapsed 60 minutes is 72.8 %. The amount of the coarse mode at time elapsed 70 minutes increased significantly but the proportion is decreased to 68.1 % as the result of an increase in the proportion of fine mode. This is an indication that the bed formed by antecedent flow UF 2-9 was less stable than the bed formed by antecedent flow UF 2-6 particularly in regard to the amount of coarse grains transported during the high flowrates.

In terms of the total amount of bedload transported during the stability flow of Experiment UF 2-9, grains in the coarser mode contributes 67.9 % while grains in the fine mode is 19.7 % (Table 5.1). These proportions are almost similar to those obtained in stability test UF 2-6 with a slightly higher proportion in the coarse mode and slightly less proportion in the fine mode.

The results of stability test of experiment UF 2-12 suggest the removal of grains both in the fine and coarse modes were extremely difficult. The stability test UF 2-12 defining a very low transport rate of bedload even at the peak flowrate that it is almost incomparable to the stability test experiment UF 2-6 and UF 2-9. The bedload transport rate decreased from the last 10 minutes of the rising limb to the corresponding discharge in the first 10 minutes of the falling limb. This pattern was not found in the stability tests UF 2-6 and UF 2-9. A considerably longer declining flowrates of 9 hours is believed to be the main factor in forming the strong and stable bed condition. The low transported rate suggests that both the finer and coarser grains were strongly bounded as the result of being exposed by longer antecedent flows. Although grains in the coarse mode started to move at time elapsed 40 minutes, its amount is extremely low. Even the peak flowrate of 0.0375 m^3/s was unable to increase the amount of bedload both in the fine and the coarse mode. Proportionally, grains in the coarse mode dominated the transport until time elapsed 100 minutes. In the last 20 minutes it was hard to see bedload movement, either for grains in the fine mode or grains in the coarse mode.

Unlike the other two stability tests which have different proportions of both fine and coarse mode transported during the whole duration, stability test UF 2-12 suggests different behaviour. The difference of the proportion between the fine mode and the coarse mode is narrowed. Grains in the fine mode contributed 30.1 % of the total bedload in comparison to 50.6 % grains in the coarse mode. In the other two tests the proportion of fine sediment to coarse sediment in the bedload was almost constant with approximately 67 % in the coarse mode and 20 % in the fine mode. At the end of the rising limb of stability test UF 2-12 grains in the coarse mode were slightly more dominant than grains in the fine mode with the proportion of 43.2 % and 33.7 % respectively (Table 5.1). The proportion at the first 10 minutes of the falling limb is 25.6 % for grains in the fine mode and 58.7 % for grains in the coarse mode. It is also noticed that grain diameter 8 mm in the coarse mode was absent in the

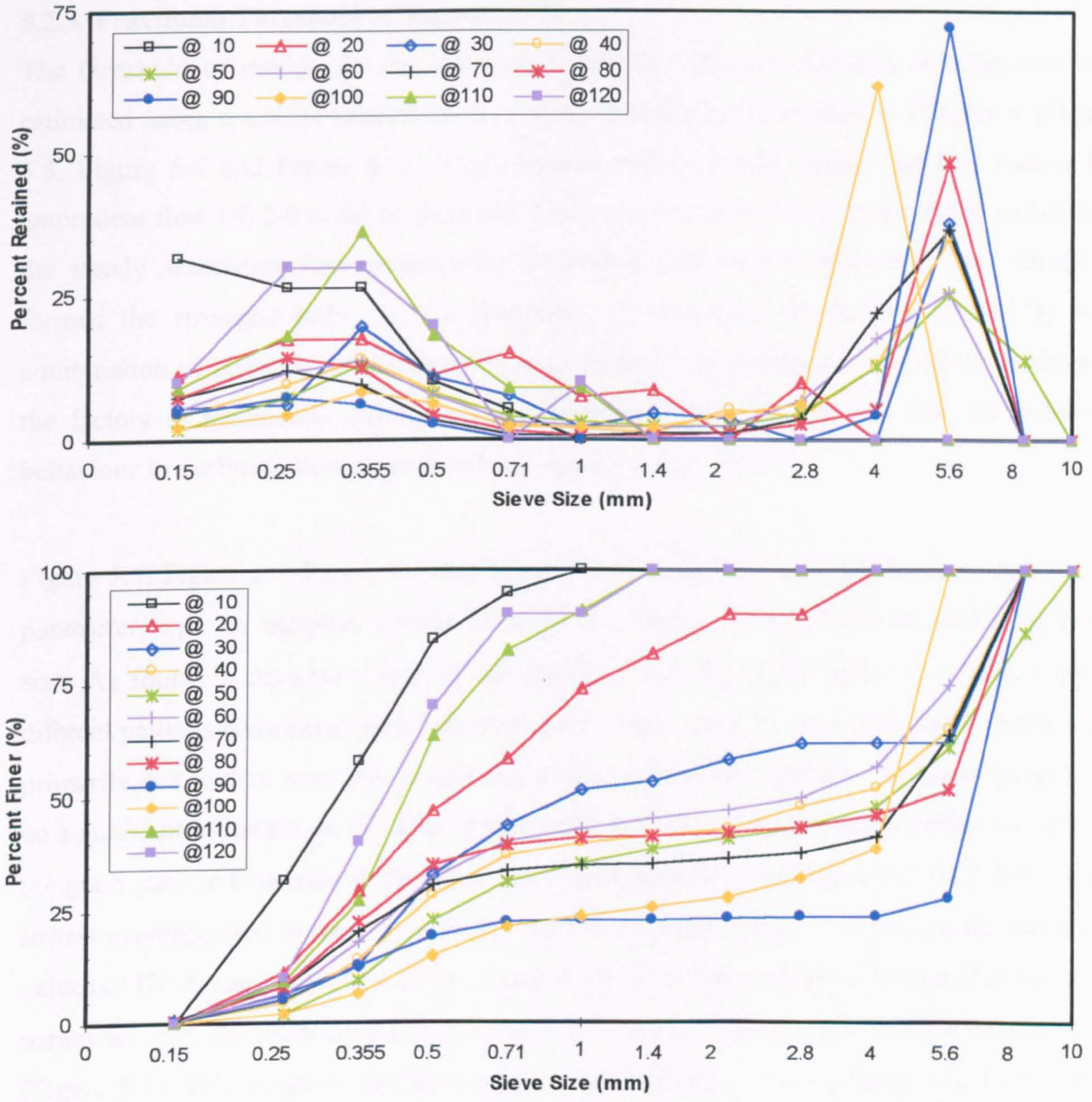

Figure 5.4. Grain size distribution of transported bedload for stability flow Experiment UF 2-12

transported bedload during the most time elapsed in this test. The only time when the appearance of this grain size was seen was at time elapsed 50 minutes, with only 1.5 grams were transported. This supported the condition that the bed formed by a long declining antecedent flow was very stable. The transport rate is very low with an increasing proportion of grains in the fine mode and significant reductions in the movement of coarse grains.

5.2.3. Fractional Threshold of Motion UF II

The threshold of motion for the individual grain size fractions for each stability test was estimated using a similar method applied in the stability tests reported in Chapter 4 (Figure 5.5, Figure 5.6 and Figure 5.7). As mentioned earlier in this chapter the bed formed by antecedent flow UF 2-9 is the weakest bed. This is a very interesting feature as the findings in the steady antecedent flow experiments underlined that longer antecedent flow durations formed the strongest beds. This is apparently not the case for the bed formed by this combination of constant and declining flow hydrograph. It is then very important to observe the factors or parameters causing these differences. The assumption is that the sediment behaviour in declining flow periods influenced the level of stability.

Figure 5.5, Figure 5.6, Figure 5.7 and Table 5.2 show that the non dimensional shear stress parameter, τ_{ri}*, for incipient motion of individual fractions decreases with increasing grain size. As found in the observation of the stability tests for steady antecedent flow, slightly diferent patterns were experienced by grain sizes 1 mm and 0.71 mm. This was thought to be primarily due to their very low availability in the original bed mixtures. As these grains have no significant influence on the amount of transport, further analysis was therefore focused on the grain sizes in both modes. The shear stress parameter, τ_{ri}*, for stability test UF 2-9 are the lowest in comparison to those for stability test UF 2-6 and UF 2-12. It is also shown that some values of UF 2-6 are very close to the values of UF 2-12. More scattered values of shear stress parameter, τ_{ri}*, for grain sizes 0.5 mm and 0.355 mm are found in the stability test UF 2-12 (Figure 5.7). This suggests that there was a wider variation in the average bed shear stress estimated from ADV measurement in comparison to those in the stability tests UF 2-6 and UF 2-9. In all stability tests the shear stress parameter, τ_{ri}*, for grains of diameter 10 mm are not available as this grain size was absent in transport. Hence no experimental information was available to derive the parameter for this grain fraction. Similar problems for the grains of diameter 8 mm in stability test UF 2-12. In stability test UF 2-12 these grains existed in transport but only at very limited time elapsed so that there was insufficient data to draw a representative value for τ_{ri}* (Table 5.2).

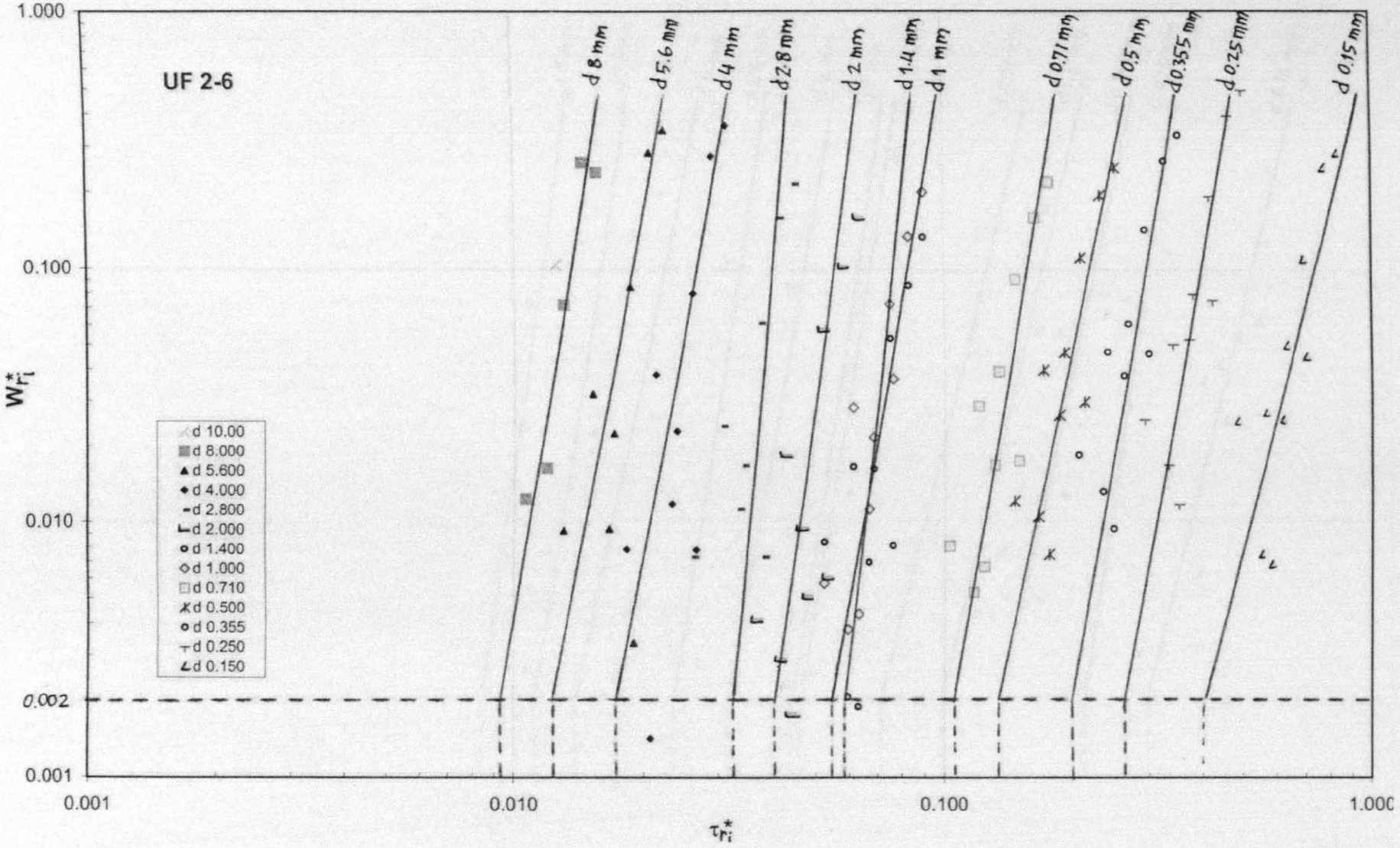

Figure 5.5. The non dimensional shear stress parameter, τ_{ri}*, determined from the low reference transport rate, W_{ri}* = 0.002, for stability tests UF 2-6

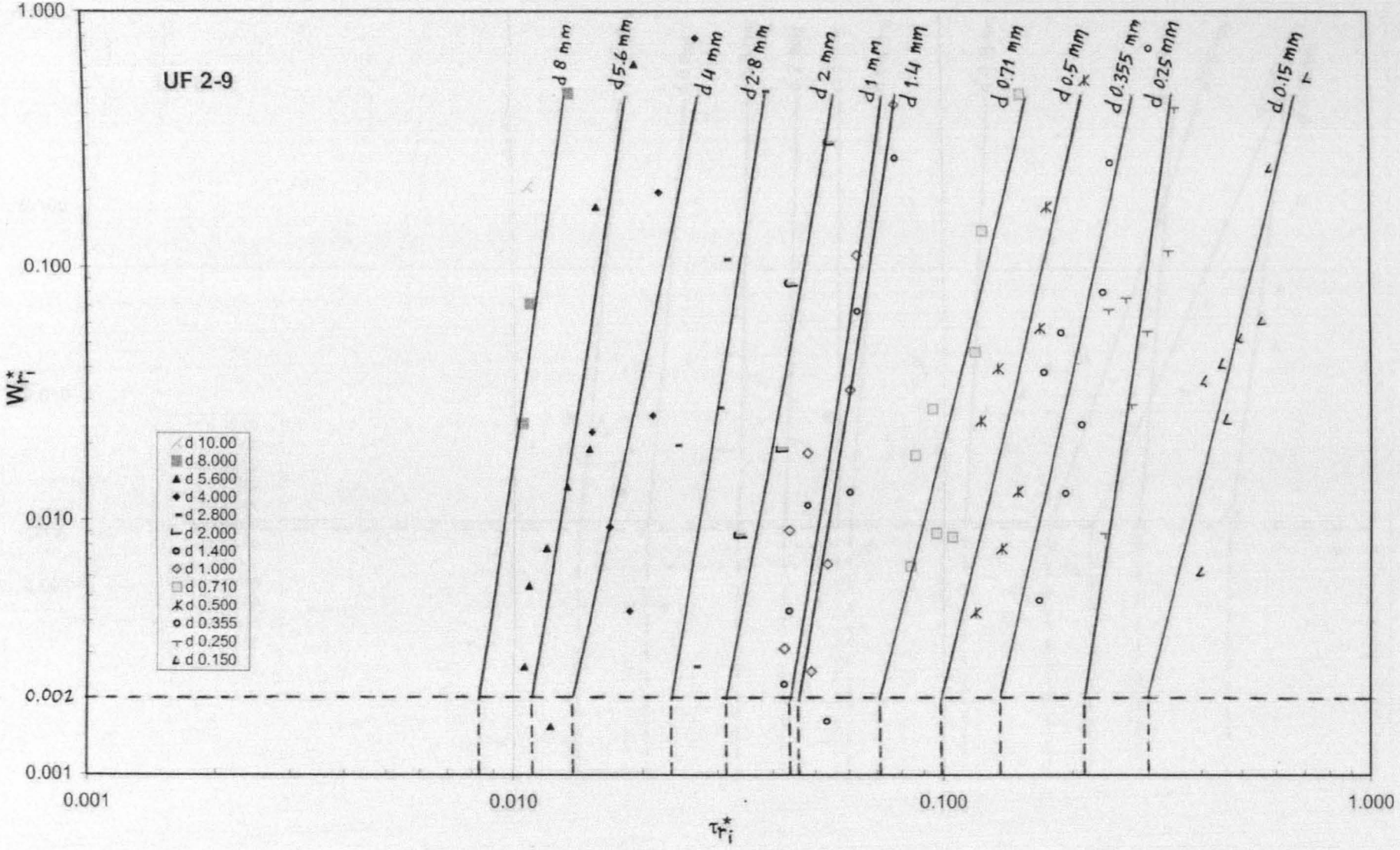

Figure 5.6. The non dimensional shear stress parameter, τ_{ri}^*, determined from the low reference transport rate, $W_{ri}^* = 0.002$, for stability tests UF 2-9

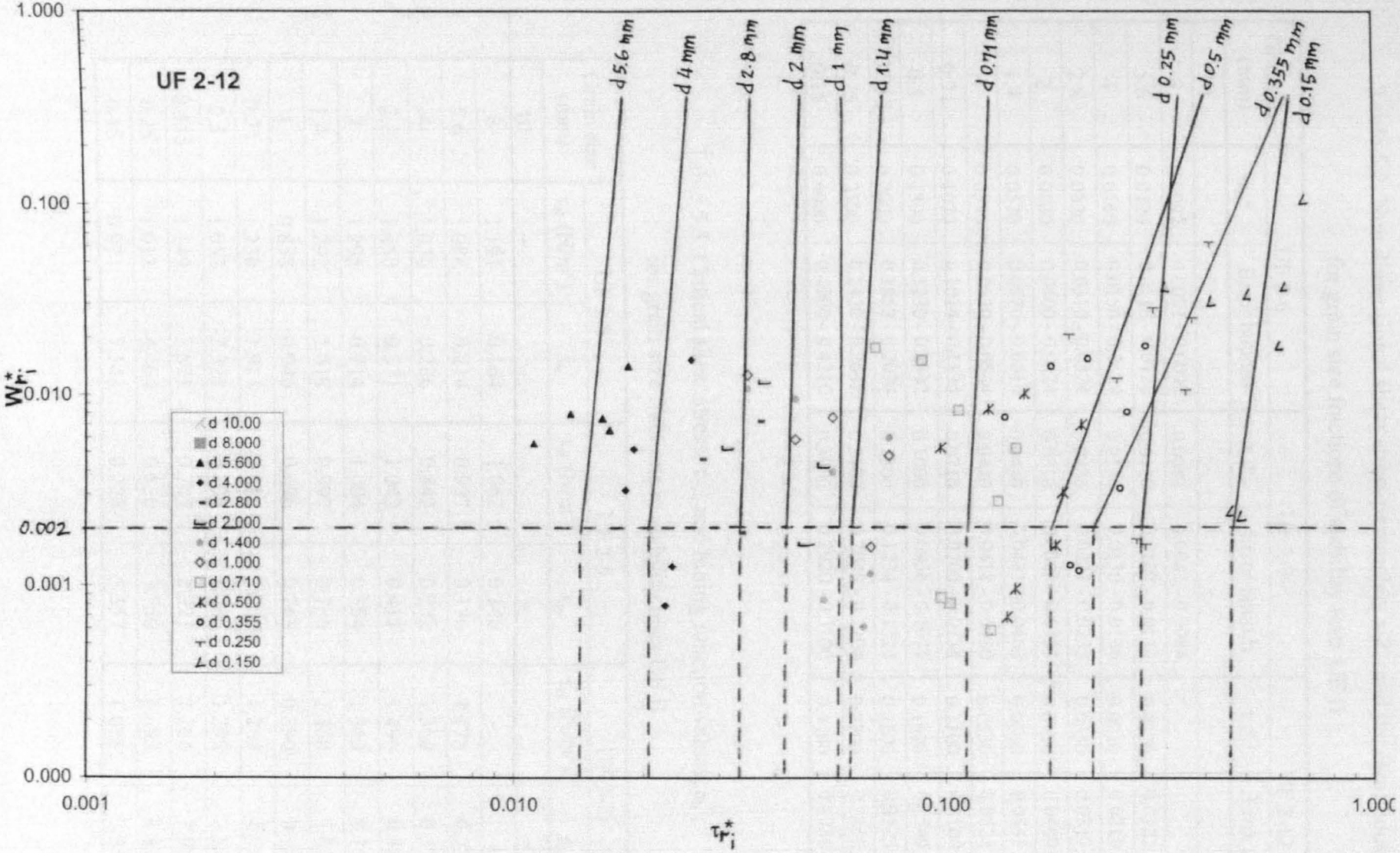

Figure 5.7. The non dimensional shear stress parameter, τ_{ri}^*, determined from the low reference transport rate, $W_{ri}^* = 0.002$, for stability tests UF 2-12

Table 5.2. Non dimensional shear stress parameter, τ_{ri}*, and the error bounds for grain size fractions of stability tests UF II

Grain size (mm)	UF 2-6		UF 2-9		UF 2-12	
	τ_{ri}*	Error bounds	τ_{ri}*	Error bounds	τ_{ri}*	Error bounds
10	-	-	-	-	-	-
8	0.0092	0.0091 - 0.0092	0.0082	0.0081 - 0.0084	-	-
5.6	0.0120	0.0118 - 0.0126	0.0110	0.0107 - 0.0114	0.0130	0.0122 - 0.0140
4	0.0160	0.0156 - 0.0179	0.0130	0.0130 - 0.0136	0.0210	0.0210 - 0.0212
2.8	0.0320	0.0310 - 0.0324	0.0230	0.0221 - 0.0232	0.0330	0.0317 - 0.0330
2	0.0400	0.0400 - 0.0424	0.0310	0.0303 - 0.0323	0.0420	0.0409 - 0.0420
1.4	0.0570	0.0570 - 0.0610	0.0440	0.0433 - 0.0463	0.0600	0.0555 - 0.0618
1	0.0530	0.0530 - 0.0544	0.0430	0.0418 - 0.0430	0.0550	0.0524 - 0.0550
0.71	0.1070	0.1014 - 0.1135	0.0710	0.0700 - 0.0734	0.1100	0.1100 - 0.1200
0.5	0.1300	0.1230 - 0.1342	0.1000	0.0936 - 0.1071	0.1600	0.1540 - 0.1600
0.355	0.2000	0.1852 - 0.2074	0.1300	0.1234 - 0.1324	0.2200	0.2123 - 0.2217
0.25	0.2500	0.2420 - 0.2642	0.2100	0.2048 - 0.2200	0.2700	0.2450 - 0.3000
0.15	0.4000	0.4000 - 0.4210	0.3000	0.2920 - 0.3100	0.4400	0.4250 - 0.4625

Table 5.3. Critical shear stress, τ_{ci}, and hiding function values, ε_{is}, for grain size fractions in stability tests UF II

Grain size (mm)	UF 2-6		UF 2-9		UF 2-12	
	τ_{ci} (N/m^2)	ε_{is}	τ_{ci} (N/m^2)	ε_{is}	τ_{ci} (N/m^2)	ε_{is}
10	-	-	-	-	-	-
8	1.191	0.164	1.062	0.146	-	-
5.6	1.088	0.214	0.997	0.196	1.178	0.232
4	1.036	0.286	0.842	0.232	1.360	0.375
2.8	1.450	0.571	1.042	0.411	1.496	0.589
2	1.295	0.714	1.004	0.554	1.360	0.750
1.4	1.292	1.018	0.997	0.786	1.360	1.071
1	0.858	0.946	0.696	0.768	0.890	0.982
0.71	1.230	1.911	0.816	1.268	1.264	1.964
0.5	1.052	2.321	0.809	1.786	1.295	2.857
0.355	1.149	3.571	0.747	2.321	1.264	3.929
0.25	1.012	4.464	0.850	3.750	1.093	4.821
0.15	0.971	7.143	0.728	5.357	1.068	7.857

The examination of the fractional critical shear stress τ_{ci} found encouraging results. The different values of non dimensional shear stress parameter τ_{ri}^* in Table 5.2 produced different critical shear stress for each grain size fraction. It was expected that the mobility of finer grains decreased while the mobility of coarser grains increased in relation to their behaviour on uniform beds. It can be seen that the weakest bed that was formed by antecedent flow UF 2-9 is clearly supported by the lower threshold of motion of all the grain size fraction available on this bed (Table 5.3 and Figure 5.8). This is reflected in the amount of bedload transported during the stability test UF 2-9 being higher than the other two tests (Figure 5.1). It can be said that the bed formed by 3 hours constant flow and 6 hours declining flow hydrograph (UF 2-9) has the lowest thresholds of motion. The bed formed by the combination of 3 hours constant flow and 9 hours declining flow hydrograph (UF 2-12) has the highest thresholds of motion for all grain sizes measured. It was impossible to make an estimate for the thresholds of motion of 8 mm grains in UF 2-12 due to the very small amount of bedload during the stability test.

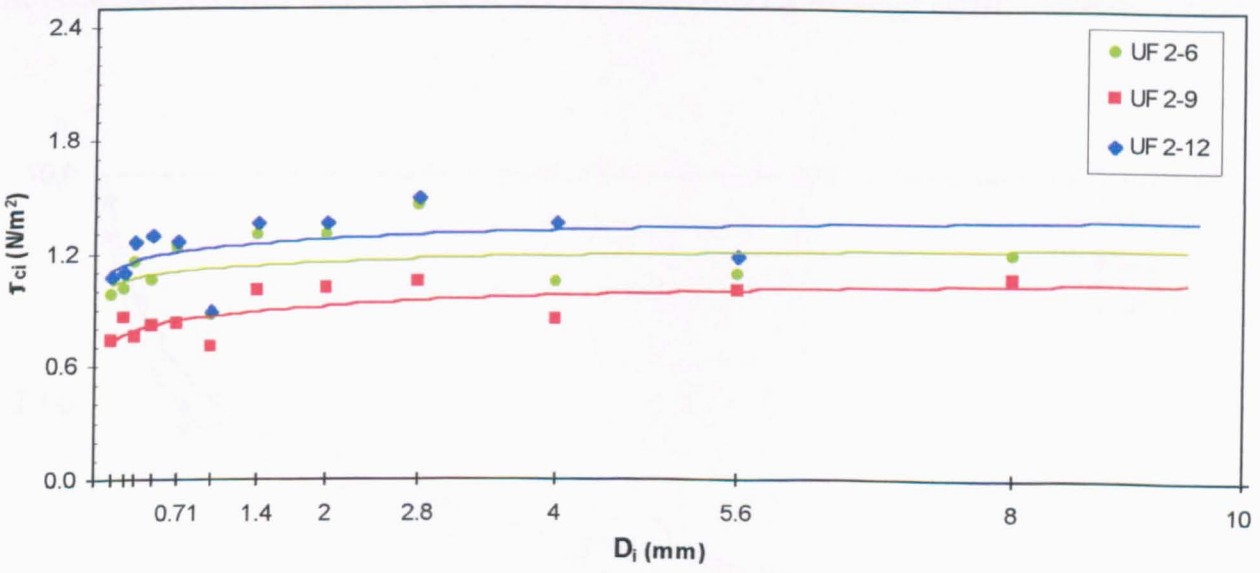

Figure 5.8. The critical shear stress, τ_{ci} , for grain size fraction in terms of grain size D_i for the stability tests UF II

Figure 5.9 shows the "hiding function type" adjustment required to predict the variation in the threshold of motion. Hiding function is calculated using Equation 4.3. It is seen that there are

wide variations throughout the grain size range unlike the constant flowrate tests in which the finer grain sizes has reach a constant stability and the coarser grains' stability varied directly with time.

In the stability tests UF II the finer grains exhibit different thresholds of motion. In the stability tests UF 2-6 and UF 2-12 the thresholds of motion up to $D_i/D_{50} = 0.2$ are very similar while in the stability test UF 2-9 the finer grains moved at considerably lower values of shear stress. In all the tests the coarser grains also exhibited different thresholds of motion. This pattern of grain size fraction thresholds suggests the following pattern of armour development. Initially only the very exposed coarse and fine grains moved. Once this has been accomplished the sediment left has a reasonable stability mainly due to the relative size of the grains, i.e. coarse grains physically shelter the fine grains. This is the end state of UF 2-6. As the higher flowrate section is extended, the flow now has a chance to sort the bed by removing the less stable fines. This also has the consequence of making the larger grains more exposed. These start to move and other deposit in more stable locations. However it is postulated that at the end of the higher flow 'mobile' section of test UF 2-9 this point had only just been reached with very few of the coarser grains finding the more stable positions. In the

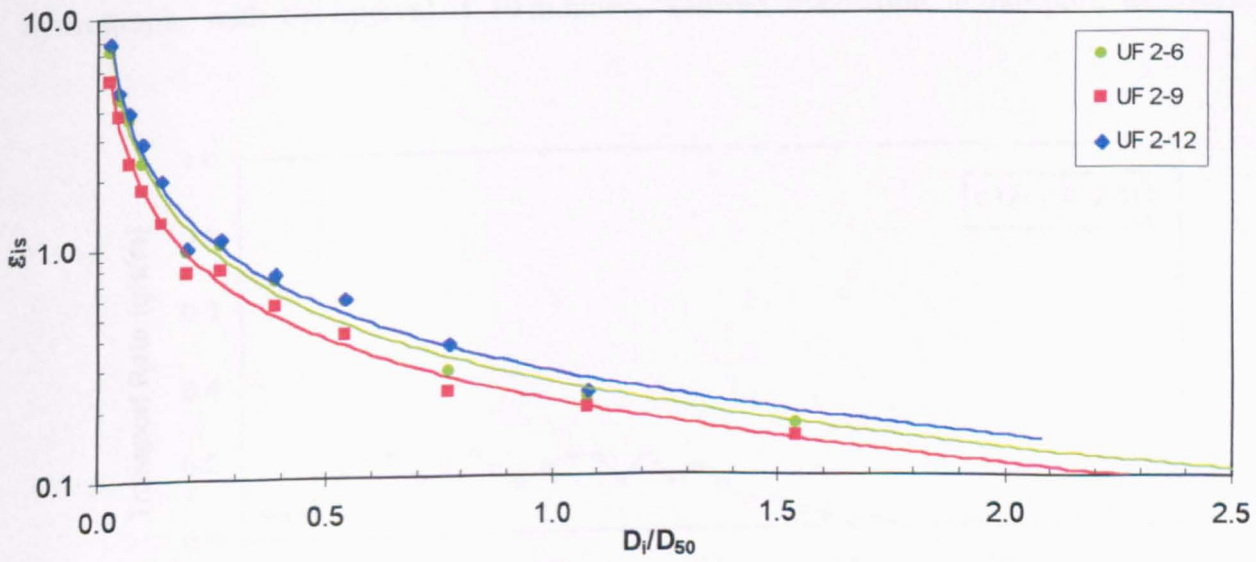

Figure 5.9. Hiding function, ε_{is}, derived from fractional threshold conditions for stability tests UF II

stability test UF 2-12 there was significantly more mobility with the coarser grains, which were able to find stable positions. The finer grains were now more able to find shelter and thus their threshold of motion also slightly increased. It is clear that the coarser grains only become more stable if they are given an extended period in which to find stable positions. If this period is further extended then the finer fractions can now find greater shelter behind these stable coarse grains. The weakest beds are formed when the fine grains are initially removed but the coarse grains have insufficient mobility to find their most stable positions. This picture of armour layer development will be confirmed by observations of bedload and composition made during the antecedent parts of the unsteady flow tests UF 2-6, UF 2-9 and UF 2-12.

5.3. OBSERVATIONS OF ANTECEDENT FLOW EXPERIMENTS UF II

5.3.1. UNSTEADY ANTECEDENT FLOW EXPERIMENT UF 2-6

5.3.1.1. Bedload Transport Rate and Composition UF 2-6

Initial stages of antecedent flow produced a low transport rate (Figure 5.10). After 30 minutes a relatively sharp increase is noted. In the first 60 minutes the average transport rate is 0.134 g/s/m. It increased in the next 120 minutes before reducing to a low value at about 240 minutes. Although the bedload collected at different time elapsed within the constant flow hydrograph, with the interval of 10 minutes, showed fluctuation in transport, the average

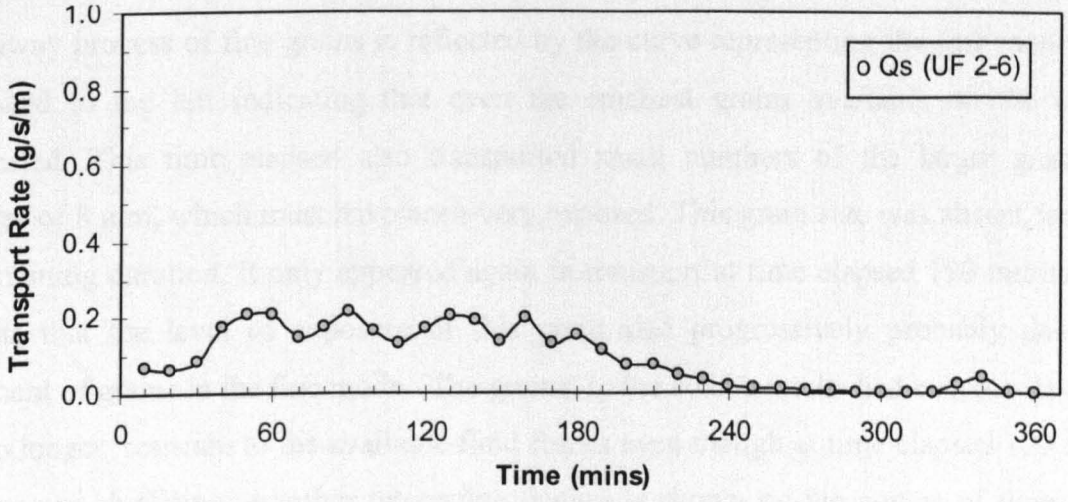

Figure 5.10. Time variation of transport rate for antecedent flow Experiment UF 2-6

hourly rates from 60 to 180 minutes are almost constant. The average transport rates at this period is 0.166 g/s/m between 60 t0 120 minutes and 0.167 g/s/m between 120 to 180 minutes respectively.

The transport rate analysis carried out in the previous chapter indicates that the bed was highly mobile during the first 180 minutes. Even though the flowrate was constant for the whole duration of experiment, the transport rate decreased after about 180 minutes. In this chapter a similar tendency is found but the declining transport rate following 180 minutes time elapsed is also due to the declining flow hydrograph. In Figure 5.10, as the flow hydrograph started to decline at time elapsed 180 minutes, the transport rate gradually decreased in the following hour. Within this period the average transport rate is 0.061 g/s/m. After this period the bedload transport rate becomes very low. The bedload decreased with an average transport rate of 0.006 g/s/m which was almost constant during the remaining hours of the test.

Observation of the bedload composition transported during antecedent flow UF 2-6 shows that the bedload was dominated by grains in the fine mode. As can be seen from Figure 5.11, the samples collected from 10 to 150 minutes indicate that sediment in the fine mode transported more than the coarse mode. The rate of transport by the fine mode then reduced. At time elapsed 160 minutes the proportion of grains in the coarse mode was slightly higher than the grains in the fine mode. Interesting features are shown by the curve of time elapsed 10-40 minutes. At this time the contribution of all grains in both modes are apparent. The wash-away process of fine grains is reflected by the curve representing the fine mode, which is skewed to the left indicating that even the smallest grains available on the bed was transported. This time elapsed also transported small numbers of the larger grains with diameter of 8 mm, which must have been very exposed. This grain size was absent for almost the remaining duration. It only appeared again in transport at time elapsed 190 minutes. This suggests that the level of exposure of this grain size progressively probably due to the movement of grains in the fine mode. The grains in the coarse mode had become less stable and no longer resistant to the available fluid forces even though at time elapsed 190 minutes the flow was declining. Another interesting feature is shown by the curves of time elapsed 230-280 minutes. No grains in the coarse mode transported during these periods. Only grains

from diameter 2 mm to the finest were transported. The distribution curve representing these times only produced a single mode, the fine mode with a considerably high proportion.

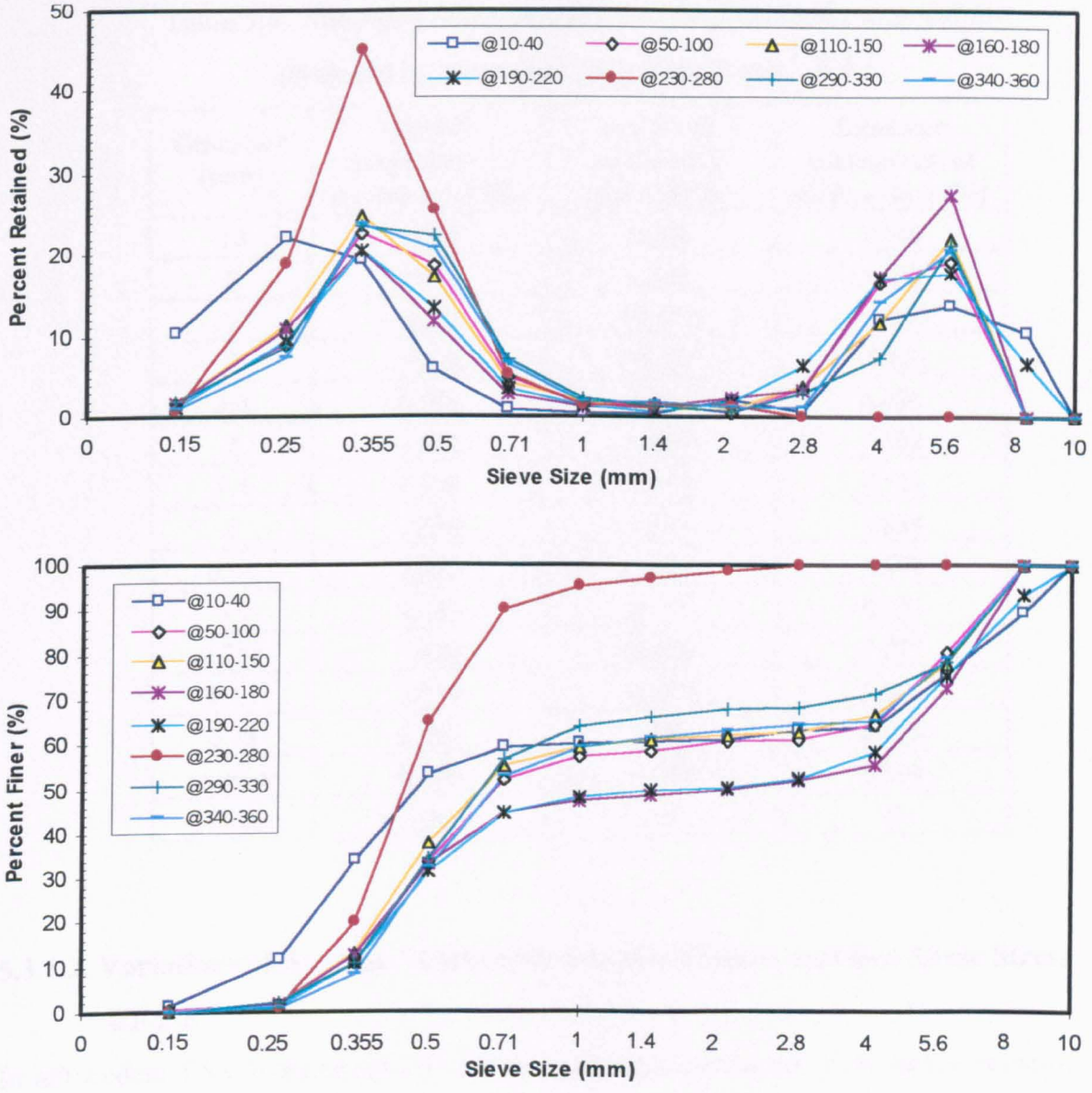

Figure 5.11. Grain size distribution of transported bedload for antecedent flow Experiment UF 2-6

The active erosion depth was estimated based on the size of the largest grain d_{100} and was used in the calculation of grain size composition left on the surface of the bed after antecedent flow. Table 5.4 shows that grains in the fine mode contributed more than grains in the coarse

mode to the transport rate as suggested by the distribution curve in Figure 5.11. The bed surface composition changed slightly but with larger variations in the finer size fractions. Little difference was noted in the surface proportions of the coarse grains.

Table 5.4. Summary of the average fractional bedload composition produced by antecedent flow Experiment UF 2-6

Grain size (mm)	Original composition of surface layer (%)	Fractional transported bedload (%)	Estimated composition of surface layer (%)
10	1.730	0.000	1.746
8	8.570	1.803	8.634
5.6	34.660	19.875	34.800
4	19.600	14.184	19.651
2.8	6.860	3.311	6.894
2	3.530	1.245	3.552
1.4	2.510	1.175	2.523
1	1.850	1.481	1.854
0.71	2.680	3.953	2.668
0.5	6.840	15.721	6.756
0.355	7.420	22.930	7.273
0.25	2.710	11.526	2.626
0.15	0.940	2.546	0.925
receiver	0.100	0.250	0.099
Total	100	100	100

5.3.1.2. Variations of Average Nearbed Streamwise Velocity and Bed Shear Stress UF 2-6

In antecedent flow Experiment UF 2-6 measurement of nearbed streamwise velocities were also carried out at a number of times at the central point of the measurement grid. Figure 5.12 shows that for the period of constant flowrate, limited observation were available because of the measurement and observation of nearbed streamwise velocity in the grid were also carried out during the course of the constant discharge section.

It can be seen from Figure 5.12 that the average nearbed streamwise velocity is sensibly constant between the start to the time elapsed 180 minutes. It is understandable since the flow

applied over the bed was kept constant at the discharge of 0.0338 m^3/s. The values of average velocity reduced slowly after 180 minutes corresponding to the declining flowrate. The variation in the average values of bed shear stress, $\overline{\tau''}$, is very small and almost constant in the first 180 minutes. The bed shear stress was estimated using Equation 3.14 and the average values was calculated using Equation 3.16. From 180 to 270 minutes the average bed shear stress drops quickly and consistently as the flowrate reduces. However an inconsistent variation is found just before the last hour of experiment. This is thought to be due to the low flow depth where the possible failure to the ADV probe influenced the measurement.

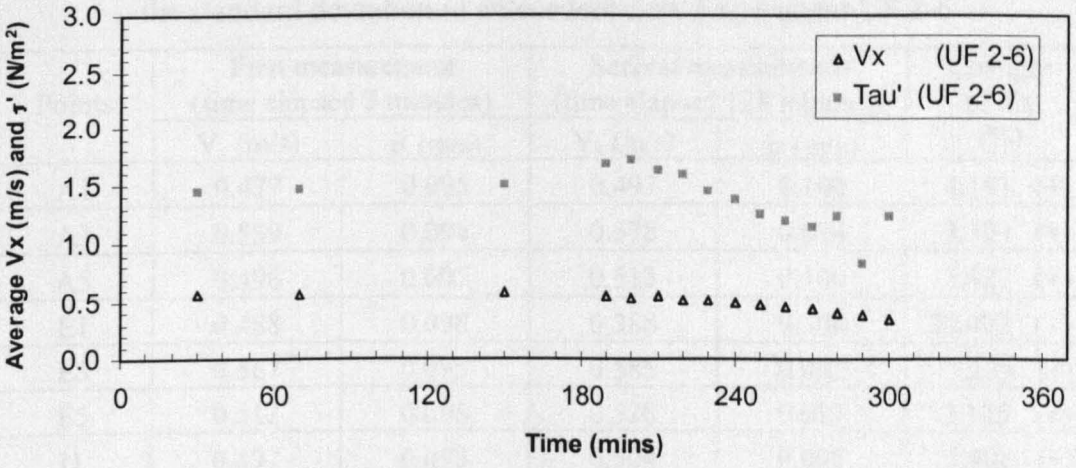

Figure 5.12. Variation of time averaged nearbed streamwise velocity and bed shear stress during antecedent flow Experiment UF 2-6

Data similar to those collected in the steady antecedent flow experiments were used to investigate the changes in the average nearbed streamwise flow velocity of the grid points by comparing the results of measurements at two series of different time elapsed. The constant flowrate lasted only 3 hours so that the time interval between measurement was relatively short (125 minutes). The results of the observations are presented in Table 5.5 and Figure 5.13. It shows that the average nearbed streamwise flow velocity of each grid point was generally increased after 125 minutes but not very significant. The range of variations is between 1.4 to 6.8 % except at point E1. This point experienced a high decrease in the average nearbed streamwise flow velocity. The second measurement gives the lowest values among all the other points. It is suspected that high fluctuation occurred at this point where

the individual values were dispersed from the mean as indicated by higher standard deviations. This pattern indicates the possibility of different distribution in the nearbed streamwise velocity over a relatively small area. As flow discharge was kept constant, it is suspected that the variations in average streamwise velocity at point E1 were subjected to the changes in the bed surface structure caused by temporal variation in sediment transport. The integrated effects of the fluid velocities over and around grains destabilise the sediment and produced movement to form different bed surface at different time.

Table 5.5. Variations of the average nearbed streamwise velocity and the standard deviation in antecedent flow Experiment UF 2-6

Points	First measurement (time elapsed 3 minutes)		Second measurement (time elapsed 128 minutes)		Changes of Vx (%)
	V_x (m/s)	σ (m/s)	V_x (m/s)	σ (m/s)	
A1	0.477	0.095	0.497	0.100	4.193 (+)
A3	0.559	0.094	0.578	0.094	3.399 (+)
A5	0.496	0.097	0.513	0.100	3.427 (+)
E1	0.488	0.098	0.388	0.308	20.492 (-)
E3	0.567	0.095	0.585	0.092	3.175 (+)
E5	0.512	0.098	0.528	0.097	3.125 (+)
I1	0.497	0.093	0.504	0.097	1.408 (+)
I3	0.559	0.097	0.575	0.092	2.862 (+)
I5	0.501	0.097	0.535	0.094	6.786 (+)
Average	0.517	0.096	0.513	0.119	

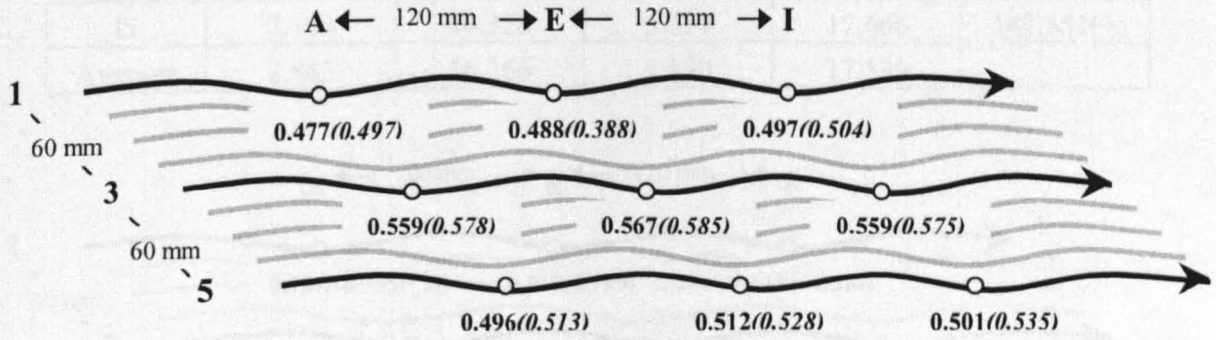

Figure 5.13. Distribution of average nearbed streamwise velocity (m/s) in antecedent flow Experiment UF 2-6 (first measurement in bold, second measurement in brackets)

Table 5.6 and Figure 5.14 shows that the patterns of average bed shear stress do not

automatically follow the pattern in average nearbed velocity. The variations of these values are much wider. The increases and reductions at the grid points indicating no systematic pattern. The most possible factor for this variation is the variation in the vertical velocity. The level of fluctuation of bed shear stress increased with time, with the standard deviation increasing at each grid point. It is very clear that the wide and scattered values of the average bead shear stress in Table 5.5 is the indication that the fluctuation of flow velocity in vertical direction was continued during the observation in constant flowrates. Normally when the streamwise velocity experience a low variation, a small variation in bed shear stress was expected if the fluctuation in vertical velocity were also small. However this appeared not to be the case.

Table 5.6. Variations of the average bed shear stress and the standard deviation in antecedent flow Experiment UF 2-6

Points	First measurement (time elapsed 3 minutes)		Second measurement (time elapsed 128 minutes)		Changes of $\overline{\tau}$ (%)
	$\overline{\tau}$ (N/m^2)	σ (N/m^2)	$\overline{\tau}$ (N/m^2)	σ (N/m^2)	
A1	0.761	14.658	-0.795	15.154	204.468 (-)
A3	8.107	16.880	3.074	18.818	62.082 (-)
A5	3.433	16.562	1.498	17.621	56.365 (-)
E1	0.015	15.525	0.199	17.411	1226.667(+)
E3	-0.890	16.964	6.992	18.466	885.618(+)
E5	4.161	16.853	4.584	17.445	10.166 (+)
I1	-2.184	15.630	-2.324	16.569	14.000 (-)
I3	10.384	17.894	9.735	18.700	6.250 (-)
I5	2.164	16.328	5.357	17.666	147.551(+)
Average	2.883	16.366	1.890	17.539	

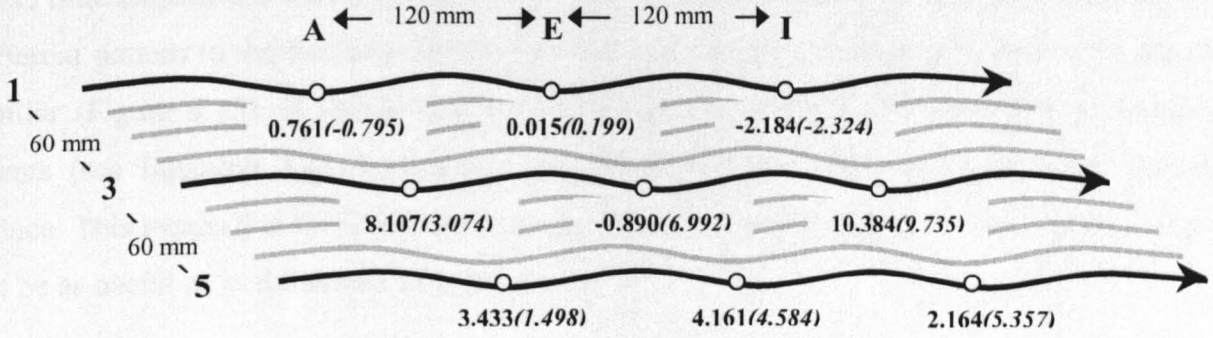

Figure 5.14. Distribution of average bed shear stress (N/m^2) in antecedent flow Experiment UF 2-6 (first measurement in bold, second measurement in brackets)

5.3.1.3. Bursting Events and Flow Momentum UF 2-6

A different pattern of bursting events than those experienced in all steady flow experiments is shown in Experiment UF 2-6. It has been found that during the constant discharge of antecedent flow experiments the ejections are generally more common than sweeps. In antecedent flow Experiment UF 2-6 the number of occurrences of sweeps is higher than ejections (Table 5.7). The difference is even lower in the falling limb. In general the average duration of both events is observed to be almost similar throughout the antecedent flow Experiment UF 2-6. The variation in the average duration is very small particularly in the falling limb. The frequency of bursting events in the falling limb is slightly higher than in the constant flowrates section. This means that in the decelerating flow more events were observed. However it is unclear whether the declining flow is the reason for this phenomenon.

Table 5.7. Time frequency and the proportion of occurrences of bursting events in antecedent flow Experiment UF 2-6

Parameter descriptions		Frequency (Hz)	Proportion (%)	Average duration (sec.)
Constant flowrate	Ejections	0.945	47.487	0.050
	Sweeps	1.045	52.513	0.053
Falling limb	Ejections	0.982	48.372	0.052
	Sweeps	1.048	51.628	0.051

Four different time elapsed are selected to observe the pattern of momentum magnitude in relation to the change in the grain size distribution of transported bedload. The summary of those time elapsed are shown in Table 5.8. Although time elapsed 150 and 290 minutes have different pattern in the bursting events, the mode of transported bedload seems to be almost similar (Figure 5.15). It should also be noted that the mathematical definition of bursting events (see Equation 2.12) means that the threshold value declines as the flow velocity reduce. This means that the information on the frequency and duration of bursting events may not be as useful as in the steady flow tests.

Table 5.8. Summary of bursting events at selected time elapsed in antecedent flow Experiment UF 2-6

Parameter descriptions	Time elapsed (minutes)			
	150	190	230	290
Threshold values (m^2/s^2)	0.0071	0.0074	0.0065	0.0049
Number of ejections	197	189	209	206
Number of sweeps	214	207	213	178
Frequency of ejections (Hz)	0.985	0.945	1.045	1.030
Frequency of sweeps (Hz)	1.070	1.035	1.065	0.890
Average duration of ejections (s)	0.050	0.051	0.052	0.049
Average duration of sweeps (s)	0.053	0.048	0.053	0.049

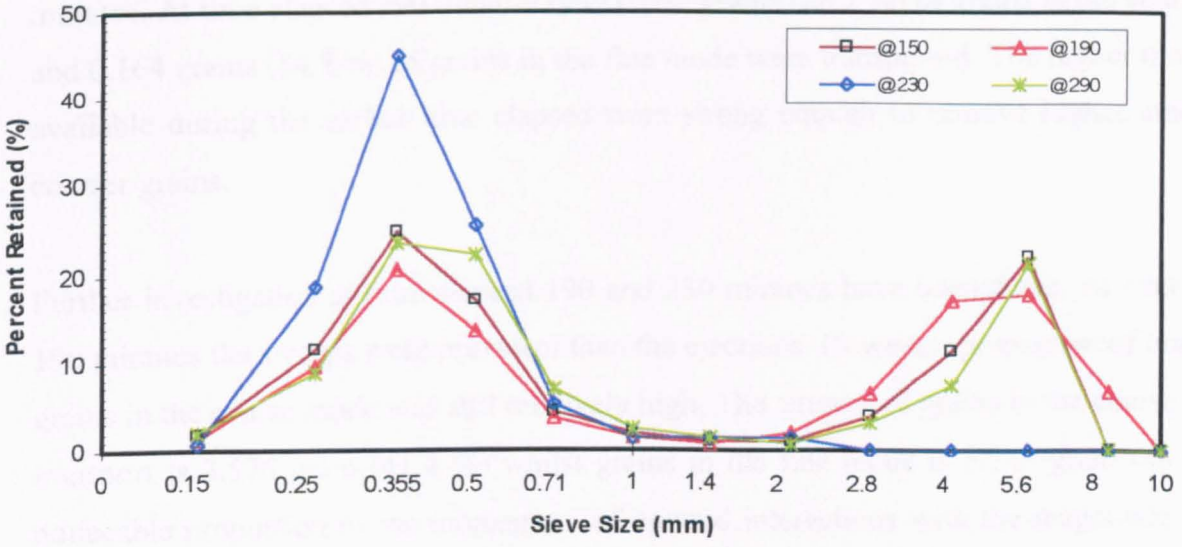

Figure 5.15. Grain size distribution of transported bedload at selected time elapsed in antecedent flow Experiment UF 2-6

The general pattern found in steady flow experiments is that the high momentum of ejections is very important in transporting coarser grains. The similarity in the modes of transported bedload at time elapsed 150 and 290 minutes may be explained by examining the probability density of the momentum per unit area of both time elapsed (Figure 5.16). The earlier time produces more sweeps in the range between -9 to -3 kg/ms. However at both time elapsed the flows were able to remove the finer grains. A more noticeable difference is found in the upward interactions. During time elapsed 150 minutes the momentum was dominated by the values between 3 and 7 kg/ms whereas time elapsed 290 minutes was clearly dominated by the lower momentum (1 to 5 kg/ms). Time elapsed 150 minutes also had many values of

momentum in the range between 15 and 19 kg/ms while time elapsed 290 minutes had many values between 5 and 11 kg/ms. This is understandable as the earlier time elapsed was in the constant flow with the higher discharge and the latter time elapsed was in the falling limb of flow hydrograph with low and declining discharge. The average instantaneous streamwise velocity at time elapsed 150 minutes was 0.585 m/s whilst at time elapsed 290 minutes was 0.384 m/s. Although the proportion of transported bedload for both modes at time elapsed 150 and 290 minutes were almost similar, the different pattern of momentum in bursting events influenced the amount of transport. At time elapsed 150 minutes 5.159 grams (33.4 %) of grains in the coarse mode and 8.226 grams (53.3 %) of grains in the fine mode were transported. These are considerably higher than the amount transported at time elapsed 290 minutes. At time elapsed 290 minutes only 0.086 grams (28.7 %) of grains in the coarse mode and 0.164 grams (54.8 %) of grains in the fine mode were transported. The higher momentum available during the earlier time elapsed were strong enough to remove higher amounts of coarser grains.

Further investigation at time elapsed 190 and 230 minutes have been made. At time elapsed 190 minutes the sweeps were prevalent than the ejections. However, proportion of transported grains in the coarse mode was still relatively high. The amount of grains in the coarse mode in transport is 3.576 gram (41.4 %) whilst grains in the fine mode is 3.749 gram (43.4 %). A noticeable proportion of the momentum of upward interactions with the magnitude between 11 to 17 kg /ms is believed to be the contributor in transportation of grains in the coarse mode at time elapsed 190 minutes. A different distribution of momentum of the ejections is shown by time elapsed 230 minutes. Theoretically, the momentum with the values in the range between 9 and 13 kg/ms would contribute to the removal of coarser grains. In fact, the coarser grains were absence in transported bedload but replaced by a high proportion of finer grains. This indicates that the ejections require a momentum threshold of approximately 13 kg/ms before they can move the coarser grains. The general pattern of grain movement in relation to the momentum found in the steady antecedent flow tests was also found in the antecedent flow Experiment UF 2-6. High momentum ejections correlated with movement of coarse grains. The number and size of the ejections after 150 minutes reduces significantly with a clear reduction between 150 and 190 minutes. This suggests very low mobilities for the coarser grains once the flowrate declines.

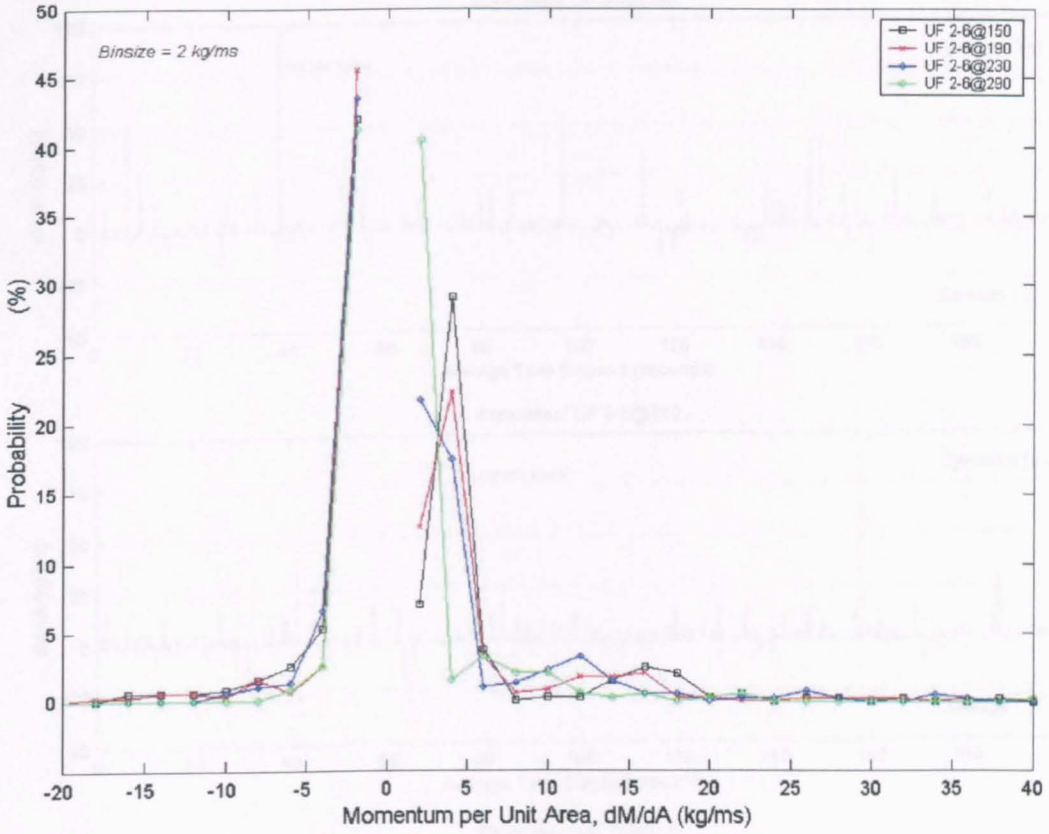

Figure 5.16. Probability distribution of momentum per unit area at selected time elapsed in antecedent flow Experiment UF 2-6 (ejections are positive and sweeps are negative)

Figure 5.17, which is presented to provide information on the sequence of momentum per unit area along with its magnitude, shown that the high momentum in upward interactions occurred at time elapsed 150 and 190 minutes. It can also be seen that the sequence with low magnitude of momentum both in the ejections and sweeps were occurred at time elapsed 290 minutes. At this time elapsed the flowrate was very low. A small variation in the streamwise and vertical flow velocity were expected and therefore low threshold value of bursting event was applied.

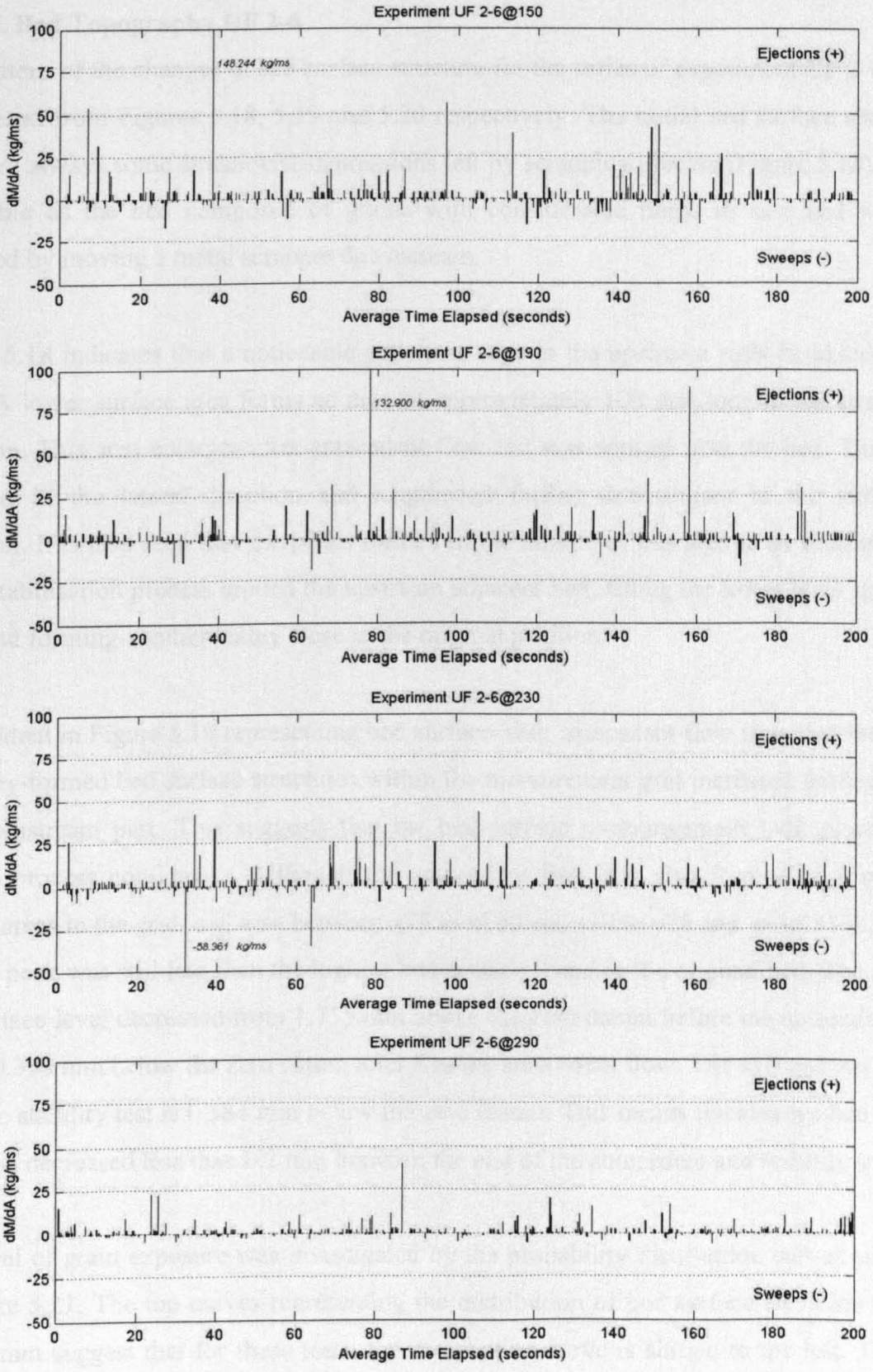

Figure 5.17. The sequence of momentum per unit area and its magnitude at selected time elapsed of antecedent flow Experiment UF 2-6

5.3.1.4. Bed Topography UF 2-6

The pattern of the changes in bed surface structure for the series of experiment UF 2-6 can be recognised from Figures 5.18, 5.19 and 5.20 respectively. The initial bed surface shows that there are always some streamwise depressions left by scrapping process (Figure 5.18). This is inevitable as the bed composed of grains with considerable range in size and was then flattened by moving a metal scrapper downstream.

Figure 5.18 indicates that a noticeable pattern is seen in the upstream right hand side of the grid. A lower surface area forms an area of approximately 100 mm long in the streamwise direction. This area enlarges after antecedent flow test was applied over the bed. The size is widened in the lateral direction and lengthened further downstream in the streamwise direction. It is also seen that the peaks formed in the middle of this area is an indication that the destabilisation process eroded the upstream adjacent bed, filling the lower level surface in front and forming another valley close to the original position.

It is evident in Figure 5.19 representing bed surface after antecedent flow tests that the spread of valley-formed bed surface structures within the measurement grid increased particularly in the downstream part. This suggests that the bed surface re-arrangement took place as the erosion process continued. Although the antecedent flow test also formed high peaks in certain areas in the grid, e.g. area between x75 to x100 and y19 to y25 and point (150,50), the highest peak was still less than the highest bed surface found in the original bed. The average bed surface level decreased from 1.755 mm above the zero datum before the antecedent flow test to 0.390 mm below the zero datum after 6 hours antecedent flow. The average bed surface after the stability test is 0.584 mm below the zero datum. This means the average bed surface elevation decreased less than 0.2 mm between the end of the antecedent and stability test.

The level of grain exposure was investigated by the probability distribution curves as shown in Figure 5.21. The top curves representing the distribution of bed surface elevation about a zero datum suggest that for these tests, the distribution curve is shifted to the left. This is a clear indication that the overall bed surface level decreased. As previously seen in the figures of bed topography, a significant decrease in positive bed surface elevation is found after the antecedent flow test. As the antecedent flow eroded the original bed, there was a decrease in

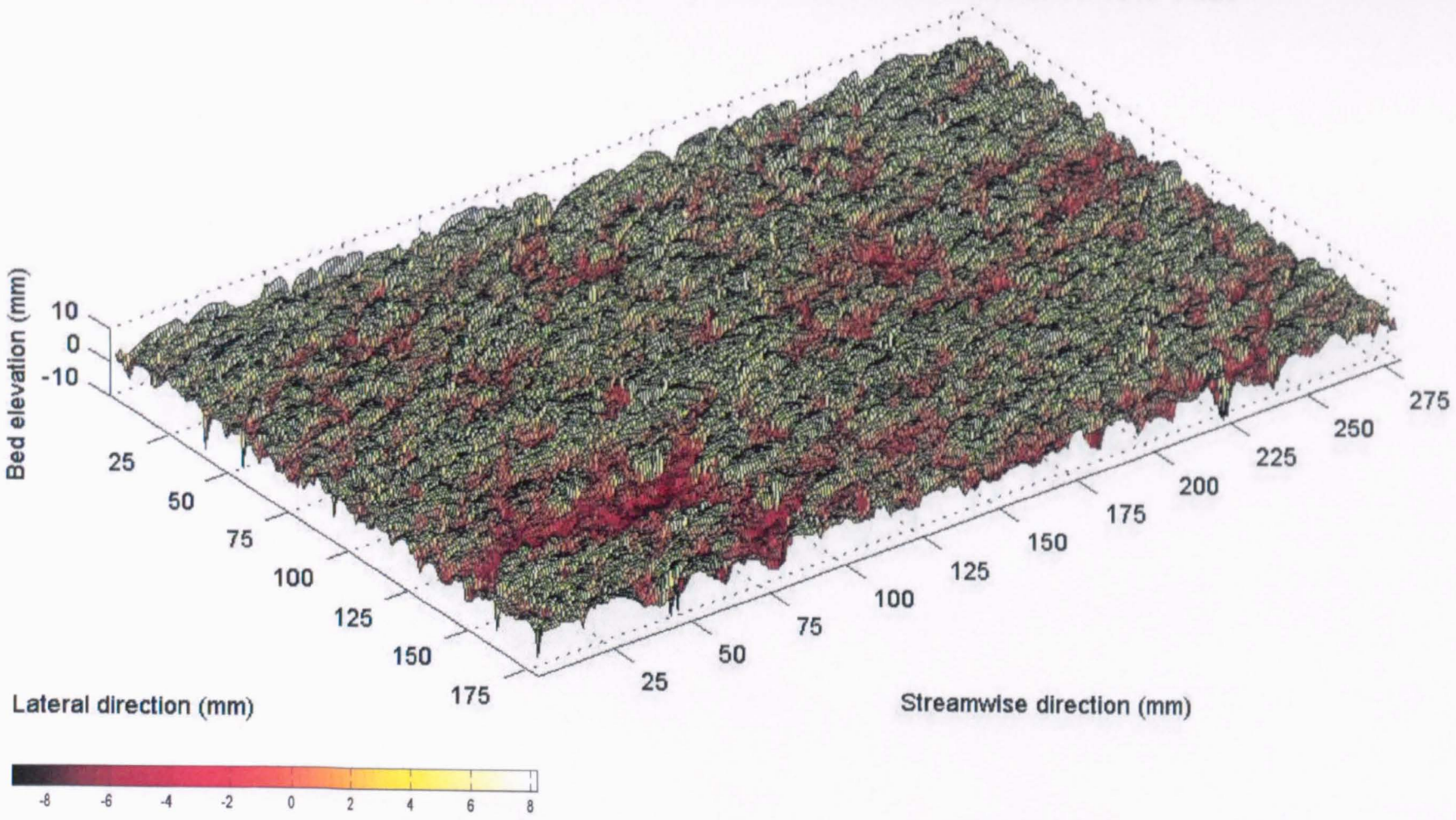

Figure 5.18. Original bed surface topography of the measurement grid Experiment UF 2-6

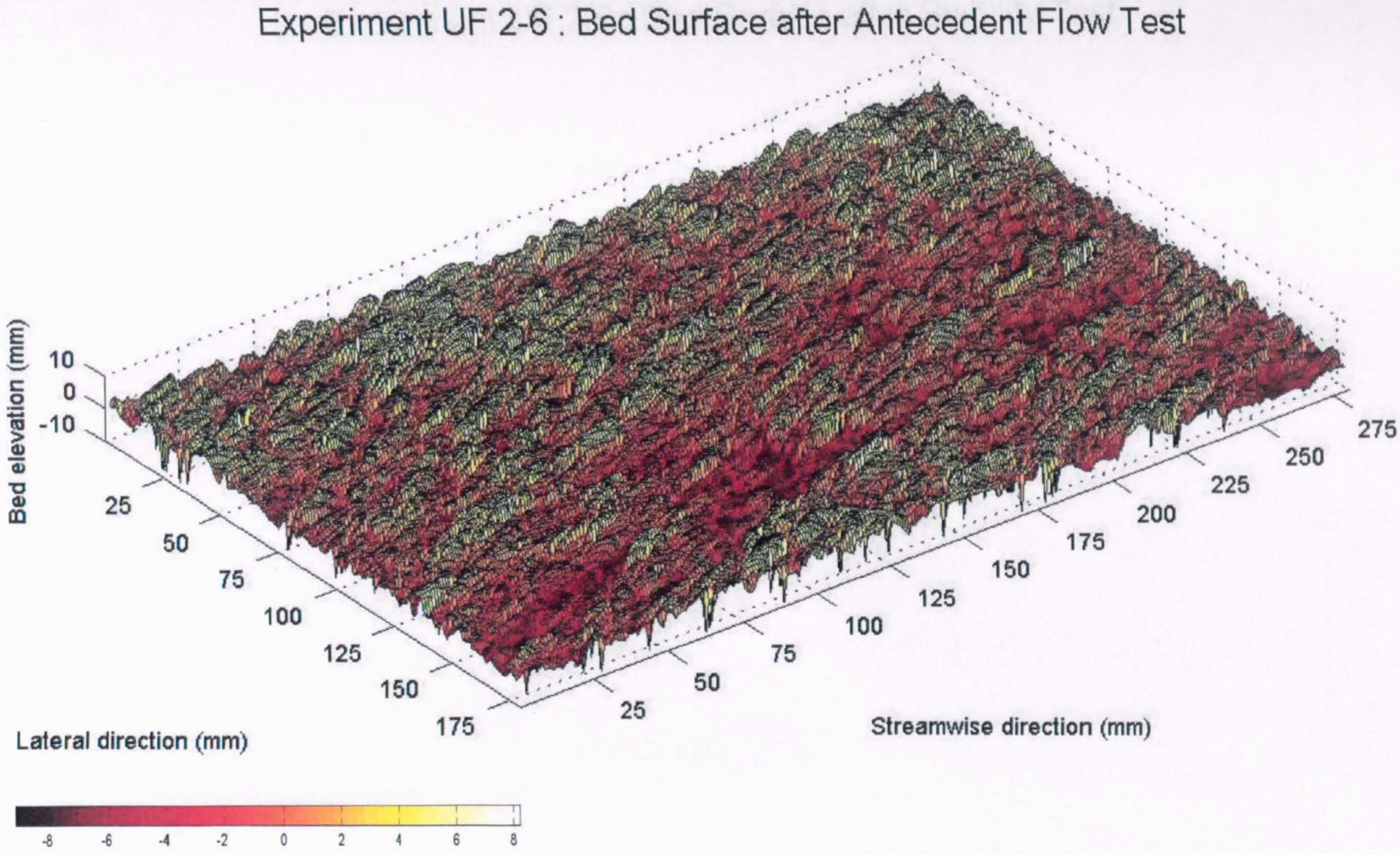

Figure 5.19. Bed surface topography of the measurement grid after antecedent flow Experiment UF 2-6

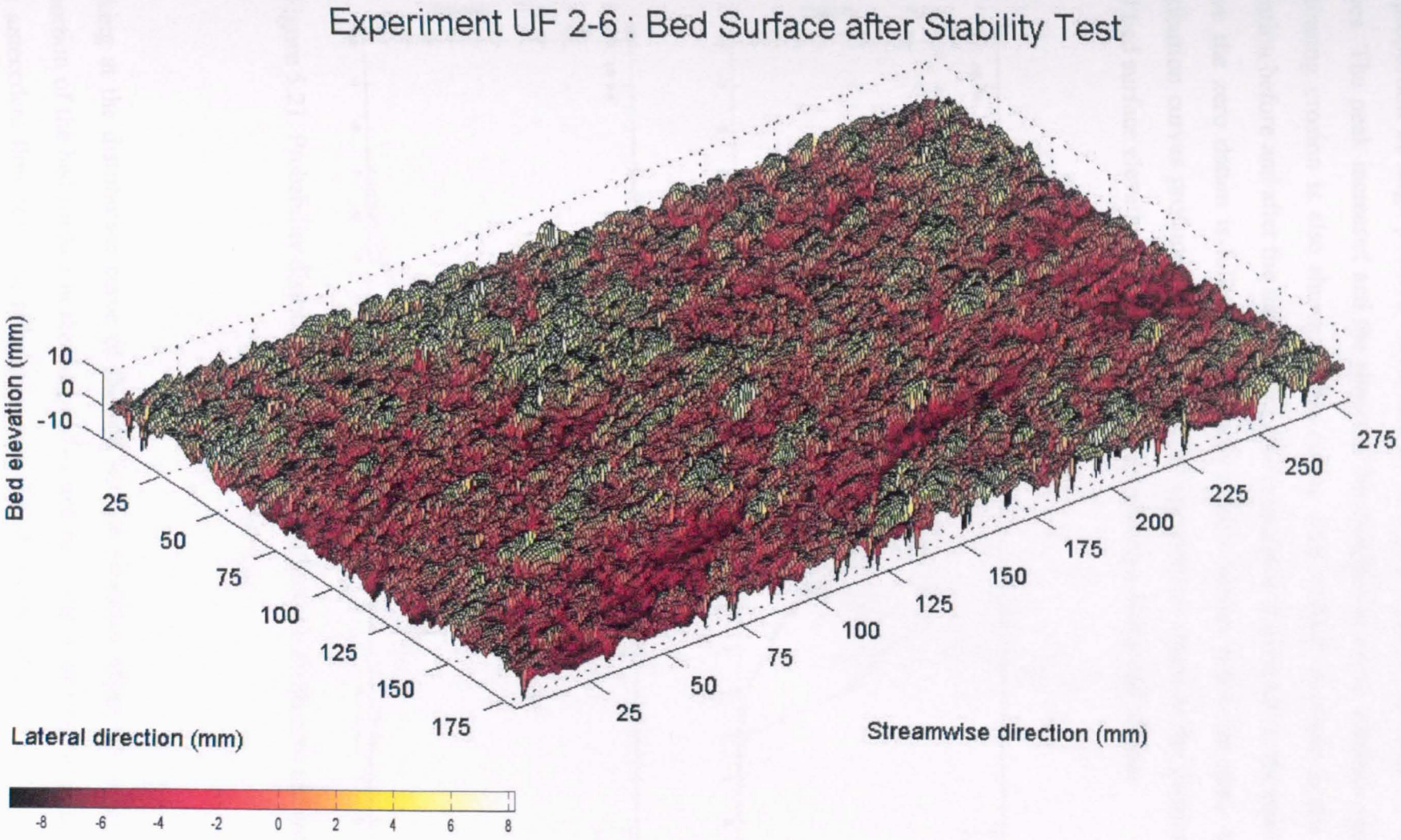

Figure 5.20. Bed surface topography of the measurement grid after stability test Experiment UF 2-6

the proportion of large positive values and an increased in the proportion of large negative values. The peak increased and the shape of the distribution curve becomes narrower. The continuing erosion is also shown by the curves with a slight decrease in the bed surface elevation before and after the stability test. The proportion of decrease in the postive elevation above the zero datum is followed by almost similar fashion below the zero datum. Both distribution curves produced an almost similar symmetrical shape as the distribution for the final bed surface elevation has higher peak, representing a flatter bed surface.

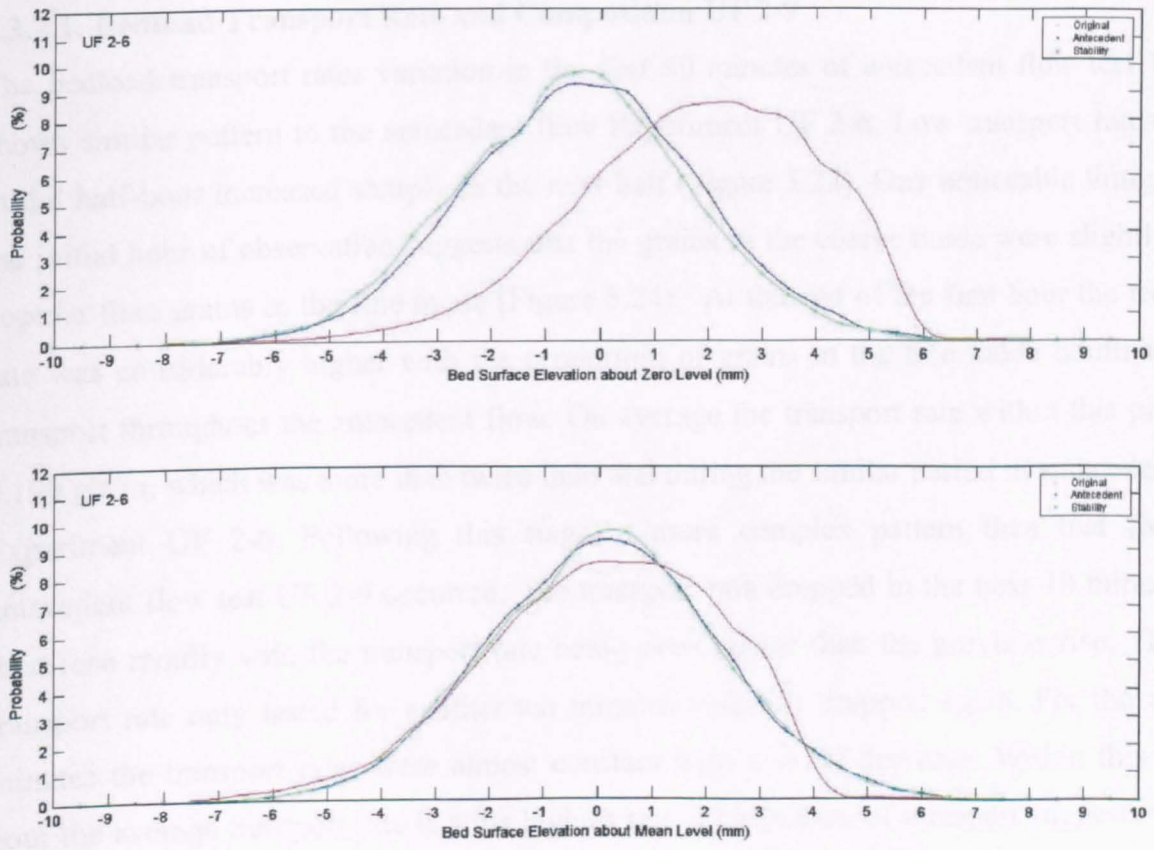

Figure 5.21. Probability distribution of bed surface elevation about zero and mean level for Experiment UF 2-6

Looking at the distribution curve of the bed surface elevation about the average level, the proportion of the bed surface in the range of -1 mm to 1 mm is also becomes more apparent after antecedent flow test. The proportion was slightly increased at the end of stability test. The positive tails shown by the curve based on the mean bed level after the antecedent flow

test suggests that the exposed large grains on the bed increased. However this is most likely caused by the removal of the surface with the exposure between 1-4 mm above the mean level. This contributed to the increasing level of exposure for other grains above 4 mm. It can be predicted that the decrease of the bed surface elevation in the high positive values leads to a slight increase in the smaller elevations from the mean. The shape of distribution would have a high and more symmetrical peak around the zero.

5.3.2. UNSTEADY ANTECEDENT FLOW EXPERIMENT UF 2-9

5.3.2.1. Bedload Transport Rate and Composition UF 2-9

The bedload transport rates variation in the first 60 minutes of antecedent flow test UF 2-9 shows similar pattern to the antecedent flow Experiment UF 2-6. Low transport rates in the initial half-hour increased sharply in the next half (Figure 5.22). One noticeable thing is that the initial hour of observation suggests that the grains in the coarse mode were slightly more popular than grains in the fine mode (Figure 5.24). At the end of the first hour the transport rate was considerably higher with the proportion of grains in the fine mode dominated the transport throughout the antecedent flow. On average the transport rate within this period is 0.199 g/s/m, which was more than twice than that during the similar period in antecedent flow Experiment UF 2-6. Following this stage, a more complex pattern than that found in antecedent flow test UF 2-9 occurred. The transport rate dropped in the next 10 minutes and then rose rapidly with the transport rate being even higher than the previous rise. The high transport rate only lasted for another ten minutes before it dropped again. For the next 30 minutes the transport rates were almost constant with a small decrease. Within this second hour the average transport rate is at its highest rate. This pattern of transport suggests that the bed was highly mobile. The average transport rate during the second hour is 0.286 g/s/m.

The next 60 minutes or the last hour of constant flow rate was characterised by a period of fairly erratic and fluctuating bedload transport rates. The average transport rate at this time is 0.188 g/s/m. Starting with a relatively high transport rate at the beginning of declining flow hydrograph, the transport rate was then decreased with a slight fluctuation at time elapsed 240 minutes. After this stage a gradual decrease in transport was observed and eventually the bedload reached a relatively more stable bed. The hourly average transport rates in the

remaining duration are 0.032 g/s/m, 0.011 g/s/m, 0.007 g/s/m and 0.001 g/s/m respectively. In the last hour when the flowrate was very small the average transport rate diminished to almost zero.

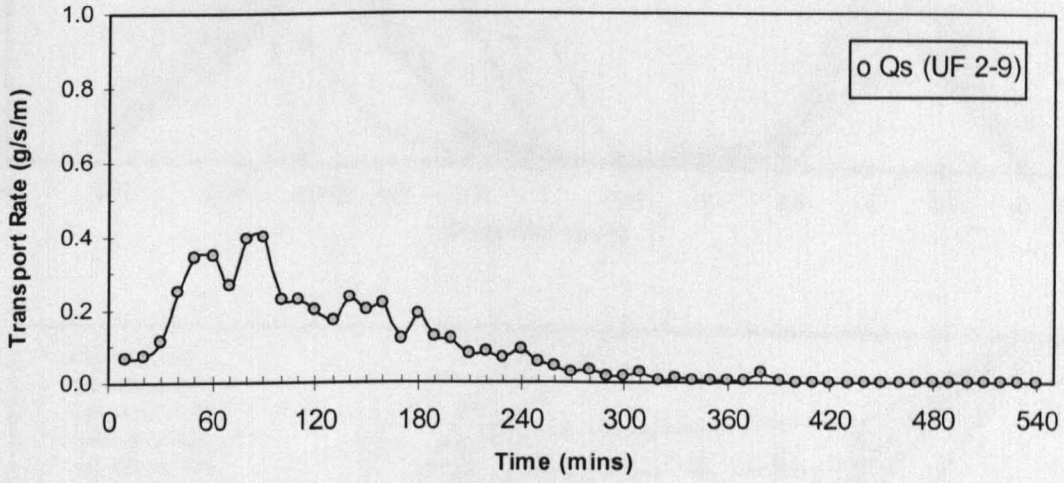

Figure 5.22. Time variation of transport rate for antecedent flow Experiment UF 2-9

Initially grains in the coarse mode were slightly more dominant in transport than grains in the fine mode (Figure 5.23). After an hour of antecedent flow grains in the fine mode were dominant for the rest of the test. This underlined the importance of grains in the fine mode in antecedent flow test UF 2-9. At time elapsed 50 - 100 minutes more than 50 % of bedload consists of grains in the fine mode whilst grains in the coarse mode contributed less than 35 %. The gap of the proportions between the two modes increased in almost all of the remaining observations indicating the dominance of grains in the fine mode throughout the rest of the experiment. It is worth noting that the observation at the last stage of constant flowrates (time elapsed 160 - 180 minutes) shows the existence of larger grains with diameter 8 mm. Only in this time elapsed were this grains found in the collection. The proportion of grains in the coarse mode increased to almost 44 % before dropped again following the decreased of flowrates in the falling limb.

Apart from grain diameter 8 mm, the fluid forces were still able to transport grains in the finer mode until time elapsed 340 minutes. In the last 200 minutes or more than 3 hours, the fluid

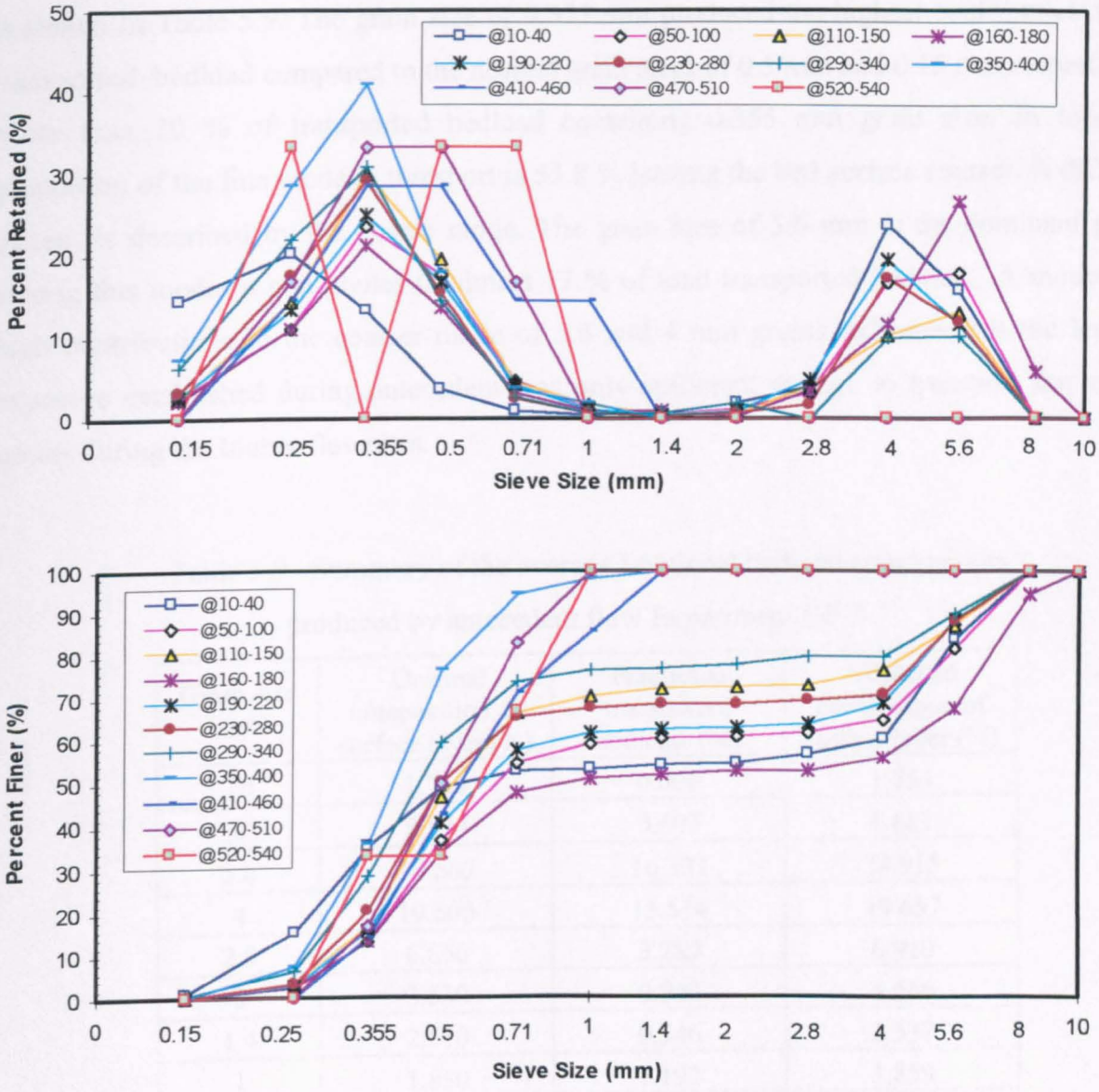

Figure 5.23. Grain size distribution of transported bedload for antecedent flow Experiment UF 2-9

forces carried only the finer grains with diameter 1 mm and less. The coarser grains were strong enough not to be transported by the available fluid forces. They were totally absent in transport for the rest of the duration of antecedent flow test whilst grains in the fine mode were still exist with the lower amount than in the early time elapsed of antecedent flow test. Within the last 200 minutes the average proportion of grains in the fine mode is almost 80 %.

The domination of grains in the fine mode transported in antecedent flow Experiment UF 2-9

is shown in Table 5.9. The grain size of 0.355 mm produced the highest contribution to the transported bedload compared to the nearest grain sizes of 0.5 mm and 0.15 mm respectively. More than 20 % of transported bedload containing 0.355 mm grain size. In total the proportion of the fine mode in transport is 53.8 % leaving the bed surface coarser. A different pattern is described by the coarse mode. The grain size of 5.6 mm is the dominant grains among this mode. It contributes to almost 17 % of total transported bedload. A moderately high contributions to the coarser mode of 5.6 and 4 mm grains indicates that the level of exposure established during antecedent was only sufficient enough to transport few coarse grains during the higher flowrates.

Table 5.9. Summary of the average fractional bedload composition produced by antecedent flow Experiment UF 2-9

Grain size (mm)	Original composition of surface layer (%)	Fractional transported bedload (%)	Estimated composition of surface layer (%)
10	1.730	0.000	1.754
8	8.570	0.607	8.681
5.6	34.660	16.337	34.915
4	19.600	15.514	19.657
2.8	6.860	3.289	6.910
2	3.530	0.942	3.566
1.4	2.510	0.546	2.537
1	1.850	1.192	1.859
0.71	2.680	3.767	2.665
0.5	6.840	15.887	6.714
0.355	7.420	24.383	7.184
0.25	2.710	13.565	2.559
0.15	0.940	3.770	0.901
receiver	0.100	0.202	0.099
Total	100	100	100

5.3.2.2. Variations of Average Nearbed Streamwise Velocity and Bed Shear Stress UF 2-9

The average nearbed streamwise velocity and the average bed shear stress during the antecedent flow Experiment UF 2-9 are shown in Figure 5.24. Because of the measurement of

nearbed streamwise flow velocity at different point in the grid, few measurement points were obtained during the constant flowrate section of 180 minutes. The average nearbed stramwise velocities during this period indicate relatively small differences in the first 180 minutes. The values were almost constant throughout the constant flowrates. It is apparent that the declining flowrates are shown by a steady decline of average nearbed streamwise velocity from time elapsed 180 minutes to 420 minutes. The last point available in Figure 5.24 suggests that the value dropped considerably. This was because of the measurement carried out at a very low water flow so that a good observation with the ADV probe could not be obtained.

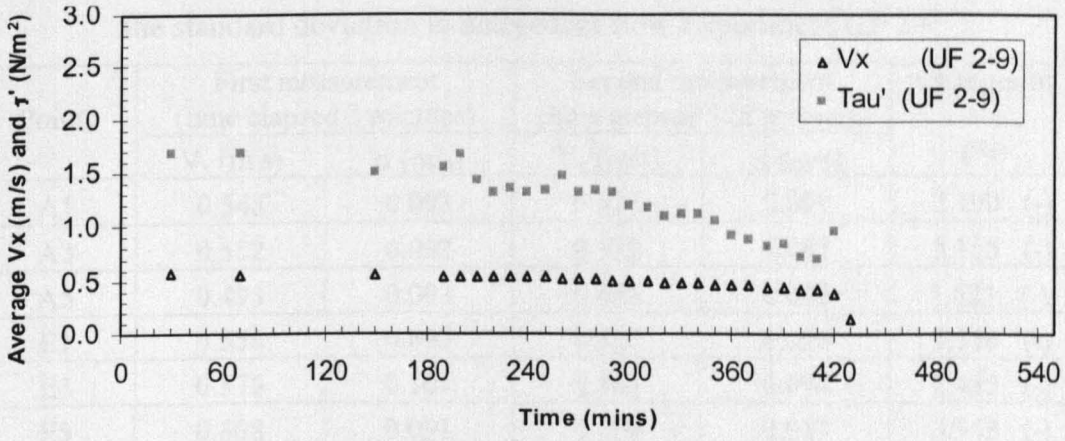

Figure 5.24. Variation of time averaged nearbed streamwise velocity and bed shear stress during antecedent flow Experiment UF 2-9

Although there are few points showing higher values than expected the distribution of the average bed shear stress is generally a reflection of flow hydrograph. Little variation is shown in the first 180 minutes and then it generally decreased in the falling limb. No measurements were carried out in the last 2 hours or so. The flowrates and therefore water depths were very low with the water surface below the ADV probe position.

The results of observation of the changes in average nearbed streamwise velocity for different points in the measurement grid in antecedent flow experiment UF 2-9 are presented in Table 5.10 and Figure 5.25. It is apparent that the average nearbed streamwise velocity at all points in the measurement grid decreased after 125 minutes even though the discharge was constant.

The changes are relatively small with the range of decrease from 1.6 to 6.8 % of the original values. The small differences in standard deviations suggest that the distribution of nearbed streamwise velocity in the constant flowrates section of antecedent flow UF 2-9 were also constant throughout the observation. In the first measurement the variation of point average velocity to the average of all measurement points is ranging from -9.5 % at point A5 to +7.5 % at point I3. In the second measurement the lowest and the highest average values are found at the same points observed in the first measurement with the range of variation between -7.8 % below and +8.5 % above the average values of all grid points.

Table 5.10. Variations of the average nearbed streamwise velocity and the standard deviation in antecedent flow Experiment UF 2-9

Points	First measurement (time elapsed 3 minutes)		Second measurement (time elapsed 128 minutes)		Changes of Vx (%)
	V_x (m/s)	σ (m/s)	V_x (m/s)	σ (m/s)	
A1	0.548	0.093	0.536	0.099	2.190 (-)
A3	0.582	0.092	0.552	0.097	5.155 (-)
A5	0.493	0.093	0.485	0.092	1.623 (-)
E1	0.558	0.092	0.527	0.096	5.556 (-)
E3	0.575	0.101	0.561	0.094	2.435 (-)
E5	0.508	0.091	0.490	0.087	3.543 (-)
I1	0.551	0.097	0.529	0.096	3.993 (-)
I3	0.586	0.091	0.571	0.092	2.560 (-)
I5	0.501	0.099	0.467	0.100	6.786 (-)
Average	0.545	0.094	0.526	0.095	

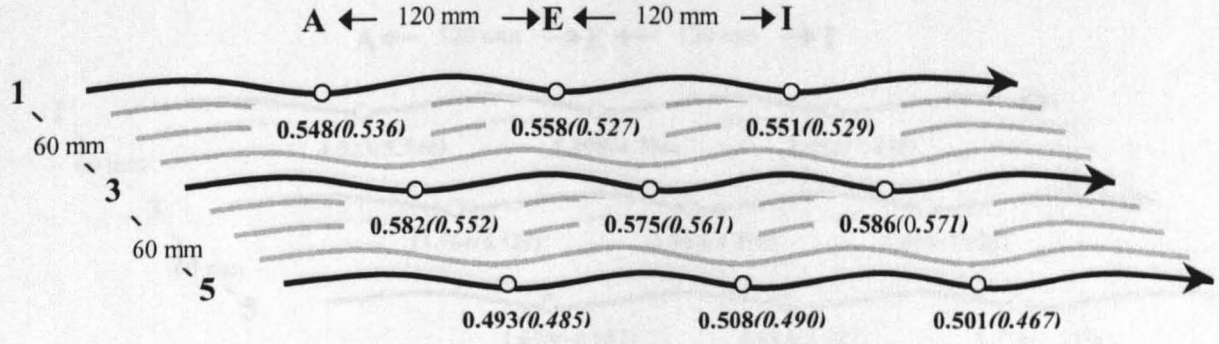

Figure 5.25. Distribution of average nearbed streamwise velocity (m/s) in antecedent flow Experiment UF 2-9 (first measurement in bold, second measurement in brackets)

Wide variations in the average bed shear stress, calculated using Equations 3.9 and 3.15, within the measurement grid occurred in antecedent flow UF 2-6 are also found in antecedent flow UF 2-9 (Table 5.11 and Figure 5.26). Although most points exhibit a decrease after 125 minutes from the first measurement, no systematic pattern in the changes of average bed shear stress is observed. The highest increase occurred at point E3. Negative values obtained at the first measurement and increased to highly positive values in the second measurement taken after 125 minutes from the first measurement. Point A5 exhibits different features than point E3. Negative values in the second measurement indicating the average bed shear stress decreased after 125 minutes from the first measurement.

Table 5.11. Variations of the average bed shear stress and the standard deviation in antecedent flow Experiment UF 2-9

Points	First measurement (time elapsed 3 minutes)		Second measurement (time elapsed 128 minutes)		Changes of $\overline{\tau}$ (%)
	$\overline{\tau}$ (N/m^2)	σ (N/m^2)	$\overline{\tau}$ (N/m^2)	σ (N/m^2)	
A1	4.023	18.252	5.546	17.969	37.857 (+)
A3	13.764	19.150	6.521	18.509	52.623 (-)
A5	3.699	16.341	-0.981	15.130	126.521 (-)
E1	5.998	17.835	4.726	17.400	21.207 (-)
E3	-0.599	18.821	9.590	18.611	1701.002 (+)
E5	6.684	16.399	5.527	14.854	17.310 (-)
I1	3.456	18.273	7.458	18.122	115.799 (+)
I3	9.678	19.708	7.923	19.222	18.134 (-)
I5	3.334	16.934	1.523	15.384	54.319 (-)
Average	5.560	17.968	5.484	17.245	

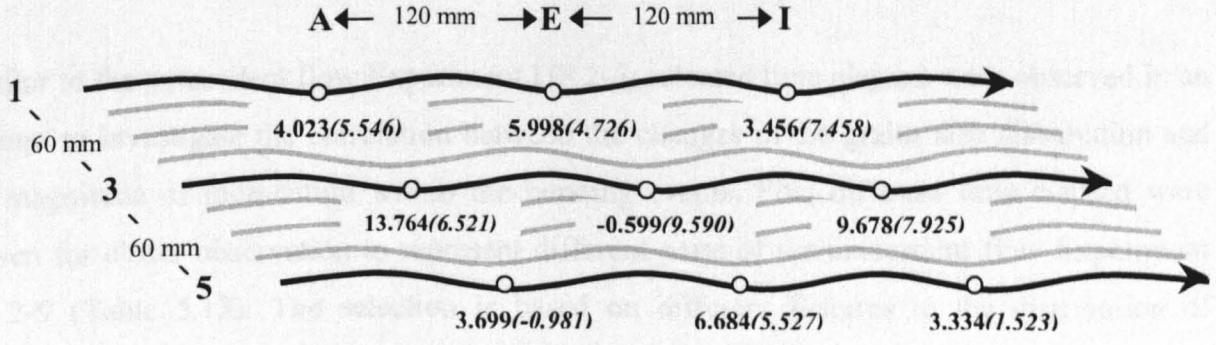

Figure 5.26. Distribution of average bed shear stress (N/m^2) in antecedent flow Experiment UF 2-9 (first measurement in bold, second measurement in brackets)

5.3.2.3. Bursting Events and Flow Momentum UF 2-9

The number of downward-looking bed interactions during the antecedent flow Experiment UF 2-9 is more than the upward interactions (Table 5.12). This is similar to the Experiment UF 2-6 in that the number of ejections exceeds the number of sweeps. Interestingly the proportion of the ejections in the constant flowrate section is lower than the proportion in the falling limb whilst the proportions of sweeps suggest otherwise. While the time frequency of the ejections increased in the falling limb, the sweeps is observed to experience a similar frequency irrespective of the phase of the flow hydrograph. With 1.013 ejections per second, the falling limb section of antecedent flow Experiment UF 2-9 produced more frequent upward interactions than the corresponding section of antecedent flow Experiment UF 2-6. Interestingly this section also produced more downward-looking bed interactions indicating that the bursting events are relatively more frequent than in the falling limb of antecedent flow Experiment UF 2-6. It is also observed that the average duration of ejections and sweeps is similar both in the constant flowrate section and in the falling limb.

Table 5.12. Time frequency and the proportion of occurrences of bursting events in antecedent flow Experiment UF 2-9

Parameter descriptions		Frequency (Hz)	Proportion (%)	Average duration (sec)
Constant flowrate	Ejections	0.940	46.192	0.051
	Sweeps	1.095	53.808	0.050
Falling limb	Ejections	1.013	48.033	0.053
	Sweeps	1.095	51.967	0.052

Similar to the antecedent flow Experiment UF 2-6, selected time elapsed were observed in an attempt to investigate the correlation between the changes in the grains size distribution and the magnitude of momentum within the bursting events. Five different time elapsed were chosen for closer observation to represent different parts of the antecedent flow Experiment UF 2-9 (Table 5.13). The selection is based on different features in the distribution of fractional transported bedload produced by these time elapsed (Figure 5.27).

Table 5.13. Summary of bursting events at selected time elapsed in antecedent flow Experiment UF 2-9

Parameter descriptions	Time elapsed (minutes)				
	150	190	280	390	410
Threshold values (m^2/s^2)	0.0072	0.0072	0.0062	0.0041	0.0038
Number of ejections	200	207	215	179	200
Number of sweeps	218	206	230	217	222
Frequency of ejections (Hz)	1.000	1.035	1.075	0.895	1.000
Frequency of sweeps (Hz)	1.090	1.030	1.150	1.085	1.110
Average duration of ejections (s)	0.050	0.050	0.053	0.053	0.051
Average duration of sweeps (s)	0.050	0.052	0.056	0.049	0.049

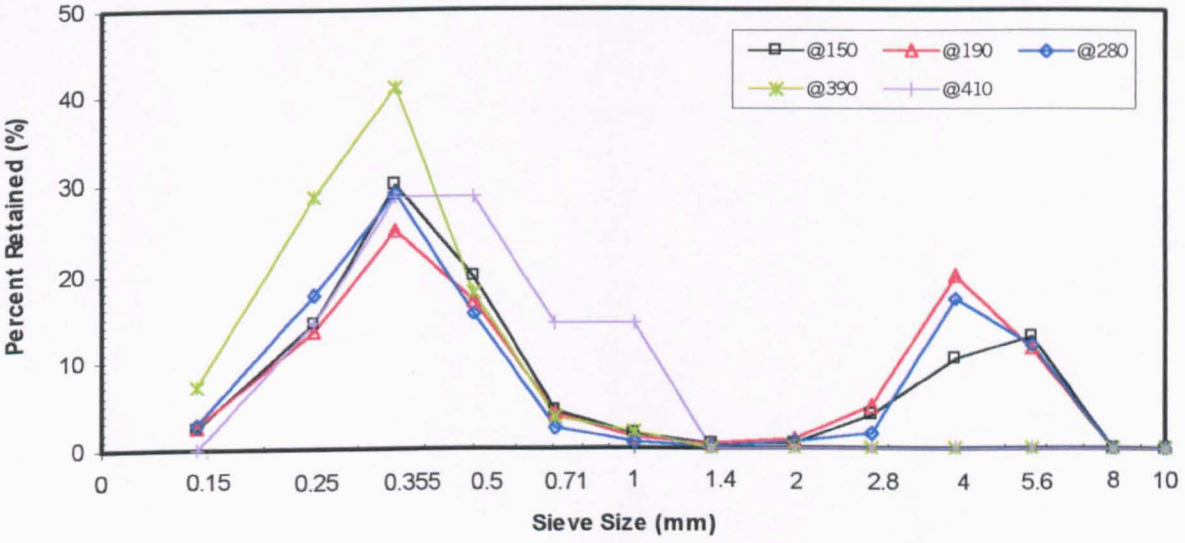

Figure 5.27. Grain size distribution of transported bedload at selected time elapsed in antecedent flow Experiment UF 2-9

Time elapsed 150 minutes has been chosen to represent the constant flow section while the others are the representatives of times during the falling limb. As shown in Figure 5.27, the transported bedload was clearly dominated by grains in the finer mode. Time elapsed 150 minutes transported more grains in the fine mode than time elapsed 190 minutes. This is likely because of the proportion of the downward-looking bed interactions (sweeps) with the momentum per unit area in the range between -11 and -3 kg/ms during this time elapsed was more frequent than in time elapsed 190 minutes (Figure 5.28). The proportion of upward interactions (ejections) with the magnitude of momentum per unit area between 11 to 17

kg/ms at time elapsed 150 minutes are also higher than all the other times. This is suspected as the main contributor to the larger amount and higher modal grain size in the coarse mode found in transported bedload (Figure 5.27). During time elapsed 150 minutes 5.269 grams of grains in the coarse mode were transported in comparison to 4.531 grams and 1.070 grams during time elapsed 190 and 280 minutes respectively. This also suggests that although the flowrates started to decline at time elapsed 190 minutes, the amount of grains in the coarse mode was still reasonably high. Although the amounts of grains in the coarse mode is slightly less than that transported at time elapsed 150 minutes and the modal grain size reduced to 4 mm, the proportion is increased. By looking at the probability distribution of momentum magnitude, it was seen that the ejections with momentum in the range between 17 and 19 kg/ms at time elapsed 190 minutes was more frequent. The existence of these momentum maintained the ability of the flow to carry the grains in the coarse mode.

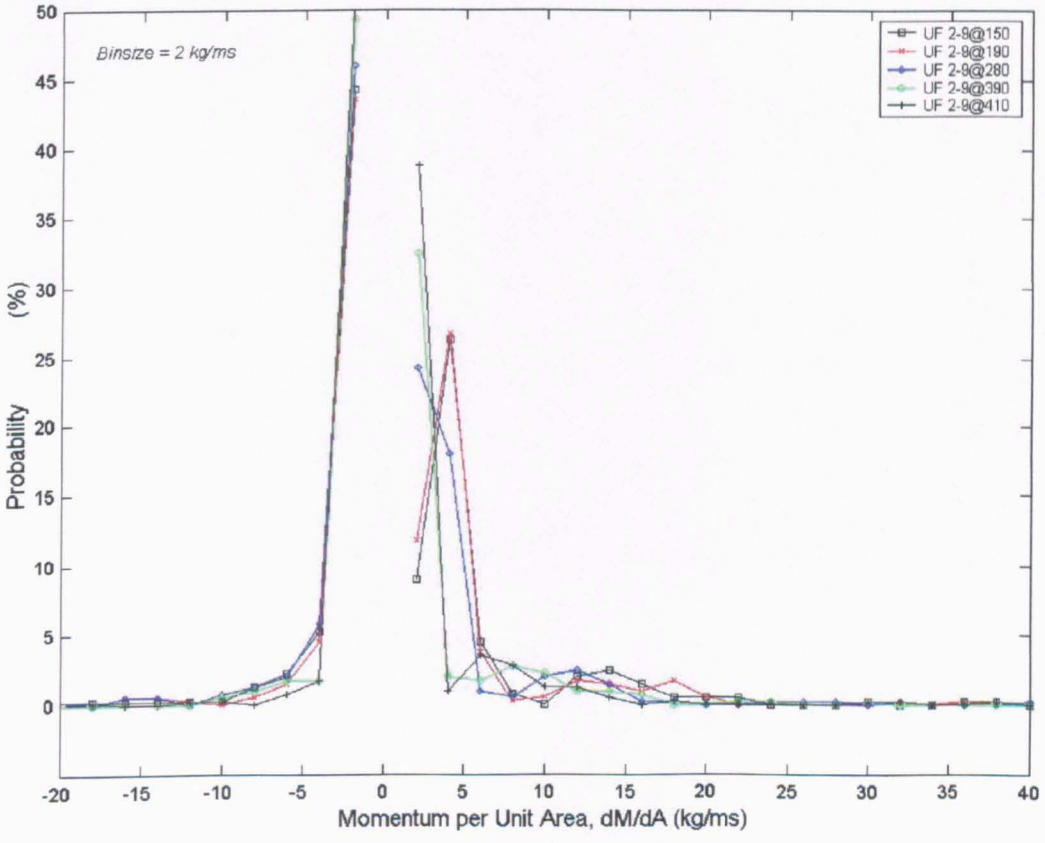

Figure 5.28. Probability distribution of momentum per unit area at selected time elapsed in antecedent flow Experiment UF 2-9 (ejections are positive and sweeps are negative)

Extended observation shows the similarity in the proportion of negative momentum between time elapsed 280 minutes and time elapsed 150 minutes (Figure 5.28). This coincides with the closeness of grain distribution in the finer mode at these two times shown in Figure 5.27. The frequency of positive momentum of higher magnitudes in the range between 11 to 13 kg/ms is the most likely factor in the production of grains in the coarse mode which still appear at time elapsed 280 minutes but with reducing quantities. As the discharge decreased, the proportion of strong momentum events both in the upward and downward-looking bed direction was also reduced. It is very clear from Figure 5.27 that the coarser grains were no longer be transported. This was seen at time elapsed 390 and 410 minutes where the distribution of ejections momentum is relatively similar, with no events above a 17 kg/ms threshold (Figure 5.28). At this stage, the momentum available in the flow removed only finer grains with a considerably high proportion.

The sequence and the magnitude of momentum both in upward and downward looking-bed interactions are presented in Figure 5.29. It is evident that the higher flowrates produced more rigorous interactions, particularly ejections at time elapsed 150, 190 and 280 minutes. As the flow decreased the interactions still exist but produced relatively low magnitude of momentum (time elapsed 390 and 410 minutes). These lower momentum were still able to move the finer grains.

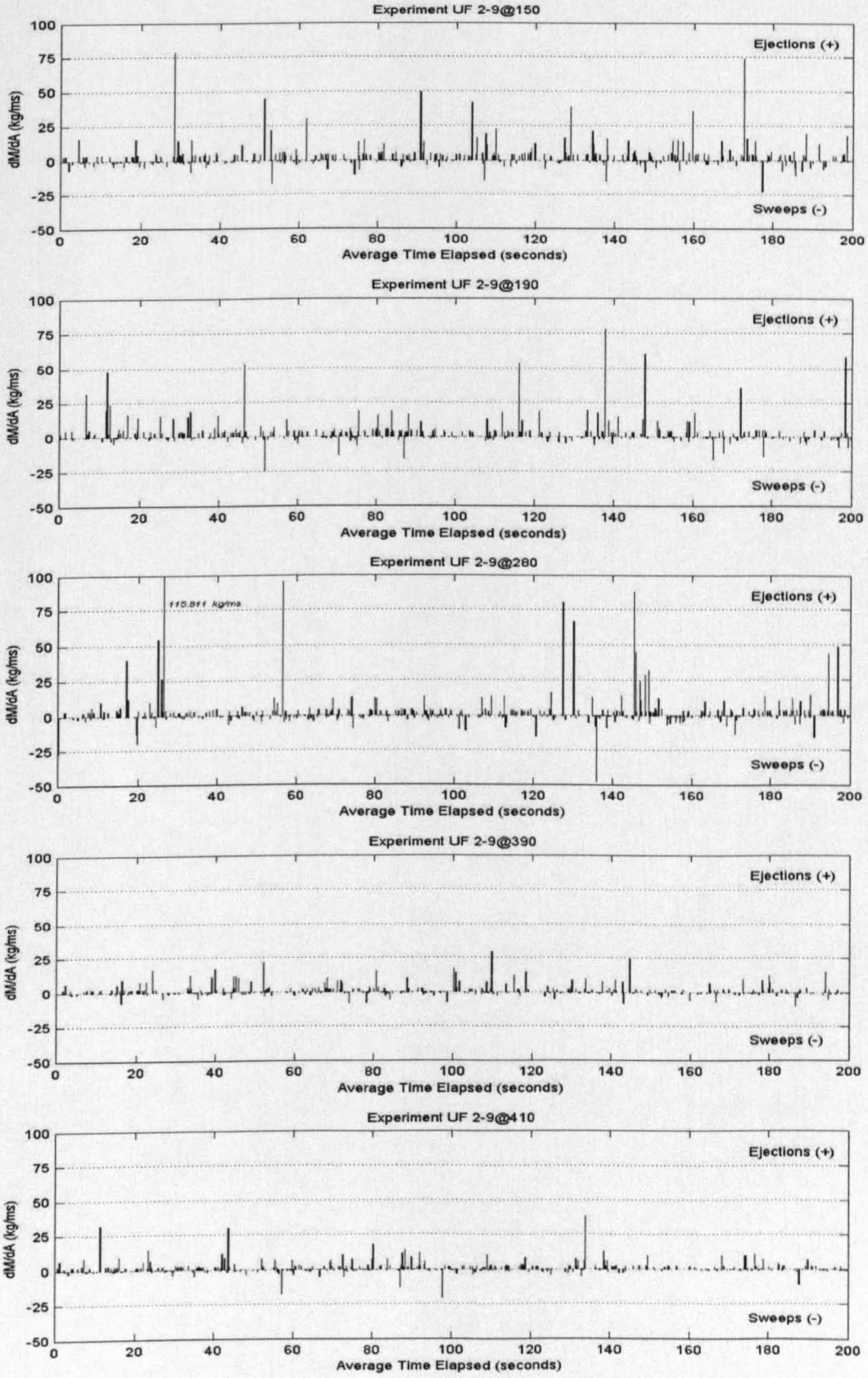

Figure 5.29. The sequence of momentum per unit area and its magnitude at selected time elapsed in antecedent flow Experiment UF 2-9

5.4.3.4. Bed Topography UF 2-9

The application of the UF 2-9 antecedent flow hydrograph consists of 3 hours constant flow and 6 hours of declining flowrate produce significant changes in the bed surface structure (Figure 5.31). A considerable amount of bed material is eroded during this test producing a low mean bed surface elevation. It can be seen from Figure 5.31 that after antecedent flow the bed were covered with valley type structures over almost all of the measurement grid. The darker areas indicate the area of the high levels of degradation. This degradation covered the centre part of the measurement grid mainly in the streamwise direction. On the rest of the surface smaller scale the undulations are observed. By looking at the average bed surface elevation before and after antecedent flow (Figures 5.30 and 5.31) it is very clear that the reduction in bed level is much higher than in the same test applied to the bed formed by 6 hours antecedent flow of UF 2-6 (Figures 5.18 and 5.19). The average bed surface elevation reduced almost 5 mm from the original bed. This suggests that significantly more erosion occurred in the longer declining flow phase.

At the end of experiment the bed topography indicated further erosion during the stability test, which had changed the bed surface arrangement. Less "deep valleys" are shown in Figure 5.32 indicating re-organisation of the bed surface structure. The movement of some grains downstream from the upstream edge of the valley covered the previously eroded surface. This resulted in the valley structure appearing to "translate" in an upstream duration. Meanwhile new valley type structure also formed in different area of the bed due to the same process. This suggests that a relatively high transport rate was experienced during the stability test of experiment UF 2-9 so that further erosion not only removed the exposed grains but also continuously eroded the previously low bed surface formed by the antecedent flow experiment. An interesting feature in Figure 5.32 is the diagonal valley extended to the left hand side of the measurement area. Similar valleys can be recognised after the stability test (Figure 5.32) with new and parallel bed features appearing. Some of the exposed large grains deposited before and after the stability test also tend to create diagonal undulations with a small angle to the streamwise direction.

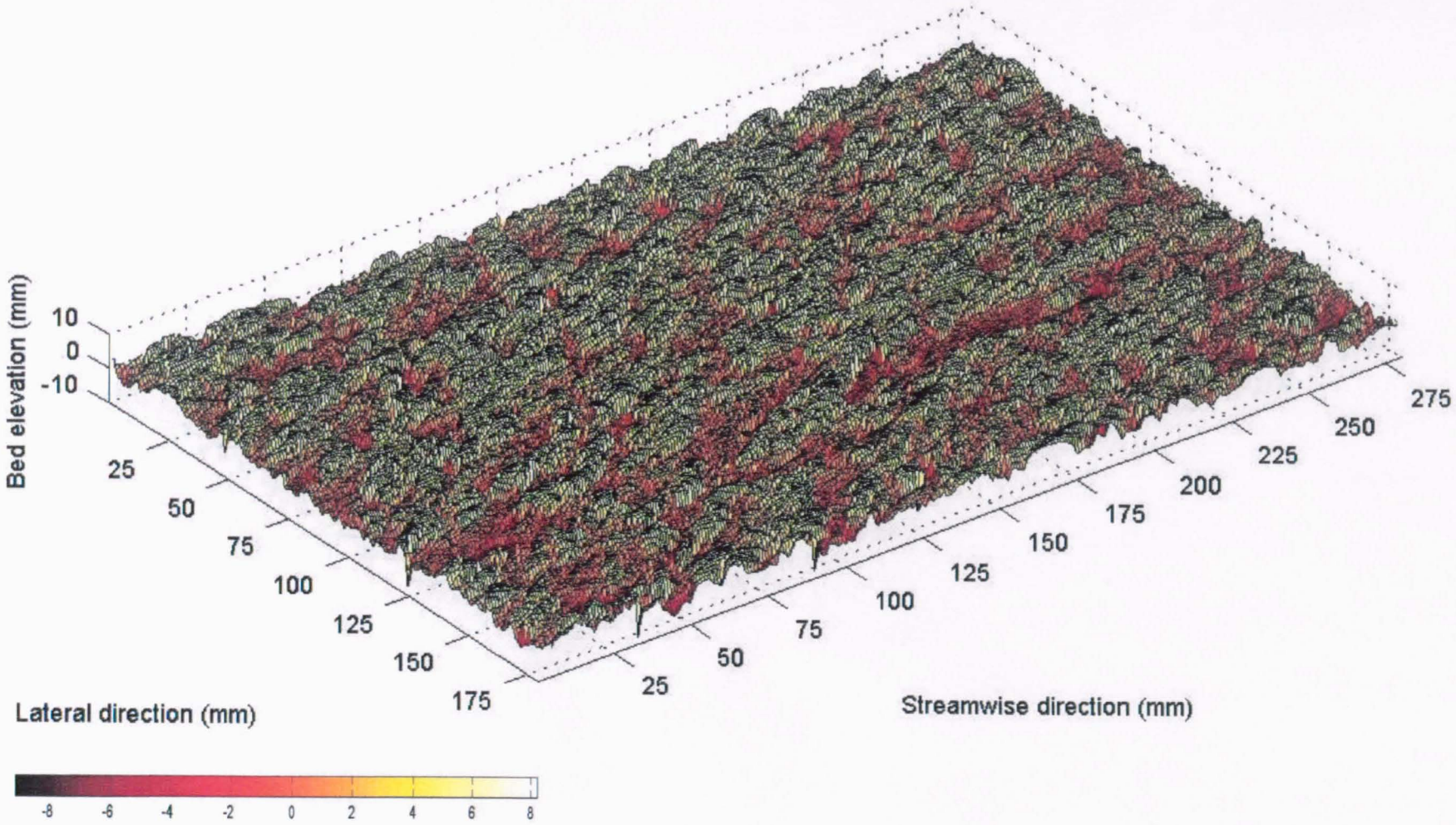

Figure 5.30. Original bed surface topography of the measurement grid Experiment UF 2-9

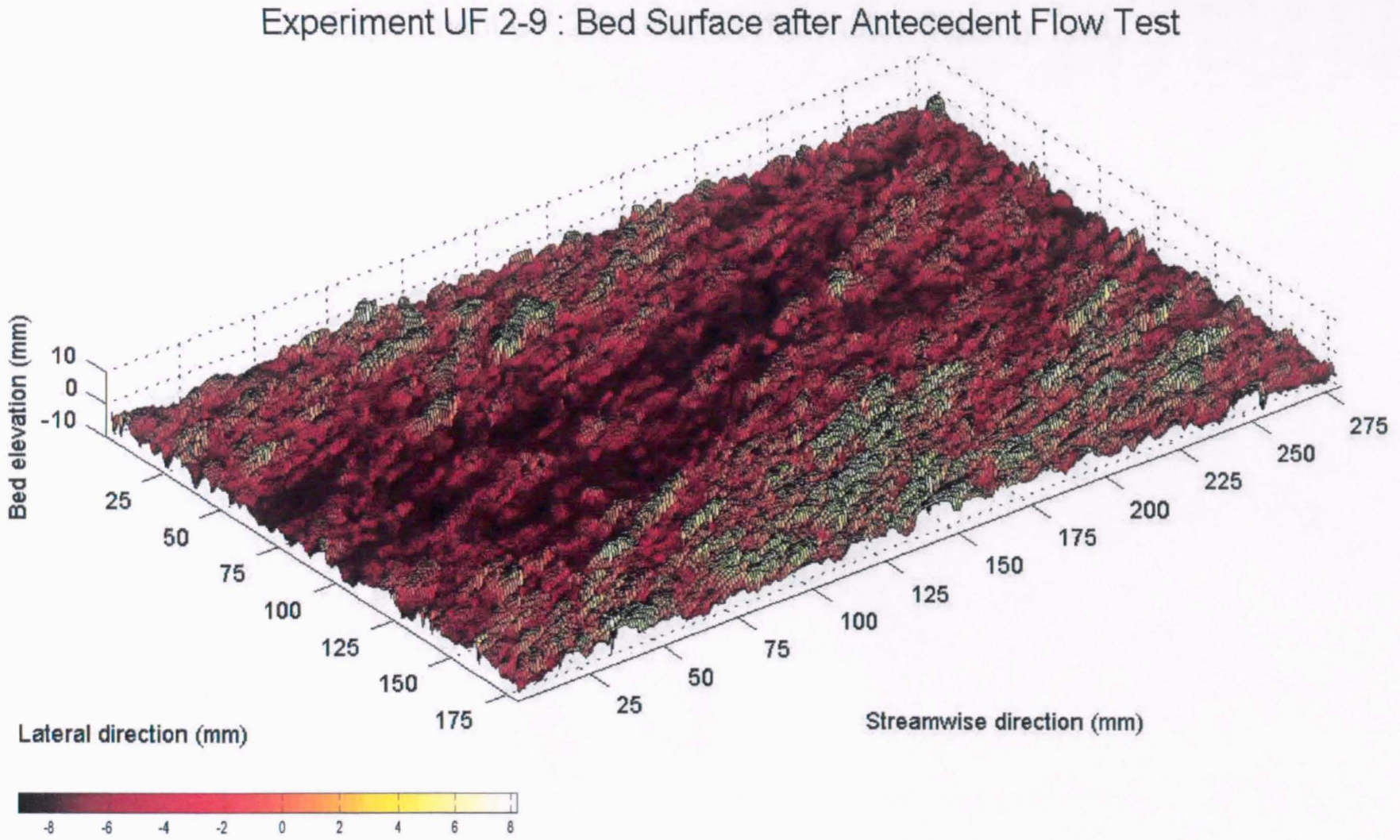

Figure 5.31. Original bed surface topography of the measurement grid after antecedent flow Experiment UF 2-9

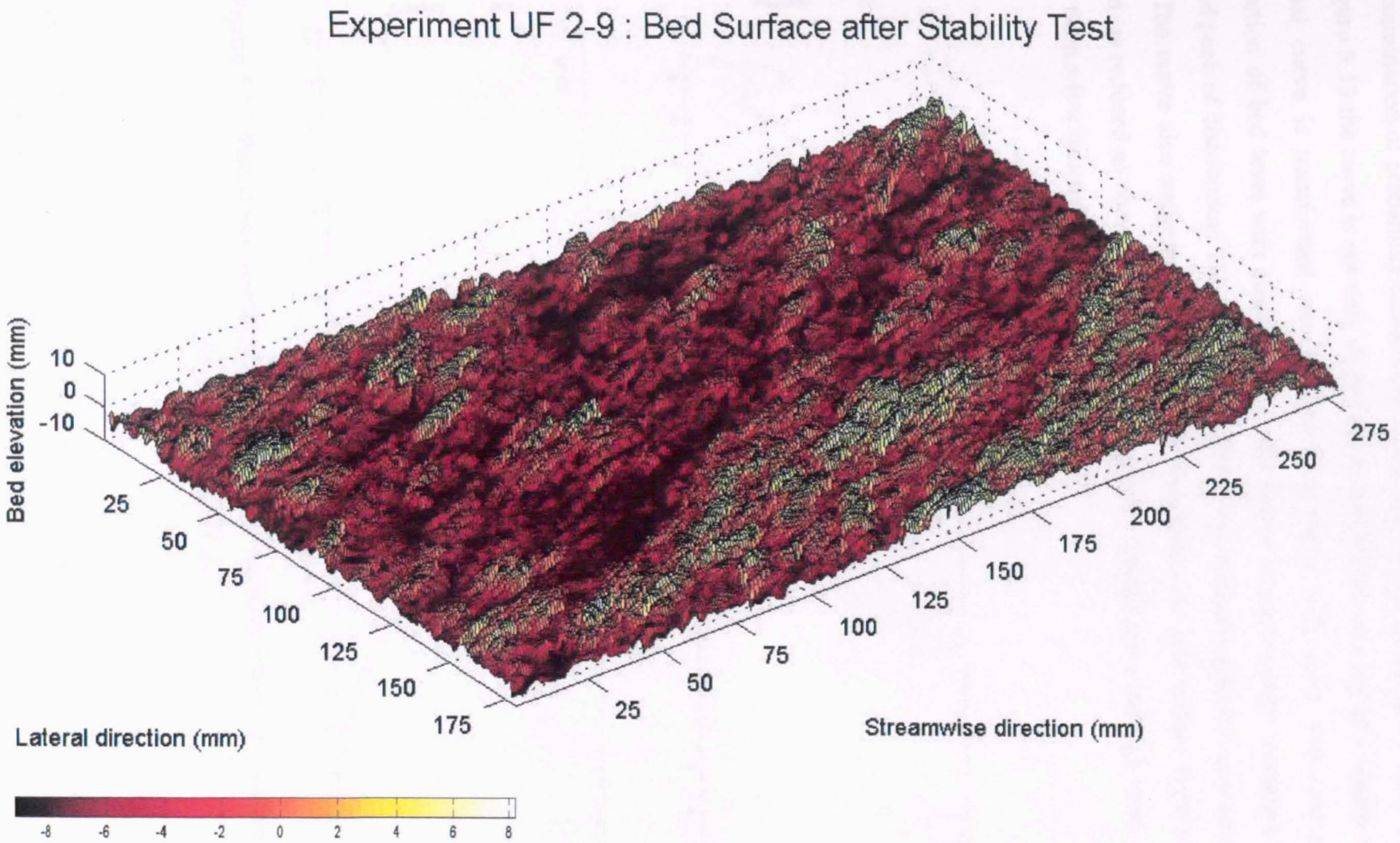

Figure 5.32. Bed surface topography of the measurement grid after stability test Experiment UF 2-9

The examination of probability distribution of bed surface elevatiosn shows a distinct pattern. In Figure 5.33 the curve is not only shifted far to the left but also has an irregular form. The original curve is transformed into a distribution curve with more than one peak. The proportion of bed level with elevation of 9 mm below the zero datum increased to form a second peak of distribution. This coincides with the high transport rate during antecedent flow test. The curve also suggests that the positive distribution of bed surface level above zero datum is reduced as observed in the bed topography which shows the high level of erosion apart from a few isolated positions.

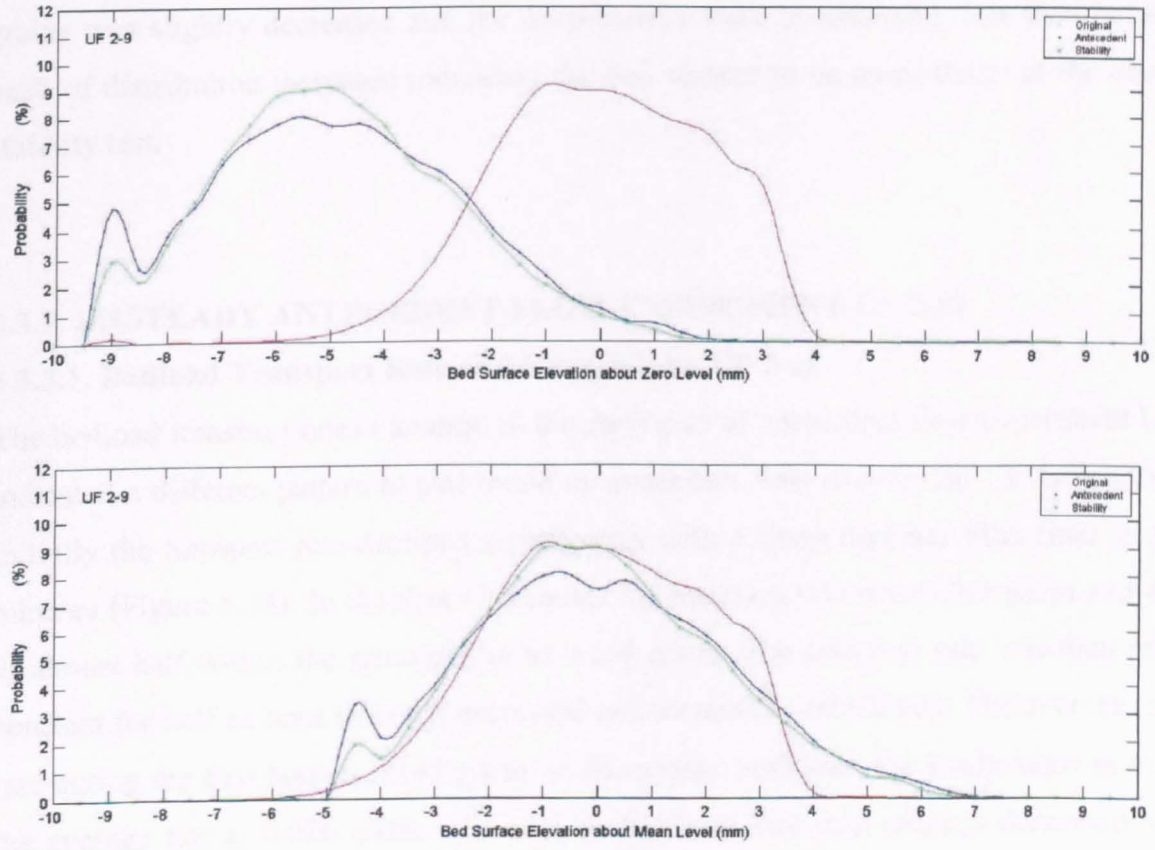

Figure 5.33. Probability distribution of bed surface elevation about zero and mean level for Experiment UF 2-9

The bed surface elevation distributions at the end of experiment UF 2-9 indicates a different pattern to that observed at the end of the antecedent flow test. The proportion of "deep valleys" with the elevation of -9 mm below the zero datum has decreased. It can be assumed

that during the stability test the degradational process removed bedload that moved into adjacent valleys, thus reducing their. This is reflected by the increasing proportion of the bed surface level in the height range between -7 mm to -4 mm about the zero datum level.

The bed surface distribution about the average level clearly indicates the existence of a considerable proportion of large exposed grains with the elevation of at least 3.5 mm above the average after the antecedent flow experiment. The eroded bed surface with the low elevation at least 2 mm below the average also increased after the antecedent flow experiment. The significant increase in the elevation of 4.5 mm below the average (Figure 5.33) representing the darker spots in Figure 5.31. After stability test the exposed larger grains was slightly decreased and the deep-valleys were considerably less than before. The peak of distribution increased indicating the bed surface to be more flatter at the end of the stability test.

5.3.3. UNSTEADY ANTECEDENT FLOW EXPERIMENT UF 2-12

5.3.3.1. Bedload Transport Rate and Composition UF 2-12

The bedload transport rates variation in the early part of antecedent flow experiment UF 2-12 indicated a different pattern to that found in antecedent flow experiment UF 2-6 and UF 2-9. Initially the transport rate declined significantly with a sharp decrease after time elapsed 10 minutes (Figure 5.34). In the first 10 minutes the transport rate was 0.268 g/s/m and dropped to almost half within the same period to 0.136 g/s/m. The transport rate was then relatively constant for half an hour before it decreased and increased periodically. The average transport rate during the first hour is 0.145 g/s/m. In the second hour with the fluctuations in transport, the average rate is 0.076 g/s/m. The average transport rate then steadily decreased to 0.060 g/s/m in the last hour of the constant flowrate. As the flowrates decreased in the falling limb of hydrograph, the transport rate continued to decrease. The average transport rate in the fourth, fifth and sixth hours are 0.034 g/s/m, 0.013 g/s/m and 0.017 g/s/m respectively. After this period, the transport rates were considerably low with the average rate within the corresponding duration are 0.008 g/s/m, 0.003 g/s/m and 0.001 g/s/m for the seventh, eighth and ninth hour respectively. The transport rate almost diminished to zero in the remaining 3 hours.

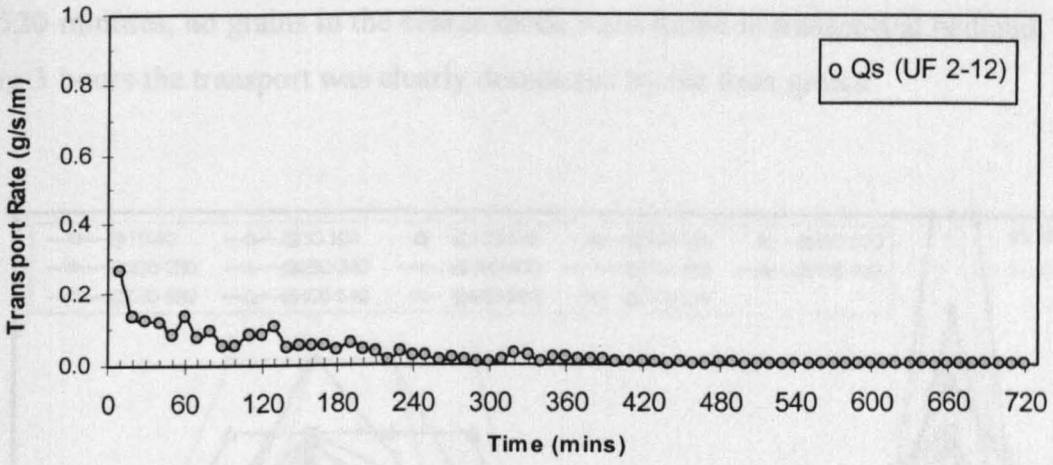

Figure 5.34. Time variation of transport rate for antecedent flow Experiment UF 2-12

The grain distribution of bedload in antecedent flow experiment UF 2-12 indicated more complex pattern than the antecedent flow experiment UF 2-6 and UF 2-9. In Figure 5.35 the transport was initially dominated by grains in the coarse mode. More than 63 % of collection at time elapsed 10 - 40 minutes was grains in the coarse mode whilst the proportion of grains in the fine mode is a mere 16 %. In the second period of observation covering time elapsed between 50 - 100 minutes the contribution of the coarse mode decreased to 34 % with an increase to 50 % in the fine mode. The contribution of the coarse mode increased again and dominated the transport in the period of time elapsed 110 and 150 minutes. At this stage the comparison between the coarse and the fine mode is 60 % to 32 %. Within the next 30 minutes of observation it was grains in the fine mode that are dominant in transport. In the following 40 minutes (time elapsed 190 - 220 minutes) the proportion of both modes changed again with the domination of the coarse mode shown. In the declining flowrates the dominant mode was always changing. Time elapsed 230 to 280 minutes was dominated by grains in the fine mode whereas the next 50 minutes was dominated by grains in the coarse mode. After this time elapsed grains in the fine mode dominated the transport for almost 2 hours. An interesting feature was found at time elapsed 410 to 460 minutes where the grains in the coarse mode were totally absent. This is an indication that the larger grains were at a stable condition. However, in the following hour grains diameter 5.6 appeared and dominated the relatively low transport rate at time elapsed 470 - 520 minutes. As the other grains in the coarse mode were not found in transport, this may be assumed that a small amount of grains of diameter 5.6 mm had become more exposed and were therefore transported. After time

elapsed 520 minutes, no grains in the coarse mode were found in transported bedload. For the remaining 3 hours the transport was clearly dominated by the finer grains.

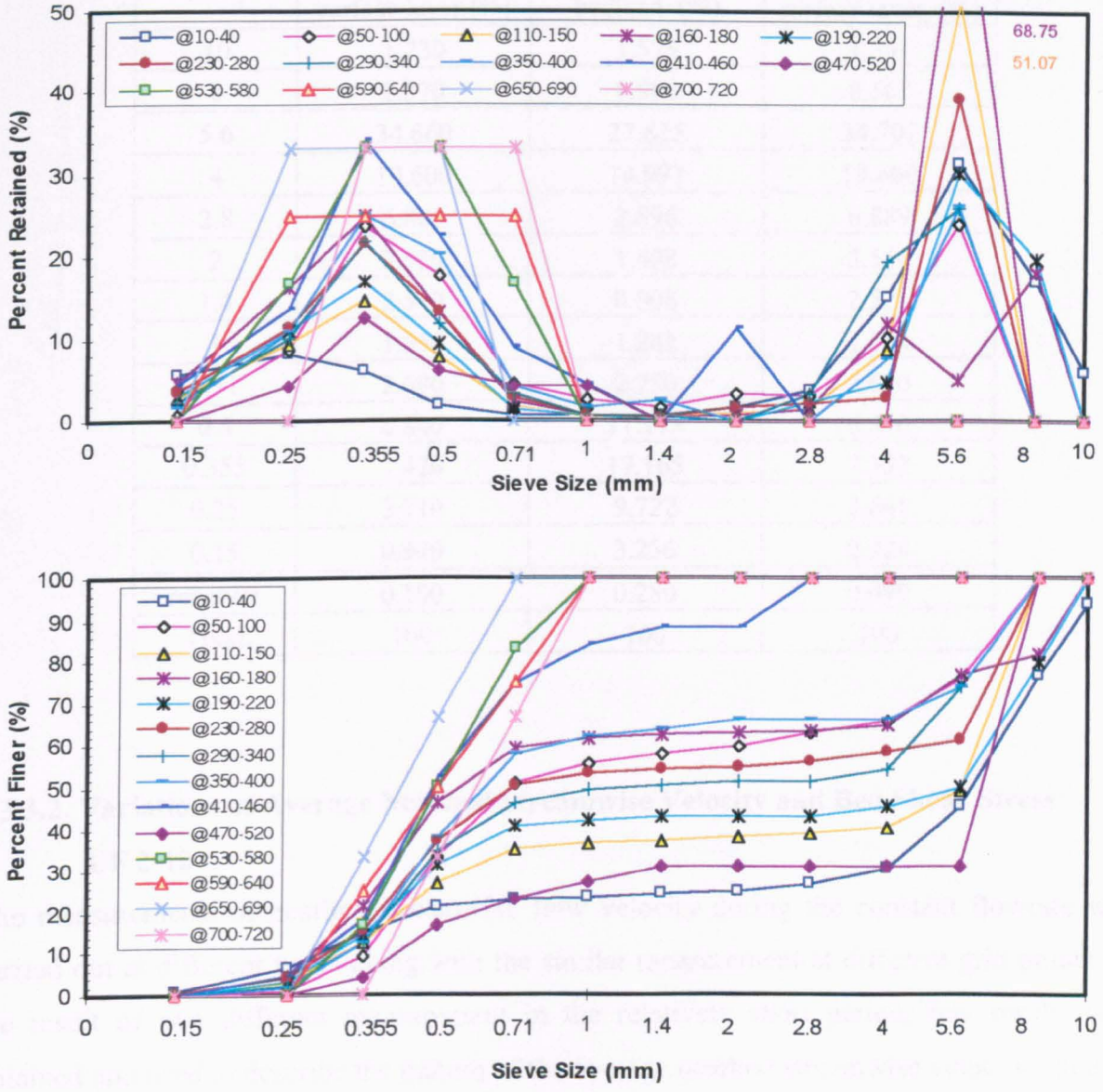

Figure 5.35. Grain size distribution of transported bedload for antecedent flow Experiment UF 2-12

By examining the composition of the total bedload, it is found in Table 5.14 that the antecedent flow experiment UF 2-12 proportionally transported more grains in the coarse mode than the antecedent flow experiments UF 2-6 and UF 2-9. The opposite pattern is shown by grains in the fine mode where less proportion than that in experiment UF 2-6 and UF 2-9 was transported during the antecedent flow Experiment UF 2-12.

Table 5.14. Summary of the average fractional bedload composition produced by antecedent flow Experiment UF 2-12

Grain size (mm)	Original composition of surface layer (%)	Fractional transported bedload (%)	Estimated composition of surface layer (%)
10	1.730	1.575	1.731
8	8.570	8.986	8.567
5.6	34.660	27.825	34.707
4	19.600	10.997	19.660
2.8	6.860	2.696	6.889
2	3.530	1.498	3.544
1.4	2.510	0.908	2.521
1	1.850	1.242	1.854
0.71	2.680	2.750	2.680
0.5	6.840	11.118	6.810
0.355	7.420	17.165	7.352
0.25	2.710	9.722	2.661
0.15	0.940	3.236	0.924
receiver	0.100	0.280	0.099
Total	100	100	100

5.3.3.2. Variations of Average Nearbed Streamwise Velocity and Bed Shear Stress UF 2-12

The measurements of nearbed streamwise flow velocity during the constant flowrate were carried out at different times along with the similar measurement at different grid points. As the result of two different measurement in the relatively short period, few results were obtained and used to describe the pattern of the average nearbed streamwise velocities and the average bed shear stress in the constant flowrate section. Again, similar patterns of those found in the antecedent flow experiment UF 2-9 were found to exist in experiment UF 2-12. In Figure 5.36 the values of the average nearbed streamwise velocity were almost constant throughout the constant flowrate. It is apparent that in the declining flowrates the of average nearbed streamwise velocity decreased from time elapsed 180 minutes onwards. The data form a declining line indicates a steady decrease in average velocity values. As experienced in antecedent flow experiment UF 2-9 the last point available in Figure 5.36 suggests that the value dropped considerably. However, this low value was because of the measurement was

carried out at a very low flowrate. At this water depth it was difficult to obtain good results from the ADV probe.

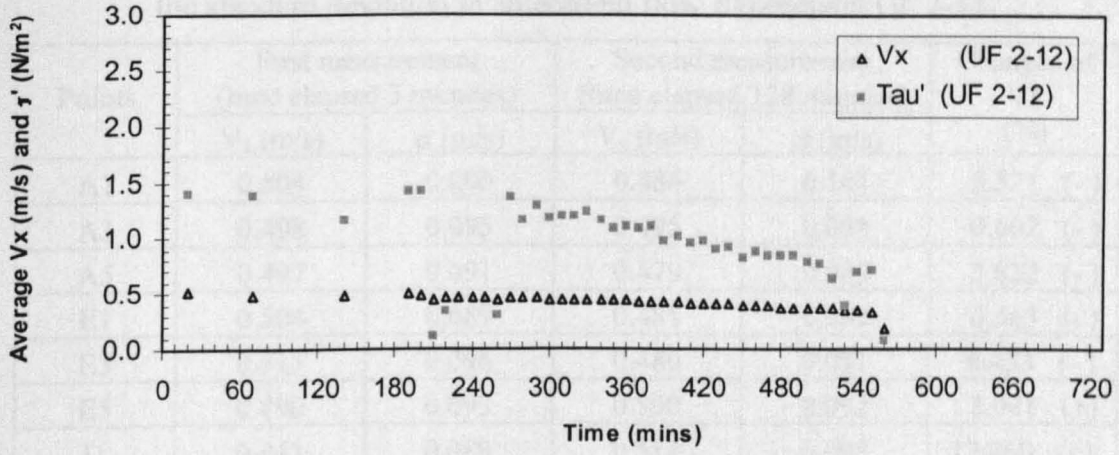

Figure 5.36. Variation of time averaged nearbed streamwise velocity and bed shear stress during antecedent flow Experiment UF 2-12

In Figure 5.36 a slightly different pattern than the average nearbed streamwise velocity is experienced by the average bed shear stress. Time elapsed 140 minutes shows a lower value than the other points in the constant flow hydrograph. By examining the transport rate it is found that there is coincidence that the lower amount of bedload were transported at this time elapsed in comparison to the adjacent time elapsed. In the falling limb there are also few points showing higher values of bed shear stress than expected. However, the distribution of the average bed shear stress is generally decreasing in accordance to the decreasing flowrates in the falling limb of hydrograph. No measurements were carried out in the last 160 minutes as the flowrate was very low and the water surface was below the position of ADV probe.

Observation to the average nearbed streamwise velocity of different points in the measurement grid indicates that in the antecedent flow experiment UF 2-12 the average values in the second measurement were generally decreased after 125 minutes from the first measurement (Table 5.15 and Figure 5.37). Although one point (I1) showed a significant increase, the standard deviation of nearbed streamwise velocity at each point is also seen to remain fairly constant. In the first measurement the range of variation is ranging from -10.9 % below and +3.6 % above the average values of all points. The range is decreased in the second

measurement from -2.8 % to +5.1 % from the average grid values.

Table 5.15. Variations of the average nearbed streamwise velocity and the standard deviation in antecedent flow Experiment UF 2-12

Points	First measurement (time elapsed 3 minutes)		Second measurement (time elapsed 128 minutes)		Changes of Vx (%)
	V_x (m/s)	σ (m/s)	V_x (m/s)	σ (m/s)	
A1	0.504	0.096	0.486	0.101	3.571 (-)
A3	0.498	0.095	0.495	0.098	0.602 (-)
A5	0.497	0.091	0.479	0.089	3.622 (-)
E1	0.504	0.089	0.481	0.092	4.563 (-)
E3	0.513	0.096	0.480	0.091	6.433 (-)
E5	0.490	0.093	0.500	0.092	2.041 (+)
I1	0.441	0.089	0.518	0.095	17.460 (+)
I3	0.501	0.095	0.501	0.094	0
I5	0.507	0.097	0.497	0.096	1.972 (-)
Average	0.495	0.093	0.493	0.094	

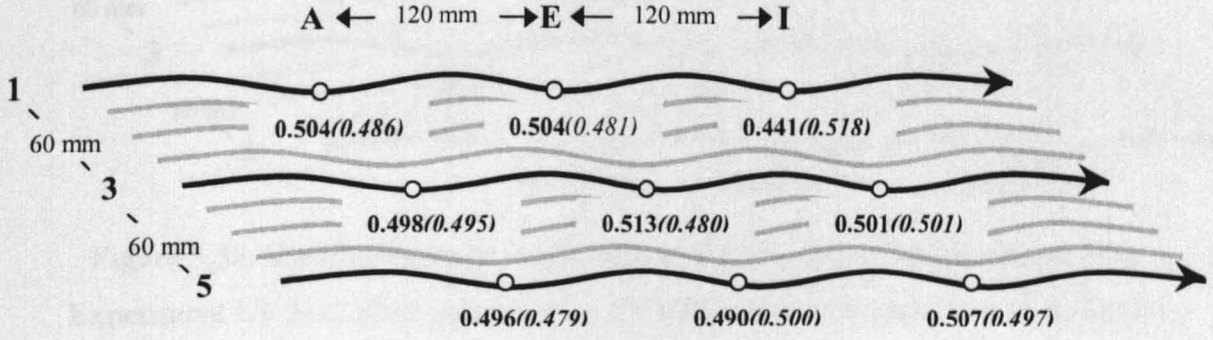

Figure 5.37. Distribution of average nearbed streamwise velocity (m/s) in antecedent flow Experiment UF 2-12 (first measurement in bold, second measurement in brackets)

Table 5.16 and Figure 5.38 shows the average bed shear stress, estimated using Equation 3.4, at different grid points. It can be seen that the average bed shear stresses are generally increased in the second measurement. After 125 minutes only three points exhibit a decrease. Another two points had negative values in the first measurement but increased quite significantly in the second measurement. The standard deviation at each point is quite considerable and like the mean values of bed shear stress show no consistent temporal pattern.

Table 5.16. Variations of the average bed shear stress and the standard deviation in antecedent flow Experiment UF 2-12

Points	First measurement (time elapsed 3 minutes)		Second measurement (time elapsed 128 minutes)		Changes of $\overline{\tau}$ (%)
	$\overline{\tau}$ (N/m^2)	σ (N/m^2)	$\overline{\tau}$ (N/m^2)	σ (N/m^2)	
A1	3.614	14.807	1.090	15.451	69.840 (-)
A3	5.588	15.238	6.109	15.122	9.324 (+)
A5	1.571	13.537	5.150	14.211	227.817 (+)
E1	-0.230	14.244	0.317	13.670	237.826 (+)
E3	3.337	15.669	4.741	14.187	42.074 (+)
E5	1.451	13.906	5.773	14.991	297.864 (+)
I1	-1.125	10.290	5.682	15.321	605.067 (+)
I3	5.471	14.880	2.856	15.155	47.797 (-)
I5	6.128	16.765	0.645	15.065	89.475 (-)
Average	2.867	14.371	3.596	14.797	

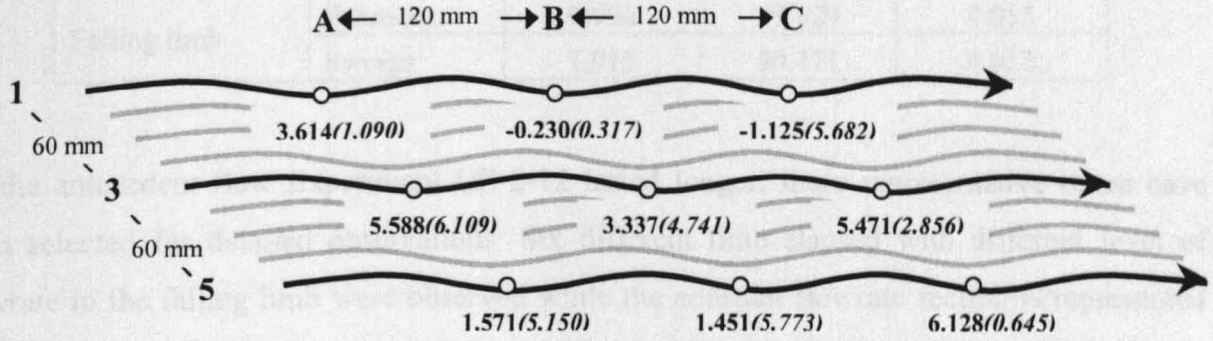

Figure 5.38. Distribution of average bed shear stress (N/m^2) in antecedent flow Experiment UF 2-12 (first measurement in bold, second measurement in brackets)

5.3.3.3. Bursting Events and Flow Momentum UF 2-12

Different flow features than those in the antecedent flow experiments UF 2-6 and UF 2-9 were found in antecedent flow Experiment UF 2-12. In this antecedent flow experiment the declining flow hydrograph was flatter in comparison to the previous two experiments. The flowrates decelerated from constant discharge of 0.0338 m^3/s to zero in the longest duration of 9 hours. It can be seen in Table 5.17 that the bursting events contained more sweeps than ejections either in the constant flowrates section or in the falling limb. This means the occurrence of downward-looking bed interactions is more frequent than the upward interactions throughout the antecedent flow. The wider variation occurred in the constant

flowrates section with the lower time frequency of ejections and the higher frequency of sweeps than in the falling limb. In this constant flowrate section the average duration of ejection is slightly longer than the average duration of sweeps. As the proportion of ejections in the falling limb increased and the sweeps decreased, the gap of proportion become closer indicating a relatively more stable bursting events where the upward interactions occurred as frequent as the downward-looking bed interactions (less than 1 % difference). In the falling limb the average duration of both ejections and sweeps are relatively similar.

Table 5.17. Time frequency and the proportion of occurrences of bursting events in antecedent flow Experiment UF 2-12

Parameter descriptions		Frequency (Hz)	Proportion (%)	Average duration (sec.)
Constant flowrate	Ejections	0.960	47.291	0.061
	Sweeps	1.070	52.709	0.051
Falling limb	Ejections	0.996	49.529	0.055
	Sweeps	1.015	50.471	0.052

As the antecedent flow Experiment UF 2-12 lasted longer, more representative times have been selected for detailed observations. Six different time elapsed with different level of flowrate in the falling limb were observed while the constant flowrate section is represented by one available data set (see Table 5.18 and Figure 5.39). Similar to the observation made in the previous antecedent flow experiments the selection of time elapsed was based on the pattern of grains size distribution of the transported bedload. This was intended to observe the

Table 5.18. Summary of bursting events at selected time elapsed in antecedent flow Experiment UF 2-12

Parameter descriptions	Time elapsed (minutes)						
	30	190	270	320	400	480	570
Threshold values (m^2/s^2)	0.0081	0.0079	0.0073	0.0067	0.0056	0.0048	0.0025
Number of ejections	192	204	204	197	219	200	156
Number of sweeps	214	196	205	187	219	205	164
Frequency of ejections (Hz)	0.960	1.020	1.020	0.985	1.095	1.000	0.780
Frequency of sweeps (Hz)	1.070	0.980	1.025	0.935	1.095	1.025	0.820
Average duration of ejections (s)	0.061	0.056	0.056	0.055	0.053	0.056	0.045
Average duration of sweeps (s)	0.051	0.054	0.051	0.053	0.056	0.052	0.045

influence of momentum in the bursting events on the changes of grains size distribution of transported bedload.

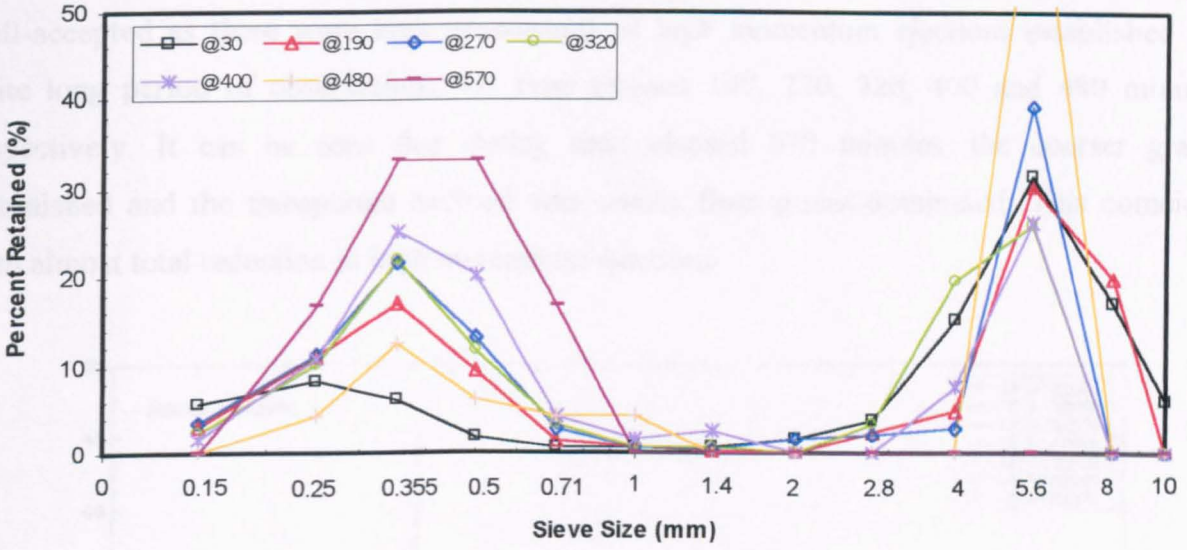

Figure 5.39. Grain size distribution of transported bedload at selected time elapsed in antecedent flow Experiment UF 2-12

At the earliest time elapsed (30 minutes) more grains in the coarse mode were transported than grains in the fine mode. Figure 5.39 shows that even grains with diameters 8 and 10 mm were removed and transported during this time. Closer observation on the probability distribution of momentum in Figure 5.40 found the answer to this pattern. It is apparently shown that the proportion of momentum with the magnitude in the range between 15 and 19 kg/ms during this time elapsed exceeds any other times. The frequency of the moderately sized ejections (11 - 15 kg/ms) is also high. It is believed that the ejections with high levels of momentum contribute to the removal of grains in the coarse mode. More than 64 % of grains in the coarse mode and almost 17 % of grains in the fine mode were transported at this time elapsed (30 minutes).

At time elapsed 190 minutes when the declining hydrograph had started, the domination of grains in the coarse mode in transport was still apparent. This coincides with data from the probability distribution curve in Figure 5.40 that shows that ejections with momentum

magnitude between 13 - 15 kg/ms is still quite frequent. The probability is almost 3 %. The transporting coarse grains phase continued until the latter time of 480 minutes in which an increasing amount of coarser grains was found in transported bedload. This coincided with an increase in ejections in the 15 - 19 kg/ms size range. This phenomenon is now reasonably well-accepted as there were high proportions of high momentum ejections established for quite long period of observations, i.e. time elapsed 190, 270, 320, 400 and 480 minutes respectively. It can be seen that during time elapsed 570 minutes, the coarser grains diminished and the transported bedload was clearly finer grains-dominated. This coincides with almost total reduction in high momentum ejections.

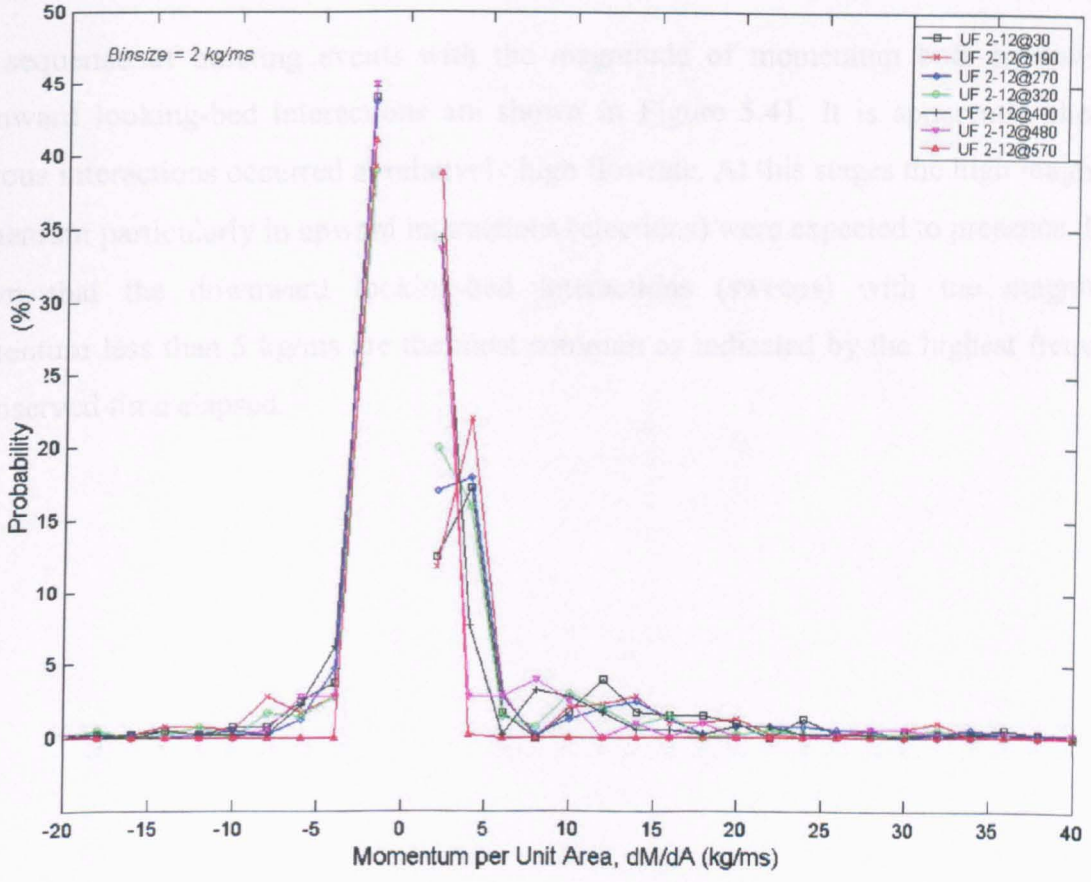

Figure 5.40. Probability distribution of momentum per unit area at selected time elapsed in antecedent flow Experiment UF 2-12 (ejections are positive and sweeps are negative)

A noticeable feature is presented by time elapsed 480 minutes. The proportion of grains in the coarse mode is extremely higher than grains in the fine mode. Although this time elapsed was in a low discharge with the average streamwise velocity of 0.380 m/s, it still produced a

considerable proportion of upward interactions with a magnitude of momentum in the range between 5 and 11 kg/ms and a measurable number of events in 15 - 19 kg/ms range. No wonder that a high proportion of coarser grains were transported during this time elapsed. Coarse grains contributes to almost 70 % of total transported bedload during this time elapsed. However, without arguing the important role of upward interactions to the entrainment process of coarser grains, it has to be remembered that there is always a possibility when the bed has reached its armouring state, i.e. time elapsed 480 minutes, only a small portion of transport in existence. At this stage the removal of a small number of exposed large grains can make a considerable proportion in the small amount of transported bedload.

The sequence of bursting events with the magnitude of momentum both in upward and downward looking-bed interactions are shown in Figure 5.41. It is apparently shown that rigorous interactions occurred at relatively high flowrate. At this stages the high magnitude of momentum particularly in upward interactions (ejections) were expected to presence. It is also shown that the downward looking-bed interactions (sweeps) with the magnitude of momentum less than 5 kg/ms are the most common as indicated by the highest frequency at all observed time elapsed.

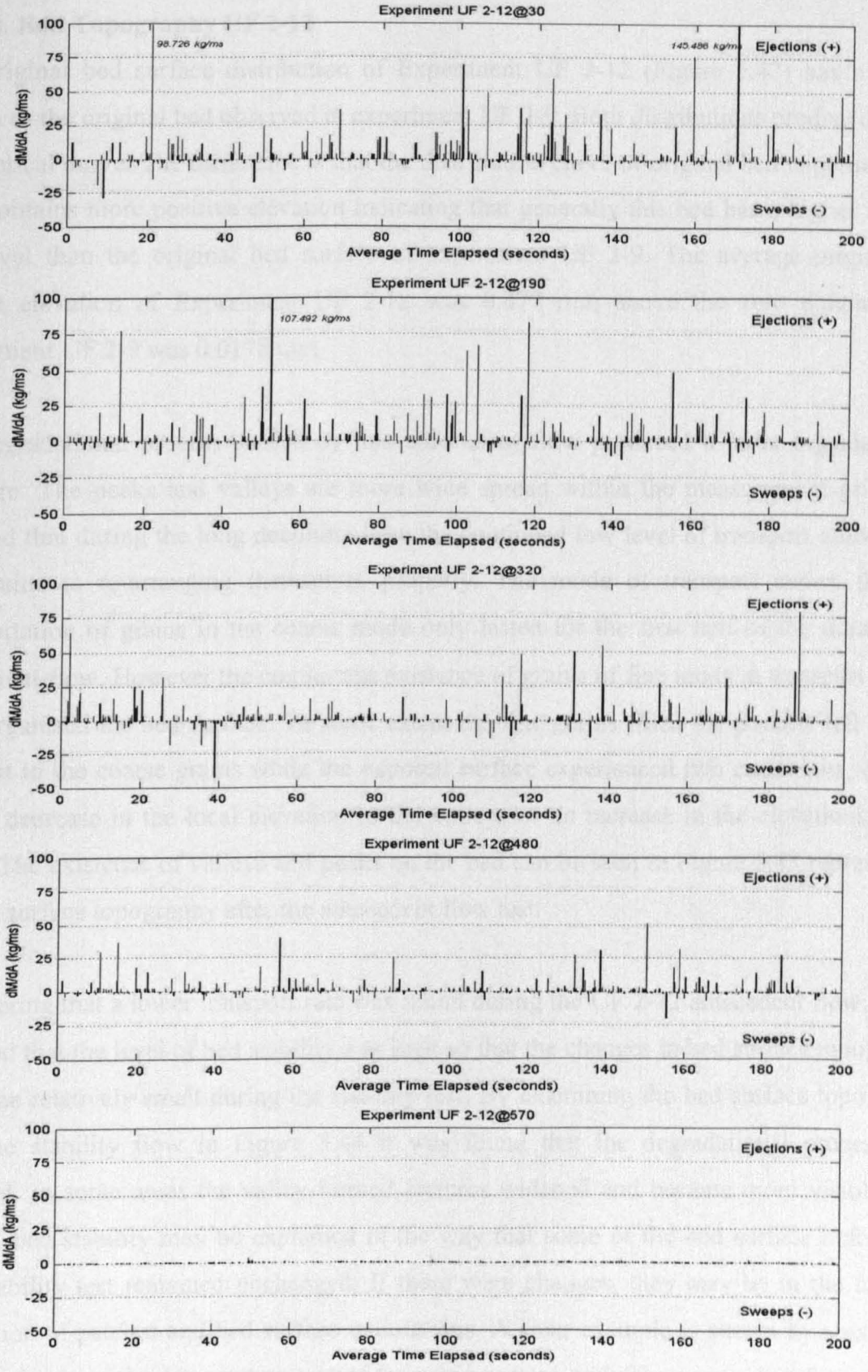

Figure 5.41. The sequence of momentum per unit area and its magnitude at selected time elapsed in antecedent flow Experiment UF 2-12

5.3.3.4. Bed Topography UF 2-12

The original bed surface distribution of Experiment UF 2-12 (Figure 5.42) has a similar pattern to the original bed observed in experiment UF 2-9. Both distributions produced almost an identical curve. The difference is that the distribution curve of original bed experiment UF 2-12 contains more positive elevation indicating that generally this bed has a higher average bed level than the original bed surface of experiment UF 2-9. The average original bed surface elevation of Experiment UF 2-12 was 0.477 mm above the zero datum whilst Experiment UF 2-9 was 0.0178 mm.

The degradational process caused by this antecedent flow produced a more organised bed structure. The peaks and valleys are more wide spread within the measurement grid. It is believed that during the long declining flow the continued low level of transport allowed the bed grains to re-arranging themselves properly. The mode of transport shows that the transportation of grains in the coarse mode only lasted for the first half of the duration of antecedent flow. However the continuous existence of grains of fine mode in transport helped to re-organised the bed surface. To some extent the fine grains filled the pockets left by and adjacent to the coarse grains while the exposed surface experienced two conditions, either a further decrease in the local elevation of the valleys or an increase in the elevations of the peaks. The existence of valleys and peaks on the bed can be seen in Figure 5.43 representing the bed surface topography after the antecedent flow test.

Considering that a lower transport rate was found during the UF 2-12 antecedent flow, it was expected that the level of bed stability was high so that the changes in bed surface topography would be relatively small during the stability test. By examining the bed surface topography after the stability flow in Figure 5.44 it was found that the degradational process still occurred. In some areas the valley-formed features widened and became more visible. The level of bed stability may be explained in the way that some of the bed surface before and after stability test remained unchanged. If there were changes, they may be in the form of dislocation of patches and bed surface undulations. A clear example is shown by area in the right hand side of the downstream part of the measurement grid. The exposed surface at point (130,100) created by antecedent flow test remain in existence after stability test whilst the bed surface undulation adjacent to it and those located further downstream and other areas show

small dislocation.

The changes in the bed surface level after the antecedent flow is shown by the distribution curve in Figure 5.45. The distribution curve is shifted to the left indicating the considerable decreased in the bed surface level. A distinct feature is shown in which the existence of valley-formed bed with many elevations up to 9 mm below the zero level is apparent. The existence of these valleys must be taken into account as they formed a second peak, which clearly marked the left tail and changes the shape of distribution. After the stability test the distribution is shifted to the right and parallel to the distribution of bed surface elevation formed by antecedent flow experiment. This suggests that there was continuing process of erosion although the bed surface structure was not significantly changed.

The observation of the distribution about mean level shows that after antecedent flow the large tail exist in the right hand side of the distribution. This is the indication that a number of grains resting on the bed surface increased. After the stability test, the tail was almost unchanged. The bed surface formed by antecedent flow test was relatively stable. The increased of the peak caused by the increasing proportion of the bed surface close to the mean level indicated that the bed surface become flatter. The second peak, which is skewed to the right after the stability test, is a reflection of the decrease in the depth of valley-type bedforms. The antecedent flow experiment eroded the bed surface and formed a noticeable amount of valleys with elevation of 5.5 mm below the average. During the stability test some grains were deposited in these valleys. The elevation of the valley was then increased to become closer to the average bed surface. This is indicated by the second peak that is shifted to the right hand side suggesting the less variation of the bed surface from the average level.

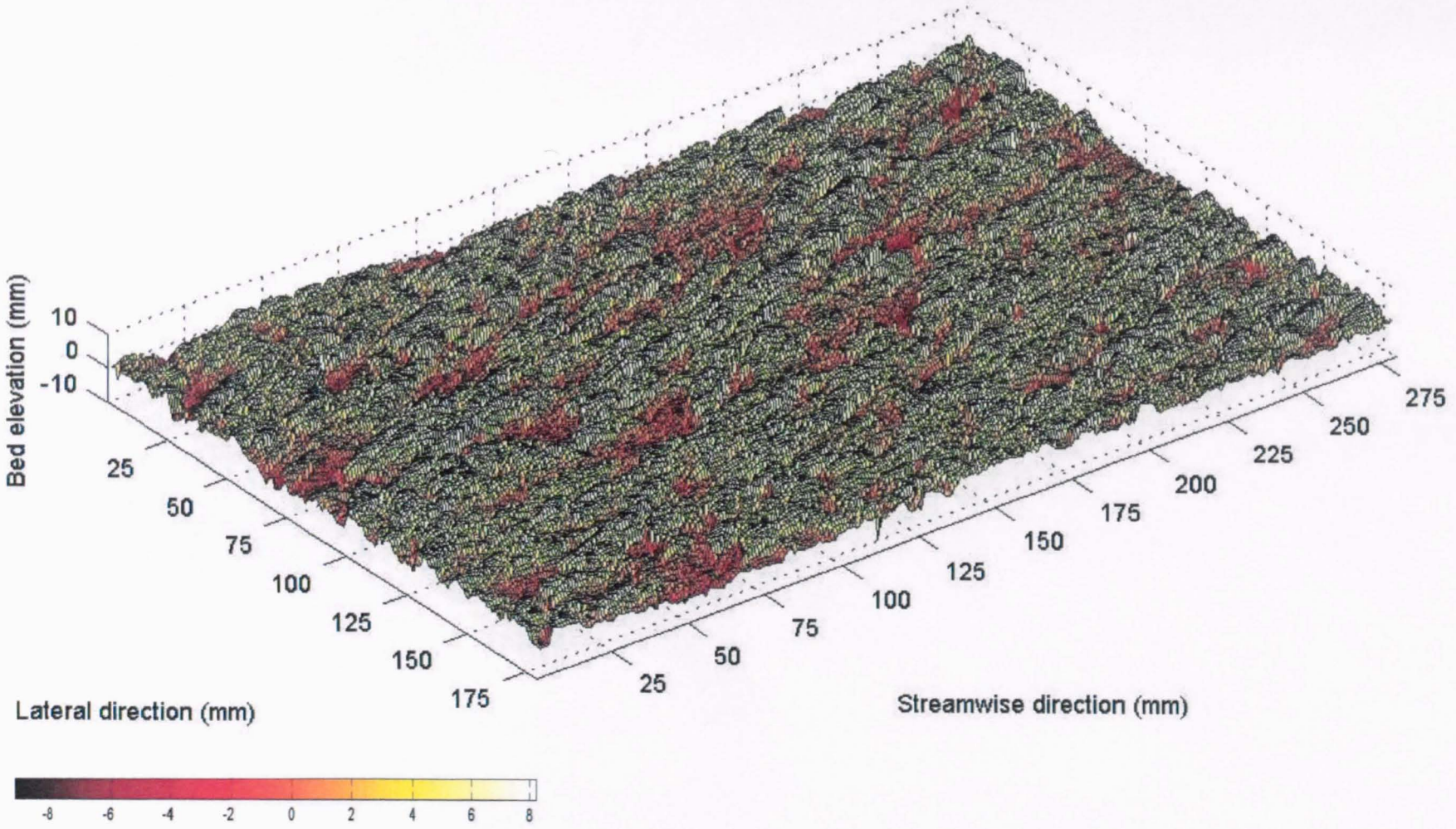

Figure 5.42. Original bed surface topography of the measurement grid Experiment UF 2-12

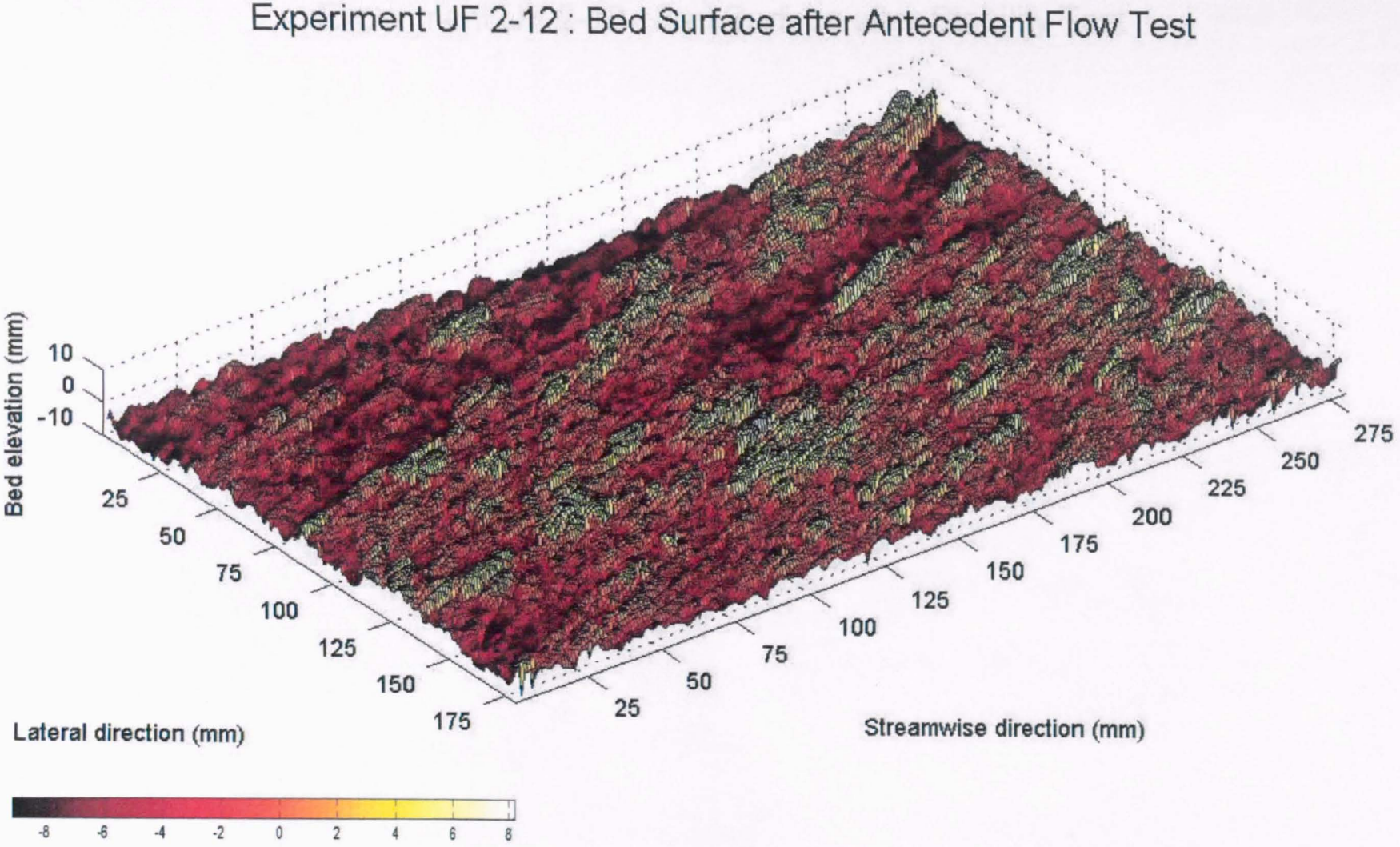

Figure 5.43. Bed surface topography of the measurement grid after antecedent flow Experiment UF 2-12

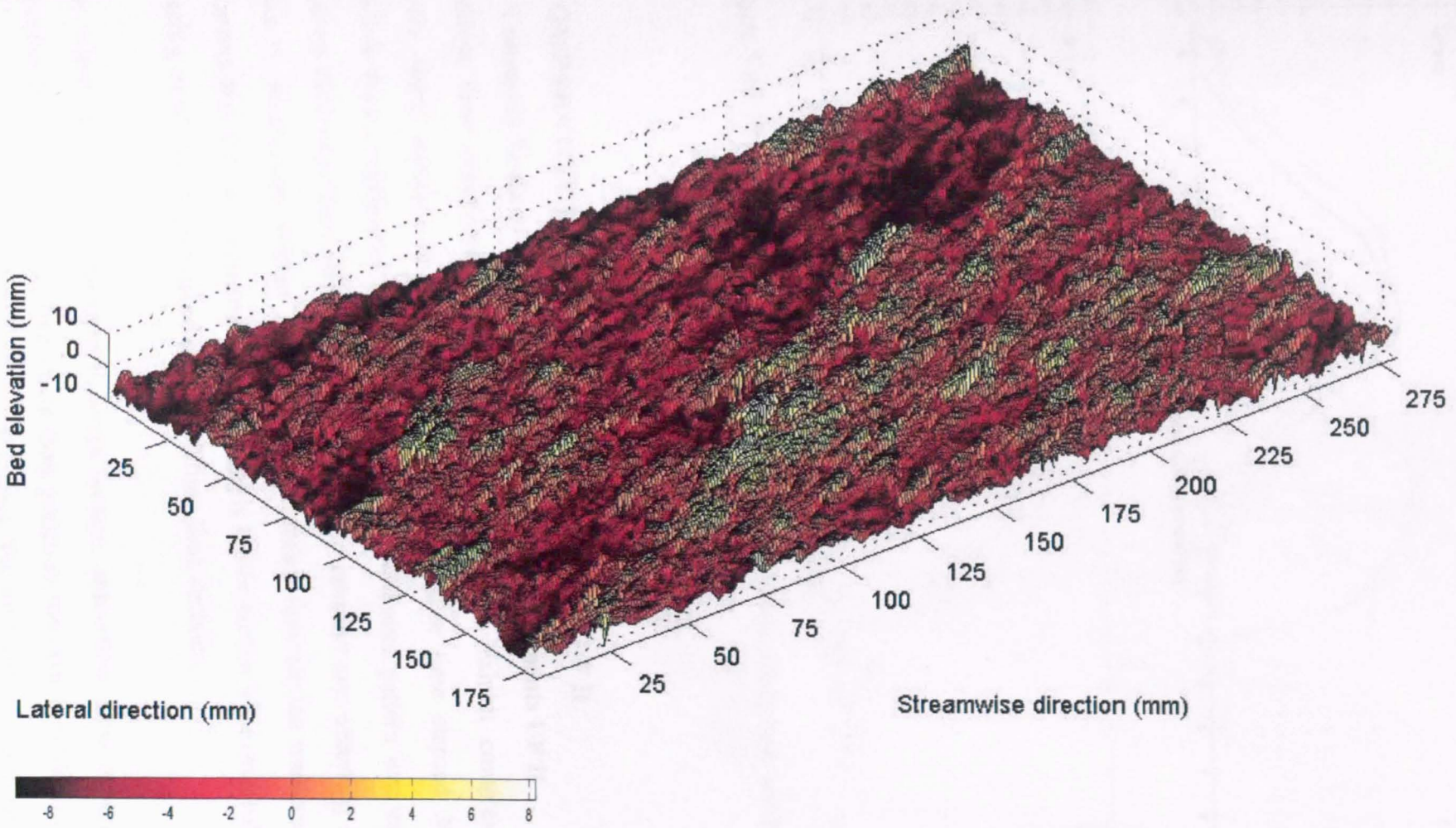

Figure 5.44. Bed surface topography of the measurement grid after stability test Experiment UF 2-12

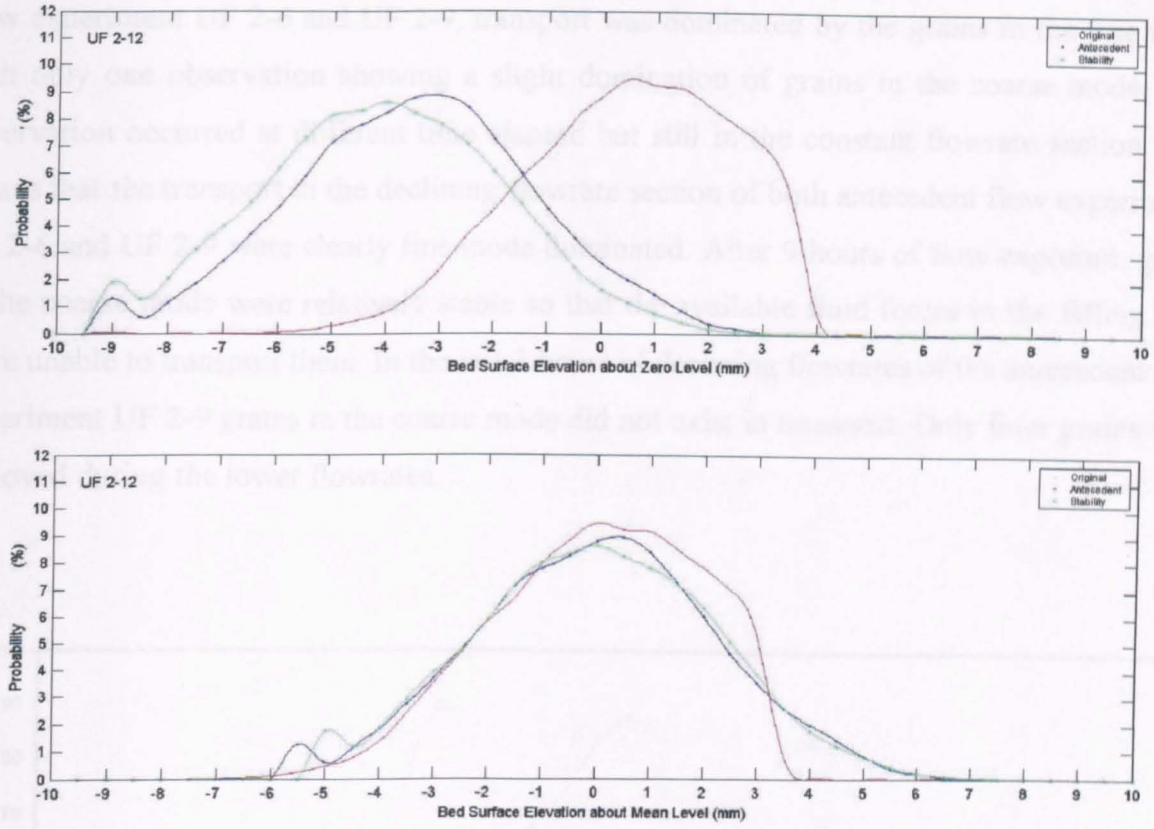

Figure 5.45. Probability distribution of bed surface elevation about zero and mean level for Experiment UF 2-12

5.4. COMPARATIVE RESULTS AND DISCUSSIONS OF UF II

5.4.1. Transport Mode of Declining Antecedent Flow Experiments UF II

Antecedent flow experiments with time varying flowrates exhibit complex patterns. A relatively sharp increase in transport rate was noted after time elapsed 30 minutes in antecedent flow experiments UF 2-6 and UF 2-9. A different pattern was experienced by antecedent flow experiment UF 2-12 with the highest transport rate occurring in the first 10 minutes of observation. Within 180 minutes of constant flowrate the transport rates for all three antecedent flow experiments fluctuated. Fairly erratic curves were established before the decreasing trend in transport found in all the falling limb sections.

In the initial hour of the constant flowrate section, antecedent flow experiment UF 2-6 transported more grains in the fine mode than grains in the coarse mode whilst antecedent flow experiment UF 2-9 and UF 2-12 are vice versa (Figure 5.46). Throughout the antecedent

flow experiment UF 2-6 and UF 2-9, transport was dominated by the grains in the fine mode with only one observation showing a slight domination of grains in the coarse mode. This observation occurred at different time elapsed but still in the constant flowrate section. This means that the transport in the declining flowrate section of both antecedent flow experiments UF 2-6 and UF 2-9 were clearly fine mode dominated. After 9 hours of flow exposure, grains in the coarse mode were relatively stable so that the available fluid forces in the falling limb were unable to transport them. In the last 3 hours of declining flowrates of the antecedent flow experiment UF 2-9 grains in the coarse mode did not exist in transport. Only finer grains were removed during the lower flowrates.

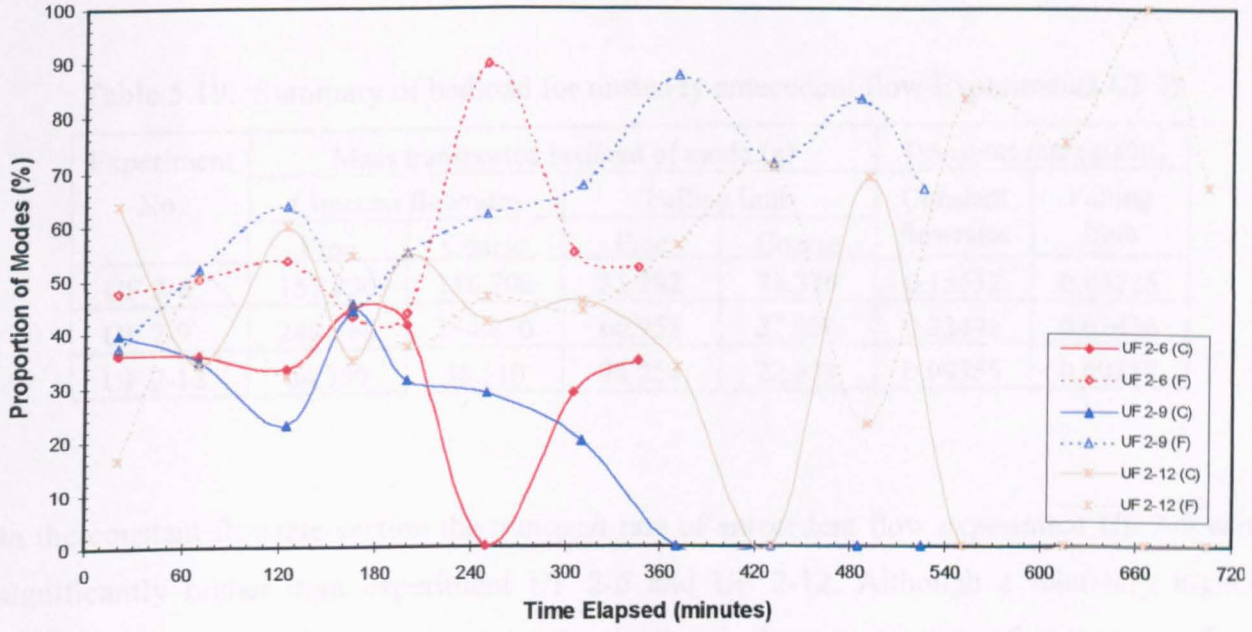

Figure 5.46. Proportion of two modes during the unsteady antecedent flow Experiments UF II (coarse and fine mode are represented by solid and dotted line)

A more complex pattern was experienced by antecedent flow experiment UF 2-12. The dominant mode of transport changed every hour of observation including in the first 3 hours of declining flowrates. After time elapsed 430 minutes the available fluid forces were unable to transport grains in the coarse mode. However this was not lasted very long. The domination of grains in the coarse mode was seen again at time elapsed 490 minutes but with a very small

amount. In the remaining hours after time elapsed 490 minutes grains in the coarse mode were not exist in transport (Figure 5.46).

Table 5.19 shows that the antecedent flow Experiment UF 2-9 transported more material than antecedent flow experiments UF 2-6 and UF 2-12. Interesting feature shown in constant flowrates section. Both antecedent flow experiments UF 2-6 and UF 2-9 transported more grains in the fine mode than the coarse mode. This coincides with the early explanation that grains in the fine mode dominated the transport in the two antecedent flow experiments. Antecedent flow experiment UF 2-12 shows a different pattern in which the transport is not only very low in comparison to the other two experiments but also has more grains moving in the coarse mode than in the fine mode.

Table 5.19. Summary of bedload for unsteady antecedent flow Experiments UF II

Experiment No.	Mass transported bedload of mode (g)				Transport rate (g/s/m)	
	Constant flowrates		Falling limb		Constant flowrates	Falling limb
	Fine	Coarse	Fine	Coarse		
UF 2-6	157.830	116.700	35.282	21.330	0.15532	0.03225
UF 2-9	240.760	154.870	60.958	27.050	0.22441	0.02436
UF 2-12	64.390	98.510	24.254	22.839	0.09355	0.00859

In the constant flowrate section the transport rate of antecedent flow experiment UF 2-9 was significantly higher than experiment UF 2-6 and UF 2-12. Although a relatively higher amount of grains was transported in the declining flowrate section of antecedent flow experiment UF 2-9, the transport rate is lower than that in the declining flowrate section of antecedent flow experiment UF 2-6. These results indicate that the unsteadiness of the flow influences the transport. Table 5.24 suggests that the maximum transport rate is highest when the duration of the falling limb is short. In antecedent flow experiment UF 2-6, the declining flowrate dropped in a very short time. It is suspected that after the destabilisation process in the relatively high constant flowrate, the grains have not sufficient time and mobility to find shelter in the falling limb. When the declining flowrate reduced at slower pace, the fluid forces decreased very slowly allowing the moving grains time to find shelter. It was expected that in the falling limb of antecedent flow experiment UF 2-12 the slower transition of the

flow allowed the grains moving in a rolling fashion more chance to find shelter and develop stability. Therefore the sheltering processes were more likely to occur in the slower declining flowrates where the transport rate was low but lasted for a long duration.

As shown in Table 5.20 the composition of both modes of transport in antecedent flow experiments UF 2-6 and UF 2-9 are relatively close with the domination of grains in the fine mode. Meanwhile, the antecedent flow experiment UF 2-12 has a different pattern where the grains in the coarse mode clearly dominated the transport during the antecedent flow experiment.

Table 5.20. Total mass and proportion of sediment modes for unsteady antecedent flow Experiments UF II

Experiment No.	Bedload transport		Mass and proportion of mode			
	Mass (g)	Rate (g/s/m)	Fine mode		Coarse mode	
			(g)	(%)	(g)	(%)
UF 2-6	384.860	0.094	193.120	50.179	138.020	35.862
UF 2-9	560.480	0.091	301.730	53.834	181.920	32.458
UF 2-12	244.850	0.030	88.630	36.198	121.340	49.557

5.4.2. Stability of the Antecedent Flow Beds and Mode of Transport UF II

The importance of high fluid forces in mobilising the surface can be described in terms of the pattern of bedload transported in the stability tests. At the lower discharges the transport rate was very low indicating an inability of available fluid forces to destabilise the armoured bed. The transport rate was considerably increased when the flowrate was about 0.0300 m^3/s. After the peak flowrates of 0.0375 m^3/s passed, the transport rates increased significantly. Even at corresponding discharges the transport rates in the falling limb were still higher than in the rising limb.

Investigation on transport rates suggest that the bed formed by the combination of 3 hours constant flowrates and 6 hours declining flow hydrograph (antecedent flow experiment UF 2-9) is the weakest. The amount of bedload transported in the stability test applied to this bed is 1040.78 grams. A similar stability test applied to the bed formed by antecedent flow

experiment UF 2-6 and UF 2-12 eroded 690.06 grams and 45.93 grams respectively. In the stability test UF 2-6 and UF 2-9, a large increase in transport rates found after the peak flowrate of 0.0375 m^3/s. Significant increases from the last 10 minutes of the rising limb to the corresponding flowrates (first 10 minutes of falling limb) were noticed.

Stability test UF 2-12 suggests a different pattern. The amount of bedload transported in the first 10 minutes of the falling limb shortly after the peak flowrates was not increased. The transport rate was slightly lower. The difference in the transport rate is even lower in the next 10 minutes in comparison to the corresponding discharge in the rising limb. This suggested that the longer duration of declining antecedent flow formed a strong pavement. The peak flowrate of this stability test was unable to destabilise the armoured bed. The increasing proportion of grains in the fine mode and the decreasing proportion in the coarse mode for the whole duration of the stability test UF 2-12 as presented in Table 5.21 also indicates that the bed formed by a long declining hydrograph is the most stable one.

Table 5.21. Transport mode of the stability tests applied to antecedent flow-formed bed UF II

Stability Test	Time elapsed of coarse grain domination (mins)	Mass of bedload and proportion				Total	
		Fine mode		Coarse mode		Fine mode	Coarse mode
		Rising	Falling	Rising	Falling		
UF 2-6	@60 - @120	52.45 gr	87.52 gr	172.49 gr	292.36 gr	139.97 gr	464.85 gr
		7.601 %	12.683 %	24.996 %	42.367 %	20.284 %	67.364 %
UF 2-9	@20 - @90	67.94 gr	136.60 gr	275.22 gr	431.54 gr	204.54 gr	706.76 gr
		6.528 %	13.125 %	26.444 %	41.463 %	19.653 %	67.907 %
UF 2-12	@40 - @90	9.44 gr	4.39 gr	13.16 gr	10.09 gr	13.83 gr	23.25 gr
		20.553 %	9.558 %	28.652 %	21.968 %	30.111 %	50.621 %

It is also seen in Table 5.21 that there are differences in the period of domination of coarse mode in transport. The weakest bed formed by antecedent flow UF 2-9 is clearly indicated by the early appearance of grains in the coarse mode in transport. The grains in the coarse mode started to dominate the transport at time elapsed 20 minutes. This means the exposed coarse grains on the bed were not stable enough to resist the small fluid forces produced at the low

flowrates. Although the domination of grains in the coarse mode established earlier in the stability test UF 2-12 than in the stability test UF 2-6, the bed formed by antecedent flow experiment UF 2-12 is more stable than the bed formed by antecedent flow UF 2-6. The period of domination of grains in the coarse mode was shorter in UF 2-12 with very low transport rates. Meanwhile the stability test UF 2-6 indicates the influence of peak flowrates on the destabilisation of the bed surface structure. It is believed that this bed structure was composed of many exposed and isolated larger grains resting on the bed so that the low fluid forces at time elapsed 120 minutes were still able to transport grains in the coarse mode. It is also seen in Table 5.21 that the transport with the domination of grains in the coarse mode was over a longer period in the stability tests UF 2-9 than the other two stability tests.

5.4.3. The Distribution of Average Nearbed Streamwise Flow Velocity and Average Bed Shear Stress UF II

The average nearbed streamwise velocity in antecedent flow Experiment UF 2-6, UF 2-9 and UF 2-12 are sensibly constant throughout the constant flowrate section (Figure 5.47). The observation of three different time elapsed representing every hour of constant flowrate section indicated that the range of variation of time averaged nearbed streamwise velocity from the average values of all measurement is less than 4 %. The narrowest range is found in the constant flowrate section of UF 2-6 with the range of ± 2 % while in the constant flowrate section of UF 2-9 the range slightly increased to ± 3 %. In constant flowrate section of UF 2-12 the variation has a range between +4 % and -3 %. These variations correlate with the observation in the steady antecedent flow Experiment SF I that the range of variation for the shorter interval between time elapsed is very low. The time averaged nearbed streamwise velocities are also generally decreased at the later time elapsed indicating an increased in the hydraulic roughness of the bed.

In the average bed shear stress the variation in the unsteady antecedent flow UF 2-6 is also small and has relatively similar range with the variation in the average nearbed streamwise velocity. The range of variation is wider in the unsteady antecedent flow UF 2-9 and UF 2-12 where the variations are ranging from -11 to +8 % and +7 to -12 % respectively (Figure 5.48). The increase in the variation of the average bed shear stress in comparison to the variation of

the average nearbed streamwise velocity is thought to be caused by the variation in the distribution of "instantaneous" vertical velocity.

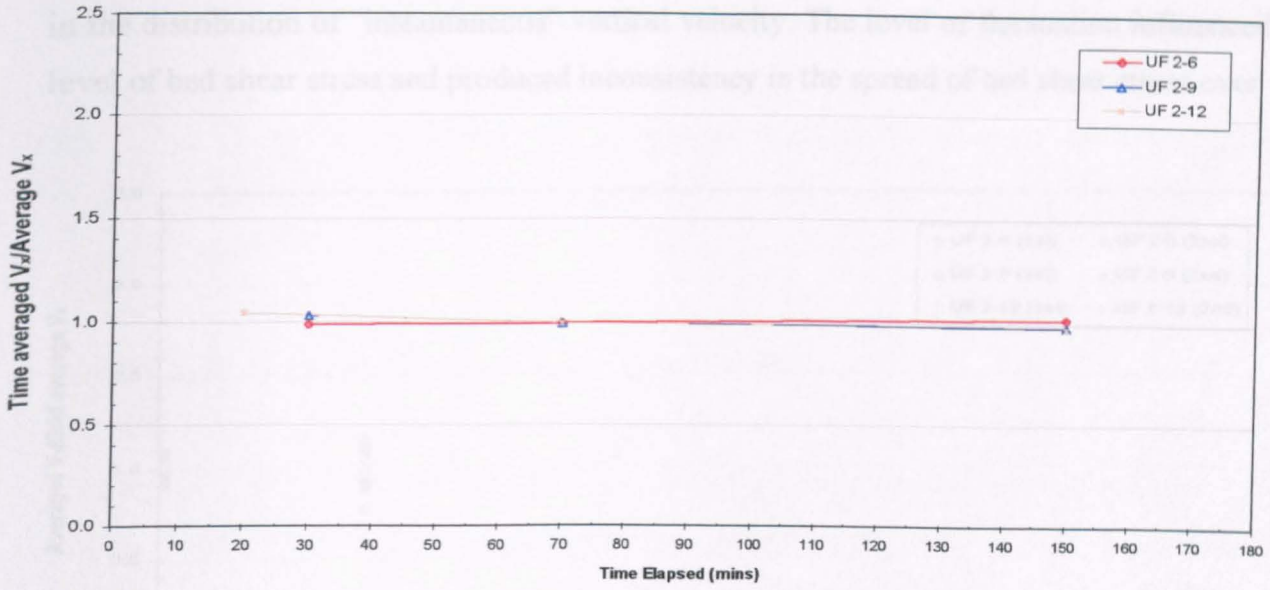

Figure 5.47. Variation of time averaged nearbed streamwise velocity during the constant flowrate section in antecedent flow Experiment UF II

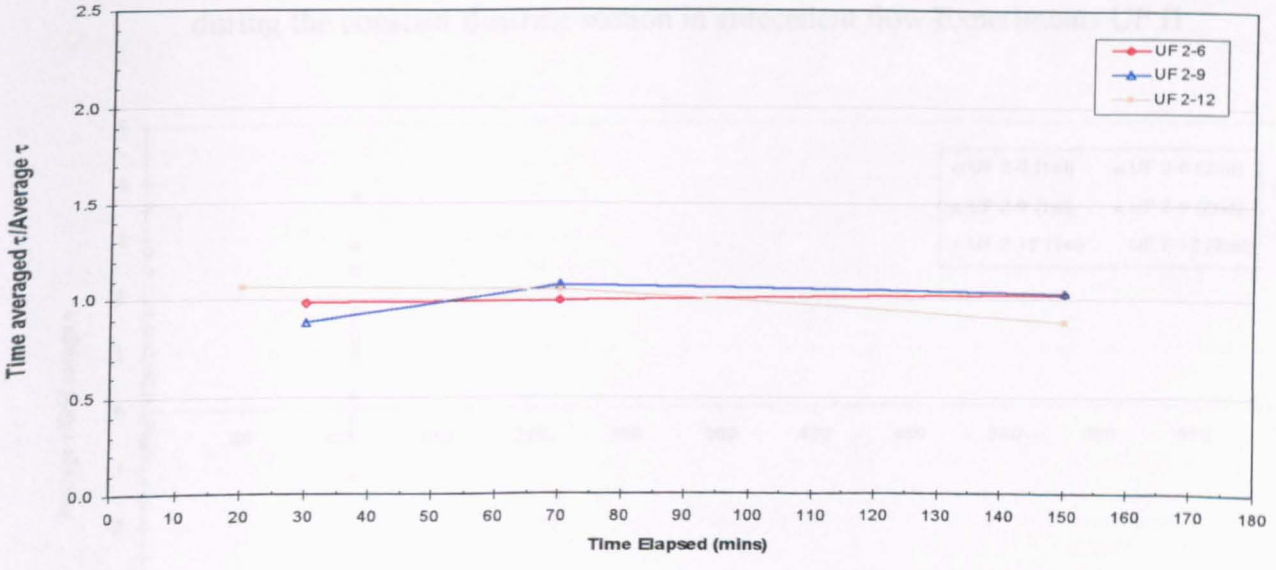

Figure 5.48. Variation of time averaged bed shear stress during the constant flowrate section in antecedent flow Experiment UF II

Similar observation to different grid points in the measurement area show that the variations in the average bed shear stress (Figure 5.50) do not automatically follow the pattern of

average nearbed streamwise velocity (Figure 5.49). The variations have no systematic pattern as some points exhibited decreasing values whilst other points increased in the second measurement. Again the most likely factor for the variation in bed shear stress is the variation in the distribution of "instantaneous" vertical velocity. The level of fluctuation influenced the level of bed shear stress and produced inconsistency in the spread of bed shear stress over the

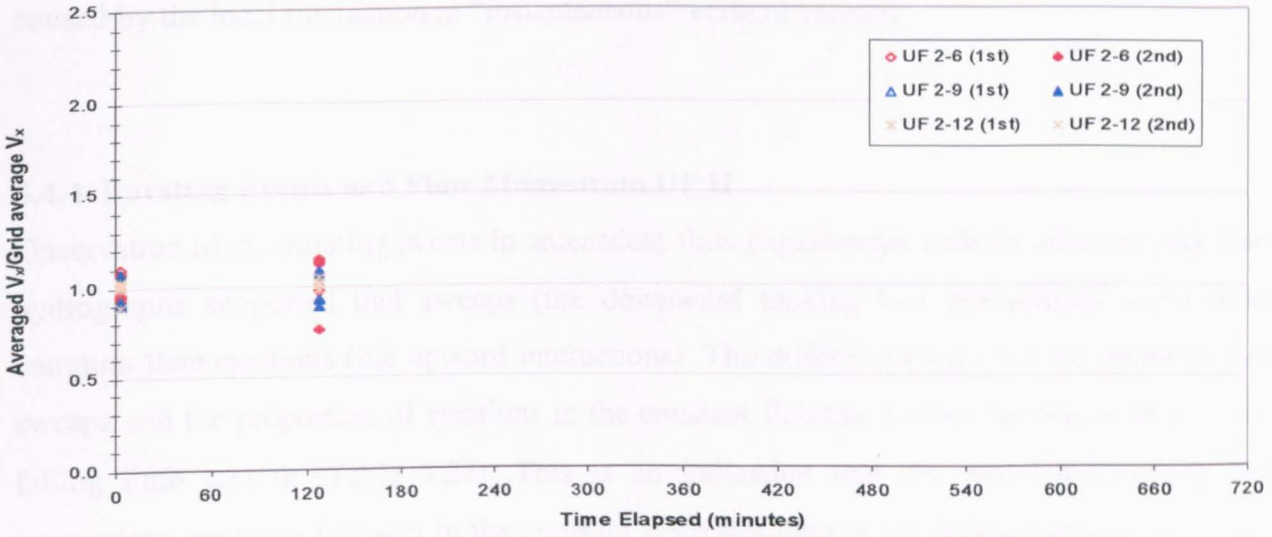

Figure 5.49. Variation of average nearbed streamwise velocity in the measurement grid during the constant flowrate section in antecedent flow Experiments UF II

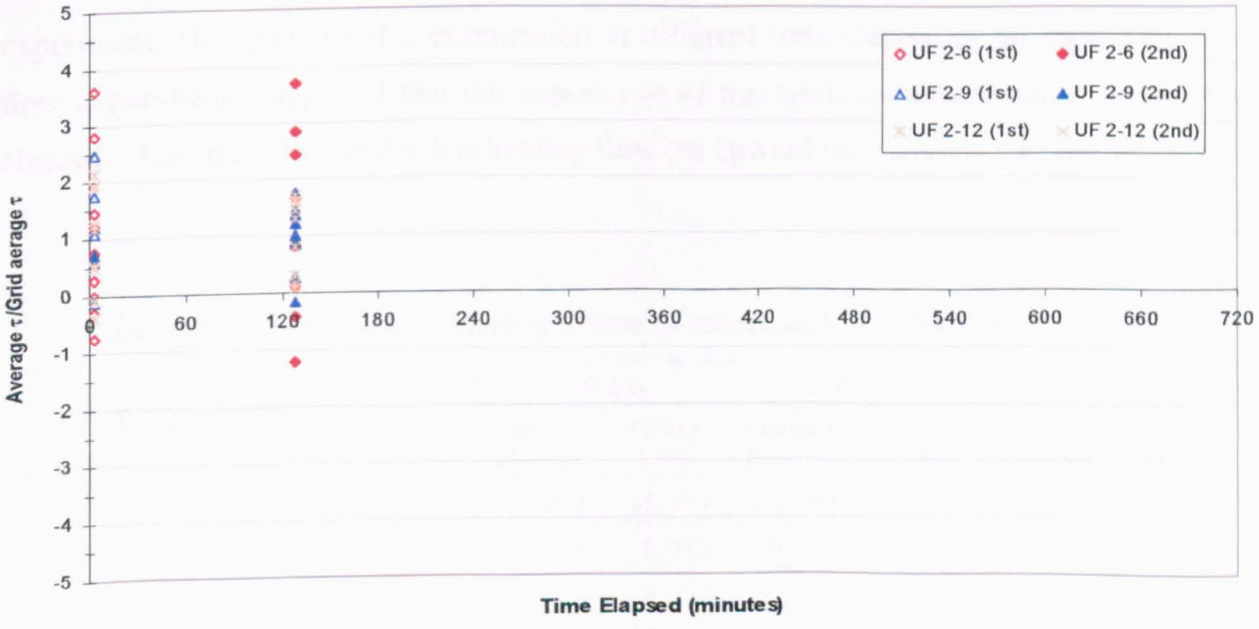

Figure 5.50. Variation of average bed shear stress in the measurement grid during the constant flowrate section in antecedent flow Experiments UF II

observation area. It is very clear that the scattered values of bed shear stress are the indication that the fluctuation of flow velocity in vertical direction continued during each test. Normally when the streamwise velocity experienced a low variation, a smaller variation in bed shear stress was produced only if the fluctuation in vertical velocity were also small. It is then assumed that the variation of bed shear stress in antecedent flow Experiment UF 2-6, UF 2-9 and UF 2-12 within an interval of 125 minutes between the measurements are primarily caused by the local fluctuation in "instantaneous" vertical velocity.

5.4.4. Bursting Events and Flow Momentum UF II

Observation of the bursting events in antecedent flow experiments with the time varying flow hydrographs suggested that sweeps (the downward looking bed interactions) were more common than ejections (the upward interactions). The differences between the proportion of sweeps and the proportion of ejections in the constant flowrate section are higher than in the falling limb section (Table 5.22). This is an indication that the downward-looking bed interactions are more frequent in the constant flowrates than in the falling limbs even though the flow decelerated in the latter sections. At the beginning it was assumed that the decelerating flow tended to produce more downward looking-bed interactions than upward interactions and hence dominated the bursting events in the duration of each antecedent flow experiment. However, careful examination at different time elapsed in all three antecedent flow experiments suggested that the importance of the ejections also found in certain time elapsed. This means that in the decelerating flow the upward interactions have the opportunity

Table 5.22. Summary of bursting events of antecedent flow Experiments UF II

Parameter descriptions		UF 2-6		UF 2-9		UF 2-12	
		Constant Flowrate	Falling Limb	Constant Flowrate	Falling Limb	Constant Flowrate	Falling Limb
Ejections	Proportion (%)	47.487	48.372	46.192	48.033	47.291	49.529
	Frequency (Hz)	0.945	0.982	0.940	1.013	0.960	0.996
	Average duration (s)	0.050	0.052	0.051	0.053	0.061	0.055
Sweeps	Proportion (%)	52.513	51.628	53.808	51.967	52.709	50.471
	Frequency (Hz)	1.045	1.048	1.095	1.095	1.070	1.015
	Average duration (s)	0.053	0.051	0.050	0.052	0.051	0.052

to dominate the bursting events in certain periods although this may not be as frequent as the downward looking-bed interactions.

In antecedent flow experiments UF 2-6 and UF 2-12 the proportion of events for both types of interactions are almost the same in the constant flowrate sections whilst in the antecedent flow Experiment UF 2-9 the proportion of ejections is slightly lower and the proportion of sweeps is slightly higher. However the frequency of occurrences for both interactions are relatively similar for all antecedent flow experiments with very close values in the constant flowrate sections. It is also seen that the average duration of both events are similar in all tests. In Table 5.22 the frequency of ejections in the falling limb section of antecedent flow Experiment UF 2-9 is higher than the antecedent flow experiments UF 2-6 and UF 2-12. It is likely that the more numerous ejections ocurring in the falling limb of Experiment UF 2-9 coincides with the pattern of transport in Table 5.19. This shows higher bedload in the coarse mode transported during antecedent flow Experiment UF 2-9 than in other two tests.

5.4.5. Bed Topography UF II

The original bed of Experiment UF 2-9 was aggressively eroded by the antecedent flow. A significantly higher amount of bedload in comparison to the other two tests was transported during the constant flowrates and during the falling limb (see Table 5.19). This is the main factor that the bed surface topography before and after antecedent flow shows a significant difference. The bed surface elevation distribution shows that there was a significant quantity of large grains resting on the bed after antecedent flow (Figure 5.51). It is also believed that during antecedent flow UF 2-9 further erosion increased the number of valleys, most notably in the surface elevation range between 4 to 5 mm below the mean bed level as shown by the bed surface distribution curve in Figure 5.51. The bed surface after antecedent flow UF 2-9 less flatter and the exposed larger grains more spread. The application of stability flow with peak flowrate higher than the maximum discharge in the antecedent flow destabilise the bed and the exposed large grains were less easy to move and transported downstream. This stability test produced extremely high transport in comparison to the other two stability tests applied to the bed formed by antecedent flow experiments UF 2-6 and UF 2-12.

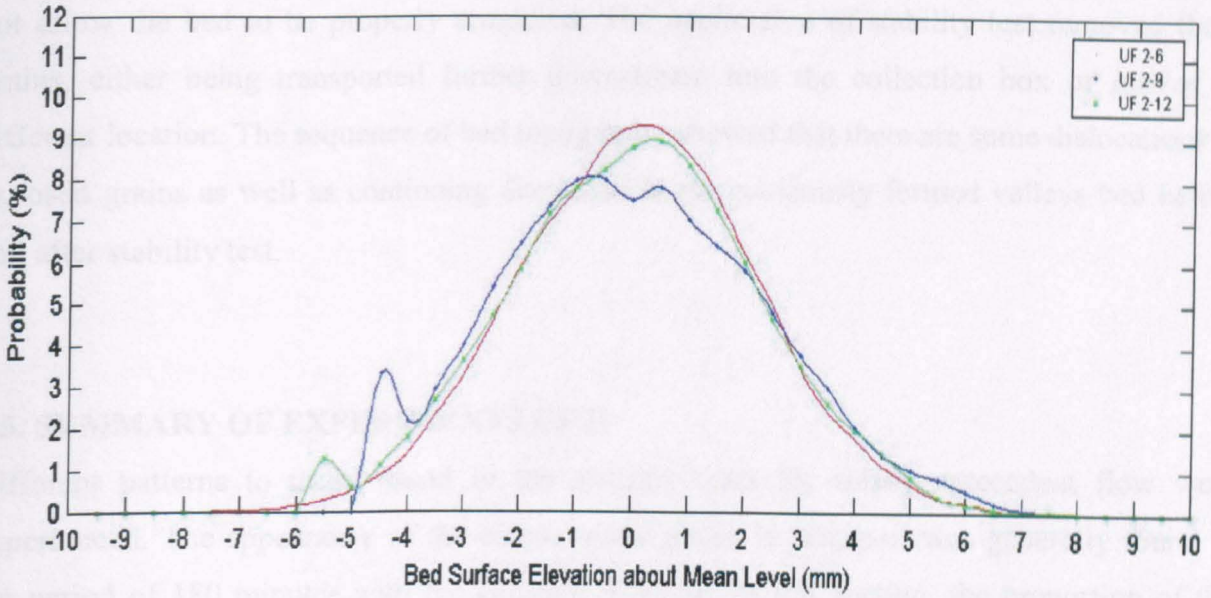

Figure 5.51. The comparison of the bed surface distribution about mean level after antecedent flow tests Experiments UF II

A relatively high number exposed grain was also found after antecedent flow experiment UF 2-12. Irregular shape of distribution curve in the negative values exist but with the lower proportion than in experiment UF 2-9. After the stability test was introduced to this bed, the distribution curves showing relatively little change. There is an increase in the proportion of the bed surface about the mean level but not to the extent experienced after the stability test experiment UF 2-9. The bed formed by antecedent flow with the combination of 3 hours constant flowrates and 9 hours declining flowrates is more stable. It is believed that for a long time period the stability test was only able to remove the coarser grains in a rolling fashion rather than in saltation so that the structures in the bed surface became progressively better developed and stronger. This is indicated by the final curves, most notably the irregular shape, which was shifted to the right indicating the eroded fine materials were not transported far away downstream but moved to and increased the bed surface elevation in adjacent neighbouring areas.

A different pattern of bed surface distribution is presented by experiment UF 2-6. The distribution curve is quite symmetrical. The distribution after antecedent flow indicated a lower number of isolated larger grains resting on the bed than in UF 2-9 and UF 2-12. These grains were relatively not in stable condition as the shorter period of decelerating flowrate did

not allow the bed to be properly armoured. The application of stability test removed these grains, either being transported further downstream into the collection box or moved to different location. The sequence of bed topography showed that there are some dislocations of exposed grains as well as continuing decreased in the previously formed valleys bed before and after stability test.

5.5. SUMMARY OF EXPERIMENTS UF II

Different patterns to those found in the stability tests for steady antecedent flow were experienced. The appearance of the coarse mode grains in transport was generally found in the period of 180 minutes with the constant flowrate. In this section, the proportion of the coarse mode in the antecedent flow experiments UF 2-6 and UF 2-9 show a decrease while UF 2-12 indicates a fluctuation. In the falling limb the contribution of the fine mode was generally increased while the coarse mode decreases in all the tests. The higher transport rates after the peak discharge of stability tests found in two experiments with the declining flow sections of 3 and 6 hours (UF 2-6 and UF 2-9). It is found that the bed formed by the medium duration of decelerating flowrate UF 2-9 is the weakest followed by the bed formed by antecedent flow with the shortest declining flow section (UF 2-6). In stability test UF 2-12 where identical stability hydrograph was applied to the bed formed by antecedent flow with 9 hours declining flowrates, the transport rate was very small. This underlines the importance of a relatively long duration of decelerating antecedent flow. The decelerating flows of antecedent flow were found to have transported mostly grains in the fine mode but coarse grains were also mobile. At this stage the armouring process was expected to properly develop. The coarse grains first became more organised and then the finer grains became more sheltered. This is indicated in the changes in the empirical hiding functions. The hiding function of grain size fractions in the stability tests UF 2-12 are slightly higher than UF 2-6 while in the stability test UF 2-9 the hiding function values are considerably lower. The thresholds of motion for finer grains in the stability tests UF 2-6 and UF 2-12 are relatively similar. In the stability test UF 2-9 the finer grains moved at considerably lower values of shear stress. Coarser grains also exhibited different thresholds of motion. It seemed that at the end of 6 hours decelerating flowrate large grains more exposed but an extended period allowed these grains to find more stable position. The finer fractions also found greater shelter

behind the stable coarse grains.

The observation of bursting events suggested that the downward looking bed interactions are more common in the antecedent flow with declining flowrates. The pattern found in antecedent flow experiment is that the high momentum of upward interactions is very important in transporting coarser grains. The frequency of occurrences and momentum magnitude determines the mode of transport. If the frequency of ejections higher than sweeps and the magnitude of momentum ejections is also high, it is expected that the transport is coarser grains-dominated. This pattern is similar to that found in the steady antecedent flow tests.

The bed topography observations displayed a similarity in which the erosion caused by the antecedent flow tends to form diagonal patches on the surface. The patches are stretched to the downstream and left side direction of the measurement grid. Although further erosion occurred in the stability tests the patches were maintained and still exist at the end of the final tests. The bed topography before and after the stability tests are relatively similar although the amount of bedload transported in this tests is higher than in the longer duration of the antecedent flow tests. This can be explained that the coarse grains dominated the transport during stability test and their movement did not considerably change the bed surface level. The distribution curves were slightly narrowed as the bed surface becoming relatively flatter.

Similar to observation in the steady antecedent flow tests, it is found that the average nearbed streamwise velocities were relatively constant throughout the constant flowrate sections. Only a small variation is noticed with the tendency to slightly decreases at the later time elapsed. Observation of the points in the measurement grid also has a similar pattern. Most points displayed a decrease in the average nearbed streamwise velocity and the average values of different measurement indicate that the second measurements always have slightly lower values. This is strongly supported the statement that as the constant flowrate progressed the average nearbed streamwise velocity would decrease slightly. In the average bed shear stress the tendency of decrease is also observed. This is thought to be due to the variation in the distribution of "instantaneous" vertical velocity as the hydraulic roughness of the bed increased.

VI. EXPERIMENTAL RESULTS OF UNSTEADY FLOW EXPERIMENTS UF III

6.1. INTRODUCTION

In this chapter three antecedent flow experiments run with three different hydrographs are reported. The hydrographs were a combination of different duration of increasing flow sections followed by 3 hours declining flowrate, which was the same in each test. The duration of the rising limbs were 3, 6 and 9 hours with a maximum discharge of 0.0338 m^3/s. This was followed by declining flow with the duration of 3 hours to form experiments with total durations of 6, 9 and 12 hours respectively. The results of each experiment, which have been identified as UF 3-6 (6 hours duration), UF 3-9 (9 hours duration) and UF 3-12 (12 hours duration), are described and then discussed together with the observations made during the subsequent stability tests.

The aim of these experiments was to examine the influence of different increasing rates of flow discharges on grain sorting and the stability of water worked sediment bed. For a comprehensive comparison between these experiments and others, which have previously been reported in Chapter 4 and Chapter 5 (Experiment SF I and Experiment UF II), this chapter is divided into four sections. The first section is focused on the stability analysis where the results of a short duration of 'standard' hydrographs applied at the end of all experiments were described. The standard hydrograph lasted 120 minutes and had a peak discharge of 0.0375 m^3/s, which was larger than the maximum discharge applied during the antecedent flows. The application of the standard hydrograph was intended to assess the stability of water worked bed at the end of each of the antecedent flow experiment.

The second section describes the observations made during each antecedent flow before the stability tests were applied. The observations consist of bedload transport pattern and composition, nearbed flow observations including the investigation of bursting events and bed topography analysis. The comparative results of all antecedent flow and stability tests form the third section in which links between the observation in the first and the second section are examined. The final part of this chapter comprises a summary or short conclusion section.

6.2. STABILITY TESTS OBSERVATIONS UF III

6.2.1. Transport Rate Measurement UF III

It has been found that the results of stability tests in Chapter 5 produced a different pattern from the results of the stability tests in Chapter 4, which showed that the bed formed by the longest constant flowrate is the strongest. Although at the end of each of these antecedent flow experiments the transport rate was very low indicating a stable bed condition, the level of armouring is believed to be different. This was proved by the stability test results. For the conditions where the constant flowrates were applied, it can be assumed that the stability of the bed is a function of time. However stability tests to beds formed by hydrographs, which combine constant flowrates and different durations of decelerating flowrates have suggested a different pattern. These findings led to the initial conclusion that the application of different types of time varying antecedent flow is likely to result in another pattern of stability in water worked beds. Because of this pattern it was decided to examine the stability of beds formed by different types of antecedent flow hydrographs, principally one with different durations of rising limb.

Figure 6.1 shows that the weakest bed was the one formed by antecedent flow test UF 3-6. Surprisingly it was the antecedent flow test UF 3-9 that formed the strongest bed. It suggests the possibility that medium duration of rising limbs sufficiently reorganised the bed structure so that the following identical falling limb strengthens the stability of the bed. However, it is too early to come to a conclusion as further investigation is necessary. It can be seen from Figure 6.1 that the transport rate of stability test UF 3-6 was extremely high in comparison to those during stability tests UF 3-12 and UF 3-9. A relatively small transport rate is evident during the early stages of rising limb. As flow strength increased, an increasing proportion of bedload was entrained into transport. This is the common pattern that was also found in the stability tests examined in the previous chapters. The transport rate was significantly increased when the flowrate was approaching its peak at 60 minutes. The bed formed by all antecedent flows were weakened at the highest discharge (time elapsed 60 minutes). It is believed that the destabilisation process took place during this particular time as the corresponding discharges after the peak flowrate produced even higher transport rates.

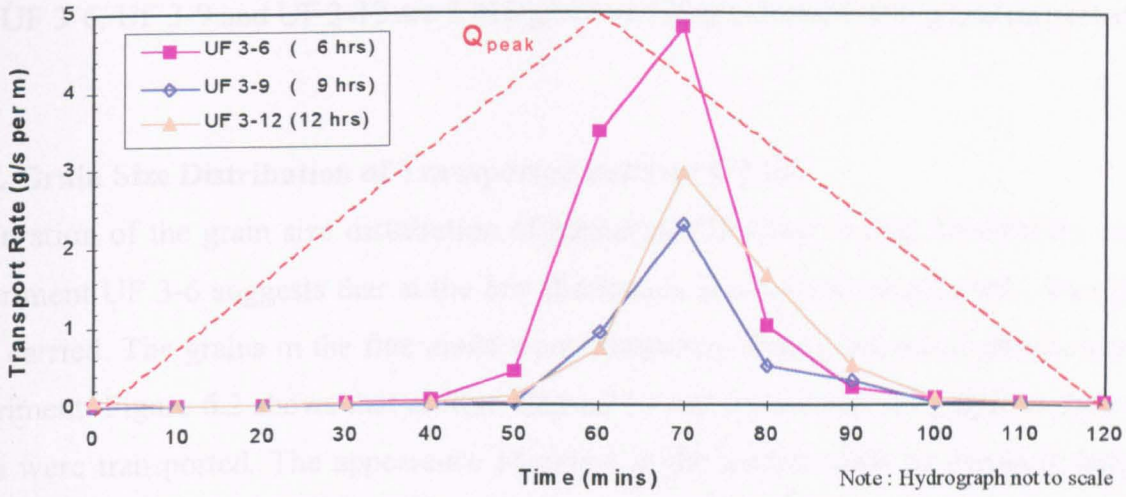

Figure 6.1. Bedload transport rate pattern during stability tests UF III

In terms of proportion of increased bedload for corresponding discharge in the rising and the falling limb, stability test UF 3-12 experienced the highest changes. Between time elapsed 50 to 60 minutes the transport rate is 0.704 g/s/m. This was increased more than threefold to 2.945 g/s/m during the time elapsed 60 - 70 minutes. The level of increased was even higher at latter times in comparison to the corresponding discharge in the rising limb. The bedload diminished to an almost-zero transport rate in the last ten minutes of the falling limb. However, the highest transport rate among the test is observed in the stability test UF 3-6 at time elapsed 60 - 70 minutes. At this time elapsed, the transport rate was 4.813 g/s/m while stability test UF 3-9 had 2.286 g/s/m and UF 3-12 had 2.945 g/s/m.

Although the stability test indicated that the antecedent flow experiments produced different levels of bed stability, Figure 6.1 confirms that only the higher discharges were able to destabilise the previously formed armoured bed. This is supported by the observation that the average transport rates in the falling limb are significantly higher than the transport rates in the rising limb. The average transport rates in the rising limb are 0.663 g/s/m for UF 3-6, 0.163 g/s/m for UF 3-9 and 0.149 g/s/m for UF 3-12. This suggest that the bedload transport rates for stability tests UF 3-9 and UF 3-12 are relatively similar in the rising limb. However different level of increase in transport after the peak flowrate was attained indicating that each bed has different level of stability. The average transport rate in the falling limbs of stability

tests UF 3-6, UF 3-9 and UF 3-12 are 1.026 g/s/m, 0.528 g/s/m and 0.865 g/s/m respectively.

6.2.2. Grain Size Distribution of Transported Bedload UF III

Observation of the grain size distribution of transported bedload during the stability test for Experiment UF 3-6 suggests that at the low discharges in the initial stages only finer grains were carried. The grains in the fine mode were transported during the whole duration of this experiment. Figure 6.2 shows that at time elapsed 10 and 20 minutes no grains in the coarse mode were transported. The appearance of grains in the coarse mode in transport was first noticed at time elapsed 30 minutes. However the fluid forces were not able to remove grains of diameter 8 mm. The higher fluid forces at time elapsed 40 minutes were also removed only grains with diameter 5.6 mm and 4 mm without diameter 8 mm. The dominance of the coarse mode was started at time elapsed 50 minutes and continued until 90 minutes. The fluid forces at time elapsed 100 minutes were still able to transport all grain sizes in the coarse mode whilst at time elapsed 110 and 120 minutes only grains of diameter 5.6 and 4 mm were transported.

It is apparent that during the stability test of experiment UF 3-6 the movement of grains in the coarse mode is more important than the movement of grains in the fine mode. Although the domination of grains in the coarse mode in transport lasted only 40 minutes with grains diameter 8 mm did not make a regular contribution and only started to move downstream when the fluid forces was sufficient enough, i.e. at time elapsed 50 minutes (Figure 6.2), their contribution to the total amount of bedload is considerably high. This is shown in Table 6.1 where a significant amount of the transported bedload was of grains in the coarse mode. More than 65 % of the total transported bedload is grains in the coarse mode whilst the proportion of grains in the fine mode is less than 20 %.

The grain size distribution of transported bedload during stability hydrograph of experiment UF 3-9 shown in Figure 6.3 suggests that grains in the coarse mode started to move at time elapsed 40 minutes, 10 minutes after the time in UF 3-6. Although the grains in the fine mode appeared from the early times with low flowrates, the amount is very small. At time elapsed 40 minutes only grains of diameter 4 mm were found in the coarse mode. The larger grains

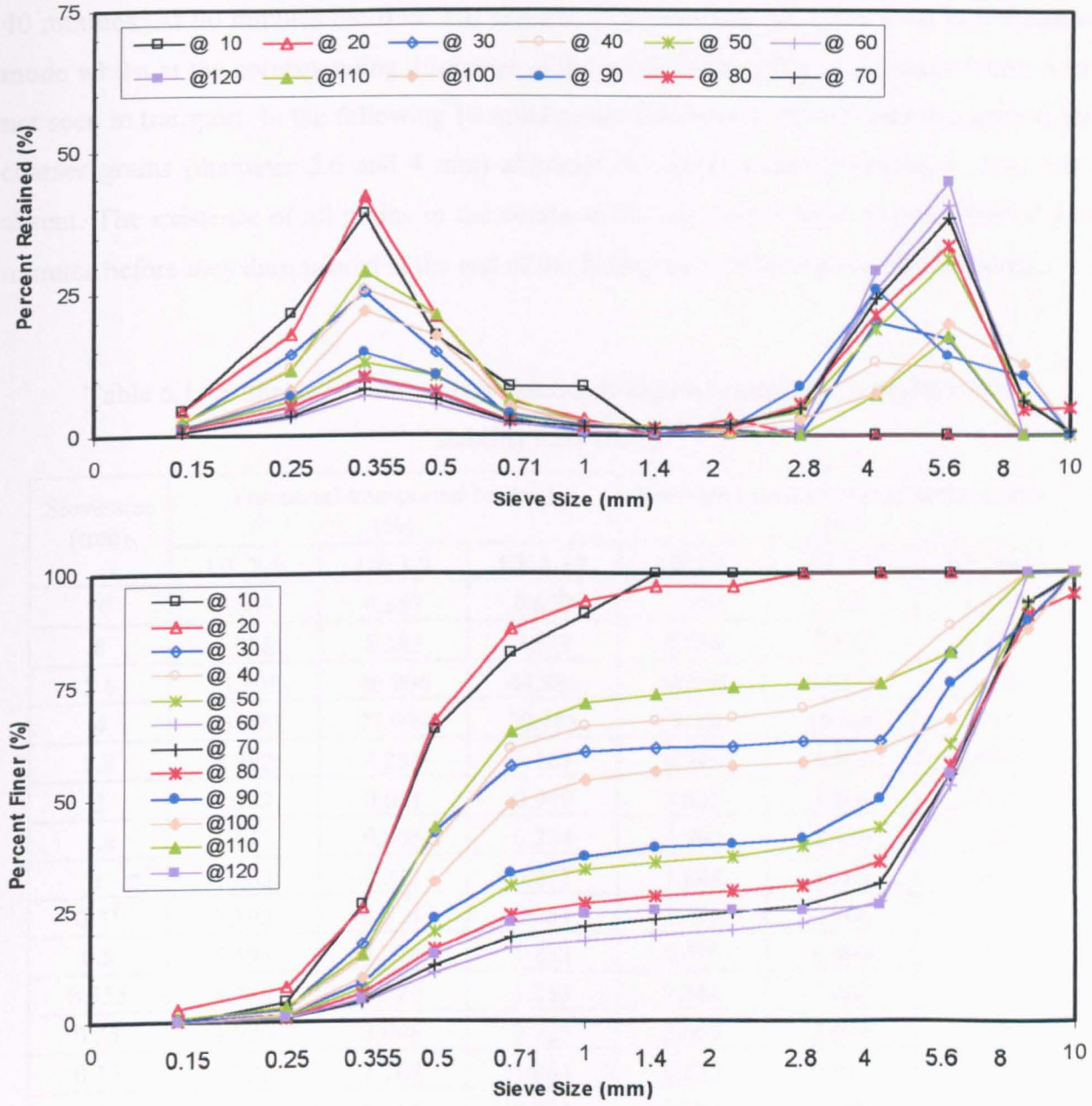

Figure 6.2. Grain size distribution of transported bedload for stability flow Experiment UF 3-6

were stable and remained so until 60 minutes. All grains in the coarse mode appeared in transport at time elapsed 60 minutes. The peak flowrates disrupted the armoured bed and transported all grain sizes in the coarse mode. The disruption caused by the peak flowrates allowed the lower fluid forces in the falling limb to remove the coarser grains. This is indicated by the appearances of all grain sizes in the coarse mode for a continuous period of

40 minutes. At 90 minutes the flow was capable of transporting all grain sizes in the coarse mode whilst at the corresponding discharge in the rising limb grains of diameter 8 mm were not seen in transport. In the following 10 minutes the flowrates were still able to transport the coarser grains (diameter 5.6 and 4 mm) although the larger grains (diameter 8 mm) were absent. The existence of all grains in the coarse mode was found again at time elapsed 110 minutes before they disappeared at the end of the falling limb (time elapsed 120 minutes).

Table 6.1. Summary of the average fractional bedload composition produced by stability tests UF III

Sieve size (mm)	Fractional transported bedload (%)			Estimated composition of surface layer (%)		
	UF 2-6	UF 3-9	UF 3-12	UF 2-6	UF 3-9	UF 3-12
10	1.005	0.857	0.879	1.760	1.741	1.746
8	5.978	8.583	7.577	8.716	8.571	8.595
5.6	37.208	46.904	44.886	34.694	34.525	34.491
4	23.997	27.994	30.188	19.495	19.506	19.424
2.8	4.782	4.259	5.163	6.949	6.892	6.891
2	1.777	0.641	0.949	3.603	3.565	3.575
1.4	1.253	0.305	0.284	2.562	2.536	2.550
1	1.463	0.311	0.277	1.864	1.868	1.877
0.71	2.392	0.521	0.851	2.676	2.706	2.712
0.5	6.695	1.774	1.833	6.775	6.900	6.925
0.355	8.735	3.520	3.253	7.264	7.462	7.485
0.25	3.920	3.048	2.725	2.608	2.699	2.699
0.15	0.721	1.168	1.064	0.933	0.932	0.931
receiver	0.074	0.114	0.072	0.100	0.099	0.099
Total	100	100	100	100	100	100

The transport at the higher discharges contained substantial amounts of grains in the coarse mode. As previously mentioned the corresponding flowrates in the rising limb and falling limb do not automatically feature similar compositions in transport. For instance, it can be seen in Figure 6.3 that the cumulative distribution curves for time elapsed 50 and 80 minutes are significantly different. Time elapsed 50 minutes indicates the dominant of grains in the fine mode whilst time elapsed 80 minutes indicates the domination of grains in the coarse mode. The plateau in both distributions is a reflections of bimodality of the bedload.

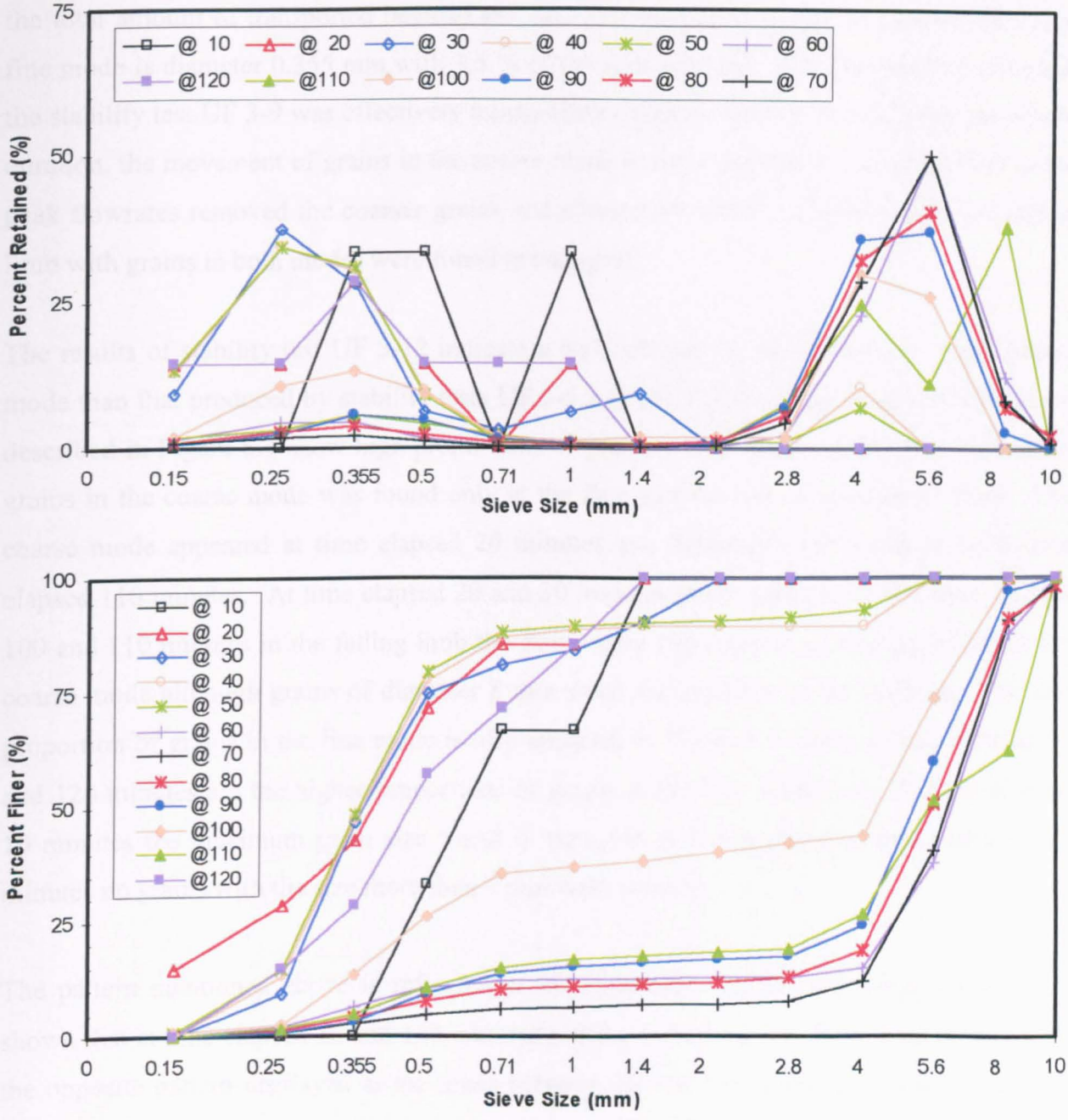

Figure 6.3. Grains size distribution of transported bedload for stability flow Experiment UF 3-9

In terms of the total amount of bedload transport, the stability flow Experiment UF 3-9 transported considerably more material in the coarse mode than in the fine mode. As shown in Table 6.1 the transported bedload consists more than 80 % of grains in the coarse mode and less than 10 % of grains in the fine mode. The grain size of 5.6 mm contributes almost half of

the total amount of transported bedload (47 %). The most popular grains transported in the fine mode is diameter 0.355 mm with 3.5 % of the total bedload. This suggests that although the stability test UF 3-9 was effectively transporting grains in the fine mode during the whole duration, the movement of grains in the coarse mode is more important. The disruption at the peak flowrates removed the coarser grains and change the pattern of transport in the falling limb with grains in both modes were found in transport.

The results of stability test UF 3-12 indicate a different pattern of domination of the coarse mode than that produced by stability tests UF 3-6 and UF 3-9. It is very clear that the curves described in Figure 6.4 show high proportions of grains in the coarse mode. The absence of grains in the coarse mode was found only at the first and the last 10 minutes of flow. The coarse mode appeared at time elapsed 20 minutes and dominated the transport until time elapsed 110 minutes. At time elapsed 20 and 30 minutes in the rising limb and time elapsed 100 and 110 minutes in the falling limb the flows were still capable of moving grains in the coarse mode although grains of diameter 8 mm were not available in the bedload. The low proportion of grains in the fine mode is also apparent in Figure 6.4. Only at time elapsed 10 and 120 minutes are the higher proportions of grains in the fine mode seen. At time elapsed 10 minutes the maximum grain size found in transport is 2 mm whilst at time elapsed 120 minutes no grains with the size more than 1 mm were moving.

The pattern mentioned above is reflected in the cumulative grain distribution curves. It is shown that at time elapsed 10 and 120 minutes a sharp increase in the finer sizes is seen with the opposite pattern displayed at the times between 20 and 110 minutes. Again the relative paucity of grains in the range from 0.71 to 2.8 mm are indicated by the plateau in the size distribution curve reflecting the bimodality of the bedload. The importance of coarse mode during stability test UF 3-12 has clearly been shown in Table 6.1. More than 82 % of the total transported bedload contains grains in the coarse mode (diameter 4 mm, 5.6 mm and 8 mm) in comparison to less than 8 % contribution of grains in the fine mode (0.25 mm, 0.355 mm and 0.5 mm).

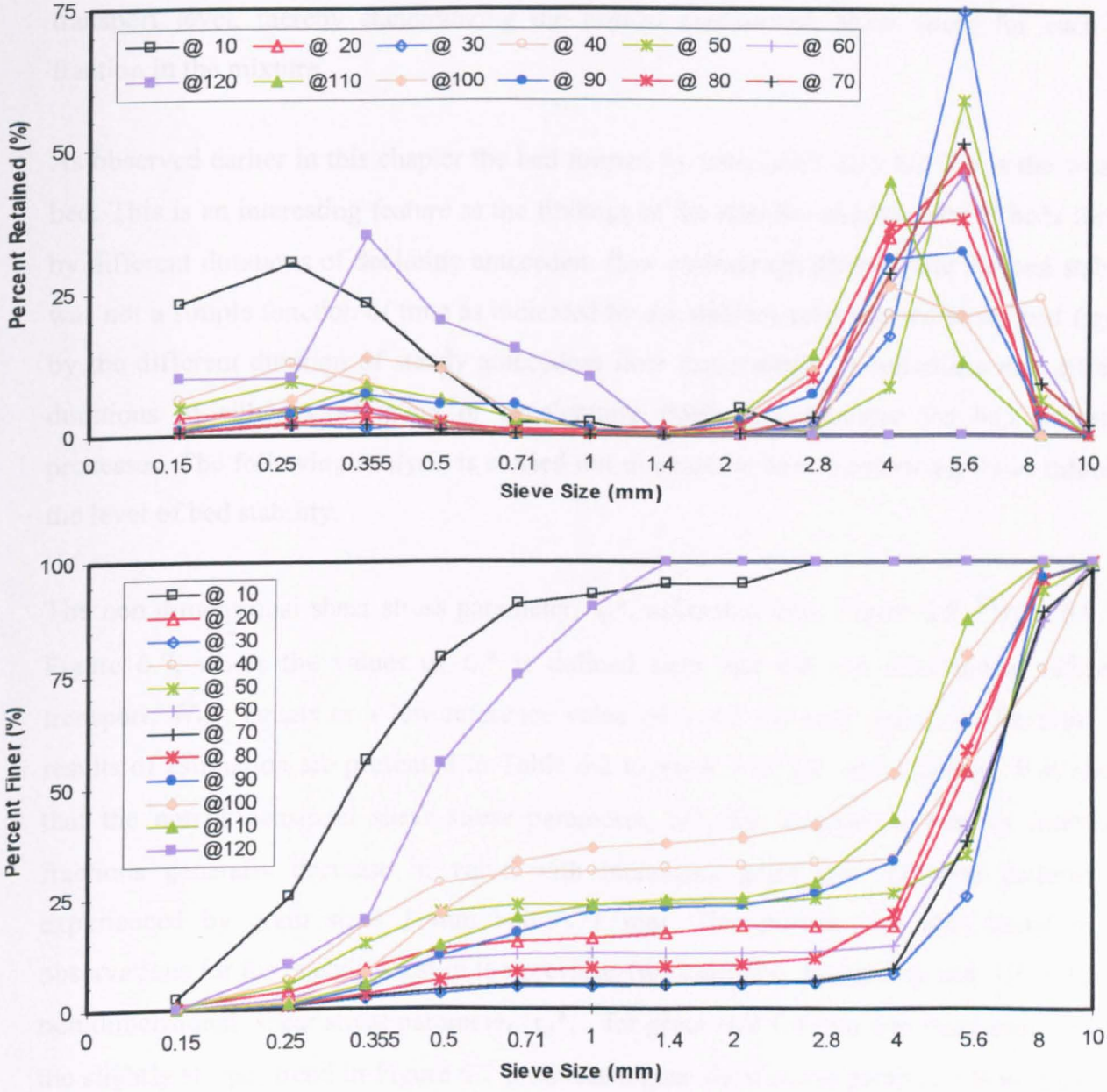

Figure 6.4. Grain size distribution of transported bedload for stability flow Experiment UF 3-12

6.2.3. Fractional Threshold of Motion UF III

Similar to the observations in the previous two chapters the threshold of motion for individual grain size fraction for each stability test was examined using the reference transport method. This method has been used in several previous studies (e.g. Parker et al, 1982 ; Wilcock and Southard, 1988 ; Kuhnle, 1993a ; Wilcock and McArdell, 1993 ; Shvidchenko et al, 2001) as it relies upon the extrapolation of gathered sediment transport measurement to a low reference

transport level, thereby standardizing the critical entrainment shear stress for each size fraction in the mixture.

As observed earlier in this chapter the bed formed by antecedent flow UF 3-6 is the weakest bed. This is an interesting feature as the findings of the stability observations of beds formed by different durations of declining antecedent flow hydrograph showed that the bed stability was not a simple function of time as indicated by the stability tests applied to the bed formed by the different duration of steady antecedent flow experiments. It underlines that different durations of either accelerating or decelerating flows can influence the bed armouring processes. The following analysis is carried out to examine how accelerating flows influence the level of bed stability.

The non dimensional shear stress parameter, τ_{ri}^*, estimated from Figure 6.5, Figure 6.6 and Figure 6.7, where the values of τ_{ri}^* is defined such that the non dimensional reference transport, W_{ri}^*, equals to a low reference value of 0.002 for each grain size fraction. The results of estimation are presented in Table 6.2 together with the error bounds. It is shown that the non dimensional shear stress parameter, τ_{ri}^*, for incipient motion of individual fractions generally decrease in value with increasing grain size. Diferent patterns are experienced by grain sizes 1 mm and 0.71 mm. This pattern was also found in the observations for the stability test in the previous two chapters. In stability test UF 3-12 the non dimensional shear stress parameter, τ_{ri}^*, for grain size 1.4 mm was more scattered and the slightly steeper trend in Figure 6.7 produces higher shear stress parameter than grain size 1.0 mm. This inconsistency is thought to be due to their low availability in the mixtures. As these grains have no significance influence on transport, further analyses are focused on the more popular grains in the fine and coarse mode.

It can be seen in Table 6.2 that the shear stress parameters for stability test UF 3-6 are the lowest in comparison to those for stability test UF 3-9 and UF 3-12. It is also shown that the values of shear stress parameter of individual grain size fraction are generally very similar in each stability test in particular tests UF 3-9 and UF 3-12. In all stability tests the non dimensional shear stress parameter, τ_{ri}^*, of grains of diameter 10 mm are not available as these grains were not transported in all the observed time elapsed.

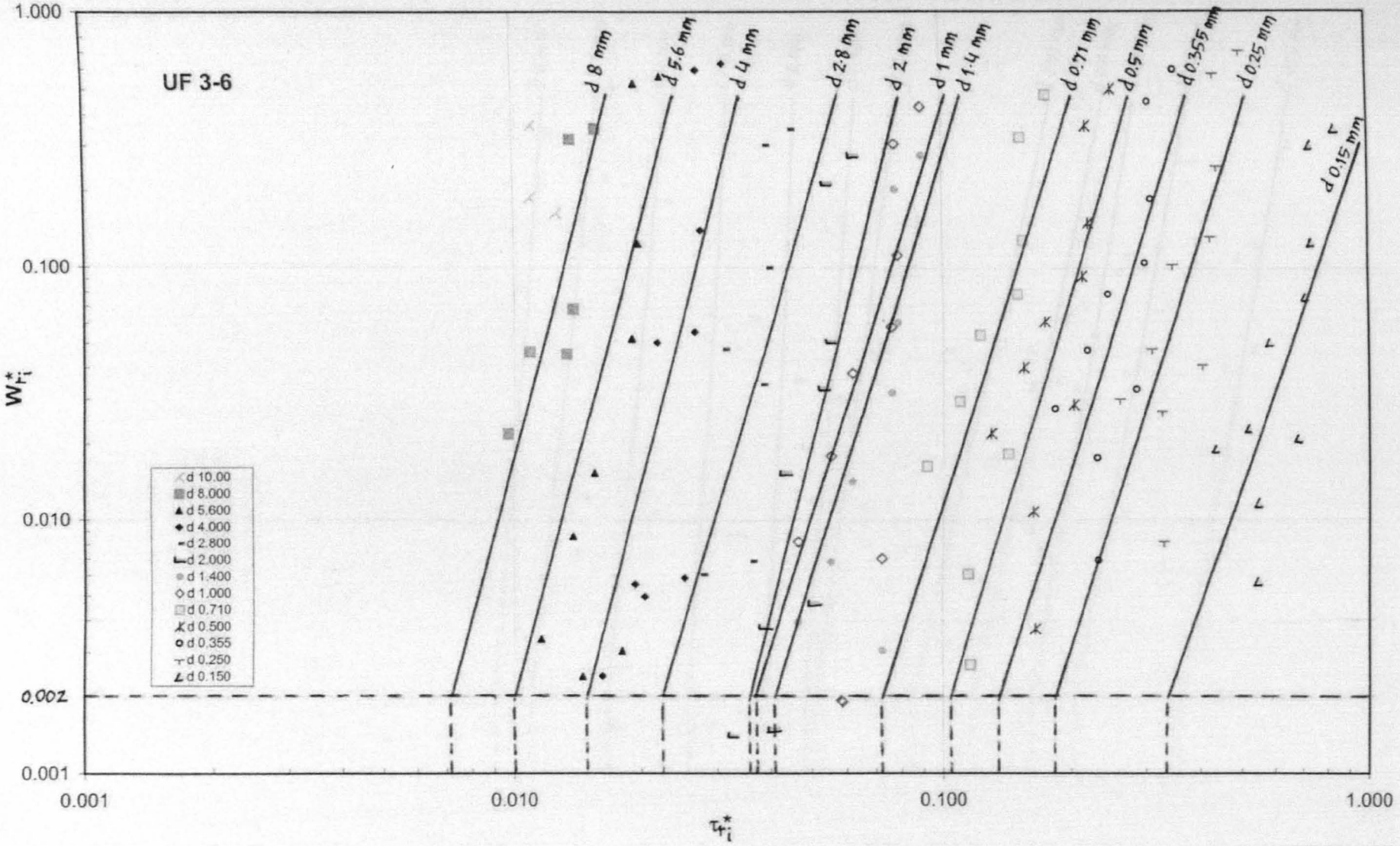

Figure 6.5. The non dimensional shear stress parameter, τ_{ri}*, determined from the low reference transport rate, W_{ri}* = 0.002, for stability test UF 3-6

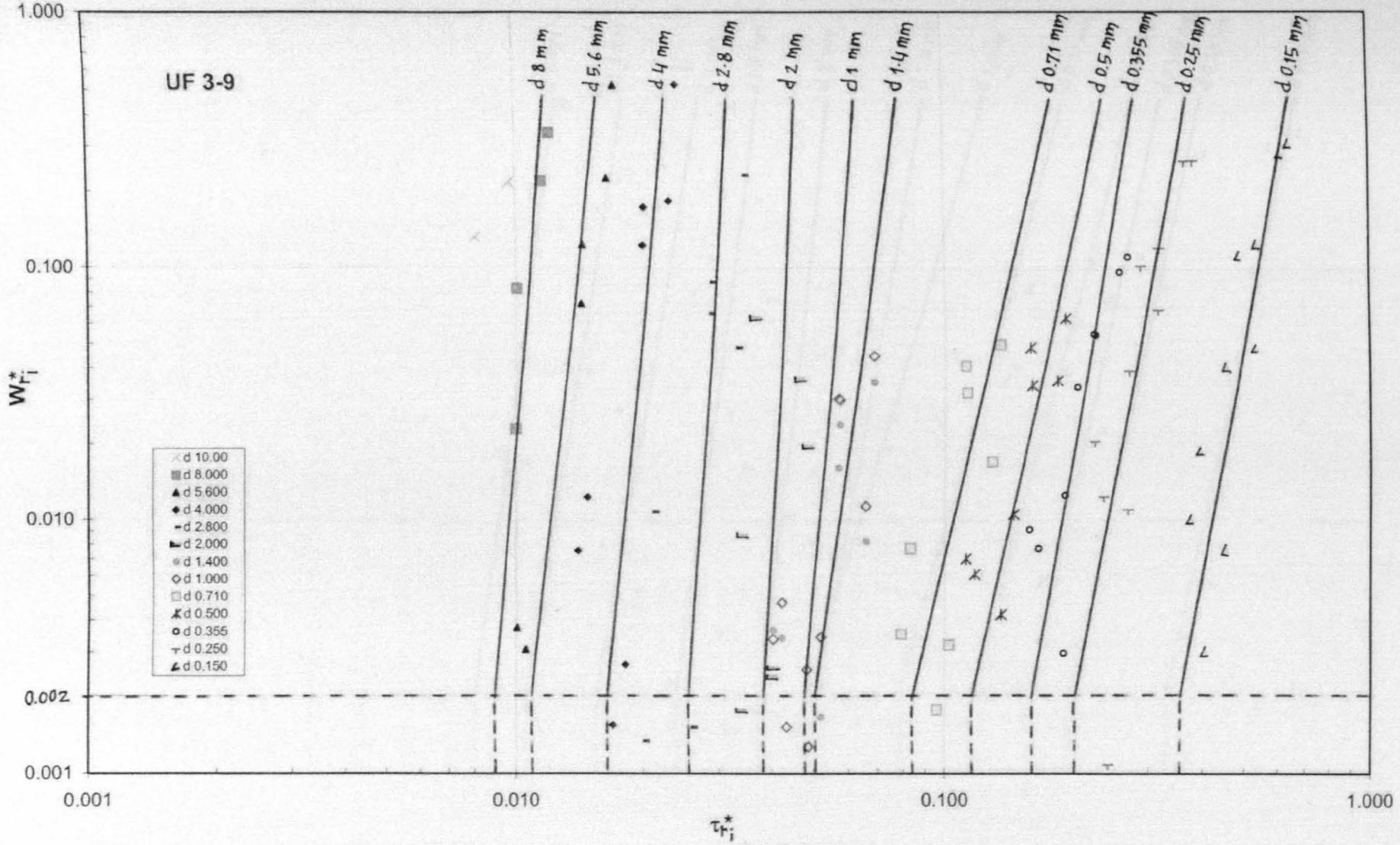

Figure 6.6. The non dimensional shear stress parameter, τ_{ri}^*, determined from the low reference transport rate, $W_{ri}^* = 0.002$, for stability test UF 3-9

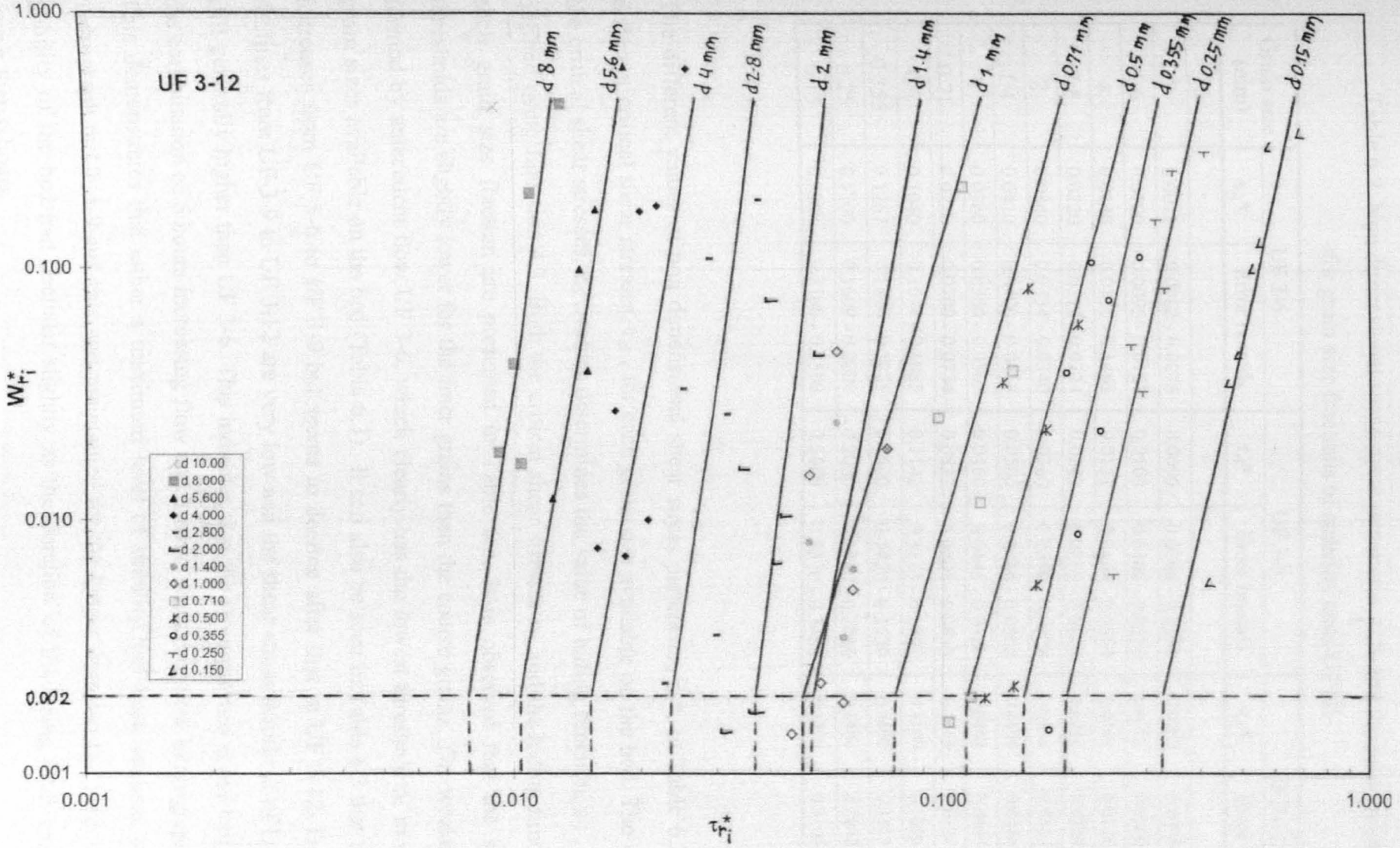

Figure 6.7. The non dimensional shear stress parameter, τ_{ri}^*, determined from the low reference transport rate, $W_{ri}^* = 0.002$, for stability test UF 3-12

Table 6.2. Non dimensional shear stress parameter, τ_{ri}*, and the error bounds for grain size fractions of stability tests UF III

Grain size (mm)	UF 3-6		UF 3-9		UF 3-12	
	τ_{ri}*	Error bounds	τ_{ri}*	Error bounds	τ_{ri}*	Error bounds
10	-	-	-	-	-	-
8	0.0071	0.0062 - 0.0076	0.0090	0.0084 - 0.0091	0.0080	0.0075 - 0.0082
5.6	0.0100	0.0095 - 0.0107	0.0109	0.0106 - 0.0110	0.0103	0.0100 - 0.0107
4	0.0140	0.0136 - 0.1463	0.0151	0.0144 - 0.0160	0.0141	0.0136 - 0.0144
2.8	0.0220	0.0214 - 0.0224	0.0240	0.0233 - 0.0240	0.0224	0.0220 - 0.0232
2	0.0340	0.0334 - 0.0340	0.0360	0.0350 - 0.0370	0.0350	0.0340 - 0.0371
1.4	0.0410	0.0400 - 0.0418	0.0500	0.0484 - 0.0500	0.0490	0.0484 - 0.0515
1	0.0360	0.0360 - 0.0363	0.0460	0.0445 - 0.0460	0.0463	0.0445 - 0.0463
0.71	0.0720	0.0700 - 0.0734	0.0822	0.0808 - 0.0853	0.0745	0.0734 - 0.0817
0.5	0.1040	0.1014 - 0.1085	0.1142	0.1113 - 0.1207	0.1100	0.1099 - 0.1200
0.355	0.1267	0.1226 - 0.1275	0.1500	0.1426 - 0.1530	0.1400	0.1355 - 0.1500
0.25	0.1700	0.1609 - 0.2000	0.2000	0.1926 - 0.2010	0.1900	0.1800 - 0.2049
0.15	0.3200	0.3100 - 0.3500	0.3400	0.3370 - 0.3430	0.3200	0.3100 - 0.3400

The different values of non dimensional shear stress parameter, τ_{ri}*, in Table 6.2 produced different critical shear stresses, τ_{ci} , for each grain size available on the bed. The variation in the critical shear stresses, τ_{ci} , values determines the value of hiding function, ε_{is} , which was defined using Equation 4.3. Both the critical shear stresses τ_{ci} and the hiding function ε_{is} for each grain size fraction are presented in Table 6.3. It is observed that the shear stress thresholds are slightly lower for the finer grains than the coarse grains. The weakest bed was formed by antecedent flow UF 3-6, which clearly has the lowest threshold of motion for all grain sizes available on the bed (Table 6.3). It can also be seen in Table 6.3 that the stability increases from UF 3-6 to UF 3-9 but seems to decline after that in UF 3-12. However the declines from UF 3-9 to UF 3-12 are very low and the shear stress threshold of UF 3-12 was still generally higher than UF 3-6. This indicates that the strongest bed is the bed formed by the combination of 6 hours increasing flow and 3 hours declining flow hydrograph (UF 3-9). This demonstrates that either a maximum level of stability had been attained by the flow hydrograph in UF 3-9 and this was maintained for the longer duration UF 3-12, or that the stability of the bed had declined slightly as the duration of the rising limb was extended longer than 6 hours.

Table 6.3. Critical shear stress, τ_{ci} , and hiding function values, ε_{is} , for grain size fractions in stability tests UF III

Grain size (mm)	UF 3-6		UF 3-9		UF 3-12	
	τ_{ci} (N/m^2)	ε_{is}	τ_{ci} (N/m^2)	ε_{is}	τ_{ci} (N/m^2)	ε_{is}
10	-	-	-	-	-	-
8	0.919	0.127	1.140	0.157	1.036	0.143
5.6	0.906	0.179	0.988	0.195	0.934	0.184
4	0.906	0.250	0.978	0.270	0.913	0.252
2.8	0.997	0.393	1.088	0.429	1.015	0.400
2	1.101	0.607	1.165	0.643	1.133	0.625
1.4	0.929	0.732	1.133	0.893	1.110	0.875
1	0.583	0.643	0.745	0.821	0.749	0.827
0.71	0.827	1.286	0.942	1.464	0.856	1.330
0.5	0.842	1.857	0.924	2.039	0.890	1.964
0.355	0.728	2.263	0.862	2.679	0.804	2.500
0.25	0.688	3.036	0.809	3.571	0.769	3.393
0.15	0.777	5.714	0.826	6.071	0.777	5.714

The grains in the fine mode for all stability tests have a relatively similar stability. It can be seen in Figure 6.8 that the grains of sizes less than 0.71 mm have a very close shear stress threshold. The difference in the shear stress thresholds increased for the larger grains where the most stable grains found in the stability test UF 3-9.

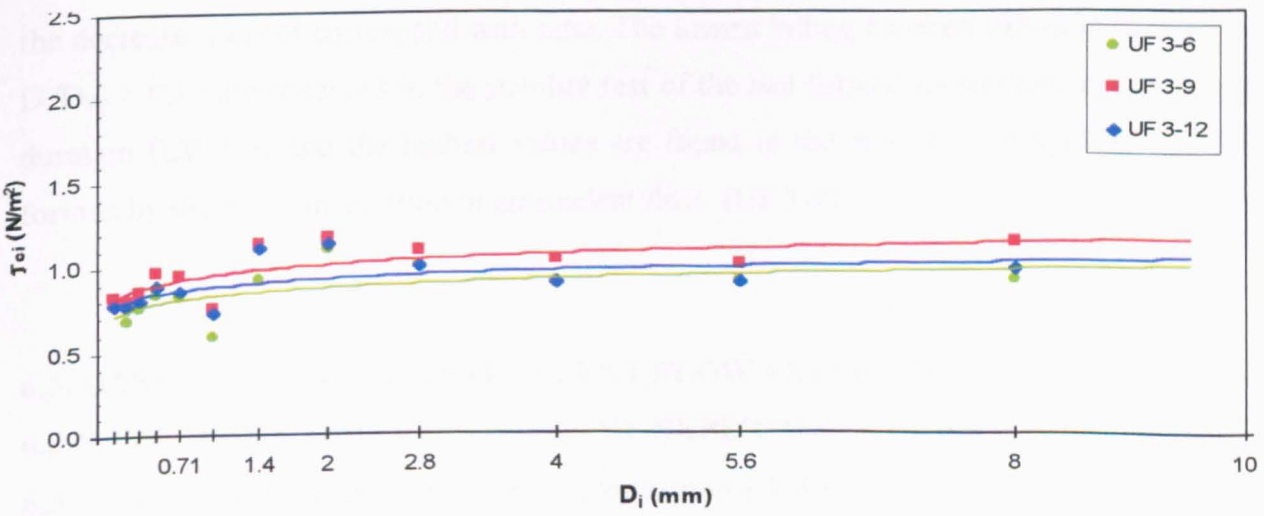

Figure 6.8. The critical shear stress, τ_{ci} , for grain size fractions in terms of D_i for the stability tests UF III

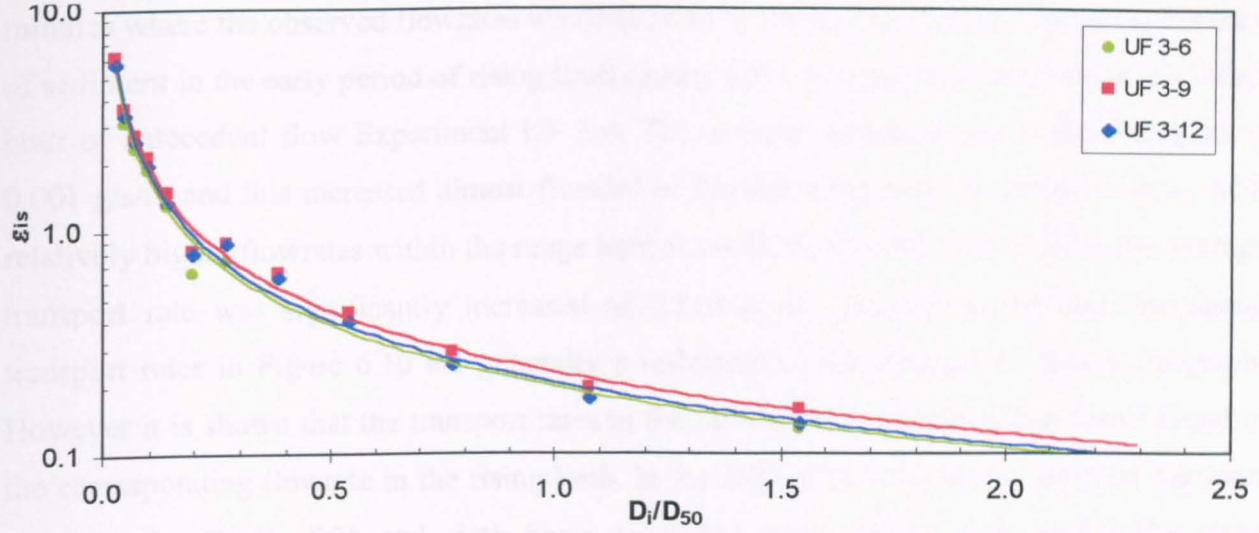

Figure 6.9. Hiding function, ε_{is} , derived from fractional threshold conditions for stability tests UF III

In Figure 6.9 the size ratio of each grain size fraction (D_i/D_{50}) was used to observed the hiding function. As applied by Wilcock and Southard (1988), the size ratio of the fraction is one of variables used to describe the relative grain size, which has a central role in mixed size sediment transport because of the size of each grain relative to others in the mixture controls the variation from fraction to fraction of both the value of bed shear stress acting on individual grains and the resistance of those grains to movement. It can be seen in Figure 6.9 that the hiding functions in the region $D_i/D_{50} < 0.15$ are similar for stability tests UF 3-6, UF 3-9 and UF 3-12. The hiding function value reduces in the region of $D_i/D_{50} > 0.15$. However the decrease was not correspond with time. The lowest hiding function values in the region of $D_i/D_{50} > 0.15$ are observed in the stability test of the bed formed by shortest antecedent flow duration (UF 3-6) and the highest values are found in the stability test applied to the bed formed by the medium duration of antecedent flow (UF 3-9).

6.3. OBSERVATIONS OF ANTECEDENT FLOW EXPERIMENTS

6.3.1. UNSTEADY ANTECEDENT FLOW EXPERIMENT UF 3-6

6.3.1.1. Bedload Transport Rate and Composition UF 3-6

The accelerating flow in antecedent flow experiment UF 3-6 transported no material in the first 20 minutes. The appearances of sediment in transport were started at time elapsed 30

minutes where the observed flowrates was 0.0056 m^3/s. As shown in Figure 6.10 the absence of sediment in the early period of rising limb caused a low average transport rate in the initial hour of antecedent flow Experiment UF 3-6. The average transport rate in the first hour is 0.001 g/s/m and this increased almost fivefold in the following hour. In the third hour, with relatively higher flowrates within the range between 0.0225 m^3/s and 0.0338 m^3/s, the average transport rate was significantly increased to 0.219 g/s/m. The increasing and decreasing transport rates in Figure 6.10 are generally a reflection of the changes in flow hydrograph. However it is shown that the transport rates in the falling limb are higher than those found in the corresponding flowrate in the rising limb. In the falling limb the hourly average transport rates for the fourth, fifth and sixth hours are 0.313 g/s/m, 0.031 g/s/m and 0.028 g/s/m respectively. Overall the transport rate during the rising limb of antecedent flow experiment UF 3-6 is 0.075 g/s/m and increased in the falling limb to 0.124 g/s/m.

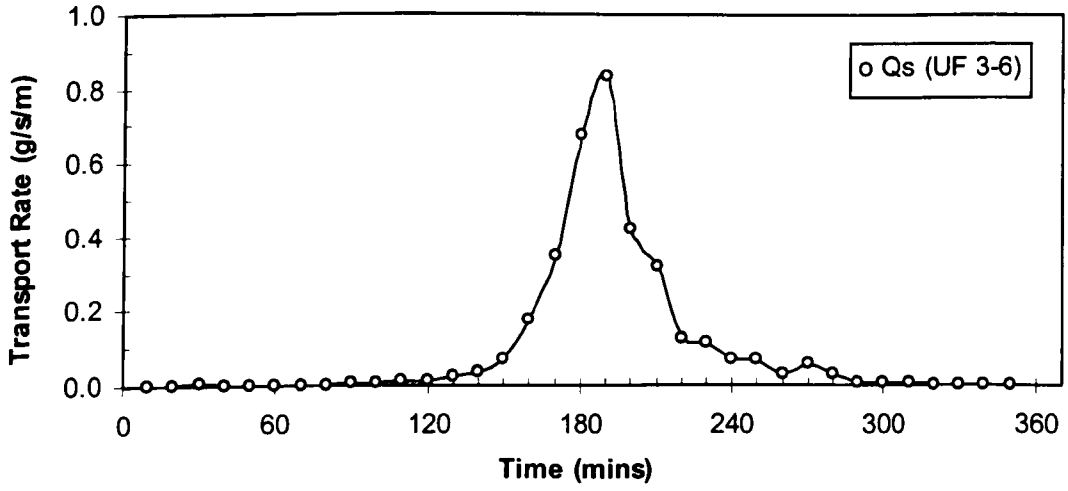

Figure 6.10. Time variation of transport rate for antecedent flow Experiment UF 3-6

The composition of the transported bedload observed during the antecedent flow UF 3-6 was dominated by grains in the fine mode. As can be seen from Figure 6.11, from the start to the time elapsed 160 minutes of observation, grains in the fine mode were transported more than grains in the coarse mode. It is noted that grains in the coarse mode did not appear in transport until time elapsed 110 minutes. In the following time elapsed (between 120 to 160 minutes) the amount of grains in the fine mode increased but proportionally decreased because of the

existence of coarse grains in transport. It was during the latter stage of rising limb and in the initial stage of falling limb when the transport were dominated by grains in the coarse mode (time elapsed 170 to 210 minutes). This means that the removal of considerable amounts of grains in the coarse mode only occurred for a relatively short period around the peak flowrate. In this case the coarse mode domination only occurred when the discharge was at least 0.0300 m^3/s. It is found that the amount of grains in the coarse mode was higher in the corresponding flowrates of the falling limb. This increase in amount was coupled with an increase in the proportion of grains in the coarse mode, which resulted in the contribution of grains in the fine mode being significantly less than at the corresponding flowrates in the rising limb.

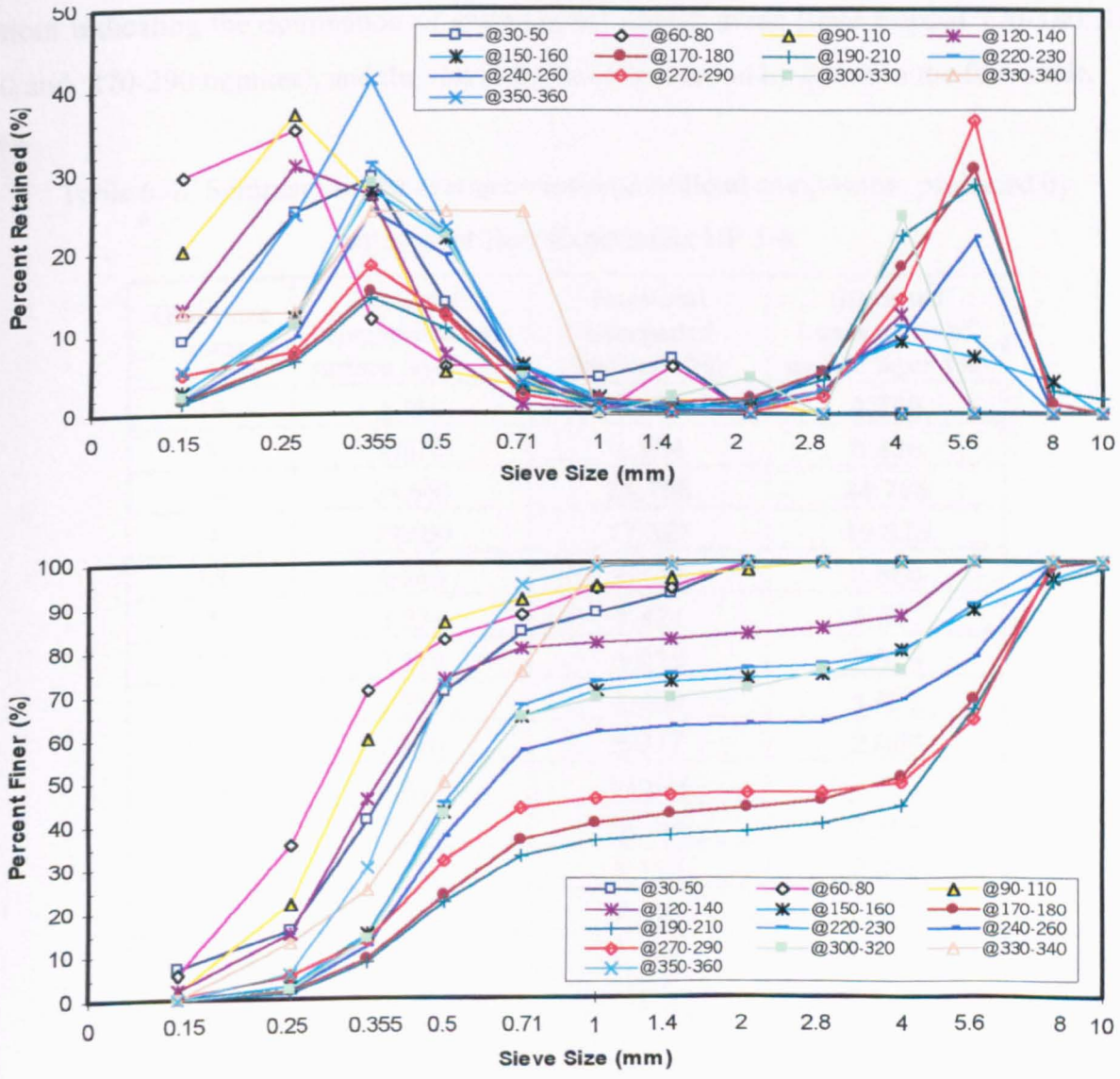

Figure 6.11. Grain size distribution of transported bedload for antecedent flow Experiment UF 3-6

The domination of grains in the fine mode in transport started again at time elapsed 220 minutes and then continued for the rest of the falling limb except at time elapsed 270-290 minutes where slightly more than half of transport contains grains in the coarse mode. This is suspected to be caused by the increasing exposure of the coarse grains as grains in the fine mode were continually transported. The loss of finer grains around the coarser grains increased the instability of larger grains so that the relatively low fluid forces were still able to transport them. The appearance of grains in the coarse mode continued in the following half-hour with a lower proportion and then diminished in the last 20 minutes of falling limb. The period or time elapsed with the domination of grains either in the fine or coarse mode in the transport can also be seen in the cumulative distribution curves where the three curves in the bottom indicating the domination of grains in the coarse mode (time elapsed 170-180, 190-210 and 270-290 minutes), and the rest indicate a domination by grains in the fine mode.

Table 6.4. Summary of the average fractional bedload composition produced by antecedent flow Experiment UF 3-6

Grain size (mm)	Original composition of surface layer (%)	Fractional transported bedload (%)	Estimated composition of surface layer (%)
10	1.730	0.851	1.739
8	8.570	1.834	8.638
5.6	34.660	24.168	34.766
4	19.600	17.327	19.623
2.8	6.860	4.128	6.888
2	3.530	1.431	3.551
1.4	2.510	1.018	2.525
1	1.850	1.609	1.852
0.71	2.680	3.877	2.668
0.5	6.840	13.548	6.772
0.355	7.420	18.683	7.306
0.25	2.710	9.139	2.645
0.15	0.940	2.191	0.927
receiver	0.100	0.197	0.099
Total	100	100	100

Overall considering the whole test, the proportion of grains in the fine mode is slightly less than the proportion of grains in the coarse mode. In Table 6.4 the proportion of the fine mode

is 41 % whilst the proportion of the coarse mode is 43 %. Although the domination of the coarse mode in transport was limited to 80 minutes, the amount transported during this period was considerable. This removal assumed to be caused by the assumption that the continuous transport of grains in the fine mode increased the level of exposure of grains in the coarse mode. The increase in the fluid forces at the higher flowrates coupled with the increased exposure and of larger grains resulted in the high amount of grains in the coarse mode being transported at this particular stage of hydrograph. It can be seen in Table 6.4 that the bed surface slightly coarsened after the antecedent flow.

6.3.1.2. Bursting Events and Flow Momentum UF 3-6

During antecedent flow Experiment UF 3-6 only the measurement of average nearbed streamwise velocity at the central point of measurement area was carried out. There was no flow velocity observation at different grid points because of the continuous changes in the flowrates where no section in the hydrograph contained a constant discharge. The results of observations of the average nearbed streamwise velocity are displayed in Figure 6.12. It can be seen that the average values of nearbed streamwise velocity were generally increased in line with the flowrates. It is also shown that although the average bed shear stress at time elapsed 180 and 210 minutes are noticeably smaller, the values generally increased with the increasing flowrates. This is indicated by the pattern of the average bed shear stress, which follow the shape of hydrograph to some extent (Figure 6.12).

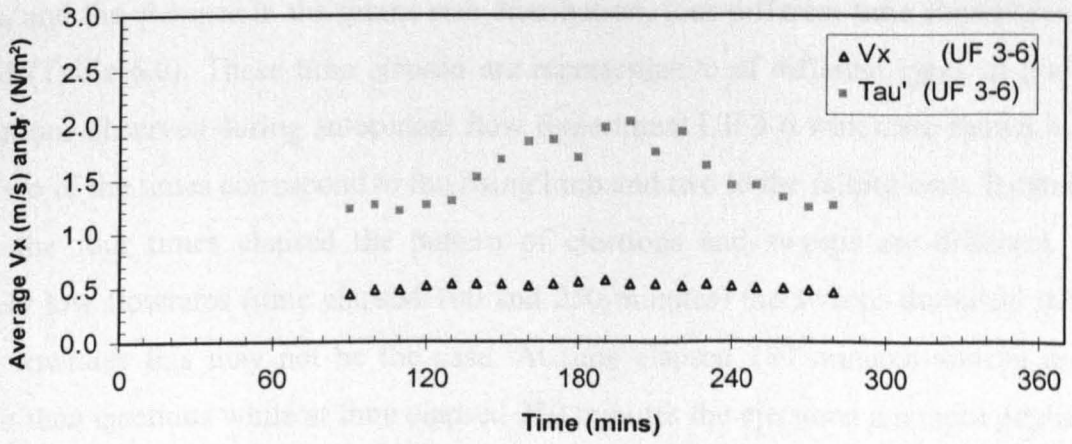

Figure 6.12. Variation of time averaged nearbed streamwise velocity and bed shear stress during antecedent flow of Experiment UF 3-6

The observation of the mean flow variables, average nearbed streamwise velocity and bed shear stress indicated a dependence with flowrate. More careful observations were made of the turbulence to examine more subtle links with the movement of the bedload. The bursting events in antecedent flow experiment UF 3-6 suggests that overall the occurrence of sweeps is higher than ejections. In the rising limb where the flowrates increased in a relatively short period, the proportion of ejections is less than the proportion in the falling limb. This is reflected in that the frequency of occurrence of ejections in the rising limb is higher than the frequency in the falling limb. However the average duration of both events either in the rising limb or in the falling limb are similar. This suggest that in the antecedent flow Experiment UF 3-6 the duration of upward and downward-looking bed interactions were not affected by the type of flow hydrograph. The accelerating and decelerating flowrates section produced events with identical duration.

Table 6.5. Time frequency and the proportion of occurrences of bursting events in antecedent flow Experiment UF 3-6

Parameter descriptions		Frequency (Hz)	Proportion (%)	Average duration (sec.)
Rising limb	Ejections	1.049	48.596	0.052
	Sweeps	1.110	51.404	0.054
Falling limb	Ejections	0.999	49.019	0.052
	Sweeps	1.039	50.981	0.053

In order to observe the relationships between the magnitude of momentum of ejections and sweeps, and the changes in the grains size distribution, four different time elapsed have been selected (Table 6.6). These time elapsed are representative of different types of grains size distributions observed during antecedent flow Experiment UF 3-6 which are shown in Figure 6.11. Two of the times correspond to the rising limb and two to the falling limb. It can be seen that in the four times elapsed the pattern of ejections and sweeps are different. At the relatively low flowrates (time elapsed 100 and 250 minutes) the sweeps dominate but at the higher flowrates this may not be the case. At time elapsed 180 minutes sweeps are more frequent than ejections while at time elapsed 220 minutes the ejections are more popular than sweeps. It is also observed that the average duration of both events are generally similar. Again no coincidence between the average duration and the level of flowrates are observed.

However the summary in Table 6.6 is not sufficient to describe the influence of ejections and sweeps to the grains size distribution as the magnitude of momentum produced in the bursting events are not known. Therefore further investigation on the probability of momentum per unit area is carried out.

Table 6.6. Summary of bursting events at selected time elapsed in antecedent flow Experiment UF 3-6

Parameter descriptions	Time elapsed (minutes)			
	100	180	220	250
Threshold values (m^2/s^2)	0.0059	0.0078	0.0072	0.0062
Number of ejections	203	207	211	188
Number of sweeps	243	218	200	225
Frequency of ejections (Hz)	1.015	1.035	1.055	0.940
Frequency of sweeps (Hz)	1.215	1.090	1.000	1.125
Average duration of ejection (s)	0.051	0.053	0.051	0.053
Average duration of sweeps (s)	0.052	0.053	0.057	0.052

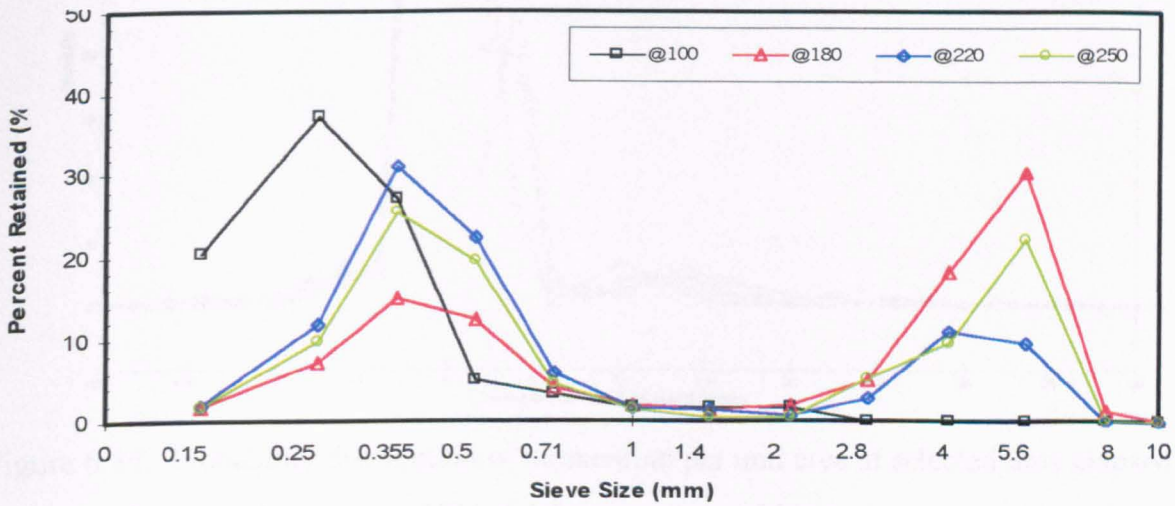

Figure 6.13. Grain size distribution of transported bedload at selected time elapsed in antecedent flow Experiment UF 3-6

The pattern found in the previous investigations of different antecedent flow experiments was that the high momentum of upward interactions (ejections) is the controlling factor in transporting coarser grains. This pattern was also found in this analysis. The absence of grains in the coarse mode in transport at time elapsed 100 minutes can be explained by examining the probability distribution of momentum per unit area presented in Figure 6.14. It is believed

that only momentum with the magnitude higher than 13 kg/ms was able to transport grains in the coarse mode. At time elapsed 100 minutes there were practically no ejections with momentum above this level and so the flow bursting events were sufficient enough to transport larger grains. As compensation, a high proportion of grains in the fine mode existed at this time elapsed (see Figure 6.13). Meanwhile at time elapsed 180 minutes a higher proportion of ejections with momentum magnitude between 13 and 15 kg/ms is noticed (Figure 6.14). It was observed that the grains in the coarse mode dominated the transport at

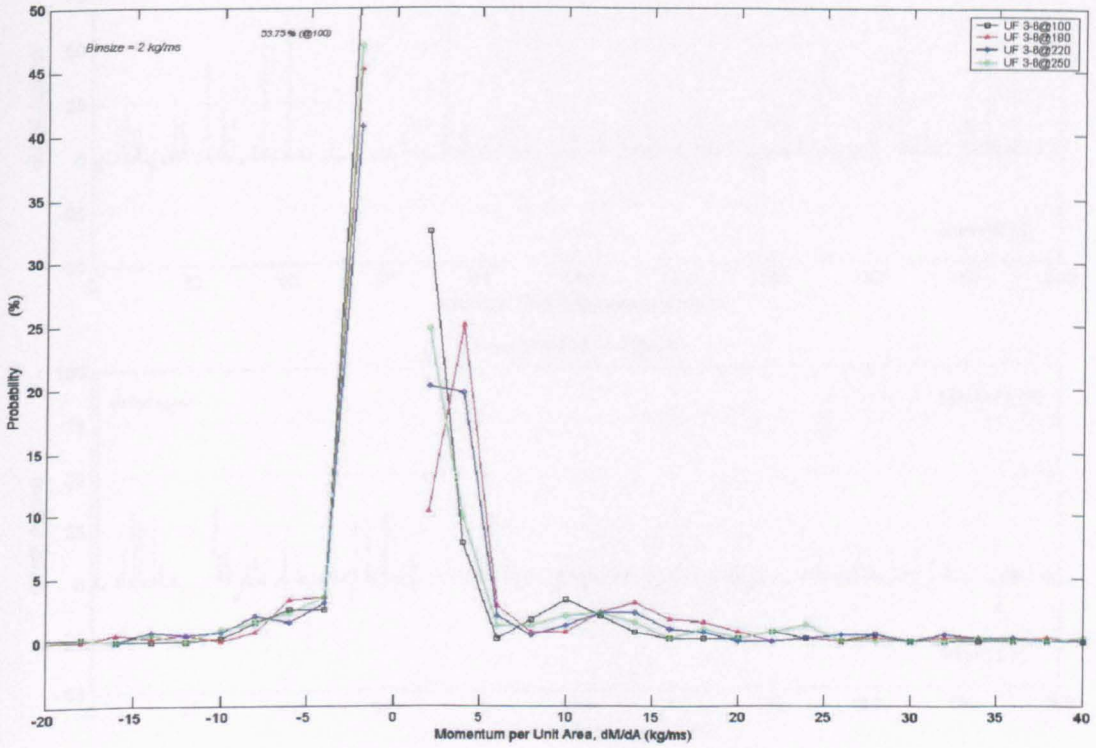

Figure 6.14. Probability distribution of momentum per unit area at selected time elapsed in antecedent flow Experiment UF 3-6 (ejections are positive and sweeps are negative)

this time elapsed. It is believed that this large transport of coarse grains was due to the occurrence of ejections with a momentum magnitude of 13 kg/ms or larger. The existence of momentum with similar magnitude but with lower proportion at time elapsed 220 and 250 minutes transported grains in the coarse mode but at the lower proportion and amount than at time elapsed 180 minutes. An interesting aspect of this plot is that the very high momentum

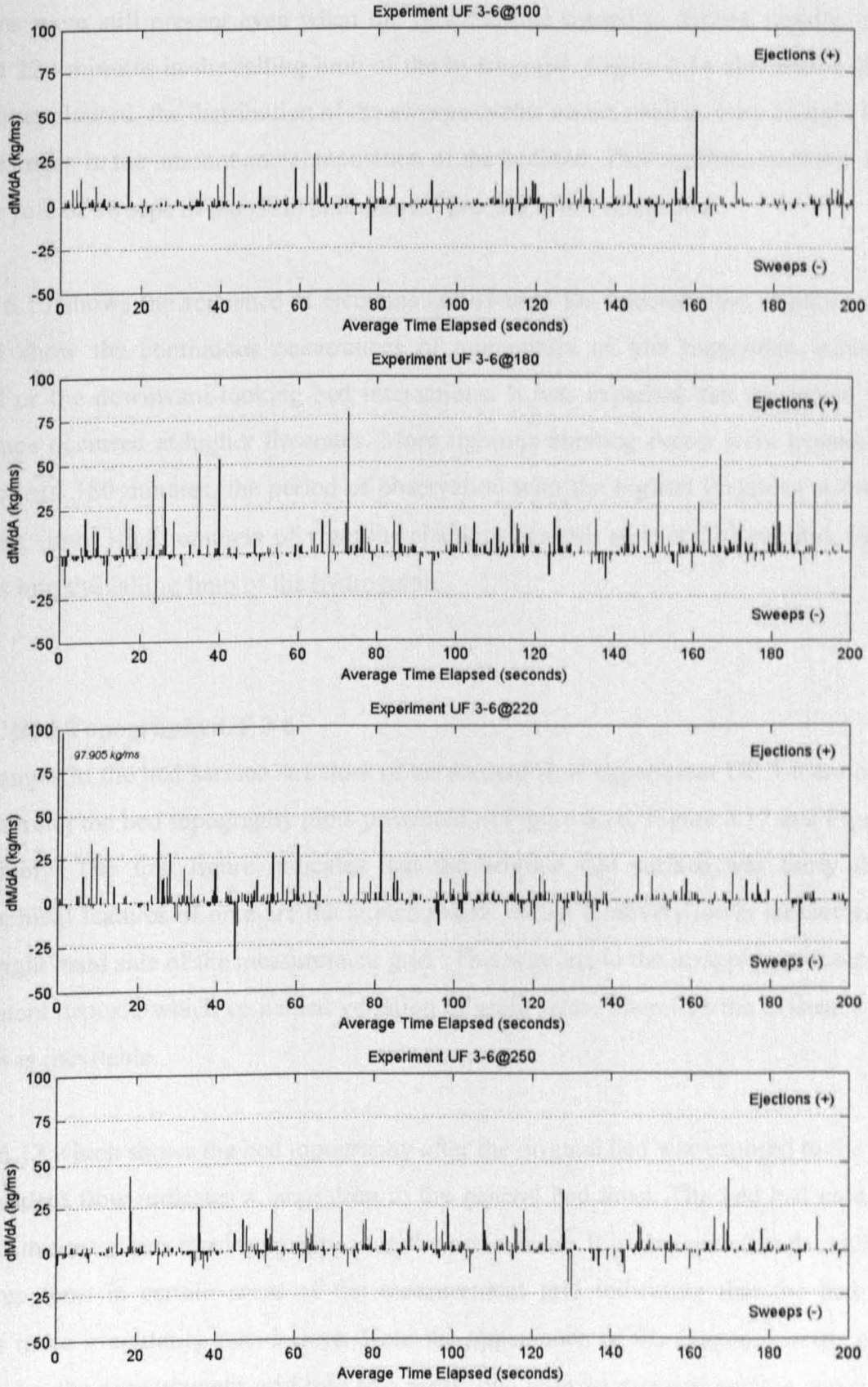

Figure 6.15. The sequence of momentum per unit area and its magnitude at selected time elapsed in antecedent flow Experiment UF 3-6

ejections were still present even when the flowrate had started to decline rapidly, e.g. time elapsed 220 minutes in the falling limb of the hydrograph. Figure 6.14 also shows that at all of the time elapsed, the distribution of the sweeps events seems similar, even thought there are large changes in the amount and composition of the bedload. This confirms previous thoughts that the role of sweeps in the grain entrainment process is not substantial.

Figure 6.15 shows the sequence of ejections and sweeps for selected time elapsed. All time elapsed show the continuous occurrences of momentum of low magnitude either in the upward or the downward-looking bed interactions. It was expected that the higher level of turbulence occurred at higher flowrates. More rigorous bursting events were experienced by time elapsed 180 minutes, the period of observation with the highest flowrates at the end of the rising limb. High numbers of vigorous ejections are still seen at 220 minutes, that is 40 minutes into the falling limb of the hydrograph.

6.3.1.3. Bed Topography UF 3-6

The changes in the bed surface structure of antecedent flow experiment UF 3-6 are observed by examining the bed topography plots presented in Figure 6.16, Figure 6.17 and Figure 6.18 respectively. The first figure indicates that the original bed surface was fairly flat. The topographical features of note are the stretch marks with a relatively lower surface elevation on the right hand side of the measurement grid. This was due to the scrapping process applied to sediment deposit, which contained variation of grain sizes. Therefore the existence of such marks was inevitable.

Figure 6.17 which shows the bed topography after the original bed was exposed to the 6 hours of antecedent flow indicates a large drop in the general bed level. The bed had eroded with some prominent grains starting to appear on the bed surface. It is also seen that the valley-type structures form in certain areas of the measurement grid indicating that the bed surface exhibits more irregularity than before. Note the appearance of the diagonal linear structure that divides the measurement grid into two areas, one with an exposed surface and the other with a generally lower level of bed surface. Having observed that the proportion of grains in the both modes transported during antecedent flow experiment UF 3-6 was almost in balance

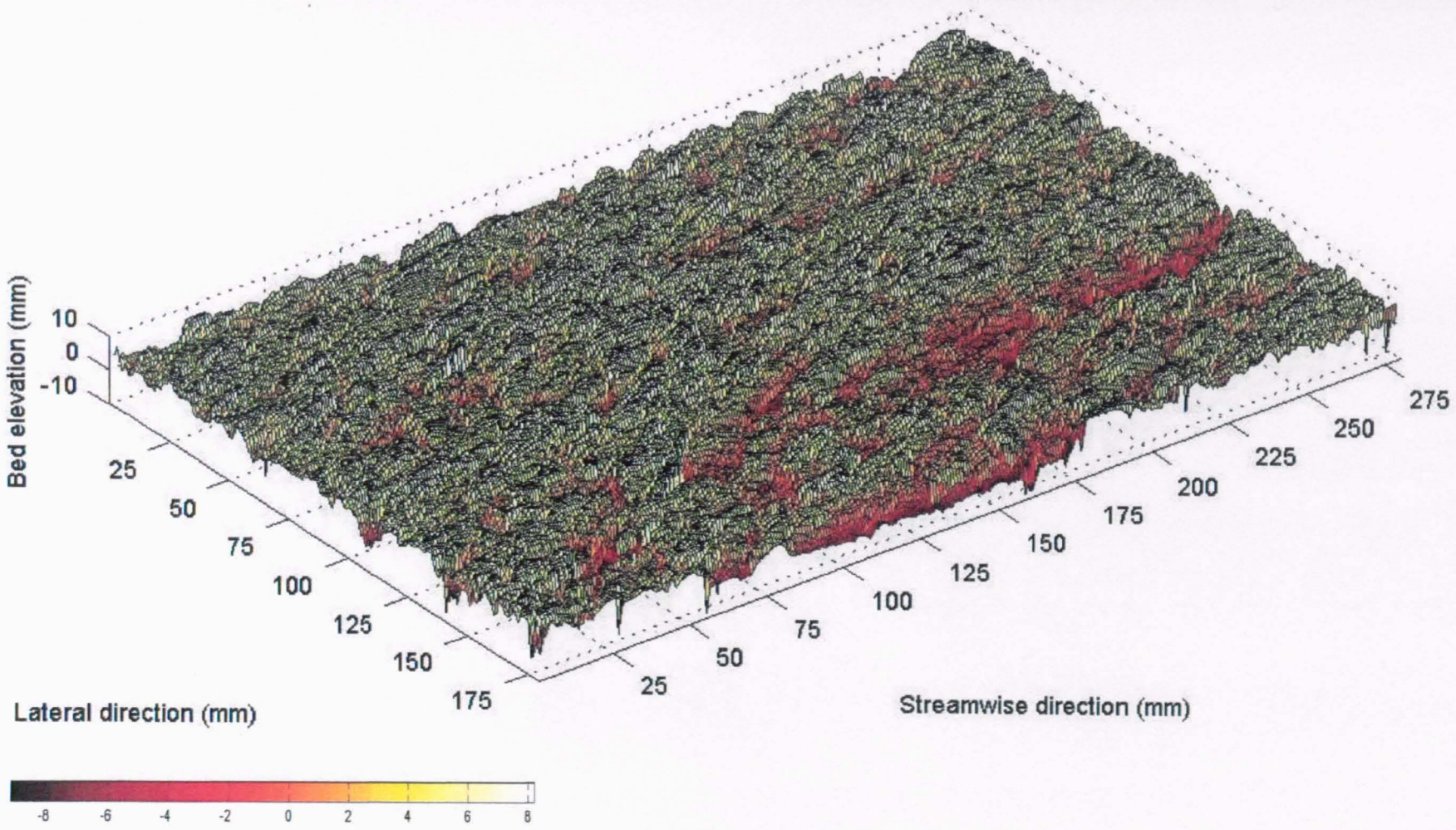

Figure 6.16. Original bed surface topography of the measurement grid Experiment UF 3-6

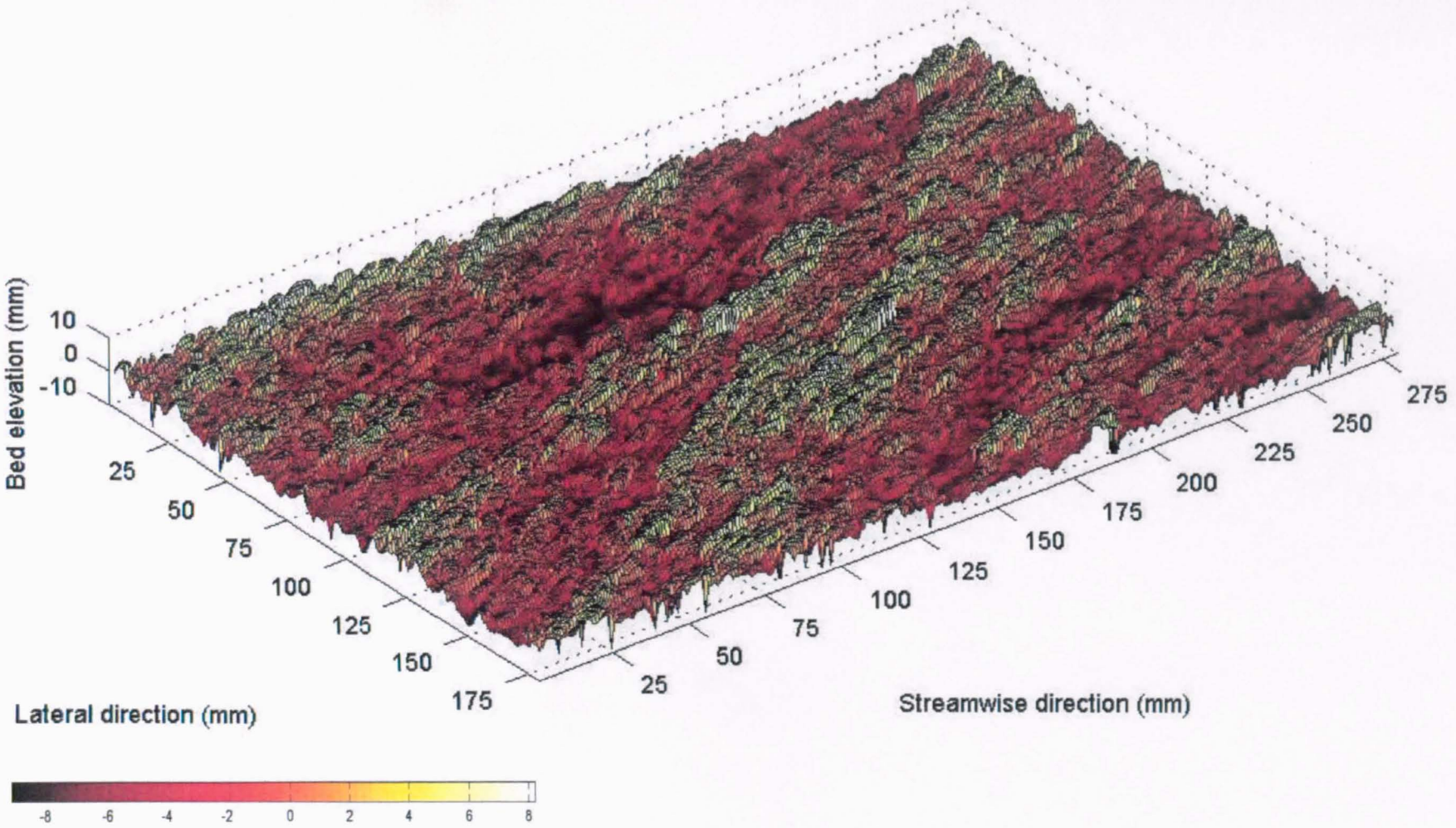

Figure 6.17. Bed surface topography of the measurement grid after antecedent flow Experiment UF 3-6

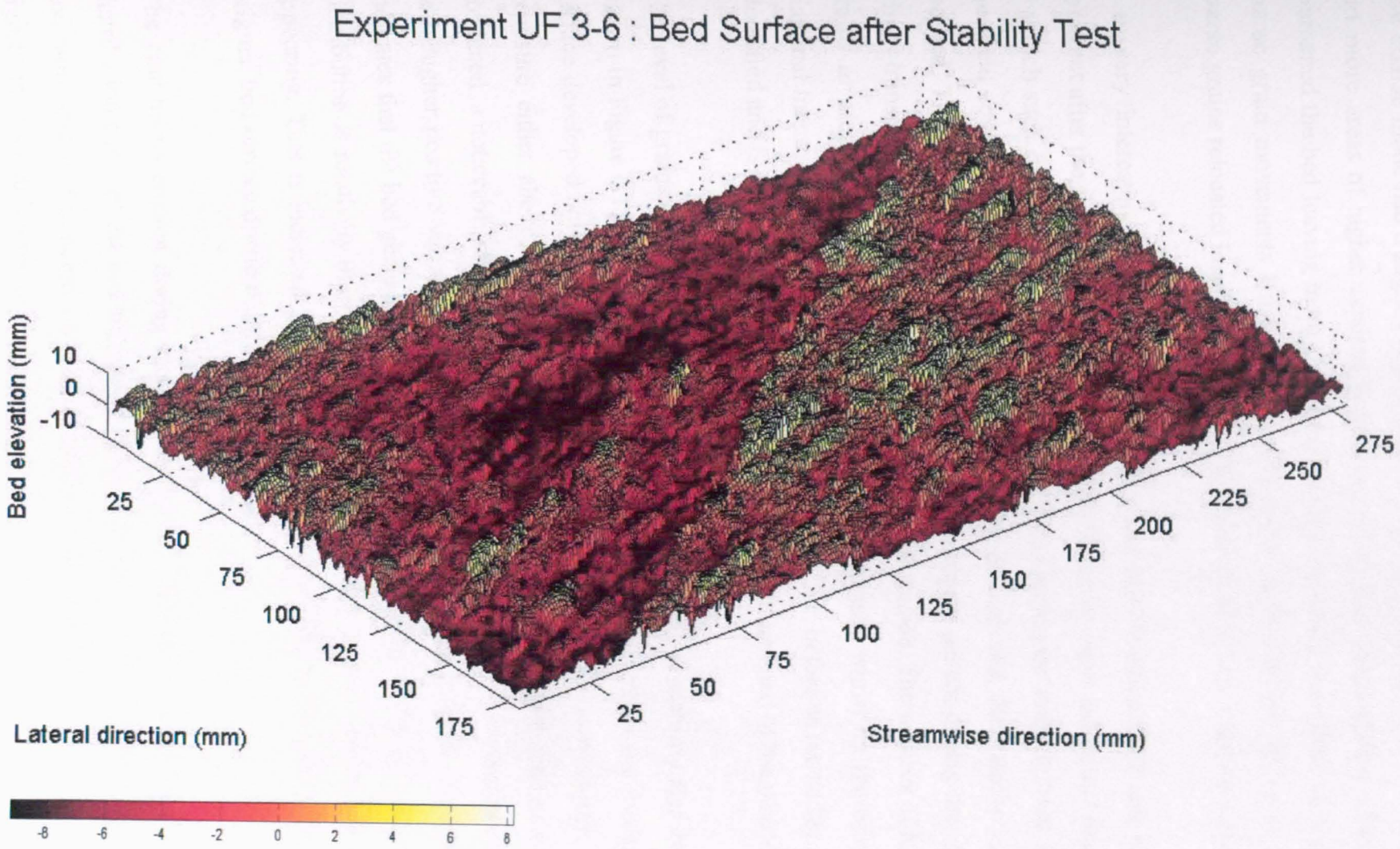

Figure 6.18. Bed surface topography of the measurement grid after stability test Experiment UF 3-6

(the coarse mode had a slightly higher proportion), the combination of low elevation valleys and more areas of higher exposed beds is expected. The transportation of the finer grains coarsened the bed leaving more exposed larger grains, which were then subsequently. These coarse grain movements left bed areas with lower surface levels. Many of the dislodged coarse grains relocated in adjacent areas to form new areas of high exposed surfaces.

It is very interesting to find out that the diagonal line is maintained and becomes more apparent after the stability test. This did not occur in the previous steady and time varying test in which such structures seemed to move "upstream" during the stability tests. In Figure 6.18 the areal coverage of the darker zones increased indicating that the stability test had eroded the bed. This seems to correspond well with the transport pattern during the stability test in which transport was dominated by grains in the coarse mode. The number of highly exposed grains or areas in the valley-type structures has decreased whilst on the other side of the diagonal line the exposed surfaces are more organised than before as the valley can be clearly identified and is now located in the right corner of downstream part of the measurement grid.

The level of grains exposure was investigated by plotting the probability distribution curve as shown in Figure 6.19. The distributions are quite revealing as to how the variation in the bed surface developed both after antecedent flow experiment and the stability test. The level of exposure either about zero level or the average bed level before and after stability test produced a noticeably different curve. The initial bed shows an unsymmetrical distribution with higher positive variations from the mean. The steep curve in the high positive values indicates that the bed generally formed by a scrapping process. After the antecedent flow the distribution is relatively more symmetrical with the large exposed grains resting on the bed appearing. This is indicated by the positive tail of the distribution exceeding the curve of original bed surface distribution.

The continuous erosion during the stability test is reflected by significant changes in the distribution curve of the bed surface elevation after this test. The distribution becomes flatter and more spread. The number of bed elevation closed to the mean level decreased indicating significant reorganisation of the bed surface during the stability tests. The positive tail continues to exceed the previous distribution indicating more large exposed grains were

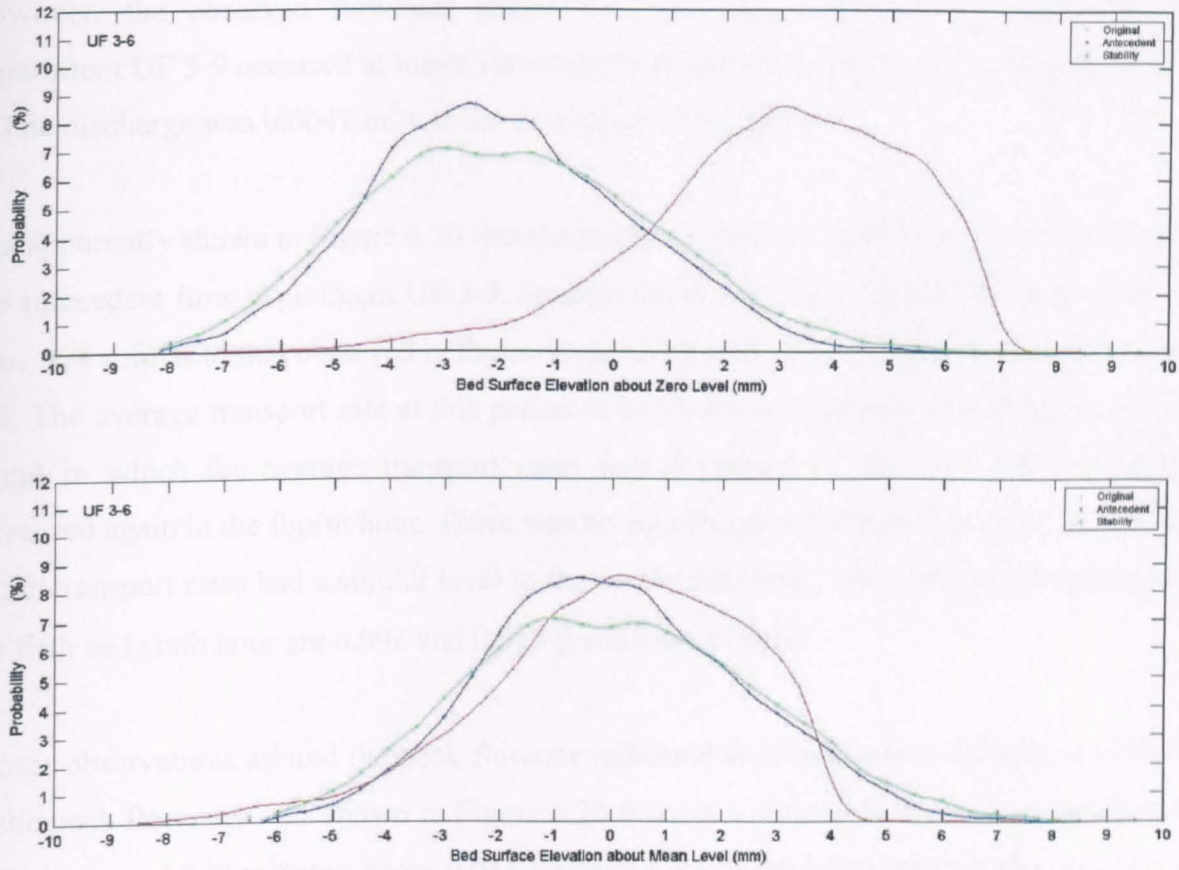

Figure 6.19. Probability distribution of bed surface elevation about zero and mean level for Experiment UF 3-6

presence. Another noticeable feature of the distribution of bed surface elevation after the stability test is that the proportion of negative elevations is also higher. This type of distribution is the characteristic of a bed with a greater number low level of valleys in the measurement area. The erosion and removal of larger grains formed new valleys as well as increasing the depth of the previously formed valleys. Most importantly the changes in the last distribution curve correlates with the transport rate observed during the stability test.

6.3.2. UNSTEADY ANTECEDENT FLOW EXPERIMENT UF 3-9

6.3.2.1. Bedload Transport Rate and Composition UF 3-9

The longer duration of rising limb in antecedent flow experiment UF 3-9 delayed the start time of transport. Material trapped in the collection box was only found at time elapsed 50 minutes or 20 minutes after the first collection in antecedent flow experiment UF 3-6.

However, the observed flowrates shows that the initial transport in antecedent flow experiment UF 3-9 occurred at lower flowrates than that in antecedent flow experiment UF 3-6. The discharge was 0.0047 m^3/s at the time of the first collection.

It is apparently shown in Figure 6.20 that the transport rates are generally very low throughout the antecedent flow experiment UF 3-9. Despite the slower start, the average rates in the first hour was similar to that observed in the corresponding time of antecedent flow experiment UF 3-6. The average transport rate at this period is 0.001 g/s/m. However a different pattern was found in which the average transport rates was decreased in the next 2 hours before it increased again in the fourth hour. There was no significant increase at this stage (fourth hour) as the transport rates had a similar level to that in the first hour. The average transport rates in the fifth and sixth hour are 0.002 and 0.015 g/s/m respectively.

Closer observations around the peak flowrate indicated that there was a disruption to the bed at the peak flowrates. As shown in Figure 6.20 there is a noticeable increase in transport rate at time elapsed 360 minutes. From 0.011 g/s/m at time elapsed 350 minutes the transport rate increased to 0.062 g/s/m at time elapsed 360 minutes. It was expected that the transport rate would be relatively high in the following time elapsed. However there was no further impact of the peak flowrates. In the initial stage of falling limb the transport rate dropped quite significantly. The transport rate at time elapsed 370 minutes is 0.012 g/s/m and thus subsequently decreased as the flowrates decreased.

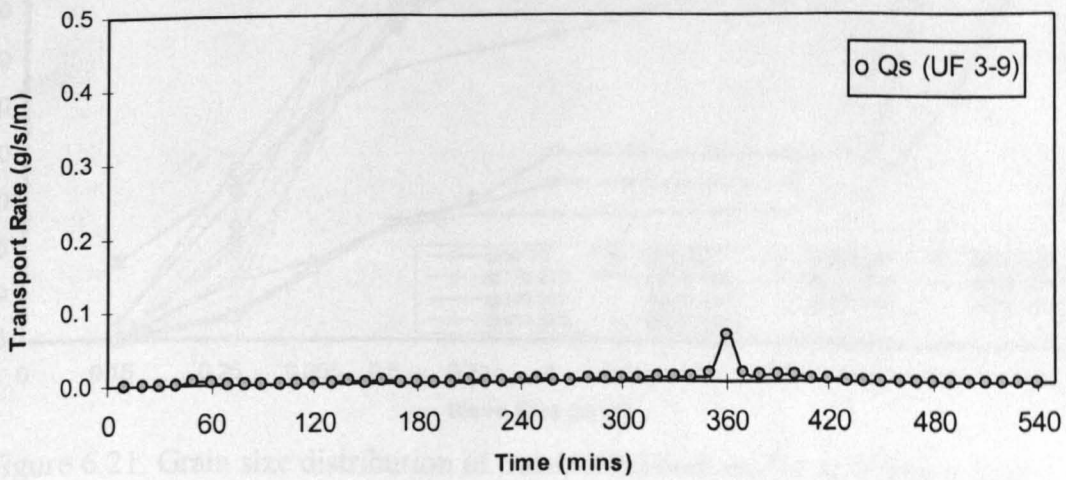

Figure 6.20. Time variation of transport rate for antecedent flow Experiment UF 3-9

The composition of the transported bedload during the whole duration of antecedent flow Experiment UF 3-9 showed the existence of grains in the fine mode throughout the test (Figure 6.21). However only small amounts were transported so that the contribution of the grains in the fine mode to the total transport is slightly less than grains in the coarse mode. Although the existence of grains in the coarse mode was rarely seen in transport, their amounts were relatively high. Coarse grains were particularly present when the peak flowrate was attained at time elapsed 360 minutes. At this time the amount of grains in the coarse mode makes up more than 30 % of the total transport. Grains in the coarse mode were still

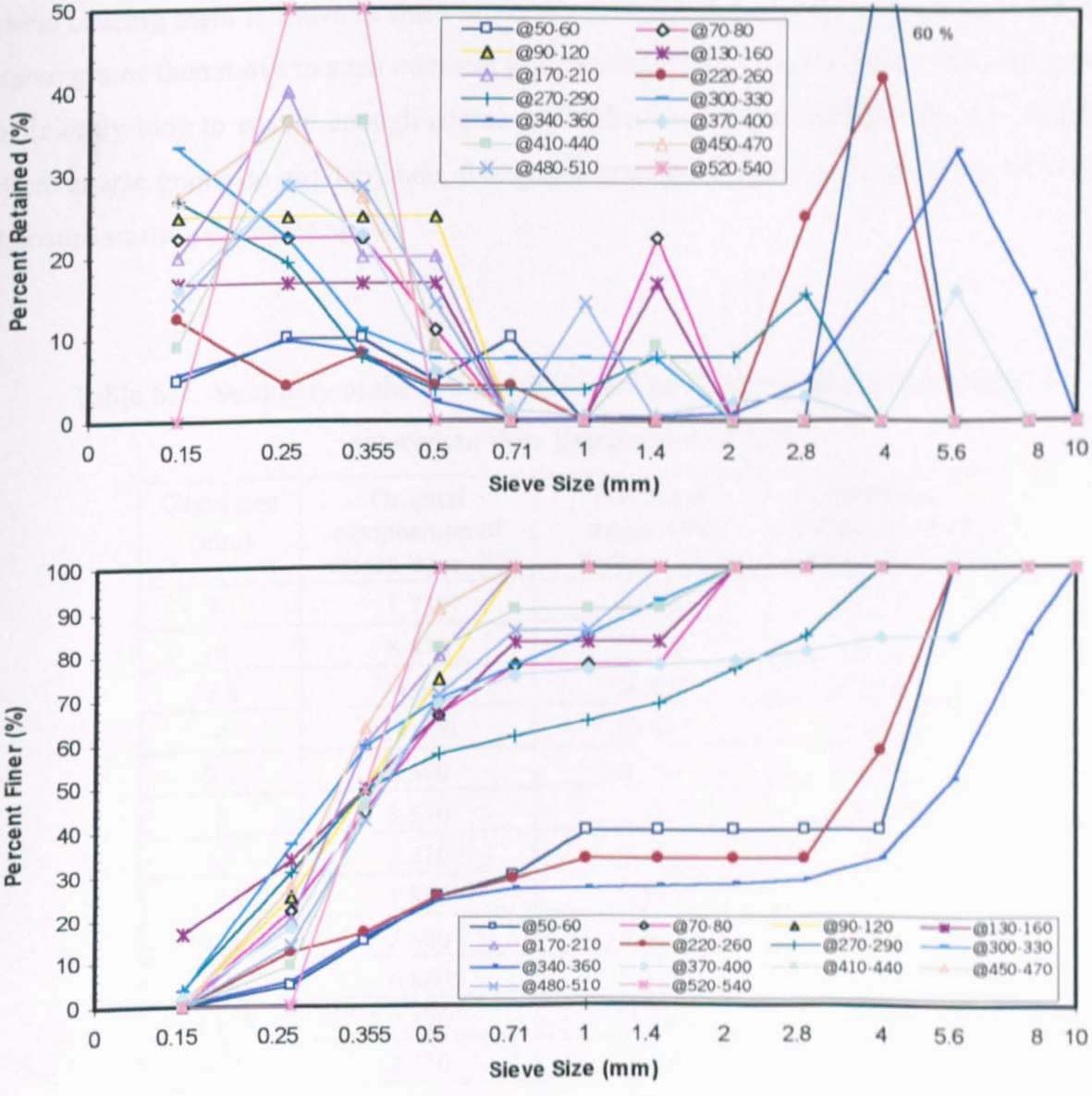

Figure 6.21. Grain size distribution of transported bedload for antecedent flow Experiment UF 3-9

moving in the following time elapsed but not in considerable amounts. At this time the transport was dominated by grains in the fine mode. The domination of grains in the coarse mode also found at time elapsed 50-60 minutes and 220-260 minutes.

The inconsistency in the pattern of the domination of the coarse mode may be a reflection of the stabilising armouring processes. It is believed that the movement of large amounts of coarse grains reorganised the bed structure. To some extent the fluctuation between the movement of coarse grains and then fine grains caused the bed to become more stabilised. It is believed that the initial transport of fine grains increased the level of exposure of the coarse grains causing them to move at shear stress levels below that than would be expected. These coarse grains then move in such numbers to form bed stabilising structures. The rising limb is sufficiently long to ensure enough coarse grains have moved to stabilise the bed. In periods where coarse grains do not dominate, fine grains are then removed increasing the coarse grain exposure starting the cycle again.

Table 6.7. Summary of the average fractional bedload composition produced by antecedent flow Experiment UF 3-9

Grain size (mm)	Original composition of surface layer (%)	Fractional transported bedload (%)	Estimated composition of surface layer (%)
10	1.730	0.000	1.731
8	8.570	7.135	8.571
5.6	34.660	18.402	34.668
4	19.600	12.632	19.603
2.8	6.860	4.343	6.861
2	3.530	1.157	3.531
1.4	2.510	2.198	2.510
1	1.850	1.159	1.850
0.71	2.680	1.801	2.680
0.5	6.840	5.303	6.841
0.355	7.420	14.153	7.417
0.25	2.710	17.721	2.703
0.15	0.940	12.535	0.934
receiver	0.100	1.460	0.099
Total	100	100	100

As mentioned earlier, the occasionally transported grains in the coarse mode contributed slightly more than grains in the fine mode. This can be seen in Table 6.7 where the proportion of the total transport in the coarse mode is 38.2 % in comparison to 37.2 % of grains in the fine mode. It can also be seen that the grains of diameter 0.15 mm have a relatively high proportion in transport with more than 12 %. This supports the earlier assumption that the periodic transports of grains in the coarse mode were primarily due to the increasing exposure caused by the continuing transport of the finer grains surrounding them.

6.3.2.2. Bursting Events and Flow Momentum UF 3-9

The observations to the average nearbed streamwise velocity indicate that the average values generally increased with increasing flowrates and decreased with the decreasing flowrates (Figure 6.22). These values confirm satisfactorily to the form of the antecedent flow hydrograph with the maximum average values is obtained at time elapsed 360 minutes. It is also shown in Figure 6.22 that the average bed shear stress at certain time elapsed did not follow a totally consistent pattern but generally followed the trend in which the values increased as the flowrate increased in the rising limb and decreased as the flowrate decreased in the falling limb. Before time elapsed 140 minutes and after time elapsed 470 minutes the water depths were below the operating depth of the ADV probe and thus no measurements were possible at these stages.

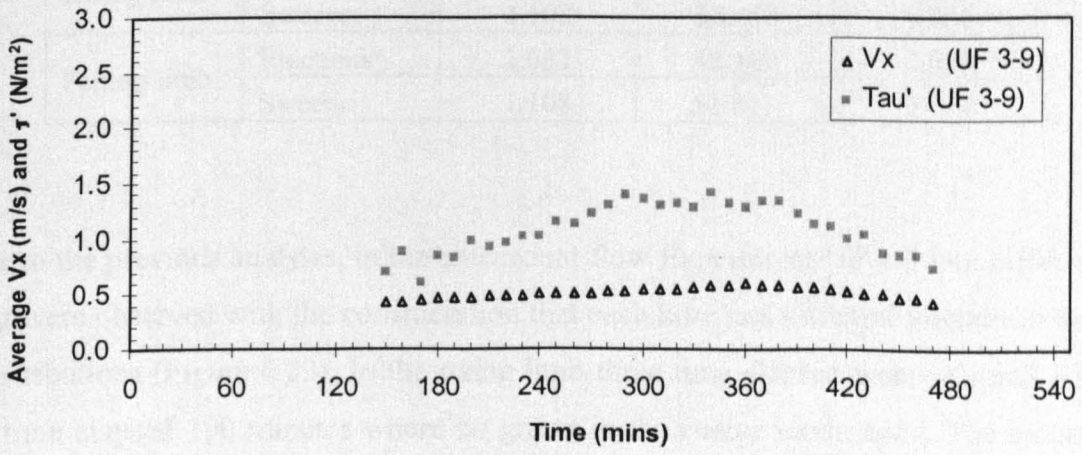

Figure 6.22. Variation of time averaged nearbed streamwise velocity and bed shear stress during antecedent flow Experiment UF 3-9

Again given that the pattern of the average nearbed streamwise velocity and average bed shear stress do not follow the patterns in the composition of the bedload it was decided to examine the nearbed flow in more detail. The observation of bursting event in the antecedent flow Experiment UF 3-9 indicates that the number of downward-looking bed interactions both in the rising limb and in the falling limb is higher than the upward interactions. The frequency of sweeps is higher than the frequency of ejections. The sweeps frequency is fairly constant while the frequency of ejections increase in the falling limb. With 47.3 % of the total bursting events, the frequency of ejections in the rising limb of antecedent flow experiment UF 3-9 is relatively low. This coincides with the early observation that the grains in the coarse mode in transport were rarely seen in the rising limb. The periodical existence of coarse grains was due to the increasing exposure rather than the frequency of ejections. In Table 6.8 it can also be seen that the frequency of ejections in the falling limb increased to 1.031 Hz. The proportion of ejections also increased to 48.2 % whilst the proportion of sweeps decreased from 52.7 % in the rising limb to 51.8 % in the falling limb. The average duration of both events is similar throughout the antecedent flow.

Table 6.8. Time frequency and the proportion of occurrences of bursting events in antecedent flow Experiment UF 3-9

Parameter descriptions		Frequency (Hz)	Proportion (%)	Average duration (sec.)
Rising limb	Ejections	0.990	47.343	0.055
	Sweeps	1.102	52.657	0.056
Falling limb	Ejections	1.031	48.189	0.053
	Sweeps	1.108	51.811	0.054

Similar to the previous analysis, in the antecedent flow Experiment UF 3-9 five different time elapsed were observed with the consideration that each time had different features in the grain size distributions (Figure 6.23). In the rising limb three time elapsed were selected. The first one is time elapsed 190 minutes where no grains in the coarse mode exist. The second time elapsed is 250 minutes where grains in the coarse mode dominate and the third selection is time elapsed 360 minutes which is the final time elapsed in the rising limb. In the falling limb,

which had shorter duration than the rising limb, two different time elapsed of 430 and 460 minutes were selected. At these times only finer grains moved. A summary of the characteristics of the bursting events for all the selected time elapsed is presented in Table 6.9.

Table 6.9. Summary of bursting events at selected time elapsed in antecedent flow Experiment UF 3-9

Parameter descriptions	Time elapsed (minutes)				
	190	250	360	430	460
Threshold values (m^2/s^2)	0.0044	0.0056	0.0063	0.0051	0.0040
Number of ejections	185	206	192	216	201
Number of sweeps	222	214	220	209	214
Frequency of ejections (Hz)	0.925	1.030	0.960	1.080	1.005
Frequency of sweeps (Hz)	1.110	1.070	1.100	1.045	1.070
Average duration of ejections (s)	0.054	0.052	0.054	0.054	0.051
Average duration of sweeps (s)	0.051	0.052	0.057	0.051	0.053

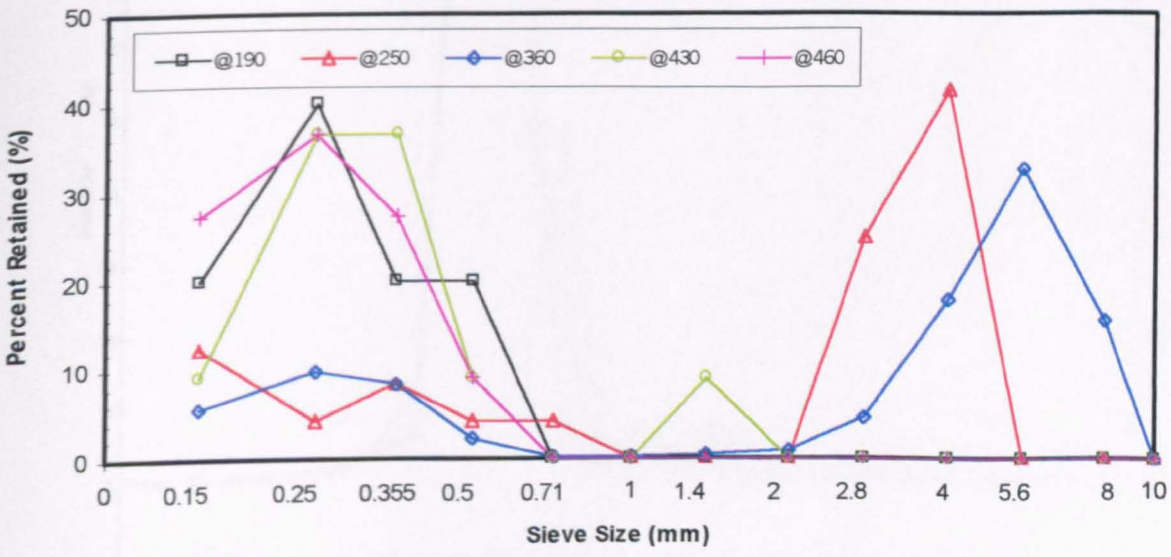

Figure 6.23. Grain size distribution of transported bedload at selected time elapsed in antecedent flow Experiment UF 3-9

It has been discussed in previous sections that the proportion of grains in the coarse mode of the total bedload is slightly higher than the proportion of grains in the fine mode. However there were certain time elapsed which contained only grains in the fine mode. At time elapsed 190, 430 and 460 minutes only fine grains are observed (Figure 6.23). In Table 6.9 although

there is similarity between time elapsed 190 and 250 minutes in which the occurrence of ejections is less than the frequency of sweeps, the pattern in transported grains size is different. It is believed that the higher proportion of momentum with the magnitude in the range between 9 and 15 kg/ms were the main factor in the transportation of grains in the coarse mode at time elapsed 250 minutes (Figure 6.24). Time elapsed 190 minutes has a relatively high proportion of ejections with the magnitude of momentum ranging from 7 to 9 kg/ms. This level of magnitude is not sufficient to transport grains in the coarse mode. Time elapsed 460 minutes has a relatively similar distribution to that found in time elapsed 190 minutes and again no grains in the coarse mode were in transport.

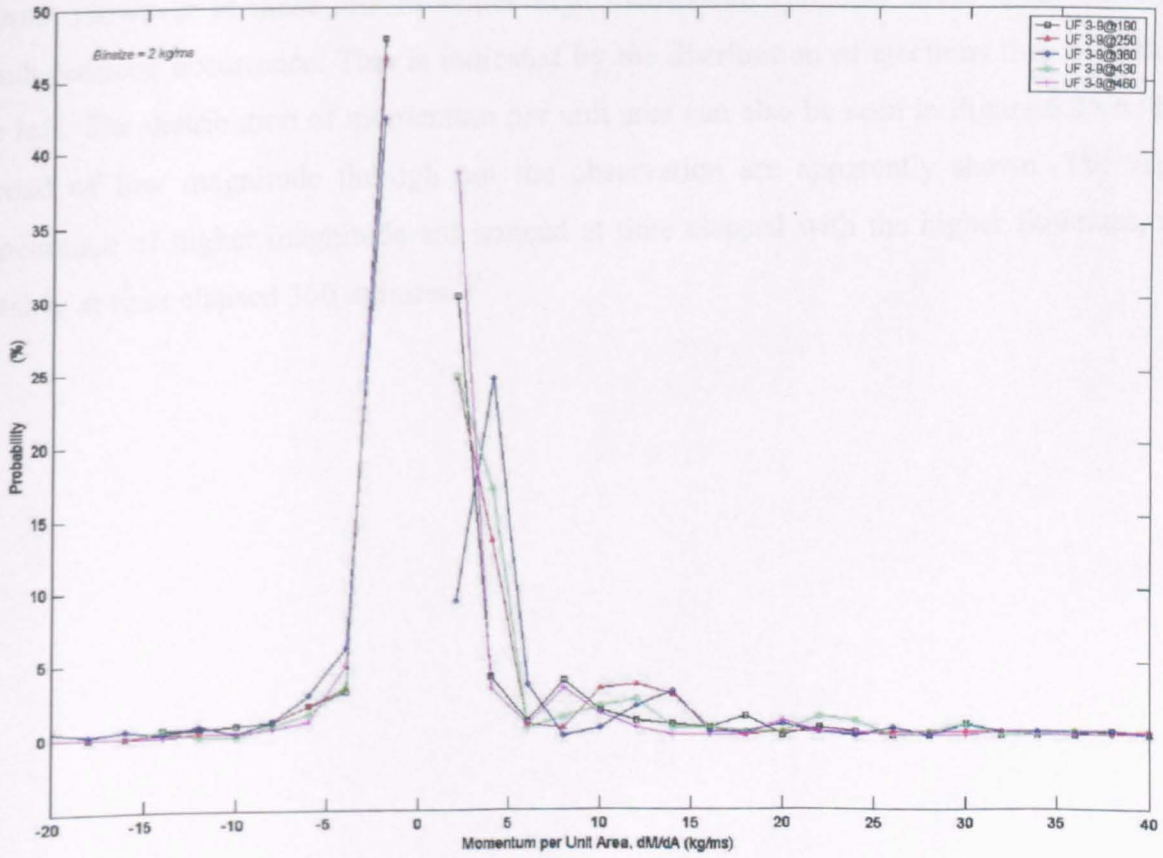

Figure 6.24. Probability distribution of momentum per unit area at selected time elapsed in antecedent flow Experiment UF 3-9 (ejections are positive and sweeps are negative)

In Figure 6.24 time elapsed 360 minutes has considerable proportion of ejections with magnitude of momentum in the range between 11 and 15 kg/ms. This is believed to be the main factor that causes grains in the coarse mode to be transported at this time elapsed. A

noticeable proportion of momentum with the magnitude ranging from 9 to 13 kg/ms occurred at time elapsed 430 minutes. However as the bed becoming more stable, only grains of diameter 1.4 mm were transported along with grains in the fine mode and other finer grains available in the mixture.

Overall the probability distribution of momentum shown in Figure 6.24 indicate that the bursting events with low momentum are a common feature. The downward-looking bed interactions always exist irrespective of the flowrates and that their magnitude is strongly linked to flowrate. A different pattern is established by the ejections (upward interactions). The lower flowrates also produced a considerable proportion of low magnitude momentum events. However at these low flowrates high momentum ejections could occur but with a much reduced occurrence. This is indicated by the distribution of ejections that is shifted to the left. The distribution of momentum per unit area can also be seen in Figure 6.25 with the spread of low magnitude through out the observation are apparently shown. The regular appearance of higher magnitude are noticed at time elapsed with the higher flowrates, most notably at time elapsed 360 minutes.

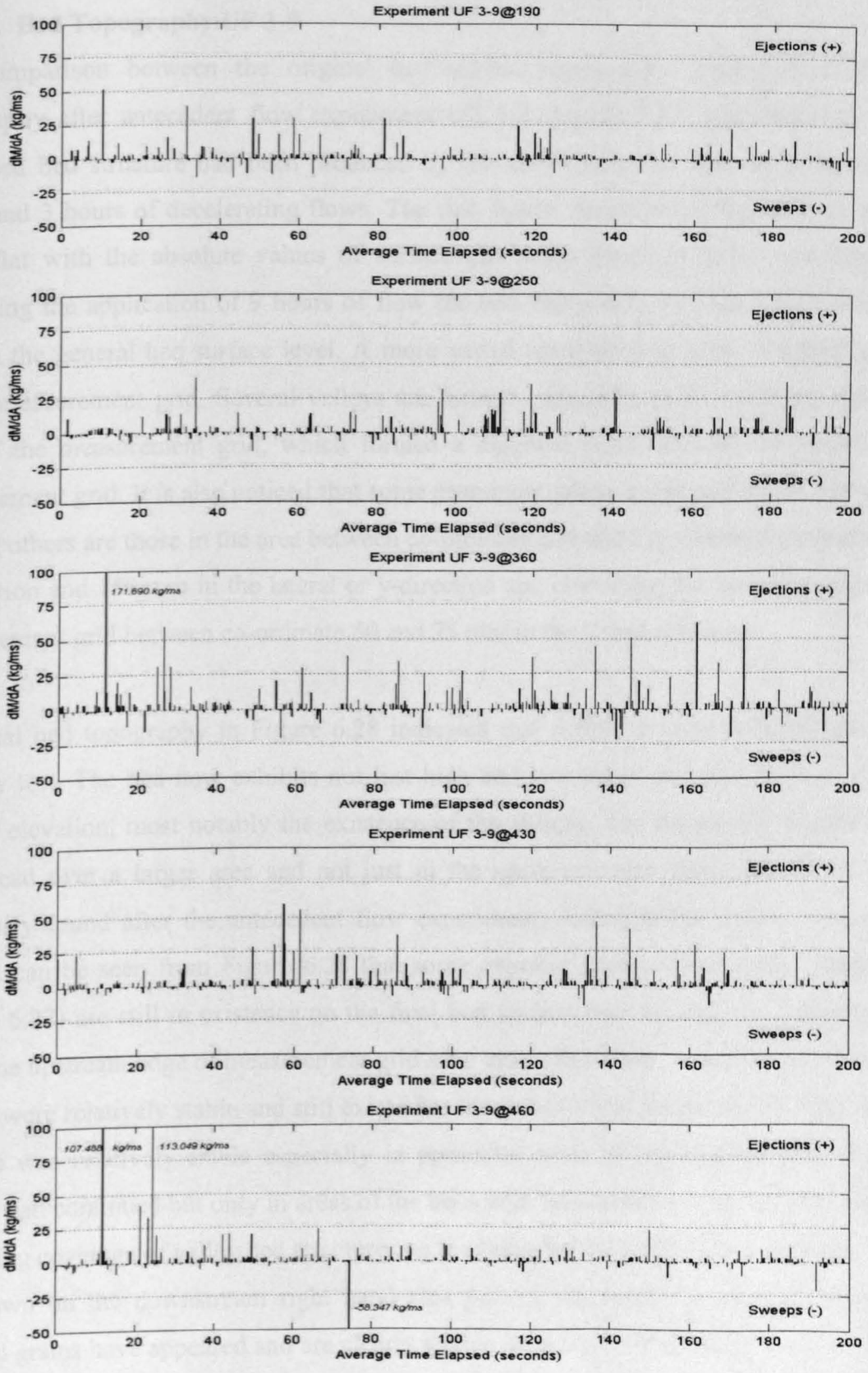

Figure 6.25. The sequence of momentum per unit area and its magnitude at selected time elapsed in antecedent flow Experiment UF 3-9

6.3.2.3. Bed Topography UF 3-9

The comparison between the original bed surface topography (Figure 6.26) and the topography after antecedent flow experiment UF 3-9 (Figure 6.27) indicated that a more organised bed structure had been produced by the combination of 6 hours of accelerating flows and 3 hours of decelerating flows. The first figure indicates that the original bed was fairly flat with the absolute values of surface elevations being generally relatively high. Following the application of 9 hours of flow the bed topography in Figure 6.27 indicates a drop in the general bed surface level. A more varied topography is seen to spread over the whole measurement grid. Several valleys are formed especially in the upstream right hand side of the measurement grid, which formed a diagonal patch towards the centre of the measurement grid. It is also noticed that some prominent grains are at rest on the bed surface. Among others are those in the area between co-ordinate 200 and 225 mm in the streamwise or x-direction and 150 mm in the lateral or y-direction and also along the upstream edge of the measurement grid between co-ordinate 50 and 75 mm in the lateral direction.

The final bed topography in Figure 6.28 indicated that further erosion occurred during the stability test. The bed now exhibits not just high and low points but also areas of different surface elevation, most notably the existence of the valleys. The diagonally aligned valleys are spread over a larger area and not just in the upstream right hand side of the grid as previously found after the antecedent flow experiment. Although the erosion process took place it can be seen from Figure 6.28 that some exposed grains found before stability test (Figure 6.27) are still in existence on the final bed surface. For example the exposed grains along the upstream edge of measurement grid after antecedent flow, which already mentioned earlier, were relatively stable and still exist after the stability test (Figure 6.28). This suggests the bed was relatively stable especially in particular areas of the measurement grid. The erosion had continued but only in areas of the beds with less stability. This is indicated by the increasing coverage of valley bed structures on the bed after the stability test. Notable features are shown on the downstream right hand side part of the measurement grid. More large exposed grains have appeared and are clearly visible on the bed. In this case the valleys at the end of the antecedent flow test have been covered by grains from upstream. This has increased the local surface elevation. Another good example of this pattern is on the left-hand side of the measurement grid, which covered by the area of 200 to 225 mm in streamwise

direction. After antecedent flow experiment this area has a relatively identical bed surface but after the application of the stability test the bed surface is considerably different with degradation occurring at the upstream edge which has led to aggradation in this area.

Observation of the probability density of the bed surface elevations (Figure 6.29) correlates with the previous explanation that the original bed was fairly flat with the surface elevations were generally relatively high. A decreased in the overall bed surfaces level after antecedent flow is shown by the distribution curve that is shifted to the left. The symmetrical shape of the curve indicates that the valley and the exposed grains were relatively balanced. Further erosion and the larger spread of valleys is represented by the distribution curve after stability test. The curve is furtherly shifted to the left indicating the lower bed surface level established on the bed.

Examinations of the bed surface elevation distribution about the average level suggest that after antecedent flow experiment there was exposed grains resting on the bed. The distribution curve narrowed with an increased in the proportion of elevation closed to the average bed level. This is the indication that the bed surface in general became more flatter. However after the application of stability test, the distribution lowered and widened. Further destabilisation of the bed during stability test not only increased the spread of the lower bed elevation but also more exposed grains were established.

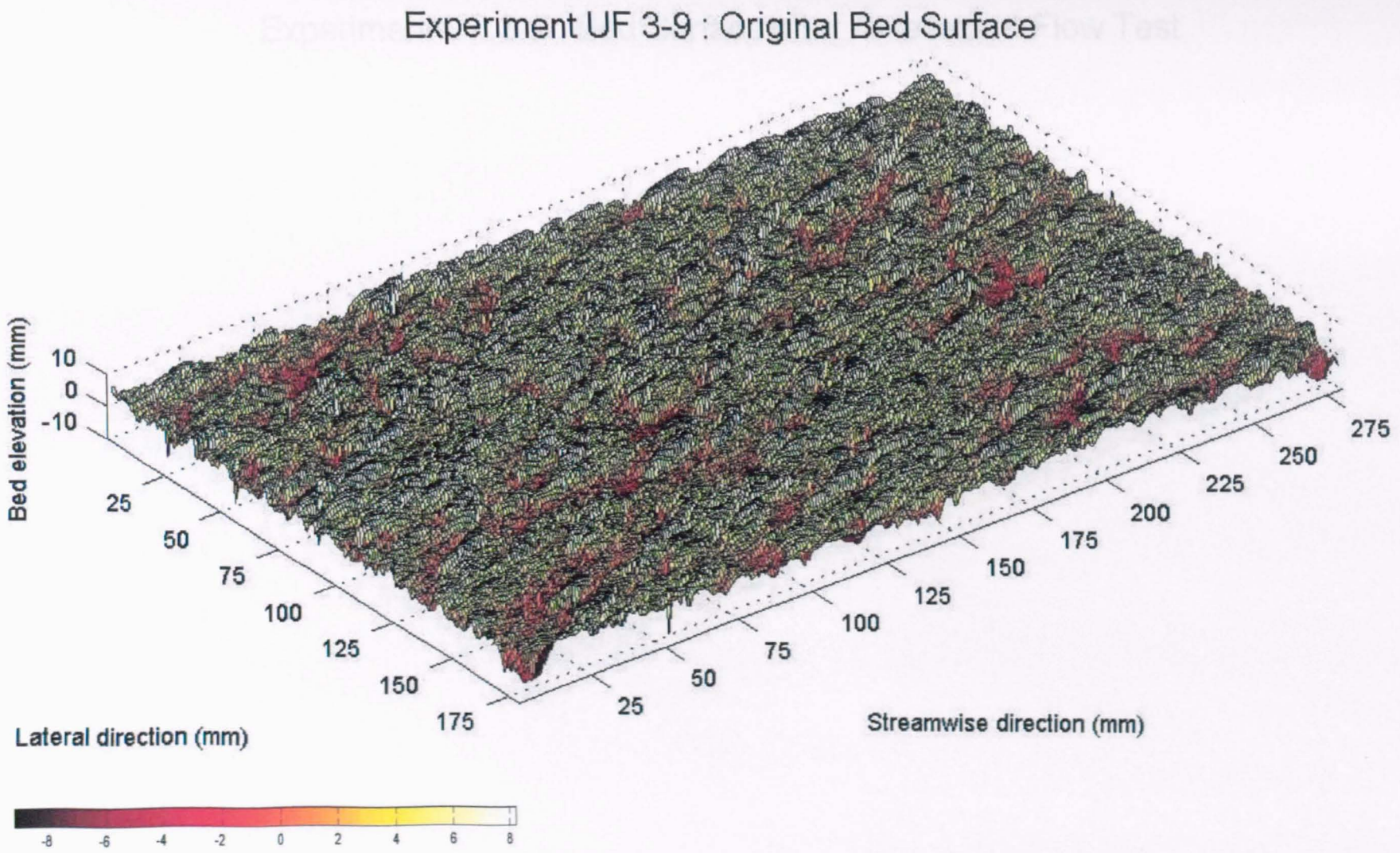

Figure 6.26. Original bed surface topography of the measurement grid Experiment UF 3-9

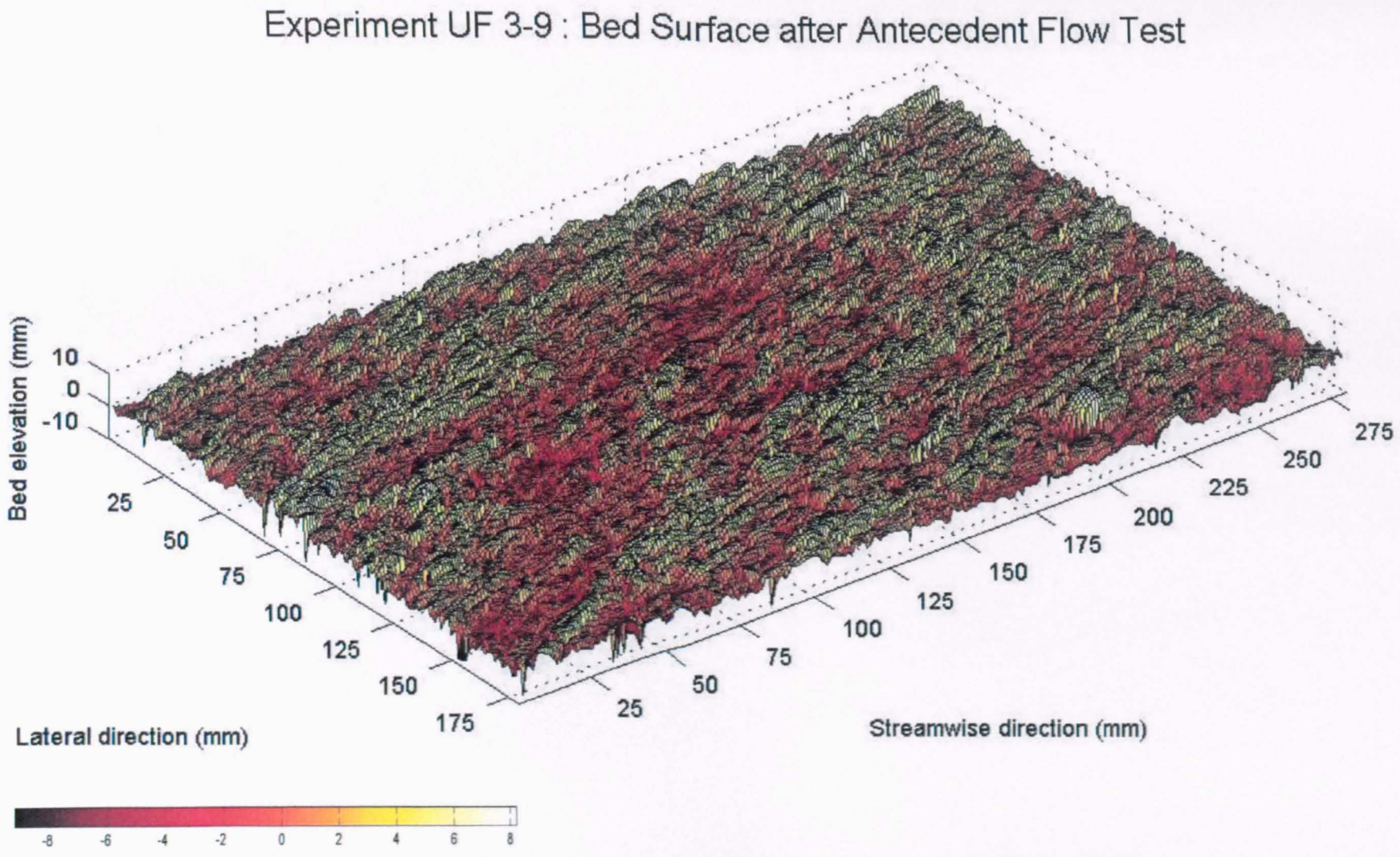

Figure 6.27. Bed surface topography of the measurement grid after antecedent flow Experiment UF 3-9

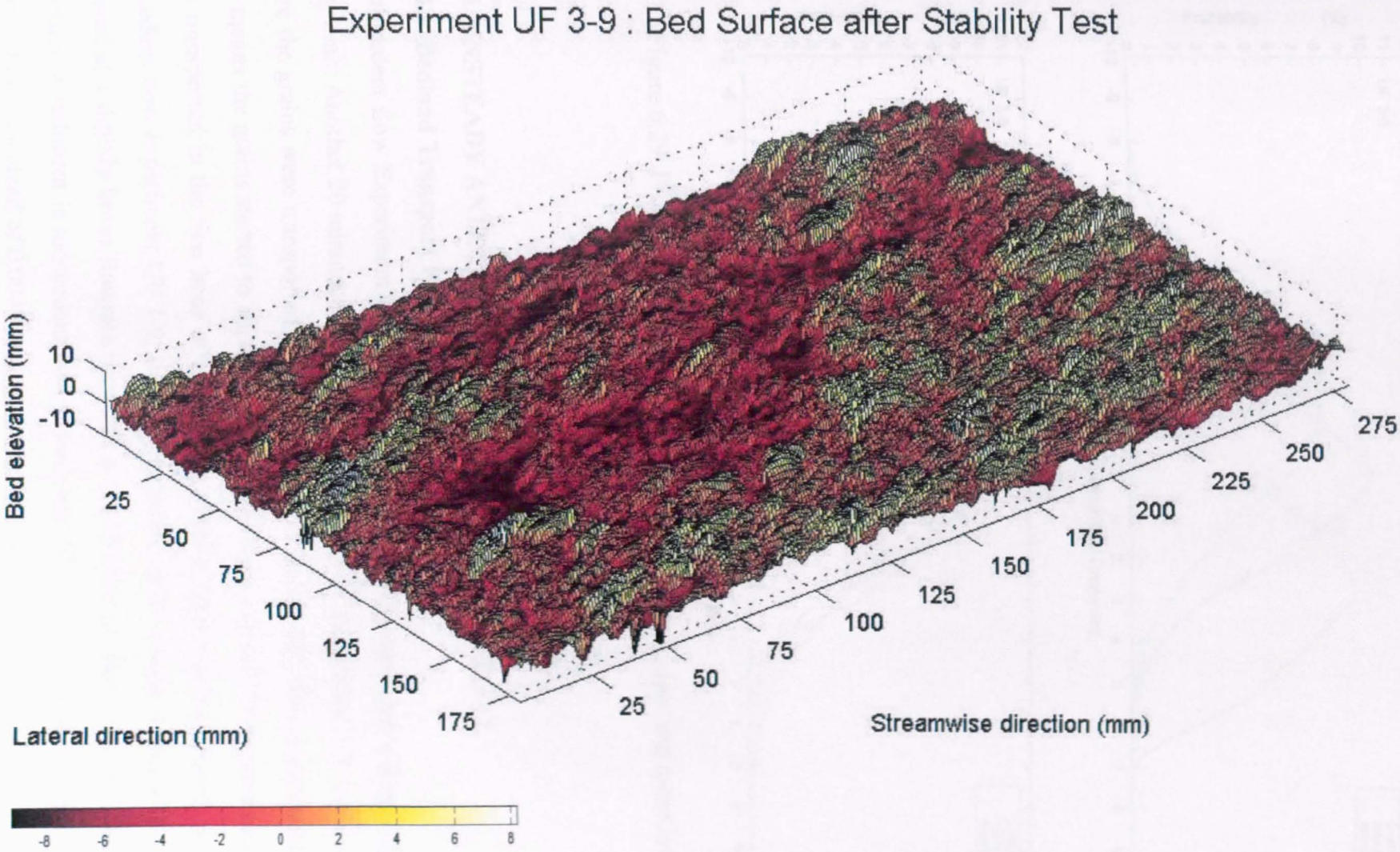

Figure 6.28. Bed surface topography of the measurement grid after stability test Experiment UF 3-9

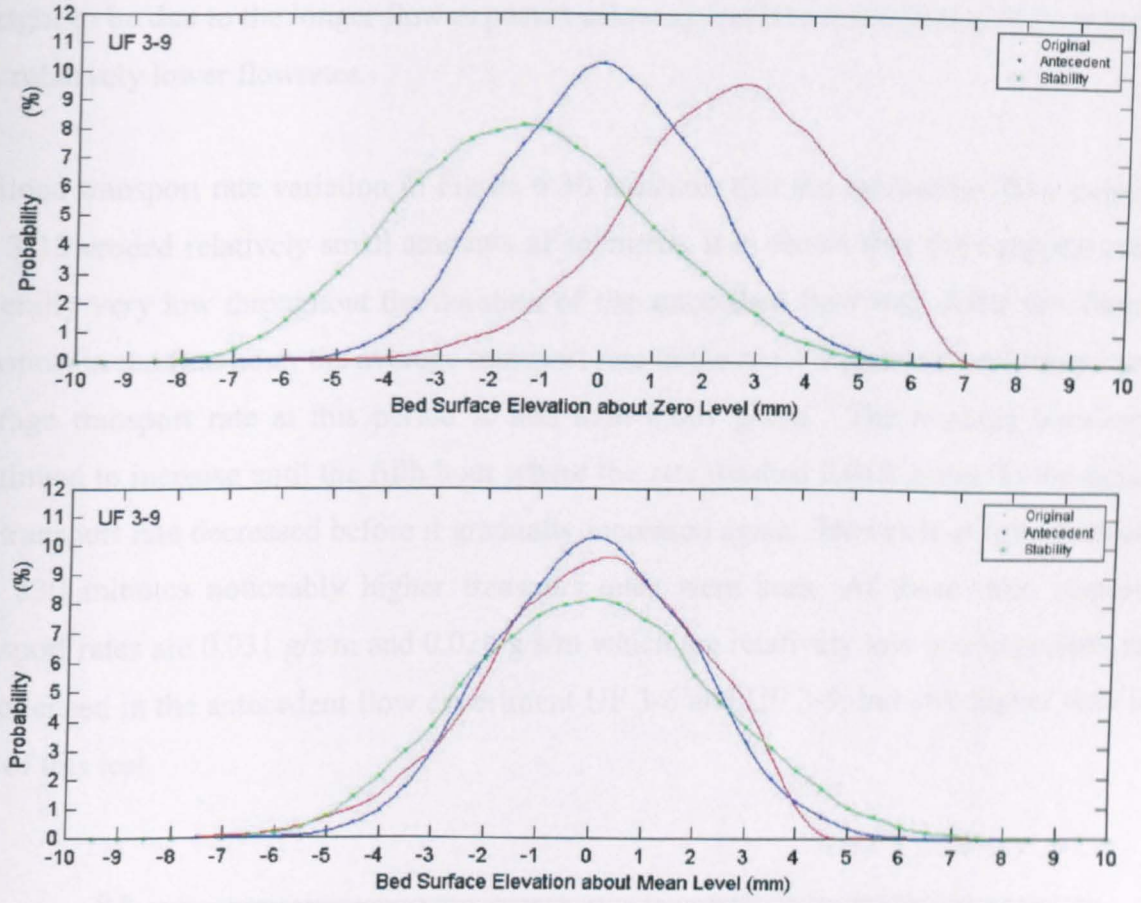

Figure 6.29. Probability distribution of bed elevation about zero and mean level for Experiment UF 3-9

6.3.3. UNSTEADY ANTECEDENT FLOW EXPERIMENT UF 3-12

6.3.3.1. Bedload Transport Rate and Composition UF 3-12

In antecedent flow Experiment UF 3-12 the flow hydrograph contained a longer duration of rising limb. Another 20 minutes than that in antecedent flow experiment UF 3-9 was required before the grains were transported for the first time in antecedent flow experiment UF 3-12. This means the grains started to appear in transport at time elapsed 70 minutes and no grains were transported in the first hour of experiment. Similar to the pattern found previously in antecedent flow experiment UF 3-9, the first collection in the longer duration of rising limb occurred at a slightly lower flowrate than that in the shorter duration of rising limb. The first collection of sediment in antecedent flow experiment UF 3-12 was taken when the discharge was 0.0044 m^3/s instead of 0.0047 m^3/s in antecedent flow Experiment UF 3-9. This again is

thought to be due to the longer flow exposure allowing the less stable grains to be transported at a relatively lower flowrates.

Bedload transport rate variation in Figure 6.30 indicates that the antecedent flow experiment UF 3-12 eroded relatively small amounts of sediment. It is shown that the transport rates are generally very low throughout the duration of the antecedent flow test. After the absence of transport in the first hour, the average transport rate in the second hour was still very low. The average transport rate at this period is less than 0.001 g/s/m. The average transport rate continued to increase until the fifth hour where the rate reached 0.013 g/s/m. In the next hour the transport rate decreased before it gradually increased again. However at time elapsed 300 and 530 minutes noticeably higher transport rates were seen. At these time elapsed the transport rates are 0.031 g/s/m and 0.020 g/s/m which are relatively low in comparison to that experienced in the antecedent flow experiment UF 3-6 and UF 3-9, but still higher than in the rest of this test.

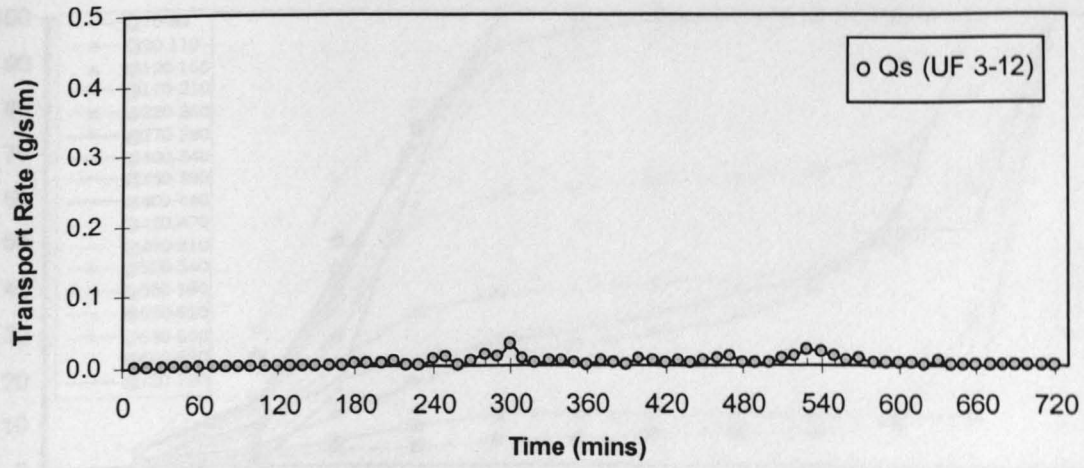

Figure 6.30. Time variation of transport rate for antecedent flow Experiment UF 3-12

One important point to note was that no significant peaks in transport rate occurred, even at the peak flowrate. By looking at the time elapsed around the peak flowrate no significant changes in transport rates were observed. Only a relatively small increase and decrease were experienced. For instance the transport rates at time elapsed 540 minutes is 0.018 gr/s/m and this decreased to 0.012 gr/s/m in the following 10 minutes at the start of the falling limb of the

hydrograph. Having observed this pattern it can be said that the bed structure was sufficiently stable as the peak flowrates were not able to transport considerable amounts of grains as in the previous tests.

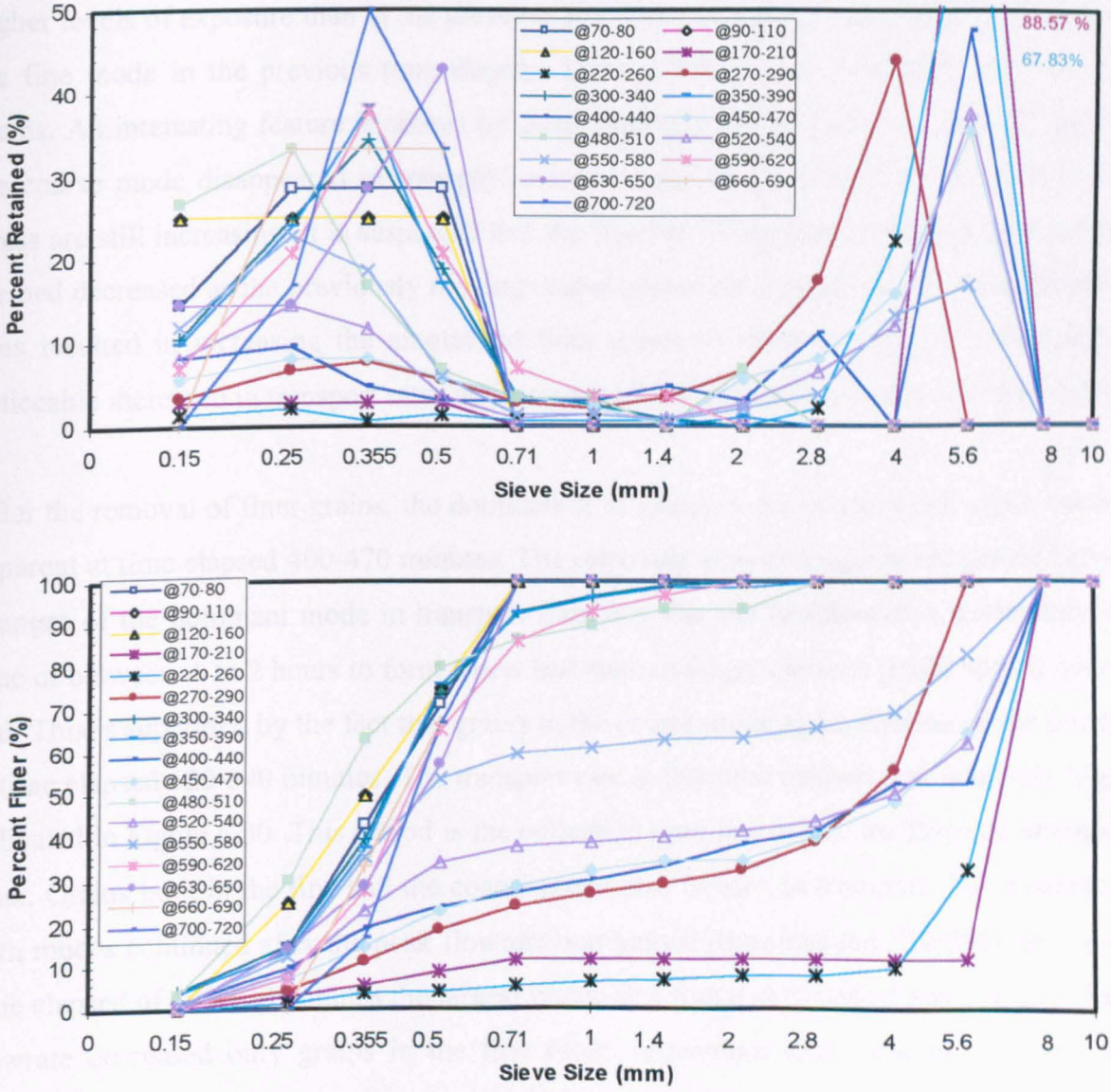

Figure 6.31. Grain size distribution of transported bedload for antecedent flow Experiment UF 3-12

In order to examine the pattern mentioned above, more depth observation to the changes in the compositions of bedload transported in antecedent flow experiment UF 3-12 was carried out (Figure 6.31). A different pattern than that seen in antecedent flow experiment UF 3-6 and

UF 3-9 is observed where the existence of grains in the coarse mode was more frequent. Initially only grains in the fine mode were transported at time elapsed 70-160 minutes. In the next observation at time elapsed 170-210 minutes grains of diameter 5.6 mm were found and started to dominate the transport. The flowrate at this particular time elapsed was 0.0106 m^3/s. This is less than in the previous test so that the removal of the 5.6 mm grains is thought to higher levels of exposure than in the previous test. The continuous transportation of grains in the fine mode in the previous time elapsed increased the level of exposure for the larger grains. An interesting feature is shown by time elapsed 300-390 minutes where the grains in the coarse mode disappeared in transport even thought the flowrate and average bed shear stress are still increasing. It is suspected that the number of exposed, isolated larger grains on the bed decreased as the previously moving coarse grains have found stable resting positions. This resulted in increasing the amount of finer grains in transport. This is reflected by a noticeable increased in transport rates at time elapsed 300 minutes as shown in Figure 6.30.

After the removal of finer grains, the domination of grains in the coarse mode again becomes apparent at time elapsed 400-470 minutes. The relatively similar length in the period between changes of the dominant mode in transport indicates that the bed needed a moderately long time of between 1 to 2 hours to form a new bed state of larger exposed grains spread over the bed. This is supported by the fact that grains in the coarse mode again dominated the transport at time elapsed 520-540 minutes. The transport rate at this time elapsed was relatively high as indicated in Figure 6.30. This period is the collection time just before the flowrate attained its peak. Grains both in the fine and the coarse mode now existed in transport. The existence of both modes continued after the peak flowrate was passed (time elapsed 550-580). In the next time elapsed of 590-620 minutes the largest grains size found in transport was 1.4 mm. As the flowrate decreased only grains in the fine mode (maximum grain size of 0.5 mm) were transported in the remaining time elapsed (630-720 minutes).

In Table 6.10 it can be seen that the proportion of grains in the fine mode in the total amount transported is slightly higher than the proportion of grains in the coarse mode. This is different than the proportions of transported sediments in the antecedent flow experiments UF 3-6 and UF 3-9 where the proportion of grains in the fine mode are slightly less than the proportion of grains in the coarse mode. In antecedent flow experiment UF 3-12 the fine

mode has contribution of 38.7 % whilst the coarse mode contributes 37.8 %. Table 6.10 also shows that the available fluid forces in antecedent flow experiment UF 3-12 were unable to transport the grains of diameter 8 mm. This means there is a possibility that the bed formed by antecedent flow experiment UF 3-12 is coarser than the bed formed by antecedent flow experiment UF 3-6 and UF 3-9.

Table 6.10. Summary of the average fractional bedload composition produced by antecedent flow Experiment UF 3-12

Grain size (mm)	Original composition of surface layer (%)	Fractional transported bedload (%)	Estimated composition of surface layer (%)
10	1.730	0.000	1.732
8	8.570	0.000	8.578
5.6	34.660	25.873	34.668
4	19.600	11.924	19.607
2.8	6.860	5.426	6.861
2	3.530	2.707	3.531
1.4	2.510	1.275	2.511
1	1.850	1.976	1.850
0.71	2.680	2.399	2.680
0.5	6.840	8.702	6.838
0.355	7.420	15.310	7.413
0.25	2.710	14.735	2.699
0.15	0.940	8.216	0.934
receiver	0.100	1.457	0.099
Total	100	100	100

6.3.3.2. Bursting Events and Flow Momentum UF 3-12

As expected Figure 6.32 shows that the average values of instantaneous nearbed streamwise velocity and the average instantaneous bed shear stress were generally increased with increasing flowrates and decreased with the decreasing flowrates. The average instantaneous streamwise velocity distribution coincides with the increasing and decreasing sections of the flow hydrograph. It is also shown that the peak of distribution is at time elapsed 540 minutes, the time which the peak flowrates was attained. Although there are some points at which the

average instantaneous bed shear stress was lower than expected, most notably at time elapsed 640 minutes, the average values generally following the trend. Similar to the antecedent flow experiments UF 3-6 and UF 3-9 all distribution values presented in Figure 6.32 accommodate only the measurement at sufficient water depths. Because of the slower increased of the rising limb and, thus a slower increased in water depths, a relatively long duration of 220 minutes in the early period is not presented as the water depth was still below the ADV probe position. In the falling limb of antecedent flow experiment UF 3-12 the measurement were possible until time elapsed 650 minutes.

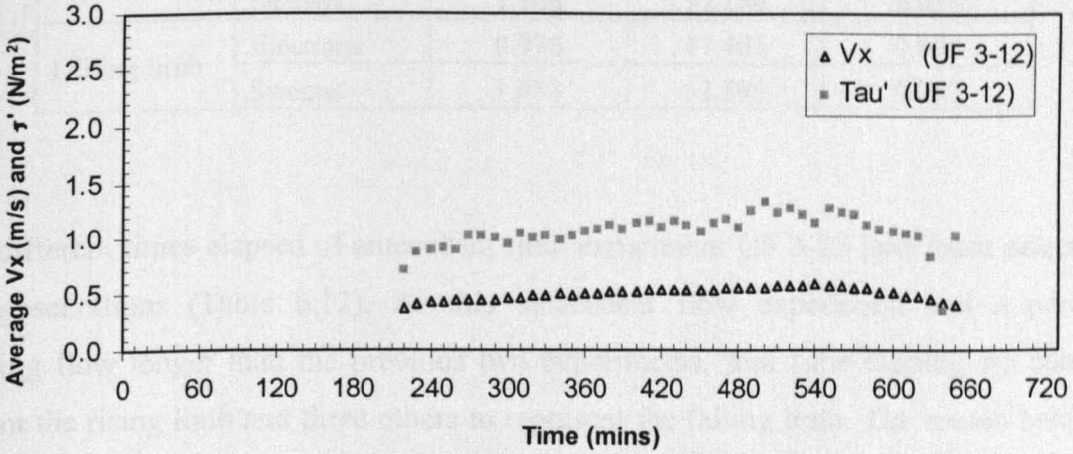

Figure 6.32. Variation of time averaged nearbed streamwise velocity and bed shear stress during antecedent flow Experiment UF 3-12

Closer observation on the nearbed flow was carried out as the information on the average nearbed streamwise velocity and bed shear stress do not provide an information on how the composition changes in relations to the pattern of nearbed flow. A similar pattern in which the occurrences of downward-looking bed interactions (sweeps) are more frequent than the upward interactions (ejections) were also experienced in antecedent flow Experiment UF 3-12. The proportion of the ejections in the rising and falling limb are relatively stable with less than a 0.5 % decrease in the falling limb. This decrease is matched by a decrease in the frequency of occurrence. In the rising limb the ejections are slightly more frequent with the time frequency of 1.015 Hz and this decreased in the falling limb to 0.976 Hz. It is clear in Table 6.11 that the frequency of sweeps is slightly less in the falling limb than in the rising

limb. It decreased from 1.108 to 1.083 Hz. However the decrease is not matched by a decrease in the proportion. In the falling limb the proportion of sweeps in the falling limb is more frequent than in the rising limb.

Table 6.11. Time frequency and the proportion of occurrences of bursting events in antecedent flow Experiment UF 3-12

Parameter descriptions		Frequency (Hz)	Proportion (%)	Average duration (sec.)
Rising limb	Ejections	1.015	47.811	0.051
	Sweeps	1.108	52.189	0.053
Falling limb	Ejections	0.976	47.405	0.053
	Sweeps	1.083	52.595	0.052

Seven different times elapsed of antecedent flow experiment UF 3-12 have been selected for detail observations (Table 6.12). As this antecedent flow experiment had a period of increasing flow longer than the previous two experiments, four time elapsed are chosen to represent the rising limb and three others to represent the falling limb. The reason behind the selection was different types of distribution of grain size were produced at each time elapsed particularly changes of the mode in transport. The grain size distribution curves for the observed time elapsed are presented in Figure 6.33.

Table 6.12. Summary of bursting events at selected time elapsed in antecedent flow Experiment UF 3-12

Parameter descriptions	Time elapsed (minutes)						
	250	300	370	430	550	620	650
Threshold values (m^2/s^2)	0.0043	0.0051	0.0055	0.0059	0.0071	0.0049	0.0059
Number of ejections	190	217	192	220	195	194	141
Number of sweeps	196	235	225	241	233	229	163
Frequency of ejections (Hz)	0.950	1.085	0.960	1.100	0.975	0.970	0.705
Frequency of sweeps (Hz)	0.980	1.175	1.125	1.205	1.165	1.145	0.815
Average duration of ejections (s)	0.052	0.050	0.051	0.054	0.053	0.053	0.048
Average duration of sweeps (s)	0.051	0.049	0.053	0.053	0.050	0.053	0.055

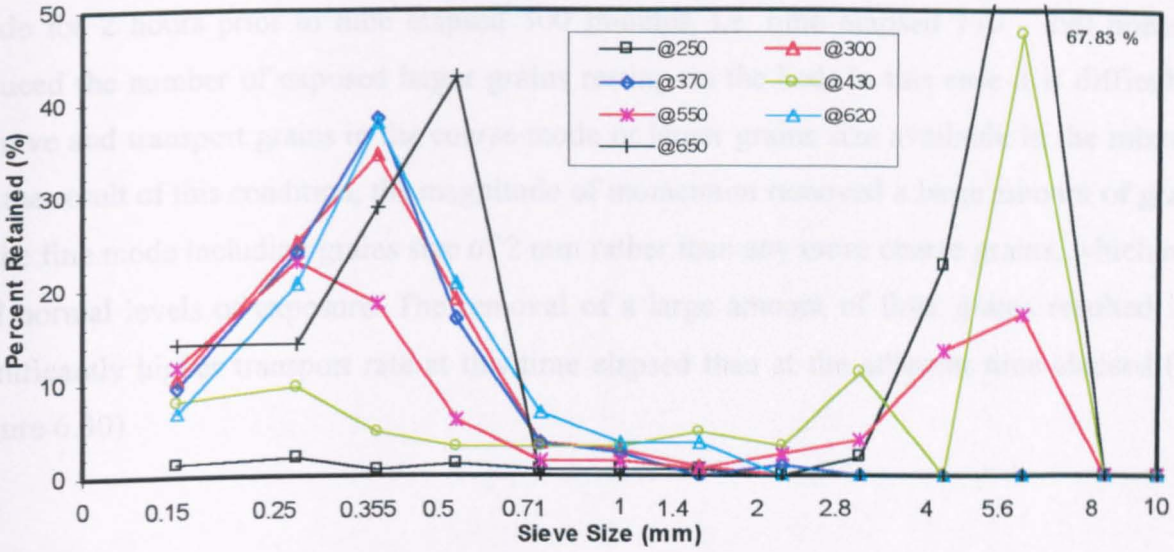

Figure 6.33. Grain size distribution of transported bedload at selected time elapsed in antecedent flow Experiment UF 3-12

It can be seen in Figure 6.33 that at time elapsed 250 minutes the transport is dominated by grains in the coarse mode. Although the flowrates was relatively low at 0.0150 m^3/s, the factor behind the transportation of grains in the coarse mode was not solely due to the instability of the grains caused by the early and continuous transport of finer grains increasing the level of exposure of the larger grains. Observation to the probability distribution of momentum per unit area shown in Figure 6.34, suggests a considerable proportion of momentum in the range between 5 and 9 kg/ms established at time elapsed 250 minutes. As the previous finding shows that grains in the coarse mode were transported by a higher level of momentum of ejections, i.e. at least 13 kg/ms, it is believed that the coarse grains were relatively unstable. This suggests that the level of exposure of the coarse grains was higher so that the momentum ejections in the range of 5 and 9 kg/ms were able to transport these grains.

Interesting features is shown by time elapsed 300 minutes. In Figure 6.34 it is very clear that a considerable proportion of ejections have momentum with magnitude ranging from 7 - 9 kg/ms. It was expected that such momentum would also be able to transport coarser grains similar to time elapsed 250 minutes. In fact only finer grains were transported at this time elapsed. By looking at the pattern of transport at different time elapsed, which has been discussed in sub chapter 6.4.1, it can be explained that the domination of grains in the coarse

mode for 2 hours prior to time elapsed 300 minutes, i.e. time elapsed 170 - 290 minutes, reduced the number of exposed larger grains resting on the bed. In this case it is difficult to remove and transport grains in the coarse mode or larger grains size available in the mixture. As the result of this condition, the magnitude of momentum removed a large amount of grains in the fine mode including grains size of 2 mm rather than any more coarse grains, which now had normal levels of exposure. The removal of a large amount of finer grains resulted in a significantly higher transport rate at this time elapsed than at the adjacent time elapsed (see Figure 6.30).

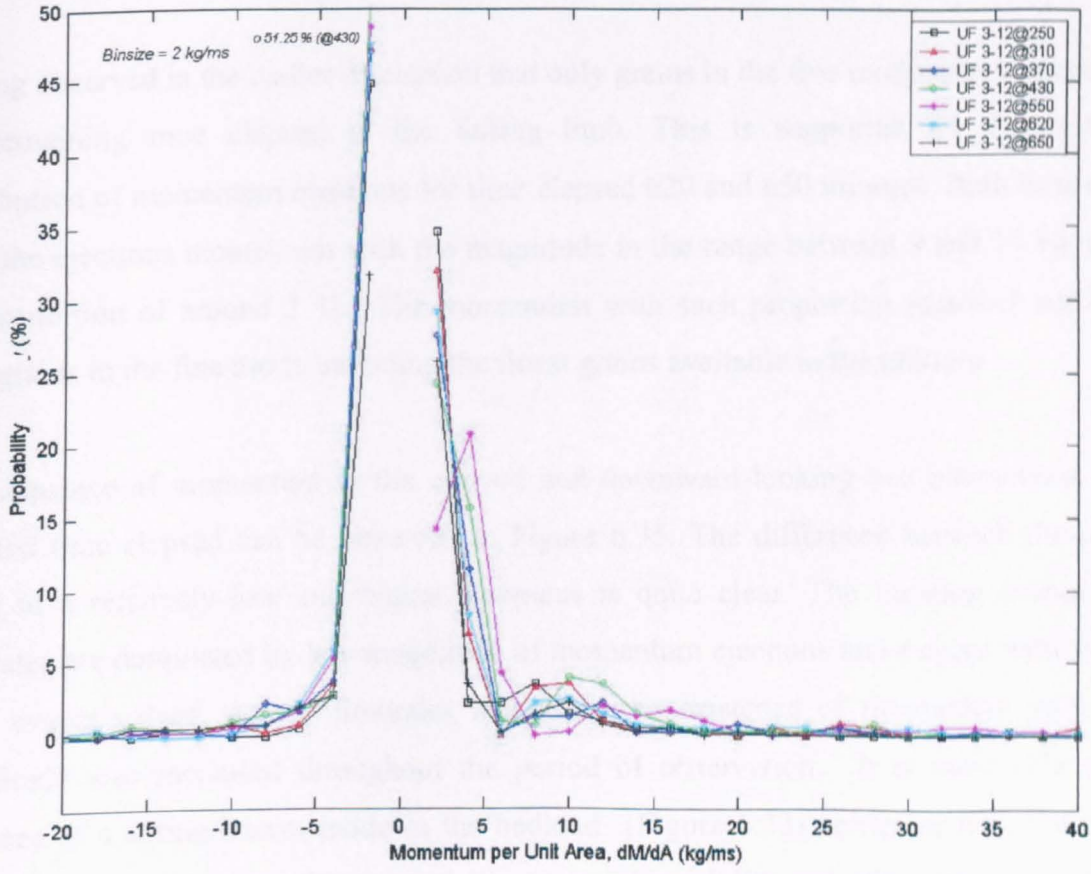

Figure 6.34. Probability distribution of momentum per unit area at selected time elapsed in antecedent flow Experiment UF 3-12 (ejections are positive and sweeps are negative)

In Figure 6.34 time elapsed 430 minutes there was a measurable proportion of higher momentum ejections ranging from 9 to 13 kg/ms. These momentum levels were sufficiently

high to remove and transported a high proportion of larger grains including grains of diameter 5.6 mm in the coarse mode (see Figure 6.33). It was expected that the higher flowrates would produce bursting events with higher magnitudes of momentum. The observation at time elapsed 550 minutes, which was the initial stage of falling limb, indicates that the momentum of ejections with the magnitude ranging from 5 to 7 kg/ms is considerably more frequent than at any other time elapsed. It is also noticed that the distribution of momentum ejections with the magnitude between 3 and 7 kg/ms are apparent as indicated by the position of the curve, which is slightly shifted to the right hand side. Although grains of diameter 4 and 5.6 mm existed in transport at this time elapsed, the amount is very small and only weak coarse grains were transported by the momentum ejections with the magnitude between 5 and 7 kg/ms.

Having observed in the earlier discussion that only grains in the fine mode were transported in the remaining time elapsed in the falling limb. This is supported by the probability distribution of momentum ejections for time elapsed 620 and 650 minutes. Both time elapsed have the ejections momentum with the magnitude in the range between 9 and 11 kg/ms with the proportion of around 2 %. The momentum with such proportion removed and carried only grains in the fine mode including the finest grains available in the mixture.

The sequence of momentum in the upward and downward-looking bed interactions for the selected time elapsed can be observed in Figure 6.35. The difference between the bursting event in a relatively low and higher flowrates is quite clear. The bursting events at low flowrates are dominated by low magnitude of momentum ejections and sweeps with very few large events values. As the flowrates increased, the existence of momentum with higher magnitude also increased throughout the period of observation. It is noticeable that the presence of a strong coarse mode in the bedload (Figure 6.33) coincides with the times at which there are a few very large ejections at time elapsed 430 and 550 minutes and to some extent at 250 minutes.

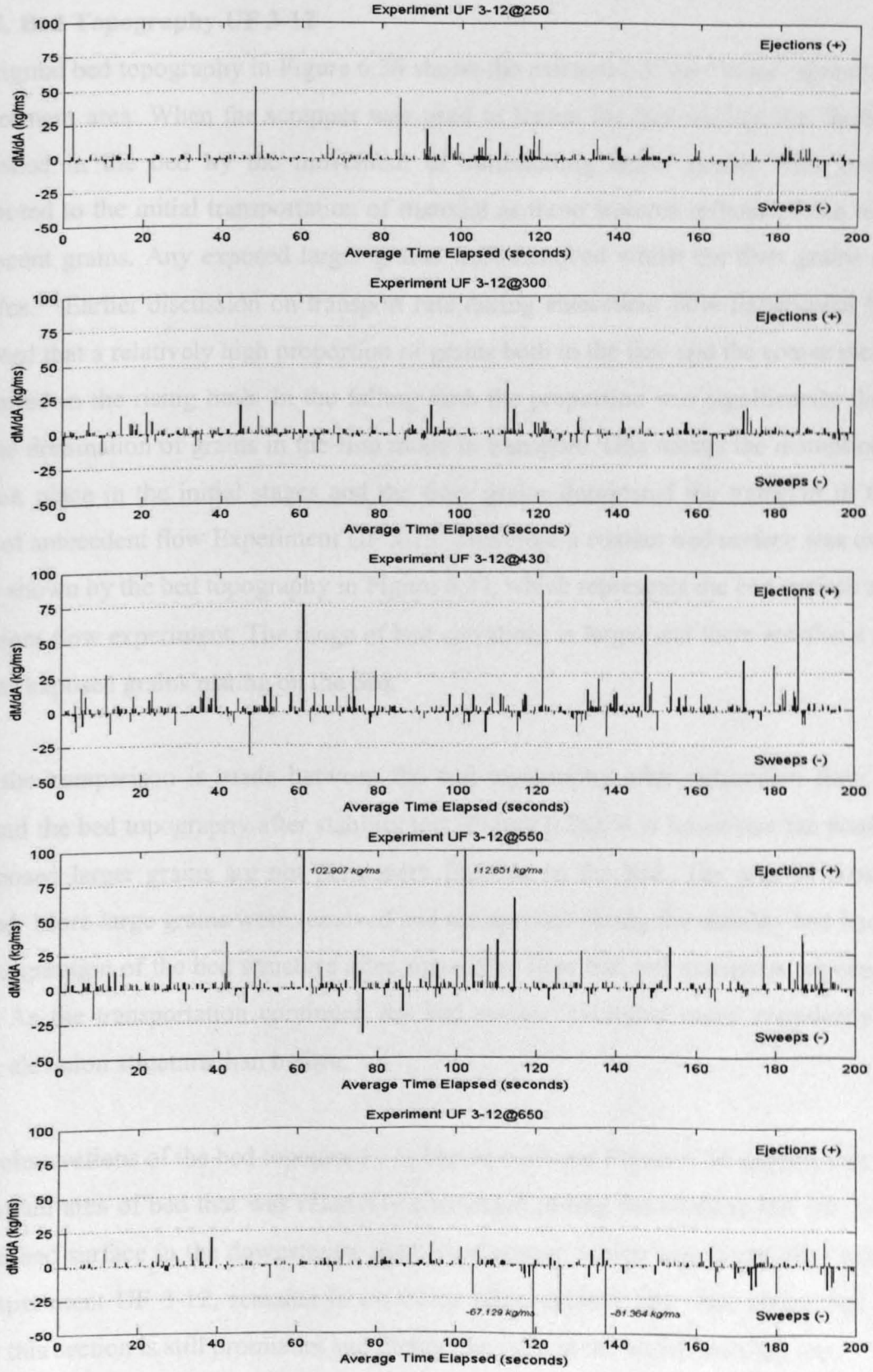

Figure 6.35. The sequence of momentum per unit area and its magnitude at selected time elapsed in antecedent flow Experiment UF 3-12

6.3.3.3. Bed Topography UF 3-12

The original bed topography in Figure 6.36 shows the existence of the "holes" spread over the measurement area. When the scrapper was used to flatten the bed surface the "holes" were established in the bed by the movement of surrounding larger grains. This irregularity contributed to the initial transportation of material as these features influenced the resistance of adjacent grains. Any exposed larger grains were removed whilst the finer grains re-filled the holes. Earlier discussion on transport rate during antecedent flow Experiment UF 3-12 suggested that a relatively high proportion of grains both in the fine and the coarse mode were transported in the rising limb. In the falling limb the proportion was significantly decreased with the domination of grains in the fine mode in transport. This means the disruption of the bed took place in the initial stages and the finer grains dominated the transport in the later stages of antecedent flow Experiment UF 3-12. Therefore a coarser bed surface was expected. This is shown by the bed topography in Figure 6.37, which represents the bed surface after the antecedent flow experiment. The range of bed elevations is larger and there are also a number of larger exposed grains resting on the bed.

When the comparison is made between the bed topography after antecedent flow (Figure 6.37) and the bed topography after stability test (Figure 6.38), it is found that the positions of the exposed larger grains are not permanent features on the bed. The area of erosion has enlarged. More large grains were removed and transported during the stability test because of the configuration of the bed structure after antecedent flow had left numerous exposed larger grains. As the transportation continued the bed surface exhibited more irregularity in bed surface elevation structure than before.

Closer observations of the bed topography in Figure 6.37 and Figure 6.38 suggest that there is also a small area of bed that was relatively unchanged during the stability test UF 3-12. The exposed bed surface in the downstream right hand corner, which was found after antecedent flow experiment UF 3-12, remains in existence after stability test. The higher bed surface level in this section is still prominent and distinctive even at the end of stability test.

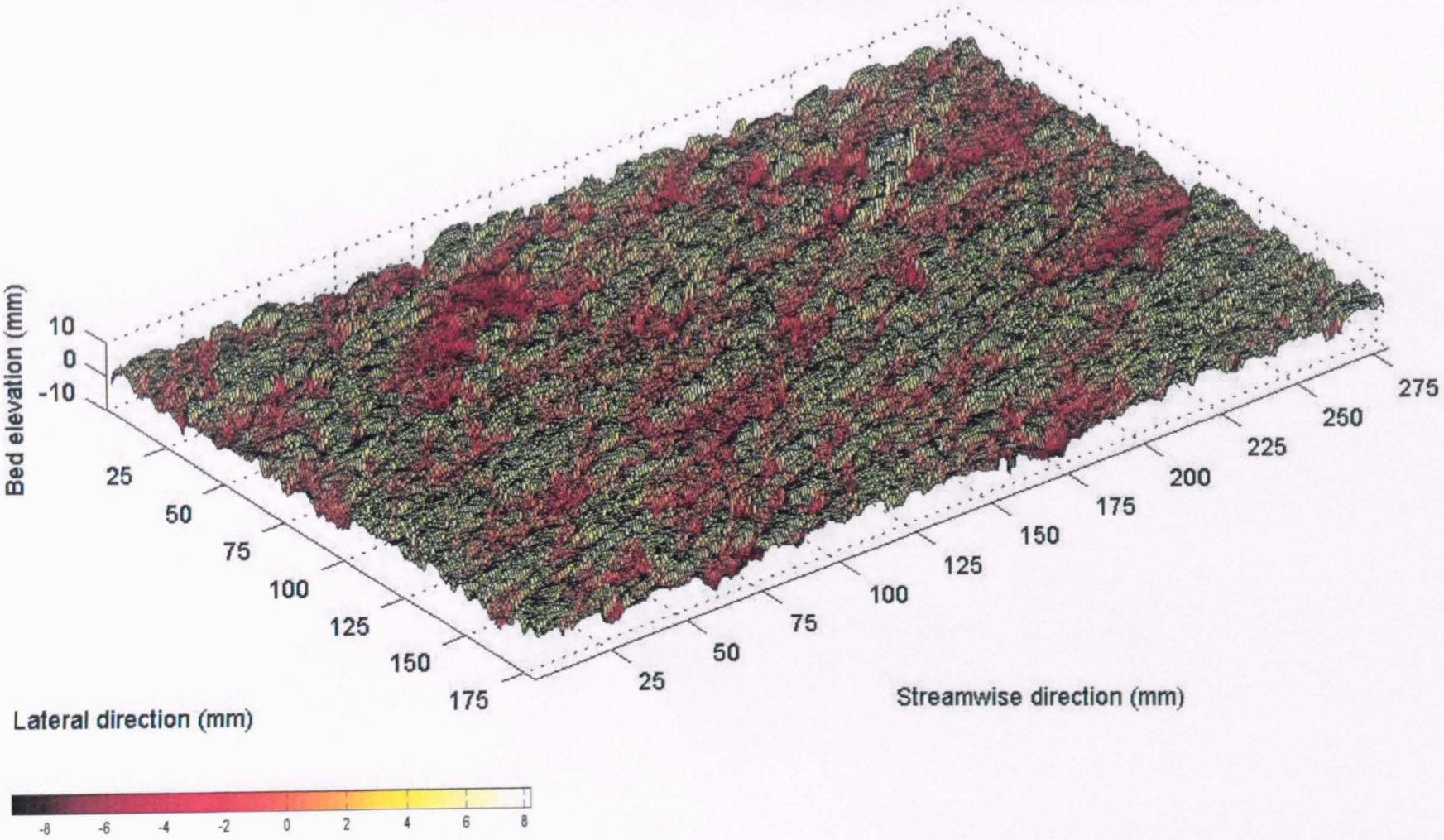

Figure 6.36. Original bed surface topography of the measurement grid Experiment UF 3-12

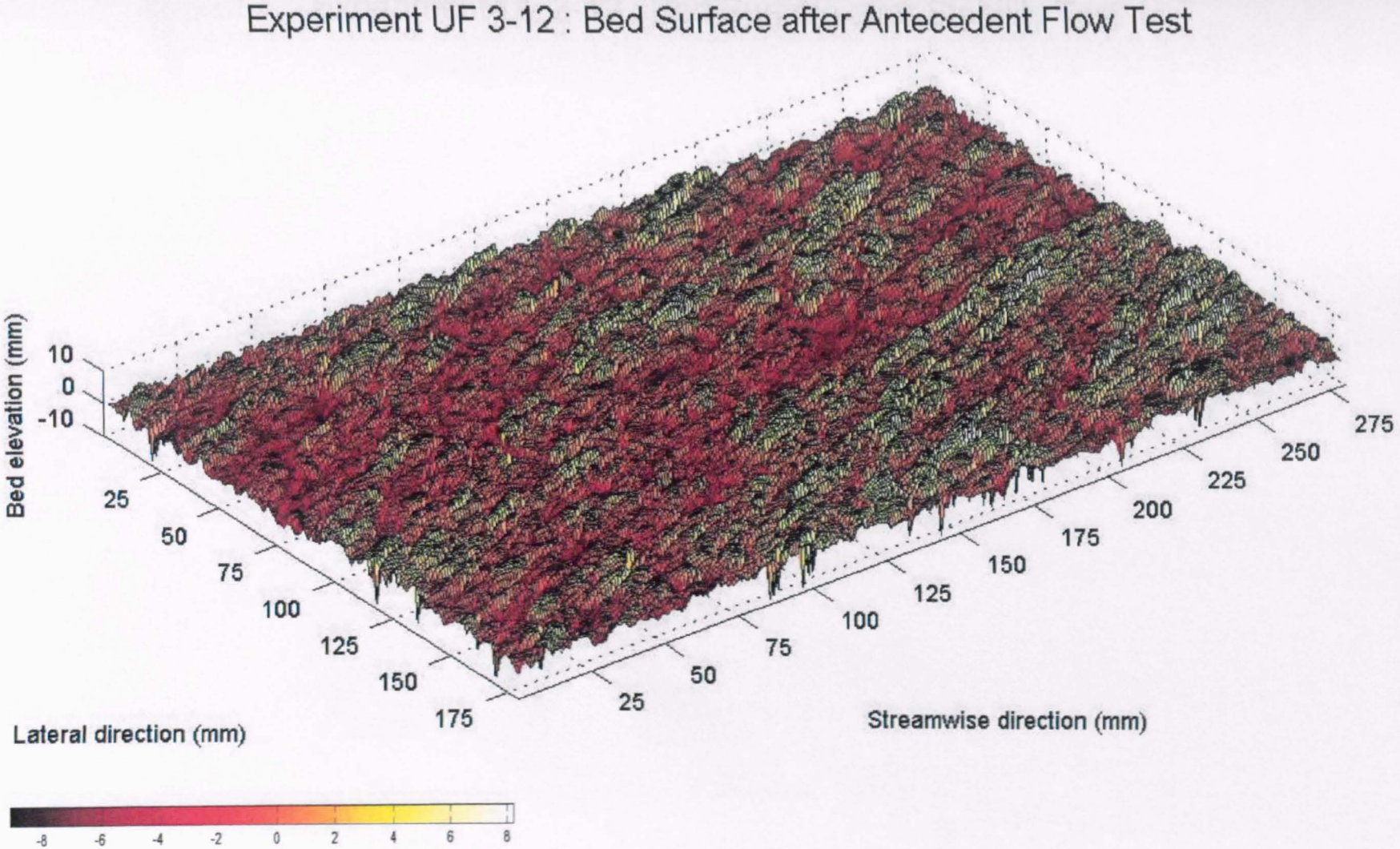

Figure 6.37. Bed surface topography of the measurement grid after antecedent flow Experiment UF 3-12

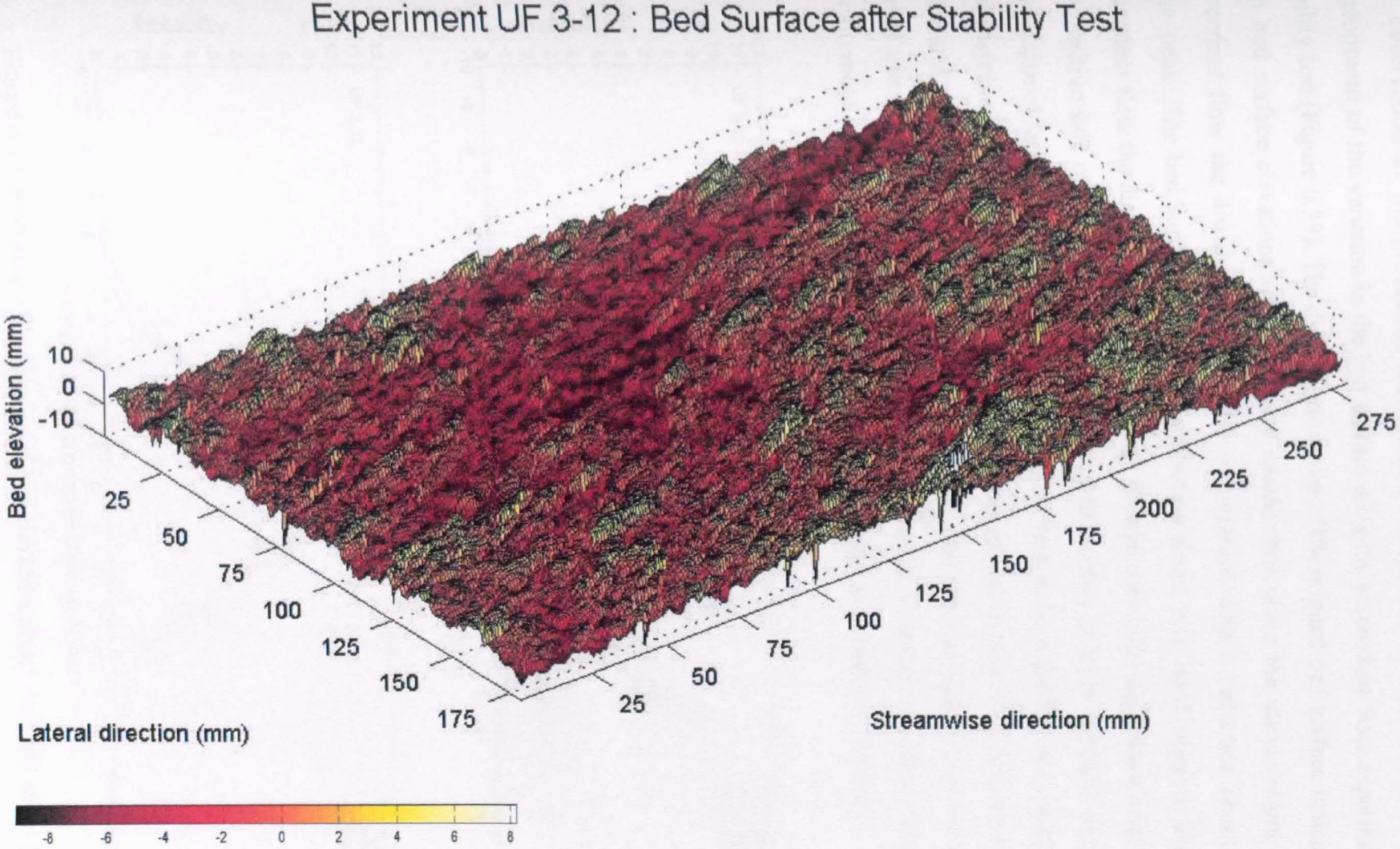

Figure 6.38. Bed surface topography of the measurement grid after stability test Experiment UF 3-12

The observation of the probability distributions of the bed surface elevation reveals the development of the variation in the bed surface after the antecedent flow experiment and the stability test (Figure 6.39). The distribution curve of the original bed surface indicates that the high bed surface elevations were generally spread throughout the measurement area. After antecedent flow the distributions are more symmetrical with a reduction about the modal value peak. The bed surface elevation distribution about zero level suggests that after the antecedent flow the distributions are negatively skewed indicating significant areas of erosion. The positive side of the distribution shows a small number of more exposed areas, probably more exposed larger grains. The continued erosion during the stability test is indicated by the final distribution curve that is further skewed to the negative side. This distribution becomes flatter and wider by increasing the areas of erosion and the numbers of exposed grains. This type of distribution is the characteristic of the bed with the spread of valleys throughout the measurement area as well as the existence of exposed surface grains on the bed.

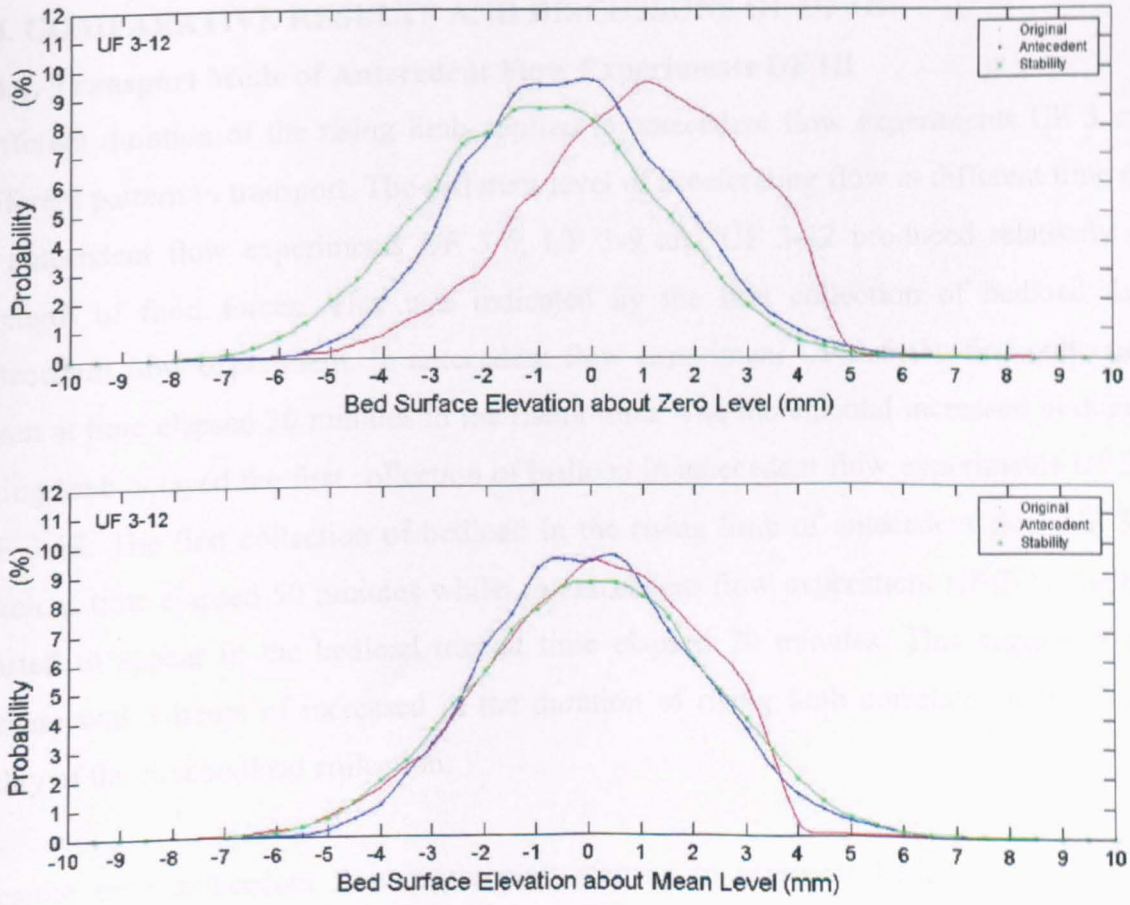

Figure 6.39. Probability distribution of bed elevation about zero and mean level for Experiment UF 3-12

By looking at the distribution of bed surface elevation about the average level, it is apparent that after antecedent flow experiment a considerable number of larger exposed grains are resting on the bed. This is indicated by the gap in the positive tail of the distribution, which exhibits a substantial number of positive bed variations from the mean. The drop in the bed surface is also shown in Figure 6.39. The distribution of bed surface elevation after antecedent flow is wider not only with the positive elevations but also with the negative levels indicating the spread of areas of eroded bed. After the stability test the distribution is more symmetrical with the extreme high and low bed surfaces decreasing slightly. The peak distribution is lowered and the bed surface around 2 and 4 mm above and below the mean level are proportionately increased. It is also noticed that the bed surface level around 1 and 2 mm above and below the mean was increased indicating a more organised bed surface is obtained at the end of the stability test.

6.4. COMPARATIVE RESULTS AND DISCUSSONS OF UF III

6.4.1. Transport Mode of Antecedent Flow Experiments UF III

Different duration of the rising limb applied in antecedent flow experiments UF 3 exhibits different pattern in transport. The different level of accelerating flow at different time elapsed in antecedent flow experiments UF 3-6, UF 3-9 and UF 3-12 produced relatively similar strength of fluid forces. This was indicated by the first collection of bedload for each antecedent flow experiment. In antecedent flow experiment UF 3-6 the first collection was taken at time elapsed 30 minutes in the rising limb. The incremental increased in duration of rising limb delayed the first collection of bedload in antecedent flow experiments UF 3-9 and UF 3-12. The first collection of bedload in the rising limb of antecedent flow UF 3-9 was taken at time elapsed 50 minutes whilst in antecedent flow experiment UF 3-12 the bedload started to appear in the bedload trap at time elapsed 70 minutes. This suggested that the incremental 3 hours of increased in the duration of rising limb correlates with 20 minutes delay of the first bedload collection.

Despite each antecedent flow experiment starting to transport bedload at different time elapsed, it was expected that this would occur at similar level of flowrates. It is found that the minimum flowrate, which was able to transport bedload was 0.0038 m^3/s. This flow contained

only finer grains in UF 3-6 and 3-12 (Figure 6.40). However a different pattern was observed in UF 3-9 where the existence of grains in the coarse mode was found in the first bedload collection. Grains in the coarse mode dominated the transport at this time elapsed but the fact that with only a mere of 0.492 gram it is believed that these grains were accidentally transported and dropped into bedload trap. This is supported by the transport pattern following this time elapsed where grains in the coarse mode were absence almost in entire period of rising limb. The small amount of grains in the coarse mode in the rising limb of antecedent flow experiment UF 3-9 was found again at time elapsed 220 minutes. After disappeared in the following period, the existence of grains in the coarse mode were considerably dominant at time elapsed 340 minutes or relatively shortly before the peak flowrate was attained. The general pattern seen in Figure 6.40 is that the fine mode started with a relatively high proportion and then dropped after about 120 minutes. The proportion increased again from 240 minutes toward the end of each test. Meanwhile the coarse mode in experiments UF 3-9 and UF 3-12 shows an erratic pattern in the rising limb while experiment UF 3-6 has a period of coarse mode domination just before the peak flowrate. In the initial and the final stages of each test the coarse mode were generally not transported although in certain time elapsed it is occasionally existed in transport.

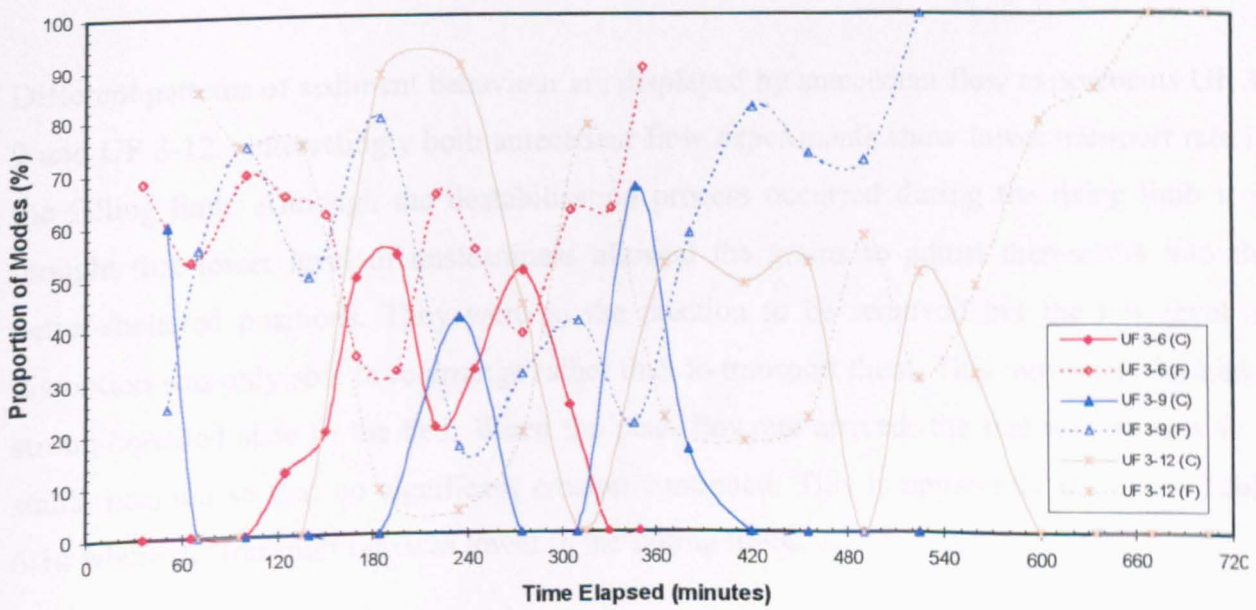

Figure 6.40. Proportion of two modes during the unsteady antecedent flow Experiments UF III (coarse and fine mode are represented by solid and dotted line)

By looking at the hourly average transport rate it can be seen that in antecedent flow Experiment UF 3-6 the hourly average transport rate was relatively high (Table 6.13). This is thought to be due to the relatively higher level of accelerating flows. An interesting feature is that the transport rate in the falling limb is higher than in the rising limb. It is believed that the accelerating flows with short duration have the capability to destabilise the bed structure. However, the short duration limits the time to transport all materials available on the bed. This resulted in unstable materials resting on the surface at the end of the test. The condition of the bed was weakened by the peak flowrate so that the corresponding flowrate in the falling limb were able to transport more grains both in the fine and the coarse mode. As seen in Table 6.13 the transport rate in the falling limb of antecedent flow Experiment UF 3-6 is extremely higher than the transport rate in the rising limb.

Table 6.13. Summary of bedload for unsteady antecedent flow Experiments UF III

Experiment No.	Mass transported bedload of mode (g)				Transport rate (g/s/m)	
	Rising limb		Falling limb		Rising limb	Falling limb
	Fine	Coarse	Fine	Coarse		
UF 3-6	64.059	63.980	105.159	113.252	0.07535	0.12399
UF 3-9	3.949	6.939	3.461	0.668	0.00351	0.00269
UF 3-12	10.324	12.497	3.556	1.042	0.00474	0.00279

Different patterns of sediment behaviour are displayed by antecedent flow experiments UF 3-9 and UF 3-12. Interestingly both antecedent flow experiments show lower transport rate in the falling limb. Although the destabilisation process occurred during the rising limb it is thought that lower level of unsteadiness allowed the grains to adjust themselves into the better-sheltered positions. They were in the position to be removed but the low level of disruption was only able to re-arrange rather than to transport them. This movement formed a strong-bounded state in the bed. When the peak flowrate arrived, the bed was already in a stable position so that no significant erosion continued. This is apparently shown in Table 6.14 where the transport rate was lower in the falling limbs.

In terms of bedload proportion, antecedent flow Experiment UF 3-6 transported more grains in the fine and in the coarse modes. Although grains in the coarse mode were hardly seen in

the individual time elapsed, their domination at the higher flowrate ensures a high proportion of total transport (Table 6.13). Meanwhile experiments UF 3-9 and UF 3-12 transported grains at very low transport rates in comparison to the Experiment UF 3-6. They also have lower proportions of sediment in both modes. Quite interestingly the antecedent flow experiments UF 3-9 and UF 3-12 have a relatively similar proportion in both modes with slightly less proportion of grains in the coarse mode transported throughout experiment UF 3-12 than in experiment UF 3-9. This suggests that longer exposure of the bed to the flow carried grains in both modes but in the coarse mode not all of the grains size were represented. In antecedent flow UF 3-12 the maximum size of grains in transport was 5.6 mm. In antecedent flow UF 3-9 grains with sieve size 8 mm existed in transport which and had a proportion of more than 7 % of the total bedload.

6.4.2. Stability of the Antecedent Flow Beds and Mode of Transport

From data collected in the stability tests UF 3 it is found that the bed formed by antecedent flow UF 3-6 is the weakest. Generally there was a significant increase in transport rate when the flowrates approached their peak. In all the stability tests the highest transport rate was found at time elapsed 70 minutes, shortly after the peak flowrates was attained. The transport rate is much higher than at the corresponding flowrates in the rising limb (see Figure 6.1). This suggests the importance of the high fluid forces in destabilising the bed structure. Observation of the stability test UF 3-9 indicated that the average transport dropped dramatically in comparison to that in stability test UF 3-6, although a similar trend in the transport rates around the peak flowrates was seen. The average transport rates for the whole duration of stability test UF 3-9 is less than half of the amount transported during the stability test UF 3-6.

Having observed this pattern it was thought that the level of bed stability would increase for the longer duration of accelerating flowrates and hence a lower transport rate than those observed in the stability tests UF 3-6 and UF 3-9 was expected in the stability test UF 3-12. In fact the data from experiment UF 3-12 exhibits a different pattern. The average transport rate is lower than the stability test UF 3-6 but slightly higher than in the stability test UF 3-9. For the whole duration of stability test UF 3-12 the average transport rate is 0.507 gr/s/m

compared with an average transport rate of 0.345 gr/s/m for UF 3-9. It could be argued that the levels of sediment mobility were similar.

The transport pattern established by stability test UF 3-12 suggests that the bed formed by antecedent flow Experiment UF 3-12 was slightly less stable than the bed formed by antecedent flow Experiment UF 3-9. It is believed that the inability of antecedent flow Experiment UF 3-12 to carry the larger grains and therefore the presence of more larger, exposed grains on this bed is the main factor behind this phenomenon. In the previous discussion it was found that there was an absence of larger grains in the bedload in the antecedent flow experiment UF 3-12. This is indicated by the early transport of coarse grains in the stability test UF 3-12. The transport of finer grains for the whole duration increased the exposure of larger grains. This correlates with the transport pattern during stability test as presented in Table 6.14. It is very clear that the larger grains were transported and were dominant from the relatively low discharges. The larger grains dominated the transport from time elapsed 20 minutes when the flowrates was only 0.0063 m^3/s and thus lasted for 90 minutes.

Table 6.14. Transport mode of the stability tests applied to unsteady antecedent flow-formed bed UF III

Stability Test	Time elapsed of coarse grain domination (mins)	Mass of bedload (g) and proportion (%)				Total	
		Fine mode		Coarse mode		Fine mode	Coarse mode
		Rising	Falling	Rising	Falling		
UF 3-6	@50 - @90 & @120	82.35 g	141.14 g	315.13 g	460.80 g	223.49 g	775.93 g
		7.130 %	12.220 %	27.285 %	39.897 %	19.350 %	67.182 %
UF 3-9	@60 - @110	14.80 g	24.61 g	90.62 g	303.79 g	39.41 g	394.41 g
		3.133 %	5.209 %	19.181 %	64.301 %	8.342 %	83.482 %
UF 3-12	@20 - @110	11.83 g	42.34 g	84.52 g	488.73 g	54.17 g	573.25 g
		1.706 %	6.105 %	12.186 %	70.465 %	7.810 %	82.651 %

It is apparent in Table 6.14 that in all tests the transport rate is always higher in the falling limb than in the rising limb irrespective of the bed stability level. It is clear that the high flowrates around the peak of the flow hydrographs roughly disrupted and then weakened the

bed. Stable coarse grains were dislodged and the instability of the grains increased. As a result of these conditions, more grains were transported in the falling limb even at lower fluid discharges.

6.4.3. Bursting Events and Flow Momentum UF III

Observation of the bursting events for all the antecedent flow experiments suggested that sweeps (downward-looking bed interactions) were more common than ejections (upward interactions). Initially it was assumed that the accelerating flows tend to produce more upward interactions than downward looking-bed interactions. This is based on the findings in the previous chapter in which the decelerating flows produced more downward-looking bed interactions than upward interactions. Detailed examination on different time elapsed in all these antecedent flow experiments showed that the domination of ejections occasionally occurred both in the rising and in the falling limb. This means the ejections have the opportunity to dominate at certain periods although overall they are not as frequent as the sweeps.

Table 6.15. Summary of bursting events of unsteady antecedent flow Experiments UF III

Parameter descriptions		UF 3-6		UF 3-9		UF 3-12	
		Rising limb	Falling limb	Rising limb	Falling limb	Rising limb	Falling limb
Ejections	Frequency (Hz)	1.049	0.999	0.990	1.031	1.015	0.976
	Proportion (%)	48.596	49.019	47.343	48.189	47.811	47.405
	Average duration (s)	0.052	0.052	0.055	0.053	0.051	0.053
Sweeps	Frequency (Hz)	1.110	1.039	1.102	1.108	1.108	1.083
	Proportion (%)	51.404	50.981	52.657	51.811	52.189	52.595
	Average duration (s)	0.054	0.053	0.056	0.054	0.053	0.052

It can be seen from Table 6.15 that the bursting events in the rising limb of antecedent flow Experiment UF 3-9 contains less frequent ejections than in the rising limb of antecedent flow experiments UF 3-6 and UF 3-12 while the frequency of sweeps is relatively constant. More frequent ejections were established during antecedent flow Experiment UF 3-12. Higher frequencies are found in the rising limb of antecedent flow Experiment UF 3-6. To some extent these pattern are believed to correlate with the transport rate pattern in which the rising

limb of antecedent flow Experiment UF 3-6 has the highest rate followed by the rising limb of antecedent flow Experiment UF 3-12. The lowest frequency of bursting events was observed in the rising limb of antecedent flow Experiment UF 3-9 and this produced the lowest transport rate.

Different and more complex patterns are shown in the falling limb. In antecedent flow Experiment UF 3-9 the falling limb contains more frequent events than in the same section of antecedent flow experiments UF 3-6 and UF 3-12. These patterns are very interesting as the transport rate patterns exhibit different features indicating no coincidence. This suggests that the link between event frequency and transport is slight or that the bed stability level formed by different level of unsteadiness in each accelerating flowrate section was the controlling factor. The shorter rising limb caused a higher disruption to the bed increasing the instability of the grains. The fluid forces in the following decelerating flowrate section transported these grains more easily. Longer period of accelerating flowrate allowed the bed to properly re-organise so that grains obtained stable positions.

It is also noticed that the existence of bursting events with the momentum magnitude less than 5 kg/ms were very popular and most common throughout the antecedent flow experiments irrespective of the form and duration of the hydrograph. Given that each antecedent flow has different pattern in transport, it is believed that the high transport mostly caused by the rigorous bursting events with high magnitude of momentum ejections. As the armoured or stable bed condition progressed the contribution of bursting event in transport may be decreased. The influence of high momentum of upward interactions may not be as significant as the early period of experiment where the bed were just started to re-arranging themselves and relatively less stable. In this case the ability of the relatively higher momentum to transport materials is also depending on the bed states. One important thing is that the existence of high momentum especially in the upward interactions determines the modes of transported bedload. The proportion of occurrences seems to be less important as all the antecedent flow tests have relatively similar proportion both in ejections and sweeps. It can also be seen that the duration of events is similar so that it is unlikely that this factor influenced the transport rate pattern. In this case it is very clear that the more the momentum of ejections with high magnitude, i.e. 13 kg/ms or higher, the more the grains in the coarse

mode are removed and then dominate the transport.

6.4.4. Bed Topography UF III

The bed topography observations of the Experiments UF 3 clearly indicated that the original beds were changed. In experiment UF 3-6 it can be seen that an area of erosion spread and that numerous large exposed grains were found on the bed (Figure 6.17). This was indicated by the distribution curve of the bed surface level after the antecedent flow. The curve was more symmetrical with the tails on both sides are widened indicating more valleys and more peaks had appeared on the bed (Figure 6.41).

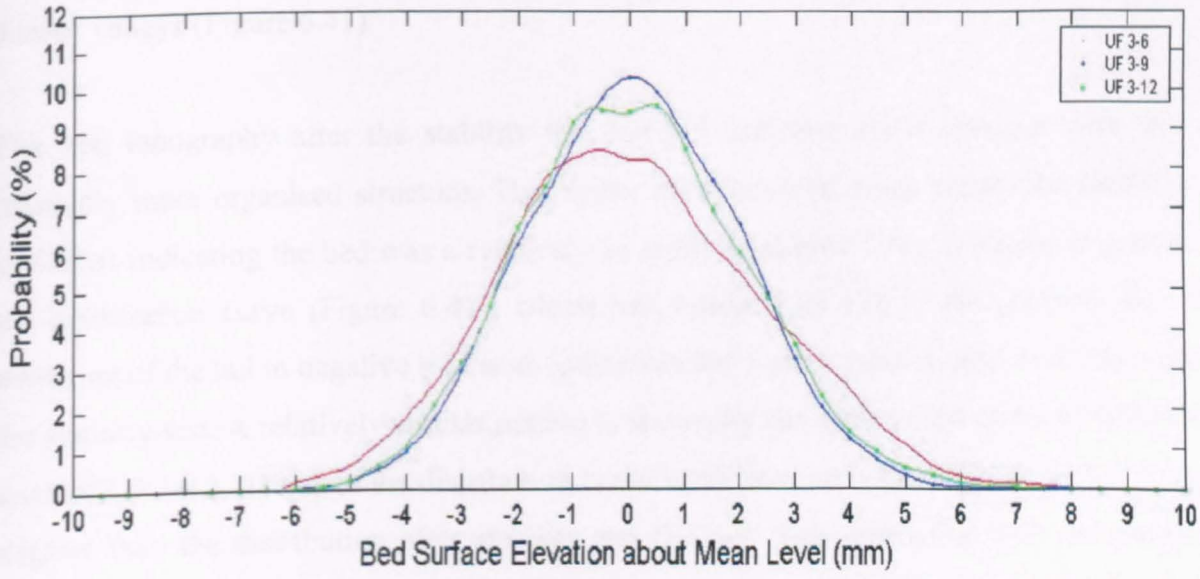

Figure 6.41. The comparison of the bed surface elevation distribution about mean level after antecedent flow Experiments UF III

The bed topography produced by antecedent flow experiments UF 3-9 and UF 3-12 are very different than the bed topography produced by antecedent flow experiments UF 3-6. Less erosion is shown, particularly after the antecedent flow Experiment UF 3-9. This is due to only small amounts of materials being transported during the antecedent flow experiment. The valleys are more spread over the bed after antecedent flow Experiment UF 3-12 in comparison to the bed after the antecedent flow Experiment UF 3-9. Isolated larger grains also appeared on more locations. This higher proportion is shown by the distribution curve. It

also noticed that the distribution of bed surface elevations after antecedent flow Experiment UF 3-9 is narrowed with an increased in the peak. This type of distribution is the characteristic of a flatter bed as the proportion of the surface close to the average level increased.

The highly unstable bed formed by antecedent flow Experiment UF 3-6 was the main factor why the bed surface topography after the stability test show significant further degradation. The exposed grains transported by available fluid forces increasing the level of erosion. The bed topography plots display darker areas reflecting the lower level of valleys formed in the bed. This is supported by the changes in the distribution curve. Although the peak of the curve decreased, both tails especially in the negative side are widened indicating the existence of deeper valleys (Figure 6.41).

The bed topography after the stability test UF 3-9 indicates some changes with still the relatively more organised structure. The higher level exposed areas before the stability test still exist indicating the bed was a relatively in stable condition. This is clearly supported by the distribution curve (Figure 6.41), which has widened its tail in the positive side. The widening of the tail in negative side is an indication that further erosion also took place during the stability test. A relatively similar pattern is shown by the distribution curve of bed surface level of UF 3-12. Although the distribution curve is widened in both tails, the peak is lowered slighter than the distribution after stability test UF 3-9. This correlates with the pattern of transport during the stability test where the proportion of grains in the fine mode in transport is higher than the proportion of grains in the coarse mode. This means the transportation of finer grains were not changing the average bed surface as much as the change in the stability test UF 3-6 and UF 3-9. This understandable as in these two stability tests grains in the coarse mode transported most than grains in the fine mode leaving more gaps or valleys at the end of the stability tests.

6.5. SUMMARY OF EXPERIMENTS UF III

Complex patterns in transport were observed. In antecedent flow Experiment UF 3-6 large amounts of material were transported in comparison to the antecedent flow experiments UF 3-

9 and UF 3-12. The lowest transport rate was experienced by UF 3-9. These patterns continued in the stability tests. The bed formed by antecedent flow experiments UF 3-9 and UF 3-12 which contained longer periods of acceleration in the rising limb exhibited relatively stable beds. Low transport rates in the rising limb of stability tests were shown by these experiments. The transport rates significantly increased in the falling limb indicating the influences of the peak flowrate.

Three stages of stabilisation process in the accelerating flowrate section were experienced. Three hours of accelerating flowrate in UF 3-6 roughly disrupted the bed. The instabilities of the grains increased. The short duration did not allow the grains to find stable positions and the flowrate easily transported them into the bedload trap. This is indicated by the stability tests in that the weakest bed was formed by the shortest accelerating flowrate. The first thought that the longer duration of accelerating flowrates formed the most stable bed are dismissed by the fact that the bed formed by antecedent flow Experiment UF 3-12 is slightly less stable than the bed formed by antecedent flow Experiment UF 3-9. This suggests that the duration of accelerating flowrate is important in the bed stabilisation process. It is believed that the level of unsteadiness in the 6 hours accelerating flowrate was sufficient to move coarse and then fine grains to form strong bounds between different fraction in the mixtures. The grains were dislodged and dislocated but the flows were not strong enough to carry considerable amounts downstream. As indicated by the bed surface distribution curves these grains were sheltered and obtained better and more stable positions instead. They formed relatively flat surfaces and were less exposed. The stability test was still able to destabilise and transported the grains but not in the same level to the other stability tests. It is suspected that a similar way of stabilisation occurred in the accelerating flowrates section of antecedent flow Experiment UF 3-12. However longer exposure to the high flowrate re-adjusted the positioning of some of these grains. More exposed grains were left on the bed, which were more easily transported during the stability test UF 3-12 than in the stability test UF 3-9. These stages suggest that a maximum level of bed stability had been attained by 6 hours accelerating flowrate but the stability declined slightly as the duration of the rising limb was extended more than 6 hours. The shear stress threshold of grain size fractions considerably increased from UF 3-6 to UF 3-9. In UF 3-12 the shear stress threshold declined but the values were still generally higher than UF 3-6.

Interesting features were found in the observation of bursting events. The downward looking bed interactions were more common in the antecedent flow experiments, even in the accelerating flowrates sections. However no strong link was found between event frequency and transport. The duration of events is also found to be relatively similar in all tests. In this case it is proven that the high magnitude of momentum ejections, particularly those in the range higher than 13 kg/ms, are very important in transporting coarser grains. The transport is coarser grains-dominated if the bursting events contained the momentum ejections with high magnitude. However the ability of the relatively high magnitude of momentum to destabilise and transported the larger grains was also depending on the bed stability. As the armoured bed progressed and developed the stable condition the ability of momentum ejections decreased accordingly.

There is distinct pattern found in the bed topography observations after antecedent flow Experiment UF 3-6 in which diagonal patches existed on the bed. The patches are stretched to the downstream left-hand side of the measurement grid dividing the grid into two sections. These patches were more apparent after the stability test. To some extent diagonal patches are also found in the bed topography after antecedent flow experiments UF 3-9 and UF 3-12. However these patches are less organised and not much in existence even after stability test UF 3-9 and UF 3-12 were applied.

It is evident that the bed formation after the antecedent flow determined the level of stability of the bed. The probability distribution of bed surface level after antecedent flow test UF 3-6 indicated more exposed larger grains resting on the bed. This caused the instability as the exposed grains were less stable to resist a similar level of flowrate applied in the stability test. The less exposed bed surface produced by antecedent flow UF 2-9 contributed to the more stable bed during the stability test. In all the test the bed topography before and after the stability tests are seen to have small changes in comparison to the original bed although the amounts of bedload transported during the stability test were higher than during the antecedent flow tests. In fact, the changes are not as extreme as the changes in the previous stage as indicated by smaller different in the distribution curve before and after stability test.

VII. CONCLUSIONS AND RECOMMENDATIONS FOR FURTHER RESEARCH

7.1. CONCLUSIONS

The works presented in this thesis comprises an attempt to compare the influence of different type of hydrographs on the stability of mixed grain size bed. The following is a review of the conclusions that have been drawn from the work within this thesis and the potential implications for river engineering.

7.1.1. Stability Tests

Considering all the stability tests it is seen that the most stable bed is the bed formed by antecedent flow Experiment UF 2-12 followed by SF 1-12, SF 1-9 and SF 1-6. Less stable bed is formed by antecedent flow UF 3-9 followed by UF 2-6, UF 3-12, SF 1-3 and UF 2-9. The weakest bed is the bed formed by antecedent flow Experiment UF 3-6. These differences underlined the importance of the antecedent flow hydrograph in determining the stability of water worked bed. The low level of unsteadiness with 9 hours duration of decelerating flowrates in UF 2-12 caused less disruption to the bed. It is most likely that the grains move in the rolling fashion allowing the grains to re-adjust their position and become better sheltered. On the contrary, the high level of unsteadiness in UF 3-6 (3 hours of increase and 3 hours of decline) caused much more disruption to the bed. The grains were suspected to be moving in suspension but the rapid decrease dropped them back to the bed surface. It is believed that these processes leave the bed surface in a disorganised condition with very low resistance level when the identical stability flow applied over the bed. These findings oppose the conclusion by Graf and Suszka (1985) who claimed that the rising branch of a hydrograph bears all the important information no matter what the slope of the descending branch. In fact the observation of different duration of accelerating flow hydrographs in this experiment produced different behaviour of transport as well as different level of bed stability.

The stability of the bed formed by antecedent flow with constant flowrates correlates with the duration. It was believed that the longer duration of constant flowrate allowed the larger grains more time to attain more stable positions so that the longer the duration the stronger the

bed. The bed formed by antecedent flow Experiment SF 1-3 is the weakest followed by the bed formed by antecedent flow experiments SF 1-6, SF 1-9 and SF 1-12. It is also seen that the constant flowrate of 0.0338 m^3/s needed more than 3 hours of flow exposure to produce a relatively stable bed. This is indicated by the almost similar increased in the amount of transport for the stability tests applied to the bed formed by 6, 9 and 12 hours of antecedent flow.

The stability of the bed formed by the combination of 3 hours constant flowrates followed by different durations of decelerating flowrates indicated that UF 2-9 with the medium duration of decelerating flowrates is weaker than the bed formed by UF 2-6 and UF 2-12. This is caused by the fact that bed surface was coarser than the other two as the antecedent flow Experiment UF 2-9 transported more amount of grains in the fine mode. It is believed that the coarse grains in antecedent flow Experiment UF 2-9 had been mobilised but had insufficient time to find stable positions as the finer grains, which expected to "cement" the coarser grains into a well developed armoured layer were washed away during this test. This resulted in the formation of less stable coarse grains in which more exposed larger grains resting on the bed and had lower resistance to the high fluid forces in the subsequent stability test. This is indicated by the pattern that in the stability test UF 2-9 grains in the coarse mode was transported earlier than in the stability test UF 2-6 and UF 2-12.

Similar conditions were experienced in the stability tests applied to the bed formed by antecedent flows with different level of accelerating flowrates. The bed formed by antecedent flow Experiment UF 3-12 was stronger than UF 3-6 but less stable than the bed formed by antecedent flow Experiment UF 3-9. The proportion of both grains in the fine mode and in the coarse mode were relatively closed but antecedent flow UF 3-12 transported more grains in the fine mode than grains in the coarse mode. The bed formed by antecedent flow UF 3-12 is slightly coarser than the bed formed by antecedent flow UF 3-9. In the stability test UF 3-12 the domination of grains in the coarse mode in transport started earlier than in the stability test UF 3-9. This characterised the pattern of bed stability for each bed.

In the stability tests the higher transport rates were found after the peak discharge and higher average bedload transport rate in the later half was common to all tests except in the stability

test UF 2-12. This pattern of behaviour demonstrates that in each stability test the bed is progressively becoming weaker once the flowrates were close to the peak. Given that there was little transport at the end of each of the steady antecedent flow test, it is reasonable to assume only the flowrates about 0.0338 m^3/s have caused significant disruption to the bed surface. Despite having similar hydrographs, the level of disruption was different in each stability test. This was thought to be due to the different levels of bed stability inherent in the beds at the end of each steady antecedent flow test.

The order of stability of the test in each series of experiments match with the fractional threshold of motion. In the stability test applied to the bed formed by steady antecedent flow, all grains size fractions in the stability test SF 1-3 moved at lower threshold of motions. This suggests that the shorter antecedent flow test formed an unstable bed with the grain size fraction has a lower critical shear stress. The threshold of motion are generally increased in the stability test for the bed formed by longer antecedent flow of SF 1-6, SF 1-9 and SF 1-12 respectively. In the stability test SF 1-9 and SF 1-12 grains in the fine mode of diameter 0.5 and 0.25 mm have a similar level of hiding whereas the modal grain size of fine mode (0.355 mm) has a larger value of hiding. This fraction was less mobile in stability test SF 1-9 than in stability test SF 1-12. In this series it is shown that the hiding function of finer grains stay the same after 3 hours exposed to the constant flowrate in antecedent flow test. The fine grains stabilised between 3 and 6 hours whereas the stability of the coarse grains were still continuing in the longer tests.

In the second series, the stability test applied to the bed formed by medium duration of decelerating flow UF 2-9 indicated a lower threshold of motion for all grain size fractions. The threshold of motion increased in the stability test UF 2-6 and UF 2-12. In stability tests UF 2-6 and UF 2-12 the level of hiding for finer grains are relatively similar while for the coarser grains the values are closed in both stability tests. In the stability test UF 2-9 all grains have a lower level of hiding. This resulted in the large amounts of grains in both modes transported during the stability test UF 2-9 compared to UF 2-6 and UF 2-12.

In the third series of experiments, the stability test UF 3-6 had lower values of threshold of motion. The beds were less stable and fractional grain size started to move at lower critical

shear stresses. This also suggests that although the threshold of motion of grains in the stability test UF 3-12 are higher than UF 3-6, the values are still lower than the stability test UF 3-9 indicating that the individual grain size in the stability test UF 3-9 are the most stable in this series. Only grain size fraction of 1 mm was more mobile in stability test UF 3-9 than UF 3-12 as indicated by the lower critical shear stress and lower level of hiding for this grain. Again, similar to the findings in the other series of stability tests, the stability tests UF III also indicated that the finer grains gained their stability within the period of 6 hours while the increase in stability of the coarser grains were continuing.

7.1.2. Antecedent Flow Experiments

Initially high transport rates were experienced in all the constant flow antecedent Experiments SF I. With no upstream sediment feed, and the same original bed composition and formation, the transport rate was a function of time. These experiments indicated that the bed started to stabilise after 3 hours of constant flow and as the experiments continued a progressively more stable bed condition was achieved. However later on in some tests the transport rates started to slightly increase. It is believed that after around 9 hours a less stable bed condition was present as finer grains were continually transported increasing the exposure of the coarser grains. This resulted in the periodic release of small amounts of coarser grains. This is the most likely factor that caused the average transport rates of SF 1-12 not to follow the trend in which average transport rate was slightly higher than SF 1-9.

The decelerating flowrate sections of antecedent flow Experiments UF II produced a trend in which the average transport rate correlates with the level of flow unsteadiness. This is not the case in the accelerating flowrate section of the antecedent flow Experiments UF III where the average transport rate patterns are more complex. The most rapid increase in flowrate produced the highest transport. However the rate of increase of flowrate in the other tests did not match the rate of change in transport.

The importance of the duration of the antecedent flow on the composition of the bedload is also noted. The application of relatively high constant discharges to the freshly laid sediment bed had different impact in the mode of transport. In the first 3 hours the transport contained

large amounts of grains both in the fine and the coarse mode in comparison to the same periods later on in the tests. In these cases, the first three hours of constant flowrate transported either the fine or coarse mode was dominant in the bedload. This pattern also applied to the 3 hours of constant flowrate in antecedent flow experiments UF 2-6, UF 2-9 and UF 2-12. After 3 hours lower transport rate were established with the domination of grains in the fine mode. Proportionally antecedent flow Experiment SF 1-3 transported more grains in the coarse mode than in the fine mode whilst the longer antecedent flow experiments SF 1-6, SF 1-9 and SF 1-12 transported more grains in the fine mode than in the coarse mode.

Three stages of stabilisation process in the accelerating flowrates were experienced. Three hours of accelerating flowrates roughly disrupted the bed. The short duration did not allow the grains to settle and the increasing flowrates comfortably transported sediment into the bedload trap. This is indicated by the stability tests that the weakest bed was formed by the shortest accelerating flowrates. Initially it was thought that the longest duration of accelerating flowrate in UF 3-12 formed the most stable bed. This was dismissed by the fact that the bed formed by antecedent flow Experiment UF 3-12 is slightly less stable than the bed formed by antecedent flow Experiment UF 3-9. This suggests certain duration of accelerating flowrate is able to form a particular level of bed stabilisation. It is believed that the level of unsteadiness in the 6 hours accelerating flowrate was sufficiently enough to form a strong bound between different fractions in the bed mixture. The coarse grains dislodged and moved but the flows were not strong enough to carry considerable amounts downstream. As the flowrate declined mostly finer grains moved. These grains were then sheltered behind the coarse grains so that fine and coarse grains obtained better and more stable positions. They formed relatively flat surfaces and the fine and coarse grains were less exposed as demonstrated by the more 'peaked' bed elevation distribution curves. The stability test was able to destabilise and transported these grains but not in a similar fashion to the other stability tests. It is suspected that the similar process occurred in the accelerating flowrate section of antecedent flow Experiment UF 3-12. However longer duration of the high increasing flowrate caused the grains to reposition and making them slightly less stable than in antecedent flow Experiment UF 3-9. More exposed grains spread on the bed, which were easier to be brought into saltation and then were transported during the stability test.

7.1.3. Bursting Events and Flow Momentum

The average nearbed streamwise velocities are sensibly constant throughout the sections of constant flow hydrograph. The time averaged nearbed streamwise velocities tend to decrease as the test progressed but the range of variation is still relatively small. Similar observations to the grid points also suggest that the variations of average nearbed streamwise velocity are smaller if the time interval between two series of measurement is shorter.

In the observation of bursting events interesting features were found. In most of the antecedent flow experiments the downward looking bed interactions (sweeps) were more common than the upward interactions (ejections), even in the accelerating and decelerating flowrate sections. Only in antecedent flow experiments SF 1-6 and SF 1-12 ejections were slightly more frequent than sweeps.

The most popular level of momentum is associated with flow structures with magnitudes less than 5 kg/ms both in the upward and downward-looking bed interactions. More than 70 % of the bursting events contain momentum of this magnitude. These features existed in all antecedent flow tests with similar shape of distribution although the levels of momentum reduced with flowrate. The different patterns in transport suggest that the downward-looking bed interactions are not important factors in determining the transport. This dismissed the findings of Nelson et al (1995) who claimed that downward-looking bed interactions collectively move more sediment than upward interactions, primarily because the downward looking-bed interactions are more common.

The magnitude of momentum caused by ejections in the range between 5 and 20 kg/ms is a distinct feature, which is apparent in different proportions in the observations in every test. The different proportion of the higher magnitude of momentum ejections observed at different time elapsed is believed to have a very important role in determining the mode of transport. Comparison of several simultaneous experimental observations of bedload composition and flowrate demonstrated that the proportion of high momentum of ejections is very important in transporting the coarser grains. The ability of the relatively high magnitude of momentum to destabilise and transport the larger grains was also depending on the bed stability. As the armoured bed progressed and developed stable conditions the ability of momentum from

these ejections decreased accordingly. To some extent the transport may be more coarse grains-dominated if the time frequency of the ejections sweeps in the bursting events is higher than sweeps. However it can generally be said that the transport was relatively insensitive to the frequency and the proportion of both types of events. It is also found that the duration of events has no influence in determining the transport pattern as the observations indicated a relatively similar duration of both types of events in each antecedent flow test.

7.1.4. Bed Topography

The bed stability is closely linked with the bed structure formed by the antecedent flow tests. It is observed that at the end of each antecedent flow test the transport rate is very low and almost diminished to zero. The different level of bed stability showed by each stability test is characterised by a different formation on the bed surface at the end of antecedent flow test.

The examination of the distribution of bed surface elevations suggests that the bed formations that contain more larger grains with high level of exposure are likely to be the weaker beds. This is indicated by the probability distribution curves from the different series of experiment. Although the bed surface elevation distributions after steady antecedent flow display relatively similar curves, closer observation shows that there is a difference in the level of grain exposure for SF 1-3, SF 1-6, SF 1-9 and SF 1-12, particularly in the surface elevation above the mean level.

The weakest bed observed in the second series of stability tests (UF II) has a distribution curve of bed surface elevations which indicates more numerous exposed large grains appeared in UF 2-9 than in UF 2-6 and UF 2-12. In the third series of experiment (UF III), the instability of the bed in the stability test UF 3-6 is also reflected by high numbers of exposed large grains left on the bed after the antecedent flow test. These exposed larger grains are less stable and contributed to considerable amounts of transport in the stability tests.

In all the tests the bed topography observations displayed a similarity in the areal pattern. The erosion caused by the antecedent flow tends to form diagonal patches on the surface. The patches are stretched to the downstream direction of the measurement grid. Although further

erosion occurred in the stability tests the patches were maintained and still exist at the end of the final tests. The bed topography before and after stability test have relatively no significant differences in pattern although the amount of bedload transported in these tests are higher than in the longer duration antecedent flow tests. This can be explained in that the coarse grains dominated the transport during stability test and their movement did not considerably change the bed surface level or its surface organisations.

The bed topography plots indicated considerable decreases in the bed surface elevation at the end of the antecedent flow experiments. It is believed that during antecedent flow vertical sorting and horizontal sorting occurred simultaneously to characterise the development of the bed surface structure. Vertical sorting is indicated by the bed surface coarsening which is the accumulation of larger particles on the bed surface whilst the smaller or finer grains lay beneath them. Horizontal sorting is characterised by the different patterns of movement and deposition of the fine and coarse grains. During the antecedent flow it was found that the proportion of grains in the fine mode was dominant in transport. After stability tests the bed topographies are seen to have produced small changes although the amount of bedload transported in the stability tests were higher than in the antecedent flow experiments. This is the characteristic that the intense transport processes were followed by re-organisation of bed surface. Peak flowrates brought grains into saltation and then transported them downstream. As the flowrates decreased the grains in saltation started to move in a rolling fashion allowing the valleys to be re-filled again. Eventually the bed topography is seen to have small changes in its pattern. In fact, the changes in bed elevation are not as extreme as the changes in the antecedent flow tests as indicated by the smaller differences in the distribution curves before and after the stability tests.

7.2. RECOMMENDED FURTHER RESEARCH

7.2.1. Type of Flow Hydrograph

Constant flow is unlikely to be seen in natural rivers. This study has shown that mixed grain sediment beds of similar surface composition but formed by unsteady time varying flows produce water worked beds of highly variable stability. It is therefore suggested that further observations should be focused on time varying flows. Shorter tests, with higher value of

flowrate acceleration and deceleration are required to more closely simulate the conditions of natural rivers with small catchment areas.

Because of the complex pattern of changes in bed stability in the tests with different decelerating and accelerating flows, there is a need for further tests with similar patterns of hydrographs but with intermediate durations. It is recommended that the measurement should cover this duration so that every level of unsteadiness could be examined to identify how the bed stabilises as well as how the period of destabilisation is affected. In this case a detailed method of investigation should be developed to assess those variables affecting the bed strength.

7.2.2. Flow Measurement

It has been identified by the author that the changes in the time averaged nearbed streamwise flow velocity within a relatively small grid are relatively small. However the spatial variation in the average bed shear stress at different grid points was much larger and thus must be considered for further observation. The existing data could be re-examined with a view to determining the different flow structures that exist in different parts of the flow cross section. The measurement of the spatial variation of the flow behaviour, e.g. bursting events, could be correlated to the transport pattern. Therefore an important recommendation for future work is that the flow measurements should not be focused on a single point to represent the flow conditions at different time elapsed.

7.2.3. Composition of Bed Sediment Mixtures and Sediment Feed

The bimodal mixture used in these experiments was based on the assumption that many natural rivers contain materials with such distribution of grain size (Shaw and Kellerhals, 1982). However it is very interesting to discover if the pattern between the two modes would be significantly different if the grain size distance between modes and/or the relative proportion of the modes of the bimodal sediment bed was significantly changed. By applying such mixtures, not only would data be collected to check calculations of the sediment transport rate based on the availability of the size fraction in the surface layer (Suzuki and

Hano, 1991) but also different grain sorting mechanisms which may occur can be investigated.

It is also recommended to investigate whether feeding sediment has an effect on the bursting events and hence the magnitude of flow momentum. This is based on the possibility that feeding sediments may be transported downstream in saltation rather than in a rolling fashion. It is therefore very interesting to observe whether the saltating grains of the feed material are less or more easy to move further by changing the magnitude of momentum of the nearbed ejections or whether the grain saltations from the recirculated sediment may reduce or increase the level of bursting events.

7.2.4. Bed Topography Analysis

A large amount of detailed bed topography data within a grid was collected using the LDM and this was used solely to calculate the distribution of bed surface elevation both from the arbitrary zero datum and the average bed level. The bed topography plot could only be used to recognise the general pattern of erosion without detailed information on the grain exposure and the protrusion of individual grains relative to adjacent grains or surrounding areas. It is therefore envisaged that the available data could be re-examined using methods to quantify the spatial distribution of grain protrusion. It will also be beneficial if the information on how the particles on the surface are aligned and orientated over a range of scales can be obtained. This may be possible using techniques such as the 2-D structure functions as proposed by Goring et al (1999).

7.2.5. Impliactions for Natural Rivers

A numerical simulation method should be developed based on the physical mechanisms of bedload transport identified in this study. It is found that the relatively short duration of accelerating flowrate had a significant impact on the stability of mixed grain size sediment beds. Experiments indicated that the stabilisation process was not properly established in a relatively short period of accelerating flowrate. This resulted in many exposed coarse grains resting on the bed surface forming generally unstable and weak beds.

Having observed this condition it is emphasised that the findings in this experiment could be beneficial in the application or investigation of bedload transport behaviour in natural rivers with small and medium catchment area, as these type of rivers normally have a rapid rise of discharge during the flood flows with relatively short recession limbs.

The most stable beds appeared to be formed by tests in which the coarse grains rolled for long periods followed by periods where the fine grains also had the appropriate conditions to roll over the bed. This pattern was found in the tests with the long durations of decelerating flowrate. This phenomenon can be associated with lowland rivers, which normally have relatively longer recession limbs following storm events. It is therefore necessary to design a modelling technique which will be able to recognise the contribution of rolling processes of the coarse and fine grains over a length of time in forming a stable bed condition.

REFERENCES

Ackers, P., and White, W.R., 1973, **Sediment Transport : New Approach and Analysis**, Journal of Hydraulic Division, ASCE, 99 (11), 2041-2060.

Ahyerre, M., Chebbo, G., and Saad, M., 2002, **Sources and Erosion of Organic Solids in A Combined Sewer**, Draft paper.

Alfredsson, P.H., and Johansson, A.V., 1984, **Time Scales in Turbulent Channel Flow**, Physical Fluids, 27 (8), 1974-1981.

Andrews, E.D., 1983, **Entrainment of Gravel from Naturally Sorted Riverbed Material**, Geological Society American Bulletin, 94, 1225-1231.

Andrews, E.D., and Parker, G., 1987, **Formation of A Coarse Surface Layer as the Response to Gravel Mobility ; in Sediment Transport in Gravel Bed Rivers**, eds. C. R. Thorne, J.C. Bathurst and R.D. Hey, John Wiley and Sons, 269-300.

Armanini, A., 1992, **Variation of Bed and Sediment Load Mean Diameters due to Erosion and Deposition Process ; in Dynamics of Gravel-bed Rivers,** eds. P. Billi et al., John Wiley & Sons, Chichester, 351-359.

Ashida, K., and Fujita, M., 1986, **Stochastic Model for Particle Suspension in Open Channels**, Journal Hydroscience and Hydraulic Engineering, 4, 21-46.

Ashida, K., and Michiue, M., 1971, **An Investigation of River Bed Degradation Downstream of A Dam**, Proc. 14th Congress of the IAHR.

Barta, A.F., Wilcock, P.R., and Shea, C.C.C., 1994, **Transport of Gravels in Boulder Bed Stream**, Proc. National Conference on Hyd. Eng., ASCE, No. 2, 780-784.

Best, J., 1992, **On the Entrainment of Sediment and Initiation of Bed Defects : Insights from Recent Developments within Turbulent Boundary Layer Research**, Sedimentology, 39, 797-811.

Bettes, R., and White, W.R., 1981, **Mathematical Simulation of Sediment Movement in Streams**, Proc. Institution of Civil Engineers, Part II, 71, 879-892.

Biran, A., and Breiner, M., 1999, **Matlab 5 for Engineers**, Addison Wesley Longman, Harlow.

Biron, P., De Serres, B., Roy, A.G., and Best, J.L., 1993, **Shear Layer Turbulence at An Unequal Depth Channel Confluence ; in Turbulence, Perspectives on Flow**

and Sediment Transport, eds. Clifford, N.J., French, J.R., and Hardisty, J., John Wiley and Sons Ltd., Chichester, 197-213.

Blair, T.C., and McPherson, J.G., 1999, **Grain-Size and Textural Classification of Coarse Sedimentary Particles**, Journal of Sedimentary Research, 69 (1), 6-9.

Borah, D.K, 1982, **Routing Graded Sediments in Streams : Formulations**, Journal of Hydraulic Divisions, ASCE, 108 (12), 1486-1503.

Bray, D.I., Church, M., 1980, **Armoured versus Paved Gravel Beds**, Journal of Hydraulic Divisions, ASCE, 106, 1937-1940.

Buffington, J.M., and Montgomery, D.R., 1997, **A Systematic Analysis of Eight Decades of Incipient Motion Studies, with Special Reference to Gravel-bedded Rivers**, Water Resources Research, 33 (8), 1993-2029.

Cao, Z., 1997, **Turbulent Bursting-Based Sediment Entrainment Function**, Proc. Am. Soc. Civ. Engrs., Journal of Hydraulic Engineering, 123 (3), 233-236.

Carling, P.A., 1983, **Threshold of Coarse Sediment Transport in Broad and Narrow Natural Stream**, Earth Surface Processes Landforms, 8, 1-18.

Chadwick, A., and Morfett, J., 1986, **Hydraulics in Civil Engineering**, Allen and Unwin, London.

Chiu, C.L., 1989, **Velocity Distribution in Open Channel Flow**, Proc. Am. Soc. Civ. Engrs., Journal of Hydraulic Engineering, 115 (5), 576-594.

Chow, V. T., 1959, **Open Channel Hydraulics**, McGraw-Hill International, Singapore.

Church, M.A., McLean, D.G., and Wolcott, J.F., 1987, **River Bed Gravels : Sampling and Analysis ; in Sediment Transport in Gravel Bed Rivers,** eds. C.R. Thorne, J.C. Bathurst, and R.D. Hey, 43-88.

Church, M., Hassan, M.A., and Wolcott, J. F., 1998, **Stabilizing Self-organized Structures in Gravel-bed Stream Channels : Field and Experimental Observations**, Water Resources Research, 34 (11), 3169-3179.

Day, T.J., 1980, **A Study of the Transport of Graded Sediments**, Report IT190, Hydraulic Research Station, Wallingford.

Defina, A., 1996, **Transverse Spacing of Low-speed Streaks in a Channel Flow over a Rough Bed ; in Coherent Flow Structures in Open Channels,** eds. P.J. Ashworth, S.J. Bennet, J.L. Best and S.J. McLelland, John Wiley and Son, Chichester, 87 - 99.

De Jong, C., 1992, **Measuring Changes in Micro and Macro Roughness on Mobile**

Gravel Beds ; in Erosion and Sediment Transport Monitoring Programmes in River Basins, Proc. Oslo Symposium, IAHS Publication 210, 31-40.

Devore, J., and Peck, R., 1994, **Introductory Statistics**, West Publishing Company, Minneapolis.

Dietrich, W.E., Kirchner, J.W., Ikeda, H., and Iseya, F., 1989, **Sediment Supply and the Development of the Coarse Surface Layer in Gravel-Bedded Rivers**, Nature, 340, 215 - 217.

Diplas, P., 1987, **Bedload Transport in Gravel-Bed Streams,** Journal of Hydraulic Engineering, 113 (3), 277-292.

Diplas, P., and Sutherland, A.J., 1988, **Sampling Techniques for Gravel Size Sediments**, Proc. Am. Soc. Civ. Engrs., Journal of Hydraulic Engineering, 114 (5), 484-501.

Diplas, P., and Fripp, J.B., 1992, **Properties of Various Sediment Sampling Procedures**, Journal of Hydraulic Engineering, 118 (7), 955-969.

Di Silvio, 1992, **Modelling Sediment Transport under Different Hydrological and Morphological Circumstances ; in Dynamics of Gravel-bed Rivers** eds. P. Billi et al., John Wiley & Sons, Chichester, 363-371.

Dittrich, A., Nestmann, F., and Ergenzinger, P., 1996, **Ratio of Lift and Shear Forces over Rough Surfaces ; in Coherent Flow Structures in Open Channels,** eds. P.J. Ashworth, S.J. Bennet, J.L. Best and S.J. McLelland, John Wiley and Son, Chichester, 125-146.

Drake, T.G., Shreve, R.L., Dietrich, W.E., Whiting, P.J., and Leopold, L., 1988, **Bedload Transport of Fine Gravel Observed by Motion Picture**, Journal of Fluid Mechanics, 192, 2193-2217.

Du Boys, P.F.D., 1879, **Le Rhone et le Rivier a Lit Affouillable**, Annales des Ponts et Chausses, 18 ser. 5.

Egiazaroff, I.V., 1965, **Calculation of Non-uniform Sediment Concentration**, Proc. Am. Soc. Civ. Engrs., Journal of Hydraulic Division, 91, 225-247.

Einstein, H.A., 1950, **The Bedload Function for Sediment Transportation in Open Channel Flows,** Technical Bulletin, No. 1026, United States Department of Agriculture.

Einstein, H.A., 1971, **Sedimentation (Suspended Solids) ; in River Ecology and Man**, eds. R.T. Oglesby, C.A. Carlson, and J.A. McCann, Proc. International

Symposium on River Ecology and the Impact of Man, 309-318.

Engelund, F., and Hansen, E., 1967, **A Monograph on Sediment Transport in Alluvial Streams**, Teknisk Forlag, Copenhagen, Denmark.

Featherstone, R.E., and Nalluri, C., 1988, **Civil Engineering Hydraulics**, BSP Professional Books, Oxford.

Ferguson, R.I., Prestegaard, K.L., and Ashworth, P.J., 1989, **Influence of Sand on Hydraulics and Gravel Transport in A Braided Gravel Bed River**, Water Resource Research, 25, 635-643.

Folk, R.L., 1954, **The Distinction between Grain Size and Mineral Composition in Sedimentary Rock Nomenclature**, Journal of Geology, 62, 344-359.

Folk, R.L., 1974, **Petrology of Sedimentary Rocks**, Hemphill Publishing Company, Austin.

Folk, R.L., Andrews, P.B., and Lewis, D.W., 1970, **Detrital Sedimentary Rock Classification and Nomenclature for Use in New Zealand**, New Zealand Journal of Geology and Geophysics, 13, 937-968.

Furbish, D.J., 1987, **Conditions for Geometric Similarity of Coarse Stream-Bed Roughness**, Mathematical Geology, 19 (4), 291-307.

Garcia, M., Nino, Y., and Lopez, F., 1996, **Laboratory Observations of Particle Entrainment into Suspension by Turbulent Bursting ; in Coherent Flow Structures in Open Channels,** eds. P.J. Ashworth, S.J. Bennet, J.L. Best and S.J. McLelland, John Wiley and Son, Chichester, 63 - 86.

Gessler, J., 1991, **Armoring on the Surface of Gravel Bed Rivers Revisited**, Proc. the International Grain Sorting Seminar, Zurich, 299 - 309.

Gilbert, G.K., 1914, **The Transportation of Debris by Running Water**, US Geological Survey, Prof. Pap. 86.

Gomez, B., 1991, **Bedload Transport**, Earth Science Review, 31 (2), 89-132.

Gomez, B., 1994, **Effects of Particle Shape and Mobility on Stable Armor Development**, Water Resource Research, 30 (7), 2229-2239.

Goring, G., and Nikora, V.I, 2002, **Despiking Acoustic Doppler Velocimeter Data**, Journal of Hydraulic Engineering, 128 (1), 117-126.

Goring, D.G., Nikora, V.I., and McEwan, I.K., 1999, **Analysis of the Texture of Gravel-Beds using 2-D Structure Functions**, IAHR Symposium River Coastal and Estuarine Morphodynamics, Geneva.

Graf, W.H., and Suszka, L., 1985, **Unsteady Flow and Its Effect on Sediment Transport**, Proc. 21st IAHR Congress Melbourne, 539-544.

Graf, W.H., and Tu, H., 1992, **Vertical Distribution of Shear Stress in Unsteady Open Channel Flow**, Proc. Inst. Civ. Engrs., 96, 63-69.

Grass, A. J., 1970, **Initial Instability of Fine Bed Sand**, Journal of Hydraulics Division, ASCE, 96 (3), 619-632.

Grass, A.J., 1971, **Structural Features of Turbulent Flow over Smooth and Rough Boundaries**, Journal of Fluid Mechanics, 50 (2), 233-255.

Grass, A.J., 1992, **Experiments in Turbulent Motion**, Proc. 23rd Convegno di Idraulica e Costruzioni Idrauliche, Firenze, Italy, 5, 41-53.

Grass, A.J., and Mansour-Tehrani, M., 1996, **Generalised Scaling of Coherent Flow Structures in the Near-wall Region of Turbulent Flow over Smooth and Rough Boundaries ; in Coherent Flow Structures in Open Channels,** eds. P.J. Ashworth, S.J. Bennet, J.L. Best and S.J. McLelland, John Wiley and Son, Chichester, 41 - 61.

Grass, A.J., Stuart, R.J., and Mansour-Tehrani, M., 1991, **Vortical Structures and Coherent Motion in Turbulent-Flow over Smooth and Rough Boundaries,** Philosophical Transactions of the Royal Society of London, Mathematical Physical and Engineering Sciences, Series A, 336, 35-65.

Guezennec, Y.G., Piomelli, U., and Kim, J., 1989, **On the Shape and Dynamics of Wall Structures in Turbulent Channel Flow**, Physical Fluids A, 1, 764-766.

Gyr, A., 1983, **Towards A Better Definition of the Three Types of Sediment Transport**, Journal of Hydraulic Research, 21 (1), 1-15.

Gyr, A., and Muller, A., 1996, **The Role of Coherent Structures in Developing Bedforms during Sediment Transport ; in Coherent Flow Structures in Open Channels,** eds. P.J. Ashworth, S.J. Bennet, J.L. Best and S.J. McLelland, John Wiley and Son, Chichester, 227 - 247.

Hayashi, T.S., Ozaki, and Ichibashi, T., 1980, **Study on Bed Load Transport of Sediment Mixture**, Proc. 24th Japanese Conference on Hydraulics.

Hey, R.D., and Thorne, C.R., 1983, **Accuracy of Surface Samples from Gravel Bed Material**, Journal of Hydraulic Engineering, 109 (6), 842-851.

Holscher, H.H., 1971, **Simplified Statistical Analysis, Handbook of Methods, Examples and Tables**, Cahners Books, Boston.

Hubbell, D.W., 1987, **Bed Load Sampling and Analysis ; in Sediment Transport in Gravel Bed Rivers,** eds. C.R. Thorne, J.C. Bathurst, and R.D. Hey, 89-118.

Iseya, F., and Ikeda, H., 1987, **Pulsations in Bedload Transport Rates Induced by A Longitudinal Sediment Sorting - A Flume Study using Sand and Gravel Mixtures,** Geografiska Annaler Series A - Physical Geography, 69 (1), 15-27.

Jiang, Z., and Haff, P.K., 1993, **Multiparticle Simulation Methods Applied to the Micromechanics of Bed Load Transport,** Water Resources Research, 29, 399-412.

Jimenez, J., Moin, P., Moser, R., and Keefe, L., 1988, **Ejections Mechanism in the Sublayer of a Turbulent Channel** , Physical Fluids, 31, 1311-1313.

Jimenez, J., and Pinelly, A., 1997, **Dynamics of the Structures of Near Wall Turbulence,** Proc. of the IUTAM Symposium, eds. J.N. Sorensen, E.J. Hopfinger and N. Aubry, Lyngby Denmark, Kluwer Academic Publisher, 41-49.

Kaftori, D., Hetsroni, G., and Banerjee, S., 1994, **Funnel-shaped Vortical Structures in Wall Turbulence,** Physical Fluids, 6, 3035-3050.

Karim, F., 1998, **Bed Material Discharge Prediction for Non-uniform Bed Sediments,** Journal of Hydraulic Engineering, 124 (6), 597-604.

Kelsey, A., Allen, C.M., Beven, K.J., and Carling P.A., 1994, **Particle Tracking Model of Sediment Transport ; in Mixing and Transport in the Environment,** eds. K. Beven, P. Chatwin, J. Millbank, 419-442.

Kim, J., 1997, **Taming Near-Wall Streamwise Vortices : A Modus Operandi for Boundary Layer Control; in Simulation and Identification of Organized Structures in Flows,** Proc. of the IUTAM Symposium, eds. J.N. Sorensen, E.J. Hopfinger and N. Aubry, Lyngby Denmark, Kluwer Academic Publisher, 3-14.

Kim, H.T., Kline, S.J., and Reynolds, W.C., 1971, **The Production of Turbulence Near A Smooth Wall,** Journal of Fluid Mechanics, 50, 133-160.

Kim, S.C., Friedrichs, C.T., Maa, J.P.Y., and Wright, L.D., 2000, **Estimating Bottom Stress in Tidal Boundary Layer from Acoustic Doppler Velocimeter Data,** Journal of Hydraulic Engineering, 126 (6), 399-406.

Kirchner, J.W., Dietrich, W.E., Iseya, F., and Ikeda, H., 1990, **The Variability of Critical Shear Stress, Friction Angle, and Grain Protrusion in Water Worked Sediments ; in Sedimentology,** 37, 647-672.

Kirkbride, A., 1993, **Observations of the Influence of Bed Roughness on Turbulence Structure in Depth Limited Flows over Gravel Beds ; in Turbulence, Perspectives on Flow and Sediment Transport**, eds. Clifford, N.J., French, J.R., and Hardisty, J., John Wiley and Sons Ltd., Chichester, 185-196.

Kline, S.J., Reynolds, W.C., Schraub, F.A., and Runstadler, P.W., 1967, **The Structure of Turbulence in Boundary Layers**, Journal of Fluid Mechanics, 30, 741-773.

Klingeman, P.C., and Emmett, W.W., 1982, **Gravel Bedload Transport Processes ; in Gravel Bed Rivers,** eds. R.D. Hey, J.C. Bathurst, and C.R. Thorne, 141-179.

Komar, P.D., 1987, **Selective Gravel Entrainment and the Empirical Evaluation of Flow Competence**, Sedimentology, 34, 1165-1176.

Komar, P.D., and Li, Z., 1988, **Applications of Grain-Pivoting and Sliding Analyses to Selective Entrainment of Gravel and to Flow-Competence Evaluations**, Sedimentology, 35 (4), 681-695.

Kottegoda, N.T., and Rosso, R., 1998, **Statistics, Probability, and Reliability for Civil and Environmental Engineers**, McGraw-Hill, Singapore.

Kramer, H., 1935, **Sand Mixtures and Sand Movement in Fluvial Models**, Trans. Am. Soc. Civ. Eng., 100, 798-878.

Kraus, N.C., Lohrmann, A., and Cabrera, R., 1994, **New Acoustic meter for Measuring 3D Laboratory Flows**, Journal of Hydraulic Engineering, 120 (3), 406-412.

Krogstad, P.A., Antonia, R.A., and Browne, W.B., 1992, **Comparison between Rough and Smooth-Wall Turbulent Boundary Layers**, Journal of Fluid Mechanics, 245, 599-617.

Krumbein, W.C., 1934, **Size Frequency Distributions of Sediments**, Journal of Sedimentary Petrology, 4, 65-77.

Krumbein, W.C., 1938, **Size Frequency Distributions of Sediments and the Normal Phi Curve**, Journal of Sedimentary Petrology, 8, 84-90.

Kuhnle, R.A., 1993, **Incipient Motion of Sand-Gravel Sediment Mixtures**, Journal of Hydraulic Engineering, ASCE, 119 (12), 1400 - 1415.

Leopold, L.B., 1992, **Sediment Size that Determines Channel Morphology; in Dynamics of Gravel-bed Rivers**, eds. P. Billi, R.D. Hey, C.R. Thorne, aand P. Tacconi, John Wiley and Son Ltd.

Ligrani, P.M., 1989, **Structure of Turbulent Boundary Layers ; in Encyclopedia of**

Fluid Mechanics, Vol. 8 Aerodynamics and Compressible Flow, Gulf Publishing Company, Houston, 165-170.

Ling, C., 1995, **Criteria for Incipient Motion of Spherical Sediment Particles**, Journal of Hydraulic Engineering, ASCE, 121 (6), 472 - 478.

Liu, Z., Landreth, C.C., Adrian, R.J., and Hanratty, T.J., 1991, **Measurements in Turbulent Channel Flow by High Resolution Particle Image Velocimetry**, Exper. Fluids, 10, 301-312.

Lu, S.S., and Willmarth, W.W., 1973, **Measurements of the Structure of the Reynolds Stress in A Turbulent Boundary Layer**, Journal of Fluid Mechanics, 60 (3), 481-511.

Luchik, T.S., and Tiederman, W.G., 1987, **Timescale and Structure of Ejections and Bursts in Turbulent Channel Flows**, Journal of Fluid Mechanics, 174, 529-552.

Luchik, T.S., and Tiederman, W.G., 1988, **Turbulent Structure in Low-Concentration Drag-Reducing Channel Flows**, Journal of Fluid Mechanics, 190, 241-263.

Math Works Inc., 2000, **Matlab The Language of Technical Computing, Using Matlab Version 6**, The Math Works Inc, Natick.

Math Works Inc., 2000, **Matlab The Language of Technical Computing, Using Matlab Graphics Version 6**, The Math Works Inc, Natick.

McEwan, I., and Heald, J., 2001, **Discrete Particle Modelling of Entrainment from Flat Uniformly Sized Sediment Beds**, Journal of Hydraulic Engineering, 127 (7), 588-597.

McLelland, S.J., Ashworth, P.J., Best, J.L., and Livesey, J.R., 1999, **Turbulence and Secondary Flow over Sediment Stripes in Weakly Bimodal Bed Material**, Journal of Hydraulic Engineering, ASCE, 125 (5), 463 - 473.

Meirovich, L., Laronne, J.B., and Reid, I., 1998, **The Variation of Water-Surface Slope and Its Significance for Bedload Transport During Floods in Gravel Bed Streams**, Journal of Hydraulic Research, 36 (2), 147-167.

Meyer-Peter, E., and Muller, R., 1948, **Formulas for Bed Load Transport**, Proc. 2nd Meeting of IAHR, 39 - 65.

Miller, M.C., McCave, I.N., and Komar, P.D., 1977, **Threshold of Sediment Motion under Unidirectional Currents**, Sedimentology, 24, 507-527.

Misri, R.L., Garde, R.J., and Ranga Raju, K.G., 1984, **Bed Load Transport of Coarse**

Non-uniform Sediment, Journal of Hydraulic Engineering, 110 (3), 312-328.

Molinas, A., and Wu, B., 1998, **Effect of Size Gradation on Transport of Sediment Mixtures**, Journal of Hydraulic Engineering, 124 (8), 786-793.

Moore, D.S., and Mc Cabe, G.P., 1999, **Introduction to the Practice of Statistics**, 3rd edition, WH Freeman and Co., New York.

Muller, A., and Gyr, A., 1996, **Geometric Analysis of the Feedback between Flow, Bedforms and Sediment Transport ; in Coherent Flow Structures in Open Channels,** eds. P.J. Ashworth, S.J. Bennet, J.L. Best and S.J. McLelland, John Wiley and Son, Chichester, 237 -247.

Nakagawa, H., and Nezu, I., 1977, **Prediction of the Contributions to the Reynolds Stress from the Bursting Events in Open Channel Flows**, Journal of Fluid Mechanics, 80, 99-128.

Neill, C.R., and Yalin, M.S., 1969, **Quantitative Definition of Beginning of Bed Movement**, Journal of Hydraulic Division, ASCE, 95, 585-588.

Nelson, J.M., McLean, S.R., and Wolfe, S.R., 1993, **Mean Flow and Turbulence Fields over Two-Dimensional bed Forms**, Water Resources Research, 29 (12), 3935-3953.

Nelson, J.M., Shreve, R.L., McLean, S.R., and Drake, T.G., 1995, **Role of Near-Bed Turbulence Structure in Bed Load Transport and Bed Form Mechanics**, Water Resources Research, 31 (8), 2071-2086.

Nezu, I., Nakagawa, H., Ishida, Y., and Kadota, A., 1993, **Bed Shear Stress in Unsteady Open Channel Flows**, Proceeding National Conference on Hydraulic Engineering, Vol. 1, Eds. Shen, H.W. et al., pp. 1458-1463.

Nikora, V.I., and Goring, D.G., 1998, **ADV Measurements of Turbulence : Can We Improve Their Interpretation?**, Journal of Hydraulic Engineering, 124 (6), 630 - 634.

Nikora, V.I., Goring, D.G., and Biggs, B.J.F., 1998, **On Gravel-bed Roughness Characterization**, Water Resources Research, 34 (3), 517 - 527.

Nikora, V.I., and Goring, D.G., 1999a, **Are Weakly Mobile-Bed Flows A Special Class of Wall-Bounded Flows?**, Internal Report, NIWA, New Zealand.

Nikora, V.I., and Goring, D.G., 1999b, **Turbulence Structure in Gravel-Bed Flows with Static and Weakly Mobile Beds : A Comparative Study**, Internal Report, NIWA, New Zealand.

Nowell,, A.R.M., and Church, M., 1979, **Turbulent Flow in A Depth-Limited Boundary Layer**, Journal of Geophysical Research, 84 (C8), 4816-4824.

Offen, G.R., and Kline, S.J., 1974, **Combined Dye-Streak and Hydrogen-Bubble Visual Observations of A Turbulent Boundary Layer**, Journal of Fluid Mechanics, 62 (2), 223-239.

Parker, G., 1990, **Surface-Based Bedload Transport Relation for Gravel Rivers**, Journal of Hydraulic Research, 28 (4), 417-436.

Parker, G., 1991, **Some Random Notes on Grain Sorting**, Proc. the International Grain Sorting Seminar, Zurich, 19 - 76.

Parker, G., 1996, **Some Speculations on The Relation Between Channel Morphology and Channel-scale Flow Structures ; in Coherent Flow Structures in Open Channels**, eds. P.J. Ashworth, S.J. Bennet, J.L. Best and S.J. McLelland, John Wiley and Son, Chichester, 423 - 458.

Parker, G., and Klingeman, P.C., 1982, **On Why Gravel Bed Streams Are Paved**, Water Resources Research, 18 (5), 1409-1423.

Parker, G., Klingeman, P.C., and McLean, D.G., 1982, **Bedload and Size Distribution in Paved Gravel-bed Streams**, Journal of Hydraulics Division, ASCE, 108(4), 544-571.

Parker, G., and Sutherland, A. J., 1990, **Fluvial Armour**, Journal Hydraulics Research, 28, 529-544.

Parker, G., and Wilcock, P.R., 1993, **Sediment Feed and Recirculating Flumes : Fundamental Difference**, Journal of Hydraulics Engineering, 119 (11), 1192-1204.

Pender, G., and Li, Q., 1995, **Comparison of Two Hiding Function Formulations for Non-Uniform Sediment Transport Calculations**, Proc. of Institution of Civil Engineers Water, Maritime and Energy, 112, 127-135.

Petruccelli, J.D., Nandram, B., and Chen, M., 1999, **Applied Statistics for Engineers and Scientists**, Prentice Hall, New Jersey.

Profitt, G.T., and Sutherland, A.J., 1983, **Transport of Non-uniform Sediment**, Journal of Hydraulics Research, 21 (1), 33-43.

Ranga-Raju, K.G., Mittal, M.K., and Porey, P.D., 1991, **Hiding and Exposure Effects in the Bed Load Transport of Non-uniform Sediments**, Proc. the International Grain Sorting Seminar, Zurich, 109 - 126.

Raudkivi, A.J., 1991, **Basic Concepts of Soil Erosion and Sediment Transport; in Scouring**, H.N.C. Breusers and A.J. Raudkivi, A.A. Balkema, Rotterdam, 7-36.

Raudkivi, A.J., 1993, **Sedimentation ; Exclusion and Removal of Sediment from Diverted Water**, A.A. Balkema, Rotterdam.

Rees, D.G., 2001, **Essential Statistics**, Fourth Edition, Chapman & Hall/CRC, Boca Raton.

Reid, I., and Frostick, L.E., and Layman, J.T., 1985, **The Incidence and Nature of Bedload Transport During Floods in Coarse-Grained Alluvial Channels, Earth Surface Processes and Landforms**, 30, 33-44.

Reid, I., and Frostick, L.E., 1987, **Toward A Better Understanding of Bedload Transport ; in Recent Development in Fluvial Sedimentology**, eds. F.G. Ethridge, R.M. Flores and M.D. Harvey, 13-19.

Robinson, S.K., 1991, **Coherent Motions in the Turbulent Boundary Layer**, Ann. Rev. Fluid Mech., 23, 601-639.

Roy, A. G., Buffin-Belanger, T., and Deland, S., 1996, **Scales of Turbulent Coherent Flow Structures in a Gravel-bed River ; in Coherent Flow Structures in Open Channels,** eds. P.J. Ashworth, S.J. Bennet, J.L. Best and S.J. McLelland, John Wiley and Son, Chichester, 147 - 164.

Saadi, Y, 2000, **The Impact of Unsteady Flows on the Erosion and Movement of Mixed Grain Size Sediment**, Transfer Report, Department of Civil and Structural Engineering University of Sheffield.

Samaga, B.R., Ranga Raju, K.G., and Garde, R.J., 1985, **Concentration Distribution of Sediment Mixtures in Open Channel Flow,** Journal of Hydraulic Research, 23 (5), 467-483.

Samaga, B.R., Ranga Raju, K.G., and Garde, R.J., 1986, **Bedload Transport of Sediment Mixtures,** Journal of Hydraulic Engineering, 112 (11), 1003-1018.

Sear, D.A., 1996, **The Sediment System and Channel Stability ; in River Channel Restoration : Guiding Principles for Sustainable Projects**, eds. A. Brookes and F.D. Shields, 149-177.

Shaw, J., and Kellerhals, R., 1982, **The Composition of Recent Alluvial Gravels in Alberta River Beds**, Bulletin 41, Alberta Research Council, Edmonton, Canada.

Shen, H.W., and Lu, J.Y., 1983, **Development and Prediction of Bed Armouring,** Journal of Hydraulic Engineering, 109 (4), 611-629.

Shields, A., 1936, **Anwendung der Aehnlichkeitsmechanik und der Turbulenszforschung auf die Geschiebebewegung**, Mitt. Preuss. Versuchsanst. Wasserbau Schiffbau, 26, 26 (English translation by W.P. Ott and J.C. van Uchelen, US Dept. of Agric. Soil Conser. Serv. Coop. Lab., California Institute of Technology, Pasadena).

Shvidchenko, A.B., and Kopaliani, Z.D., 1998, **Hydraulic Modelling of Bedload Transport in Gravel-bed Laba River**, Journal of Hydraulic Engineering, 124 (8), 779-785.

Shvidchenko, A.B., Pender, G., and Hoey, T.B., 2001, **Critical Shear Stress for Incipient Motion of Sand/Gravel Streambed**, Water Resources Research, 37 (8), 2273-2283.

Simon, A.L., and Korom, S.F., 1997, **Hydraulics, 4th Edition**, Prentice Hall, New Jersey.

Simons, D.B., and Simons, R.K., 1987, **Differences Between Gravel and Sand-bed Rivers ; in Sediment Transport in Gravel Bed Rivers,** eds. C.R. Thorne, J.C. Bathurst, and R.D. Hey, 2-15.

Sirovich, L., and Karlsson, S., 1997, **Turbulent Drag Reduction by Passive Mechanisms**, Nature, 388, 753-755.

Smart, G.M., 1999, **Turbulent Velocity Profiles and Boundary Shear in Gravel Bed Rivers**, Journal of Hydraulic Engineering, 125 (2), 106-116.

Smith, C.R., 1996, **Coherent Flow Structures in Smooth-wall Turbulent Boundary Layers : Facts, Mechanism and Speculation ; in Coherent Flow Structures in Open Channels,** eds. P.J. Ashworth, S.J. Bennet, J.L. Best and S.J. McLelland, John Wiley and Son, Chichester, 1 - 39.

Smith, C.R., and Metzler, S.P., 1983, **The Characteristics of Low-Speed Streaks in the Near-Wall Region of A Turbulent Boundary Layer**, Journal of Fluid Mechanics, 129, 27-54.

Snyder, W. H., and Castro, I. P., **Acoustic Doppler Velocimeter Evaluation in Stratified Towing Tank**, Journal of Hydraulic Engineering, 1999 125 (6), 595-603.

Song, T., and Graf, W.H., 1996, **Velocity and Turbulence Distribution in Unsteady Open-Channel Flow**, Journal of Hydraulic Engineering, 122 (3), 141-154.

SonTek, 1994, **ADV Precise Measurements of 3-D Fluid Flow**, Hydraulic Research

Station, Wallingford.

SonTek, 1995, **ADV Operation Manual Version 1.0**, SonTek Inc., San Diego, California.

Sumer, B.M., and Deigaard, 1981, **Particle Motions Near the Bottom in Turbulent Flow in An Open Channel**, Part 2, Journal of Fluid Mechanics, 109, 311-337.

Sumer, B.M., and Oguz, B.,1978, **Particle Motions Near the Bottom in Turbulent Flow in An Open Channel**, Journal of Fluid Mechanics, 86, 109-127.

Sutherland, A.J., 1967, **Proposed Mechanism for Sediment Entrainment by Turbulent Flows**, Journal of Geophys. Res., 72, 191-198.

Sutherland, A.J., 1991, **Hiding Functions to Predict Self Armouring**, Proc. the International Grain Sorting Seminar, Zurich, 273 - 298.

Sutherland, A.J., and Williman, E. B., 1977, **Development of Armoured Surfaces in Alluvial Channels**, Proc. 6th Australasian Hydraulics and Fluid Mechanics Conference, Adelaide, 352 - 355.

Suzuki, K., and Hano, A., 1991, **Grain Size Change of Bed Surface Layer and Sediment Discharge of an Equilibrium River Bed**, Proc. the International Grain Sorting Seminar, Zurich, 151 - 162.

Tait, S.J., and Willetts, B.B., 1991, **Characterisation of Armoured Bed Surfaces**, Proc. the International Grain Sorting Seminar, Zurich, 207-225.

Tait, S.J., Willetts, B.B., and Maizels, J.K., 1992, **Laboratory Observations of Bed Armouring and Changes in Bedload Composition ; in Dynamics of Gravel-bed Rivers** eds. P. Billi et al., John Wiley & Sons, Chichester, 205-226.

Tait, S.J., 1993, **The Physical Processes of Bed Armouring in Mixed Grain Sediment Transport**, PhD Dissertation, University of Aberdeen.

Tait, S. J., Willetts, B. B., and Gallagher, M.W., 1996, **The Application of Particle Image Velocimetry to the Study of Coherent Flow Structures over a Stabilizing Sediment Bed : Facts, Mechanism and Speculation ; in Coherent Flow Structures in Open Channels,** eds. P.J. Ashworth, S.J. Bennet, J.L. Best and S.J. McLelland, John Wiley and Son, Chichester, 185 - 201.

Tu, H., and Graf, W. H., 1992, **Vertical Distribution of Shear Stress in Unsteady Open-Channel Flow**, Proc. Institution of Civil Engineers, 96, 63-69.

Udden, J.A., 1914, **Mechanical Composition of Clastic Sediments**, Geological Society of America, Bulletin, 25, 655-744.

Urushihara, T., Meinhart, C.D., and Adrian, R.J., 1993, **Investigation of the Logaritmic Layer in Pipe Flow using Particle Image Velocimetry ; in Near-Wall Turbulent Flows**, eds. So, R.M.C, Speziale, C.G., and Launder, B.E., Elsevier Science Publishers B.V., 433-446.

Vanoni, V.A., 1964, **Measurements of Critical Shear Stress for Entraining Fine Sediments in A Boundary Layer**, Report No. KH-R-7, California Institute of Technology, Pasadena.

van Rijn, L.C., 1984, **Prediction of Sediment Transport and Alluvial Roughness**, Proc. ASCE, Journal of Hydraulic Division, 110, 1733-1754.

Velikanov, M.A., 1955, **Dynamics of Alluvial Streams** (in Russian), Vol. II (Sediment and Flow Bed), State Publishing House of the Theoretical and Technical Literature, Moscow.

Voulgaris, G., and Trowbridge, J.H., 1998, **Evaluation of the Acoustic Doppler Velocimeter (ADV) for Turbulence Measurements**, Journal of Atmospheric and Oceanic Technology, (15), 272-289.

Wathen, S.J., Ferguson, R.I., Hoey, T.B., and Weritty, A., 1995, **Unequal Mobility of Gravel and Sand in Weakly Bimodal River Sediments**, Water Resources Research, 31, 2087-2096.

Weedman, S.D., and Slingerland, R., 1985, **Experimental Study of Sand Streaks Formed in Turbulent Boundary Layers**, Sedimentology, 32, 133-145.

Wells, J., 1992, **Experiences sur les Impacts Liquide-solide et le Soulevement de Particular par un Tourbillon Annulaire : Application a L'Erosion des Sols et au Transport des Sediments**, Unpublished PhD Thesis, University Joseph Fourier, Grenoble I, France.

White, C.M., 1940, **The Equilibrium of Grains on the Bed of A Stream**, Proc. Royal Society London A, 174, 322-338.

White, W.R., and Day, T.J., 1982, **Transport of Graded Gravel Bed Material ; in Gravel-Bed Rivers**, eds. R.D. Hey, J.C. Bathurst, and C.R. Thorne, John Wiley and Son, 181-224.

Wiberg, P.L., and Smith, J.D., 1985, **A Theoretical-Model for Saltating Grains in Water,** Journal of Geophysical Research-Oceans, 90 (NC4), 7341-7354.

Wiberg, P.L., and Smith, J.D., 1987, **Calculations of the Critical Shear Stress for Motion of Uniform and Heterogeneous Sediments**, Water Resource Research, 23

(8), 1471-1480.

Wilcock, P.R., 1988, **Methods for Estimating the Critical Shear Stress of Individual Fractions in Mixed-Size Sediment**, Water Resource Research, 24 (7), 1127-1135.

Wilcock, P.R., 1992, **Flow Competence-A Criticism of A Classic Concept**, Earth Surface Processes Landforms, 17 (3), 289-298.

Wilcock, P.R., 1993, **Critical Shear Stress of Natural Sediments**, Journal of Hydraulic Engineering, ASCE, 119 (4), 491-506.

Wilcock, P.R.,and Southard, J. B., 1988, **Experimental Study of Incipient Motion in Mixed-Size Sediment**, Water Resource Research, 24 (7), 1137-1151.

Wilcock, P.R.,and Southard, J. B., 1989, **Bedload Transport of Mixed Size Sediment-Fractional Transport Rates, Bed Forms, and the Development of A Coarse Bed Surface Layer**, Water Resource Research, 25 (7), 1629-1641.

Wilcock, P.R., and McArdell, B.W., 1993, **Surface-Based Fractional Transport Rates: Mobilization Thresholds and Partial Transport of A Sand-Gravel Sediment**, Water Resource Research, 29 (4), 1297-1312.

Willetts, B.B., Maizels, J.K., and Florence, J., 1987, **The Simulation of Stream Bed Armouring and Its Consequences**, Proc. Institution of Civil Engineers, Part 1 (82), 799-814.

Williams, P.B., and Kemp, P.H., 1971, **Initiation of Ripples on Flat Sediment Beds**, Journal of Hydraulic Divisions, ASCE, 97, 505-522.

Willmarth, W.W., and Lu, S.S., 1972, **Structure of the Reynolds Stress Near the Wall**, Journal of Fluid Mechanics, 55, 65-92.

Wu, W., Wang, S.S.Y., and Jia, Y., 2000, **Non-Uniform Sediment Transport in Alluvial Rivers**, Journal of Hydraulic Research, ASCE, 38 (6), 427-434.

Yalin, M.S., 1977, **Mechanics of Sediment Transport**, 2nd Edition, Pergamon Press, Oxford.

Yalin, M.S., and Karahan, E., 1979, **Inception of Sediment Transport**, Journal of Hydraulic Division, ASCE, 105, 1433-1443.

Yang, C.T., 1973, **Incipient Motion and Sediment Transport**, Journal of Hydraulic Division, ASCE, 99 (10), 1679-1704.